

BIROn - Birkbeck Institutional Research Online

Enabling Open Access to Birkbeck's Research Degree output

Mobility of Pb and Zn in a neutral mine drainage setting, Gunnerside Gill, Yorkshire

<https://eprints.bbk.ac.uk/id/eprint/47623/>

Version: Full Version

Citation: Tame, Catherine Diana McLaren (2020) Mobility of Pb and Zn in a neutral mine drainage setting, Gunnerside Gill, Yorkshire. [Thesis] (Unpublished)

© 2020 The Author(s)

All material available through BIROn is protected by intellectual property law, including copyright law.

Any use made of the contents should comply with the relevant law.

[Deposit Guide](#)
Contact: [email](#)

Mobility of Pb and Zn in a Neutral Mine
Drainage Setting, Gunnerside Gill, Yorkshire

Catherine Diana McLaren Tame

Birkbeck, University of London

PhD Thesis

April 2020



Declaration

This thesis is a presentation of my original research work. Wherever contributions of others are involved, every effort has been made to indicate this clearly, with due reference to the literature.

This work was done under the guidance of Professor Karen Hudson-Edwards, Birkbeck College, University of London and Dr Hugh Potter, Environment Agency.

Name: Catherine Tame

Abstract

Numerous areas throughout the world are affected by circum-neutral pH, low iron (Fe) drainage with high concentrations of lead (Pb) and zinc (Zn) arising from discharges from, and weathering of, mine wastes. Gunnerside Gill, a small upland tributary in the headwaters of the River Swale in Yorkshire, is such a site affected by historic Pb mining. The aim of the study is to assess the controls on Pb and Zn mobilisation from the mine tailings and alluvial sediments to the river water through geochemical characterisation (including total digestion, x-ray diffraction and sequential extraction), column leaching experiments and aqueous field data. Previous studies have largely focused on the metallic element concentrations within the sediments and there has been little or no investigation into the concentrations within the mine wastes.

Total concentrations of Pb ranged from 1,840 to 70,000 mg/kg and Zn concentrations ranged from 2,000 to 64,300 mg/kg. The column leachate experiment showed that pH is the main control on the dissolution of ore minerals within Gunnerside Gill. The control of Zn mobility is largely governed by the dissolution of primary (sphalerite) and secondary minerals (for example smithsonite) within the mine waste samples and from the dissolution of secondary minerals within the alluvial sediments. In the mine waste samples Pb mobility was largely controlled by the dissolution of secondary minerals, with weathering rims were often noted on the primary ore grains. The mobility of Pb within the alluvial sediment sample appeared to be controlled by the dissolution of primary and secondary ore minerals, but also Mn oxyhydroxides that act as a temporary sink for Pb. The alluvial sediment sample was found to leach between 10 to 17 times more Pb than the mine waste samples. Similarly a higher concentration of Zn was mobilised from the sediment sample than the mine wastes. This is considered to be a function of age of the mine wastes and the location of the alluvial sample downstream of both the main mining and processing areas.

Potential management options include localised reactive barriers at the mine adits, phytostabilisation of mine wastes and sediments, and small scale civil engineering barriers to reduce the direct mobilisation of mine wastes and sediments into Gunnerside Gill.

Acknowledgements

Firstly I would like to thank my supervisors, Karen Hudson-Edwards and Hugh Potter for their support throughout my long PhD journey. I would also like to acknowledge Robert White of the Yorkshire Dales National Park Authority for his guidance during the site visit Gunnerside Gill.

I would also like to give special thanks to Professor Andy Carter, Jim Davy, Dr David Kossoff, Gary Tarbuck, Hank Sombroek and Dr Chris Hibbert for their ongoing support throughout the project. This thesis would not have been completed without the constant and unwavering support from Jim and David in particular. In addition, thank you to Professor Martin Smith for allowing me to use the XRD at the University of Brighton. Also many thanks to Keith Hardcourt for his proof reading skills.

This thesis is also dedicated to the people who started on the PhD journey but for whatever reason were not able to complete their studies. This has been an incredibly difficult, terrifying, exciting and long process and there were many points where I wanted to quit.

Finally, my thanks to my parents for moral support and allowing me to store many of my samples at their house.

Acronyms

ALKMD – alkaline mine drainage

AMD – acid mine drainage

BCR - Community Bureau of Reference

BGS – British Geological Survey

CEC – cation exchange capacity

CND – contaminated neutral drainage

CRM – certified reference material

DEFRA - Department for Environment, Food and Rural Affairs

EA – Environment Agency

EQS – environmental quality standards

G-BASE - Geochemical Baseline Survey of the Environment

HDPE – high density polyethylene

ICP-OES – inductively coupled plasma optical emission spectrometry

NMD – neutral mine drainage

SoBRA – Society of Brownfield Risk Assessment

USEPA – United States Environmental Protection Agency

Glossary

Adit – horizontal access to a mine

Battle – certified reference material from the National Water Research Institute, Environment Canada

Gangue – a mineral or rock of no economic value that is present in association with ore minerals

Isomorphic – atom of a similar size

PHREEQC – is a computer program that is designed to perform a wide variety of aqueous geochemical calculations

Rhizosphere – soil zone around roots

TMDA – a certified reference water produced by the National Water Research Institute of Canada

Mineral Formulas and Element Symbols

| MINERAL | |
|-----------------|--|
| Name | Formula |
| Akaganeite | $(\text{Fe}^{3+}, \text{Ni}^{2+})_8(\text{OH}, \text{O})_{16}\text{Cl}_{1.25} \cdot n\text{H}_2\text{O}$ |
| Anglesite | PbSO_4 |
| Arsenopyrite | FeAsS |
| Augite | $(\text{Ca}, \text{Na})(\text{Mg}, \text{Fe}, \text{Al})(\text{Si}, \text{Al})_2\text{O}_6$ |
| Ankerite | $\text{Ca}(\text{Fe}^{2+}, \text{Mg})(\text{CO}_3)_2$ |
| Barite | BaSO_4 |
| Bauxite | $\text{Al}(\text{OH})_3$ |
| Beudantite | $\text{PbFe}_3(\text{AsO}_4)(\text{SO}_4)(\text{OH})_6$ |
| Calcite | CaCO_3 |
| Cerussite | PbCO_3 |
| Chalcocite | Cu_2S |
| Chalcopyrite | CuFeS_2 |
| Dolomite | $\text{CaMg}(\text{CO}_3)_2$ |
| Feldspar | $\text{KAlSi}_3\text{O}_8, \text{NaAlSi}_3\text{O}_8, \text{CaAl}_2\text{Si}_2\text{O}_8$ |
| Ferrihydrite | $\text{FeO}(\text{OH})$ |
| Franklinite | ZnFeO |
| Galena | PbS |
| Goethite | $\text{FeO}(\text{OH})$ |
| Gypsum | $\text{CaSO}_4 \cdot 2\text{H}_2\text{O}$ |
| Hematite | Fe_2O_3 |
| Hemimorphite | $\text{Zn}_4(\text{OH})_2 \cdot \text{H}_2\text{O}$ |
| Illite | $\text{K}_{0.65}\text{Al}_{2.0}[\text{Al}_{0.65}\text{Si}_{3.35}\text{O}_{10}](\text{OH})_2$ |
| Jarosite | $\text{KFe}^{3+}_3(\text{SO}_4)_2(\text{OH})_6$ |
| Lepidocrocite | $\text{FeO}(\text{OH})$ |
| Maghemite | $\text{Fe}^{3+}_2\text{O}_3$ |
| Magnetite | Fe_3O_4 |
| Montmorillonite | $(\text{Na}, \text{Ca})_{0.33}(\text{Al}, \text{Mg})_2(\text{Si}_4\text{O}_{10})(\text{OH})_2 \cdot n\text{H}_2\text{O}$ |
| Palygorskite | $(\text{Mg}, \text{Al})_2\text{Si}_4\text{O}_{10}(\text{OH}) \cdot 4\text{H}_2\text{O}$ |
| Pyrite | FeS_2 |
| pyromorphite | $\text{Pb}_5(\text{PO}_4)_3\text{Cl}$ |
| Pyrrhotite | Fe_7S_8 |
| Quartz | SiO_2 |
| Sepiolite | $\text{Mg}_4(\text{Si}_6\text{O}_{15})(\text{OH})_2 \cdot 6\text{H}_2\text{O}$ |
| Siderite | FeCO_3 |
| Smithsonite | ZnCO_3 |
| Sphalerite | ZnS |
| Vermiculite | $\text{Mg}_{0.7}(\text{Mg}, \text{Fe}, \text{Al})_6(\text{Si}, \text{Al})_8\text{O}_{20}(\text{OH})_4 \cdot 8\text{H}_2\text{O}$ |
| Witherite | BaCO_3 |
| Willemite | Zn_2SiO_4 |
| Zinkosite | ZnSO_4 |

| ELEMENT | |
|----------------|---------------|
| Name | Symbol |
| Aluminium | Al |
| Antimony | Sb |
| Arsenic | As |
| Barium | Ba |
| Cadmium | Cd |
| Calcium | Ca |
| Chromium | Cr |
| Cobalt | Co |
| Copper | Cu |
| Fluorine | F |
| Gold | Au |
| Iron | Fe |
| Lead | Pb |
| Magnesium | Mg |
| Manganese | Mn |
| Mercury | Hg |
| Nickel | Ni |
| Oxygen | O |
| Phosphorus | P |
| Potassium | K |
| Selenium | Se |
| Silver | Ag |
| Sodium | Na |
| Strontium | Sr |
| Sulfur | S |
| Thallium | Tl |
| Zinc | Zn |

Table of Contents

| | |
|--|-----------|
| Declaration | 2 |
| Abstract | 3 |
| Acknowledgements | 4 |
| Acronyms and Glossary | 5 |
| Mineral Formulas and Element Symbols | 6 |
| | |
| Chapter 1 - Introduction | 15 |
| 1.1 Mining Catchments and Neutral Mine Drainage (NMD) | 15 |
| 1.2 Study Site - The River Swale and Gunnerside Gill | 16 |
| 1.3 Aim and Objectives | 16 |
| 1.4 Structure of the report | 18 |
| | |
| Chapter 2 – Review of Literature | 20 |
| 2.1 Mining related contamination in river systems and the assessment of such contamination | 21 |
| 2.1.1 Mining Inputs of Contaminants to River Systems | 21 |
| 2.1.2 Toxicity of Pb, Zn and Cd | 30 |
| 2.1.3. Assessment of Contamination in Mining-Affected River Systems | 32 |
| 2.1.4 Legislation Relating to Rivers and Mine Waste | 34 |
| 2.1.5 Thresholds to Determine the Impacts of Mining on Rivers Waters and Sediments | 34 |
| 2.2 Introduction to Metallic Elements Behaviour and Control | 39 |
| 2.2.1 Geochemical Behaviour of Metallic Elements | 39 |
| 2.2.1.1 pH | 42 |
| 2.2.1.2 Mineralogy | 43 |
| 2.2.1.3 Cation Exchange Capacity (CEC) | 45 |
| 2.2.1.4 Manganese and Iron Oxide, Oxyhydroxide and Hydroxide Coatings | 46 |
| 2.2.1.5 Organic Matter | 48 |
| 2.2.1.6 Microbiology | 48 |
| 2.2.1.7 Oxidic and Anoxic Conditions | 49 |
| 2.2.2 Physical Controls of Metallic Element Mobility | 51 |
| 2.3 Mine Drainage | 53 |
| 2.3.1 Definitions of Acid Mine, Circum-Neutral and Alkaline Mine Drainage | 53 |
| 2.4 Mineral Weathering Reactions | 59 |
| 2.4.1 Neutralisation Reactions | 63 |

| | |
|---|------------|
| 2.5 Worldwide Mine Drainage | 66 |
| 2.5.1 Neutralisation by Host Rock Buffering: Global Case Studies | 66 |
| 2.5.2 Changes in Mine Drainage Chemistry over Time | 72 |
| 2.6 Column Leaching Studies Mineral Weathering Processes Leading to Processes and Products of Mine Drainage | 73 |
| 2.7 Investigating Metallic Element Speciation by BCR Sequential Extractions | 77 |
| 2.8 Conclusions | 78 |
| Chapter 3 – Area of Study | 80 |
| 3.1 The North Pennine Orefield | 80 |
| 3.2 General Characteristics of the River Swale | 82 |
| 3.3 Swale Catchment Geology | 83 |
| 3.3.1 Pb-Zn Mineralisation | 84 |
| 3.4 Mining in the River Swale Catchment | 89 |
| 3.5 Mining-related metal contamination of the Swale Floodplain | 91 |
| 3.6 Gunnerside Gill | 96 |
| 3.7 Mining in Gunnerside Gill | 99 |
| 3.7.1 Blakethwaite Mines | 100 |
| 3.7.2 Lownathwaite Mines | 101 |
| 3.7.3 Old Gang Mines | 101 |
| 3.7.4 Sir Francis Level | 102 |
| 3.8 Previous studies describing mining-related metal contamination of Gunnerside Gill | 103 |
| 3.9 Summary | 107 |
| Chapter 4 – Materials and Methods | 109 |
| 4.1 Sample Collection | 109 |
| 4.2 Solid Analysis | 113 |
| 4.2.1 XRD | 113 |
| 4.2.2 Acid Digestion | 113 |
| 4.2.3 Sequential Extractions | 115 |
| 4.2.4 Electron Microprobe Analysis | 117 |
| 4.2.5 Carbon Determination | 117 |
| 4.2.6 Particle Size Analysis | 117 |
| 4.2.7 Solid pH Analysis | 118 |
| 4.3 Column Leaching Experiments | 118 |
| 4.3.1 Column Leachate Analysis | 122 |
| 4.4 Statistical Analysis | 123 |
| 4.5 Computer Modelling | 124 |
| 4.6 Precision and Accuracy | 124 |
| 4.7 Summary | 129 |

| | |
|--|------------|
| Chapter 5 – Results | 131 |
| 5.1 Characterisation of Samples | 132 |
| 5.1.1 Particle Size Distribution | 132 |
| 5.1.2 Soil pH | 133 |
| 5.1.3 Geochemical Characterisation – total digestion | 133 |
| 5.2 BCR Sequential Extraction | 139 |
| 5.2.1 BCR Sum vs Total Digestion | 145 |
| 5.3 Mineralogical Characterisation | 147 |
| 5.3.1 XRD | 147 |
| 5.3.2 EMP | 150 |
| 5.3.3 Mineralogy Summary Table | 157 |
| 5.4 Column Experiment | 159 |
| 5.4.1 Column Samples | 160 |
| 5.4.2 Leachate Volume, pH and Eh | 160 |
| 5.4.3 Physical Characteristics | 162 |
| 5.4.3.1 Visual Description of Post Column Material | 162 |
| 5.4.3.2 PSD | 162 |
| 5.4.4 Leachate Chemistry | 163 |
| 5.4.4.1 ICP | 163 |
| 5.4.5 Electron Microprobe | 170 |
| 5.4.6 Total Digestion | 174 |
| 5.4.7 BCR Sequential Extraction | 177 |
| 5.5 Summary | 181 |
| | |
| Chapter 6 – Results and Discussion of Pb and Zn Mobility and Control Mechanisms | 183 |
| 6.1 Characterisation of samples | 184 |
| 6.1.1 Particle size | 184 |
| 6.1.2 Mineralogy | 185 |
| 6.1.2.1 Mine waste mineralogy | 185 |
| 6.1.2.2 Sediment mineralogy | 187 |
| 6.1.3 Bulk Geochemistry | 188 |
| 6.1.4 Solid Phase-Speciation of Metallic Elements | 188 |
| 6.1.5 pH of Solid Phases and Column Leachate | 190 |
| 6.1.6 Comparison of Samples | 193 |
| 6.1.6.1 Gun 1 | 193 |
| 6.1.6.2 Gun 2 | 195 |
| 6.1.6.3 Gun 3 | 197 |
| 6.1.6.4 Gun 4 | 199 |
| 6.1.6.5 Gun 5 | 199 |
| 6.1.6.6 Gun 6 | 199 |
| 6.1.6.7 Gun 7 | 200 |

| | |
|--|------------|
| 6.1.6.8 Gun 8 | 200 |
| 6.1.6.9 Gun 9 | 200 |
| 6.1.6.10 Gun 10 | 202 |
| 6.1.6.11 Summary of Sample Comparison | 203 |
| 6.2 Comparison to Published Threshold Values | 208 |
| 6.2.1 Mine Wastes and Sediments | 208 |
| 6.2.2 Column Leachate | 210 |
| 6.3 Column Leachate vs EA Monitoring Data | 211 |
| 6.4 Geochemical Modelling | 217 |
| 6.4.1 Changes in pH | 221 |
| 6.5 Comparison to Previous Studies | 224 |
| 6.6 Controls on Weathering Reactions | 226 |
| 6.6.1 Eh-pH from Column Leachate Experiment | 227 |
| 6.6.2 pH from EA Monitoring Data | 231 |
| 6.6.3 Ficklin Classification | 233 |
| 6.6.4 Mineralogy | 234 |
| 6.6.5 Location of Mine Wastes and Impacted Sediments | 235 |
| 6.6.6 Grain Size | 238 |
| 6.6.7 Prediction of Metallic Element Mobility | 239 |
| 6.7 Comparison to Worldwide Drainage | 240 |
| 6.8 Summary | 243 |
| | |
| Chapter 7 Conclusions and Recommendations | 245 |
| 7.1 Conclusion | 245 |
| 7.2 Recommendations | 248 |
| 7.3 Further Work and Limitations | 251 |
| | |
| References | 243 |
| Appendix A – Summary of EA data | 270 |
| Appendix B – Summary of BCR data | 304 |
| Appendix C – Summary of column leachate data | 312 |
| Appendix D – Summary of XRD data | 323 |

Table of Figures

| | |
|---|----|
| Figure 1.1: Location of the study area Gunnerside Gill | 16 |
| | |
| Figure 2.1: Conceptual model of the main physicochemical processes occurring within a tailings or waste rock heap | 27 |
| Figure 2.2: A model for the dispersal and storage of mine waste | 29 |
| Figure 2.3: Range of pH of AMD and NMD | 54 |
| Figure 2.4: Geochemical plot for the total dissolved metals and pH | 57 |

| | |
|---|-----|
| Figure 2.5: Tools to predict the chemistry of mine drainage | 73 |
| Figure 3.1: Sketch map showing the location of the main rivers and associated orefields of the Pennines | 82 |
| Figure 3.2: Geology map of the River Swale | 84 |
| Figure 3.3: Locations of the Alston and Askrigg blocks | 85 |
| Figure 3.4: Location of Gunnerside Gill including the main Pb mining areas from A.D 1700-1900 | 91 |
| Figure 3.5: Pb vertical profiles taken from the Swale with locations indicated on map | 92 |
| Figure 3.6: Changes in downstream Pb concentration in the River Swale, arrows represent the approximate tributary locations | 93 |
| Figure 3.7: Simplified geology map of Gunnerside Gill including major faults | 97 |
| Figure 3.8: Mines and veins of Gunnerside Gill | 97 |
| Figure 3.9: Location of mining areas and scheduled monuments in Gunnerside Gill | 98 |
| Figure 3.10: Field photos of Gunnerside Gill showing the former mine structures and waste rock piles (appear as grey material in the photos). | 100 |
| Figure 3.11: Block flux diagram with the different contributions (cumulative %) of Pb, Zn and Cd in Gunnerside Gill | 106 |
| Figure 4.1: Sample location photographs | 111 |
| Figure 4.2: Gunnerside Gill sample location map | 112 |
| Figure 4.3: Experimental column set up | 120 |
| Figure 5.1: Triplot showing the particle size distribution of the samples | 132 |
| Figure 5.2: Relative concentrations of Pb, Zn and Cd | 134 |
| Figure 5.3: Total concentrations and standard error of Pb and Zn downstream of GG1 | 136 |
| Figure 5.4: Standard error based on the mean total concentrations of Gun 1 to Gun 10 solid samples | 137 |
| Figure 5.5: Zn/S and Pb/S correlation graphs | 137 |
| Figure 5.6: BCR sequential extraction relative proportions for Pb and Zn | 140 |
| Figure 5.7: BCR sequential extraction results for Mn, Fe and Mg | 142 |
| Figure 5.8: BCR sequential extraction results for S, Al and Ca | 144 |
| Figure 5.9: BCR sequential extraction sum of all steps compared to the respective total digestion relative proportions for Pb, Zn and Mn. | 145 |
| Figure 5.10: BCR sequential extraction sum of all steps compared to the respective total digestion relative proportions for Fe and S. | 146 |
| Figure 5.11: BCR sequential extraction sum of all steps compared to the respective total digestion relative proportions for Mg, Al and Ca. | 147 |

| | |
|---|-----|
| Figure 5.12: Examples of the peak locations of cerussite (Gun 1) and galena and sphalerite (Gun 5) | 148 |
| Figure 5.13: Typical galena, sphalerite and cerussite XRD spectrum | 149 |
| Figure 5.14: Backscattered electron images of Gunnerside Gill tailings and sediments. Gun 5 and Gun 7 show the highest proportion of bright grains. | 151 |
| Figure 5.15: Elemental map showing Cd-, Cu- and Zn-bearing Fe oxihydroxide rimmed by Si-Al-K bearing clay mineral (Gun 1) | 152 |
| Figure 5.16: Elemental map showing Cd- and Na- bearing Zn sulfide rimmed by Ba oxide or carbonate (Gun 5) | 153 |
| Figure 5.17: Elemental map showing Pb sulfide rimmed by Pb oxide or carbonate and clay minerals (Gun 2) | 154 |
| Figure 5.18: Elemental map showing Cu-, Cd and Mn bearing Pb sulfide rimmed by barite and Pb oxide or carbonate (Gun 5) | 155 |
| Figure 5.19: Elemental map showing Cu-, Cd- and Mn- bearing Pb sulfide rimmed by barite and Pb oxide or carbonate (Gun 10) | 156 |
| Figure 5.20: Elemental map showing Cd- bearing Pb-Zn phosphate (Gun 9) | 157 |
| Figure 5.21: Volume, pH and Eh of column leachate including 'blank' (black line) | 161 |
| Figure 5.22: Post column solids with Munsell colour chart detail | 162 |
| Figure 5.23: Post column solids particle size in comparison to pre-column experiment solids | 163 |
| Figure 5.24: Column leachate ICP data for Pb, Zn and S ($\mu\text{g/L}$) | 164 |
| Figure 5.25: Column leachate ICP data for Mn, Mg and Fe ($\mu\text{g/L}$) | 166 |
| Figure 5.26: Column leachate ICP data for Ba, Ca and Al ($\mu\text{g/L}$) | 168 |
| Figure 5.27: Column leachate anion data for chloride, NO _x and sulphate | 169 |
| Figure 5.28: General view backscattered EMP photomicrographs of post column solids | 170 |
| Figure 5.29: Backscattered EMP photomicrographs of post column solids showing grains of interest in each sample | 171 |
| Figure 5.30: Elemental maps from CGun 1 (above) and CGun 2 (below) | 172 |
| Figure 5.31: Elemental maps from CGun 3 (above) and CGun 9 (below) | 173 |
| Figure 5.32: Pre and post column solid total digestion comparison for the key elements of concern Pb and Zn (mg/kg) | 176 |
| Figure 5.33: Pre and post column BCR data for Pb and Zn | 178 |
| Figure 5.34: Pre and post column BCR data for Mn, Fe and S | 180 |
| | |
| Figure 6.1: Correlation graphs for various pairs of elements from Gun 1 leachate ($\mu\text{g/L}$) | 194 |
| Figure 6.2: Correlation graphs for various pairs of elements from Gun 2 leachate ($\mu\text{g/L}$) | 196 |
| Figure 6.3: Correlation graphs for various pairs of elements from Gun 3 leachate ($\mu\text{g/L}$) | 198 |

| | |
|--|-----|
| Figure 6.4: Correlation graphs for various pairs of elements from Gun 9 leachate ($\mu\text{g/L}$) | 202 |
| Figure 6.5: Correlation graphs for various pairs of elements from the solid phases of Gun 1 to Gun 10 (mg/kg) | 206 |
| Figure 6.6: Column leachate concentrations vs EA monitoring data for Pb | 213 |
| Figure 6.7: Column leachate concentrations vs EA monitoring data for Zn | 214 |
| Figure 6.8: Column leachate concentrations vs EA monitoring data for Mn | 215 |
| Figure 6.9: Column leachate concentrations vs EA monitoring data for Ca | 215 |
| Figure 6.10: Eh-pH diagram for Pb-O-H | 228 |
| Figure 6.11: Eh-pH diagram for Zn-O-H | 229 |
| Figure 6.12: Eh-pH diagram for Mn-O-H | 230 |
| Figure 6.13: Eh-pH diagram for Fe-O-H | 231 |
| Figure 6.14: Ficklin plot of EA data and column leaching data | 233 |
| | |
| Figure 7.1: Conceptual site model for the reactions at Gunnerside Gill | 246 |

List of Tables

| | |
|---|-----|
| Table 2.1: Typical Pb and Zn concentrations in Great Britain stream sediments | 33 |
| Table 2.2: Soil guidelines for the acceptable levels of Pb, Zn and Cd | 36 |
| Table 2.3: Drinking water guidelines for the acceptable levels of Pb, Zn and Cd | 37 |
| Table 2.4: Mineralogy of selected clays, surface area and CEC | 45 |
| Table 2.5: Electron acceptor reaction sequence | 50 |
| Table 2.6: Examples of the geochemistry of NMD and ALKMD | 57 |
| Table 2.7: Relative resistance to alteration of sulfides in oxidised tailings | 61 |
| | |
| Table 3.1: Minerals of the Yorkshire Dales | 86 |
| Table 3.2: Estimated Pb production and storage in the tributaries of the River Swale | 95 |
| Table 3.3: Previous studies of Pb, Zn and Cd concentrations in floodplain sediments of the Upper Swale and Gunnerside Gill. | 103 |
| | |
| Table 4.1: Sample descriptions | 110 |
| Table 4.2: Sequential extraction target phases | 116 |
| Table 4.3: Volume of water added to columns to represent the seasons | 121 |
| Table 4.4: Average precision values for BCR sequential extraction results ($\pm\%$) | 124 |
| Table 4.5: Average accuracy values for BCR CRM 701 (%) | 125 |
| Table 4.6: Average accuracy values for the BCR sequential extraction for the water step (CRMs – TMDA-64 and Battle) (%) | 125 |
| Table 4.7: Absolute differences between the BCR CRM pairs as a percentage of the average (%) | 126 |

| | |
|--|-----|
| Table 4.8: Limit of detection and limit of quantification for the BCR sequential extraction procedure (ppm) | 126 |
| Table 4.9: Average precision values for the column leachate ($\pm\%$) | 127 |
| Table 4.10: Average accuracy values for the column leachate (TMDA-64 and Battle) (%) | 127 |
| Table 4.11: Limit of detection and limit of quantification for the column leachate (ppm) | 128 |
| Table 4.12: Average accuracy values for the total digestions and residual BCR step (TMDA-64 and Battle) (%) | 128 |
| Table 4.13: Average precision values for the total digestions (%) | 128 |
| Table 4.14: Limit of detection and limit of quantification for the total digestions (ppm) | 129 |
| | |
| Table 5.1: pH values of solid samples | 133 |
| Table 5.2: Total digestion concentrations for all ten samples (mg/kg) | 135 |
| Table 5.3: Pearson coefficients for key elements | 138 |
| Table 5.4: Relative proportions of Zn and Pb in pre column solids compared to total concentrations | 138 |
| Table 5.5: XRD results for mine wastes (Gun 1 to Gun 8) and sediments (Gun 9 and Gun 10) from Gunnerside Gill | 158 |
| Table 5.6: Average column leachate pH values | 161 |
| Table 5.7: Pre and post column particle size distribution data (%) | 163 |
| Table 5.7: Total digestion concentrations of the post column solids and pre column solids (mg/kg) | 175 |
| | |
| Table 6.1: Spearman and Pearson correlation for Gun 9 leachate | 207 |
| Table 6.2: Average aqueous concentrations of Pb and Zn from the column leachate experiment | 211 |
| Table 6.3: Saturation indices of key minerals from EA monitoring data | 219 |
| Table 6.4: Saturation indices from column leachate experiments | 221 |
| Table 6.5: Summary of the saturation indices from EA monitoring data for pH's 8, 7.5, 7, 6.5, 6, and 5.5 | 222 |
| Table 6.6: Summary of saturation indices from column leachate data for pH's 8, 7.5, 7, 6.5, 6, and 5.5 | 223 |
| Table 6.7: Total Pb and Zn concentrations (mg/kg) compared to calculated 'pre-mining' background values from Brewer at al. (2005). | 225 |
| Table 6.8: pH values reported following EA water monitoring campaign (EA 2013) | 232 |
| Table 6.9: Summary of key primary and secondary minerals for mine wastes (Gun 1 to Gun 8) and sediments (Gun 9 and Gun 10) | 234 |

Chapter 1

Introduction

Contents

| | |
|---|----|
| 1.1 Mining Catchments and Neutral Mine Drainage (NMD) | 15 |
| 1.2 Study Site - The River Swale and Gunnserside Gill | 16 |
| 1.3 Aim and Objectives | 17 |
| 1.4 Structure of the report..... | 18 |

1.1 Mining Catchments and Neutral Mine Drainage

Neutral mine drainage (NMD) is a worldwide problem but has been subject to less research than acid mine drainage (AMD). This is partly due to its lack of visibility, since it does not create the bright colours associated with AMD. Many historical mining areas in the British Isles are characterised by circum-neutral, low-Fe drainage, with high levels of dissolved Zn, Pb and Cd, these include Wales, the Irish Republic and North Pennines (Warrender and Pearce, 2007).

Problems associated with NMD extend to Europe as studied by various researchers including;- Alvarez-Ayuso et al. (2013); Sterckeman et al. (2000); Resongles et al. (2014); Tesser et al. (2011); Pavoni et al. (2018); Strzebońska et al. (2017); Postawa and Motyka (2018); Gomes et al. (2010); and worldwide, for example, Carroll et al. (1998); Kelley and Taylor (1997); Lindsay et al. (2009); Hammarstrom et al. (2002), Desbarats and Dirom (2007); Sracek et al. (2011); Sanusi et al. (2017); Ramos Arroyo and Siebe (2007); Chappell and Craw (2002); and Argane et al. (2015). Although AMD is a widely used term, only a small number of polluting mine waters are actually acid (Younger et al., 2001). This idea is further supported by recent industry guidance published on abandoned mine workings (CIRIA, 2019), which reports that there are less acidic and more neutral and alkaline mine waters within the British Isles. It has been estimated that 12,000 km² of river catchments in the north of England are directly affected by historical mining (Johnston et al., 2008) and in Scotland most of the polluting mine drainage is circum-neutral and alkaline in nature (Younger et al., 2001).

The overarching objective of this study is to increase the understanding of the mechanisms controlling NMD in a historically mined catchment in the North Pennines. The implications for NMD are environmental (including water, soil, sediments, flora and fauna) and may adversely impact the health of people living nearby, or even downstream of the affected area.

1.2 Study Site - The River Swale and Gunnerside Gill

The River Swale and more specifically Gunnerside Gill (Figure 1.1) was selected as the location for the study as they are circum-neutral water courses, and the area has been investigated previously, by Macklin et al. (1994), Dennis et al. (2003, 2009), and as a result there is background data available. The history of mining is relatively well understood and much of Gunnerside Gill is accessible on foot. Furthermore, the Environment Agency (EA) undertook a campaign of water sampling and testing in 2010 and 2011 to better understand the effects of historical mining on water quality and aqueous ecology within Gunnerside Gill. Further work was required to identify the mechanisms responsible for transfer of Pb, Zn and Cd from the mine wastes and sediments to the catchment waters, which this project has to address.

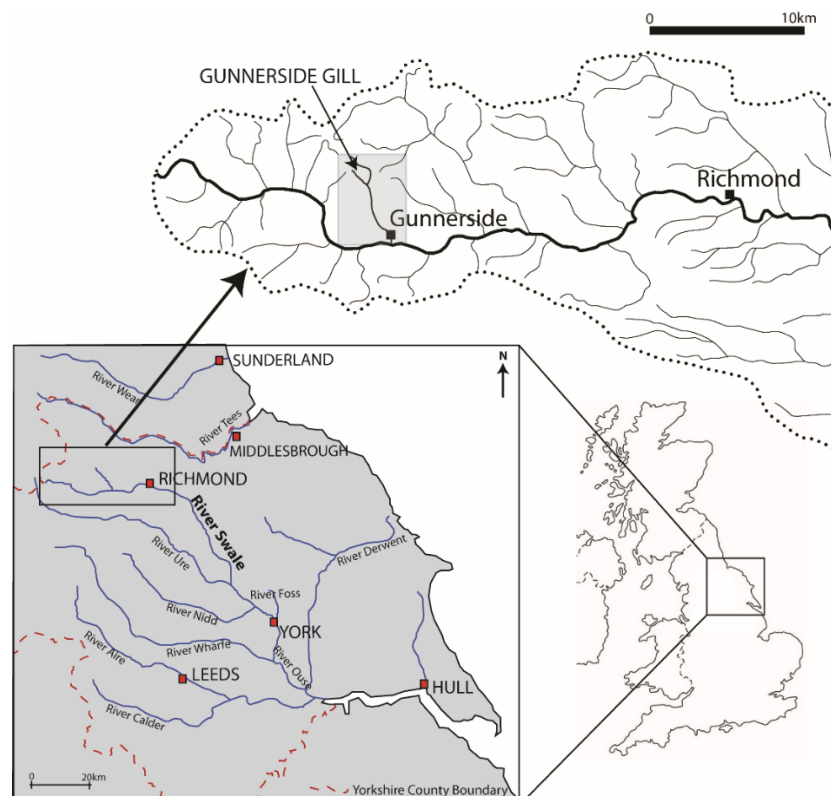


Figure 1.1: Location of the study area Gunnerside Gill (after coolgeography.co.uk 2019 and Dennis, 2005)

Dennis et al. (2003) have recorded concentrations of Pb up to 8,000 mg/kg and Zn up to 14,000 mg/kg (channel edge and overbank sediments respectively) within the River Swale as a result of sediment input from Gunnerside Gill. Stream sediment mean concentrations UK wide of Pb and Zn were recorded as 84.6 mg/kg and 152.4 mg/kg, respectively, in the British Geological Surveys (BGS) Geochemical Baseline Study of Great Britain (BGS 2009a/2009b). The values recorded by Dennis et al. (2003) indicate that the concentrations of Pb and Zn within Gunnerside Gill are well above average concentrations when compared to the rest of England and Wales and therefore the gill is a representative highly contaminated site to study the mechanisms and controls of NMD.

Given that the sediments within Gunnerside Gill are largely derived from the upstream mine wastes it is considered that the concentrations of metallic elements are likely to be higher in the mine wastes, as these are the source materials. Dennis et al. (2009) estimated that the Pb retention and storage in Gunnerside Gill was 1,602 tonnes, with a total estimated production of 17,796 tonnes from the associated mines. Previous studies have focused on the concentrations of Pb and Zn within the channel and overbank sediments. This study aims to investigate the metallic element concentrations within both the mine wastes and the sediments. In order to guide this study, the current hypothesis is that 'higher concentrations of metallic elements are released from the solid mine wastes than the sediments into the catchment waters of Gunnerside Gill as a result of historical mining activities'.

1.3 Aim and Objectives

The aim of the study is to determine the controls on Pb and Zn mobility from the mine tailing / waste and river bank sediments in a NMD setting, namely Gunnerside Gill.

The aim will be fulfilled by carrying out the following specific objectives:

1. Characterisation of the solid-phase speciation of the metallic elements present in mine waste and sediments;
2. Determining the major factors influencing the transfer of metallic elements from solids into the waters, e.g. mineralogy, grain-size,

location of the mine tips and/or contaminated sediments, pH, reductive dissolution of the Fe/Mn oxyhydroxides, or solution chemistry;

3. Using column leaching experiments, aqueous field data and geochemical modelling to determine the influence of changes in the environmental setting, i.e. reduction of pH, increased or decreased rainfall due to the effects of climate change.

The results of the study will be compared to other NMD settings around the British Isles and worldwide to see if any significant trends can be identified. The results will help to predict how Pb, Zn and Cd cycle through mining affected catchments with the intention to reduce the environmental and human health impacts.

1.4 Structure of the thesis

Chapter 1 is a short introduction into the nature and extent of NMD. This chapter also outlines the aims and objectives of the work. The background of the problem is expanded in Chapter 2, which is a review of existing scientific publications and available industry guidance. This includes the mining inputs to river systems, the toxicity of Pb, Zn and Cd, national and international legislation and published threshold concentrations, metallic element behaviour and controls, definition of NMD and mineral weathering reactions and the worldwide nature of the problem. Investigation techniques including column leachate studies and sequential extraction procedures are considered. Chapter 3 describes the Gunnerside Gill study site in detail with regards to geology, historical mines and mining techniques, and previous studies undertaken. Chapter 4 presents the sampling, laboratory, statistical analysis and computer modelling methodologies used in the study. It also includes a section detailing the precision and accuracy of the techniques where possible. The results of the study are reported in Chapter 5. The first half of the chapter (5.1 to 5.3) relates to the characterisation of the samples. The second half of the chapter (5.4) focuses on the results of the column leaching experiment. Chapter 6 is a discussion of the controls of Pb and Zn mobility within Gunnerside Gill, aiming to address the objectives outlined in Section 1.3. The characterisation of the samples is discussed in Section 6.1 to 6.3, looking at

the mineralogy and geochemistry of the samples initially and then comparing the data to the published threshold values to better assess the human and environmental risks. Then the results are compared to the EA data and previously published studies. Section 6.4 takes the data from the study and the EA data to create geochemical models to try and determine the effects of changes within the environment, i.e. changes in pH, on the potential metallic element release into the catchment waters. The results are compared to previous studies, worldwide mine drainage and the controls on weathering reactions are examined. Section 6.7 is a comparison to worldwide NMD. The main findings and conclusions of the thesis are outlined in Chapter 7. This also includes potential further work and management options for the metallic element contamination within Gunnerside Gill.

Chapter 2: Review of Literature

Mining Contamination in River Catchments

Contents

| | |
|---|----|
| Chapter 2..... | 20 |
| 2.1 Mining-related contamination in river systems and the assessment of such contamination..... | 21 |
| 2.1.1 Mining Inputs of Contaminants to River Systems..... | 21 |
| 2.1.2 Toxicity of Pb, Zn and Cd..... | 30 |
| 2.1.3 Assessment of Contamination in Mining-Affected River Systems..... | 32 |
| 2.1.4 Legislation Relating to Rivers and Mine Waste..... | 34 |
| 2.1.5 Thresholds to Determine the Impacts of Mining on Rivers Waters, Sediments and Soils | 34 |
| 2.2 Introduction to Metallic Elements Behaviour and Control..... | 39 |
| 2.2.1 Geochemical Behaviour of Metallic Elements | 39 |
| 2.2.1.1 pH..... | 42 |
| 2.2.1.2 Mineralogy | 43 |
| 2.2.1.3 Cation Exchange Capacity | 45 |
| 2.2.1.4 Manganese and Iron Oxide, Oxyhydroxide and Hydroxide Coatings | 46 |
| 2.2.1.5 Organic Matter..... | 48 |
| 2.2.1.6 Microbiology | 48 |
| 2.2.1.7 Oxidic and Anoxic Conditions..... | 49 |
| 2.2.2 Physical Controls of Metallic Element Mobility | 51 |
| 2.3 Mine Drainage..... | 53 |
| 2.3.1 Definitions of Acid Mine, Circum-Neutral and Alkaline Mine Drainage | 53 |
| 2.4 Mineral Weathering Reactions | 59 |
| 2.4.1 Neutralisation Reactions..... | 63 |
| 2.5 Worldwide Mine Drainage..... | 66 |
| 2.5.1 Neutralisation by Host Rock Buffering: Global Case Studies | 66 |
| 2.5.2 Changes in Mine Drainage Chemistry over Time..... | 72 |
| 2.6 Column Leaching Studies Mineral Weathering Processes Leading to Processes and Products of Mine Drainage | 73 |
| 2.7 Investigating Metallic Element Speciation by BCR Sequential Extractions..... | 77 |
| 2.8 Conclusions | 78 |

Chapter 2 will give the context for this work. It will describe mining-related contamination in river systems and the assessment of such contamination (Section 2.1). Metallic element geochemistry will be covered in Section 2.2. Section 2.3 will look at the different types of mine drainage and Section 2.4 will detail some relevant mineral weathering reactions. Towards the end of this chapter, examples of worldwide mine drainage (Section 2.5) and methods for studying mineral weathering processes (Section 2.6 and 2.7) will be discussed.

2.1 Mining-related contamination in river systems and the assessment of such contamination

2.1.1 Mining Inputs of Contaminants to River Systems

A mining catchment can be broadly defined as the drainage basin of a specific watercourse where mining activities, such as extraction, processing, storage of ores and wastes, or disposal, have been or are being undertaken. As is the case with many aspects of environmental geology, contaminated sites can vary hugely depending on the historic activities undertaken and the nature of the site itself, including the underlying geology, land use, hydrogeology and hydrology. It is also the case that no two river systems are ever the same; although general similarities and differences can often be observed. In many historic mining areas, the metallic elements (including metalloids for the purposes of this discussion) released by mining activities are likely to have obscured the natural background contribution to stream sediments. For example, in some cases finely-ground waste rock and tailings were discharged directly into any nearby waterway, thereby masking the background concentrations of natural metallic element load of the river (Helgen and Moore, 1996). As the population of the world increases, so does the need for metallic elements resulting in the potential for soil, sediment and water contamination to increase, especially in developing nations (Sparks, 2005). Surface water and groundwater throughout Europe has been and remains heavily impacted by historical mining activities, for example Italy

(Drescher-Schneider et al., 2007; Tesser et al., 2011; Cidu et al., 2012), France (Resongles et al., 2014) and Germany (Kalbitz and Wennrich, 1998). The result of this is the reduced potential for these water bodies reaching a 'good status' as required by the Water Framework Directive (Gandy et al., 2007), see Section 2.1.4.

Environmental contamination resulting from the mining, processing and subsequent utilisation of metallic elements forms one of the earliest changes to geochemical cycles by human activity (Macklin, 1992). Mining has been undertaken for coal, metalliferous ores and minerals in Britain since the Bronze Age, and has often resulted in environmental contamination (Johnston et al., 2008). Mining activities generally affect reasonably small geographical areas, however in those areas can have huge impacts on the local environment (Salomons, 1995). Whilst it is the case that contamination can reduce with distance from a point source, the effects can often be far reaching. For example, metallic element contamination has been recorded around 40 km downstream of the nearest mine site within the River Tyne basin in the British Isles (Macklin et al., 1997).

Although modern mining techniques and environmental legislation have been put in place to limit the input of mine wastes into rivers, this has not always been the case, so historical mining waste has been and is still being incorporated into fluvial systems today (Lewin et al., 1977). Modern mines collect water and discharge it to settling ponds or tailings dams, but historically mine wastes caused contamination at local or regional scales as they often discharged directly into the surrounding environment from adits and shafts (Lottermoser, 2010). Even though adit and shaft discharges are often more visible sources, mineral processing, tailings heaps and waste disposal are also important spatially as they are often spread over a large area (Johnson et al., 2008).

Early studies of mining areas often investigated the concentrations and spatial extent of metallic elements within the vicinity of the mining activities (for example Li and Thornton, 1993; Jung and Thornton, 1996), but they did

not necessarily investigate the mechanisms that control the mobility of metallic elements.

The impact of mining on the natural environment is also a worldwide issue. Examples of mine drainage issues include, but are in no way limited to; America (Carroll et al., 1998; Kelley and Taylor, 1997; Lindsay et al., 2009; Hammerstrom et al., 2002), Canada (Desbarats and Dirom, 2007), Spain (Alvarez-Ayuso et al., 2013), France (Strerckeman et al., 2000 and Resongles et al., 2014), Italy (Tesser et al., 2011; Pavoni et al., 2018), Poland (Strzebonska et al., 2017; Postawa and Motyka, 2019), Portugal (Gomes et al., 2010), Zambia (Sracek et al., 2011), Nigeria (Sanusi et al., 2017), Mexico (Ramos Arroyo and Siebe, 2007), New Zealand (Chappell and Craw, 2002) and Morocco (Argane et al., 2015). For example, Pb-Zn mines are common worldwide around 240 are thought to still be active, but most have been abandoned and can represent hazard as a result of metallic element release to the surrounding environment and rivers (Gutierrez et al., 2016). In mining regions one of the most common and important sources of metallic element-bearing particles in rivers are the direct discharges of mine tailings, effluent and waste rock from mining activities (Hudson-Edwards, 2003). In addition, unplanned mining-related metallic element-bearing releases to surface waters occur, including accidental discharge of mine and processing of wastes, failures of tailings dams, remobilisation of mining contaminated sediments, and abandoned mine drainage (Hudson-Edwards, 2003).

It is well recognised in the British Isles that managing the environmental effects resulting from abandoned metalliferous mines is often based on water quality being the main remediation driver (Johnston et al., 2008). In the British Isles there is a substantial amount of water quality data for specific mine sites, particularly for some of the worst affected locations. Nationally our understanding of mining impacts on river catchments is not entirely complete, this is partly due to a limited understanding of how significant diffuse mine water contamination can be in mining affected catchments (Jarvis et al., 2007). To emphasise the geographical extent of the problem it has been

estimated that 12,000 km² of river catchments in the north of England are directly affected by historical mining (Johnston et al., 2008). To give this more context, the Humber River basin covers an area of around 26,100 km², the Northumbria River basin covers around 9,000 km² and the North West river basin covers around 13,200 km² (Ordnance Survey, 2018). This indicates that approximately 25 % of the river catchments in the north of England are impacted by historical mining. This figure is likely to be less nationally given the spatial distribution of metallic element mine sites around the British Isles.

Such historic contamination by metalliferous mining of fluvial sediments can result in the formation of stratigraphic horizons with distinctive geochemical fingerprints (Brewer and Taylor, 1997) and in large volumes of waste rock often being stored in unsaturated heaps at or near the mine location (Amos et al., 2015). One problem with the management of older mines and their associated infrastructure is the evolution of a mine site over time is commonly undocumented, including changes in mine ownership resulting in the loss of records of mining and waste disposal procedures (Younger and Robins, 2002). Up until the mid-18th century, wastes from mines were of little interest, the volumes produced were not recorded and often they were disposed of by the cheapest and most convenient methods available, generally by dumping in or close to the nearest river (Hochella et al., 2005; Palumbo-Roe and Colman, 2010). It is difficult to investigate problems associated with historical metalliferous mining and smelting because of the absence of information with regards to the location of 'hot spots', such as tailing heaps and pits (Stefanowicz et al., 2014) and processing areas. There is still no national record of mine waste products in the British Isles; although there is an inventory for England and Wales which details closed and/or abandoned mine waste sites that could seriously impact the surrounding environment (Potter and Johnston, 2014). This complies with a European Commission Directive (2006/21/EC) in which member states are required to create an inventory of closed waste facilities. In addition, there was little or no understanding of the broad environmental impacts until relatively recently, with the exception of localised and extreme cases (Palumbo-Roe and Colman, 2010). In England and Wales, a major continuing impact of metallic

element mining is the contamination of suspended, channel and floodplain sediments by metallic elements and metalloids including As, Cd, Cu, Pb and Zn in the 2 mm and finer fraction (Hudson-Edwards et al., 2008). Whether sediment-bound mining waste will become a source of toxic elements to water bodies is essentially controlled by water-rock interactions, discussed in more detail in Section 2.3. It is therefore important to carefully characterise the reactive minerals present within both fresh and weathered samples, so that the chemical reactions taking place can be better understood (Jamieson et al., 2015).

The nature and volume of tailings and waste rock can vary enormously depending upon the mineral of interest, the types of processes involved and the mineralogy of the area being mined. These variations result from many factors including particle size, permeability, secondary mineral formation, and the concentration and distribution of metallic elements (Palumbo-Roe and Colman, 2010). Tailings from grinding and numerous chemical and physical separation processes, typically comprise of fine-sand and silt-sized materials that contain metallic element and non-metallic residues from the ore and may also contain various process chemicals (Macklin et al., 2006). The composition of fresh tailings is often dominated by silicate, carbonate and sulfide minerals; including gangue and ore minerals that were not removed during the processing phases (Lindsay et al., 2015). The nature of the waste rock produced changes over time with evolving technologies and mining techniques. In the past, mining waste would have been comprised of relatively large pieces of rock and resulting waste heaps would have been free draining with a limited surface area (Palumbo-Roe and Colman, 2010). Notwithstanding this, the particle size within waste rock piles can vary significantly from >1 m to sub-millimetre clay and silt sized fractions (Amos et al., 2015). Generally, accumulation of metallic elements is related to the surface area of a grain, normally surface area increases as a function of decreasing grain size (Miller and Orbock-Miller, 2007). Sulfide ores are often crushed and ground to reduce the size of the particles and separate the ore minerals from the gangue minerals (Lindsay et al., 2015) using density

separation techniques. Mechanical crushing and grinding machinery would have increased the proportion of finer waste particle with a larger surface area and increased the retention of water within the waste heaps, increasing the potential for the oxidation of any sulfide minerals present (Palumbo-Roe and Colman, 2010). The milling and resulting storage of mine wastes and tailings produced by mining activities is considered to contribute to the largest proportion of inputs to metallic element contaminants in solution and particulate form in river channels and floodplains (Macklin et al., 2006).

It is not only the nature of the tailings but also the physical characteristics of the waste rock pile itself, including the size and morphology of the pile, the size distribution of the particles, the thermal conductivity of the rock, and the surface area of the minerals within the pile and external factors such as temperature and precipitation that can also impact the type and volume of drainage generated, which can make definitive classification both challenging and expensive (Amos et al., 2015). Mine tailings and waste piles are often inhomogeneous with layers of sand, silt and clay horizons resulting in a complicated hydrological regime (Dold, 2005).

The mobility of metallic elements present within tailings or spoil / waste heaps may depend on their location relative to the upper oxidised zone or the lower reduced zone (Figure 2.1; Palumbo-Roe and Colman, 2010). Often waste rock piles are located close to the river given the use of the water during the processing stage.

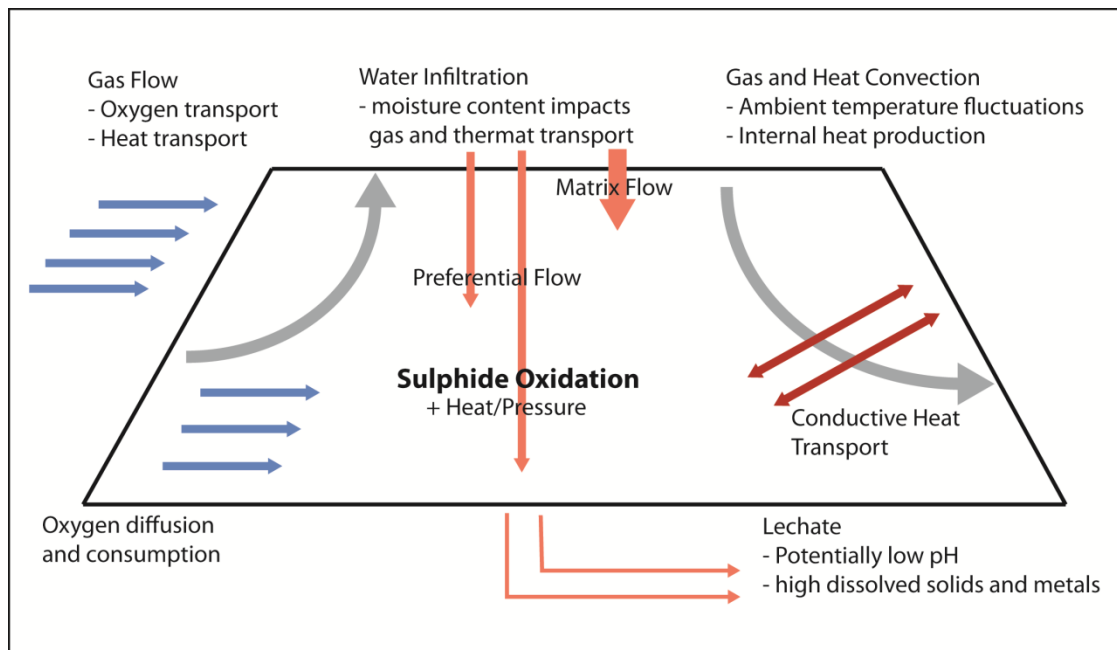


Figure 2.1: Conceptual model of the main physicochemical processes occurring within a tailings or waste rock heap (after Lefebvre et al., 2001 and Amos et al., 2015).

Fluvial processes are fundamentally important to the transport and redistribution of metallic elements on the Earth's surface (Miller, 1997). Fluvial systems can be characterised as erosion, transport and deposition environments within a channel confining the flow of fresh water which carries and deposits gravel and sand on bars (Reid et al., 1997). Metallic element-rich sediment may temporarily accumulate in channels or become spread across the floodplain during a flood event (Lewin and Macklin, 1987). The dispersal of mining wastes by fluvial systems is both physically and chemically complex.

Mining processes and fluvial activity may converge in several ways, including;

- solutes and sediments from mine waste that can be dispersed and redeposited;
- the channel morphology can be altered by the input of additional materials and discharges (Lewin et al., 1977).

A high proportion of metallic element load in aquatic systems is bound to particulate matter and sediments (Calmano et al., 1993). The capacity of sediments to adsorb and retain metallic elements is constrained by the mineralogy, surface area, and surface properties of the particles (Filgueiras et al., 2004), discussed further in Section 2.2. Such contaminated sediments may be transported over large distances, tens of kilometres, and may result in the damage to aquatic environments and even agricultural land present on floodplains (Hudson-Edwards et al., 2008). An example of this was investigated by El Azhari et al. (2017) when they undertook a study on the soil and water environment around a historical Pb-Zn mining area in north east Morocco. As expected, the tailings piles recorded the highest concentrations of Pb, Zn, Cu, Cd and As, with concentrations decreasing with increasing distance from the tailings piles. The waters of the Moulouya River, which passes through the area of tailings storage, did not record significantly elevated concentrations of the metallic elements studied. This indicates that the metallic elements are likely to accumulate or remain in the sediments and are then transported 'particle-bound' to the sediments as they move through the fluvial system (El Azhari et al., 2017).

Solutes, sediments and bedload rich in metallic elements can be produced as a result of rainsplash, wash, creep and subsurface flow from solid mine waste and sediments (Figure 2.2; Hudson-Edwards et al., 2008). The solid fractions are transported downstream and can be deposited, for example, as point and channel bars where they can re-join the sediment cycle (Hudson-Edwards et al., 2008). This was observed in the Gardon River, France, where after around 50 years after the closure of the local mines, these sites were the main source of several metallic elements including Pb and Zn. The metallic elements were initially sediment associated and due to changes in the environmental parameters were then mobilised in the aqueous phase (Resongles et al., 2014).

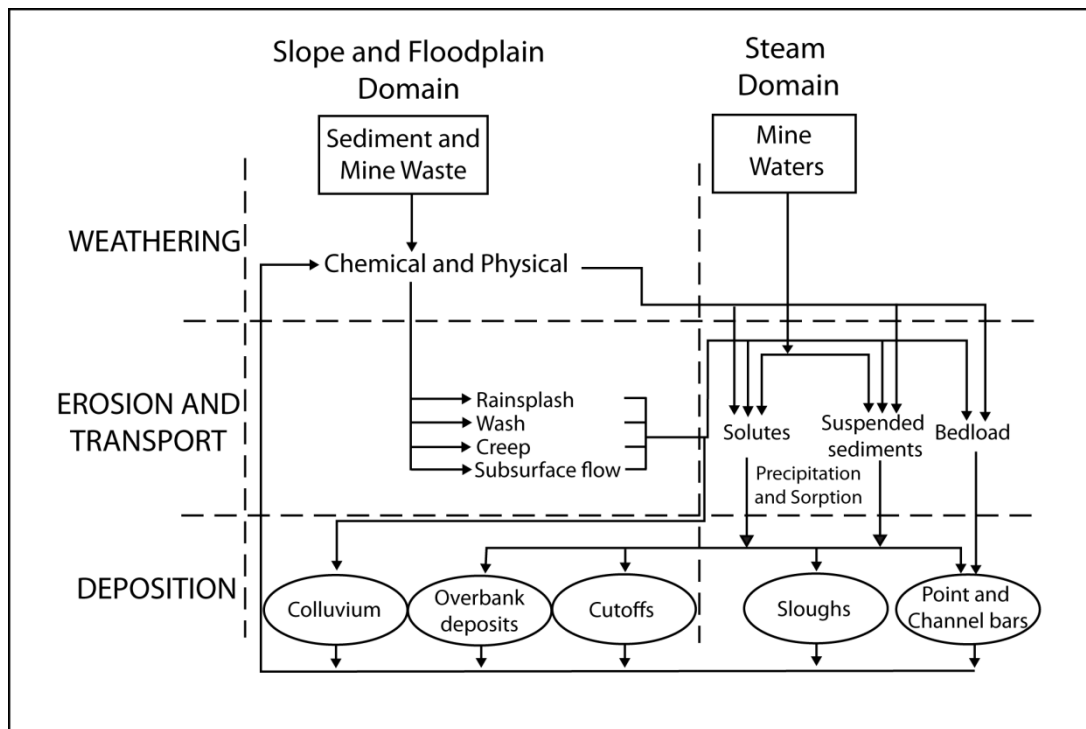


Figure 2.2: A model for the dispersal and storage of mine waste (after Lewin et al., 1977; Hudson-Edwards et al., 2008)

Sediments at the base of a river are often considered as a ‘legacy of the past’, especially in mining affected catchments. Suspended particulate matter may also be used to differentiate between historic and current sources of anthropogenic inputs (Strzebońska et al., 2017). For example, samples of river water and bottom sediments were collected from the Vistula River and one of its tributaries, the Przemsza River, Poland, an area of Pb-Zn mining since the Middle Ages. The water from the Przemsza River, Poland, and its tributaries was found to be between pH 7.01 and 8.19 (Strzebońska et al., 2017). The Zn (48 to 5,020 $\mu\text{g}/\text{dm}^3$), Pb (0.99 to 145.7 $\mu\text{g}/\text{dm}^3$) and Cd (0.19 to 12.72 $\mu\text{g}/\text{dm}^3$) concentrations of the river water varied based on the bedrock geology and point sources of contamination. Within the suspended particulate matter, the concentrations of Zn varied from 2,431 to 39,097 mg/kg, Pb from 1,206 to 21,898 mg/kg and Cd from 37 to 340 mg/kg, the highest concentrations were recorded in the Biala tributary. Concentrations of Zn in the bottom sediment ranged from 765 to 28,158 mg/kg, Pb varied from 670 to 8,872 mg/kg and Cd from 13 to 167 mg/kg. Concentrations of the Pb,

Zn and Cd increased downstream from where the Przemsza River reached the Vistula River. The Przemsza River was found to contain higher concentrations of metallic elements within the water, suspended particulate matter and bottom sediments. Based on this study it was concluded that 20 to 50 % more Pb, Zn and Cd was present in the suspended particulate matter than the bedload, which was related to both the reworking of the bottom sediments but also continued inputs of contamination into the rivers (Strzebońska et al., 2017). This study indicates that the fluvial system is complicated and that there are multiple interactions and environments that impact the contaminant load. The issue is how best to understand these to help with the prediction and remediation of NMD.

In summary, the mining inputs to contaminated river systems are potentially a matter of serious environmental concern with significant implications for the environment and human health of surrounding communities.

2.1.2 Toxicity of Pb, Zn and Cd

The term 'heavy metal' has come into question due to its ambiguity (Duffus, 2002; Hodson, 2004). No strict definition exists in the relevant literature, and researchers normally define the term when and as they use it (Duffus, 2002). For example, Sparks (2003) states that 'heavy metals are elements with densities greater than 5.0 g cm^{-3} , e.g.; Cd, Cr, Co, Cu, Pb, Ni and Hg'. In this thesis, the term 'metallic element' (Duffus, 2002) will be used in place of the out-dated term 'heavy metal', even though the latter is still widely used in the literature. The term 'metallic element' refers to both pure metals and metalloids.

The potential pathways that humans may be affected by metallic elements from mining-contaminated rivers include ingestion of contaminated water (including private water supplies), soil, fruit and vegetables, fish and livestock; inhalation of contaminated dust and adsorption through the skin (Hudson Edwards et al., 2008; Palumbo-Roe and Colman, 2010). Iron, Cu, Co, Mn and Zn are essential elements for humans, but they can be harmful at high levels, whereas metallic and metalloid elements such as Hg, Pb, Cd and As are not essential to any animals (Caussy et al., 2003). The exposure

pathway may also affect how harmful a metallic element can be to human health. Metallic elements have a variety of serious toxic effects; for example Cd can progressively impair kidney function in humans, the mental function of children can be weakened as a result of Pb exposure, and plant growth can be inhibited and anaemia induced in animals as a result of high Zn concentrations (Palumbo-Roe and Colman, 2010).

The key metallic elements of this study are Zn, Pb and Cd, each of which have different toxicities and effects on the environment and human health. Aquatic organisms are very sensitive to Zn, but humans much less so (Tirutabarna et al., 2007). In water, Zn generally occurs as Zn^{2+}_{aq} , and is relatively soluble and therefore bioavailable. Zn^{2+}_{aq} can be retained on solids by ion exchange, chemisorption by hydrous oxides and complexation with organic matter (Pulford and Flowers, 2006). In acidic waters Zn is predominantly in solution, which can be treated with alkali dosing to make a hydroxide solid, or by reducing sulfate to sulfide (Nuttall and Younger, 2000). In net-alkaline mine waters Zn is predominantly found in a carbonate complex ($ZnCO_3$) and will not react readily to form non-carbonate solids (Nuttall and Younger, 2000). In mine tailings sphalerite is the main source of Zn and Cd (Moncur et al., 2009) and sphalerite may also contain ecotoxic amounts of thallium (Tl) and Cd (Dold, 2005).

Lead is not volatile, has low solubility, and has low mobility in the environment; it sorbs with Fe-Mn-Al oxyhydroxides and complexes with soil organic matter, this means soils are a major sink for Pb (SoBRA, 2011). Lead is highly toxic to animals and plants and generally occurs in the aqueous environment as Pb^{2+}_{aq} , which can form stable complexes with organic matter, be precipitated with phosphate and chemisorbed by hydrous oxides (Pulford and Flowers, 2006). Toxicity from Pb-contaminated soils is largely as a result of direct ingestion (Schwab et al., 2005). Typical symptoms of Pb poisoning include abdominal pain, anaemia, headaches, convulsions, kidney damage and brain damage (Maria das Graças et al., 2006). The main mineral source of Pb is galena, alongside cerussite and anglesite, and Pb can also exist in trace amounts in feldspars and clays, as it can substitute for Ca and K in the atomic structure (SoBRA, 2011).

Cadmium can persist in soils for decades and when taken up by plants and crops can bio-accumulate up the food chain (Bernard, 2008). Cadmium has been found in batteries, pigments, metal coatings, plastics (Martin and Griswold, 2009), fertilisers, sewage sludge (Satarug et al., 2003) and occurs naturally in ore mixtures with Zn, Pb and Cu (Järup, 2003). In most parts of the world, the main human exposure pathway to Cd is through diet, however smoking is also an important source, one cigarette may contain 1-2 µg (Järup and Akesson, 2009). It has a long half-life in the human body and as a result once absorbed can continue to accumulate over time (Bernard, 2008). Cadmium is known to be cancer causing in humans and long-term exposure can result in kidney, lung and bone damage (Martin and Griswold, 2009).

2.1.3 Assessment of Contamination in Mining-Affected River Systems

In the aquatic environment it is nearly impossible to separate natural and man-made sources of metallic elements and the processes controlling their release and mobility (Fernandez and Borrok, 2009). Indeed, more than 90 % of metallic elements in rivers are sediment associated and follow the same transport routes as the natural load of the river. This means that if the long-term and large-scale movement and storage can be modelled then so can the fate of sediment-associated metallic elements (Brewer et al., 2005). The mobility and transportation of metallic elements in soils, sediments and waters is controlled by a variety of chemical and physical processes. These include grain size, pH of waters, soils and sediments, chemical speciation, local vegetation, rainfall, wind strength and direction, slope stability, drainage, and connectivity between the mine workings and surface waters (Palumbo-Roe and Colman, 2010). In order to assess the impact of contamination in river systems affected by mining, it is necessary to understand the processes ongoing within the natural system. Metallic elements can become enriched in river water via several processes including direct discharge from mines, chemical weathering of *in situ* contaminated soils, sediments and mining waste, and through the movement of metallic element-rich sediments during flood events (Hudson-Edwards et al., 2008).

The presence of elevated concentrations of metallic elements in the environment does not necessarily indicate there is a significant risk. The level of risk depends on the chemical form, concentration, behaviour, bioavailability, mineral particle size, pH (soil or water), and the existence of both pathways and receptors (Palumbo-Roe and Colman, 2010). The form of the element of concern and underlying geochemical environment come together to influence the mobility of contaminants and therefore the risks to both the environment and human health (Jamieson et al., 2015). In the British Isles the risk assessment of contaminated land is based on a source-pathway-receptor model (EA, 2004). In order for a risk to occur all three components must be present, if one or more are missing then the risk is negligible or absent. For example, if there are elevated concentrations of Pb in soils but no humans live and work at the affected site, then there is no pathway between the source and receptor and therefore no significant risk, although visitors to the site might be exposed on a short-term basis.

One of the main problems of trying to achieve an integrated approach to river basin management of catchments affected by historic mining processes is the absence of an acceptable maximum concentration of metallic elements in sediments and soils (Hudson-Edwards et al., 2008). As part of the British Geological Survey (BGS) Geochemical Baseline Study of Great Britain (GBASE), the typical concentrations of Pb and Zn in sediments were analysed and are shown in Table 2.1.

Table 2.1: Typical Pb and Zn concentrations in Great Britain stream sediments (mg/kg) (BGS 2009a/2009b)

| | Minimum | Median | Mean | Maximum |
|----|---------|--------|-------|---------|
| Pb | <1 | 33.8 | 84.6 | 22,982 |
| Zn | <1 | 108.0 | 152.4 | 16,070 |

There are several ways to tackle this including national and international legislation and industry standards.

2.1.4 Legislation Relating to Rivers and Mine Waste

The European Water Framework Directive (WFD) (2000/60/EC) was published in 2000 with the aim of improving the quality of surface waters in all member states of the European Union, putting aquatic ecology at the centre of management decisions (Hering et al., 2010). The impacts from historic mining on river catchments have been identified as a significant risk of the British Isles not achieving good chemical or ecological status in many rivers, as demanded by the WFD (Johnston et al., 2007).

In line with the EU Dangerous Substances Directive (2008/105/EC) Pb is considered a priority substance and Zn is a specific pollutant. The Water Environment (Water Framework Directive) (England and Wales) (2017) is designed at least in part to help implement the WFD in England and Wales on a legal basis.

In addition to the WFD, the EU Mine Waste Directive (MWD) was published in March 2006 and relates to wastes from mines, quarries and other mineral extraction industries (DEFRA, 2010). The overall aim of the MWD is to provide measures to effectively manage the waste from extractive industries, and to reduce or prevent the risk to the environment (including water, soil, air and ecology) and human health (DEFRA 2010). The directive aims to mitigate the environmental impacts of mine wastes, including by preventing the failure of waste containment structures such as tailing dams, and by trying to increase the sustainable reuse of mine wastes (Palumbo-Roe and Colman, 2010).

2.1.5 Thresholds to Determine the Impacts of Mining on Rivers Waters, Sediments and Soils

The bedrock geology can influence the metallic element concentrations of overbank and stream sediments, but this can be masked by anthropogenic contamination of fluvial sediments (Swennen and Van der Sluys, 1998) including but not limited to mining related activities.

In order to assess the level of contamination in the environment, assessment criteria or numerical limits have been approved at a national, European or

international level. Regulators and countries aim to address human health concerns of direct contact with potentially contaminated soils by developing threshold values that specify the maximum amount of a contaminant that may be present without prompting a regulatory response (Jennings, 2013).

When developing acceptable human health guideline values, assumptions must be made to define the person or people coming in contact with the contaminant in question, such as body mass, soil inhalation rate, ingestion rate and skin exposure area, the exposure scenario, for example, frequency and duration of contact, and the acute and/or chronic health impact of the contaminant (Jennings, 2013; Nathanail et al., 2015). Several countries worldwide have developed human health guideline values including USA, Great Britain, Australia and Canada. Often various countries agree that certain contaminants should be regulated, however they often disagree on the guidance values themselves. It is not uncommon for such thresholds to differ by several orders of magnitude (Jennings, 2013). To illustrate this Table 2.2 records the threshold values from various countries based on a 'residential' setting, which includes ingestion, inhalation of dust and direct dermal contact of potentially contaminated soils.

Table 2.2: Soil guidelines for the acceptable levels of Pb, Zn and Cd

| | Residential Guideline Value | Country of Origin | Reference |
|---------|------------------------------------|--------------------------|---|
| Lead | 400-1,200 mg/kg | USA | USEPA 2018 |
| | 140 mg/kg | Canada | Government of Alberta 2016 |
| | 300 mg/kg | Australia | Department of Environment and Conservation 2010 |
| | 200 mg/kg | Great Britain | Nathanail et al., 2015 |
| Zinc | 23,500 mg/kg | USA | USEPA 2018 |
| | 200 mg/kg | Canada | Government of Alberta 2016 |
| | 7,000 mg/kg | Australia | Department of Environment and Conservation 2010 |
| | 3,700 mg/kg | Great Britain | Nathanail et al., 2015 |
| Cadmium | 71 mg/kg | USA | USEPA 2018 |
| | 10 mg/kg | Canada | Government of Alberta 2016 |
| | 20 mg/kg | Australia | Department of Environment and Conservation 2010 |
| | 11 mg/kg | Great Britain | Nathanail et al., 2015 |

Drinking water standards have been published both nationally (UK Drinking Water Standards for England and Wales (DWS) DWI 2009) and internationally (the World Health Organisation (WHO) 2011). The aim of these guidelines is to manage the risks posed to the safety of drinking water from all forms of contamination from biological; chemical including hydrocarbons and metallic elements; and even radiological substances. The guidelines also cover 'acceptability aspects' including taste odour and appearance (WHO 2011). Chemical contaminants present in water are generally of concern over the longer timescales, years rather than months. This results from them being subject to changes in concentration depending upon the source of the contaminants, e.g., intermittent discharges and leaching from landfills (WHO, 2011), flooding of mine workings, low flow

conditions or diffuse sources. These guidelines are based on long-term exposure in humans and are not necessarily the best way to directly assess the risks present in mining areas; however, they do give a useful indicator of acceptable levels of total Pb, Zn and Cd in drinking water.

Table 2.3: Drinking water guidelines for the acceptable levels of Pb, Zn and Cd

| | Drinking Water | Country of Origin | Reference |
|---------|---|-------------------|--|
| Lead | 0.015mg/L | USA | USEPA 2009 |
| | 0.01 mg/L | Canada | Health Canada 2017 |
| | 0.01 mg/L | Australia | Australia Drinking Water Guidelines 2017 |
| | 0.001 mg/L | UK | DWI 2009 |
| | 0.01 mg/L | WHO | WHO 2011 |
| Zinc | NA | USA | USEPA 2009 |
| | <5.0mg/L | Canada | Health Canada 2017 |
| | 3 mg/L | Australia | Australia Drinking Water Guidelines 2017 |
| | NA | UK | - |
| | Not of health concern at levels found in drinking-water | | WHO 2011 |
| Cadmium | 0.005 mg/L | USA | USEPA 2009 |
| | 0.005 mg/L | Canada | Health Canada 2017 |
| | 0.002 mg/L | Australia | Australia Drinking Water Guidelines 2017 |
| | 0.005 mg/L | UK | DWI 2009 |
| | 0.003mg/L | WHO | WHO 2011 |

In addition to the WHO guidelines countries including the USA, Australia, UK and Canada have all produced their own safe drinking water standards, as

detailed in Table 2.3. The standards for drinking water are understandably strict and may not be applicable in determining acceptable contamination level in surface waters such as rivers and streams as the distance to the compliance point (i.e. potable water abstraction) is an important factor on the concentration of contaminants as they may be diluted by other sources. As such, drinking water standards are likely to be overly conservative for most mine water discharges. For example, in New Zealand there are no universal water quality standards, as the preferred option is a limiting threshold relating to the specific aquatic environment (Pope et al., 2009).

The WFD requires more directly applicable Environmental Quality Standards (EQS) to be set in order to protect aquatic life from metallic elements present within the water column, food chain and contaminated sediments (Hudson-Edwards et al., 2008). For example, the EA calculated the EQS (annual averages) for Gunnerside Gill based on a hardness of 70 mg/L sampled in February 2010 as; 50 µg/L for Zn, 7.2 µg/L for Pb and 0.09 µg/L Cd (EA, 2013). More recently the EQS have been updated to be based on bioavailability (WFD UKTAG 2014), for Gunnerside Gill this means the EQS values have reduced to 6.1 µg/L for Pb and 28 µg/L for Zn. Metallic element concentrations can often exceed the EQS in mining-contaminated rivers, but for some metallic elements, such as Pb, Zn and Cd, this is not necessarily the case as they can be removed from the water column via precipitation and sorption especially in rivers underlain by carbonate-dominated rocks (Hudson-Edwards et al., 2008).

Examples of limited regulation within current mining areas and the surrounding waters, such as Nigeria (Sanusi et al., 2017), could act as an analogy for the historical mining within Swaledale which was undertaken before legislation was even conceived. Illegal mining is commonplace in Nigeria. Rivers and lakes are often used in the removal of metallic elements from the ore minerals after crushing via floatation. Sanusi et al. (2017) undertook a study of the soils and water around a historical Pb-Zn mines in Yelu, Nigeria. The mines were officially abandoned in the mid-1990s and no treatment of the mine wastes was undertaken, however local miners have

started to work in the mines again. Both soil and water samples were collected and analysed, the results show that the pH of the soils ranged from 7.10 to 8.92. Lead was found in all the tested samples, mean concentrations ranged from 65 to 658 mg/kg. Similarly, Zn was detected in all the soil samples with mean concentrations ranging from 185 to 373 mg/kg. Cadmium was only found to be present in soil samples from two of the four tested locations ranging from 12.62 to 20.70 mg/kg. Within the water samples, three of six concentrations of Pb and Zn exceeded the WHO permissible value of 0.01 mg/L and 3 mg/L, respectively. In addition, one sample recorded Cd in excess of the corresponding WHO value of 0.003 mg/L. The pH of the waters was not reported. The study concluded that the soils close to the abandoned mines have a high risk of having concentrations of Pb, Zn and Cd in excess of regulatory thresholds. The study also noted that the surface water and borehole waters generally complied with the WHO standards. It was recommended that the activities of any 'artisan' miners be monitored, mining activities should be undertaken away from drinking water resources, and both local people and miners be educated about the potential risks to human health from contact with Pb, Zn and Cd (Sanusi et al., 2017).

2.2 Introduction to Metallic Elements Behaviour and Control

2.2.1 Geochemical Behaviour of Metallic Elements

The mobility of metallic elements, weathering products and pH within tailings are controlled by precipitation-dissolution, reduction-oxidation and sorption-desorption reactions (Lindsay et al., 2015). These reactions are also important in controlling metallic elements concentrations in the soils and sediments, groundwater, and bioavailability for uptake by plants (Schwab et al., 2005). Dissolved phases in natural waters are mobilised by weathering, transportation through the hydrological cycle, and are often impacted on or even aided by bacterial mechanisms (Nordstrom, 2011). The distribution of metallic elements in soil and pore waters is related to variations in soil properties, including pH, organic matter content and quality, texture, the quantity and quality of sorption sites (Barančíková and Makovníková, 2003) and the extent of their sorption with solid phases (Singh and Oste, 2001). In

soils and pore waters metallic elements generally occur in inorganic forms (as ions or salts) and occasionally as organic forms complexed with organic compounds (Caussy et al., 2003). The oxidation state and hydrated ionic radius of the metallic element affects the soil-element bonding strength, which generally increases with the valence and decreases with increasing ionic radius (Covelo et al., 2007).

In aqueous environments, metallic elements can exist in various forms that vary in toxicity and mobility, furthermore the physio-chemical conditions present mean metallic element associations are reversible and changeable (Warren and Haack, 2001). In addition, the bioavailability of metallic elements depends upon their chemical and mineralogical form (Wilson and Bell, 1996). For a metallic element to be mobile in river systems it must be present in the source rock, present in sufficient concentrations, soluble, and in the flow path of the water (Nordstrom, 2011). From a purely geochemical perspective, the main processes involved in metallic element binding and mobility in sediments are as follows (Calmano et al., 1993):

- sorption and desorption;
- formation and dissolution of carbonate-bound metallic elements;
- formation and decomposition of soluble and insoluble metallic element organic complexes;
- formation and dissolution of hydroxides and oxyhydroxides;
- sorption and co-precipitation of metallic elements by Fe and Mn oxides, particularly in oxic environments at neutral pH;
- precipitation of metallic element-bearing sulfides in strong reducing environments and dissolution as sulfates under oxic conditions.

Solid surface reactions in an aqueous medium result from: unfulfilled charges of functional groups or molecules on the surface of the solid; dissolved metallic elements with unbalanced charges; and the fact that aqueous systems are constantly changing and are not in equilibrium (Warren and Haack, 2001). Over time, mining wastes containing metallic elements move through a variety of complex redox and pH environments that affect the solid

and dissolved phases, which in turn impact on their toxicity and bioavailability (Hochella et al., 2005).

The effect of increasing metallic element concentrations with decreasing particle size are thought to be due to three main processes; firstly the influence of surface area, secondly the larger quantity of reactive coatings (i.e. organic matter and iron/manganese oxides), and thirdly differences in the mineralogy of the grains (Miller and Orbock-Miller, 2007). How metallic elements become sediment-associated is somewhat uncertain, however it is generally assumed co-precipitation and adsorption of the metallic element ions are the main responsible mechanisms (Klarup, 1997).

Sorption is a general term used when the exact retention mechanism of a surface is unknown. Adsorption can be defined as 'the accumulation of a substance or material at an interface between the solid surface and the bathing solution' (Sparks, 2003). The retention of metallic elements by sorption on clay minerals, metallic oxides and hydroxides, and soil organic matter is a major factor controlling their mobility and fate in soil and water systems (Sparks, 2005). Soil systems are nearly always heterogeneous, consisting of both organic and inorganic constituents that have different affinities for sorption of metallic elements and the metallic elements themselves have differing affinities for soil surfaces (Shaheen, 2009).

Sorption involves covalent bonds and electrostatic complexes (Warren and Haack, 2001). A covalent bond can form between the solute ion and the solid surface, also referred to as an 'inner sphere complex' and also as adsorption or being 'adsorbed'. Whereas outer sphere complexes are weaker bonds resulting from electrostatic forces and can be more easily remobilised (Warren and Haack, 2001).

If there is more than one metallic element species present in natural waters, then competitive adsorption might take place. For example, alkali earth metallic cations such as Mg^{2+} and Ca^{2+} compete for adsorption sites with other metallic elements (Salomons, 1995). When metallic elements are in a soluble form the type of solid soil constituents present (i.e. silicates, carbonates, oxides, and organic matter) can have a strong influence on the

retardation of the metallic elements, reflecting the different type and degree of adsorption capacity of the individual components themselves (García-Sánchez et al., 1999). Aqueous Pb has a tendency to sorb to surfaces of natural solids, especially Fe and Mn oxyhydroxides and organic matter (Morin et al., 1999). In floodplain soils an important sorption mechanism is considered to be a single stage during which dissolved metallic elements reach rapid equilibrium with the weak binding sites on the surfaces of sediments (Laing et al., 2009). Additional stages can be theorised during which the metallic elements move to the pores and/or go through solid-state reactions with higher energy binding sites (Laing et al., 2009).

It has been shown that swelling clay particles have the highest capacity for sorbing Cu, Pb and Zn, followed by mixed clay structures with swelling components and illites had the least capacity (Sipos et al., 2008). In addition organic matter and Fe-oxides preferentially immobilise Pb, while Zn mostly sorbs to clay mineral particles; and Fe oxide coatings have been found to provide a sorption capacity for minerals that otherwise do not adsorb metallic elements, for example, silica and feldspar (Sipos et al., 2008). Similarly, soils with the greatest capacity for metallic element sorption are those with the most organic matter present and clay fractions with a significant proportion of vermiculite (Covelo et al., 2007).

Sorption is heavily influenced by pH. It has been shown that Pb is mostly sorbed to Fe oxide-coated suspended sediments at pH 5 and above, while Zn is mostly dissolved from pH 3 to 8 in waters affected by mine drainage in Colorado (Smith et al., 1992).

The key factors effecting metallic element mobility in the fluvial environment are discussed further in the following sections.

2.2.1.1 pH

pH is one of the most important factors that describes adsorption behaviour. Typically metallic element adsorption increases from virtually nothing to nearly 100 % as the pH changes through a critical range of 1-2 units

(Salomons, 1995), this is especially true of divalent cations (Warren and Haack, 2001) such as Pb and Zn. This means that a small change in pH in the associated aqueous fluid, i.e. water, causes a sharp increase or decrease of the dissolved metallic element concentration (Salomons, 1995). Neutral pH conditions may allow for dissolved metallic elements to precipitate or co-precipitate with carbonates or hydroxides, including siderite, smithsonite and cerussite (Nejeschlebová et al., 2015).

Metallic elements that become more soluble and mobile under acidic conditions include Cd, Co, Cr, Cu, Mn, Ni, Pb and Zn (Wilson and Bell, 1996). In calcareous and clay soils, metallic element solubility is relatively low, but in more acidic soils the metallic elements can dissolve and become more available for uptake by plants (García-Sánchez et al., 1999). The amount of Pb that is released into solution when the pH drops from 5 to 4.5 was found to increase from 200 $\mu\text{m/g}$ to more than 27,000 $\mu\text{m/g}$ (Gee et al., 2001). Within Coldale Beck, Cumbria, England, it was noted that reductions in pH due to run off from surrounding peat resulted in an increase in the release of metallic elements, for example Zn increased from 160 $\mu\text{g/L}$ at a pH 7.42 to 5,530 $\mu\text{g/L}$ at a pH 4.66 (Jarvis et al., 2018). The pH of a solution can not only affect the dissolution of metallic elements, but also the formation or dissolution of 'sorbents' including Fe/Mn oxyhydroxides; the charge on the surface of the sorbents; and the fractionation of the metallic elements (Munk et al., 2006).

2.2.1.2 Mineralogy

The metallic element-bearing minerals in a mining catchment are heavily influenced by the underlying geology and the mineralogy of the mining site and sediment inputs. In addition, weathering and degradation of the primary minerals plays a role, as primary minerals can be altered or even completely destroyed over time.

The particle size of fine sediment within a river is in part controlled by its mineralogy and geochemistry. For example, material finer than 2 μm are often composed of secondary silicate minerals, whereas quartz, feldspar and carbonate dominate in larger size fractions (Walling et al., 2000; Miller and

Orbock-Miller, 2007). Knowledge of the mineralogy of the metallic element-associated phases is important for a variety of reasons, including understanding the stability, solubility, mobility, bioavailability and toxicity, modelling future behaviour, and considering potential remediation approaches (Hudson-Edwards, 2003). The mineralogical composition of the particles influences the type and extent of surface irregularities such as cracks, ridges, micropores and depressions, can increase the surface area (Miller and Orbock-Miller, 2007). Solid phases in natural waters that interact with dissolved contaminants include clay minerals, carbonates, quartz, feldspar and organic solids, these are often coated with Fe/Mn oxyhydroxides and organic matter (Salomons, 1995).

Soil chemical characteristics have been shown to be better at predicting the mobility and retention of metallic elements in soils than mineralogical characteristics in certain cases (Matos et al., 2001). In the River Tees the overbank sediments were shown to be composed of three major groups of mineral and rock fragments comprising quartz, sandstone and shale (derived from the underlying strata including the Whin Sill) (Hudson-Edwards et al., 1997). Within the Tees sediments four groups of contaminant-bearing minerals were identified; the first group included sulfides such as galena, sphalerite and chalcopyrite; the second group were made up of cerussite, smithsonite and occasional Pb phosphates; Fe oxyhydroxides comprised the third and most common contaminant-bearing mineral group; and fourth were Mn oxides. The Fe and Mn oxyhydroxides were pseudomorphs of sphalerite, cerussite, chlorite, siderite, pyrite and augite (Hudson-Edwards et al., 1997). Direct observations of metallic element mineral associations in the Clark Ford Superfund Complex, Montana, have shown that in the shallower oxic environment the metallic elements were present in sulfides and hydrous metallic element oxides. Whereas in the anoxic environment metallic element oxides were found along with sulfides in sulfate reducing conditions and clays carried large amounts of Zn and Cu (Hochella et al., 2005). Similarly the Lot River, France, has historically been impacted by mining and smelting activities. The mineralogy of the river is characterised by the spinel group including franklinite and magnetite, sulfates such as barite, gypsum, anglesite

and jarosite, willemite and phyllosilicates, they are either in the form of primary residual phases or authigenic, as a result of precipitation (Audry et al., 2010).

2.2.1.3 Cation Exchange Capacity

A high cation exchange capacity (CEC) can reduce metallic element mobility and result in the retention of metallic cations (Laing et al., 2009).

Table 2.4: Mineralogy of selected clays, surface area and CEC (from García-Sánchez et al., 1999)

| Clay | Mineral | % present in sample ^a | Specific surface area (m ² g ⁻¹) | Cation exchange capacity (mEq. 100 g ⁻¹) |
|-----------------------------|-----------------|----------------------------------|---|--|
| Palygorskite (Bercimmuelle) | Palygorskite | 80 | 157 | 15.5 |
| | Quartz | 17 | | |
| | Calcite | 3 | | |
| Palygorskite (Torrejon) | Palygorskite | 66 | 93 | 9.2 |
| | Quartz | 34 | | |
| | Chlorite | Trace | | |
| Sepiolite (Vallecas) | Sepiolite | 95 | 271 | 5.2 |
| | Calcite | 5 | | |
| Sepiolite (Orera) | Sepiolite | 87 | 272 | 9.1 |
| | Dolomite | 7 | | |
| | Quartz | 4 | | |
| | Illite | 2 | | |
| Bentonite (Almeria) | Montmorillonite | 100 | 57 ^b | 89 |
| | Illite | Trace | | |
| | Quartz | Trace | | |

^a Semi quantitative analysis, ^b Outer surface area

The CEC of a soil or sediment is generally as a result of the clay content (Covelo et al., 2007), however other minerals also exhibit CEC but often to a lesser extent (Table 2.4). The CEC of clay minerals varies depending upon the crystal lattice structure and the degree of isomorphous substitution, because of this it is always useful to identify the clay minerals present, their densities and abundance (Vega et al., 2004). García-Sánchez et al. (1999)

carried out an investigation into the adsorption of metallic elements by different minerals in relation to remediation of contaminated soils, specifically from the Guadiamar Valley, Spain. Four topsoils were sampled from the flooded areas and the soil properties and potential adsorption capacity of the local soils were determined. As part of their work they carried out a comparative study of Zn adsorption capacity of different clay minerals. Table 2.4 shows the semi-quantitative mineral compositions of the selected clays, their surface area and the CEC.

2.2.1.4 Manganese and Iron Oxide, Oxyhydroxide and Hydroxide Coatings

In alluvial settings grains, such as clay minerals, quartz and feldspar, may be partially or entirely coated by reactive substances (Miller and Orbock Miller, 2007; Filgueiras et al., 2004). The exact oxyhydroxide present, its crystallinity, any impurities present, size, weathering, and co-precipitates, all influence the reactivity of that oxide and in turn its ability to attract metallic elements (Warren and Haack, 2001).

In oxic environments Fe oxides, oxyhydroxides and hydroxides such as hematite, magnetite, goethite, akaganeite, lepidocrocite, ferrihydrite and maghemite are produced by oxidising dissolved Fe(II) or by the oxidation of pyrite (Waychunas et al., 2005; Laing et al., 2009). A study by O'Reilly and Hochella (2003) investigating Pb absorption by natural and synthetic Mn and Fe oxides found that generally the Mn oxides were better at sorbing Pb than Fe oxides, which was concluded to be as a result of 'internal reactive sites' within the Mn oxides. Iron and Mn oxides, oxyhydroxides and hydroxides (hereafter known collectively as oxyhydroxides) in aqueous environments act as scavengers of metallic elements and accumulate them by co-precipitation and adsorption (Miller and Orbock Miller, 2007). Metallic element sorption by oxyhydroxides generally increases with increasing pH over a narrow range referred to as the 'sorption edge', this range is different for each metallic element and is influenced by the sorbate to sorbent ratio (Smith et al., 1992).

These phases are all important in biogeochemical reactions in natural environments due to their wide occurrence, tendency to nucleate and grow

on other phases, redox capabilities, and reactivity (Waychunas et al., 2005). With the exception of ferrihydrite, Fe oxides are often crystalline, ferrihydrite is poorly ordered and unstable in aquatic environments, commonly it changes to a more stable Fe oxide like goethite (Warren and Haack, 2001).

In oxidised tailings as the system matures the Fe oxyhydroxides gradually become more crystalline reducing their ability to sorb metallic elements (Moncur et al., 2009). Poorly crystalline and microcrystalline Mn and Fe oxyhydroxides have a large sorption capacity for metallic elements, in a dry oxidising environment they recrystallise and become more stable with greater capacities for immobilising their incorporated metallic elements (Tack et al., 2006).

Within the sediments of the Guadalquivir estuary, Spain, Fe is most associated with the lithogenic fraction, whereas Mn appears in the Fe-Mn oxyhydroxide fraction. Lead is associated with both the residual and the Fe-Mn oxyhydroxide fractions, and Fe, Mn and Pb have similar distribution patterns with increasing depth (Riba et al., 2002). The influence of release rates of metallic elements (specifically Cu, As and Zn) from the Fe and Mn oxyhydroxides in contaminated river sediments when oxalic acid was applied has been carried out on samples from the Clark Fork River, USA. At pH 1.85 around 90 % of the Mn was removed from the sample without the addition of any oxalic acid. Around 60 % of the Cu was removed quickly from the sediment, likely to be due to the dissolution of salts (Klarup, 1997). In this case the oxalic acid assisted the release of the Zn, although around 40 % of the Zn was removed independently of the oxalic acid. In the Clark Fork River the 63-250 μm fraction samples reacted with oxalic acid confirm that Cu, Zn and As in the sediments are not associated with the same oxides (Klarup, 1997). Iron oxyhydroxides appear to be unimportant for Cu and Zn, whereas Zn shows a close association with Mn oxyhydroxides. This is a relatively small-scale study with a narrow remit, however it does give some indication as to how Zn interacts with Fe and Mn oxyhydroxides.

In reality it these processes do not happen singularly and are heavily dependent upon the environmental conditions at particular times.

2.2.1.5 Organic Matter

Organic matter includes humic acids, fulvic acids, and bacteria (Warren and Haack, 2001). Organic matter is complex, variable and can have several different functional groups at the surface (Warren and Haack, 2001). Roots of higher plants exude organic acids, fatty acids, oxalic, glycolic, lactic and tartaric acids and aromatic acids (Burckhard et al., 1995). Metallic elements sorbed to organic matter are generally more strongly bound than those sorbed to Fe oxyhydroxides (Warren and Haack, 2001) and complexes can be formed with dissolved organic matter in soils, sediments or organic systems (Weng et al., 2002).

Some studies have found that dissolved organic matter has a very limited influence on the mobilisation of metallic elements, depending upon other soil properties. For example, Kalbitz and Wennrich (1998) analysed five soils from the Mulde River, Germany. It was found that in some locations low pH resulted in high metallic element mobility and that highly protonated dissolved organic matter has a low affinity for positively charged elements.

A column leaching study was used to investigate the effect of organic acids on the leaching of metallic elements. It was found that rhizosphere organic acids had an effect on the mobility of Zn and that citric acid released more Zn than formic, succinic and oxalic acids (Burckhard et al., 1995).

2.2.1.6 Microbiology

Microorganisms can influence metallic element mobility in mine wastes in various ways, some microorganisms act to aid the mobilisation of metallic elements, while others do not (Ledin and Pedersen, 1996). Soil bacteria have surfaces that interact with metallic ions in solution. The mechanisms and adsorption kinetics regarding how bacteria influence the speciation and distribution of metallic elements in the soil are not well understood, especially under field conditions (Wu et al., 2006). In some bacteria the outer wall appears to selectively retain metallic elements that are useful for structure, function or both (Hoyle and Beveridge, 1983). Microbial activity can change the chemical and physical characteristics of the environment and so may

indirectly influence chemical speciation and mobility of metallic elements (Joubert et al., 2007). Wu et al. (2006) found that water-soluble Pb was reduced as a result of adsorption by bacteria cell walls and possible sedimentation reactions with phosphate or other available anions.

Soil bacteria can influence the amount of oxygen present by carrying out aerobic and anaerobic respiration, this in turn can influence the chemistry and redox potential.

2.2.1.7 Oxidic and Anoxic Conditions

Redox potential (E_H) is a measure of the electron availability and can predict the stability of metallic elements in floodplain sediments and soils. It changes from high to low as the soil or sediment moves from aerobic to anaerobic. Natural waters rich in dissolved organic carbon tend to result in the consumption of the dissolved oxygen present, once the dissolved oxygen has been used up the next electron acceptor will be consumed according to the following sequence in Table 2.5 (Langmuir, 1997). This may lead to the development of discrete redox zones (Petrunic et al., 2005; Laing et al., 2009). At the oxic-anoxic boundary and in the anoxic floodplain sediments, redox-sensitive processes occur that result in metallic elements becoming included in precipitates or released from the dissolution of precipitates. Water saturation for extended periods may result in changes in the chemical properties of soils and sediments, soils undergo a series of redox reactions when the environment changes from aerobic to anaerobic (Laing et al., 2009).

Changes in redox conditions can affect soil pH, as during reduction protons are consumed and during oxidation acidification occurs. Increased activity of protons reduces negative surface charges on organic matter, clay particles, and Fe/Mn oxyhydroxides and can increase the solubility of precipitates and carbonates (Laing et al., 2009).

Table 2.5: Electron acceptor reaction sequence (Langmuir, 1997)

| | Reaction | E _H value for each change at pH 7 (mV) |
|------------|---------------------|---|
| Reaction 1 | Aerobic respiration | 816 |
| Reaction 2 | Denitrification | 713 |
| Reaction 3 | Mn(IV) reduction | 544 |
| Reaction 4 | Fe(III) reduction | 14 |
| Reaction 5 | Sulfate reduction | -217 |
| Reaction 6 | Methanogenesis | -260 |

Overall the controls on the availability of metallic elements is generally a complex interaction of the various processes described in Sections 2.2.1.1 to 2.2.1.7. An example of this is a study undertaken by Sharafi et al. (2018) of the Angouran mine located in Iran (a predominantly Zn mine with lesser concentrations of Pb and Ag) with the Calcimin Zn-Pb processing plant located some 20 km south east of the mine itself. Rock samples of both sulfide and non-sulfide ore were recovered from the pit and adit of the mine and sediment samples were recovered from the pit and a tailings dam. In addition, ten water samples were collected from around the mine and the plant. The sulfide ore was found to comprise sphalerite, galena, smithsonite and quartz. The non-sulfide ore contained smithsonite and hemimorphite. The sulfide ores were found to contain higher concentrations of Zn, whereas the non-sulfide ores contained higher concentrations of Pb. The pH of the water samples varied from 5.2 to 8.25, the lowest pH was found within the tailings water. The waters from the tailings pond were found to be near neutral with a high metallic element content, however the waters from the Angouran mine were found to have high alkalinity and low to high metallic element concentrations. The water samples from the processing plant were found to contain bivalent Pb and Zn, the speciation was controlled by the high sulfate concentrations within these samples. Within the tailings pond there is evidence of weathering of the primary ore minerals to anglesite, Pb-

As jarosite and beudantite. In addition, the precipitation of Al and Fe oxyhydroxides in some of the tested waters indicate that the metallic elements may be being removed by 'scavenging' (Sharafi et al., 2018).

2.2.2 Physical Controls of Metallic Element Mobility

Metallic element concentrations in rivers and sediments can be changed greatly by deposition and remobilisation processes (Filgueiras et al., 2004). Sediment transportation is directly related to the movement of water within the channel, during transportation the sediments can be categorised into three groups: suspended sediment, bedload and the saltation load (Ongley, 1996). Physical controls that influence the distribution of metallic elements at mining sites include; differential transport of mine waste according to size and density, abrasion, mining of trunk-stream sediment including bank and tributary material and floodplain deposition (Macklin et al., 1997).

Lewin and Macklin (1987) identified four main mechanisms of fluvial storage and dispersal, namely: hydraulic sorting, based on differences in particle density; chemical dispersion, including adsorption and complexation, by solution or biological uptake; mixing with clean sediment, reducing contaminant concentrations; and loss to or exchange with floodplain sediments.

As a result of extended residence times of metallic elements in rivers and floodplain sediments of tens to thousands of years, metallic element-contaminated sediments could become sources of contamination in the future following remobilisation (Taylor and Hudson-Edwards, 2008). It is thought the River Swale catchment has been influenced by Pb mining since Roman times (further information in Section 3.4). As a result, concentrations of Pb, Zn and Cd have been recorded above background levels in previous studies by Dennis et al. (2003), Walling et al. (2003), Brewer et al. (2005), Macklin et al. (2006) and Dennis et al. (2009), summarised in Section 3.5 which includes a vertical core study. It has also reported that rare metallic-tolerant plant communities have been noted downstream from historical Pb-Zn mining areas. For example alluvial deposits as Ninebanks, Northumberland, have been designated a site of special scientific interest as

a result of metallic element input from the Pennine Orefield and metallophyte plants found living there (Hudson-Edwards et al., 2008). This indicates that there can be ongoing mining influences on whole catchments, not just the main mining locations.

Accelerated sedimentation studies have produced estimates of floodplain sediment accumulation rates, however dating of the sediments is limited so the averages produced can underestimate maximum sedimentation rates, miss short term variations, and / or overestimate minimum rates. Also if lateral variation of sediment rates are locally significant, they may not represent the sedimentation rates across whole valleys (Lecce and Pavlowsky, 2001).

Mechanical erosion of the waste piles and tailings results in the metallic element associated sediments directly entering the fluvial system (Audry et al., 2006). For example, in the Nant Gwynant (a tributary of the River Conwy in Wales, British Isles) gully erosion by surface drainage, bulk erosion and leaching of the tailings lead to contamination of metallic elements in the channel and floodplain (Gao and Bradshaw, 1995). Similarly, in Toka Creek in Hungary, a mining-derived, sulfide-rich 'yellow sand' was continuously remobilised laterally and vertically by flooding and oxidation (Ódor et al., 1998).

During times of low to mean river discharges, metallic element-associated sediments accumulate within the channels (Hudson-Edwards, 2003). The residence time of the contaminants in floodplains is dependent upon the rates of post-deposition physical, biological and chemical remobilisation, and the geomorphology of the catchment (Hudson-Edwards, 2003). Overbank deposition on floodplains represents a loss of sediment in the system as it enters long-term storage, conversely channel storage is usually shorter-term and results in the transport of sediment to the catchment outlet (Walling et al., 2003).

2.3 Mine Drainage

2.3.1 Definitions of Acid Mine, Circum-Neutral and Alkaline Mine Drainage

Abandoned mine wastes with a high sulfide content are among some of the most severe sources of environmental contamination worldwide (Gieré et al., 2003). Understanding the underlying geochemical processes, such as the controls of precipitation and dissolution of secondary minerals, is imperative so that models can be formulated to predict possible future impacts from mining sites. A better knowledge of these processes may also allow tailored remediation at existing sites and a reduction in impact of proposed and future sites (Gieré et al., 2003).

During mining operations large volumes of rock are excavated and processed to remove the ore from the host rock, this results in the production of waste rock. This waste material is often stockpiled or used in the construction during other mining operations. The consequence of the excavation is that sulfide minerals come into contact with the atmosphere and oxygen, and therefore oxidation can begin (Blowes et al., 2013). When in contact with oxygen and water, sulfide minerals are thermodynamically unstable (Lindsay et al., 2015). The oxidative weathering of sulfide-rich minerals and rocks is a primary control of the release of associated metallic elements and sulfate ions into shallow soils and the aquatic environment (Fernandez and Borrok, 2009).

Mine drainage is most commonly defined based on the pH of the discharge, for example acid mine drainage (AMD), neutral mine drainage (NMD) (sometimes referred to as contaminated neutral drainage (CMD)) and alkaline mine drainage (ALKMD) (Figure 2.3). AMD is produced when the neutralisation capacity of the tailings is used up as a result of continuing sulfide oxidation reactions, which can result in high dissolved concentrations of metallic elements including Fe, Al, Mn, Zn, Ni, Cu and Pb (Lindsay et al., 2015). NMD is normally present when the carbonate dissolution within the tailings is able to neutralise the acid produced from the sulfide oxidation reactions and can be characterised by elevated Fe(II), Zn, Cd and hydroxide-forming elements such as As, Se and Sb (Lindsay et al., 2015).

However, other types of NMD have been described such as the impact of the host rock and changes in chemistry over time, as detailed in Section 2.5.2.

NMD has been divided by some researchers (Bright and Sandys, 2015) into two main categories, mineral types and in-situ weathering reactions. Firstly the oxidation of sulfide minerals coupled with neutralisation reactions and secondly dissolution at the surface of a non-sulfide mineral, e.g. oxides (magnetite or hematite). The mineralisation within a mine is often a complex assemblage of both ore and gangue minerals that result in various chemical weathering interactions and rates (Bright and Sandys, 2015). As a result, the prediction of the drainage chemistry of mine waste is challenging.

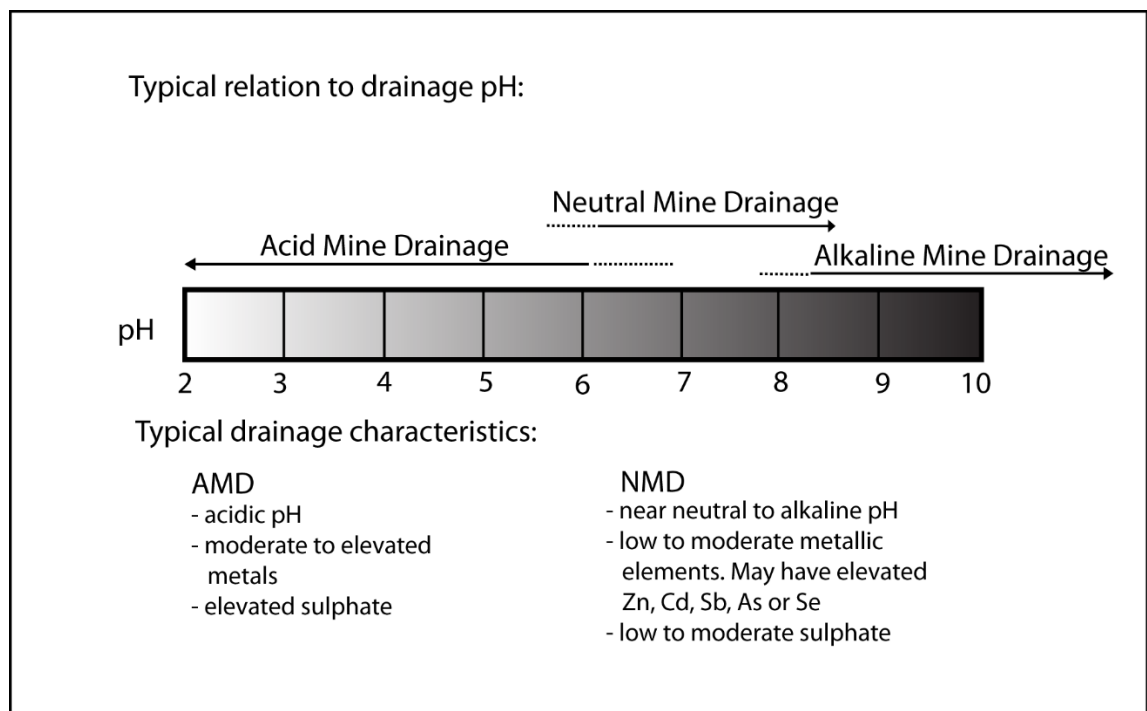


Figure 2.3: Range of pH of AMD and NMD (after Chatwin et al., 2009; Nordstrom et al., 2015)

Mineralogy is a significant influencing factor as it is can be the difference between AMD, NMD and mine drainage that does not adversely impact the surrounding and wider environment. Nordstrom (2011) made reference to different pH bands 0-5 as AMD, pH 6-8 as NMD and pH 8-12 ALKMD, as shown in Figure 2.3. It should be noted that ALKMD is very rare and will not

be discussed further as part of this study. Rainwater has a pH of 5.6 and AMD is considered to occur if the mine effluent had a pH below 5.5 as this is when the biota is adversely impacted (Blowes et al., 2013). AMD is often caused by the oxidation of pyrite and other Fe-bearing sulfide minerals resulting in the release of protons into the waters and a low pH, as shown in equation 1 below.



In turn this acidity then releases metallic elements and sulfate from the surrounding minerals (Lottermoser, 2010), often due to the infiltration of oxygen-rich water (Gomes and Favas, et al., 2006). A consequence of S oxidation is the formation of sulfuric acid, sulfate and if Fe is present in an aqueous form then ferric iron and Fe hydroxide may also be precipitated (Bell, 2004). High sulfate, Fe and Al, elevated Cu, Cr, Ni, Pb and Zn are characteristic of AMD (Lottermoser, 2010). Often at mine sites, anthropogenic activity has caused or intensified AMD by increasing the exposure of sulfide minerals to the atmosphere resulting in oxidation and associated generation of acid (Blowes et al., 2013). Although AMD often receives more attention than NMD, NMD is still important as it has the ability to transmit significant concentrations of metallic elements (Jamieson et al., 2015). NMD and ALKMD may result from a variety of causes. These include residues from alkaline leaching within the tailings/waste rock or water flow path, non- or low-sulfide ores and tailings, ores or tailings that were totally oxidised as a result of pre-mining weathering, the presence of abundant neutralising minerals, for example, carbonate, and sulfide ores with high amounts of non-acid producing sulfides (including galena (equation 2), sphalerite (equation 3), arsenopyrite, and chalcocite) and low quantities of acid producing sulfates (pyrrhotite) (Lottermoser, 2010).



Plumlee et al. (1992) analysed over 25 sites that suffered from impacted mine drainage and natural springs in mineralised areas of Colorado in order

to design a classification scheme for mine drainage. This work demonstrated that mine drainage chemistry reflects the ore deposit itself: its composition, texture, host geology, structure and trace element chemistry (Plumlee et al., 1992). In addition the presence of oxygen, water, evaporation, and existence or lack of mine waste deposits/tailing piles; and geochemical mechanisms, including precipitation, dissolution, sorption and desorption are also important (Plumlee et al., 1992).

Ficklin et al. (1992) used the metallic element concentrations and pH data from the sites analysed by Plumlee et al. (1992), which were plotted against each other resulting classification scheme (Figure 2.4). This is designed to extend beyond the Colorado sites to any mine drainage site. It was found that the lowest pH and highest metallic element concentrations were found in oxygenated waters flowing through mine wastes and acid-sulfate epithermal (warm temperature, shallow depth) ores. These were associated with a low buffering capacity of the country rock, and highly fractured ores allowing oxidation by water or oxygen, classified as 'high acid/extreme metal'. 'High acid/high metal' and 'acid/high metal' waters are characterised by sulfide rich deposits with low to moderate acid buffering capacities, with high concentrations of dissolved oxygen and drain directly from mine workings not dumps or tailings piles with limited access to sulfide minerals. Acid pH with low dissolved metallic element concentrations fall in to the 'acid/Low metal' category, the waters contain limited dissolved oxygen and high sulfate concentrations. 'Near neutral/Low metal' waters resulted from carbonate or reactive aluminosilicate hosted ores, with variable dissolved oxygen concentrations (Ficklin et al., 1992; Plumlee et al., 1992).

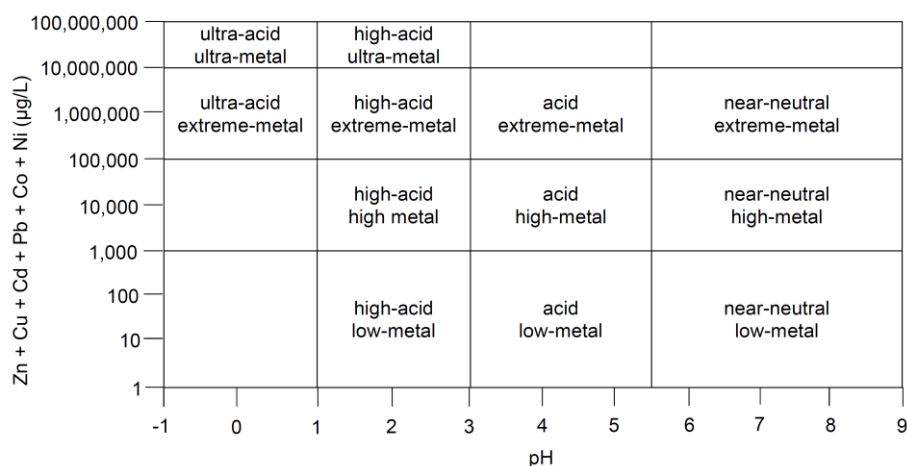


Figure 2.4: Geochemical plot for the total dissolved metals and pH (after Ficklin et al., 1992)

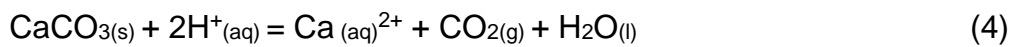
Many of the most problematic mine drainage waters around the world are alkaline or circum-neutral (Younger et al., 2002). Table 2.5 shows a range of pH settings varying from around 6 up to 8.22 and metallic element concentrations vary widely.

Table 2.6: Examples of the geochemistry of NMD

| | Mike Horse Mine, Montana ^a | Frazer's Grove Mine, British Isles ^b | Bwlch Mine, Wales, UK ^c | Green Creek Mine, Alaska ^d | Rio Mannu Basin, Sardinia ^e | Kocacay River, Turkey ^f (average) | |
|------------------|---|---|--|--|--|--|----------------|
| | | | | | | Arid period | After rainfall |
| pH | 6.2-6.6 | 6.7-7.4 | 6.2 | 6.82-8.22 | 7.0-8.0 | 7.69 | 5.63 |
| SO ₄ | 1150 | 60-1080 | - | 971-2673 | 32-242 | - | - |
| Cl | - | 16-42 | - | - | 57-157 | - | - |
| HCO ₃ | - | - | - | - | 41-325 | - | - |
| Na | - | 7-83 | - | - | 41-83 | - | - |
| K | - | 4-26 | - | - | 2.1-4.6 | - | - |
| Ca | 310 | 29-313 | 26 | 52-389 | 19-130 | - | - |
| Mg | 207 | 8.2-86 | 8 | 173-468 | 11-30 | - | - |
| Fe | 49 | 0.3-11 | 0.02 | <0.1-17 | - | 0.05 | 40.44 |
| Mn | 37 | - | - | 0.1-4.1 | - | 2.04 | 4.49 |
| Cu | - | - | - | 1.9-4.1 | - | <0.01 | 1.01 |
| Pb | - | 0.02-3.83 | 2.40 | - | - | <2 | 0.65 |
| Zn | 57 | 0.4-27 | 22 | <0.1-1.91 | - | 1.68 | 47.88 |
| Key Ore Minerals | Pyrite, galena, sphalerite, chalcopyrite, | Galena, chalcopyrite, fluorite, siderite | Galena, sphalerite, siliclastic host rocks | Sphalerite, tetrahedrite, galena, pyrrargyrite, electrum, pyrite | Sphalerite, galena, pyrite | Pyrite, galena, sphalerite, chalcopyrite | |

Concentrations in mg/L: a) Hochella et al., 1999, data from time of solid sampling b) Younger, 2001, c) Warrender and Pearce 2007, initial concentrations d) Lindsay et al., 2009, e) Cidu et al., 2012, f) Aykol et al., 2003.

Numerous historical mining areas in the British Isles, for example, are characterised by circum-neutral, low-Fe drainage, with high levels of dissolved Zn, Pb and Cd; these include Wales, the Irish Republic, England, (for example the North Pennines (Warrender and Pearce, 2007)) and in Scotland the majority of contaminated mine drainage is circum-neutral or alkaline in nature (Younger, 2001). In a mine setting, the most important pH-buffering reactions are from the dissolution of gangue minerals, the most significant are carbonates (equation 4), Al hydroxides, Fe oxyhydroxides and aluminosilicates (Blowes et al., 2013).

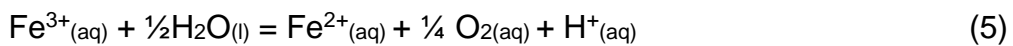


Banks et al. (2002) investigated alkaline mine drainage from metallic sulfide and coal mines. They concluded that NMD and ALKMD may be as a result of:

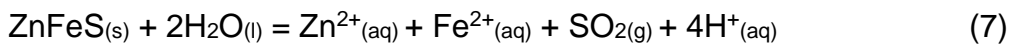
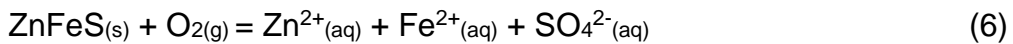
- a low concentration of sulfide minerals;
- the occurrence of monosulfides rather than Fe sulfides including pyrite and marcasite;
- neutralisation of AMD by carbonate or basic silicate minerals within the surroundings;
- engineering factors, for example, explosion prevention using lime dust or the use of cement during construction;
- neutralisation of AMD by natural alkaline groundwater;
- water within the system not effectively interacting with the sulfide minerals present; and/or
- oxygen not being in direct contact with sulfide minerals or the presence of highly reducing influent water (Banks et al., 2002).

2.4 Mineral Weathering Reactions

Weathering rates of sulfides in tailing deposits and waste rock are largely dependent on the mineralogy of the ore residues, humidity, and particle size distribution (Ramos Arryo and Siebe, 2007). Acid can be produced via two processes, either by the oxygen and ferric Fe oxidation of sulfide minerals (equation 5) or hydrolysis of ferric Fe resulting in the precipitation of ferrous oxyhydroxides and/ or sulfate oxyhydroxides (Dold, 2005; Seal II et al., 2008).



Sulfide containing mine wastes with a high concentration of Fe sulfides, such as pyrite and marcasite, or sulfides with a major Fe component, such as Fe-rich sphalerite (Zn,Fe)S, are able to generate more acidity than sulfide wastes with a low concentration of Fe sulfides or Fe concentrations (equations 6 and 7), such as galena and Fe-poor sphalerite (Lottermoser, 2010).



Chemical weathering of rocks is a spontaneous and irreversible thermodynamic process that results in a more stable state of the minerals under a given set of conditions (Viers et al., 2013). Many minerals are formed at elevated temperatures and pressures, and as a result they are not thermodynamically stable at earth surface conditions (Langmuir, 1997; Deutsch and Siegel, 1997). As a result chemical weathering occurs when minerals are in contact with atmospheric conditions, precipitation and shallow soil moisture in humid climates (Langmuir, 1997). Sulfides are insoluble and stable under reducing conditions, but they oxidise when they come into contact with the atmosphere, as shown in equation 2 and 3 (Gomes et al., 2010).

Sphalerite and galena do not generally produce acid when oxygen is the oxidant, but aqueous ferric Fe (a by-product of pyrite oxidation) is an

aggressive oxidant when it reacts with sulfide minerals and generates greater quantities of acid than generated by oxygen alone (Plumlee and Nash, 1995). Generally sulfide-rich mineral assemblages with high percentages of Fe will produce more acid than those without Fe (Plumlee and Nash, 1995).

Galena is often associated with pyrite and pyrrhotite. The latter oxidise to form acid ferric sulfate solutions, which in turn can enhance the oxidation of Pb-bearing sulfide minerals (Blowes et al., 2013). If Fe-rich and acid-generating waste materials are present, surface coatings can develop on the ore minerals, thus reducing their access to oxygen and reducing the initial rate of dissolution (Weisener et al., 2003). When oxidised Zn becomes more soluble as it changes from sphalerite to Zn sulfate (e.g. zinkosite) and Pb becomes less soluble as it oxidises from galena to Pb sulfate (e.g. anglesite), which coats the galena and stops it from being oxidised further (Nuttall and Younger, 2002). Under low pH conditions, the weathering of galena can result in high concentrations of Pb reaching downstream receiving waters in the form of sulfate (anglesite) (Palumbo-Roe and Colman, 2010). Sphalerite is commonly weathered by particle-size reduction rather than secondary mineral replacement (Moncur et al., 2009).

Banwart et al. (2002) described two different kinds of mineral weathering: 'vestigial contamination' and 'juvenile contamination.' Vestigial contamination refers to the accumulation of secondary minerals that result from the weathering of sulfide minerals in dewatered voids. The problem occurs when the mine workings are flooded causing the secondary precipitates to dissolve. Juvenile contamination is as a result of soluble contaminants being released due to the weathering of sulfide minerals controlled by oxygen. The soluble contaminants can then be transported to potential receptors such as rivers and aquifers. Vestigial contamination is more of a short-term issue and is controlled by the flooding of the workings. Juvenile contamination is a longer-term problem and is controlled by the rate of weathering of the sulfide minerals present and the amount of mineral present within the active weathering zone (Banwart et al., 2002).

Table 2.7: Relative resistance to alteration of sulfides in oxidised tailings (from Moncur et al., 2009)

| Mineral | Chemical Composition | Resistance |
|--------------|------------------------------|--|
| Pyrrhotite | Fe_{1-x}S | <p style="text-align: center;">Low resistance</p>  <p style="text-align: center;">High resistance</p> |
| Galena | PbS | |
| Sphalerite | (Zn,Fe)S | |
| Bornite | Cu_5FeS_4 | |
| Pentlandite | $(\text{Fe,Ni})_9\text{S}_8$ | |
| Arsenopyrite | FeAsS | |
| Marcasite | FeS_2 | |
| Pyrite | FeS_2 | |
| Chalcopyrite | CuFeS_2 | |
| Molybdenite | MoS_2 | |

The 'resistance' of various sulfide minerals to weathering was described by Moncur et al. (2009) in an oxidising environment, Table 2.7. Galena and sphalerite are similarly reactive, but galena tends to form a coating of anglesite early during oxidation. The formation of the anglesite rim results in a slowing of any further replacement, but it does not fully stop it. Therefore, galena may be present longer in oxidising conditions that have resulted in the removal of sphalerite (Moncur et al., 2009).

Galena is one of the most important sulfide minerals, is often the most economically viable Pb mineral (Acero et al., 2007). As a result it is also major source of Pb in aqueous environments, which are dominated by low pH and high oxygen saturation (De Giudici and Zuddas, 2001). An understanding of galena dissolution is important as it could potentially predict the long-term mobility and availability of Pb in the natural environment (Liu et al., 2008). The mobility of Pb is often controlled by sorption on clays, organic matter and Fe/ Mn oxyhydroxides or the formation of less soluble Pb minerals (Palumbo-Roe and Colman, 2010).

When galena and sphalerite are found together, a 'galvanic cell' can be set up. This is when one mineral acts as a cathode and the other as an anode, the former being the mineral with the higher residual potential, under redox conditions (Urbano et al., 2007). In the case of galena and sphalerite, the

presence of Zn results in the preferential oxidation of the sphalerite over galena.

Short duration experiments for galena, i.e., hours to days, usually result in a more rapid measured rate of dissolution than those measured over months or years. This means the rates obtained over short durations do not accurately predict the rate of dissolution of galena during extended interactions with solutions, for example, pore waters in mine tailings and mining-affected surface waters (Acero et al., 2007). The reason for the limited research over longer timescales tends to be due to high costs and lack of time available for long term experiments when deciding the fate and management options for a mine (Ramos Arroyo and Siebe, 2007).

The mineral surface, on a microscopic scale, is complex, consisting of terraces and numerous edges formed by steps, kinks, and cavities, not dissimilar to topographic features (De Giudici and Zuddas, 2001). Changes in the surface topography of galena may also influence the dissolution reaction rate. At pH 1 to 3, surface pits form over part of the galena surface and then 'protrusions' form covering the entire surface, stopping the nucleation and growth of the pits. During the protrusion formation the Pb concentration in the solution drops, showing a reduction in the surface reactivity (De Giudici and Zuddas, 2001). By reacting natural galena (99.7% pure) with aqueous solutions of differing pHs, Kim et al. (1995) aimed to detail the oxidation/dissolution processes that occur. It was found that the dissolution is generally consistent and the rate of surface dissolution increases as the pH decreases or with increasing oxygen within the water. The amount of Pb^{2+} in the surrounding solution increased due to surface product formation, in this case verified as Pb hydroxide (Kim et al., 1995).

The composition of sphalerite varies depending upon the chemistry of the environment of formation. Iron can substitute for Zn in significant quantities (Dold 2005), the higher the amount of Fe, the higher the rate of leaching observed for Zn and Fe (Weisner et al., 2004). Divalent cations including Cd

and Mn also commonly substitute for Zn, and Cu and Pb may occur in trace concentrations within sphalerite (Stanton et al., 2008).

Goethite (FeO(OH)) absorbs Pb easily and is frequently found in soils and wastes (Kleszczewska-Zeębala et al., 2016). As a result goethite may represent a bioavailable source of Pb in soils and sediments as given a reduction in pH, for example when rain water percolates through Pb contaminated soils, it will result in the Pb being released into solution (Zhang et al., 1997) as Pb²⁺.

The size of the mineral grain can also have an effect on its interaction with the environment. Mineral nanoparticles can behave differently in the micro- and the macro-scale as a function of their size and shape (Liu et al., 2008). This is also true for galena. Differences in the rates of surface etching matched that of existing knowledge relating to bulk crystals on the macroscale. In addition, nanocrystals of galena dissolved at a much slower rate when adjacent to other nanocrystals rather than when exposed to the bulk solution (Lui et al., 2008). This potentially relates to the altered properties and/or movement of the solution in a confined space, this may help when trying to understand weathering in confined spaces. Predictably the nanocrystals of galena dissolved faster than bulk crystals due to their increased surface to volume ratio and also possibly the presence of more crystal faces (Liu et al., 2008).

2.4.1 Neutralisation Reactions

Carbonate minerals including calcite (CaCO₃), ankerite and siderite are often present in a variety of economic mineral deposits, and are especially important when the deposits contain sulfide minerals as they may be able to prevent the formation of AMD (Al et al., 2000). The most mobile elements, such as Na and Ca, are often removed from soils in dissolved form, less mobile elements such as Al and Fe tend to be incorporated into stable secondary mineral phases such as clays and metallic oxyhydroxides (Viers et al., 2013). Alkalinity is generally characterised as the ability of water to

neutralise a strong acid to an exact end point, for example using bromocresol green-methyl red colour change at pH 4.5 (Younger, 2001). A substantial alkalinity can neutralise natural or even man-made contaminant acidity (Langmuir, 1997).

Carbonate dissolution consumes protons (H⁺) and generates alkalinity, which can therefore decrease the acidity of mine waters (Lindsay et al., 2009). Carbonate dissolution is 'congruent', as shown in equation 4 (Viers et al., 2013). The pH of mine drainage is dependent upon sulfide hydrolysis and oxidation reactions, which result in a cycle of pH decrease, buffering of carbonates and then an increase in pH (Pavoni et al., 2018).

Wetting and drying cycles of the mine waste can affect the potential acid production, frequent wetting generates a more constant volume of acid and other contaminants as the water infiltrates and removes the oxidation products (USEPA, 1994). When the oxidising sulfide minerals come into contact with water, the oxidation stops and the metallic ions dissolve and the sulfate becomes sulfuric acid (equation 8).



The overall impact of this process depends upon the mineralogy of the surrounding rocks, if they are carbonate-rich the water may be neutralised and the metallic elements immobilised (Johnson et al., 2008). Soil cover remediation systems, can in theory, reduce the infiltration of water and air into mine wastes, thereby reducing the longer-term acid and metallic element loadings to receiving waters and environments (Cheong et al., 2012). Galena and other Pb sulfides may persist in alkaline pH waters and mine waste due to the formation of low-solubility outer coatings, which are dependent upon the supply of dissolved SO₄²⁻, CO₃²⁻ and PO₄³⁻, and include anglesite, cerussite and pyromorphite (Palumbo-Roe and Colman, 2010).

Similar to mining locations, smelting sites also have a legacy of metallic element contamination within the shallow soils. Where the buffering capacity of the soil is increased by the presence of Ca-rich slag and gangue minerals, the soil pH is relatively high and is likely to remain so (Gee et al., 2001). Lead

mobilisation is reduced where soil pH is maintained around pH 8 to 5. However, between pH 5 to 4 calcite and cerussite may become involved in the buffering reactions. The overall effect is slower drops in pH and as a result a slower rate of release of Pb into the surrounding pore waters (Gee et al., 2001).

Lara et al. (2011) carried out an investigation into the weathering of galena under simulated calcareous soil conditions. It was found that galena surface initially oxidises to an anglesite-like phase, which decreases the reactivity of the galena and goes on to form cerussite-like phases. The cerussite-like phase results in a porous layer, meaning the underlying surface of the galena is accessible to continuous dissolution. The cerussite-like phase is a major hazard, as it is the most bioavailable Pb phase in soils (Lara et al., 2011). During laboratory leaching of sphalerite, it was found that the initial high rate of dissolution decreased as metallic element-deficient polysulfide layers formed on the mineral surface (Weisener et al., 2003).

During the evolution of the Magellen non-sulfide Pb deposit, Western Australia, it has been proposed that the original Pb sulfate and Pb carbonate were precipitated out of solution resulting in the partial dissolution of the surrounding carbonate rock (Pirajno et al., 2010). The Zn was then flushed out as it was more mobile, leaving the Pb behind as anglesite. Weathering and ingress of carbon dioxide-rich meteoric waters meant the anglesite was later replaced by cerussite. This has left behind a sulfide ore body fully weathered by oxidising infiltrating waters. This evolution requires some specific conditions in order to occur; the presence of a shallow sulfide ore body and hot/ wet climatic conditions to allow for the infiltration of oxidising meteoric waters (Pirajno et al., 2010). This non-sulfide Pb deposit gives an insight into the range of reactions that can occur when Pb sulfides react with carbonates in the absence of major Fe interactions.

In summary the reactions that occur and result in NMD are complex and do not take place in isolation. Changes in the environmental conditions will result in changes in the reactions taking place.

2.5 Worldwide Mine Drainage

Mine drainage is a serious problem affecting the environment (Smith et al., 1992). In the British Isles NMD and ALKMD are less researched than AMD, often due to the fact AMD is highly visible to both the authorities and the public.

The exact number of non-coal mines in the British Isles is unknown, but in Wales, Northumbria and the south west there are estimated to be over 3,700 sites, although not all result in contamination of the environment (Johnston et al., 2008). The WFD River Basin Characterisation study identified approximately 2,840 km to be at high or moderate risk from non-coal mining contamination (Johnston et al., 2008).

2.5.1 Neutralisation by Host Rock Buffering: Global Case Studies

NMD commonly results from the buffering capacity of the surrounding host rock mineralogy and weathering reactions, as described in Section 2.4. For example, Red Dog, Lik and Drenchwater are carbonaceous black shale-hosted Ag-Pb-Zn sulfide deposits in northwest Alaska. Drenchwater and Lik were investigated as at the time they had not been mined and could provide natural baseline data (Kelley and Taylor, 1997). Drenchwater Creek flows into Discovery Creek, the pH in the creeks was found to be 7.2 and 4.3 respectively. Discovery Creek was also found to be enriched in Al, Fe, Mn, Cd, Co, Cu, Ni, Pb and Zn. Mining commenced at Red Dog in 1990 and the main deposit is exposed on both sides of Red Dog Creek. The pH of the creek was found to be similar to Discovery Creek, however the metallic element concentrations were significantly higher. The water chemistry of the streams near the Lik deposit differed from the waters of Drenchwater and Red Dog, the Lik samples were found to be near-neutral and the only metallic element that was consistently high in concentration was Zn. Discovery Creek is naturally enriched due to the underlying mineralisation. Red Dog has a higher metallic element concentration in the ore, which is reflected in the water chemistry. Although the Lik deposit is dominated by Fe-sulfide, waters draining the deposit were found to be near-neutral and only elevated in Zn,

due to the buffering action of the surrounding carbonate rocks (Kelley and Taylor, 1997).

The Rosh Pinah mine, Namibia, is a Zn-Pb-Cu mine hosted in black shale, arenites and carbonates. A study of the soils and sediments found the tailings to have a near neutral pH as a result of the presence of dolomite (Nejeschlebová et al., 2015). The metallic elements, Zn, Cu and Pb, were generally found to be bound to Fe/Mn oxyhydroxides and also carbonates. Although Fe oxyhydroxides are relatively resistant to weathering, Mn oxyhydroxides and carbonates are less so and may therefore release associated metallic elements to the surrounding environment and as a result of ongoing weathering reactions (Nejeschlebová et al., 2015).

In addition to carbonate host rocks, aluminosilicates can also neutralise mine waters. For example, the Clayton mine in Cluster County, Idaho, is an Ag-Pb-Zn replacement deposit hosted within dolomite and quartzite (Hammarstrom et al., 2002). The mine waste and mill tailings were found to have the same mineralogy as the deposit itself, although they had different degrees of heterogeneity. The primary ore minerals present were identified as galena and sphalerite. All pH measurements, of the mine waste, mill tailings, adit water, surface water and leachates, were found to be near neutral. Any potential acidity generated by oxidation of the sulfide minerals present is readily neutralised by the surrounding dolomite and quartzite, meaning AMD is not considered to be a problem. Zinc and Mn, on the other hand, showed enhanced mobility at near-neutral pHs resulting in elevated aqueous concentrations at some carbonate-hosted deposits (Hammarstrom et al., 2002).

Similarly, the host rocks of the Colline Metallifere Park near Tuscany, Italy, are not all carbonate-based. The three main geological formations are Permian schist, highly karstified dolomitic limestone and clayey schist (Drescher-Schneider et al., 2007). Three mines within the Colline Metallifere Park were also investigated by Tesser et al. (2011), and it was found that the mines, Niccioleta, Boccheggiano and Gavorrano, produced NMD, rather than

AMD. The pH values were found to be 6.6, 7.4 and 6.7, respectively. All of the mines extracted pyrite and in the case of Boccheggiano pyrite and other sulfides were mined. Within the discharges concentrations of metallic elements and sulfate often exceeded the Italian regulatory guideline values for reclaimed wastewater disposal (Tesser et al., 2011). It is likely that the discharges emanating from the three mines would be highly acidic based on the presence of pyrite and other sulfide minerals; notwithstanding this, the discharge then undergoes neutralisation due to the weathering of the surrounding dolomitic limestone and schists.

Neutral mine drainage developed near Montevecchi, Sardinia, as a result of Pb-Zn mining since the mid-nineteenth century until the 1960s to 1980s. Galena and sphalerite veins were dominant alongside minor pyrite, chalcopyrite, barite, cerussite, anglesite, and smithsonite were present with quartz, siderite, ankerite, dolomite and calcite country rock. Scanning electron microscope analysis identified that the galena had been oxidised to anglesite and cerussite, and Fe-rich sphalerite had rims of Zn-rich Fe oxyhydroxides (Fanfani et al., 1997). In addition, Fe-oxide pseudomorphs were found to be present on siderite and less commonly pyrite and chalcopyrite, and Fe-Mg-Zn sulfates were present on weathered mineral surfaces (Fanfani et al., 1997).

Postawa and Motyka (2019) undertook a study of metallic elements within groundwater in a Pb-Zn mining district in Southern Poland. Three Pb-Zn mines, Boleslaw, Olkusz and Pomorzany, were active in this region in the latter half of the 20th century. When Boleslaw closed in the mid-1990s, the mine workings were 'spontaneously' flooded. The Olkusz mine started to close in the late 1990s, however dewatering of the mine was maintained. Over 400 water samples were collected from 1967 to 2016 from various 'leaks' and monitoring boreholes. Not all the samples were subject to a full suite of testing and samples were very rarely collected from 1980 to 1995 so the dataset is incomplete. However, it was found that, during the initial stage of sampling, the mine drainage exhibited distinct chemical zonation. Over the longer term readily soluble Ca, Mg and Fe hydroxysulfates were produced as

a result of oxidation of sulfide containing ore minerals. The oxidation of the sulfide minerals present produced large quantities of acidic drainage, allowing for metallic elements present to become mobile. The authors concluded that the surrounding carbonate rocks buffered the AMD such that the pH had not changed significantly (Postawa and Motyka, 2019), however the pH data was not reported in the paper so it is difficult to assess this. The assumption of NMD could be made given the presence of limestones within the surrounding rocks.

The Salafossa mining area, Italy, is one of the biggest Pb-Zn deposits in Europe (Pavoni et al., 2018). The region drains into the Piave River. Both water and sediment samples were collected from the river to gain a better understanding of the concentrations of metallic elements within the catchment. The water samples in this study recorded a pH range of 7.15 to 8.21, considered to be as a result of buffering from the surrounding carbonate rocks. The drainage directly from the mine galleries is diluted after the confluence with the Piava River, such that the Piava River downstream of the mine was found to be near neutral with a relatively low metallic element load. In addition, As, Cd, Pb, Tl and Zn were found to accumulate within the Fe-Mn oxyhydroxides and carbonates within the sediments of the mine galleries themselves (Pavoni et al., 2018). This study highlights the complexity of mine drainage where there are several processes involved in the attenuation of the contaminants of concern.

The Myra mine is a volcanogenic massive sulfide deposit hosted by andesitic to rhyolitic volcanic rocks located on Vancouver Island, Canada. Mining for Zn, Cu and Pb has been undertaken since 1966. Waters draining from the 10-Level portal were found to be oxidising and circum-neutral, with moderate total dissolved base metallic elements dominated by Zn (Desbarats and Dirom, 2007). An adit draining from the volcanic massive sulfide deposits was found to be much more acidic and had higher dissolved metallic element concentrations. The primary process for the water chemistry is sulfide oxidation by oxygen and subsequent neutralisation by calcite. This process shows that at some point the waters draining from the 10-Level portal came

into contact with calcite-based minerals, whereas the waters from the adit did not (Desbarats and Dirom, 2007).

The Fonte Santa tungsten mine area, Portugal, was mined for wolframite (WO_4) and scheelite (CaWO_4) until 1982. There is no significant AMD associated with the old mine workings, which is due to the carbonates within the country rock, which neutralise the water and reduce the concentration of metallic elements (Gomes et al., 2010). Carbonate minerals also have an important influence at the Greens Creek Mine, Alaska, where the tailings deposits have been characterised as containing pyrite, sphalerite, galena, tetrahedrite ($\text{Cu}_{12}\text{Sb}_4\text{S}_{13}$), arsenopyrite (FeAsS) and chalcopyrite. Pyrite constitutes approximately 20 to 35 wt.% of the tailings and dolomite and calcite are also present at approximately 30 and 3 wt.%, respectively. The tailings deposit had nearly neutral pH pore water and drainage. The acidity generated as a result of pyrite oxidation is neutralised by the dissolution of the carbonate minerals present, this means that the near neutral pH is maintained throughout the tailings facility and the discharges (Lindsay et al., 2009).

Leachate from mine tips around Rookhopen, Weardale were reported to have a neutral pH and maximum concentrations of 1,520 mg/L SO_4 , 0.3 mg/L Pb, 1 mg/L Zn and 1.9 mg/L F. Metallic element mobility was shown to be limited as a result of the surrounding carbonate rock (Palumbo-Roe and Colman, 2010).

The Nent Valley in the nearby North Pennines was mined for Pb and Zn for over 200 years. The mines are hosted in calcareous rocks, which means the water draining from the mine has a circum-neutral pH in the range of 7.4 to 8.0 (Nuttall and Younger, 2000, Warrender and Pearce, 2007). Similarly, the Bwlch Pb-Zn mine hosted by siliciclastic rocks, near Aberystwyth, was worked for galena and sphalerite during the 19th century. The waters draining from the mine contain high concentrations of Zn but due to the very low concentration of pyrite the pH was recorded as circum-neutral (Warrender and Pearce, 2007). Frazer's Grove mine, in the north Pennines, British Isles,

is also carbonate hosted with a high dissolved metallic element content although the associated waters are circum-neutral (Johnson and Younger, 2002).

A study of Holden Beck, a tributary of the River Wharfe in the north Pennines was undertaken in relation to NMD from coal and Pb-Zn mines and deposits in a carboniferous upland catchment. Mining was undertaken using hushing and density sorted on the dressing floor (Valencia-Avellan et al., 2017), similar to the activities undertaken at Gunnerside Gill. The study was undertaken to gain a better understanding of metallic element concentration and mobility in the dissolved phase of a carboniferous catchment affected by historical metallic element mining, specifically Pb and Zn. The results have the potential to improve the management of catchments impacted by NMD. Monthly water samples were collected from sixteen sites down Holden Beck, covering a stretch of 5 km. In addition, four sediment samples and three spoil samples were recovered to assess the mineralogical composition. The mean pH was found to be 6.8 in 80% of the samples. Dissolved Zn was found to be the most common contaminant with concentrations ranging from 67.8 to 4,252.3 µg/L and dissolved Pb ranging from 4.4 to 284.2 µg/L. Within the solid phases the highest concentrations of Pb and Zn were recorded within the spoil samples and the highest Pb and Zn concentrations were noted within sediment samples from the headwaters, where the majority of the mines were present. The concentrations of Pb and Zn were found to decrease downstream within the sediment samples. The researchers concluded that metallic element mobility was controlled by the pH and weathering reactions which are in turn influenced by the underlying limestone geology. The mobilisation of Zn and Pb were strongly linked to site specific hydrological and biogeochemical conditions. Within Holden Beck dissolved Pb and Zn were derived from galena and sphalerite respectively but also from secondary minerals including cerussite and smithsonite. These secondary minerals contribute to the Pb and Zn concentrations within the catchment due to continuous leaching, which would be an issue should remediation be considered (Valencia-Avellan et al., 2017).

2.5.2 Changes in Mine Drainage Chemistry over Time

The dissolution of primary minerals and the precipitation of secondary minerals can result in changes to the mine drainage chemistry over time. The depletion of carbonate minerals as a result of continuing sulfide mineral oxidation can occur before a change in pH to acidic conditions (Lindsay et al., 2015). In this case the pH will remain neutral until the carbonate mineral content is exhausted and the rate of acid generation exceeds acid consumption (Nordstrom et al., 2015). This phase of neutral pH before acid generation begins is called the 'lag period' and may last anywhere between months and years (Nordstrom et al., 2015).

Within the gold and silver Guanajuato mining region, Mexico, the surface tailings give an opportunity to look at the changes over time (Ramos Arroyo and Siebe, 2007). This is because the tailings have been exposed to the atmospheric conditions for known amounts of time, including 0, 2, 4, 16, 70, 75, and 100 years. The Au and Ag are associated with pyrite, chalcopyrite, sphalerite and galena. As the ages of the tailings increase, the proportion of metallic elements associated with the sulfide phases decreases and the proportion associated with Fe oxide increases reaching equilibrium between 40 and 60 years. In this case Pb has a limited affinity with Fe oxides, this has been attributed to the alkaline conditions meaning the Pb from galena is precipitated as anglesite or cerussite (Ramos Arroyo and Siebe, 2007).

Resongles et al. (2014) demonstrated that following the closure of mines in the Gardon River, France, the mines were the main source of Pb, Zn, Cd, Tl, Hg, As and Sb within the sediments. As a result of changes in the environmental conditions following the mine closures some of these metallic elements within the sediments were mobilised within the dissolved fraction.

2.6 Column Leaching Studies Mineral Weathering Processes Leading to Processes and Products of Mine Drainage

There are several ways to study the impacts that mining can have on the environment. One of these is by using prediction methods, such as a combination of laboratory and field-based tests.

While it may not be necessary to use all tests for each and every site, multiple tests and data are required to develop a better understanding of the influence of potential mine drainage on the environment (Bright and Sandys, 2015). One of the kinetic laboratory tests denoted in Figure 2.5 is a column leaching experiment. Column leaching studies are used to evaluate mineral weathering processes and determine the effects of rainfall, infiltration, leaching and chemical reactions on these processes (for example Abumaizar and Smith, 1999; Yukelsen and Alpaslan, 2001; Matos et al., 2001; Yong et al., 2001; Voegelin et al., 2003; Hauser et al., 2005; Navarro et al., 2008; Chen et al., 2010; Kossoff et al., 2011).

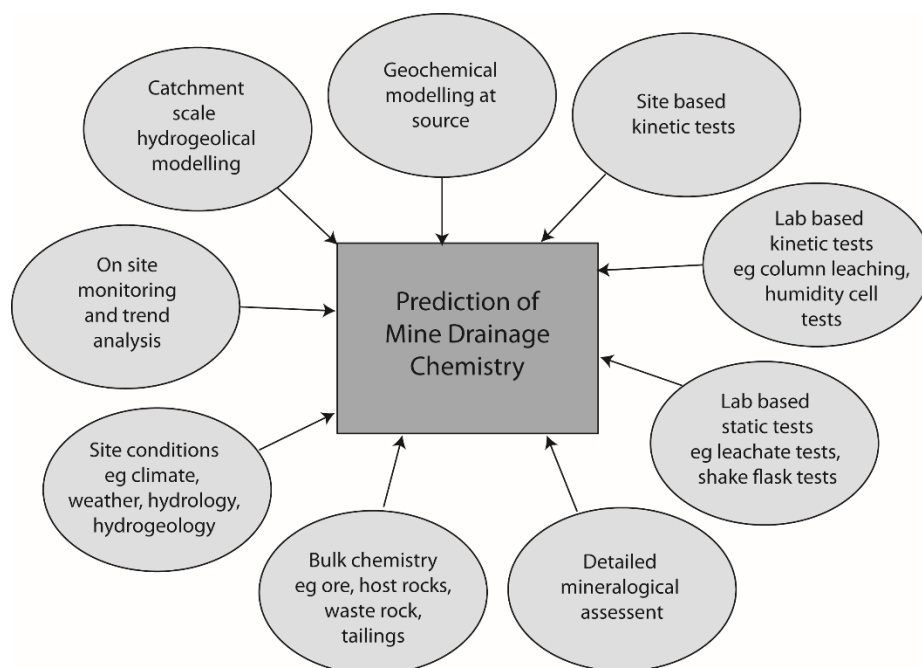


Figure 2.5: Tools to predict the chemistry of mine drainage (from Bright and Sandys, 2015)

Hirsche et al. (2017) studied the attenuation of Zn by layering different waste rocks in field barrels and humidity cells. As a result, they were able to

investigate the mechanisms that control Zn in a neutral mine drainage setting. Following geochemical modelling it was concluded that the precipitation of secondary Zn minerals is not enough to explain the degree of attenuation observed. It was thought that the Zn may have been incorporated into clay minerals, but the mechanism was unclear and required further investigation (Hirsche et al., 2017).

While column studies are commonly used it should be noted that there has been no standardisation of the technique (Lewis and Sjöström, 2010), and there is no ideal length or diameter of the columns. This is in part because each experiment is different and therefore requires a different approach (Lewis and Sjöström, 2010). In the design of a column leaching study, various considerations need to be taken into account including: length, diameter, overall aim (e.g. to recreate the infiltration rates from the field setting), external temperature, bulk density, number of cycles of leaching, how long after the samples were recovered should they be analysed, what to analyse for at the time of collection of leachate, filter system, and the occurrence or formation of preferential fluid pathways.

For example, samples collected from the Guangdong Dabaoshan Mine, China, were sieved to below 2 mm and placed in columns 300 mm in length (Chen et al., 2010). Following daily additions of deionised water for 30 cycles it was found that less than 20 % of the total acidity was removed from the soil column. This means there was acidity remaining in the soil that could be released by percolating water over a long period of time. Dissolved Cu and Pb were rapidly leached out, soluble Fe concentrations in the soil were found to be low, and Zn and Mn continuously decreased over the length of the experiment, with the exception of the organic bound Zn and Mn fractions (Chen et al., 2010).

A column leaching study was carried out to evaluate metallic element attenuation in tailings from southeast Spain (Flores and Sola, 2010). The main ore minerals galena, barite, siderite, and Ag-Pb sulfosalts, were extracted by crushing, grinding and flotation. The tailings were then dumped

in the catchment of the Canalejas River. Samples were recovered from the main ore deposit and various wastes including the tailings. The columns comprised a water reservoir, a column 15cm diameter x 75 cm long, and a series of instruments to measure various parameters. The mine wastes were found to contain high concentrations of Ag, As, Ba, Cu, Pb, Sb and Zn and the column experiments showed that Al, Ba, Cd, Cu, Mn, Pb and Zn were all found to be relatively immobile when the water was added, while Fe and Sr became mobile. The immobilisation was thought to be as a result of calcite dissolution causing an increase in pH, leading to adsorption and co-precipitation of the metallic elements (Flores and Sola, 2010).

The Montevecchio-Levante Pb-Zn mine in Sardinia has resulted in the contamination of the surrounding area, with metallic elements in the waste dumps found to be around 12,245 mg/kg Pb, 3,366 mg/kg Zn, 444 mg/kg Cu and 25 mg/kg Cd (Ciccu et al., 2003). Column experiments were carried out using this contaminated material to determine the immobilisation potential of fly ash and residual 'red mud' material from bauxite processing. The columns were 1.4 cm in diameter and 40 cm high and after filling with the mine wastes were allowed to 'age' for 60 hours before starting any tests. The experiment was carried out over 30 months, 150 ml of distilled water was added every day in a single addition, and water was stopped occasionally for 20 to 30 days to simulate a 'dry period' of weather. It was found that the addition of fly ash and red mud reduced the metallic element concentration of the resulting leachates, which was attributed to the alkalinity of these materials and their potential absorption capacity (Ciccu et al., 2003).

The release of Cd and Zn from mine tailings from weathering was determined using tailings and soil from Potosi, Bolivia (Kossoff et al., 2011). The columns comprised 5.5 cm diameter by 55 cm high HDPE pipe. The weather of Bolivia was replicated using six-week cycles, adding simulated water for three weeks and allowed to dry for three weeks, this was carried out for 15 cycles or modelled years. In the initial three cycles, a 'first flush' effect was noted, when a high concentration of Zn and Cd were mobilised as a result of the dissolution of soluble Cd and Zn salts. The results tended to be cyclical, the

first addition of water increased the concentrations above the year before; concentrations rose dramatically after the second week water addition and then reduced after the third. Overall Cd and Zn concentrations were highest in years one and two, decreasing in year three, then increasing slightly to year 9 and reducing again to year 15. The decline around year three is thought to result from the formation of secondary minerals or a reduction in the rate of mineral dissolution (Kossoff et al., 2011).

Contaminant transport and fate may be governed by soil dispersivity, which can be considered to be an intrinsic property of the soil (Bromly et al., 2007). Bromly et al. (2007) found that the dispersivity increased with increasing column diameter of repacked soil columns, with clay content being the second most important factor reflecting the dispersivity. They concluded that the main considerations of column design are inlet mixing (can increase dispersion in shorter columns), column size, and soil packing.

The packing and saturation of a column are also important. Soil columns that are unsaturated and repacked from disturbed samples contain both water and air and are often used to mimic the conditions at the surface above the groundwater table within the vadose zone (Lewis and Sjöstrom, 2010). One of the key advantages of using packed rather than undisturbed soil columns is their reproducibility as it is possible to more easily control the bulk density of the soils (Lewis and Sjöstrom, 2010). Undisturbed soil columns have the advantage of being more similar to the actual field conditions as the soil structure has been preserved (Lewis and Sjöstrom, 2010).

Plante et al. (2014) used various methods including column experiments, weathering cells, humidity cells, field cells and waste rock piles to study the influence of scale effects of lab to field tests on NMD prediction. They found that the volume-normalised release reaction rates can be up to 4 orders of magnitude different and the surface normalised release rates were found to vary by up to 3 orders of magnitude between lab and field scale. In addition, column experiments appear to increase the rate when compared to field

scale tests, where neutralisation and oxidation ratios remain similar to those in the field.

Additional methods of investigation include laboratory testing, such as, total digestion and sequential extraction.

2.7 Investigating Metallic Element Speciation by BCR Sequential Extractions

The forms of metallic elements within soils and sediments depend heavily upon their nature and origin (Ma and Uren, 1997), the aim of chemical extraction techniques is to assess metallic element (bio)availability and mobility within soils (Verner et al., 1995; Ma and Rao, 1997). Sequential extractions have been used by many researchers to study the fractionation of Pb, Zn and Cd in mining affect environments, including; Verner et al. (1996); Fafani et al. (1997); Li and Thornton (2001); Wang et al. (2005); Audry et al. (2006); Vaněk et al. (2008); Pulford et al. (2009). An example of this is a study on smelter-impacted soil in the north of France which looked at the geochemical speciation and oral bioaccessibility of Pb, Zn and Cd. The soils were found to have a pH of 6.7 to 8.2. It was found the metallic elements were bioaccessible in the gastric and gastrointestinal stages generally in soluble forms, bound to organic matter and associated with carbonates and Fe/Mn oxyhydroxides (Waterlot et al., 2017).

Mouni et al. (2017) undertook a study of soils from the Pb-Zn Amizour-Bejaia mining area, Algeria. The soils were analysed using a five-step sequential extraction procedure based on Tessier et al. (1979). The tested soils were found to have a pH of 7.5 to 8.3 and a low organic matter content. Concentrations of Pb ranged from 102 to 144 mg/kg, Zn ranged from 206 to 293 mg/kg and Cd from 1.3 to 5.4 mg/kg. Following the sequential extraction Pb and Zn were found to be associated mostly with the organic and reducible fractions, and less than 20 % with the residual fraction. It was noted that Cd was likely to be more mobile as it binds preferentially to carbonates. As a result of this study the researchers concluded that organic matter and Fe/Mn oxides were most important for Pb and Zn, and carbonate is the most

important for Cd. It was found that in these mine soils the relative mobility is likely to be Zn>Cd>>Pb (Mouni et al., 2017).

The Zanjan province of Northern Iran is an area known for Pb-Zn mining and smelting. The National Iranian Lead and Zinc (NILZ) smelter is located some 11 km east of Zanjan (Gharyoraneh and Qishlaqi, 2017). Waste materials are known to have been dumped to the east of the smelter itself for a number of years. This means the wastes have been subjected to erosion by both wind and water. Analysis of the waste filter cakes recorded average concentrations of 12,900 mg/kg of Pb, 450,000 mg/kg of Zn and 139,000 mg/kg of Cd. The wastes themselves had a low pH due to the use of acid during the processing, however topsoil samples from a 10 km transect southeast from the smelter generally recorded neutral pH values of 6.98 to 7.18. It was found that concentrations of Pb, Zn and Cd generally decreased with increasing distance from the smelter, however concentration of Cu, Cr and Ni remained relatively consistent along the length of the transect. Following a four-stage BCR sequential extraction Pb was found to be mostly present within the Fe/Mn oxyhydroxide fraction, Zn and Cd were found to be mostly present within the reducible fraction (Gharyoraneh and Qishlaqi, 2017).

2.8 Conclusions

Historical mining operations have resulted in significant metallic element release into many river basins worldwide (Hudson-Edwards et al., 2008). Nordstrom (2015) noted that metallic element concentrations of AMD can be 1 to 3 orders of magnitude greater than NMD. Despite this, NMD can still result in an increase of metallic element concentrations within affected catchments. Compared to AMD not as much is known about NMD and more research is required to bridge this gap. What literature there is tends to focus on experimental techniques for remediation. There is a gap in knowledge about the actual mechanisms that control NMD, although there are variations on how NMD occurs including neutralisation of AMD by host rock buffering and changes in mine drainage over time. The aim of this study is to look at

the mechanisms of classic low Fe NMD and how they can be used in a wider context to help predict and hopefully contribute to the remediation of NMD worldwide.

In summary:

- the impact of mining on the natural environment is a worldwide issue;
- Pb-Zn mines are common worldwide, around 240 are still active, however most have been abandoned and can represent hazard as a result of metallic element release to the environment and rivers;
- in many parts of the world over 50 % of the population is living on an alluvial plain and industrial activities are concentrated in these areas;
- ore geology is a major influence of mine drainage chemistry and therefore mine drainage should be predictable if the geology of the mining area has been extensively researched;
- over the past two decades a lot of research has been undertaken with regards to mine drainage and the reactions that control it; however the complexity of these reactions and uniqueness of each site means there is no 'one-size-fits-all' answer to the problem. There is a particular lack of information on NMD and the relative contributions of metallic elements from mine waste and mining-contaminated alluvial sediment weathering to this drainage;
- studies on carbonaceous catchments are required to better understand the differences in chemistry in AMD and NMD, specifically the concentration of protons, how Al and Fe solubility is controlled by pH, and the differences in the bioavailability of metallic elements for aquatic organisms (Valencia-Avellan et al., 2017).

Chapter 3

Area of Study

Contents

| | |
|---|-----|
| Chapter 3..... | 80 |
| 3.1 The North Pennine Orefield..... | 80 |
| 3.2 General Characteristics of the River Swale..... | 82 |
| 3.3 Swale Catchment Geology..... | 83 |
| 3.3.1 Pb-Zn Mineralisation..... | 84 |
| 3.4 Mining in the River Swale Catchment..... | 89 |
| 3.5 Mining-related metallic element contamination of the Swale Floodplain..... | 91 |
| 3.6 Gunnerside Gill..... | 96 |
| 3.7 Mining in Gunnerside Gill..... | 99 |
| 3.7.1 Blakethwaite Mines..... | 100 |
| 3.7.2 Lownathwaite Mines..... | 101 |
| 3.7.3 Old Gang Mines..... | 101 |
| 3.7.4 Sir Francis Level..... | 102 |
| 3.8 Previous studies describing mining-related metallic element contamination of Gunnerside Gill..... | 103 |
| 3.9 Summary..... | 107 |

Chapter 3 will describe the project's area of study, including Yorkshire (Section 3.1) and the River Swale in terms of its catchment (Section 3.2), geology (Section 3.3), mining (Section 3.4) and mining-derived contamination (Section 3.5). The sampling site, Gunnerside Gill, will be discussed in more detail in Section 3.6, with particular emphasis on the underlying geology, historical mining (Section 3.7) and previous research quantifying the mining-related contamination of Gunnerside Gill (Section 3.8). Finally a summary will be given in Section 3.9.

3.1 The North Pennine Orefield

Yorkshire is the largest county in England and it is situated in the northeast of the country. Historically Yorkshire was an important area for mining and extracting Pb, which peaked during the 18th and 19th centuries (Palumbo-Roe and Colman, 2010). Some of the former extractive industrial sites lie within

the area comprising the Yorkshire Dales National Park. This Park covers an area of approximately 1,770 km² and has a population of around 20,000 (National Parks, 2015). The geology of Yorkshire mostly comprises Carboniferous limestone overlain by the Millstone Grit Series (Edwards and Trotter, 1954). The main mining areas of Yorkshire include Swaledale, Arkengarthdale, Wensleydale, Greenhow Hill and Wharfedale (Raistrick and Jennings, 1965).

The Pennines are an area of high ground running the length of the county along its western margin. This range comprises a dissected plateau of Carboniferous strata that rise up to 600 m above sea level (Jarvie et al., 1997). The mineralised rocks of Yorkshire are located within the southern part of the Northern Pennine Orefield, known as the Askrigg Block (Dunham and Wilson, 1985). The orefield is incorporated parts of Yorkshire, Westmoreland, Cumberland, Durham and Northumberland (North Mines Research Group, 2017).

The North Pennine Orefield deposits have been worked over thousands of years since pre-Roman times. By the nineteenth century the orefield was the biggest producer of Pb and associated Ag in England (Dunham and Wilson, 1985; Macklin et al., 1997). Ore production was greatest during the second half of the 18th century when most of the remaining accessible veins were exploited, following this the industry went into decline once the most easily reached sources had been worked (Jarvie et al., 1997). In addition, a fall in Pb prices from the mid-1870s made the downturn worse (Mills et al., 2014). The estimated mine waste production from the Northern and Southern Pennine Orefields combined is thought to be in the order of up to 50 million tonnes with a Pb production of 7.5 million tonnes (Palumbo-Roe and Colman, 2010). The environmental impacts from metallic element mining in the region did not become large-scale until the middle of the 19th century when, with the expansion of the industry, smelting, dumping mine wastes on land and uncontrolled fine-grained discharges to rivers resulted in extensive contamination (Macklin et al., 1997). The spoil heaps and floodplains contaminated by these historic mining activities are currently the primary

source of contaminant metallic elements (Macklin et al., 1997) within the region's catchments.

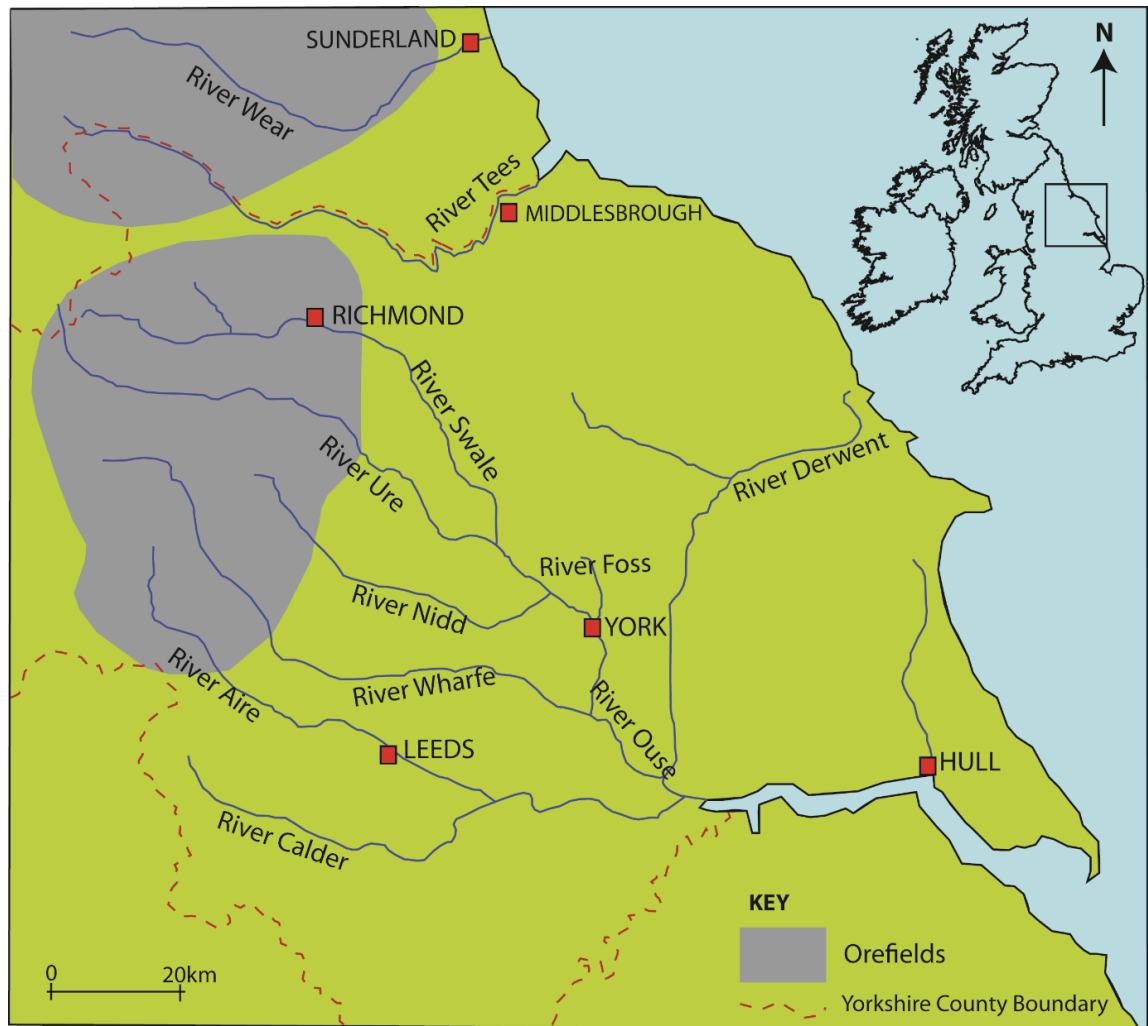


Figure 3.1: Sketch map showing the location of the main rivers and associated orefields of the Pennines (after coolgeography.com 2017)

According to the EA many of the catchments of the Yorkshire Dales and Northern Pennines are among the most affected by metalliferous mining in England and Wales. These include the Swale, Wharfe, Nidd, Ure, Wear and Tees catchments (Hudson-Edwards et al., 2008), Figure 3.1.

3.2 General Characteristics of the River Swale

The River Swale, with headwaters located in the Yorkshire Dales, is the northernmost tributary of the Yorkshire Ouse (Dennis, 2005), as shown in

Figure 3.1. The River Swale has a total catchment area of 1,446 km² and the main channel is 117 km in length (Dennis et al., 2003; 2009). The catchment is rural with a low population density (Walling et al., 2003) and the water has a characteristic brown colour as a result of drainage through the upland peat (House and Warwick, 1998b). The upland areas support sheep grazing whereas arable, sheep, cattle and poultry farming are carried out in lowland catchment areas (House and Warwick, 1998a).

According to the UK National Flow Archive (nrfa.ceh.ac.uk consulted 2015) the annual historic rainfall from 1961 to 1990 in the River Swale catchment varied from 3,000 mm high in the Pennines to 700 mm on lower ground near Richmond. The average annual hydrograph, based on data from 1961 to 1980, generally shows higher flow rates from September to May, and lower flows from June to August. During the winters of 2013-2014, 2015-2016 and 2019 there was an unprecedented volume of rainfall which resulted in widespread flooding not only of this catchment, but also across the UK. In some areas the main channel has been straightened to reduce the potential impact of flooding and the banks have been reinforced to protect the surrounding farmland (House and Warwick, 1998b).

3.3 Swale Catchment Geology

The River Swale is underlain by Carboniferous strata in the west, becoming progressively younger moving eastwards through Permian and Triassic strata (Figure 3.2) (House and Warwick, 1998a; 1998b). The limestones, shales and sandstones of the Lower Carboniferous appear at the surface in the valleys of the upper Swale and its various tributaries (Dunham and Wilson, 1985). The sandstones, shales and limestones of the Upper Carboniferous overlie the Lower Carboniferous strata and appear on the higher ground in the upper part of the catchment (Dunham and Wilson, 1985). For the sake of clarity a search of the BGS website (September 2017) indicated that the Stainmore Group and Wensleydale Group are terms that have been amalgamated and superseded by the Yoredale Group. Similarly the Magnesian Limestone has been superseded by the Zechstien Group.

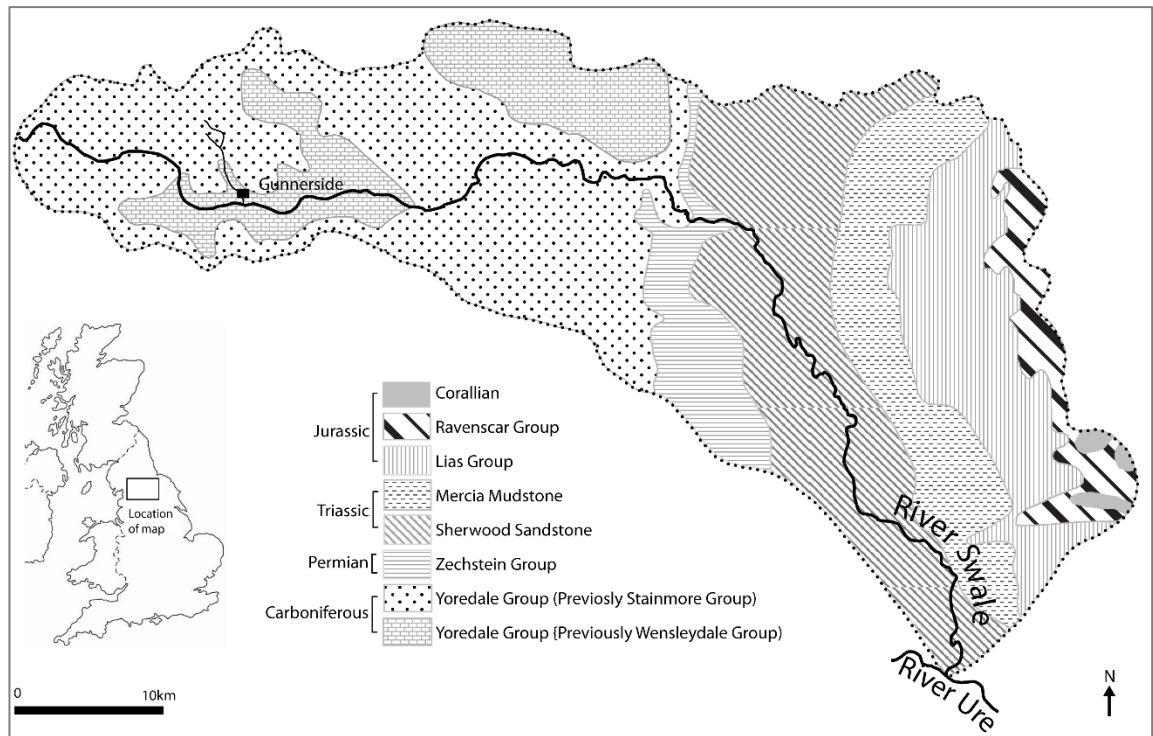


Figure 3.2: Geology map of the River Swale (after Dennis, 2005; BGS website 2017)

The upland tributaries of the River Swale cross the most heavily mineralised areas of the southern region of the north Pennine Orefield, including Gunnerside Gill, Barney Beck, Arkle Beck and Marske Beck (Dunham and Wilson, 1985). Historic Pb and Zn mining was widespread within these upland tributaries (Dennis et al., 2003).

3.3.1 Pb-Zn Mineralisation

A sequence of carbonate and shale rocks were laid down across a large part of southern Britain during the Carboniferous within shallow water environments and marginal basins respectively (Bevins et al., 2010). The combination of these strata resulted in the formation of localised Pb-Zn-F mineralisation within the Alston and Askrigg blocks of the north Pennine orofield (Bevins et al., 2010). The Alston and Askrigg Blocks, combined with the intervening Stainmore Trough, form a graben structure that trends generally east-west (Waters et al., 2011). Both of the blocks have granite cores (Smith and Murphy, 2011), as denoted in Figure 3.3.

The mineralised Askrigg Block is defined by the Craven Fault to the south and west, the Dent Fault to the north, and to the east the Askrigg Block disappears below younger sediments towards the Vale of York and Vale of Mowbray (Yorkshire-dales.com, 2017). The Askrigg block has a mining history dating back to the Roman times, but the output was significantly less than for the Alston block to north (BGS, 1996). The locations of the Askrigg and Alston blocks are shown on Figure 3.3, the River Swale is present on the northern portion of the Askrigg block (Figure 3.2).

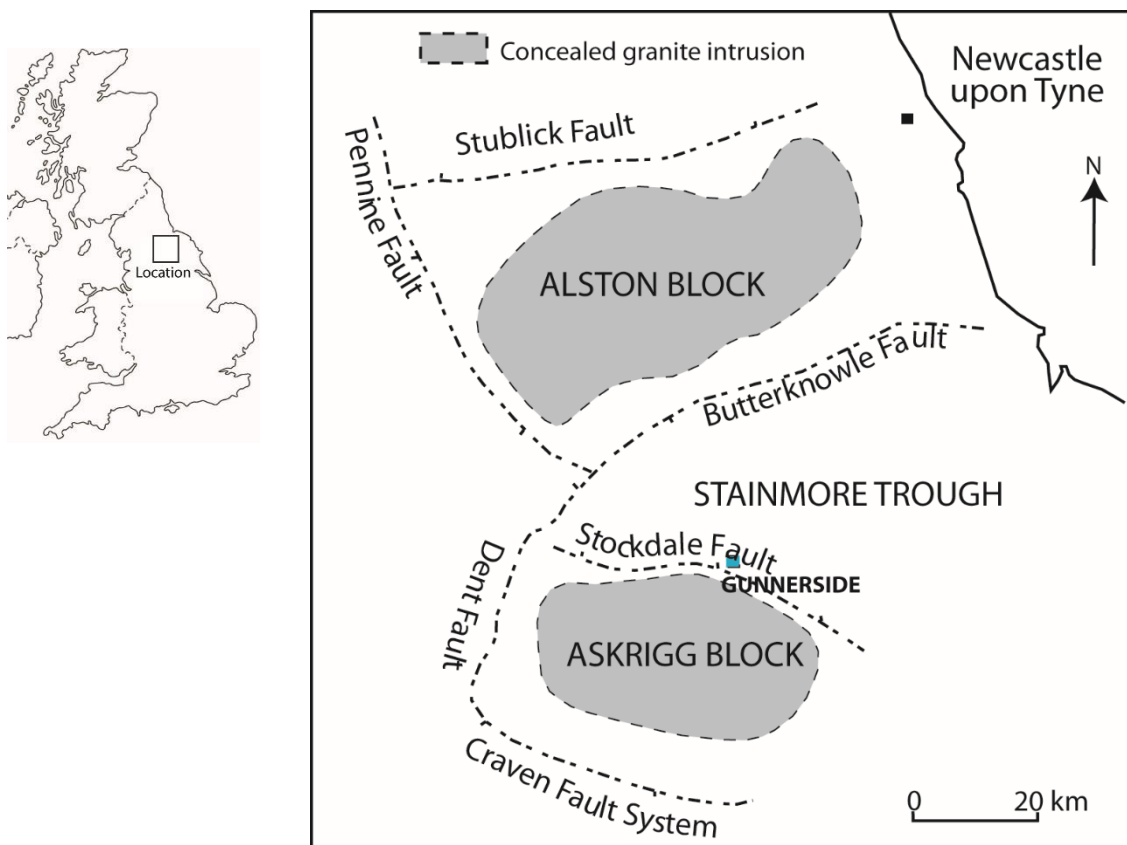


Figure 3.3: Locations of the Alston and Askrigg blocks (adapted from Geological Conservation Review 2018 and Earthwise.bgs.ac.uk 2018)

The ore bodies are primarily orientated in an east-west or southeast-northwest direction and are gently inclined or nearly horizontal (Dunham and Wilson, 1985). The main minerals found within North Pennine Orefield are listed in Table 3.1.

Table 3.1: Minerals of the Yorkshire Dales (after Dunham, 1959). Principal secondary minerals are italicised.

| Primary and secondary minerals of the North Pennine Orefield | |
|--|--|
| galena PbS | <i>cerrusite PbCO₃, anglesite PbSO₄</i> |
| sphalerite ZnS | <i>hemimorphite Zn₄Si₂O₇(OH)₂H₂O,</i> |
| smithsonite ZnCO ₃ , | <i>hydrozincite Zn₅(CO₃)₂OH)₆</i> |
| chalcopyrite CuFeS ₂ | <i>malachite Cu₂CO₃(OH)₂</i> |
| bornite Cu ₅ FeS ₄ | <i>azurite Cu₃(CO₃)₂(OH)₂</i> |
| covellite CuS | <i>goethite FeO(OH)</i> |
| chalcocite Cu ₂ S | <i>barytocalcite BaCa(CO₃)₂</i> |
| pyrite FeS ₂ | aragonite CaCO ₃ |
| quartz SiO ₂ | calcite CaCO ₃ |
| fluorite CaF ₂ | dolomite CaMg(CO ₃) ₂ |
| barite BaSO ₄ | ankerite Ca(Mg,Fe,Mn)(CO ₃) ₂ |
| witherite BaCO ₃ | siderite FeCO ₃ |

The mineralisation of the North Pennine orefield is zonal. Within the Askrigg Block fluorite is considered to be an indicator of the zonal centres, surrounded by and/or interbedded with barium minerals (BGS, 1996). The concentration of galena is often highest between the outer section of the fluorite zone and inner portion of the barium zone (BGS, 1996).

Within the Askrigg Block the Pb-Zn mineralisation generally consists of fissure veins within conjugate fault fissures and limestone replacement related to the veins themselves (Dunham, 1959; BGS, 1996). Four types of ore body have been identified:

- veins, large ribbon-shaped deposits formed in fissures mainly within the brittle limestones and cherts;

- scarns, deposits within vertical or steeply dipping discontinuities;
- pipes, formed at the intersection of two fractures or a fracture and bedding plane;
- flots, floats and flats, replacement features formed generally parallel to bedding planes (Dunham and Wilson, 1985; Ixer and Vaughan, 1993).

Initially it was thought that during the late Carboniferous or early Permian Pb, Zn, Ba and F-rich fluids associated with the concealed Wensleydale Granite were introduced into Carboniferous strata (Ixer and Vaughan, 1993). Some geologists also believe that the Pb veins formed as a result of hot saline solutions moving through sandstone aquifers in the region (Gill, 2001).

More recently the role of the intruded granites in the mineralisation of the area has come into question. Following the drilling of exploratory boreholes, it was found that the limestones were unconformably laid down upon the granite and that it was unlikely to have been intruded but rather an earlier Caledonian granite (Dempsey, 2016). As a result the mineral veins of the orefield are unlikely to be associated with the formation of the Weardale granite (Dempsey, 2016).

Cann and Banks (2001) undertook a review of the literature and crush/leach investigations of fluid inclusions to try and determine the constraints of the mineralisation within the North Pennine Orefield. The researchers put forward that following a phase of tectonic inactivity ore genesis commenced as the basement heated up during 'pulse extension'. As a result the overlying sedimentary rocks were faulted and fractured into the basement allowing the overlying brine water of the Zechstein Sea to penetrate some 8 km deep. This resulted in hot hydrothermal fluids interacting with the fissured basement rocks. The heat of the Weardale Granite and surrounding rocks set up a convection cell that allowed the heated fluids to rise and then water moved down the sides of the granite. Cann and Banks (2001) refer to at least four different fluids being involved in the reactions and that the majority of the mineralisation occurred where the fluids mixed.

Lady's Rake Mine, a geological conservation review site, has been used to date the mineralisation of the north Pennine orefield as it indicates the Pb-Zn mineralisation came after the emplacement of the Whin Sill (Bevins et al., 2010). This is considered to be between the upper Carboniferous and lower Permian times, represented by an unconformity in the sequence (Bevins et al., 2010).

Dempsey (2016) hypothesized that the metallic elements within the North Pennine Orefield were unlikely to be related to leaching of sediments due to the underlying hot granite, but are more likely to have resulted from a 'mantle source' namely the Whin Sill. In addition, the orefield appears to be controlled structurally, when there was a change from north-south compression to north-south extension (Dempsey, 2016).

The presence of the Weardale and Wensleydale granite intrusions controlled the development of the Alston and Askrigg blocks, as from the mid-Devonian onwards these were 'positive highs' that resulted in the deposition of the Yoredale facies (Bevins et al., 2010). The deposits occur within Carboniferous rocks within five distinct facies: massive limestone (the Great Scar), reef limestone, Yoredales (an upwards cyclothemic sequence of limestone-shale-sandstone with occasional coal), Bowland Shale (black shale with impure limestone) and Millstone Grit (Dunham, 1959). The Yoredales facies is characterised by thin bands of rhythmic sedimentary deposits (Bevins et al., 2010).

The economic minerals of the Swale deposits principally comprise galena, barite, sphalerite, witherite, and more generally, gangue calcite (Dunham, 1959; Ixer and Vaughan, 1993). The metallic element-bearing veins comprise coarse-grained aggregates of these hosted minerals that are commonly banded parallel to the sides of the fissures where they were emplaced (Dunham, 1959). Galena is the most important Pb-bearing mineral comprising around 90 % of the Pb-bearing ores within the orefield (Ixer and Vaughan, 1993).

Secondary minerals form as a result of weathering of the primary ore minerals. This weathering may occur before, after or during mining

(Lottermoser, 2010). However, because weathering is largely a surficial process post-mining is the most significant source of secondary minerals. The oxidation of galena to anglesite and cerrusite, sphalerite to smithsonite and hydrozincite, chalcopyrite to malachite and azurite, Fe sulfides to ankerite and siderite and to Fe oxyhydroxides such as goethite is widespread. Other secondary minerals are also present in minor amounts (Table 3.1., Ixer and Vaughn 1983).

3.4 Mining in the River Swale Catchment

A 'pig' (also known as an ingot) of Pb engraved with the name of Hadrian (the Roman Emperor who reigned from AD 117 until AD 138) was discovered at Hurst Mine (Raistrick and Jennings, 1965; Raistrick, 1975). This suggests that Pb mining has been an industrial activity since at least Roman times in Swaledale. There is little evidence of mining for centuries after the Romans, however in 690 AD Pb from Yorkshire was possibly used to repair an early church at the site of York Minster as it could have easily been transported via the River Swale (Raistrick, 1975). Lead mining in northern Britain resumed in the 9th century, from existing locations such as the Old Gang mines (Raistrick and Jennings, 1965). Mining in the Swale area was recorded over the next few hundred years. Indeed a working mine was present in Arkengarthdale in 1285, which was reported to have a profit of £4 (presumably per year, however not stated within the text) (Raistrick, 1975). The mines were again mentioned in documentation from the 14th century, which suggests they were being worked regularly at this time. Further, in the 16th century Pb was purchased by York merchants who moved it to Hull for exportation or transit to London (Raistrick, 1975). In the late 16th and early 17th centuries the mines of Swaledale were prosperous as a result of demand for Pb being high due to its increasing use in construction of new houses and buildings (Raistrick, 1975) likely to be for plumbing and roofing.

Early mining methods were labour intensive, relying on hand tools and the forces of gravity and water. The ore deposits of the upper reaches of the River Swale were mined by 'hushing', a form of hydraulic open cast mining

(Gill, 2001). This involved the release of water from a turf dam constructed on a hillside, which when broken resulted in a torrent of water (Gill, 2001). The water eroded and transported surface soil and broken rock in its path, exposing fresh veins and removing waste materials (Raistrick and Jennings, 1965). The resulting debris spread out at the foot of the slope where it could be sorted through by hand (Raistrick, 1975). Miners would also have used hushing to clear out accumulated waste materials and as a result significant amounts of fine-grained metallic element-contaminated sediments were released into the catchment (Hudson-Edwards et al., 2008).

Later the veins were worked at the surface from narrow open pits without supports; as the workings became deeper the veins were accessed by adits and shafts (Palumbo-Roe and Colman, 2010). The shafts could only be extended to as far as air circulation would allow, then another shaft would be sunk further along the vein and the previous one abandoned (Raistrick, 1975). The sulfides would then have been separated by crushing the ore and gravity sorting in the nearby waterway and both liquid and solid mining wastes were often directly disposed of into the nearest water course (Hudson-Edwards et al., 2008). In larger mines mechanical crushers would have been used, whereas in smaller mines 'hand cobbling' was more common (Palumbo-Roe and Colman, 2010) to process the ore. On the dressing floor ores were separated by density using water; often inefficient operations meant much of the ore was lost (Palumbo-Roe and Colman, 2010). Mining methods evolved during the 16th century when levels were driven following the ore veins horizontally and the 18th century saw the use of steam engines to pump mines and water wells (Raistrick, 1975) to remove the excavated rock from the mines. In addition, the pumping of water also enabled miners to work below the level of the water table. Large quantities of mine waste were released into the River Swale during the late 18th and 19th centuries. Mines around this time were primarily located in Gunnerside Gill and the surroundings (Figure 3.4, Dennis et al., 2003). High channel and overbank sedimentation during this time caused aggradation of the valley floor and burial of the earlier fluvial sediments, to depths of between 1 m and 1.5 m (Brewer et al., 2005).

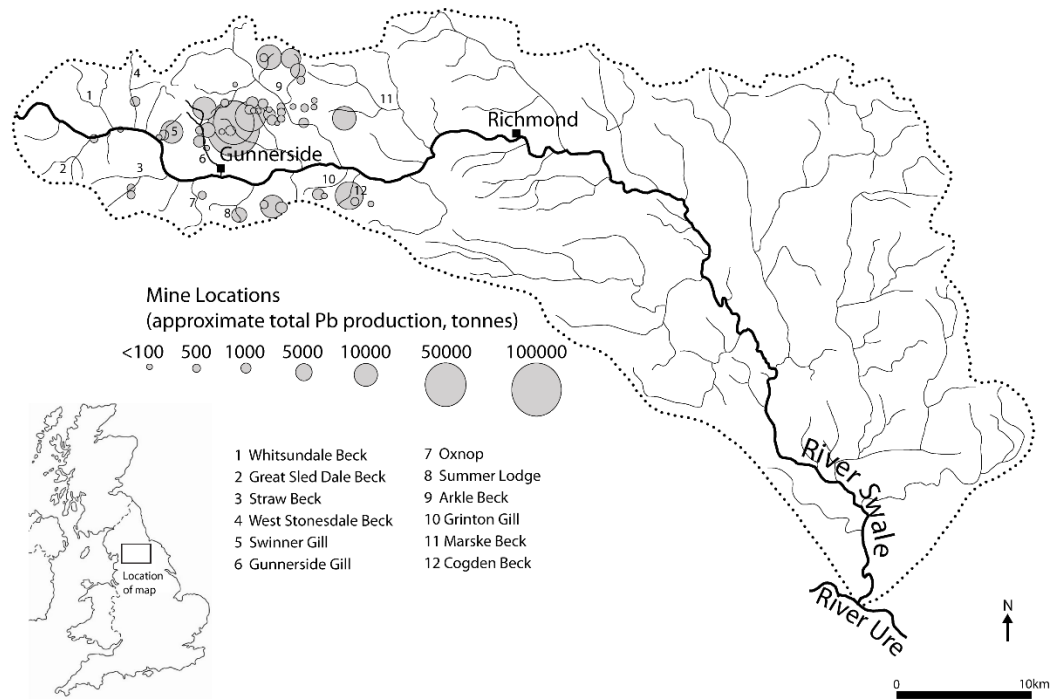


Figure 3.4: Location of Gunnerside Gill including the main Pb mining areas from A.D 1700-1900 (from Dennis et al., 2003)

Metallic element-contaminated alluvial deposits can be easily identified by their alternating layers of light sand and dark silty sand, which overlies pre-mining sediments that contain more clay and silt, are more cohesive, contain fossilised wood and lack obvious bedding structures (Brewer et al., 2005).

3.5 Mining-related metallic element contamination of the Swale Floodplain

Although mining finished during the early 20th century, metallic element-rich sediments are still present and due to remobilisation still contribute to floodplain contamination in the present day (Dennis et al., 2003; Walling et al., 2003; Hudson-Edwards et al., 2008). In the North Pennine Orefield, the potential for acid mine drainage is considered to be low, a result of the low concentrations of pyrite present and associated acid-buffering minerals in the form of the carbonate host rocks (Palumbo-Roe and Colman, 2010).

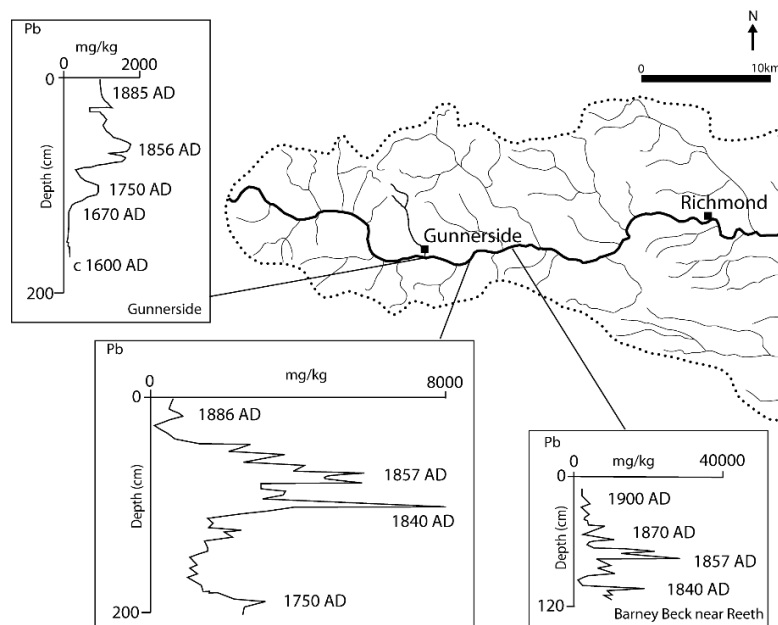


Figure 3.5: Pb vertical profiles taken from the Swale with locations indicated on map (after Macklin et al., 1994)

Various studies have been undertaken on the mining contamination within the River Swale catchment. Macklin et al. (1994) carried out chemostratigraphic analysis (using ^{14}C) of three vertical profiles from the River Swale (Figure 3.5). The furthest upstream site was taken from Gunnerside Gill, where the longest record of overbank sedimentation spanning from 1600 AD to 1885 AD was found. At the base of the section (1.7 m below ground level (bgl)) the sediments were found to be relatively uncontaminated and were thought to have been deposited before the extensive development of mining in the mid-18th century. The authors go on to state that further downstream, the overbank sediments dated from around 1750 AD to 1890 AD show the rise and demise of Pb mining in the catchment from the late 18th century (1.9 m bgl) and the mid-late 19th century (1.1 to 0.6 m bgl), respectively. The final profile was taken from a site just downstream of the Barney Beck, where the overbank sediments appear to have been deposited between 1840 AD and 1900 AD. The metallic element concentrations here are the highest of the three sites. Lead values were found to be up to 30,000 mg/kg and Zn exceeded 8,000 mg/kg. At all three locations the highest levels of contamination in the alluvial sediments were found to be deposited in the mid-19th century and were located around 0.7 m bgl to 1.0 m bgl.

Dennis et al. (2003) undertook a study looking at the impact of the severe flooding in 2000 on the dispersal of Pb, Zn and Cd in the River Swale. The autumn floods of 2000 resulted in erosion of the channels and slopes in the headwaters and of the banks in the middle and lower sections of the catchment. Upstream of Richmond samples of overbank and channel edge flood sediment were recovered from downstream of the major tributaries, confluences and downstream of Richmond they were recovered every 5 km. The samples were divided by size into two separate fractions, sand (2,000-63 μm) and silt and clay (<63 μm). Figure 3.6 denotes the Pb concentrations in the overbank sediment in the River Swale moving downstream.

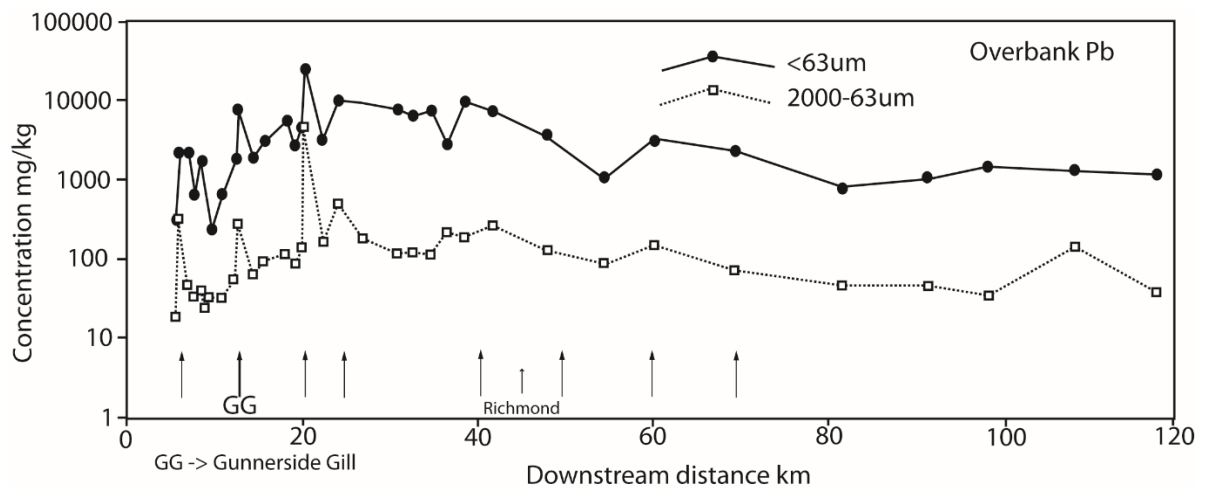


Figure 3.6: Changes in downstream Pb concentration in the River Swale, arrows represent the approximate tributary locations (adapted Dennis et al., 2003)

Elevated concentrations of Cd, Pb and Zn were noted in both the overbank and channel edge sediments in both size fractions at 6 km and 12 km downstream, these elevations were attributed to Swinner Gill and Gunnarside Gill respectively. Further concentration peaks were noted along the length of the River Swale likely resulting from Barney Beck (c. 20 km), Arkle Beck, Grinton Gill and Cogden Gill (25 to 35 km), Marske Beck (35 to 40 km), and Colburn Beck and Skeeby Beck (c. 50 km). Elevated concentrations of Cd, Pb and Zn were also noted at around 60 km and 70 km downstream; these are considered to be a result of reworking of contaminated upstream materials rather than local inputs of metallic element contaminated sediments. From 80 km onwards the concentrations of metallic

elements reduce and remain relatively constant. Overall the study concluded the channel edge and overbank sediments deposited in the River Swale contained elevated concentrations of Cd, Pb and Zn. Furthermore, concentrations of Cd, Pb and Zn were highest in the finer silt and clay sized fraction and elevated concentrations of these metallic elements were noted along the whole length of the channel. The source of the contaminated sediments was considered to be mining waste from the tributaries and reworking of the historically contaminated floodplain sediments already present within the River Swale (Dennis et al., 2003). A similar trend was identified by Walling et al. (2003) who reported that Pb and Zn concentrations in the river-bed sediments decrease downstream in the River Swale, which they considered to be at least in part due to downstream dilution from the input of uncontaminated sediment.

Another approach used to study the contamination of the River Swale was geomorphological mapping undertaken by Brewer et al. (2005). The aim of the study was to test geomorphological mapping techniques for the assessment of hazards resulting from metallic element contamination of floodplains at the field scale. Two sites were selected, a section of river just south of Reeth located some 2.3 km downstream of the heavily mined Barney Beck together with a 'control' section at Brompton-on-Swale which is 15 km downstream of the nearest mine. Sampling of the floodplain was undertaken on a 25 m grid in smaller fields and a 100 m grid in larger land areas. Samples of both surface (0 to 20 cm) and sub-surface (20 to 50 cm) sediments were recovered for analysis. In addition to this information supplementary data from both published and unpublished studies was collated. This database was then interrogated to examine the relationship between flooding and metallic element concentrations within the floodplain soils, the geographical variation in concentrations of metallic elements within the Swale Valley and to map the extent of the contamination along the River Swale. The results indicated that over 55 % of the valley floor of the River Swale is likely to be contaminated, suggesting that previous studies appeared to underestimate the degree and geographical extent of contamination (Brewer et al., 2005).

A study by Macklin et al. (2006) involving the analysis of 264 soil and sediment samples from nine valley floor sites showed that the local background Pb concentration was exceeded by a maximum factor of up to 10. These calculated background concentrations refer to those published by Brewer et al. (2005) of 212 mg/kg for Pb, 105 mg/kg for Zn and 1.0 mg/kg for Cd, as recorded from River Swale floodplain soils.

In a study which emphasized the very large scale of contamination, Dennis et al. (2009) estimated that there are around 30,000 tonnes of Pb stored within historically mined areas in the upper catchment of the River Swale (Table 3.2). The estimated values were based on extrapolation of the results of the Gunnerside Gill study, presuming similar mining and processing techniques within the Swale catchment and the assumption that 9 % of Pb was retained as metal-rich sediment within the floodplain (Dennis et al., 2009).

Table 3.2: Estimated Pb production and storage in the tributaries of the River Swale (after Dennis et al., 2009)

| Tributary | Catchment area (km²) | Total Pb production (tonnes) | Estimated Pb retention (tonnes) |
|---------------------|--|-------------------------------------|--|
| Great Sleddale Beck | 10 | 461 | 42 |
| Whitsundale Beck | 19 | 173 | 16 |
| Swinner Gill | 3 | 11187 | 1007 |
| Straw Beck | 20 | 774 | 70 |
| Oxnop Beck | 6 | 299 | 27 |
| Gunnerside Gill | 14 | 17796 | 1602 |
| Summer Lodge Beck | 5 | 3103 | 279 |
| Barney Beck | 17 | 236844 | 21315 |
| Arkle Beck | 67 | 37887 | 3410 |
| Grinton Gill | 3 | 1607 | 145 |
| Cogden Beck | 4 | 19460 | 1751 |
| Marske Beck | 39 | 13167 | 1185 |
| TOTAL | 207 | 342848 | 30820 |

In 2003 DEFRA commissioned a report to examine the use of geochemical mapping for identifying metallic element contamination of floodplains, using the River Swale as the case study. The main findings of the report were (Brewer et al., 2005):

- Pb, Zn and Cd contamination is likely in 29.1 km² of the valley floor;
- in upper Swaledale the contaminated sediments and soils reach up to 2 m above the river channel;
- sub-surface samples contain higher concentrations of Pb, Zn and Cd than the topsoil;
- 91 % of topsoil and 94 % of sub-surface samples were elevated in Pb above the local background concentrations;
- between 90 % and 95 % of samples exceeded the local background concentrations of Cd and Zn;
- calculated background 'pre-mining' concentrations were 212 mg/kg for Pb, 105 mg/kg for Zn and 1.0 mg/kg for Cd.

The report further concluded that within the Swale catchment low flow conditions were shown to result in contaminated sediments and mining wastes being deposited as banks, river-bed or on bars. Conversely, high flows result in the mining-contaminated sediments entering the river system and being diluted by the addition of uncontaminated sediment. This dilution allows for the reduction in metallic element concentrations within the sediments but can also result in contaminated material being transported further downstream (Brewer et al., 2005).

3.6 Gunnerside Gill

Gunnerside Gill is a c. 7 km long small upland tributary in the headwaters of the River Swale. The mineralization here is considered to be representative of a typical 'fissure-vein Pb-Zn-F deposit' (Bevins et al., 2010).

A series of Carboniferous strata underlie Gunnerside Gill. The Stainmore Group (part of the Yoredale Group (BGS.co.uk, 2020) comprising silica-cemented sandstones, grey to dark grey limestones and cherts of the outcrop in upland areas of the catchment (Figure 3.7) (Dunham and Wilson, 1985). Lower down the valley fluvial erosion has exposed the limestones and sandstones of the upper Yoredale Group (Dunham and Wilson, 1985). Figure 3.7 also denotes the major faults within the catchment, which coincide with the main veins as shown on Figure 3.8.

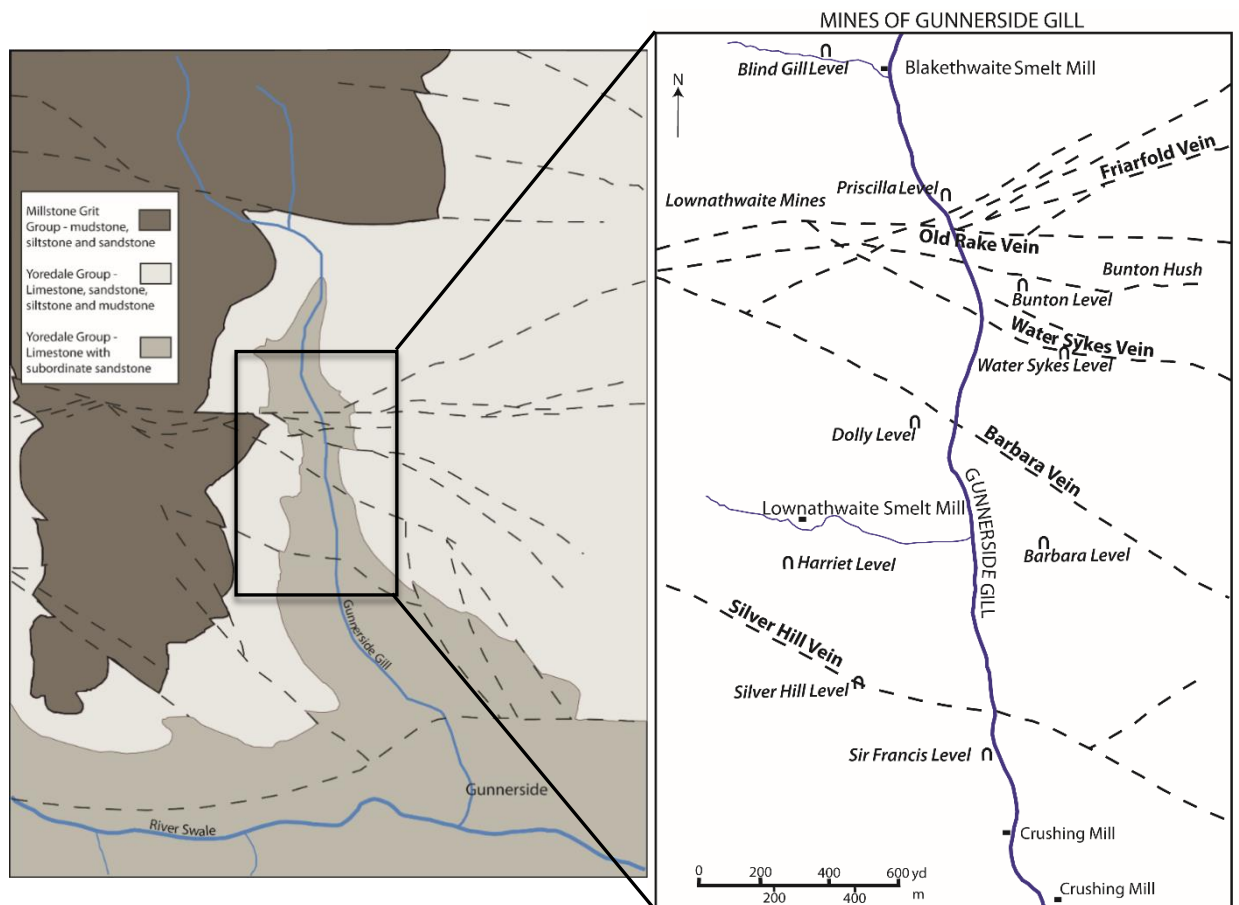


Figure 3.7: Simplified geology map of Gunnerside Gill including major faults denoted by dashed lines (adapted from BGS, 2015).

Figure 3.8: Mines and veins (denoted by dashed lines) of Gunnerside Gill (adapted from Raistrick, 1975)

The Gunnerside Gill catchment is subject to several designations, including the North Pennines Moor Special Protection Area and Special Area of Conservation, and three Sites of Special Scientific Interest (Arkengarthdale,

Gunnerside and Reeth Moors) for blanket bog, heather moorland and their breeding bird populations (EA, 2013).

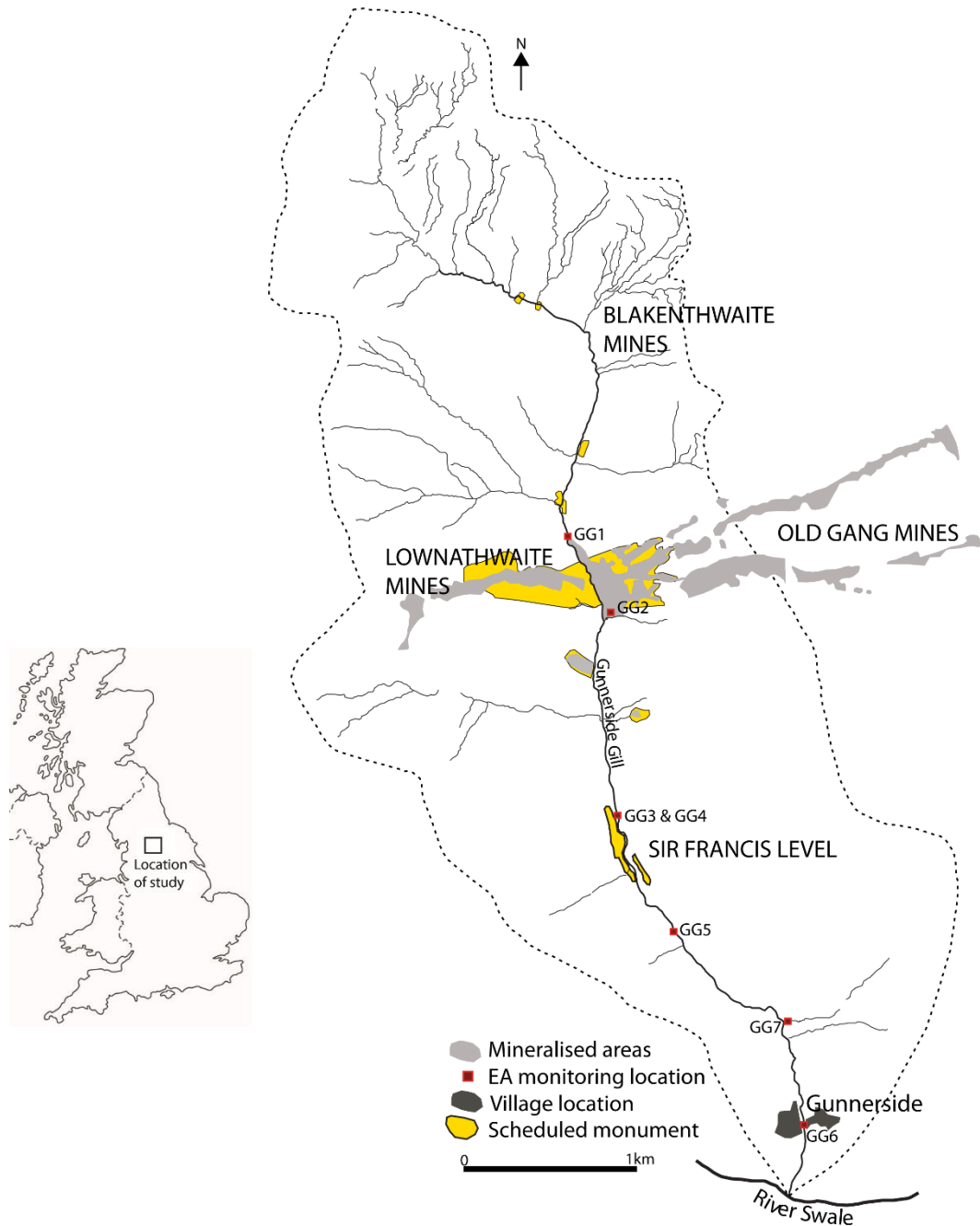


Figure 3.9: Location of mining areas and scheduled monuments in Gunnerside Gill (adapted Dennis et al., 2005 and magic.defra.co.uk)

In addition, several of the dams, dressing floors and mine waste tips are protected as they are scheduled ancient monuments (EA, 2013). These are concentrated in the areas of Lownathwaite and Old Gang Mines and Sir Francis Level (Figure 3.9). Modern uses of the area surrounding Gunnerside

Gill include sheep grazing, walking and grouse hunting. Much of the length of the Gill is uninhabited until it reaches the village of Gunnerside where it converges with the River Swale. Based on data from the UK National River Flow Archive, the average rainfall from 1961 to 1990 in Gunnerside Gill catchment was 1,200 to 1,400 mm per year (CEH webpage, 2017).

The River Swale catchment was adversely impacted by the floods in 2000 (Section 3.5, Dennis et al., 2003). A significant proportion of the Cd, Pb and Zn contamination immediately downstream of Gunnerside Gill (as denoted on Figure 3.6) was attributed to the remobilisation of sediments as a result of these floods (Dennis et al., 2003).

3.7 Mining in Gunnerside Gill

Various mining techniques were employed over the centuries to exploit the Pb ores in and around Gunnerside Gill. Although present, it is understood that Zn was not commercially worked in Swaledale (Gill, 2001). One of the main techniques was hushing (see Section 3.4), which may have started in Roman times and remained in use until the end of the 19th century (Raistrick and Jennings, 1965). Hushing was not only used as a production tool but also for exploration with the hope of exposing buried ore veins

Gunnerside Gill and its immediate surroundings had four main areas of mining: Blakethwaite mines to the north, Lownathwaite mines to the west, the Old Gang Mines to the east, and Sir Frances Level in the south (Figures 3.8 and 3.9) (Dennis et al., 2009).



A) Remains of Blakethwaite Smelt Mill



B) Example of a waste rock pile



C) Evidence of hushing



D) Sir Frances Level dressing floor

Figure 3.10: Field photos of Gunnerside Gill showing the former mine structures and waste rock piles (appear as grey material in the photos).

3.7.1 Blakethwaite Mines

In 1710 the eastern tip of the Blakethwaite Vein was being worked on a small scale near Little Prichard Gill, with production ceasing in 1797 by which time the ore was being raised from several deep shafts (Gill, 2001). Later work started on two new levels of Blakethwaite Mine in 1812 and 1814 (Raistrick, 1975). The first vein cut was an extension of the Rigg Vein, named the Red Sun Vein by the miners and in 1818 the Blakethwaite Vein was cut (Gill, 2001). Production was stable between 1820 and 1831; however, it dropped

quickly between 1830 and 1831 due to a fall in ore prices (Gill, 2001). The mine changed hands in 1836 and production increased and was again relatively stable between 1839 and 1847, but archaeological evidence suggests production stopped at Blakethwaite around 1860 (Gill, 2001).

3.7.2 Lownathwaite Mines

North Vein and Sun Vein (part of the Friarfold and Old Rake Veins, respectively) meet at the Lownathwaite mines, where they have been exploited on both sides of Gunnerside Gill (Gill, 2001). The Lownathwaite Mines reached as far east as Gunnerside Gill where the veins passed into the Old Gang Mines (Dunham and Wilson, 1985). The Lownathwaite Mines were the largest group of workings associated with the Friarfold Complex and the mines extended towards Swinnergill Level in the west (Rastrick, 1975). Several hushes are associated with Lownathwaite including North, Sun (or Clifton) and Watersikes hushes (Gill, 2001). The hushes at Lownathwaite Mine are thought to have been worked prior to 1676 (Rastrick and Jennings, 1965), when the majority of the shallow ore would have been extracted by hushing (Dunham and Wilson, 1985). The exact ages of the hushes are still unknown, however late 18th century plans of the area show many shafts where the hushes are located (Gill, 2001). In the 1680s shafts were sunk at the Lownathwaite Mines and the mines were worked through much of the 18th century, with production rising in the latter half of the period (Gill, 2001). New levels were still being driven in the early 19th century including Dolly or Barbara Level and Priscilla Level, followed by Blind Gill Level in the 1840s, which were worked until the 1860s (Gill, 2001). Several of the levels were briefly reopened in the 1870s, but moved to Sir Francis Level around this time (Gill, 2001).

3.7.3 Old Gang Mines

The Friarfold Vein continues east from the Lownathwaite Mines and having crossed Gunnerside Gill becomes the Old Rake Vein through the Old Gang Mines (Rastrick, 1975). The most important veins in the vicinity included the

Friarfold, Merryfield, North Rake, Old Rake and Watersikes Veins (Gill, 2001). A series of hushes, opencast workings and mine tailings/ waste tips show the outcrop of Old Rake Vein at the surface (Dunham and Wilson, 1985).

Gorton, Friarfold, Old Rake and Bunting (or Bunton) Veins also reach the surface at Gunnerside Gill and before the end of the 18th century appear to have been worked by hushing, then levels were later being driven into them early in the 1800s (Gill, 2001). The Old Gang Mines comprised many levels and shafts including Gorton, Barbara, Brandy Bottle, Watersikes, Bunton, and Sir George Levels (Rastrick, 1975). All of the Old Gang Mines were abandoned in 1887 but some were later reopened in 1889 (Gill, 2001). By 1890 ore was being raised from Rigg String, Rigg Vein, Bunting Sun Vein and Watersikes Vein, however production fell in the 1890s and Bunton Level was abandoned in 1898 (Gill, 2001). The last working at Old Gang Mine was a branch of Alderson's vein, thought to be around 1900 (Dunham and Wilson, 1985).

3.7.4 Sir Francis Level

Sir Francis Level was designed to explore the strata below the Friarfold Vein complex to allow lateral exploration and dewater an extensive area (Rastrick, 1975). Work commenced in 1864, the Friarfold Vein was reached in 1877 and by the end of 1878 480 tonnes of ore had been raised (Gill, 2001). Work stopped on the Old Rake and Friarfold Veins towards the end of the 19th century when attention turned to the North Vein and Priscilla Level (Gill, 2001). In 1887 Sir Francis Level was extended to the Watersikes Vein and then the Blind Gill Vein in 1889 (Gill, 2001). During its operation large amounts of ore were obtained from the veins served by Sir Francis Level and as a result two crushing mills and dressing floors were constructed there (Rastrick, 1975). Mining ceased in Gunnerside Gill in 1906 when the last miners left Priscilla Level (Gill, 2001).

3.8 Previous studies describing mining-related metallic element contamination of Gunnerside Gill

Hushing and mineral processing in Gunnerside Gill released large volumes of metallic element-rich sediment directly into the catchment. In addition, it is likely that the presence of spoil heaps and mine waste piles adjacent to the water's edge may be influencing the water quality today. In 1941 it was estimated that at least 100,000 tonnes of mine waste had been dumped along the course of Old Rake Vein alone (Dunham and Wilson, 1985). In addition, rough dressing of the ore often resulted in losses of Pb into the catchment (Dunham and Wilson, 1985).

Table 3.3: Previous studies of Pb, Zn and Cd concentrations in floodplain sediments of the Upper Swale and Gunnerside Gill

| Description | Pb (mg/kg) | Zn (mg/kg) | Cd (mg/kg) | Reference |
|---|---------------|------------|------------|---------------------|
| Overbank sediments from the Upper Swale at the surface | ~10-30,000 | ~50-8,000 | - | Macklin et al. 1994 |
| Channel edge sediment resulting from input of Gunnerside Gill sediments within the River Swale after the 2000 floods (silt- and clay-sized fraction). | 8,000 | 4,500 | 32 | Dennis et al. 2003 |
| Overbank flood sediment resulting from input of Gunnerside Gill sediments within the River Swale after the 2000 floods (silt- and clay-sized fraction). | 7,500 | 14,000 | 53 | Dennis et al. 2003 |
| Floodplain sediments within Gunnerside Gill (clay- and silt-sized fraction) | 11,000-14,500 | - | - | Dennis et al. 2009 |
| Floodplain sediments within Gunnerside Gill (sand-sized fraction) | 21,500-22,400 | - | - | Dennis et al. 2009 |
| Overbank sediments in the Upper Swale, Dec 1997 to Dec 1999 (mean values of clay- and silt-sized fractions) | 361-1602 | 884-1070 | - | Walling et al. 2003 |

As a result of the historical mining various studies have been undertaken within the Upper Swale and Gunnerside Gill itself, as shown in Table 3.3, which compiles ranges and maximum concentrations of Pb, Zn and Cd within various sedimentary units including the channel edge and overbank sediments. The values within Table 3.3 indicate that the sediments within Gunnerside Gill are contaminated when compared to the acceptable soil guideline values as described in Section 2.1.5. In the UK the thresholds for proposed residential end use are 200 mg/kg for Pb, 3,700 mg/kg for Zn and 11 mg/kg for Cd (Nathanail et al., 2015), although these are not directly applicable for risks to controlled waters.

In 2010 a single water sample recovered from the confluence of Gunnerside Gill with the River Swale indicated elevated concentrations of Pb (22 µg/L), Cd (1.7 µg/L) and Zn (199 µg/L) (EA, 2013). The EA calculated the Environmental Quality Standards (EQS) (annual averages) for Gunnerside Gill based on a hardness of 70 mg/L sampled in February 2010 as; 7.2 µg/L for Pb, 0.09 µg/L Cd and 50 µg/L for Zn (EA, 2013). More recently the EQS have been updated and are now based on bioavailability rather than hardness (WFD-UKTAG, 2014), for Gunnerside Gill this means the EQS values have reduced to 28 µg/L for Zn and 6.1 µg/L for Pb. Additional water monitoring was completed by Hull University in 2010 and the EA in 2011, which confirmed the earlier result. Following up on this, Gunnerside Gill was subject to an EA study published in October 2013 (included as Appendix A) (EA, 2013). The aim of the 2013 study was to investigate the effects of the historical mining on water quality and aqueous ecology within the Gunnerside Gill catchment. In March 2012 water quality and simultaneous flow sampling by the EA began at six locations, as shown in Figure 3.9.

Initially six locations were monitored by the EA, including GG1 (to the north of the main mining areas) GG2 (adit at Bunton Level), GG3 (river monitoring point), GG4 (Sir Francis Level mine water discharge), GG5 (river monitoring point) and GG6 (downstream river monitoring point at the village of Gunnerside). An additional monitoring point (GG7) was added in December

2012 along with two control monitoring points located in West Stonesdale Beck. Ecological monitoring was also undertaken at GG3 and GG6. In total 95 water samples were analysed (including control samples from West Stonesdale Beck) from the 13 monitoring rounds. The results show that 92 % of the Pb and Zn and 100 % of the Cd concentrations exceeded the original respective EQS. The main sources of Zn and Cd were found to be from monitoring point GG4 at Sir Francis Level under all flow conditions. Lead concentrations were found to be mainly from three diffuse sources; namely contaminated in-river sediments, wastes from Bunton Mine and wastes from Sir Francis Level (EA, 2013). The flux of Cd, Pb and Zn from the monitoring points is shown in Figure 3.11.

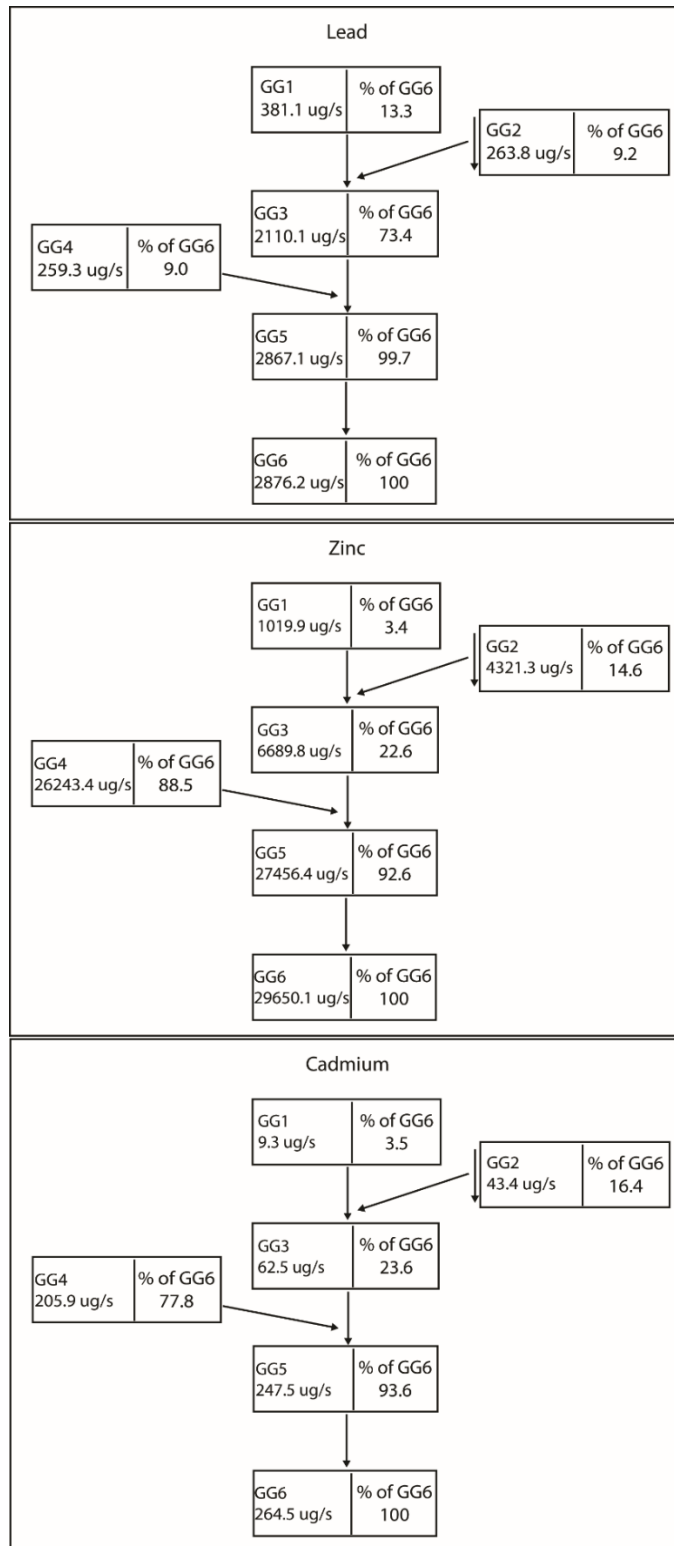


Figure 3.11: Block flux diagram with the different contributions (cumulative %) of Pb, Zn and Cd in the waters of Gunnerside Gill (from EA, 2013).

3.9 Summary

The River Swale is located in Yorkshire with the headwaters flowing through the Askrigg block of North Pennine Orefield. The underlying geology comprises Carboniferous (including limestone, sandstone and shale) strata in the west, becoming progressively younger moving east through the Permian and Triassic strata (House and Warwick, 1998a; 1998b). The key ore minerals within the orefield were galena and sphalerite.

Within the Askrigg Block, fluorite is considered to be an indicator of the mineralised zonal centres, surrounded by and/or interbedded with barium minerals, barite and witherite are the main gangue minerals (BGS, 1996). The mineralisation had previously been attributed to the intrusion of granite at depth, however more recent research indicates the Carboniferous Whin Sill is more likely to be the source of the hydrothermal fluids resulting in the ore minerals present (Cann and Banks, 2001; Bevins et al., 2010; Dempsey, 2016).

Mining for Pb is thought to have commenced in Swaledale during Roman times, since then large quantities of mining waste have been released into the River Swale catchment. Although mining finished during the early 20th century, metallic element-rich sediments are still present and due to remobilisation, still contribute to floodplain contamination in the present day (Dennis et al., 2003; Walling et al., 2003; Hudson-Edwards et al., 2008). Various studies have been undertaken of the River Swale to gain a better understanding of the contamination present within the catchment including Macklin et al. (1994), Dennis et al. (2003), Walling et al. (2003), Brewer et al. (2005), Macklin et al. (2006) and Dennis et al. (2009). It has been estimated that around 30,000 tonnes of Pb is stored within the upper catchment of the River Swale (Dennis et al., 2009). A DEFRA study in 2003 estimated that over 90 % of topsoil and sub-surface samples exceeded calculated background concentrations of Pb, Zn and Cu within the River Swale catchment (Brewer et al., 2005).

Gunnarside Gill is a tributary of the River Swale and was subjected to widespread Pb and Zn contamination from four main mining areas between 1700 and 1900. Inefficient mining and ore dressing techniques resulted in

extensive contamination of the channel and floodplains of Gunnerside Gill with Pb, Zn and Cd. As a result of ongoing natural erosion and deposition within the catchment it is likely that the impacted sediments and remaining mine wastes are frequently being reworked by rain and river water, and are consequently resulting in elevated concentrations of Pb, Zn and Cd within the waters of Gunnerside Gill (Dennis et al., 2003; Walling et al., 2003; Dennis et al., 2009; EA, 2013). Further work is required to identify the mechanisms responsible for transfer of Pb, Zn and Cd from the mine wastes and sediments to the catchment waters. This project aims to work towards identifying the processes controlling the movement of Pb, Zn and Cd within Gunnerside Gill.

Chapter 4

Materials and Methods

Contents

| | |
|--|-----|
| Chapter 4..... | 109 |
| 4.1 Sample Collection..... | 109 |
| 4.2 Solid Analysis..... | 113 |
| 4.2.1 X-Ray Diffraction | 113 |
| 4.2.2 Acid Digestion | 113 |
| 4.2.3 Sequential Extractions..... | 115 |
| 4.2.4 Electron Microprobe Analysis | 117 |
| 4.2.5 Carbon Determination | 117 |
| 4.2.6 Particle Size Analysis | 117 |
| 4.2.7 Solid pH analysis..... | 118 |
| 4.3 Column Leaching Experiments..... | 118 |
| 4.3.1 Column Leachate Analysis..... | 122 |
| 4.4 Statistical Analysis | 123 |
| 4.5 Computer Modelling | 124 |
| 4.6 Precision and Accuracy | 124 |
| 4.7 Summary | 129 |

Chapter 4 will describe the collection of the samples (Section 4.1), the characterisation of the solid samples (Section 4.2); the design of the experimental columns and leaching experiments (Section 4.3), and the analysis of the resulting leachate and post-leaching solids (Section 4.3.1). Section 4.4 describes the statistical analysis used and the computer modelling software is detailed in Section 4.5. The precision and accuracy of the techniques are reported in Section 4.6 and Section 4.7 summarises the chapter.

4.1 Sample Collection

Bulk samples of the mine wastes and sediments were collected on 7th June 2012. Ten samples were recovered from the length of Gunnerside Gill, as shown in Figure 4.1 and 4.2, and duplicate samples were recovered from locations 1, 2, 3 and 9 for use in the column leaching experiment. The

duplicate samples represent the mine wastes and alluvial sediments within Gunnerside Gill.

The samples were collected based on accessibility and type of sample; including wastes from waste piles and dressing floors, and sediments from downstream of the mining areas.

In addition, samples from similar locations but differing colours were also collected to see if there was any discernible difference in metallic element concentrations based on the colour of the material. For example, Gun 5 and Gun 6 were from two different layers at the same location, and Gun 7 and Gun 8 were from a dressing floor but varied in colour. Table 4.1 gives a short description of the samples collected, Figure 4.1 show photographs of the sampling sites and Figure 4.2 shows the locations of the samples collected. The pH was measured in the field using universal pH indicator paper to give a general indication of the pH values of the water at the sampling site (see Table 4.1), all samples were recorded as circum-neutral.

Table 4.1: Sample descriptions

| Sample | Sample Description |
|---------------|---|
| Gun 1 | Dark fine grained mine waste material. Iron weathering noted on underlying shale. Water pH 5-6 |
| Gun 2 | Dark grey mine wastes |
| Gun 3 | Dark grey mine wastes. Sir Frances Level dressing floor. Water pH around 6. Floodplain material observed below the waste pile |
| Gun 4 | Grey / brown mine wastes. Fresh overbank sediments. In line with Sir Frances Level adit, possible 'Driving waste' |
| Gun 5 | Lighter grey mine wastes – possible burning/ smelted layer (above Gun 6) |
| Gun 6 | Brown in situ sand – possible pre-mining sediment layer |
| Gun 7 | Grey mine wastes |
| Gun 8 | Brown / orange gravelly mine wastes |
| Gun 9 | Grey floodplain/ alluvial sediments |
| Gun 10 | Grey / brown floodplain /alluvial sediments, near to junction with the River Swale. |

To take into account any heterogeneity of the sediments, samples of 1-2 kg were collected from three locations within the top 10 cm of the surface and homogenised. Samples were collected using a stainless steel trowel, then placed in air tight bags and labelled. Once returned to the laboratory the

samples were oven dried at 25°C and sieved to 2 mm, with gravels greater than 2 mm removed from the samples.



a) Gun 1



b) Gun 2



c) Gun 3



d) Gun 4



e) Gun 5 (grey) and Gun 6 (brown)



f) Gun 7 (grey) and Gun 8 (brown)



g) Gun 9



h) Gun 10

Figure 4.1: Sample location photographs

It was decided that it was best to specifically study a limited number of samples in detail to try and understand the underlying processes responsible for metallic element mobility. The samples comprised a mixture of mine wastes and alluvial sediments, as denoted in Table 4.1, so as to represent the main metallic element-bearing materials within Gunnerside Gill. Additional water monitoring data was provided by the EA collected after their 2011 study in order to gain an insight into the processes occurring with respect to the solid and aqueous phases within the system (EA, 2013). The EA locations are also shown on Figure 4.2 for reference.

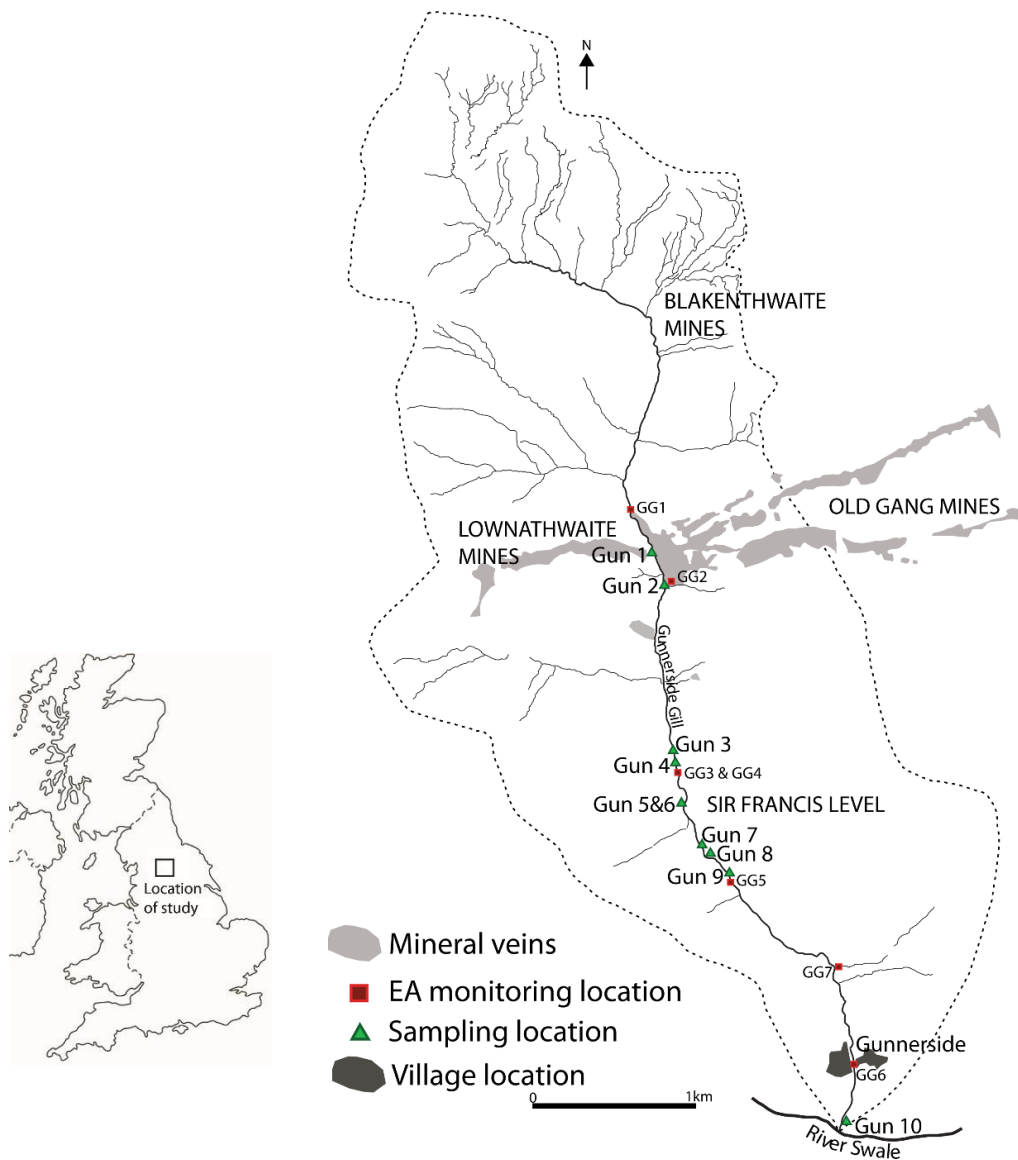


Figure 4.2: Gunnerside Gill sample location map (adapted from Dennis, 2005)

4.2 Solid Analysis

Solid analysis, including X-ray diffraction, acid digestion, and sequential extraction, were undertaken on the initial ten collected samples (Gun 1 to Gun 10) and four post-column experiment samples (CGun 1, CGun 2, CGun 3 and CGun 9; see below for description of experiments), so the samples could be compared they were analysed using the same techniques.

4.2.1 X-Ray Diffraction

Powder X-ray diffraction (XRD) analysis of the initial ten samples was undertaken at the University of Brighton using a PANalytical X'Pert PRO diffractometer using Cu-K α radiation, to investigate Objectives 1 (characterisation of the solid-phase speciation of the metallic elements present in mine waste and sediments) and 2 (determining the major factors influencing the transfer of metallic elements from solids into the waters). The oven-dried samples were first powdered using an agate pestle and mortar, then loaded into mounts being careful to make sure the surface of the samples was flat and smooth. The accelerating voltage used was 40 kV, with an operating current of 30 mA. The data was collected over a range of 2 to 70 degrees of 2θ , with a step size of 0.5 degrees 2θ . The collection time was approximately 75 minutes per sample. The data were analysed using Phillips PC-ACD software version 1.6 and MATCH (Crystal Impact, 2019), the limit of detection is approximately 1 % for each mineral phase.

4.2.2 Acid Digestion

The pre- and post-column experiment leaching solid samples were both subjected to acid digestion by hydrofluoric acid (HF), nitric acid (HNO₃), perchloric acid (HClO₄) and hydrogen peroxide (H₂O₂). The acid digestions were undertaken to study Objective 1. Approximately 0.07 g (to within 0.008 g tolerance) of material was sub-sampled from each of the main samples. Initially the samples were soaked over the weekend in 4 ml of HF (48 % w/v) and 2 ml of HNO₃ on a hotplate at 130°C. Then the acids were evaporated off and 1 ml of HF, 2 ml of HClO₄ (70 % w/v) and 1 ml of HNO₃ were added and

heated overnight at 200°C. Following evaporation, a further 1 ml of HClO₄ and 2 ml of HNO₃ were added and the solution was again heated overnight at 200°C. This was again evaporated off before 1 ml of HNO₃ and 3 ml of H₂O₂ (30 % w/v) were added and left overnight unheated. Finally the acid mixture was evaporated off, 1 ml of HNO₃ was added and evaporated off twice and the samples were diluted in 50 ml flasks with high-purity water (18 MΩ Milli-Q; Millipore). The resulting digestion data was then calculated back to give the actual metallic element concentration of the sample. The volume of the dilution (50 ml) was divided by the weight of the sample (0.07g) which was multiplied by the measured concentration (in ppm). The digestions were undertaken at the Wolfson Laboratory at the University College London – Birkbeck Institute of Earth and Planetary Sciences.

The samples were run in three batches and each batch included at least 10 % duplicate samples, a blank sample and a certified reference material (CRM) (in this case China National Analysis for Iron and Steel NCS DC73322 (GMW07404)).

A fine white solid remained in around 80 % of the samples, which could either have been as a result of incomplete digestion or precipitation once the digestion had been completed. An attempt was made to filter the solid out using vacuum filtration and filter papers. The filter papers (Whatman 42 and 41) were initially placed in the drying cabinet to eliminate any moisture present. The filter paper was weighed, the filtration undertaken and then the filter paper with remaining solids were placed back in the drying cabinet for one week and reweighed. In around 10 % of samples the filter paper weighed less once the filtration was complete. This is assumed to be as a result of incomplete drying prior to the initial weighing. The white solid was identified by scanning electron microscopy using a Jeol JSM-6480LV to be barite (BaSO₄). Given that barite was found to remain in the majority of the samples and at very low concentrations (<0.001 g) it was excluded from the results.

4.2.3 Sequential Extractions

The Commission of the European Communities Bureau of Reference (BCR) regime was selected to carry out the sequential extractions of the samples following the method described by Rauret et al. (1999). For this study the sequential extraction was undertaken in relation to Objectives 1 and 2. An end-over-end shaker was not available at the time of the experiment and was substituted by a roller mixer. In recent years the use of the modified BCR procedure has become more widely accepted (Anju and Banerjee, 2010), alongside Tessier et al. (1979), as an investigative technique for contaminated soils and sediments.

The BCR sequential extraction and modified procedure have been used by researchers investigating the fractionation of metallic elements from worldwide mine sites, for example Sardinia (Fernández-Ondoño et al., 2017), Spain (Pueyo et al., 2008; Rodriguez et al., 2009), Kosovo (Kerolli-Mustafa et al., 2015), India (Anju and Banerjee, 2010), Belgium (Cappuyns et al., 2007), Portugal (Alves et al., 2018), Scotland (Pulford et al., 2009), France (Resongles et al., 2014) and Bolivia (Kossoff et al., 2011).

In addition to the BCR method described by Rauret et al. (1999), an initial water leaching step was completed prior to the commencement of the sequential analysis. Approximately 1 g (to within 0.007 g tolerance) of sample (<2 mm fraction) was weighed into 50 ml centrifuge tube and 40 ml of 18 Mohm high-purity water was added. The tubes were then placed on the roller mixer overnight (approximately 16 hours) and were subsequently centrifuged at 3800 revolutions per minute (rpm) for 20 minutes. The supernatant was pipetted off and the sample washed with high purity water between each step. The following steps were then undertaken on each of the samples.

- Step 1: 40 ml of acetic acid was added to the remaining solids following completion of the water step and placed on the roller mixer overnight. The mixture was centrifuged at 3800 rpm for 20 minutes to separate the solid from the leachate.

- Step 2: 40 ml of hydroxylammonium chloride, adjusted with nitric acid to the pH 2, was added to the solid from step 1 and the extraction repeated as above.
- Step 3: The solid from step 2 was treated twice with 8.8 mol l⁻¹ hydrogen peroxide, evaporated to near dryness using a water bath. Then 50 ml of ammonium acetate, adjusted to pH 2 with nitric acid, was added and the extraction undertaken as above (Mossop and Davidson, 2003).

Table 4.2 indicates the phases operationally targeted by each of the steps of the sequential extraction. Once the three steps of the BCR procedure had been completed, the remaining residue was dried and subjected to the acid digestion as described in Section 4.2.2.

The BCR extracts were analysed by ICP-OES and were subject to similar procedures as detailed in Section 4.3.1. A procedural Certified Reference Material (CRM), the ‘European Commission: community bureau of reference materials BCR Reference Material No. 701 (Lake Sediment (Extractable trace elements))’, and blanks were included in all the steps undertaken including the water and residual phase. The ICP-OES standards for each step were matrix matched, except those for the ammonium acetate standard for step 3, to which hydrogen peroxide was not added. The sequential extractions were undertaken at the Wolfson Laboratory at the University College London – Birkbeck Institute of Earth and Planetary Sciences.

Table 4.2: Sequential extraction target phases (adapted from Davidson et al., 1998; Mossop and Davidson, 2003)

| Step | Fraction | Target Phases |
|-----------------|----------------------------|---------------------------|
| Water | Water soluble | Soluble species |
| 1 | Exchangeable, acid soluble | Carbonates, CEC sites |
| 2 | Reducible | Fe and Mn oxyhydroxides |
| 3 | Oxidisable | Organic matter, sulfides |
| Residual | Residual | Non-silicate bound metals |

4.2.4 Electron Microprobe Analysis

Polished resin blocks of the samples were made of each sample and these were sputter coated with a thin (<20 nm) conductive film of carbon. Point element spectral analysis and element X-ray mapping were carried out using a Jeol 8100 Superprobe (electron microprobe (EMP)) and Oxford Instrument Inca system by energy-dispersive spectroscopy (EDS). The elements mapped included O, Na, K, Zn, Pb, Al, Cd, Fe, Mn, S, P, Cu and Ba, but some of the maps excluded some of the elements due to time constraints. The EMP was calibrated using compositionally known standards of silicate minerals, oxides, sulfides and pure metals on a weekly and monthly basis. The EMP analysis was used to address both Objective 1 and Objective 2. The EMP was located in the Geology Department at University College London.

4.2.5 Carbon Determination

Total carbon (TC) concentrations of the solid samples were determined using a Laboratory Equipment Corporation (LECO) C9S 200-analyser, using FeO as an accelerant. Blanks were run at the beginning and end of the analysis. Tracking standards were run every five samples to monitor experimental calibration drift and the results were subject to drift correction. The analyses were undertaken at the Wolfson Laboratory at the University College London / Birkbeck Institute of Earth and Planetary Sciences and were used to investigate Objective 1.

4.2.6 Particle Size Analysis

Particle size analysis was completed using a Malvern Mastersizer laser particle-sizer at the department of Geography at University College London, to help assess Objective 1. A small volume of sample (less than a gram) was added to the water bath attached to the Mastersizer. The size of the particles, from 0.2 to 2000 μm , was then measured using laser diffraction. The Mastersizer automatically carries out three runs of the sample and generates a graph to compare the runs showing the grain sizes. If these are

significantly different due to the heterogeneity of the sample, then the analysis is rerun. Between each run the Mastersizer was thoroughly rinsed using tap water.

4.2.7 Solid pH analysis

The pH of the mine wastes and sediments was determined using a calibrated Hach sensION1® fitted with a Hach 51935-00® gel filled electrode. Approximately 1.0 g (± 0.03 g) was weighed out and 10 ml of 18 Mohm high-purity water was added. The samples were placed on a stirring plate for a minimum of 10 minutes and three pH readings were taken, to allow an average to be calculated.

4.3 Column Leaching Experiments

As discussed in section 2.6, column leaching studies are used widely to evaluate mineral weathering processes in the laboratory and to look at the effect of rainfall, infiltration, leaching and chemical reactions involving mine wastes (e.g., Kossoff et al., 2011). A column leaching experiment in the case of this study was considered appropriate in order to assess the mobility of metallic elements in both mine wastes (Gun 1 to Gun 3) and overbank sediments (Gun 9) in a controlled environment. These samples were chosen based on their location, visual assessment and to represent different parts of the sediment cycle within Gunnerside Gill. The samples were placed in the columns in an 'as recovered' state, not sieved to < 2 mm and air dried, to mimic the natural setting as closely as possible. The use of mine wastes and sediments was selected to determine which could have a greater potential to impact the aquatic environment and to investigate Objective 3 (using column leaching experiments, aqueous field data and geochemical modelling to determine the influence of changes in the environmental setting). The column leaching experiment was undertaken at Birkbeck College, University of London.

A wooden frame was constructed and lengths of clear plastic pipe (80 cm long and 5.5 cm diameter) were attached as shown in Figure 4.3. When considering other column studies (Section 2.6) no standard length or diameter of columns is has been prescribed previously; the columns were

designed so that they could accommodate the solids and additional water and to try and reduce the effect of preferential pathways whilst not requiring an excessive quantity of sample. The use of clear plastic was so that visual changes, if any, could be observed during the experiment. The plastic components were all soaked in 50 % v/v HNO₃ at pH 2 for 48 hours, to make sure the components were not contaminated before the commencement of the experiments.

To model the field conditions as accurately as possible, the samples were not sieved before being placed in the columns. First, a nylon mesh of 200 µm was placed at the base of each column to reduce any loss of solid sample into the leachate collection vessel below. Then 200 g of acid washed quartz sand was added at the base to allow for free drainage. Approximately 1400 g of each sample was packed uniformly in layers of 1 to 2 cm and compacted using a plastic disk on a stick with gentle pressure 20 times. The column set up is shown in Figure 4.3. A top cap with ventilation holes was present at the top of the columns to allow for evaporation and to stop any outside material falling into the columns. As the columns were constructed from clear plastic to allow for any visual changes to be observed, the columns were covered with black-out fabric to mimic the natural environment where most of the sediments and mine wastes would be below the surface.



Figure 4.3: Experimental column set up

Although other column leaching studies (e.g. Kossoff et al., 2011) created artificial ‘rainwater’ by adjusting the pH and chemistry of the water, it was considered in this case that high-purity water (18 M Ω Milli-Q; Millipore) would be sufficient to imitate UK rainwater. The use high purity water reduces the number of variables within the experimental design and means the experiment can be more easily reproduced. Due to access issues within the laboratory set up the source of high purity water changed partway through the 40 weeks of the column leaching experiment as detailed in the results in Section 5.4.2.

The volume of water to be added to the columns was calculated by first ascertaining the amount of rainfall per year within the catchment of Gunnerside Gill. This was found from the rainfall map from the Centre for Hydrology and Ecology website (Nrfa.ceh.ac.uk, 2015), approximately 1200 to 1400 mm per year, averaged to 1300 mm. Then by calculating the cross-sectional area of the column (internal diameter 5.2 cm) (πr^2 : $\pi \times 2.6^2$) 21.3

cm² multiplied by the amount of rainfall (130 cm) the yearly total is 2760.8 cm³.

Table 4.3: Volume of water added to columns to represent the seasons

| Season | Spring (Mar/April/May) | Summer (June/July/Aug) | Autumn (Sept/Oct/Nov) | Winter (Dec/Jan/Feb) |
|---|---------------------------|---------------------------|--------------------------|-------------------------|
| % of yearly rainfall | 21 | 23 | 29 | 27 |
| Seasonal column volume (cm ³) | 580 | 635 | 801 | 745 |

Starting from the spring season the water was added once a week in a single addition, working through each season in turn to mimic a year for modelling purposes. The resulting leachate was collected in a beaker beneath the columns. Water was added for a total of 40 weeks, which is equivalent to 10 years of modelling.

There is some variability in the recorded volume of leachate recovered which can be accounted for by evaporation as the overall volume recovered was recorded over the two days following the addition of the water. However, if the transit time was too slow (greater than 2 days) the remaining leachate volume would be recorded prior to the next addition a week later. This most often happened in Gun 3 and Gun 9, where a minor loss in the volume of leachate was recorded. A rudimentary experiment was run to determine the approximate rate of evaporation in the laboratory in three different weeks using a known volume of water left uncovered over one day or one week. The evaporation rates were calculated as 0.23 ml/hr, 0.23 ml/hr and 0.22 ml/hr.

During the winter of 2013/2014 and winter of 2015/2016 there was an unprecedented volume of rainfall that resulted in widespread flooding across the UK, with the area around Gunnerside Gill receiving around 150 to 175 % and 175 to 200 % of the normal annual rainfall, respectively (Met Office 2017). Additional flooding was also documented in Yorkshire in November

2019, with 160 % of the normal rainfall recorded when compared to the annual average (Met Office 2019). These are considered to be extraordinary events and therefore they have been excluded from the dataset used in the subsequent column leaching experiment. The annual averages are calculated from data collected between 1981 and 2010.

4.3.1 Column Leachate Analysis

The leachate volume, pH (Hach sensION1® meter fitted with a Hach 51935-00® gel filled electrode) and E_H (Hanna ORP meter) were recorded for the leachate and the water prior to it being added to the columns. The pH meter was calibrated with pH 4 and pH 7 standard buffer solutions on a weekly basis. The experiment-dedicated probe was stored in a pH buffering solution of pH 4 between sessions. Three repeat measurements were taken and an average of the measurements was recorded. A field ORP meter was used to measure the E_H of the leachate. The E_H was measured after the samples were filtered and collected (as described below). The probe was placed into the remaining leachate, reducing the potential for contamination of the samples. The probe was washed twice in high-purity water prior to use and between measuring each of the samples. It should be noted that the system was open to the atmosphere and as such the E_H measurements will reflect this.

The leachate collected from the columns was subsequently filtered to 0.2 μm (disposable PTFE syringe filter) and 10 ml and 30 ml sub samples were collected for anion and cation analysis, respectively. The cations were stabilised by the addition of 100 μg of 69 % v/v HNO_3 , and then stored in acid-washed bottles and were refrigerated until analysis.

Anions (Cl^- , F^- , NO_3^- and SO_4^{2-}) were analysed by ion chromatography (IC, Dionex ICS-2500). A blank and standard were run approximately every ten samples during each analytical run. In some cases the nitrate concentrations were quite variable, this was considered to be as a result of potential cross contamination (use of nitric acid to wash vessels) and possibly due to interference from organic matter. Tracking standards were run every five

samples to monitor experimental calibration drift, and the results were subject to drift correction. The analysis was undertaken at the Wolfson Laboratory at the University College London – Birkbeck Institute of Earth and Planetary Sciences.

All other elements, Al, Ba, Ca, Cd, Cu, Fe, Mg, Mn, Pb, S, Zn, K and Na, were analysed by ICP-OES (Varian VISTA PRO®) at University College London / Birkbeck Institute of Earth and Planetary Sciences. Potassium and Na were run separately after the other elements as it was decided later these would be required for later analysis including computer modelling. After each measurement the ICP-OES carried out a rinse by flushing through the spray chamber with high-purity water acidified with around 1 % nitric acid (69 % w/v). A minimum of two spectral lines were used for each element and a single line was chosen for each element for data analysis. Blanks were run at the start, finish and at regular intervals during each analysis. Tracking standards were run every eight to ten samples to monitor experimental calibration drift and all of the results were subject to drift correction calculations. The accuracy of the ICP ion determination was assessed by the analysis of CRMs, specifically TMDA-64 and Battle (National Water Research Institute, Environment Canada) periodically during each analytical run. Precision was quantified by using approximately 10 % duplicate samples. The limits of detection (LOD) and limits of quantification (LOQ) were calculated using the following equations, where σ is standard deviation:

$$LOD = \frac{\text{Conc. of standard} - \text{Conc. of blank}}{\text{Int. of standard} - \text{Int. of blank}} \times 3\sigma \text{ on blank}$$

$$LOQ = \frac{\text{Conc. of standard} - \text{Conc. of blank}}{\text{Int. of standard} - \text{Int. of blank}} \times 10\sigma \text{ on blank}$$

4.4 Statistical Analysis

Statistical analysis was used to confirm whether the methods were suitable to produce repeatable and consistent results (Hibbert 2017). The data was subjected to basic statistical analysis including Pearson correlation,

regression analysis using R^2 and standard error calculations. The statistical analysis was used in relation to all three objectives.

4.5 Computer Modelling

Computer modelling programme, PHREEQC (Parkhurst and Appelo, 2013), based on ion-association aqueous modelling, including speciation, reaction-path, advective transport, and inverse geochemical calculations (Parkhurst, 1995). PHREEQC was used to address Objective 3 and determine the saturation indices over a range of different pH values. By using the chemical analysis of the total concentration of elements in solution PHREEQC undertakes calculations to distribute these elements among aqueous species, which are then used for determining the saturation indices relative to water (Parkhurst and Appelo, 2013).

The data was input using the dissolved concentrations of the elements from both the column leaching experiment and the EA monitoring data from Gunnerside Gill. The inbuilt mineral database was used for this study.

4.6 Precision and Accuracy

This section details the precision and accuracy of the ICP results for the BCR sequential extraction procedure, the column leachate and total digestion analyses.

Table 4.4: Average precision values for BCR sequential extraction results ($\pm\%$)

| BCR | Al | Ba | Ca | Cd | Cu | Fe | Mg | Mn | Pb | S | Zn |
|----------|------|------|------|-------|------|-----|------|------|------|------|------|
| Water | 30.0 | 14.0 | 17.7 | 18.0 | - | 1.0 | 21.8 | 30.4 | 11.2 | 34.8 | 6.0 |
| Step 1 | 4.8 | 9.7 | 8.4 | 6.0* | 8.9* | 6.8 | 8.0 | 7.3 | 2.9 | 26.6 | 12.7 |
| Step 2 | 3.8 | 1.8 | 2.6 | 8.8 | 8.8 | 1.5 | 4.7 | 7.7 | 4.1 | 3.3 | 4.1 |
| Step 3 | 6.7 | 4.8 | 3.4 | 14.0* | 17.8 | 9.5 | 7.0 | 4.8 | 6.6 | 8.1 | 20.4 |
| Residual | 1.2 | 3.4 | 2.8 | 18.0 | 39.1 | 5.0 | 1.1 | 3.2 | 1.6 | 3.0 | 26.0 |

* Concentrations above LoD but below LoQ

The precision values given in Table 4.4 are average precisions based on up to four duplicate pairs of samples. The precision is dependent on the concentrations of the elements present. For example Al, Cd and Cu are often present in relatively low concentrations, so small variations result in significant changes in the perceived precision. In addition, there is the

potential for limitations in duplicate sampling due to the heterogeneity of the samples themselves, given they are naturally occurring materials that can result in inaccuracies of the data (McKillup and Dyar, 2010).

The precision values given in the table above are average precisions based on a duplicate pair of samples of the BCR CRM 701 run alongside the rest of the samples.

Table 4.5: Average accuracy values for BCR CRM 701 (%)

| BCR | Al | Ba | Ca | Cd | Cu | Fe | Mg | Mn | Pb | S | Zn |
|-----------------|------|------|------|------|------|------|------|------|------|------|-------|
| Water | 103 | 101* | 101 | - | 97.3 | 95.3 | 101 | 100 | - | 97.7 | 64.1* |
| Step 1 | 95.2 | 94.9 | 97.6 | 95.2 | 88.9 | 93.5 | 97.3 | 96.5 | - | 91.8 | 97.2 |
| Step 2 | 95.6 | 94.5 | 98 | 88.8 | 96.6 | 94.7 | 94.1 | 94.1 | 94.9 | 93.0 | 103.4 |
| Step 3 | 98.9 | 98.3 | 88.8 | 80.4 | 99.9 | 97.5 | 98.5 | 99.2 | - | 96.3 | 97.2 |
| Residual | 99.6 | 94.3 | 117 | 103 | 94.6 | 97.8 | 96.5 | 106 | - | 104 | 97.8 |

* Concentrations above LoD but below LoQ

The precision values given in the table above are average precisions based on a duplicate pair of samples of the BCR CRM 701 run alongside the rest of the samples.

The BCR CRM did not perform as expected and did not record the published concentrations of Cd, Cr, Cu, Pb and Zn in any of the BCR steps. The standards were matrix matched to each step so the water based CRMs Battle and TMDA-64 were not run as part of the analysis, with the exception of the water step.

Table 4.6: Average accuracy values for the BCR sequential extraction for the water step (CRMs – TMDA-64 and Battle) (%)

| Water Step | Al | Ba | Ca | Cd | Cu | Fe | Mg | Mn | Pb | S | Zn |
|---------------|-------|------|------|------|------|------|----|------|------|---|------|
| TMDA | 100.8 | 98.7 | - | 99.1 | 99.4 | 99.9 | - | 98.9 | 93.6 | - | 98.7 |
| Battle | - | - | 99.7 | - | - | - | - | - | - | - | - |

Table 4.6 shows the accuracy of the water step of the BCR based on Battle and TMDA-64. The results show reasonable accuracy based on the results obtained during the water step analysis. With the exception of Pb, all the other elements were accurate to within 2 % of the respective CRM. Pb

concentrations showed a slightly higher variation across the samples and therefore a lower accuracy of 93.6 %.

As it was not possible to determine the accuracy of the BCR using the method CRM the duplicate pairs of the CRM were interrogated slightly differently. The absolute difference was calculated between the pairs and then determined as a percentage of the average concentration, as shown in Table 4.7. The results indicate that the duplicate pairs showed an accuracy of between 0.1 % and 8.4 %.

Table 4.7: Absolute differences between the BCR CRM pairs as a percentage of the average (%)

| | Cd | Cu | Pb | Zn |
|---------------|-----------|-----------|-----------|-----------|
| 2014 | | | | |
| Step 1 | 8.4 | 7.3 | - | 5.5 |
| Step 2 | 6.1 | 1.9 | 5.8 | 0.6 |
| Step 3 | - | 0.5 | - | 3.8 |
| 2015 | | | | |
| Step 1 | 4.9 | 0.7 | - | 0.1 |
| Step 2 | 4.2 | 1.8 | 0.1 | 4.0 |
| Step 3 | - | 0.2 | - | 2.8 |

- Concentrations below LoQ not presented

Table 4.8: Limit of detection and limit of quantification for the BCR sequential extraction procedure (ppm)

| BCR | Al | Ba | Ca | Cd | Cu | Fe | Mg | Mn | Pb | S | Zn |
|-------------------|-----------|-----------|-----------|-----------|-----------|-----------|-----------|-----------|-----------|----------|-----------|
| Water step | | | | | | | | | | | |
| LOD | 0.03 | 0.01 | 0.1 | 0.01 | 0.01 | 0.01 | 0.001 | 0.002 | 0.1 | 0.2 | 0.02 |
| LOQ | 0.1 | 0.03 | 0.3 | 0.03 | 0.02 | 0.02 | 0.003 | 0.01 | 0.3 | 0.5 | 0.1 |
| Step 1 | | | | | | | | | | | |
| LOD | 0.2 | 0.01 | 1.8 | 0.02 | 0.1 | 0.02 | 0.1 | 0.003 | 0.1 | 1.7 | 0.1 |
| LOQ | 0.7 | 0.02 | 5.9 | 0.1 | 0.3 | 0.1 | 0.2 | 0.01 | 0.3 | 5.7 | 0.4 |
| Step 2 | | | | | | | | | | | |
| LOD | 0.01 | 0.003 | 0.8 | 0.01 | 0.02 | 0.1 | 0.01 | 0.002 | 0.03 | 0.1 | 0.03 |
| LOQ | 0.04 | 0.01 | 2.5 | 0.03 | 0.1 | 0.30 | 0.05 | 0.01 | 0.1 | 0.3 | 0.1 |
| Step 3 | | | | | | | | | | | |
| LOD | 0.01 | 0.2 | 0.8 | 0.01 | 0.02 | 0.2 | 0.05 | 0.004 | 0.2 | 0.2 | 0.1 |
| LOQ | 0.03 | 0.7 | 2.8 | 0.03 | 0.1 | 0.7 | 0.2 | 0.01 | 0.7 | 0.6 | 0.2 |

Table 4.8 details the limit of detections and quantifications from the BCR sequential extraction analysis. With the exception of Ca all the LoQs were below 0.7 ppm. Generally Ca had the highest concentrations of all the elements tested and as a result also has the highest LoQ.

The LoD and LoQ values are the same as for the total digestions and residual step as they were all analysed in the same run.

Table 4.9: Average precision values for the column leachate ($\pm\%$)

| Column Leachate | Al | Ba | Ca | Cd | Cu | Fe | Mg | Mn | Pb | S | Zn |
|-----------------|-----|-----|-----|-----|----|----|-----|-----|-----|-----|-----|
| Average | 2.3 | 0.1 | 0.1 | 1.9 | - | - | 0.2 | 0.1 | 1.5 | 2.0 | 0.1 |

Table 4.9 records the precision averages, of the column leachate, calculated from 26 duplicate pairs completed over four separate runs of the ICP. Values are not given for Cu and Fe as the concentrations remained below the calculated limit of detection. Concentrations of Al and Pb were above the limit of detection on three occasions and with the exception of Mn and Cd all the other elements recorded concentrations above the LoD at least 20 times. Manganese and Cd concentrations were above the LoD in 12 and 17 of the duplicates, respectively. Overall the precision of the recorded results is within 2.3 %.

K and Na were not included in the original element list so were subsequently run separately from the other elements and recorded precisions of $4.4 \pm\%$ and $2.8 \pm\%$, respectively. However, this was only during the first week of the column experiment as the concentrations generally remained below the instruments limit of detection in the subsequent 39 weeks.

Table 4.10: Average accuracy values for the column leachate (TMDA-64 and Battle) (%)

| Column Leachate | Al | Ba | Ca | Cd | Cu | Fe | Mg | Mn | Pb | S | Zn |
|-----------------|-----|------|------|------|-----|-----|-----|-----|-----|---|------|
| TMDA | 103 | 100. | - | 99.8 | 101 | 101 | - | 100 | 100 | - | 99.4 |
| Battle | - | - | 99.2 | - | - | - | 104 | - | - | - | - |

The accuracy of the column leachate was determined using two CRMs: TMDA-64 and Battle. Table 4.10 above shows the average values from the four runs of the ICP. The accuracy is generally good and less than 3.6 %. K and Na were completed on a run on their own recording accuracies of 115.7 % and 84.1 %, respectively.

Table 4.11: Limit of detection and limit of quantification for the column leachate (ppm)

| Column Leachate | Al | Ba | Ca | Cd | Cu | Fe | Mg | Mn | Pb | S | Zn | Na | K |
|-----------------|-----|-------|-----|-------|------|-----|------|-------|-----|-----|-----|-----|-----|
| LOD | 0.1 | 0.005 | 0.6 | 0.002 | 0.02 | 0.1 | 0.03 | 0.001 | 0.1 | 0.1 | 0.1 | 2.2 | 0.3 |
| LOD | 0.3 | 0.02 | 1.9 | 0.01 | 0.1 | 0.3 | 0.1 | 0.004 | 0.3 | 0.5 | 0.2 | 7.3 | 1.0 |

With the exception of Ca and Na, the LoQs were all less than 1.0 ppm, as shown in Table 4.11. Ca and Na had calculated LoQs of 7.3 ppm and 1.9 ppm, respectively, which is likely to be a reflection of higher concentrations and/or the range of concentrations recorded.

Table 4.12: Average accuracy values for the total digestions and residual BCR step (TMDA-64 and Battle) (%)

| Digestions | Al | Ba | Ca | Cd | Cu | Fe | Mg | Mn | Pb | S | Zn |
|------------|------|-----|-----|------|-----|-----|----|------|-----|---|------|
| TMDA | 94.8 | 101 | - | 99.2 | 102 | 102 | - | 99.5 | 100 | - | 99.1 |
| Battle | - | - | 101 | - | - | - | - | - | - | - | - |

Deionised water was used to dilute the digestions as a result the accuracy of the total digestions and residual BCR step were determined using TMDA-64 and Battle. Table 4.12 shows the accuracy of the total digestions based on Battle and TMDA-64. The results show reasonable accuracy, generally within 2 % of the respective CRM. Al recorded a lower accuracy of 94.8 %.

Table 4.13: Average precision values for the total digestions ($\pm\%$)

| Digestions | Al | Ba | Ca | Cd | Cu | Fe | Mg | Mn | Pb | S | Zn |
|------------|-----|------|-----|-----|------|------|-----|-----|------|------|------|
| Average | 3.1 | 23.0 | 9.3 | 1.3 | 13.0 | 13.0 | 1.0 | 3.0 | 29.2 | 13.0 | 15.0 |

The above precision averages are calculated from 3 duplicate pairs. Table 4.13 indicates that although the total digestions recorded reasonable

accuracy the precision is generally lower, varying between 0.3 % and 29.2 %. This could be as a result of analysing the total digestions and the residual step of the BCR together. This will have resulted in a larger range of concentrations of each of the elements as during the BCR they would have been removed during the proceeding steps.

Table 4.14: Limit of detection and limit of quantification for the total digestions (ppm)

| Digestions | Al | Ba | Ca | Cd | Cu | Fe | Mg | Mn | Pb | S | Zn |
|------------|-----|-----|-----|-------|-------|-----|------|-------|------|-----|------|
| LOD | 0.3 | 0.2 | 0.2 | 0.003 | 0.004 | 0.2 | 0.04 | 0.002 | 0.03 | 0.1 | 0.03 |
| LOQ | 0.9 | 0.6 | 0.8 | 0.01 | 0.01 | 0.7 | 0.1 | 0.01 | 0.1 | 0.2 | 0.1 |

The LoQs for the total digestions and residual BCR step were all reported below 0.8 ppm as shown in Table 4.14.

4.7 Summary

- Eight samples of mine wastes (Gun 1 to Gun 8) and two samples floodplain sediments (Gun 9 and Gun 10) were collected from the length of Gunnerside Gill in Yorkshire;
- Four laboratory columns were set up. Three of the columns contained mine wastes (Gun 1, Gun 2 and Gun 3) and the fourth column contained floodplain sediment (Gun 9) collected from downstream of the mining areas;
- High-purity water was added weekly to the columns according to the seasons (as detailed in Table 4.3) for 40 weeks, the equivalent to 10 model years;
- Leachate volume, pH and Eh were recorded at the time of collection;
- Leachate concentrations of various elements were analysed using IC and ICP-OES;
- Analytical accuracy was ascertained by using CRMs, while precision was monitored with the aid of 10 % duplicate samples;
- The ten field samples and four post-column solid materials were characterised by EMP, acid digestion, BCR sequential extraction, and

particle size analysis. The initial ten samples were also subjected to XRD analysis.

Chapter 5

Results

Contents

| | |
|---|-----|
| Chapter 5..... | 131 |
| 5.1 Characterisation of Samples | 132 |
| 5.1.1 Particle Size Distribution | 132 |
| 5.1.2 Soil pH | 133 |
| 5.1.3 Geochemical Characterisation – total digestion..... | 133 |
| 5.2 BCR Sequential Extraction..... | 139 |
| 5.2.1 BCR Sum vs Total Digestion..... | 145 |
| 5.3 Mineralogical Characterisation | 147 |
| 5.3.1 XRD..... | 147 |
| 5.3.2 EMP | 150 |
| 5.3.3 Mineralogy Summary Table | 157 |
| 5.4 Column Experiment | 160 |
| 5.4.1 Column Samples..... | 160 |
| 5.4.2 Leachate Volume, pH and Eh | 160 |
| 5.4.3 Physical Characteristics | 162 |
| 5.4.3.1 Visual Description of Post Column Material | 162 |
| 5.4.3.2 PSD | 162 |
| 5.4.4 Leachate Chemistry..... | 163 |
| 5.4.4.1 ICP | 163 |
| 5.4.5 Electron Microprobe | 170 |
| 5.4.6 Total Digestion | 174 |
| 5.4.7 BCR Sequential Extraction..... | 177 |
| 5.5 Summary | 181 |

Chapter 5 will describe the results of the study, starting with characterisation of the solid samples by particle size and total digestion (Section 5.1). The results of the sequential extraction are given in Section 5.2 to decipher how readily available the contaminants of concern may be in the environment. Section 5.3 looks at the mineralogy of the samples and Section 5.4 details the

results of the column leaching study, including comparison to the pre column solids. Finally, a summary is given in Section 5.5.

5.1 Characterisation of Samples

5.1.1 Particle Size Distribution

The triplot (Figure 5.1) shows that all the samples predominantly comprise a mixture of silt and sand with generally less than 5 % clay. Gun 5 is the sample that stands out the most for comprising 95.5 % sand and 4.4 % silt; all the other samples contain at a range of silt from 13.2 % (Gun 4) up to 51.2 % (Gun 3). The percentage of sand present in the samples varies from 44.6 % (Gun 2) up to 95.5 % (Gun 5). There are no significant relationships between grain size and location of the sample recovered. This is most likely to be as a result of the nature of the tailings and waste rock themselves, which are inhomogeneous mixtures of grain sizes.

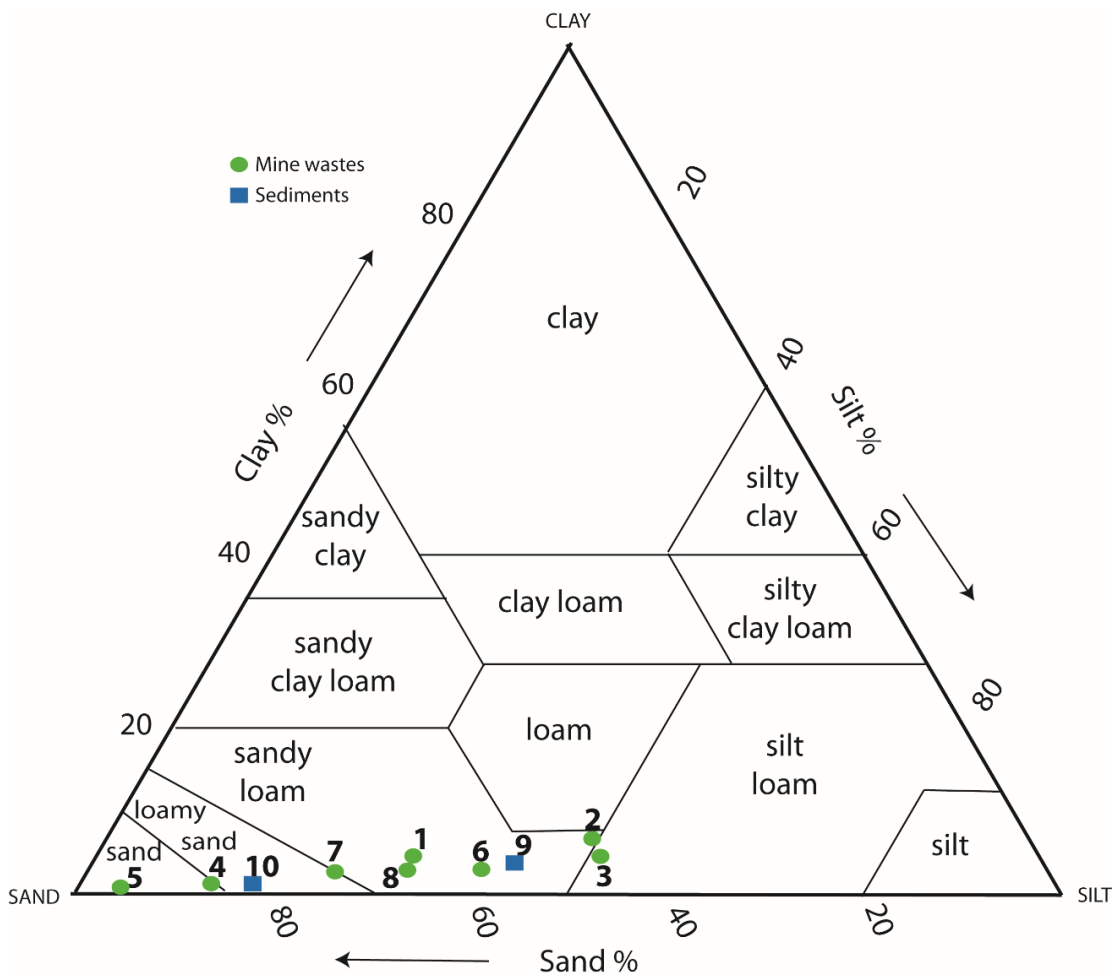


Figure 5.1: Triplot showing the particle size distribution of the samples (<2 mm sieve fraction only) (plot produced using Graham and Midgley 2000)

5.1.2 Soil pH

The soil pH values of the ten samples is shown in Table 5.1. Generally the pH values range from 7.0 (Gun 10) to 7.3 (Gun 2), with the exception of Gun 6 and Gun 7, which are slightly more alkaline and Gun 9, which is slightly more acidic.

Table 5.1: pH values of solid samples

| | Gun 1 | Gun 2 | Gun 3 | Gun 4 | Gun 5 | Gun 6 | Gun 7 | Gun 8 | Gun 9 | Gun 10 | Blank |
|-----------|--------------|--------------|--------------|--------------|--------------|--------------|--------------|--------------|--------------|---------------|--------------|
| pH | 7.2 | 7.3 | 7.1 | 7.2 | 7.1 | 7.6 | 8.0 | 7.1 | 6.8 | 7.0 | 7.1 |

5.1.3 Geochemical Characterisation – total digestion

The total digestions show that all the samples predominantly are composed of Al, Ba and Ca with relatively low concentrations of Cu and Mn. As expected Pb, Zn and S show the largest variations in total concentrations.

As Table 5.2 shows Ca concentrations vary greatly between samples and do not appear to show any trends in relation to the source material. Concentrations of Pb are highest in Gun 1 (70,000 mg/kg) and Gun 5 (49,300 mg/kg), whereas Zn is highest in Gun 5 (64,300 mg/kg) and Gun 7 (60,900 mg/kg) as shown on Figure 5.2. Similar to Zn, Gun 5 and Gun 7 have the highest concentrations of S (11,700 mg/kg and 17,100 mg/kg, respectively). Cadmium is generally below the limit of quantification (0.7 ppm) prior to multiplication with the calculating factor (converting ppm to mg/kg as described in Section 4.2.2), although the highest concentrations are also found in Gun 5 and Gun 7, which are the same as the highest concentrations of Zn. Given that concentrations of Cd are below the limit of quantification Cd results have largely been excluded from the remainder of this chapter.

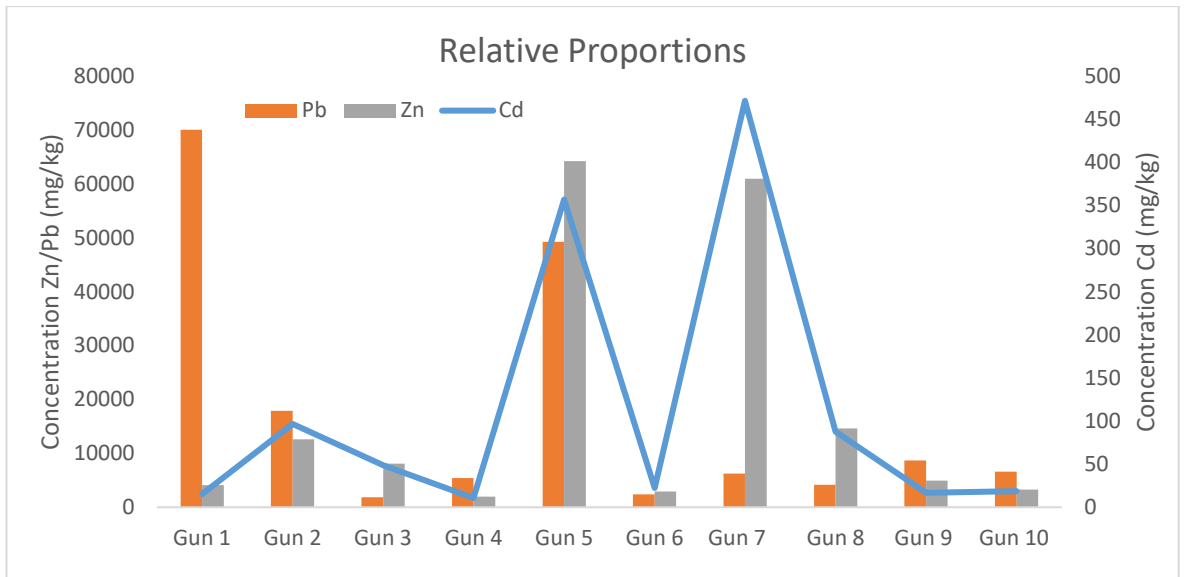


Figure 5.2: Relative concentrations of Pb, Zn and Cd (mg/kg).

Table 5.2: Total digestion concentrations for all ten samples (mg/kg)

| | Pb | Zn | Cd | Al | Ba | Ca | Cu | Fe | Mg | Mn | S | Na | K | Total C |
|---------------|-----------|-----------|-----------|-----------|-----------|-----------|-----------|-----------|-----------|-----------|----------|-----------|----------|----------------|
| | (mg/kg) | | | | | | | | | | | | | % |
| Gun 1 | 70000 | 4100 | 15 | 34200 | 11900 | 13200 | 59 | 35900 | 2860 | 1600 | 4150 | 1230 | 8520 | 1.67 |
| Gun 2 | 17900 | 12600 | 97 | 38400 | 13700 | 34300 | 119 | 26400 | 2590 | 80 | 5720 | 1330 | 11200 | 1.57 |
| Gun 3 | 1840 | 8100 | 49 | 65200 | 7380 | 51600 | 76 | 15700 | 3350 | 47 | 7160 | 2290 | 18900 | 2.57 |
| Gun 4 | 5430 | 2000 | 11 | 42600 | 12800 | 11900 | 20 | 15500 | 3010 | 890 | 4290 | 1750 | 9510 | 1.42 |
| Gun 5 | 49300 | 64300 | 357 | 6150 | 5710 | 73900 | 170 | 4870 | 370 | 50 | 11700 | 534 | 1790 | 1.92 |
| Gun 6 | 2400 | 2900 | 22 | 25300 | 15100 | 13200 | 17 | 24200 | 1220 | 1060 | 4020 | 1550 | 5220 | 0.98 |
| Gun 7 | 6260 | 61000 | 471 | 11200 | 2670 | 105000 | 71 | 5490 | 670 | 60 | 17100 | 800 | 3690 | 1.58 |
| Gun 8 | 4140 | 14600 | 88 | 24300 | 8670 | 92100 | 54 | 9920 | 1410 | 60 | 7310 | 1060 | 9000 | 2.03 |
| Gun 9 | 8710 | 4950 | 17 | 22000 | 15900 | 39500 | 67 | 18500 | 1420 | 870 | 4760 | 1690 | 5690 | 1.89 |
| Gun 10 | 6590 | 3280 | 19 | 24000 | 12100 | 12300 | 23 | 20900 | 1700 | 450 | 3970 | 1800 | 5760 | 1.87 |

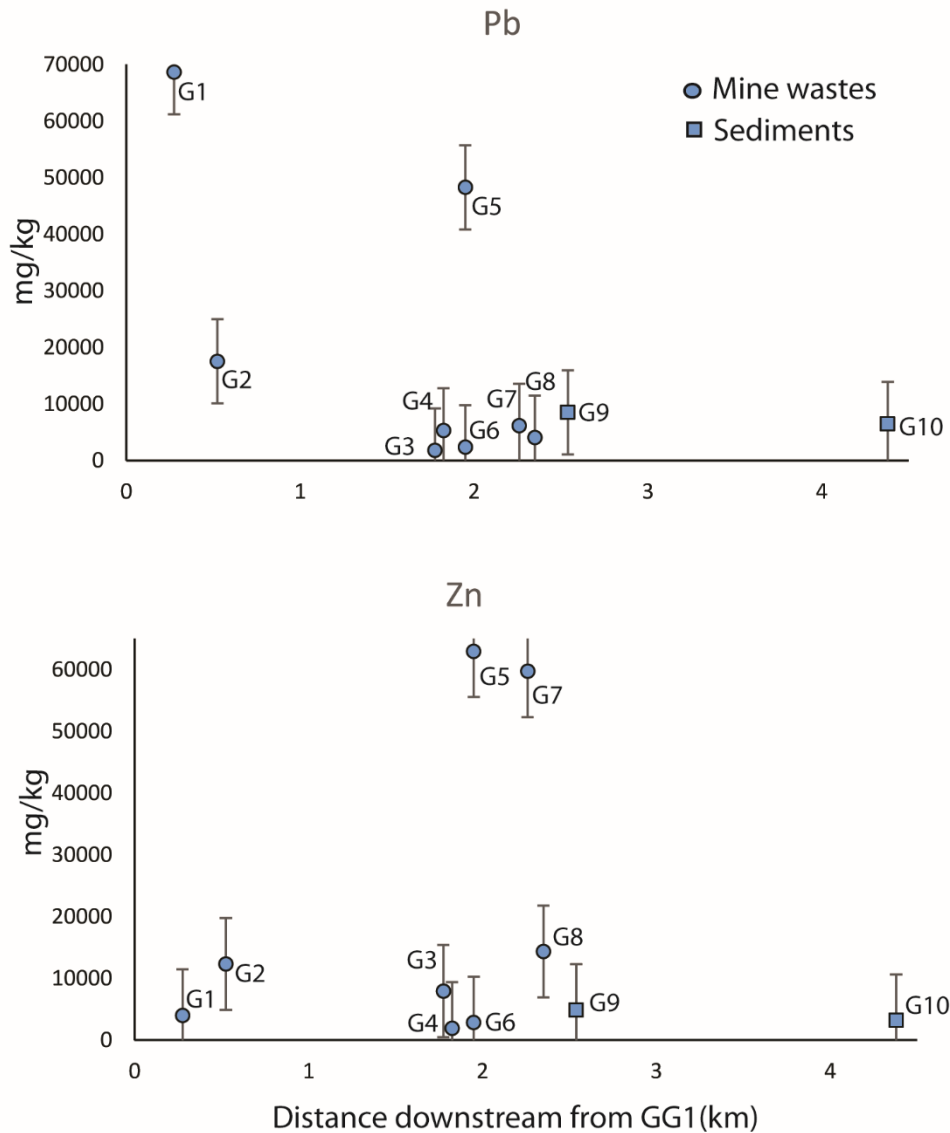


Figure 5.3: Total concentrations and standard error of Pb and Zn downstream of GG1 (most upstream EA monitoring location).

The graphs in Figure 5.3 give a general impression of the concentrations of Pb and Zn downstream along Gunnerside Gill from the initial waste rock piles of Gun 1, 2 and 3. As is evident in the Pb graph Gun 1 and Gun 5 contain significantly elevated concentrations of Pb when compared to the other samples. In contrast the highest Zn concentrations are recorded in Gun 5 and Gun 7, with significantly lower concentrations in the upper waste samples.

The standard errors of the mean concentrations reflect the variability of the total concentrations across the ten samples (Figures 5.3 and 5.4). The larger standard error bars represent higher variability within the sample ranges,

including Pb, Zn and Ca. The smaller the standard error the less variation of concentrations across the ten samples, examples include Ba, Fe and S.

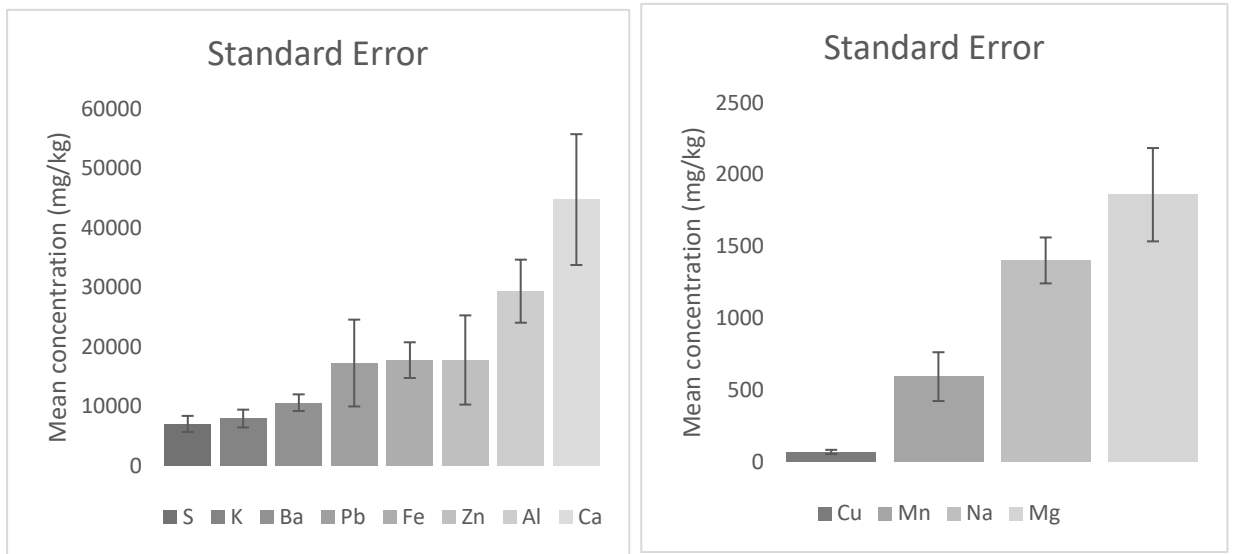


Figure 5.4: Standard error based on the mean total concentrations of Gun 1 to Gun 10 solid samples

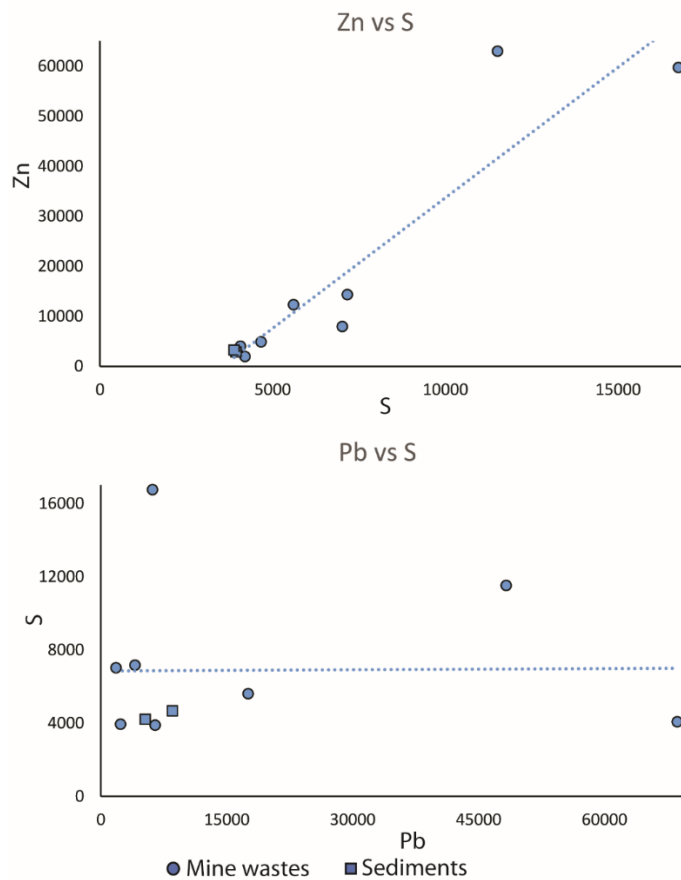


Figure 5.5: Zn/S and Pb/S correlation graphs

Zinc and S show a strong correlation based on Figure 5.5. The concentrations of Pb and S do not show any perceivable relationship; only Gun 5 and Gun 10 are really comparable.

The results of the Pearson correlation coefficient analysis indicate that Zn-S show a strong correlation (Table 5.3). Lead shows very different trends; it has limited correlations with any other tested element. In fact essentially shows no correlation with S, which would indicate that galena is unlikely to be the main Pb mineral responsible for Pb weathering in Gunnerside Gill.

Table 5.3: Pearson coefficients for key elements

| | Na | K | Al | Ba | Ca | Cu | Fe | Mg | Mn | Pb | S | Zn |
|----|-------|-------|-------|-------|-------|-------|-------|-------|-------|------|-------|-------|
| Fe | 0.38 | 0.26 | 0.39 | 0.71 | -0.79 | -0.32 | - | 0.57 | 0.88 | 0.35 | -0.74 | -0.71 |
| Mn | 0.20 | -0.03 | 0.16 | 0.75 | -0.78 | -0.35 | 0.88 | 0.40 | - | 0.40 | -0.66 | -0.59 |
| Pb | -0.48 | -0.23 | -0.21 | -0.08 | -0.12 | 0.47 | 0.35 | 0.01 | 0.40 | - | 0.01 | 0.23 |
| S | -0.64 | -0.33 | -0.47 | -0.89 | 0.86 | 0.49 | -0.74 | -0.57 | -0.66 | 0.01 | - | 0.93 |
| Zn | -0.79 | -0.51 | -0.63 | -0.81 | 0.76 | 0.67 | -0.71 | -0.68 | -0.59 | 0.23 | 0.93 | - |

The strongest correlation is between Mn and Fe, likely to be secondary oxyhydroxides. Iron and S show a very strong negative correlation, where higher concentrations of Fe are generally associated with lower concentrations of S. Similarly, Zn-Fe, Zn-Mg and Zn-Mn also show negative correlations.

Table 5.4 shows the relative proportions of Pb and Zn between the ten samples. This shows that the majority of the Pb is present in Gun 1 and the highest proportions of Zn are present in Gun 5 and Gun 7.

Table 5.4: Relative proportions of Zn and Pb in pre column solids compared to total concentrations

| | Gun 1 | Gun 2 | Gun 3 | Gun 4 | Gun 5 | Gun 6 | Gun 7 | Gun 8 | Gun 9 | Gun 10 |
|------------|-------|-------|-------|-------|-------|-------|-------|-------|-------|--------|
| Pb (wt. %) | 40.6 | 10.4 | 1.1 | 3.1 | 28.5 | 1.4 | 3.6 | 2.4 | 5.0 | 3.8 |
| Zn (wt. %) | 2.3 | 7.1 | 4.6 | 1.1 | 36.2 | 1.6 | 34.3 | 8.2 | 2.8 | 1.8 |

5.2 BCR Sequential Extraction

The BCR graphs (Figures 5.6, 5.7 and 5.8) depict the fractions within the solid in which each of the tested elements is present, based on the BCR procedure. The full methodology can be found in Section 4.2.3. Broadly speaking five steps were undertaken, targeting operationally defined specific phases:

- Step 0 (water) – water soluble phases;
- Step 1 (acid soluble and exchangeable) – carbonate and CEC sites;
- Step 2 (reducible) – Fe and Mn oxyhydroxides;
- Step 3 (oxidisable) – organic matter and sulfides;
- Residual – non silicate bound metallic elements.

With regards to Pb, less than 0.4 % was found to be present in the water soluble fraction in all of the samples (Figure 5.6). Relative proportions in the exchangeable fraction varied from 8 % (Gun 3) to 68 % (Gun 2) and from 4 % (Gun 7) to 50 % (Gun 8 and Gun 9) in the reducible fraction. The residual phase contained 4 % (Gun 1) to 67 % (Gun 5 and Gun 7) of Pb across the ten samples. Lead was mostly present in the exchangeable fraction in Gun 1 and Gun 2, conversely Pb was mainly present in the residual fraction in Gun 3, Gun 5 and Gun 7. In Gun 4, Gun 6, Gun 8, Gun 9 and Gun 10 Pb was found to be largely present in the reducible fraction with slightly lower relative proportions present in the exchangeable fraction.

Similarly, less than 0.8 % of Zn was recorded in the water fraction in any of the samples. Relative proportions varied in the exchangeable fraction between 5 % (Gun 7) to 50 % (Gun 1 and Gun 2), <1 % (Gun 7) to 22 % (Gun 1) of Zn was present in the reducible fraction and 5 % (Gun 1) to 54 % (Gun 8) was recorded in the oxidisable fraction. The residual fraction contained 14 % (Gun 10) to 77 % (Gun 5) of Zn proportionally. In Gun 1, Gun 2, Gun 4, Gun 9 and Gun 10 Zn was mostly present in the exchangeable fraction, and Gun 6 and Gun 8 contained Zn predominantly in the oxidisable fraction. Gun 3, Gun 5 and Gun 7 were dominated by Zn being present in the residual phase.

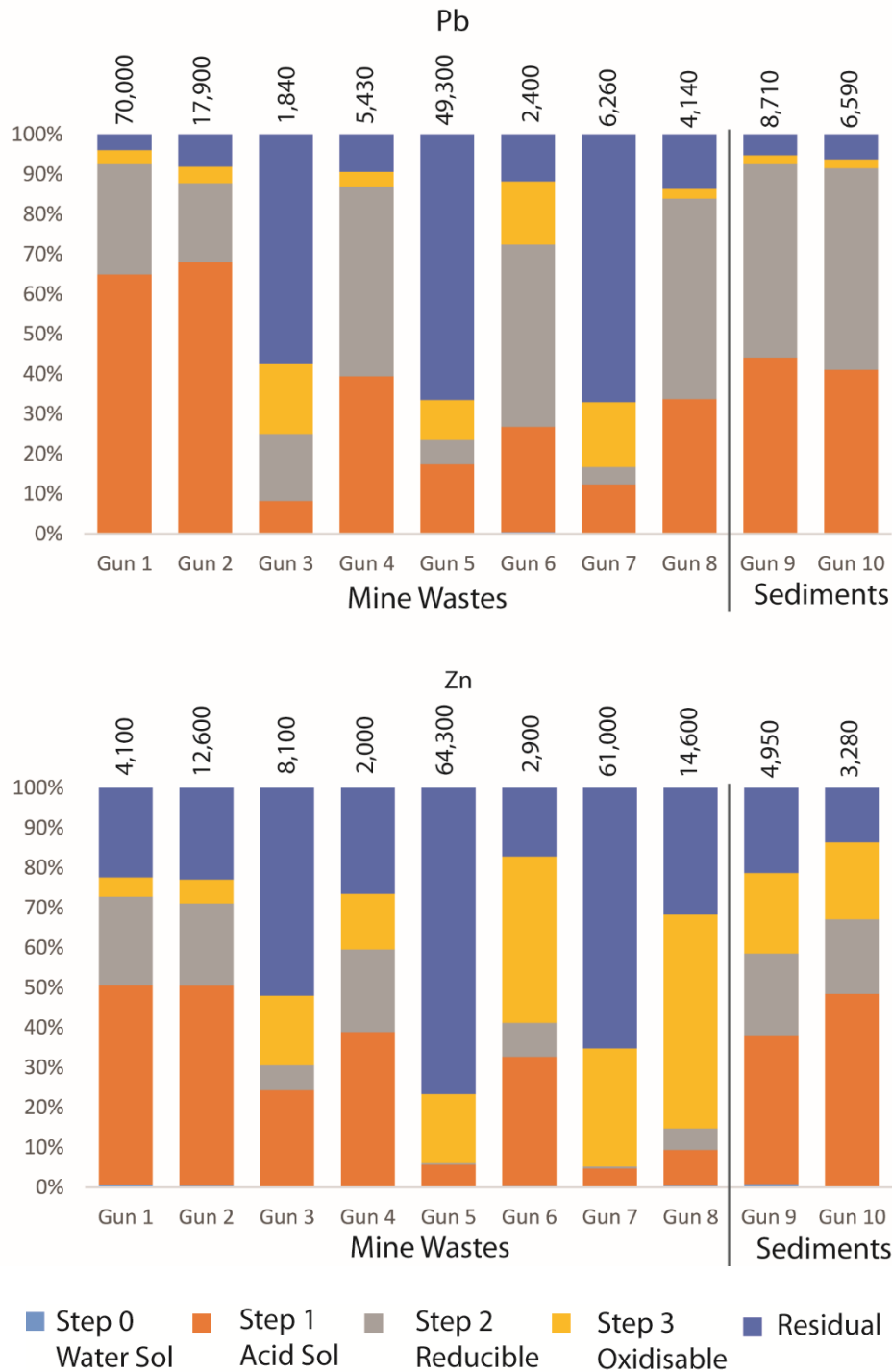


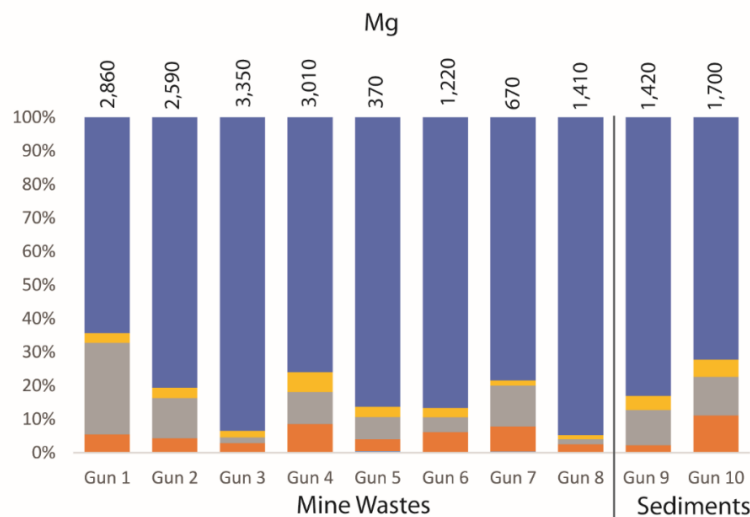
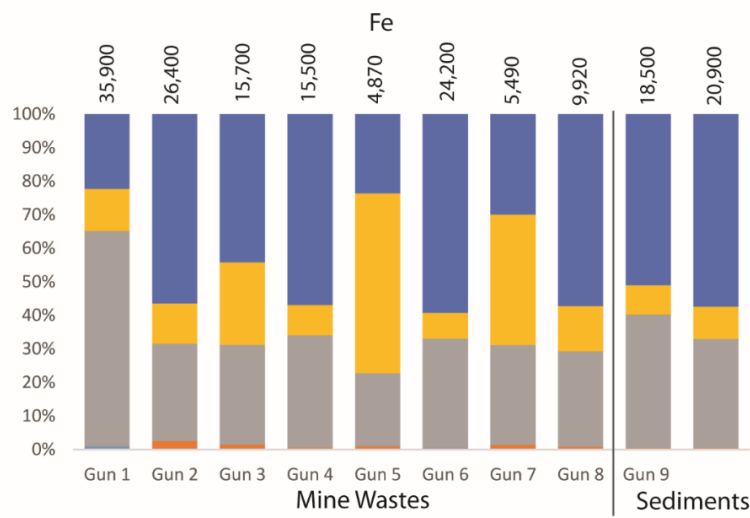
Figure 5.6: BCR sequential extraction relative proportions for Pb and Zn (total digestion concentration shown at top of column mg/kg)

With regards to Mn (Figure 5.7), generally less than 0.7 % was recorded in the water fraction, with the exception of Gun 8 which was found to be 4 %. Relative proportions in the exchangeable fraction varied from 8 % (Gun 9) to 61 % (Gun 8), in the reducible phase from 14 % (Gun 3) to 86% (Gun 9) and generally less than 5 % in the oxidisable fraction, with 11 % Mn recorded in Gun 3. The

residual phase contained 4 % (Gun 4) to 31 % (Gun 3) of Mn. Manganese was mainly present in the exchangeable fraction in Gun 3, Gun 5, Gun 7, and Gun 8, and in the reducible fraction in Gun 1, Gun 2, Gun 4, Gun 6, Gun 9, and Gun 10. The presence of Mn in the reducible fraction was to be expected as the reagents of the BCR procedure target Fe and Mn oxyhydroxides in this step.

Iron was found to have very low relative proportions of <1 % and <2 % in both the water step and exchangeable fraction, respectively. Relative proportions of Fe in the reducible fraction were found to vary from 22 % in Gun 5 to 64 % in Gun 1, with the majority of the relative proportions between 8 % and 33 %. The oxidisable fraction contained 8 % (Gun 6) to 54 % (Gun 5) Fe and 22 % (Gun 1) to 59 % (Gun 6) of Fe was recorded within the residual fraction. Similar to Mn, Fe was mainly found to be present in the reducible fraction with slightly lower relative proportions in the residual fraction.

Magnesium was found to be predominantly present in the residual phase, ranging from 72 % (Gun 10) to 95 % (Gun 9). Less than 0.5 % was recorded in any of the samples during the water step, a limited relative proportion range of between 2 % (Gun 8 and Gun 9) to 11 % (Gun 10) was recorded in the exchangeable fraction, and only 1 % (Gun 8) to 6 % (Gun 4) present in the oxidisable fraction.

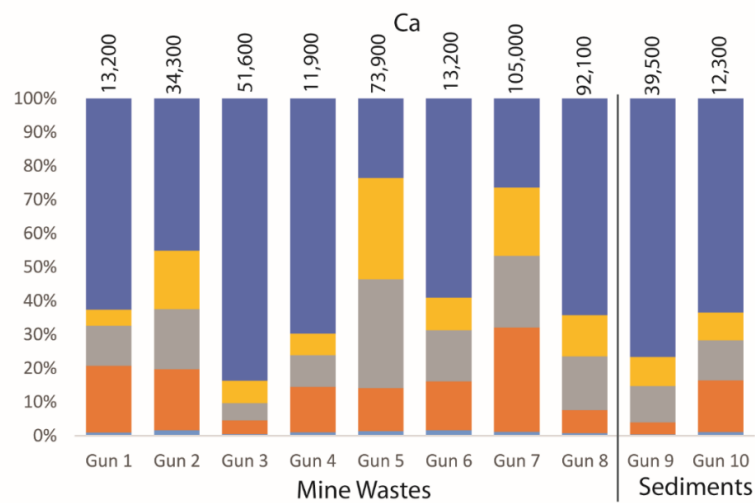
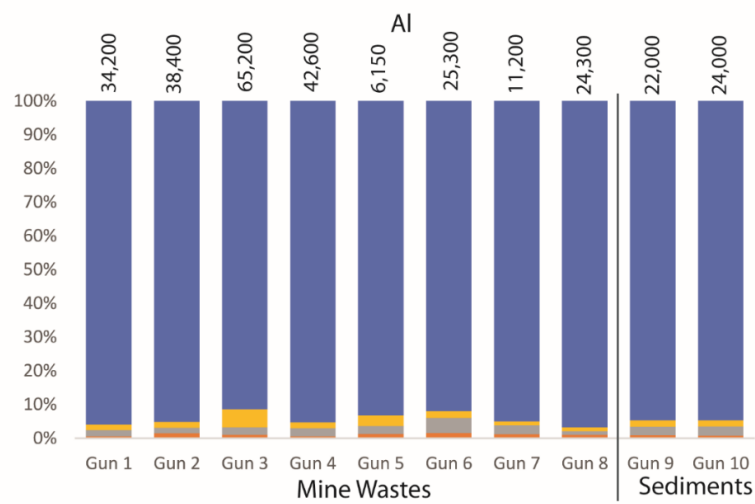


■ Step 0 ■ Step 1 ■ Step 2 ■ Step 3 ■ Residual
 Water Sol Acid Sol Reducible Oxidisable

Figure 5.7 BCR sequential extraction results for Mn, Fe and Mg (total digestion concentration shown at top of column mg/kg)

The water step and exchangeable fraction contained less than 1.1 % and 1.0 % of S, respectively, in all of the ten samples (Figure 5.8). A maximum proportion of 4 % (Gun 6 and Gun 10) of S was recorded in the reducible fraction and a range of 17 % (Gun 5) to 42 % (Gun 8) in the oxidisable step. The residual fraction contained 56 % (Gun 8) to 82 % (Gun 5) S. Sulfur was mainly present in the residual fraction, with lower relative proportions recorded in the oxidisable fraction.

Aluminium was predominantly present in the residual fraction, which contained 91 % to 97 % in all samples. Relative proportions of Ca were found to vary across the samples and the various fractions. Less than 2 % of Ca was present in the water step, a range of 4 % (Gun 3 and Gun 9) to 20 % (Gun 1) in the exchangeable fraction, 5 % (Gun 3) to 32 % (Gun 5) in the reducible phase, 5 % (Gun 1) to 30 % (Gun 5) in the oxidisable step and 24 % (Gun 5) to 77 % (Gun 9) in the residual fraction. This could imply Step 1 is not dissolving all of the carbonate present.



■ Step 0 ■ Step 1 ■ Step 2 ■ Step 3 ■ Residual
 Water Sol Acid Sol Reducible Oxidisable

Figure 5.8: BCR sequential extraction results for S, Al and Ca (total digestion concentration shown at top of column mg/kg)

5.2.1 BCR Sum vs Total Digestion

Following the completion of the BCR sequential extraction procedure the relative proportions for each step were summed to allow for comparison to the total digestion results for each sample.

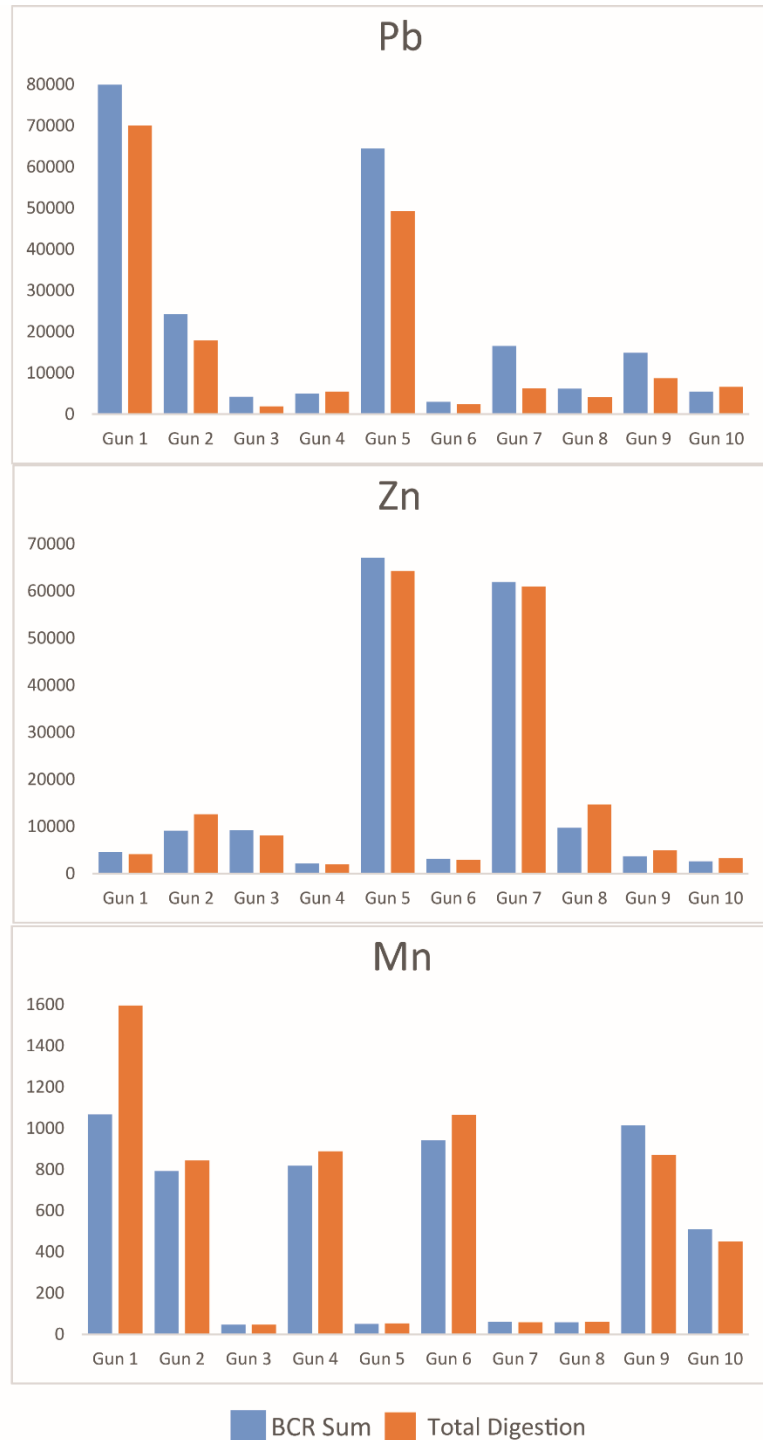


Figure 5.9: BCR sequential extraction sum of all steps compared to the respective total digestion relative proportions for Pb, Zn and Mn.

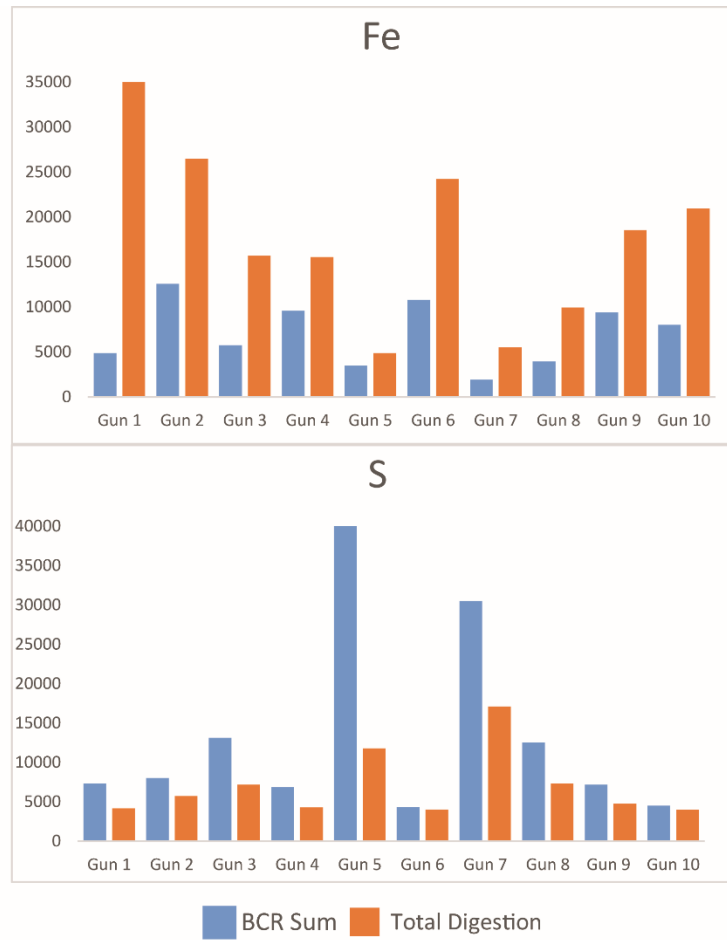


Figure 5.10: BCR sequential extraction sum of all steps compared to the respective total digestion relative proportions for Fe and S.

Generally the sum concentrations from the BCR and the total digestion concentrations for Pb, Zn, Mn, Mg and Al recorded similar values (Figures 5.9 to 5.11). There was some variation, which could be attributed to heterogeneity of the sample or losses during the sequential extraction wash phases. Eight of the ten samples showed reasonable agreement for S concentrations, however Gun 5 and Gun 7 recorded higher concentrations from the BCR procedure than the total digestion. Iron and Ca showed more variability than the other elements, but on the whole are within the same order of magnitude between the BCR sum and total digestions concentrations.

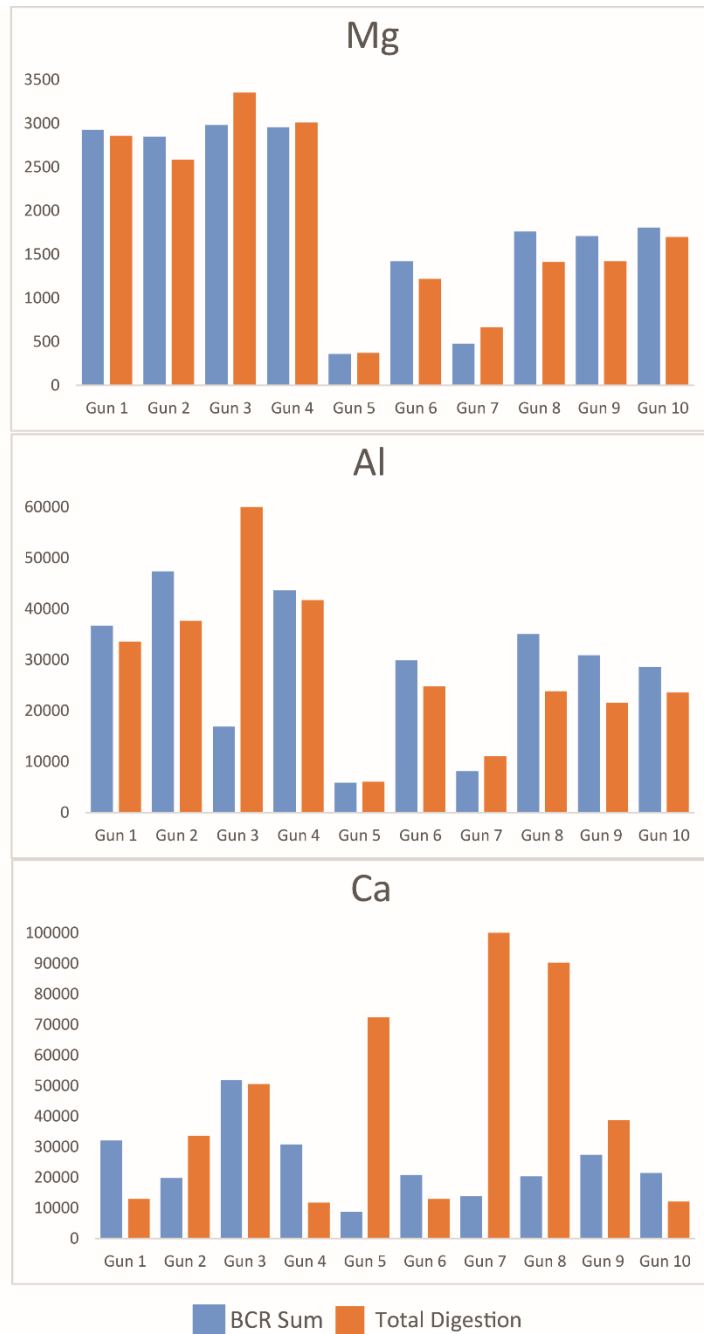


Figure 5.11: BCR sequential extraction sum of all steps compared to the respective total digestion relative proportions for Mg, Al and Ca.

5.3 Mineralogical Characterisation

5.3.1 XRD

Based on the semi-quantitative analysis, using MATCH (Crystal Impact 2019), the XRD data show that the samples primarily comprise quartz (approximately 70 % to 90 %) and barite (around 4 % to 25 %) with lesser quantities of clays (approximately 5 % to 10 %) and fluorite (typically 5 % to 10 %). Calcite (up to

5 % where present), galena (up to 8 % where present), sphalerite (between 2 % and 15 % where present) and cerussite (around 3 % in Gun 1) were also identified by XRD analysis and show greater variability across the samples.

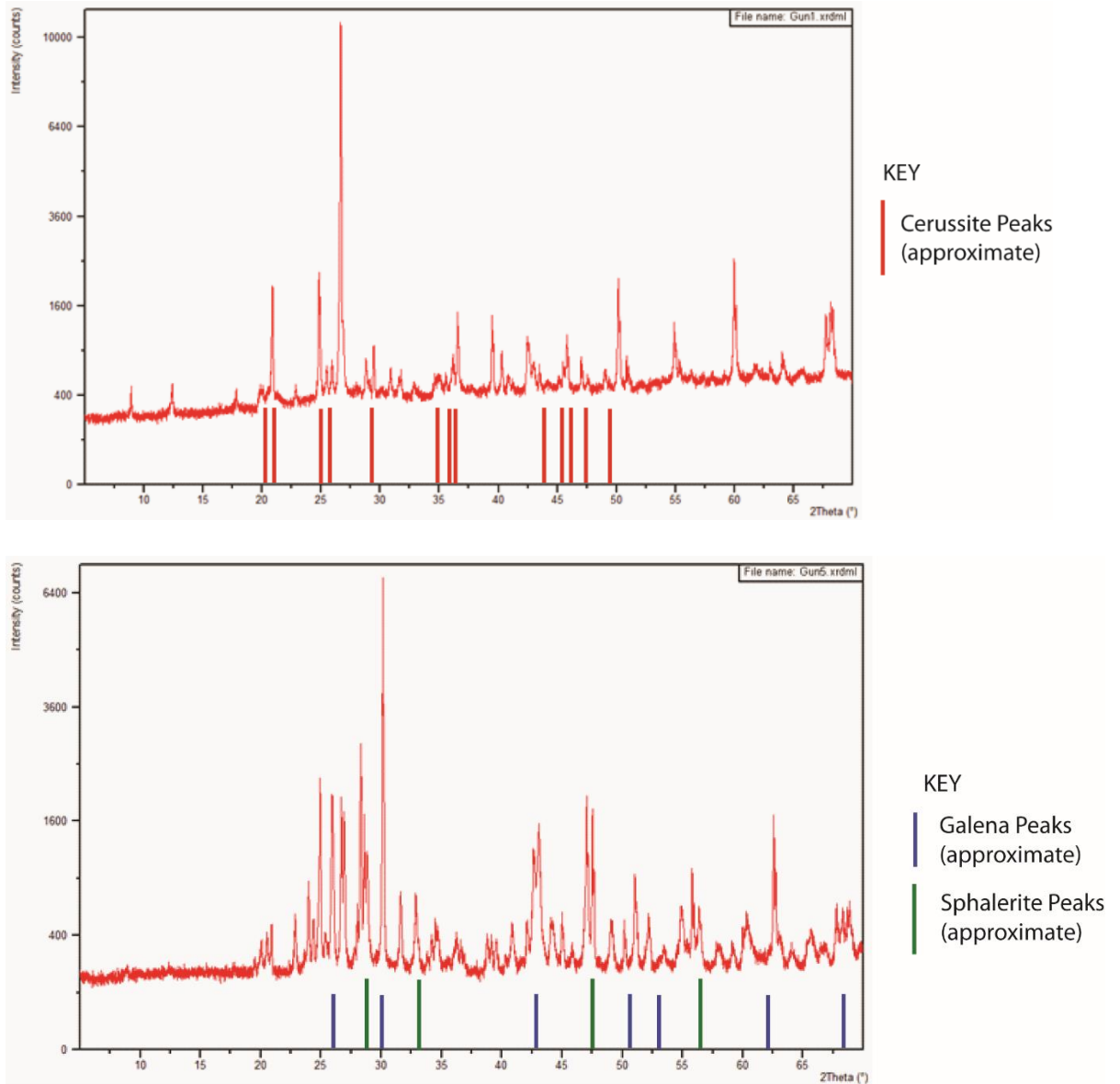


Figure 5.12: Examples of the peak locations of cerussite (Gun 1) and galena and sphalerite (Gun 5)

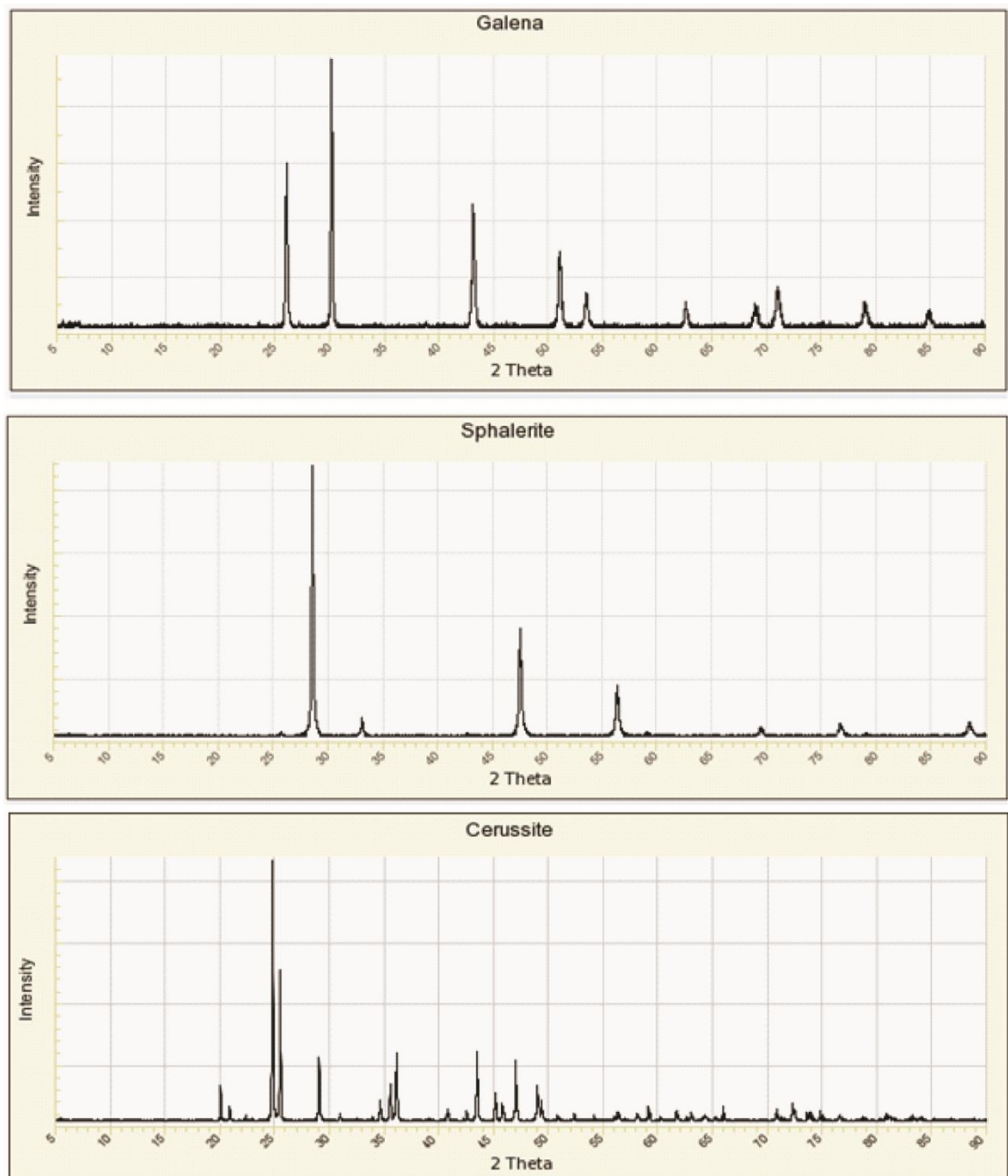


Figure 5.13: Typical galena, sphalerite and cerussite XRD spectrum (from <http://rruff.info> 2019)

The concentration of quartz within the samples was found to be relatively high, ranging from 70 % to 90 %. Barite and fluorite were present in the majority of the samples with the highest concentrations coinciding with the lowest concentrations of quartz in Gun 5 and Gun 7. Clay minerals, tentatively identified as kaolinite (however clay peaks can be difficult to assign), were present in the majority of the samples, with the exception of Gun 5. Galena

was identified in four of the samples, ranging from less than 1 % in Gun 3, Gun 6 and Gun 7 to around 8 % in Gun 5, galena peaks are shown in Figure 5.12 and 5.13. Cerussite, a common secondary Pb mineral following weathering of galena, was found to be present in Gun 1 (typical cerussite peaks are shown in Figure 5.12 and 5.13).

Sphalerite was also found to be present in four samples, ranging from around 1.5 % in Gun 9, 7 % in Gun 5 and Gun 8, to approximately 15 % in Gun 7, sphalerite peaks are also shown in Figure 5.10 and 5.11.

5.3.2 EMP

The EMP analysis showed the similarities and differences in the textural and mineralogical compositions of all the samples. When using the EMP in backscatter mode the brighter the grains the heavier the elements within it are, in the case of this study the brighter grains are likely to contain metallic elements or those with a higher atomic mass, as denoted in Figure 5.14. The brighter grains in these samples are likely to be barite, galena and sphalerite amongst others. Alongside the general analysis and photographs elemental maps were also undertaken to show the composition changes within individual grains.

Gun 1 (Figure 5.14) showed a relatively uniform texture and composition, and generally comprised grains of quartz, calcite, composite grains of clay and bright materials. Gun 2 and 3 were finer grained than Gun 1 and were composed of mostly clays and quartz with fewer bright grains. Gun 4 is similar to Gun 1 with a relatively uniform texture, but contained fewer bright grains. Although Gun 5 was texturally similar to Gun 1 and Gun 4 it had a significantly higher proportion (40-50 %) of barite and metallic element bearing grains (Figure 5.14).

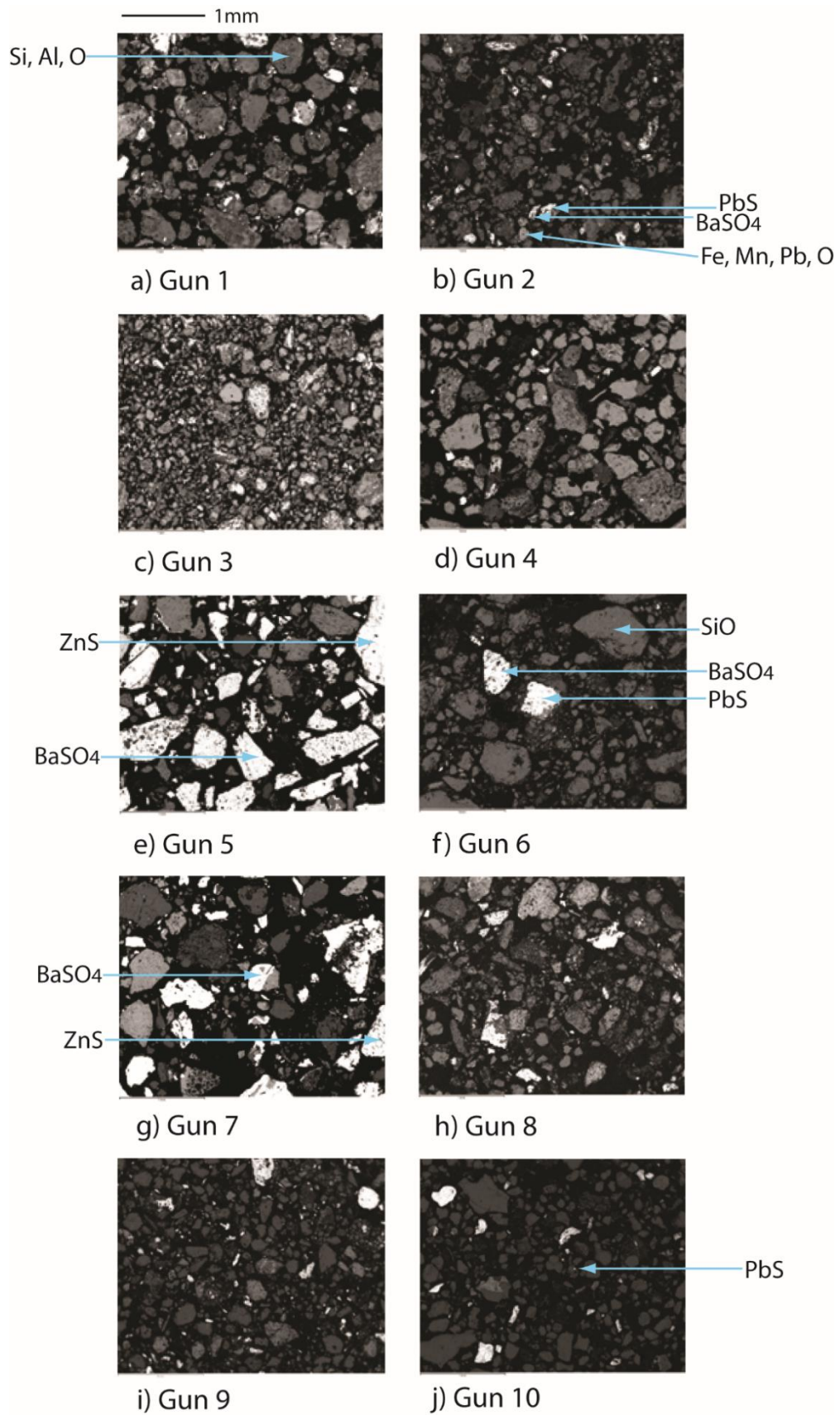


Figure 5.14: Backscattered electron images of Gunnerside Gill mine wastes and sediments. Gun 5 and Gun 7 show the highest proportion of bright grains.

Gun 6 had a wide range of grain sizes ranging from very fine to around 1 mm diameter. In addition, Gun 6 had a low proportion of bright grains and was mainly comprised of quartz and clays. Gun 7 was texturally similar to Gun 5, but contained significantly less (around 25 %) bright grains. Gun 8 was both texturally and compositionally similar to Gun 1 and Gun 4. Gun 9 and 10 were fine grained and comparable to Gun 2 and Gun 3.

In addition to looking at the texture and point composition of the samples, several grains from each sample were selected for elemental mapping.

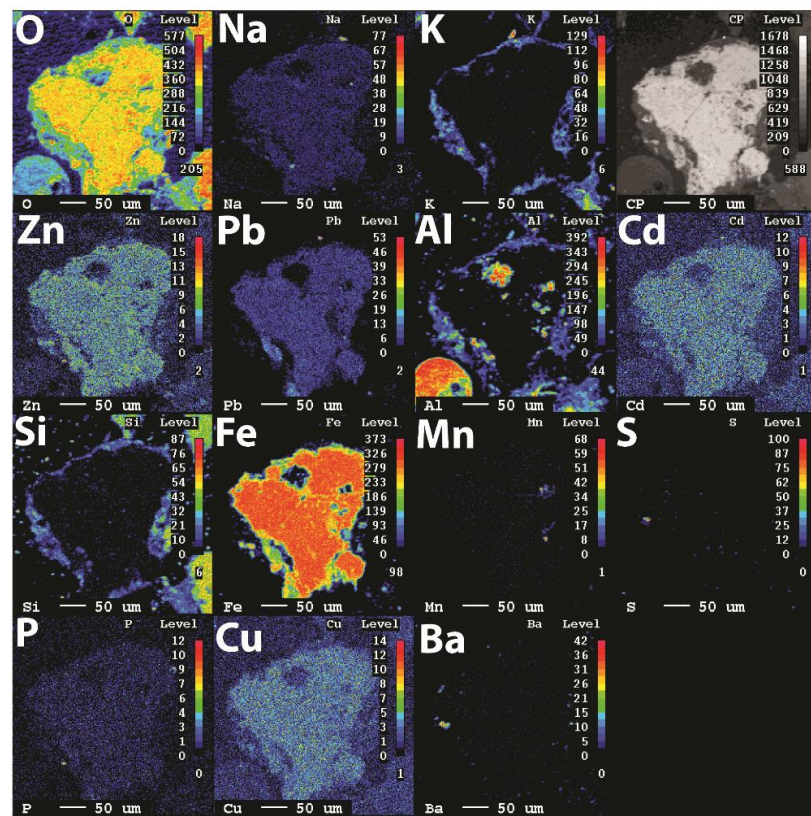


Figure 5.15: Elemental map showing Cd-, Cu- and Zn-bearing Fe oxyhydroxide rimmed by Si-Al-K bearing clay mineral (Gun 1). The colour scale reflects the intensity, red and yellows are the highest and blue the lowest intensity. The presence of Na is considered to be from spectral interference from Zn.

Several of the samples including Gun 1, Gun 2, Gun 4, and Gun 5 contained grains of Fe oxyhydroxide containing varying proportions of Cd-Cu-Zn with a rim of clay around the outer edge (Figure 5.15). Mineral rims were evident throughout all the samples including Gun 5 which contained a grain of pyrite with a corner of Cd-Cu-Mn bearing Pb oxide or carbonate. The whole grain

was surrounded by a rim of Ba oxide or carbonate. The Pb oxide appears to have a small core containing some residual S.

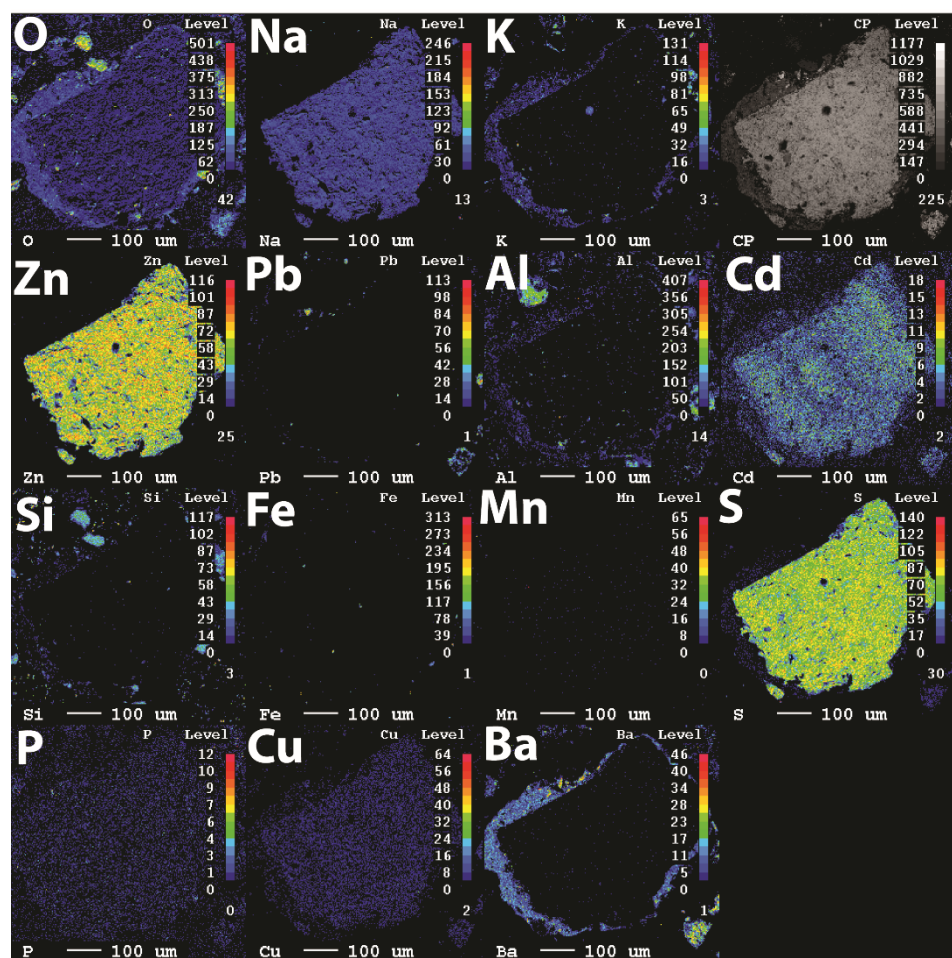


Figure 5.16: Elemental map showing Cd-bearing Zn sulfide rimmed by Ba oxide or carbonate (Gun 5). The colour scale reflects the intensity, red and yellows are the highest and blue the lowest intensity. The presence of Na is considered to be from spectral interference from Zn.

Other interesting grains were noted in Gun 3, Gun 5, Gun 6 and Gun 7 which comprised a core of Cd-bearing Zn sulfide, an example is shown in Figure 5.16. Although Na appears to be present it is more likely to be as interference from Zn peaks as a result of using energy dispersive spectroscopy (EDS). In Gun 5 and Gun 7 the outer rims also comprised Ba oxide and clay minerals. In the case of Gun 6 the core appeared to be weathering with the outer rim being less bright and surrounded by a layer of clay minerals.

Evidence of mineral reactions was also evident in Gun 2, Gun 5 and Gun 10. A grain of galena was noted in Gun 2, surrounded by Pb oxide or carbonate. The whole grain was then surrounded by a thin layer of Si-Al-K clay minerals.

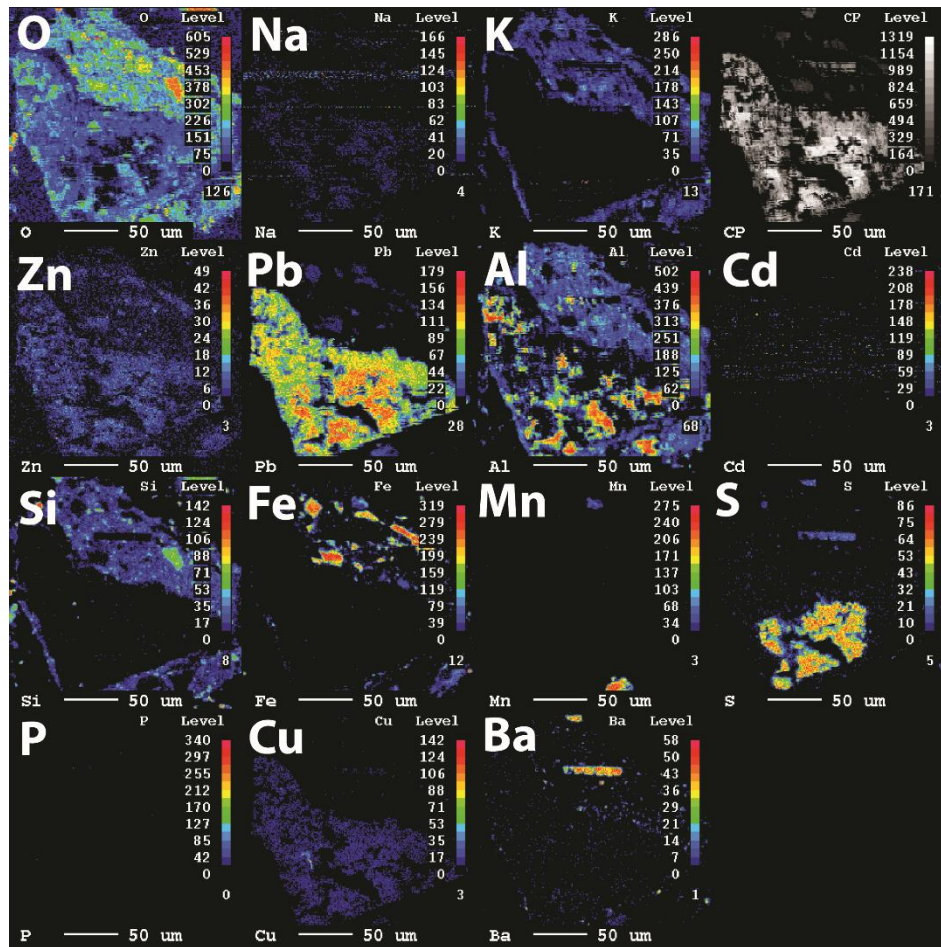


Figure 5.17: Elemental map showing Pb sulfide rimmed by Pb oxide or carbonate and clay minerals (Gun 2). The colour scale reflects the intensity, red and yellows are the highest and blue the lowest intensity

Figure 5.17 is an example of grain with a core of galena with concentrations implying lattice substitution of Cd and Cu, surrounded by an outer rim of barite and then a thin layer of possibly secondary Pb. Anglesite and cerussite are largely absent based on the XRD results implying the Ba oxide is protecting the galena core from ongoing reactions and weathering. In addition, Gun 5 also contained grains of galena with some Cd zoning and it also had an outer barite rim, again protecting it from further weathering (Figure 5.18). A thin outer rim of Pb oxide or carbonate is present around the barite, with a final layer of K-Al-Si clay minerals around the outermost edge.

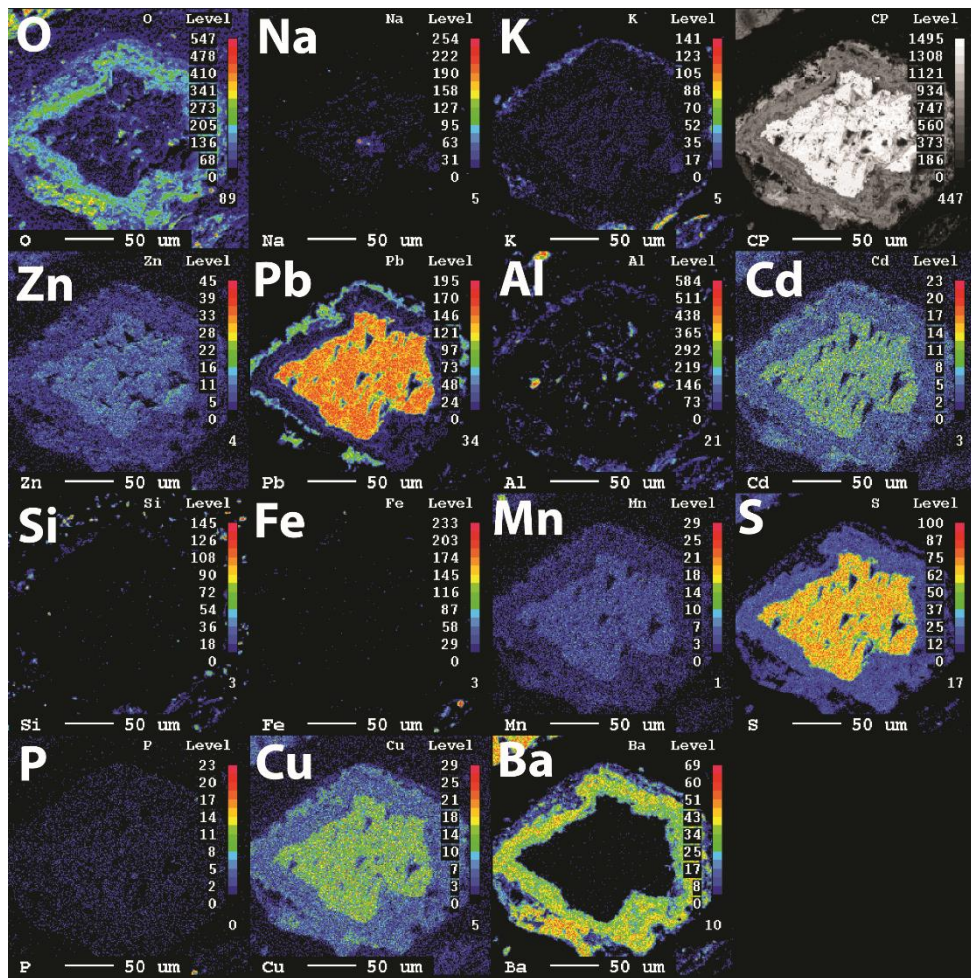


Figure 5.18: Elemental map showing Cu-, Cd and Mn bearing Pb sulfide rimmed by barite and Pb oxide or carbonate (Gun 5). The colour scale reflects the intensity, red and yellows are the highest and blue the lowest intensity

A Zn-, Cd-, and Cu- bearing Pb oxide or carbonate was noted in Gun 10, as shown in Figure 5.19. There was a distinct absence of S within the grain, however the concentrations of O, Al and Fe varied across the grain indicating it could be undergoing different weathering reactions.

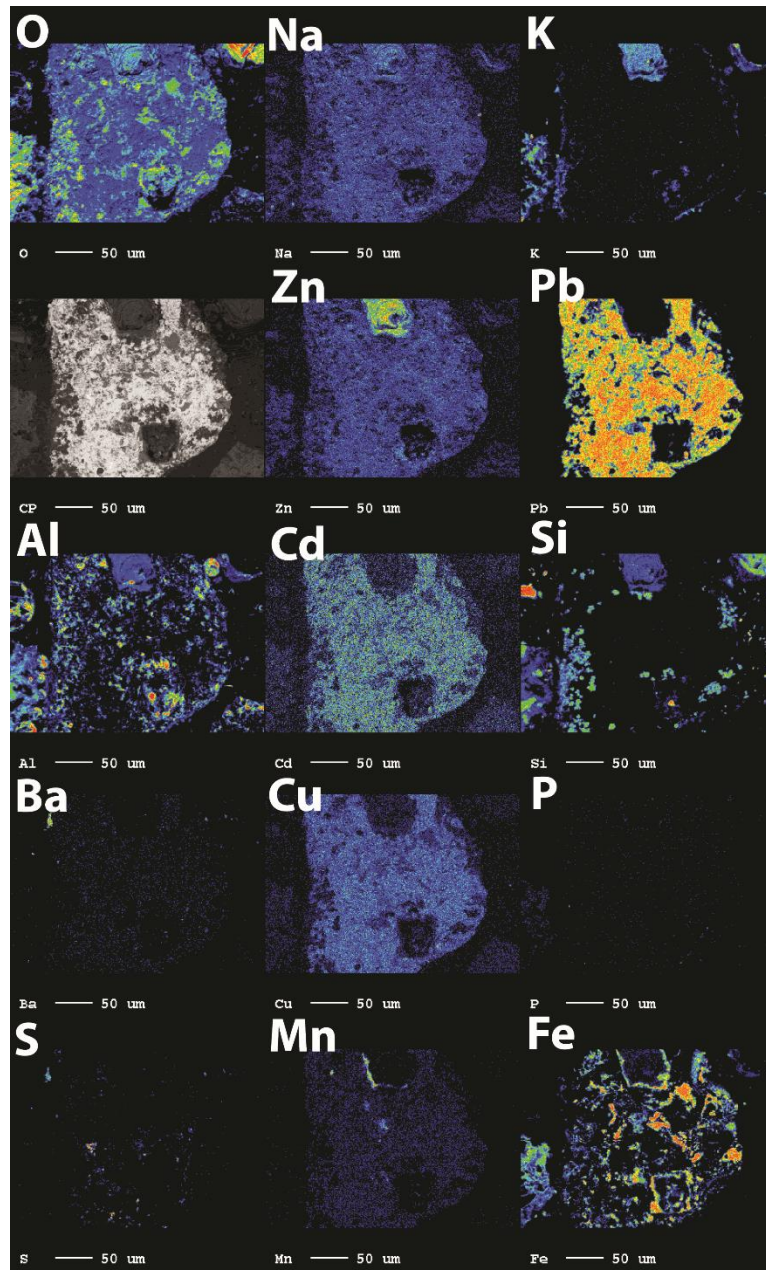


Figure 5.19: Elemental map showing Cu-, Cd- and Mn- bearing Pb oxide rimmed by barite and Pb oxide or carbonate (Gun 10). The colour scale reflects the intensity, red and yellows are the highest and blue the lowest intensity. The presence of Na is considered to be from spectral interference from Zn.

Gun 9 (Figure 5.20) showed a departure from the galena and sphalerite grains noted in the rest of the Gunnerside Gill samples and indicated the presence of a Pb-Zn phosphate with associated Cd. This could possibly be pyromorphite ($\text{Pb}_5(\text{PO}_4)_3\text{Cl}$), but Cl was not included as an element during the mapping analysis.

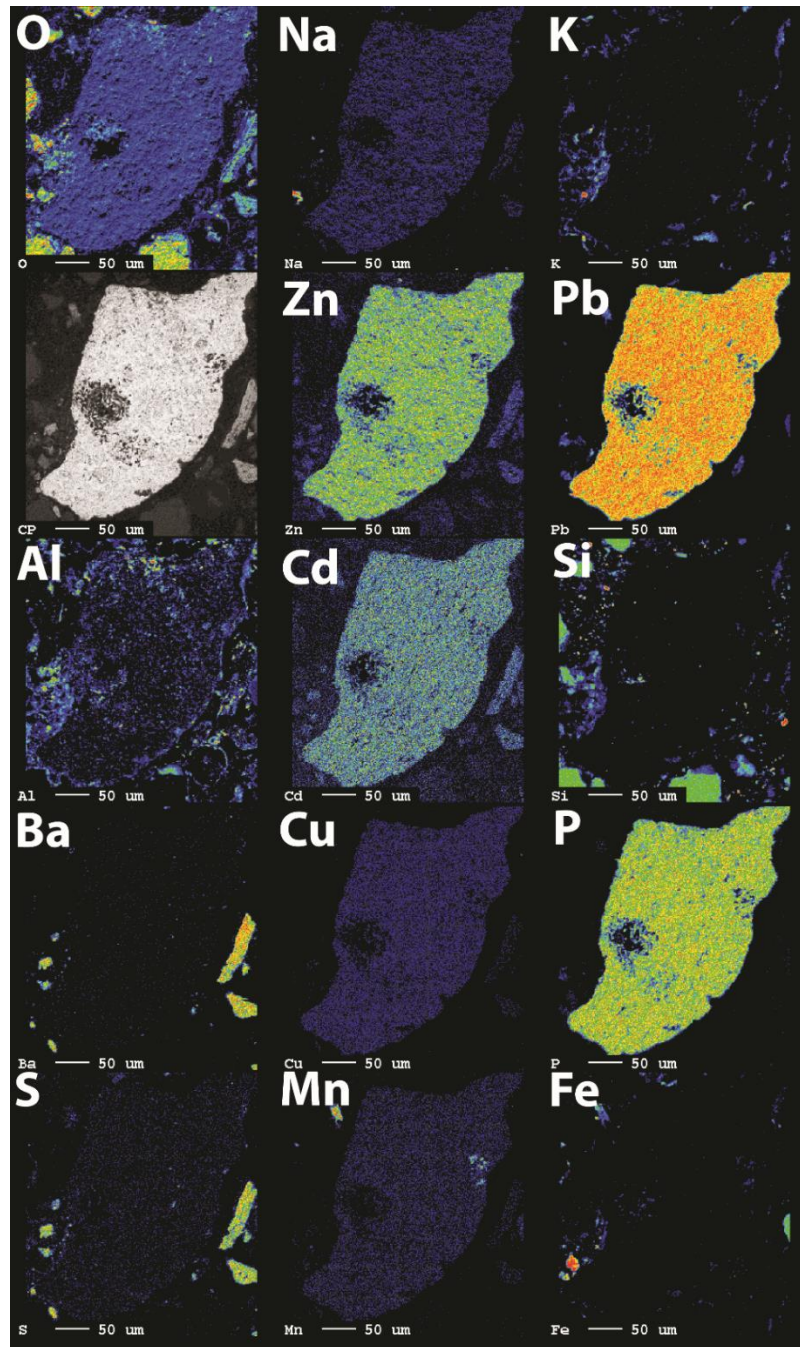


Figure 5.20: Elemental map showing Cd- bearing Pb-Zn phosphate (Gun 9). The colour scale reflects the intensity, red and yellows are the highest and blue the lowest intensity. The presence of Na is considered to be from spectral interference from Zn.

5.3.3 Mineralogy Summary Table

A summary mineralogical compositions, of both the XRD and EMP analysis, of all the Gunnerside Gill samples are shown in Table 5.5.

Table 5.5: XRD results for mine wastes (Gun 1 to Gun 8) and sediments (Gun 9 and Gun 10) from Gunnerside Gill (XXX = >70%, XX = 10-25%, X = minor component <10%, x_g = individual grains identified by EMP)

| | Quartz | Barite | Calcite | Clay | Fluorite | Galena | Sphal. | Ceru. | Fe Oxi | Pb/Zn Phosp. | Pyrite | Smiths. |
|--------|--------|----------------|---------|----------------|----------|----------------|----------------|----------------|----------------|----------------|----------------|----------------|
| Gun 1 | XXX | X | X | X | | | | X | X _g | | X _g | |
| Gun 2 | XXX | X | X | XX | X | x _g | | X _g | X _g | | | |
| Gun 3 | XXX | X | | X | XX | X | x _g | | | | X _g | |
| Gun 4 | XXX | X | X | X | X | | | | X _g | | | |
| Gun 5 | XX | XX | | x _g | XX | X | X | X _g | X _g | | X _g | |
| Gun 6 | XXX | x _g | | X | X | X | | X _g | | | X _g | |
| Gun 7 | XXX | XX | | XX | XX | X | X | | X _g | | X _g | |
| Gun 8 | XXX | XX | | X | X | | X | X _g | | | | |
| Gun 9 | XXX | X | | X | X | | X | | X _g | X _g | | |
| Gun 10 | XXX | X | | X | | | | X _g | X _g | | X _g | X _g |

* Sphal – sphalerite, ceru – cerussite, Fe oxi - Fe oxyhydroxides, smiths – smithsonite

Galena and sphalerite were both present in half of the samples recovered, although not the same samples. Cerussite was only identified in Gun 1 by XRD, but it was also suggested to be present in several other samples using EMP analysis. Pyrite and Zn-, Cd- and Cu- bearing Fe oxyhydroxides were observed by EMP in the majority of the samples. A single Pb/Zn phosphate grain, possibly pyromorphite (Pb₅(PO₄)₃Cl), was found in Gun 9 and one grain of Zn oxide or possibly carbonate was observed in Gun 10 also by elemental mapping techniques.

Many of the metallic-element bearing grains were observed to have weathering rims and/or coatings of clay when studied using the EMP. This would imply a reduction in reaction or weathering rates as the mineral surfaces

are not readily available for environmental chemical reactions, depending upon the secondary minerals formed. If the secondary minerals included oxyhydroxides, these could be more reactive than the sulfide but at the same time these weathering rims still offer some protection to the remaining metallic elements within the core. Fluorite and clay (determined by XRD) were present in the majority of the samples and calcite was only noted to be present in some of the more upstream samples.

None of the samples had the same mineralogical composition, making the prediction of the overall behaviour of the metallic elements at Gunnerside Gill difficult. This is likely to be a reflection of different origins of the mine wastes and different weathering rates and conditions. Galena was found to be present by XRD in over half of the mine waste samples but was absent from the sediment samples. Cerussite was noted to be present in several of the samples by EMP analysis of individual grains, which is likely to be present in Gunnerside Gill as a result of the weathering of galena.

Sphalerite was recorded in four of the waste samples and one of the alluvial sediment samples. The highest concentration of sphalerite was present in the sample, Gun 7, a mine waste sample recovered downstream of Sir Francis Level.

Iron oxides were also identified by EMP analysis and were recorded in seven of the samples including both the mine wastes and sediments. Pyrite was found to be slightly less common than the Fe oxyhydroxides but was also present in both the waste and sediment samples. The other interesting minerals noted within the samples include potential smithsonite, a secondary weathering product of sphalerite, observed by EMP in Gun 10.

There are similarities between the compositions of the mine tailings and sediments, which is to be expected as they are transported and redistributed along the length of the gill. The highest concentrations of galena and sphalerite were found to be present in the central portion of Gunnerside Gill, in the vicinity of Sir Francis Level.

5.4 Column Experiment

5.4.1 Column Samples

Three of the waste rock samples (Gun 1, Gun 2 and Gun 3) and one floodplain sediment sample (Gun 9) were subjected to column leaching experiments (described in Section 4.3), the results of which are presented below. Gun 1 to 3 are representative of the mine waste piles at Gunnerside Gill. These were recovered from the northern section of the study area and comprise tailings/waste rock associated with the Old Gang and Lowanthwaite mines. Gun 9, on the other hand, was located downstream in the study area, near the village of Gunnerside. It comprises overbank floodplain sediments downstream of the mining areas, which is considered to represent a potential depositional area for the transported mine wastes. The mine waste samples and sediment sample represent different parts of the weathering cycle and mobilisation of the materials within the Gunnerside Gill fluvial system. The sediments are likely to have been greatly influenced by physical transport of mine wastes down the catchment over since the mining activities ceased.

5.4.2 Leachate Volume, pH and Eh

Following the initial 'wash out' phase the pH of the columns remained relatively stable (Figure 5.21). The leachate in Gun 1 always displayed the highest pH, while that in Gun 9 nearly always recorded the lowest (Table 5.6). The leachate in Gun 2 and Gun 3 had similar pH values throughout the course of the experiment. Although the pH of the blank solution (deionised water) dropped around week 23 (as detailed in Section 4.3) the pH values of the column leachates remained stable and exhibited a buffering response to the drop.

The columns and leachate were not in a closed system and therefore were able to equilibrate with the surrounding atmosphere. There are some general trends that can be observed. Gun 9 often has the highest Eh and Gun 1 often has the lowest Eh, this is opposite to the pH results.

Table 5.6: Average column leachate pH values

| | Min | Mean | Median | Max |
|--------------|-----|------|--------|-----|
| Blank | 5.5 | 6.8 | 7.0 | 7.7 |
| Gun 1 | 6.4 | 7.1 | 7.1 | 7.6 |
| Gun 2 | 6.3 | 6.8 | 6.9 | 7.1 |
| Gun 3 | 5.5 | 6.6 | 6.8 | 7.0 |
| Gun 9 | 4.4 | 6.5 | 6.7 | 6.9 |

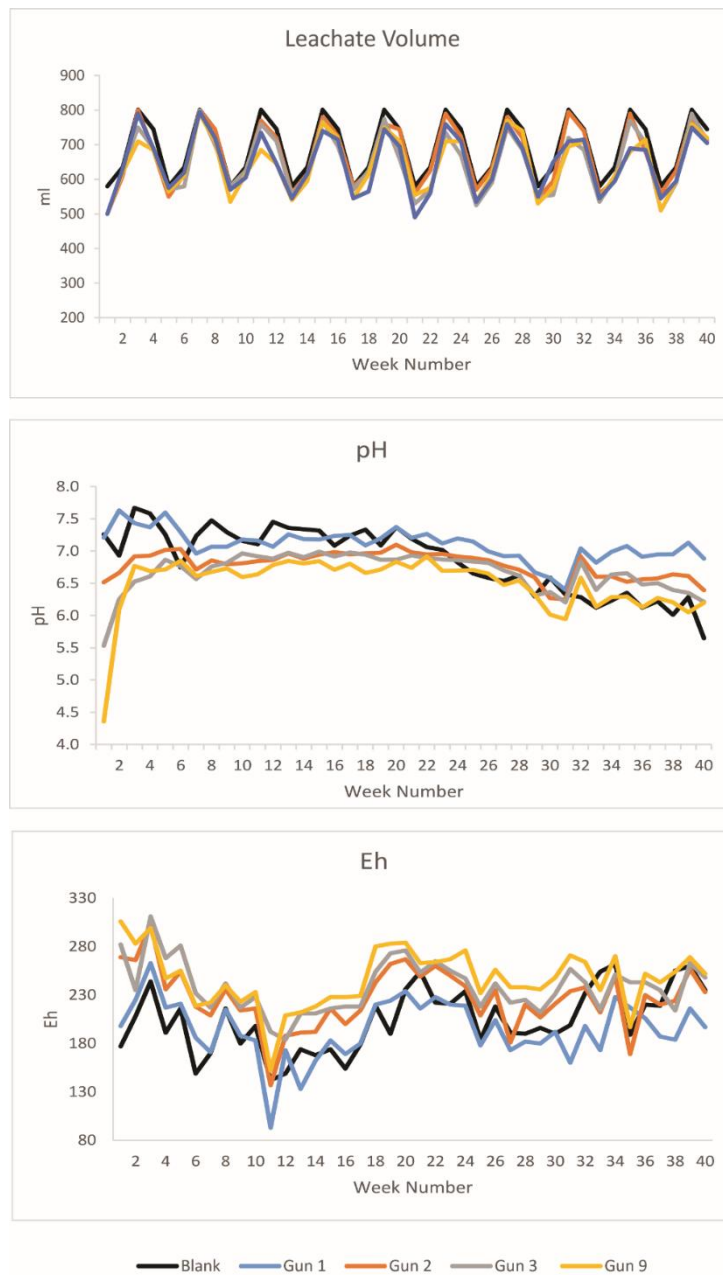


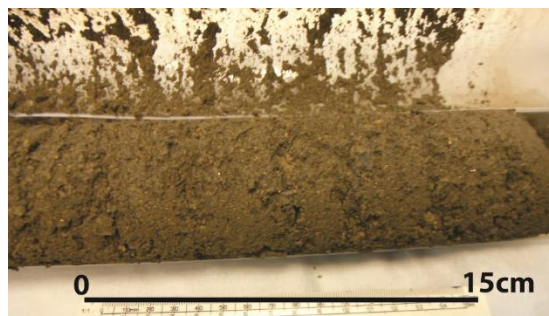
Figure 5.21: Volume, pH and Eh of column leachate including 'blank' (black line)

The volume of leachate recovered (coloured lines) generally reflected the volume added (black line). Loss by evaporation is considered to be minimal as shown by basic evaporation experiment detailed in Section 4.3.

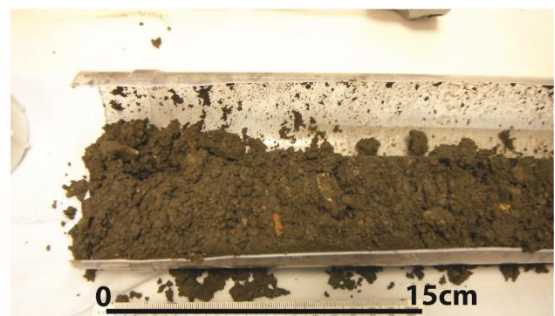
5.4.3 Physical Characteristics

5.4.3.1 Visual Description of Post Column Material

After the columns had been split open following completion of the 40 week column leaching experiment, photographs were taken of the post experimental solids and the colours were recorded using a Munsell colour chart, as shown in Figure 5.22. The post experimental material was relatively homogenous in colour and did not vary much along the length of the column.



a) CGun 1 - 7.5YR-3/2 Dark brown



b) CGun 2 - 7.5YR-2.5/1 Black



c) CGun 3 - 5YR-4/1 Grey



d) CGun 9 - 5YR-3/1 Very dark grey

Figure 5.22: Post column solids with Munsell colour chart detail

5.4.3.2 PSD

The triplot (Figure 5.23) illustrates that all the samples predominantly comprise a mixture of silt and sand with generally less than 6 % clay. CGun 1 showed a reduction in sand size grains from 63.5 % (Gun 1) to 55.1 % in the post column

solid, this coincided with a slight increase in both the silt and clay fractions. The proportions within CGun 2 and CGun 3 remained largely the same as the pre-column solids. CGun 9 recorded a slight decrease in the silt fraction and an increase in the sand fraction.

Table 5.7: Pre and post column particle size distribution data (%)

| Sample | Clay | | Silt | | Sand | |
|--------|------|------|-------|------|------|------|
| | Pre | Post | Pre | Post | Pre | Post |
| Gun 1 | 4.12 | 6.0 | 32.34 | 38.8 | 63.5 | 55.1 |
| Gun 2 | 5.9 | 7.1 | 49.6 | 57.0 | 44.6 | 35.9 |
| Gun 3 | 4.1 | 5.5 | 51.2 | 50.2 | 44.7 | 44.3 |
| Gun 9 | 3.4 | 3.9 | 43.1 | 40.0 | 53.6 | 52.1 |

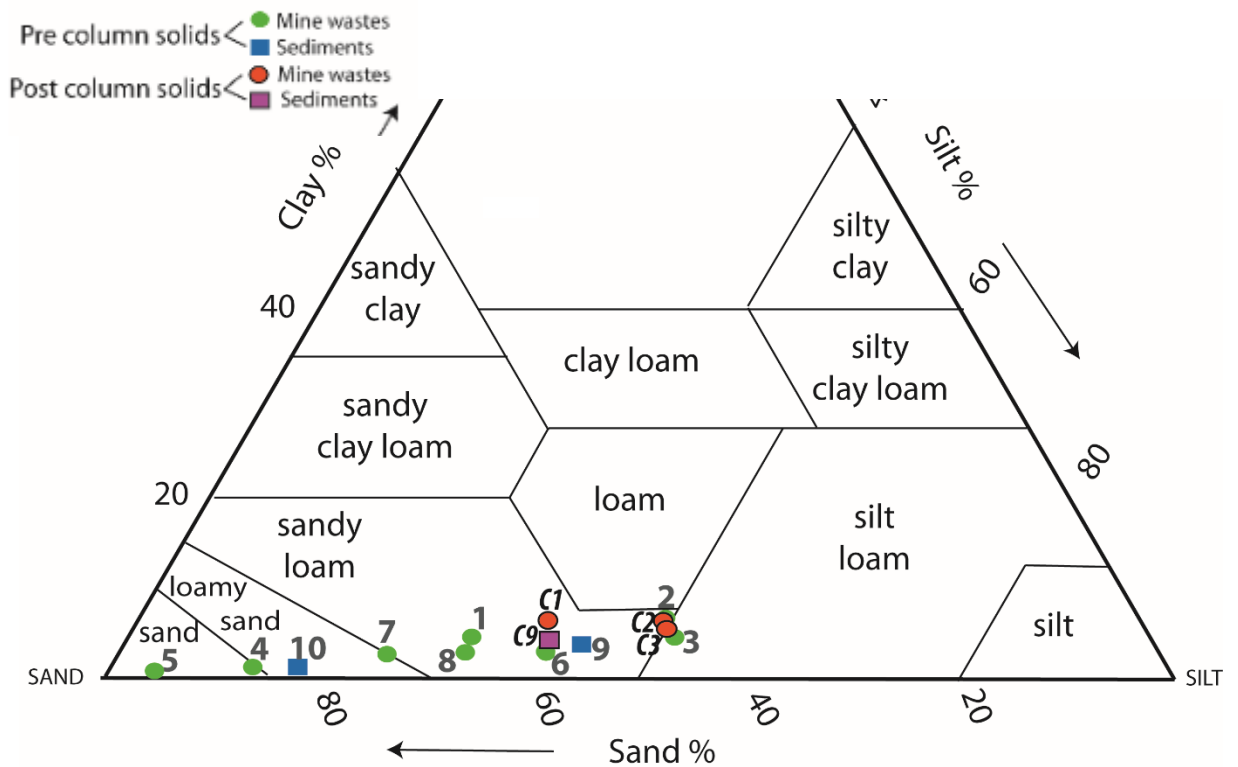


Figure 5.23: Post column solids particle size in comparison to pre-column experiment solids (plot produced using Graham and Midgley 2000)

5.4.4 Leachate Chemistry

5.4.4.1 ICP

The column leaching data for 40 week experiment for the various metallic elements are summarised in Figures 5.24 to 5.26.

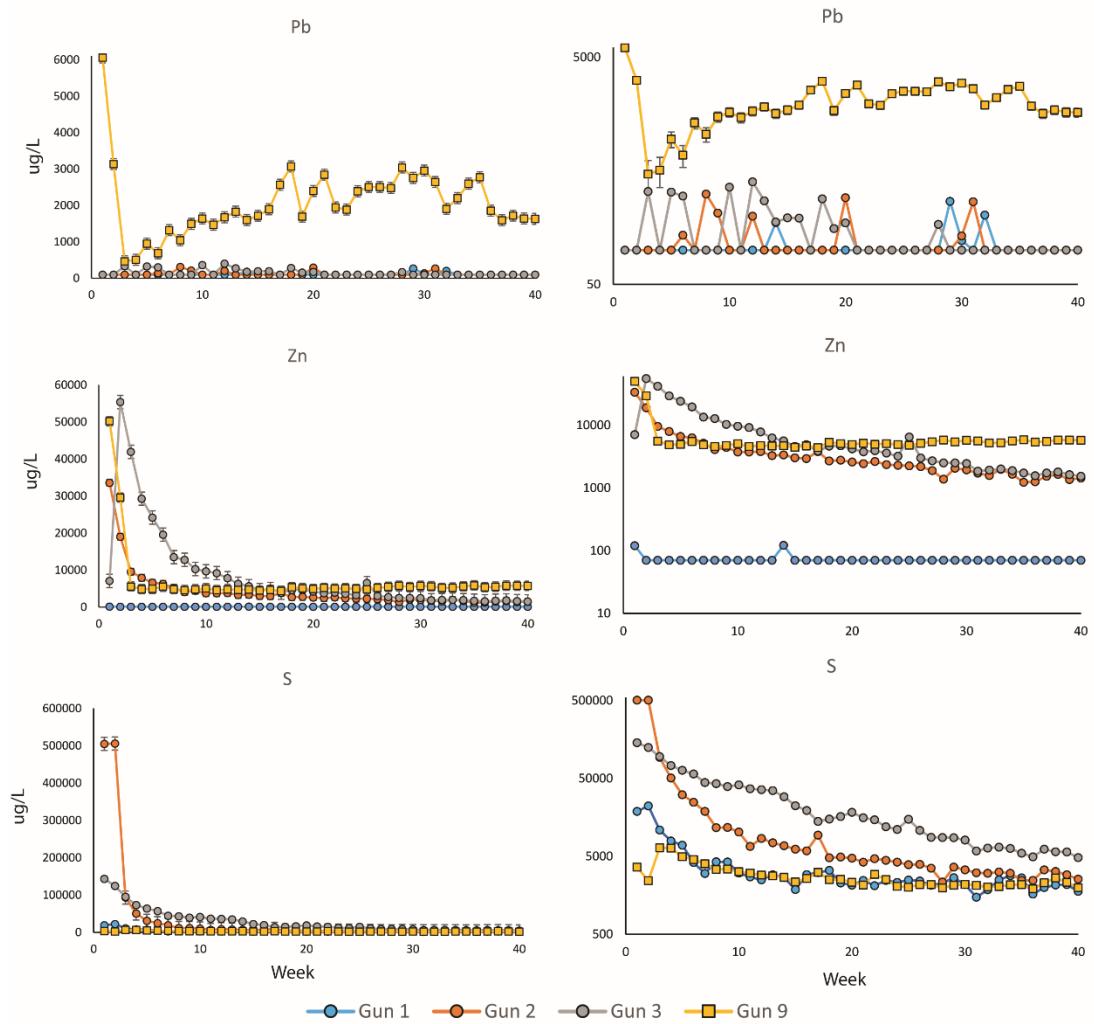


Figure 5.24: Column leachate ICP data for Pb, Zn and S ($\mu\text{g/L}$). Normal scale on the left and logarithmic scale on the right.

As shown in Figure 5.24 Pb concentrations throughout the 40 weeks generally remained consistently low in Gun 1, Gun 2 and Gun 3, whereas those in Gun 9 were significantly higher. After initial peaks in weeks 1 and 2, the Gun 9 Pb concentration dropped to $460 \mu\text{g/L}$ in week 3. Following this, Pb concentrations increased steadily to between $1,670$ and $3,070 \mu\text{g/L}$, remaining relatively stable at around $1,700 \mu\text{g/L}$ from week 36 to week 40.

The Zn concentrations in Gun 1 remained low throughout the whole 40 weeks. Gun 2 had an initial concentration of $33,500 \mu\text{g/L}$, which then reduced to $8,000 \mu\text{g/L}$ by week 3. Gun 3 and Gun 9 show the highest initial concentration of $55,000$ and $50,200 \mu\text{g/L}$ respectively, Gun 3 then reduced until around week

12 when it plateaus at around 8,000 $\mu\text{g/L}$ for the remainder of the experiment. Gun 9 reduced to around 4,800 $\mu\text{g/L}$ around week 4 and generally remained between 4,700 and 5,700 $\mu\text{g/L}$ for the remaining weeks.

The concentrations of S within Gun 1 peaked around 22,600 $\mu\text{g/L}$ in week 2 then reduced to 7,000 $\mu\text{g/L}$ in week 5, further gradually decreased to around 2,500 $\mu\text{g/L}$ from week 19 to week 40. Sulfur concentrations in Gun 2 peaked at around 505,000 $\mu\text{g/L}$ in the first two weeks, then reduced to 10,000 $\mu\text{g/L}$ by week 10. After week 10 the concentration again gradually decreased to 3,500 $\mu\text{g/L}$ in week 27 and then to 2,500 $\mu\text{g/L}$ around week 35. Initial concentrations of S peaked in Gun 3 at 143,300 $\mu\text{g/L}$ in week 1, then reduced to 43,000 $\mu\text{g/L}$ by week 7. There is a more gradual reduction to between 15,000 to 20,000 $\mu\text{g/L}$ by week 20 and then around 5,000 to 6,000 $\mu\text{g/L}$ from week 30 to week 40. Concentrations in Gun 9 peak at 6,400 $\mu\text{g/L}$ in week 3 and then reduced to around 4,500 $\mu\text{g/L}$ by week 5, and remained relatively stable for the rest of the experiment.

Gun 1 and Gun 2 show similar trends for Mn, initial concentrations peaked at 70 $\mu\text{g/L}$ in week 1 and 200 $\mu\text{g/L}$ in week 2 respectively, as shown in Figure 5.25. Concentrations reduced in week 10 to around 2 $\mu\text{g/L}$ and remained low for the remainder of the experiment. The peak concentration for Mn in Gun 3 was in week 2 (1,400 $\mu\text{g/L}$) and then reduced to around 50 $\mu\text{g/L}$ by week 20 and 2 $\mu\text{g/L}$ by week 26. Gun 9 has an initial concentration of 340 $\mu\text{g/L}$ in week 1, which decreased to 35 $\mu\text{g/L}$ by week 3. Concentrations of Mn then increase to around 420 $\mu\text{g/L}$ in week 13 before remaining between 260 and 320 $\mu\text{g/L}$ until week 33. After this the concentration of Mn in Gun 9 gradually reduced to around 70 $\mu\text{g/L}$ in week 40.

Concentrations of Fe were generally low (<100 $\mu\text{g/L}$) in all of the samples, with sporadic peaks in Gun 2 and Gun 3 of between 210 to 430 $\mu\text{g/L}$.

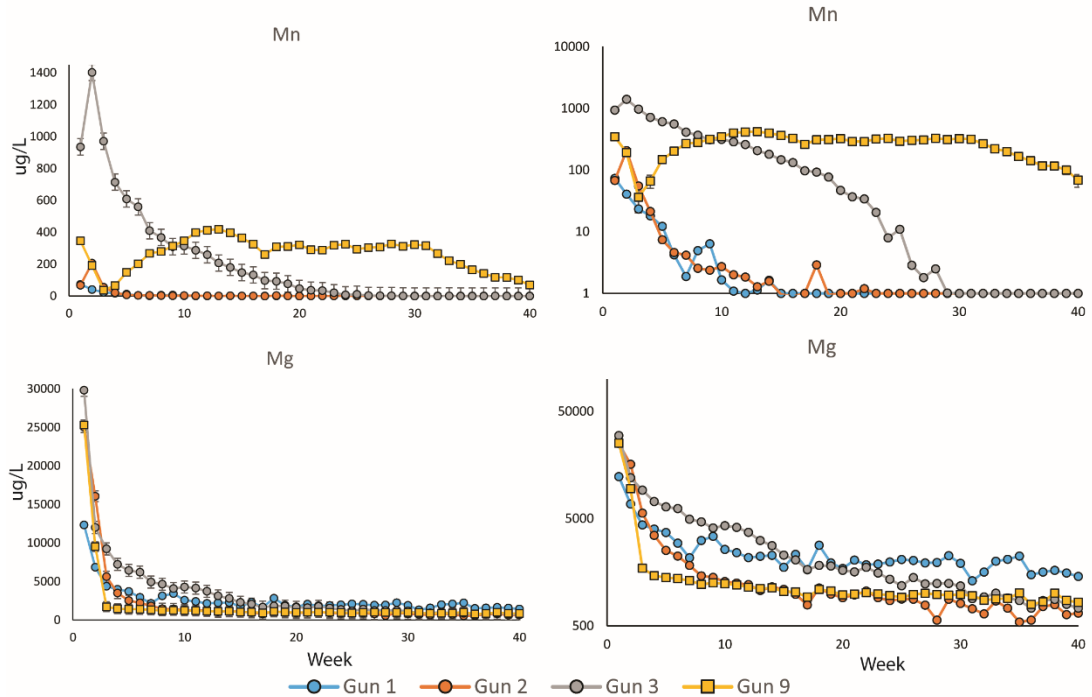


Figure 5.25: Column leachate ICP data for Mn and Mg ($\mu\text{g/L}$). Normal scale on the left and logarithmic scale on the right.

As shown in Figure 5.26 an initial peak concentration of 64,000 $\mu\text{g/L}$ Ca was recorded in Gun 1, this reduced to 24,000 $\mu\text{g/L}$ in week 6 and then remained between 15,000 to 25,000 $\mu\text{g/L}$ until week 40. Gun 2 showed a similar pattern, with an initial wash out concentration of 390,000 $\mu\text{g/L}$, reducing to 25,000 $\mu\text{g/L}$ in week 10 and then generally staying between 14,000 to 23,000 $\mu\text{g/L}$ for the rest of the experimental period. Gun initially 3 peaked at 145,300 $\mu\text{g/L}$ in week 1, reducing to around 20,000 $\mu\text{g/L}$ in week 17. Concentrations of Ca then remained between 10,000 and 20,000 $\mu\text{g/L}$ from week 18 to week 40. The concentration of Ca in Gun 9 started at 189,700 $\mu\text{g/L}$, before rapidly reducing to 8,600 $\mu\text{g/L}$ in week 3 and remaining between 6,500 and 8,500 $\mu\text{g/L}$ until week 40.

Concentrations of Ba (Figure 5.26) in Gun 1, Gun 2 and Gun 3 were initially around 50 $\mu\text{g/L}$ in week 1, and then increased to 800 $\mu\text{g/L}$ (week 35), 290 $\mu\text{g/L}$ (week 40) and 400 $\mu\text{g/L}$ (week 34) respectively. The initial concentration of Ba

in Gun 9 peaked at 7,000 µg/L in week 1, rapidly reducing to 760 µg/L in week 3 and remaining around 700 µg/L until week 40.

Magnesium had an initial concentration of 12,000 µg/L in Gun 1 in week 1, which then reduced to 2,500 µg/L in week 10. Concentrations then decreased further to between 1,500 to 2,300 µg/L until week 40. Gun 2 recorded a peak concentration of 25,000 µg/L in week 1, rapidly reducing to 2,200 µg/L in week 6. The concentration of Mg reduced further but generally remained between 650 and 1,400 µg/L for the remaining time. Similarly Gun 3 had a peak of 29,800 µg/L in week 1, which reduced to around 6,200 µg/L in week 6. Concentrations reduced further to between 800 to 1,800 µg/L until the end of the experiment. Gun 9 had an initial concentration of 25,300 µg/L before reducing to 1,700 µg/L in week 3 and generally staying between 820 to 1,300 µg/L until week 40.

For Al concentrations in Gun 1 and Gun 2 remained below 200 µg/L for the whole experiment. An initial peak of 119,000 µg/L was noted in Gun 3, which then rapidly reduced to 1,600 µg/L in week 3 and again to 210 µg/L in week 10 and remained below 200 µg/L until week 40. Gun 9 had an initial Al concentration of 940 µg/L, reducing to around 500 µg/L by week 7 and then gradually further reducing to 200 µg/L by the final week of the experiment.

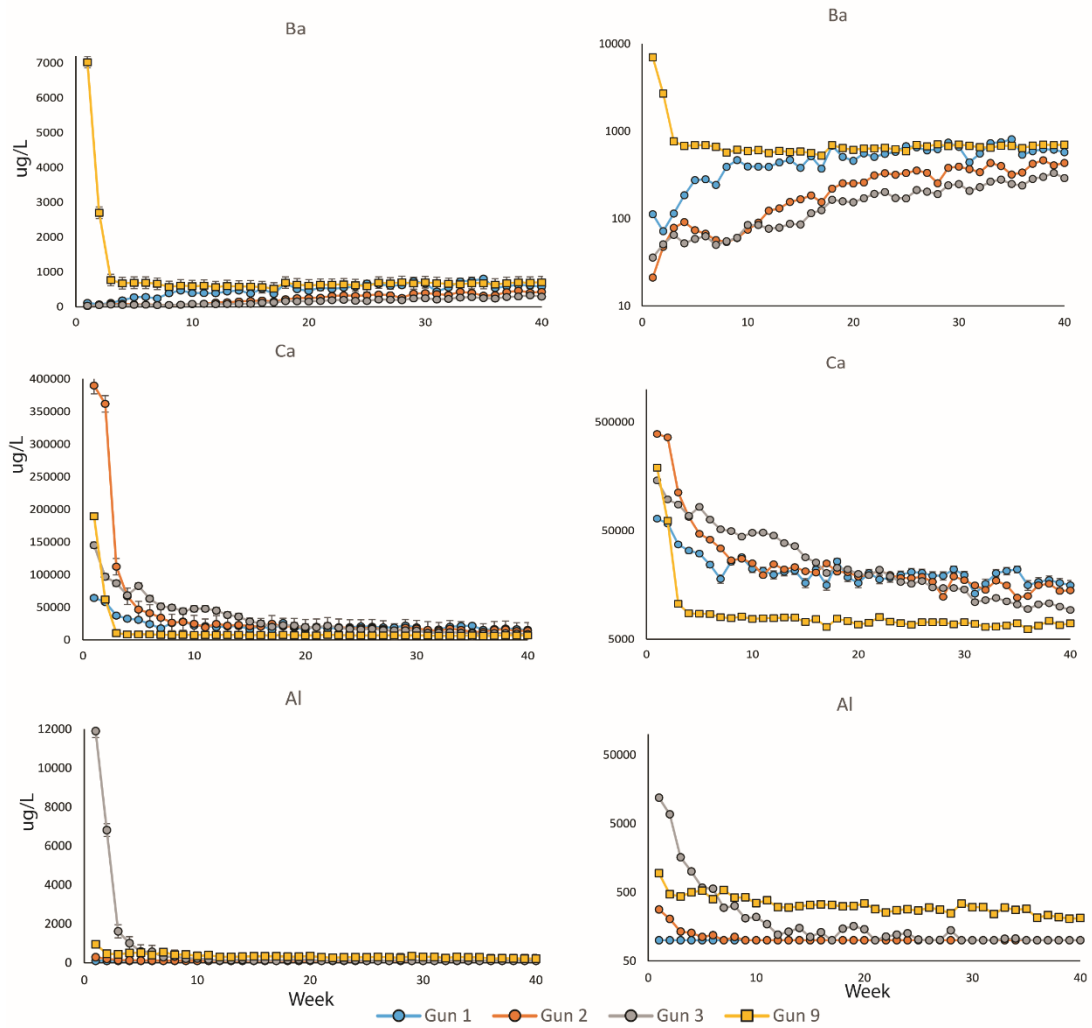


Figure 5.26: Column leachate ICP data for Ba, Ca and Al ($\mu\text{g/L}$). Normal scale on the left and logarithmic scale on the right.

The concentrations of Cl^- were low and did not show any significant trends. NO_x showed an initial peak in week 1 in Gun 9 but rapidly reduced to a background level, similar to the other samples (Figure 5.27). Sulfate showed an initial peak in Gun 2 and Gun 3 before stabilising around week 15, similar to the trend for S as denoted in Figure 5.24.

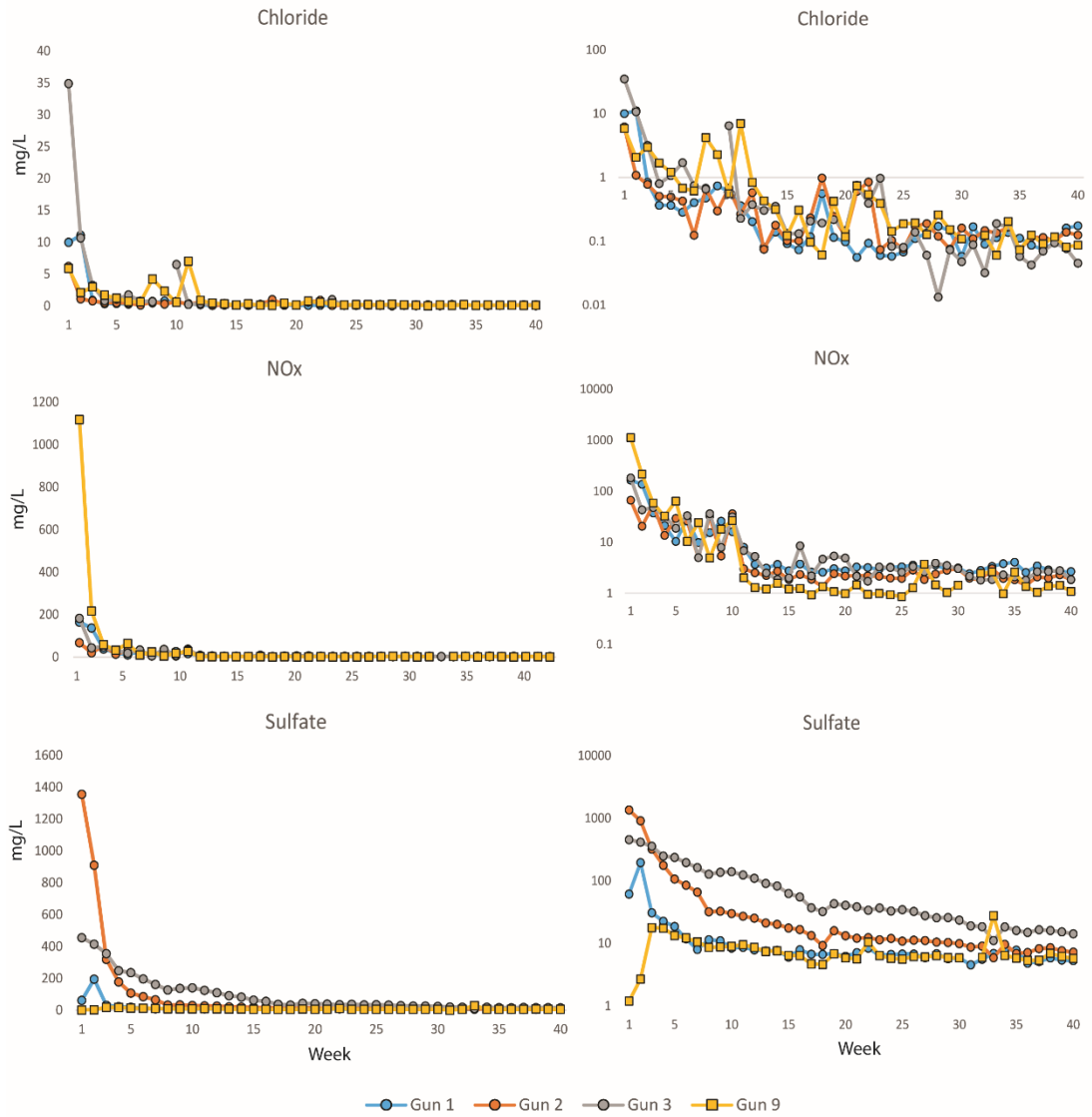


Figure 5.27: Column leachate anion data for chloride, NOx and sulphate (mg/L). Normal scale on the left and logarithmic scale on the right.

Following the completion of the column leachate experiment the post column solids were analysed by EMP, total digestion, and sequential extraction as detailed in the following sections.

5.4.5 Electron Microprobe

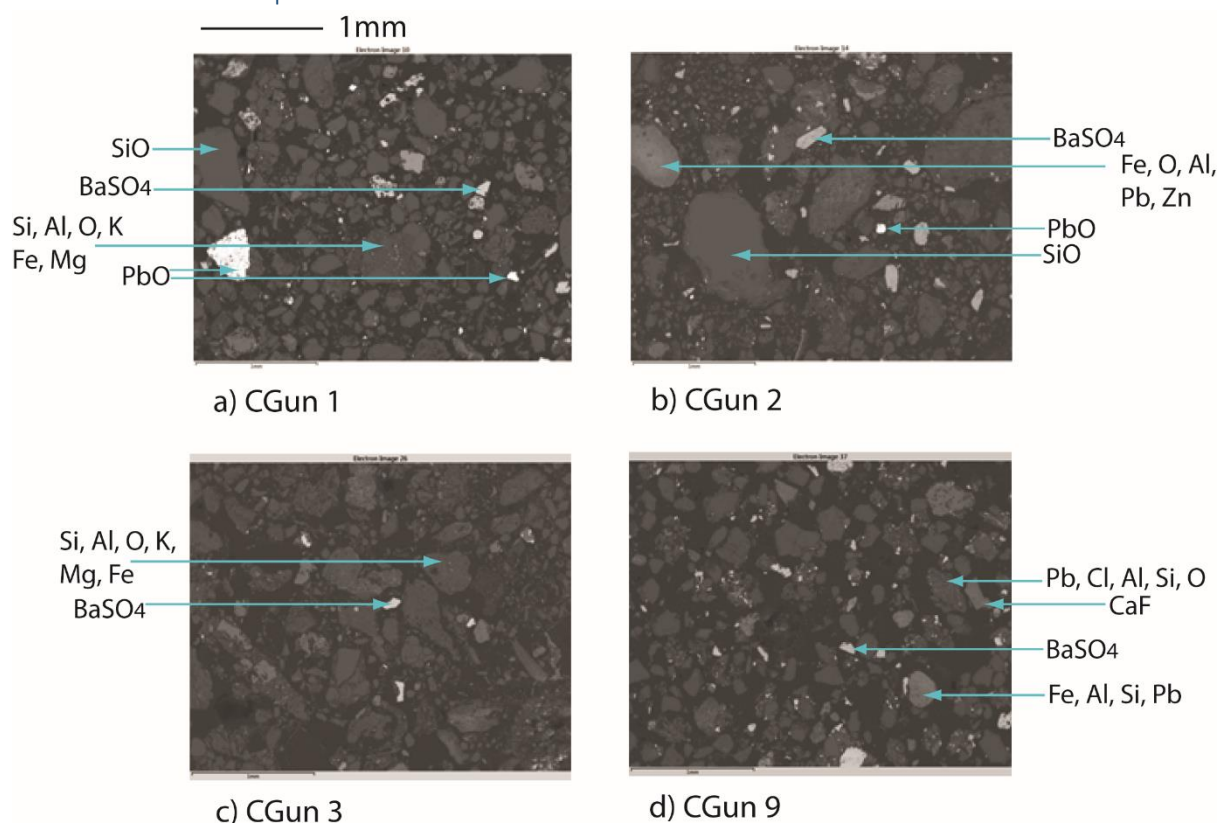


Figure 5.28: General view backscattered EMP photomicrographs of post column solids

CGun 1 and CGun 9 (Figure 5.28) showed a relatively uniform texture and composition, and generally comprised grains of quartz, calcite, composite grains of clay and bright material. CGun 2 and CGun 3 appeared to have a larger range of grain sizes but were compositionally similar to CGun 1 and CGun 9.

The minerals in CGun 1 included quartz, clay minerals, barite, Fe oxyhydroxides with Zn or Pb, and Pb oxide/carbonate. The grain in Figure 5.29 comprises a Pb oxide/ carbonate, which appears to be degrading based on the cracking and pitted texture. The weathering potential may have been reduced given the presence of clay minerals around the edge of the grain.

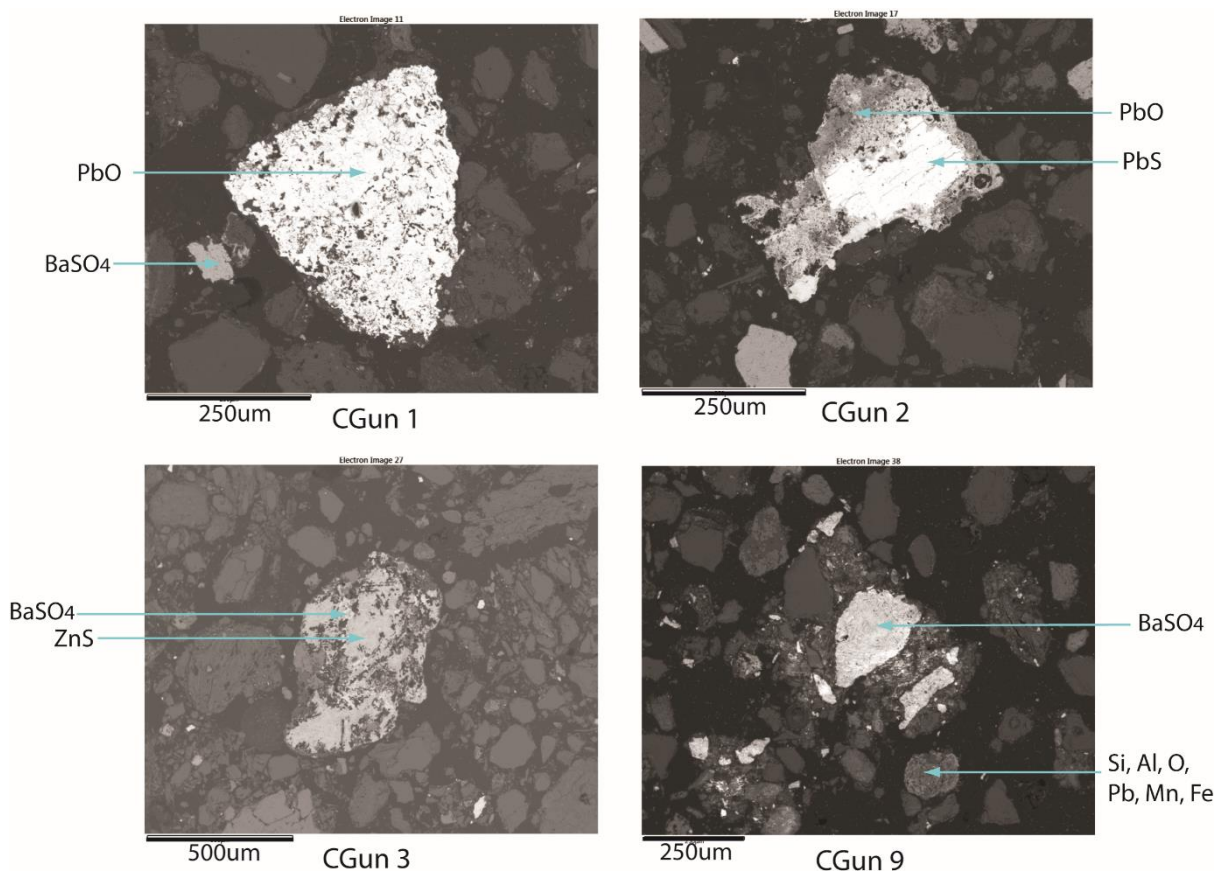


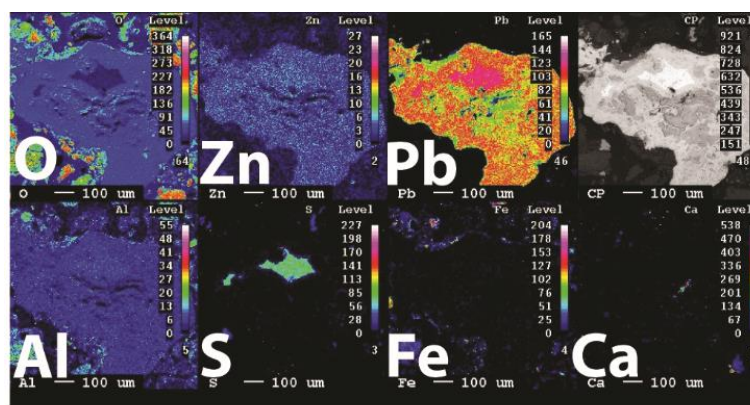
Figure 5.29: Backscattered EMP photomicrographs of post column solids showing grains of interest in each sample

CGun 2 generally comprised quartz, barite, fluoride, clays, clays with Zn/Mn/Fe, Pb oxide/carbonate, Fe oxyhydroxide with Zn and Pb, galena and sphalerite. Figure 5.29 shows a core of galena weathering to Pb oxide/carbonate around the edge, as denoted by the darker grey colour.

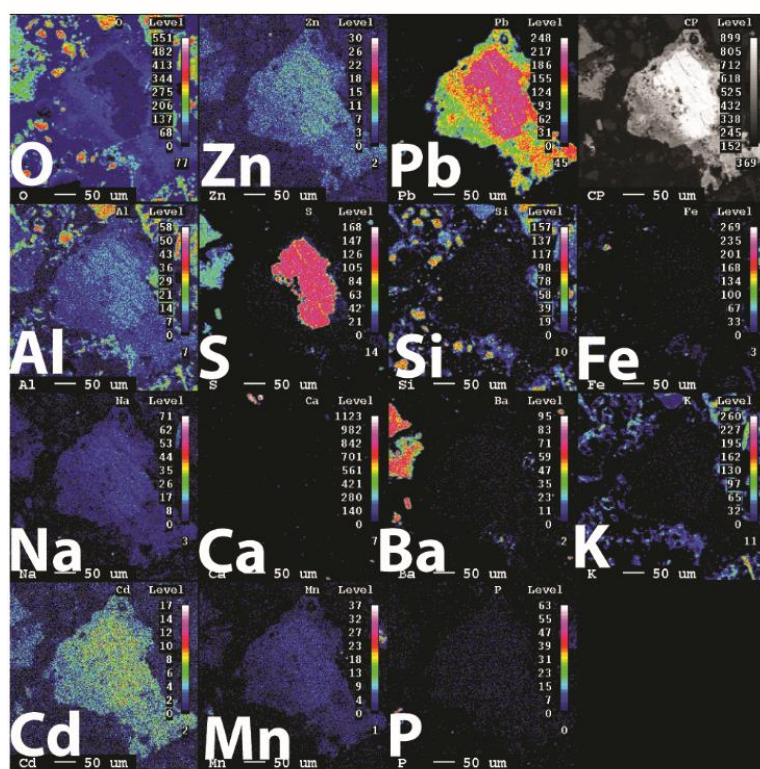
Minerals observed in CGun 3 again included mainly quartz, clay, fluorite, barite, and sphalerite. The grain in Figure 5.29 comprised a grain of sphalerite and barite and appeared to show some weathering textures.

CGun 9 mainly comprised quartz, clays, barite, pyrite, galena, Fe oxyhydroxide with Mn and Pb and Pb phosphate. The Pb phosphate grain can be seen at the centre of the photo in Figure 5.29.

Elemental mapping was undertaken on selected bright grains in all the post column solid samples. Due to time constraints not all elements were mapped for each sample.



-100um
CGun 1



-50um
CGun 2

Figure 5.30: Elemental maps from CGun 1 (above) and CGun 2 (below). The colour scale reflects the intensity, red and yellows are the highest and blue the lowest intensity. The presence of Na is considered to be from spectral interference from Zn.

CGun 1 was noted to have a grain with a core of galena surrounded by Pb oxide or carbonate (Figure 5.30). CGun 2 also had a grain with a galena core surrounded by Pb oxide or carbonate. The galena core also included concentrations of Cd, Al and Zn. The whole grain had a thin clay coating around the edge.

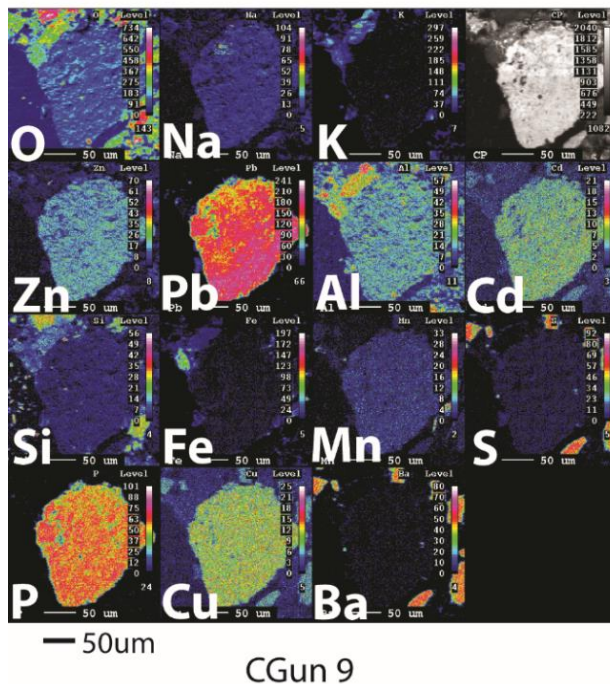
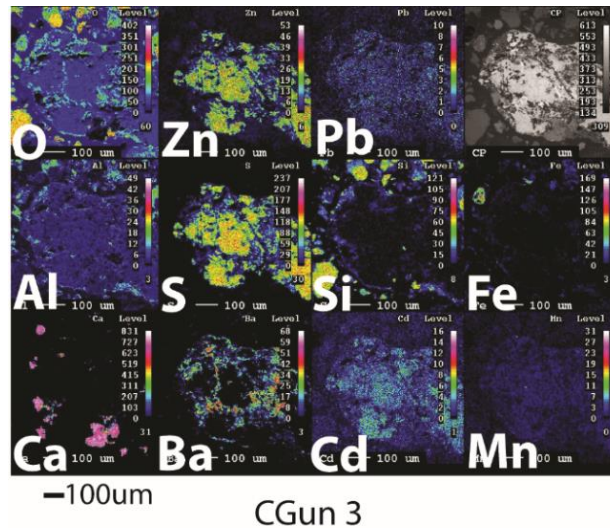


Figure 5.31: Elemental maps from CGun 3 (above) and CGun 9 (below). The colour scale reflects the intensity, red and yellows are the highest and blue the lowest intensity. The presence of Na is considered to be from spectral interference from Zn.

A sphalerite grain was mapped in CGun 3, as shown in Figure 5.31. The sphalerite also included concentrations of Cd and was surrounded by barite

with a thin outer clay rim. As with the pre-column solids the post-column solids in CGun 9 also contained Pb phosphate grains, with concentrations of Zn, Al, Cd and Cu noted.

The grains in the pre and post column solids were comparable, with similar textures and compositions found in both sample sets.

5.4.6 Total Digestion

Total digestions of the post column leachate solids, Table 5.8, were undertaken to allow for comparisons to the pre column solids.

Table 5.8: Total digestion concentrations of the post column solids (CGun) and pre column solids (Gun) for comparison (mg/kg)

| | Pb | Zn | Cd | Al | Ba | Ca | Cu | Fe | Mg | Mn | S | Na | K | Total |
|---------------|-----------|-----------|-----------|-----------|-----------|-----------|-----------|-----------|-----------|-----------|----------|-----------|----------|--------------|
| | (mg/kg) | | | | | | | | | | | | | C % |
| CGun 1 | 55400 | 4010 | 20 | 36400 | 16900 | 12000 | 88 | 39000 | 2930 | 1620 | 5140 | 1200 | 9000 | 1.67 |
| Gun 1 | 70000 | 4100 | 15 | 34200 | 11900 | 13200 | 59 | 35900 | 2860 | 1600 | 4150 | 1230 | 8520 | 1.67 |
| CGun 2 | 12100 | 7530 | 40 | 44500 | 12100 | 37600 | 181 | 16700 | 2500 | 615 | 6920 | 1600 | 13600 | 1.58 |
| Gun 2 | 17900 | 12600 | 97 | 38400 | 13700 | 34300 | 119 | 26400 | 2590 | 80 | 5720 | 1330 | 11200 | 1.57 |
| CGun 3 | 738 | 4160 | 35 | 72500 | 11200 | 31100 | 33 | 27900 | 2800 | 39 | 6480 | 2740 | 17900 | 2.52 |
| Gun 3 | 1840 | 8100 | 49 | 65200 | 7380 | 51600 | 76 | 15700 | 3350 | 47 | 7160 | 2290 | 18900 | 2.57 |
| CGun 9 | 12300 | 3070 | 15 | 23800 | 11800 | 40800 | 76 | 2760 | 1510 | 29 | 4170 | 1480 | 6010 | 1.80 |
| Gun 9 | 8710 | 4950 | 17 | 22000 | 15900 | 39500 | 67 | 18500 | 1420 | 870 | 4760 | 1690 | 5690 | 1.89 |

Concentrations of Na, Cd, Cu, Mg and Mn remain very low. The highest concentration of Pb is recorded in CGun 1, which interestingly also records the highest concentrations of Fe and Mn. This is also true of the pre-column solids in Gun 1.

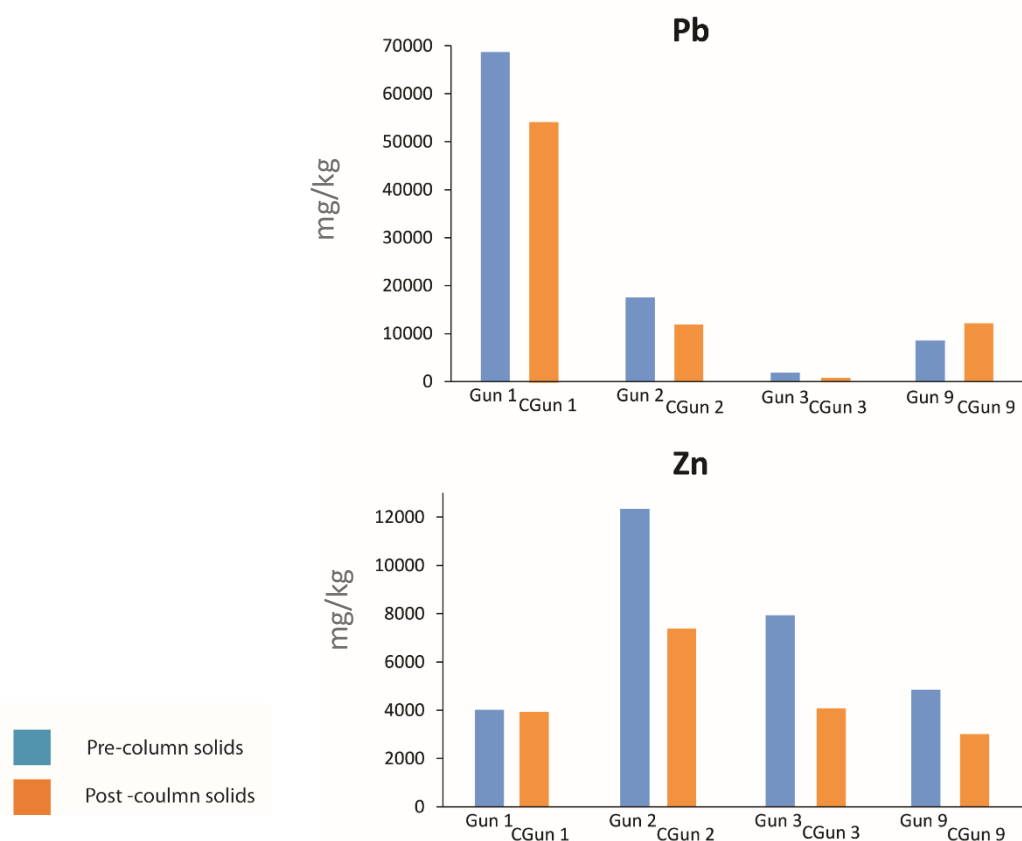


Figure 5.32: Pre (Gun) and post column (CGun) solid total digestion comparison for the key elements of concern Pb and Zn (mg/kg)

Figure 5.32 shows a comparison of the total concentrations of Pb and Zn between the pre column solids ('Gun') and the post column solids ('CGun').

With the exception of CGun 9 all of the post column solids showed a reduction in the concentration of Pb. The reductions ranged from 21 % in CGun 1, 32 % in CGun 2 and 60 % in CGun 3. CGun 9 increased by approximately 42 %, this is likely to be an effect of the inhomogeneity of the sample rather than an actual increase or decrease of Pb in the sample.

In all of the post column samples Zn was recorded at a lower concentration than in the pre column samples. This ranged from 2 % in CGun 1 to 49 % in CGun 3.

5.4.7 BCR Sequential Extraction

As with the pre column solids the proportion of Pb in the water step remained low and was <0.5 % in both the pre and post column solids. The relative proportions of Pb in CGun 1 showed a reduction in the residual (from 4 % to 2 %), oxidisable (from 4 % to 1 %) and reducible (28 % to 17 %) phases and a similar increase from 65 % to 8 % in the exchangeable fraction when compared to Gun 1. CGun 2 maintained relative proportions of Pb of 8 % in the residual fraction and 4 % in the oxidisable fraction in both the pre and post column solids. There was a slight increase of 4 % in the reducible fraction and a similar decrease of 4 % in the exchangeable fraction. The relative proportions of Pb in CGun 3 were comparable between the pre and post column solids for both the exchangeable and residual fractions. A decrease of 17 % to 9 % was noted in the oxidisable step and a similar increase of Pb from 17 % to 26 % was recorded in the reducible fraction. The changes in the relative proportions of Pb in all the fractions in CGun 9 were less than 3 %.

Similar to Pb the relative proportions of Zn in the water leaching step remained low, all below 2 %. There was little difference in the relative proportions of Zn between the pre and post column solids in Gun 1 and CGun 1, all were within 3 %. More notable changes were observed between Gun 2 and CGun 2. A 9 % reduction was recorded in both the exchangeable and reducible steps with similar increases of 9 % in both the oxidisable and residual fractions. The relative proportions of Zn in CGun 3 reduced in the exchangeable (from 24 % to 18 %) and residual (from 52 % to 22 %) fractions and increased in the reducible (6 % to 12 %) and oxidisable (from 17 % to 47 %) steps. This indicates a significant movement of Zn from the residual to oxidisable fraction. CGun 9 showed similar if less pronounced trends to CGun 3 with reductions of 37 % to 25 % and 21 % to 18 % in the exchangeable and residual phases respectively. The reducible and oxidisable steps showed slight increases of 1 % and 7 %, respectively.



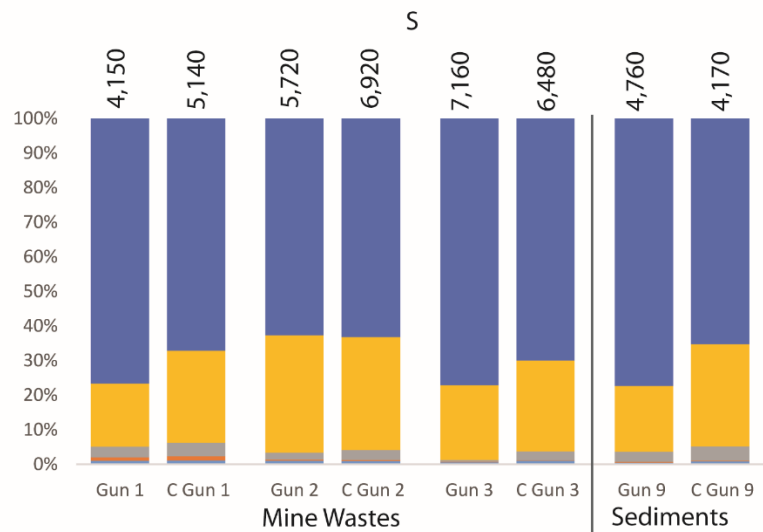
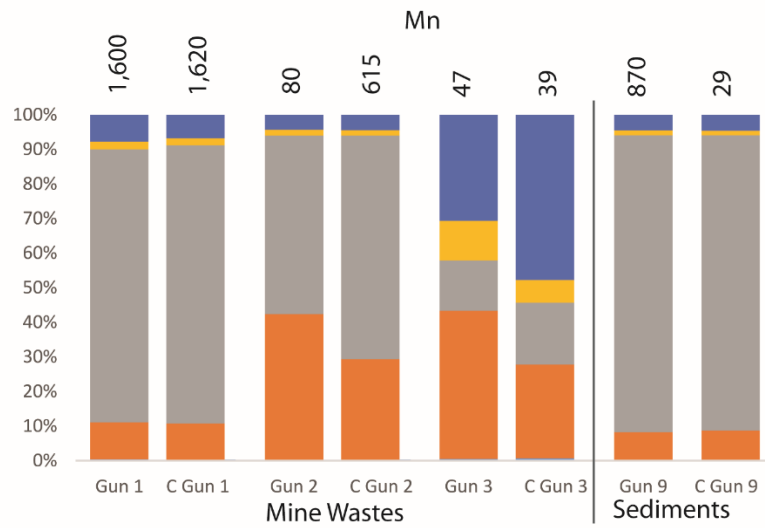
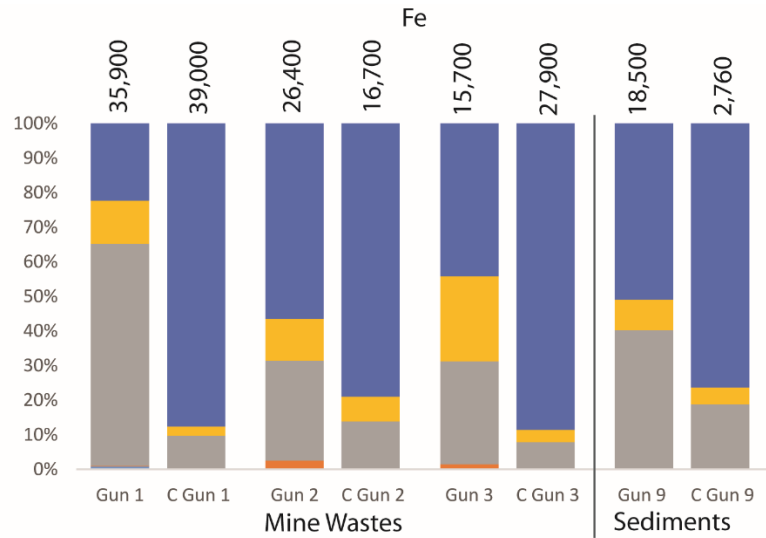
Figure 5.33: Pre and post column BCR data for Pb and Zn (total digestion concentration shown at top of column mg/kg)

Relative proportions of Fe in both the pre and post column solids in all four samples remained below 2 % in both the water and exchangeable fractions. In CGun 1 the relative proportion of Fe reduced between the pre and post column solid from 64 % to 10 % and 13 % to 3 % in the reducible and oxidisable fractions respectively. Conversely there was an increase of 66 % in the residual fraction. CGun 2 showed a similar trend with reductions of 15 % in the reducible and 5 % in the oxidisable fractions and an increase of Fe of 22 % in

the residual fraction. This trend continues in the remaining two samples, relative proportions of Fe reduce in both the reducible and oxidisable steps and increase in the residual fraction.

The pre and post column solids of CGun1 and CGun 9 showed very little variation of Mn across the five BCR steps. In CGun 2 the relative proportions of Mn essentially stayed the same in the water, oxidisable and residual fractions. Mn decreased by 13 % in the exchangeable step and similarly increased by 13 % in the reducible step. There was more variation across the steps between Gun 3 and CGun 3. Reductions in the relative proportions of Mn in the exchangeable (by 16 %) and oxidisable (by 4 %) fractions and increases of 4 % and 17 % in the reducible and residual fractions, respectively.

Relative proportions of S recorded little variation across all the samples in the water, exchangeable and reducible steps and in the remaining steps in CGun 2. In the three remaining samples S increased between 4 % (CGun 3) and 10 % (CGun 9) in the oxidisable fraction and increased a similar amount of 3 % (CGun 3) to 10 % (CGun 1) in the residual fraction.



■ Step 0 Water Sol
 ■ Step 1 Acid Sol
 ■ Step 2 Reducible
 ■ Step 3 Oxidisable
 ■ Residual

Figure 5.34: Pre and post column BCR data for Mn, Fe and S (total digestion concentration shown at top of column mg/kg)

5.5 Summary

- The particle size data of the <2 mm fraction indicates the samples generally comprise a mixture of silt and sand with less than 5 % clay;
- The results of the total digestion show that the highest concentrations of Pb were found within Gun 1 and Gun 5, and the highest Zn concentrations in Gun 5 and Gun 7;
- The correlations from the total digestions show a strong correlation between Zn and S, and no correlation between Pb and S;
- The BCR sequential extraction showed that Pb was present in the reducible fraction in half of the samples, again in half the samples Zn was mainly present in the exchangeable fraction, Mn was split between the exchangeable and reducible fractions, Fe was also mainly present in the reducible fraction, and S was largely present in the residual fraction;
- Galena and sphalerite were both present half of the samples recovered, although not the same samples. Cerussite was only identified in Gun 1 by XRD, but it was also found to be present in several other samples using EMP analysis. None of the samples had the same mineralogical composition, making the prediction of the overall behaviour of the metallic elements at Gunnerside Gill difficult. This is likely to be a reflection of different origins of the mine wastes and different weathering rates and conditions;
- The leachate from the column experiment in Gun 1 always displayed the highest pH, while that in Gun 9 nearly always recorded the lowest. Conversely Gun 9 often has the highest Eh and Gun 1 often has the lowest Eh;
- The column leachate experiment recorded low concentrations of Pb in Gun 1, Gun 2 and Gun 3. Interestingly after the initial peak and fall in concentration in Gun 9 Pb concentrations gradually increased for the remainder of the experiment, a trend that is also noted in for Mn in Gun 9. Concentrations of Zn and S show an initial 'wash out' effect in all samples before reducing for the rest of the experiment;
- The post column solids (CGun1 to CGun 3 and CGun 9) generally show a reduction in the metallic element concentrations present and there

were some variations of the relative proportions based on the results of the sequential extraction procedure.

Chapter 6

Results and Discussion of Pb and Zn Mobility and Control Mechanisms

Contents

| | |
|---|-----|
| Chapter 6..... | 183 |
| 6.1 Characterisation of Samples | 184 |
| 6.1.1 Particle Size | 184 |
| 6.1.2 Mineralogy | 185 |
| 6.1.2.1 Mine Waste Mineralogy..... | 185 |
| 6.1.2.2 Sediment Mineralogy..... | 187 |
| 6.1.3 Bulk geochemistry..... | 188 |
| 6.1.4 Solid Phase-Speciation of Metallic Elements | 188 |
| 6.1.5 pH of Solids and Column Leachate..... | 190 |
| 6.1.6 Comparison of Samples | 193 |
| 6.1.6.1 Gun 1 | 193 |
| 6.1.6.2 Gun 2 | 195 |
| 6.1.6.3 Gun 3 | 197 |
| 6.1.6.4 Gun 4 | 199 |
| 6.1.6.5 Gun 5 | 199 |
| 6.1.6.6 Gun 6 | 199 |
| 6.1.6.7 Gun 7 | 200 |
| 6.1.6.8 Gun 8 | 200 |
| 6.1.6.9 Gun 9 | 200 |
| 6.1.6.10 Gun 10..... | 202 |
| 6.1.6.11 Summary of Sample Comparison..... | 203 |
| 6.2 Comparison to Published Threshold Values | 208 |
| 6.2.1 Mine Wastes and Sediments | 208 |
| 6.2.1 Column Leachate..... | 210 |
| 6.3 Column Leachate vs EA Monitoring Data | 211 |
| 6.4 Geochemical Modelling | 217 |
| 6.4.1 Changes in pH | 221 |
| 6.5 Comparison to Previous Studies | 0 |
| 6.6 Controls on Weathering Reactions | 2 |

| | |
|--|----|
| 6.6.1 Eh-pH from Column Leaching Experiment..... | 3 |
| 6.6.2 pH from EA Monitoring Data | 7 |
| 6.6.3 Ficklin Classification | 9 |
| 6.6.4 Mineralogy | 10 |
| 6.6.5 Location of Mine Wastes and Impacted Sediments | 11 |
| 6.6.6 Grain Size | 14 |
| 6.6.7 Prediction of Metallic Element Mobility | 15 |
| 6.7 Comparison to Worldwide Drainage | 16 |
| 6.8 Summary | 19 |

Chapter 6 comprises the discussion of the results, starting with the characterisation of the samples (Section 6.1). Section 6.2 compares the results of the study to published threshold values and then compared to the EA water monitoring data for Gunnerside Gill (Section 6.3). Geochemical computer modelling is discussed in Section 6.4 and the results are compared to previous studies (Section 6.5). The controls on weathering reactions are considered in Section 6.6 and the study data are compared to worldwide drainage in Section 6.7. Finally, a summary is given in Section 6.8.

6.1 Characterisation of Samples

The first objective of this study was to characterise the solid phase speciation of the metallic elements present in the mine wastes and sediments. The composition of the samples was generally consistent with the mapped geology and the mineralogy of the North Pennine Orefield as described by Dunham (1959).

The following sections go into more detail with regards to the characterisation of the samples collected from Gunnerside Gill.

6.1.1 Particle Size

The particle size analysis of the sub 2 mm fraction shows the samples predominantly comprise a mixture of silt and sand with generally less than 5 % clay.

Gun 5 was the most unusual as it comprised 95.5 % sand and 4.4 % silt, and is therefore classified as a 'sand'. There were no significant relationships

between grain size and location of the sample recovered. This is most likely to be as a result of the nature of the tailings and waste rock themselves, which are inhomogeneous mixtures of grain sizes.

The grain sizes were further investigated using backscatter electron images from the EMP (Section 5.3.2). Gun 1 showed a relatively uniform texture of <0.1 mm to 0.5 mm. Gun 2 and 3 were finer grained than Gun 1, with grains generally <0.2 mm in size. Gun 4, Gun 5, Gun 7, Gun 8 and Gun 9 had similar textures to Gun 1. Gun 6 had a wide range of grain sizes ranging from <0.1 mm to around 1 mm diameter. Gun 9 and 10 were fine grained and comparable to Gun 2 and Gun 3.

Given that the mine wastes are heterogeneous in size within the <2 mm size fraction, it follows that the sediments are too, as they are derived from the mine waste material.

6.1.2 Mineralogy

Gun 1 to Gun 8 were recovered from the upper and central portions of Gunnerside Gill and are considered to be representative of the mine wastes present within the catchment (Figure 4.2). Gun 9 was recovered from overbank sediments on the central portion of Gunnerside Gill, not far from Gun 8. Gun 10 was from the most southerly portion of the gill near the confluence with the River Swale. Gun 9 and Gun 10 are considered to be representative of floodplain / alluvial sediments directly adjacent to Gunnerside Gill.

6.1.2.1 Mine Waste Mineralogy

As detailed in Section 5.3.1, quartz dominated the composition of the majority of the mine waste samples, typically ranging from 70 vol % to 90 vol %, with the exception of Gun 5 and Gun 7 which contained around 20 vol % quartz by weight. Barite and fluorite were present in the majority of the samples, the highest concentrations coincided with the lowest concentrations of quartz. Clay minerals were present in most of the samples, with very low quantities in Gun 5 identified by EMP. Galena was identified in four of the samples by XRD, ranging from less than <1 vol % in Gun 3, Gun 6 and Gun 7 to around 8 vol % in Gun 5. Elemental mapping shows that in some of the mine waste samples (e.g. Gun 2 and Gun 5) the grains of galena were often rimmed by other minerals, either secondary minerals (including cerussite, anglesite and / or Pb

oxides) as a result of weathering reactions or clay coatings, and in some case more than one rim of differing mineralogy (Figure 5.18). These coatings may prevent further weathering or weathering of the galena at a slower rate, and may explain why galena is recorded at relatively high concentrations within Gun 5.

Galena was found to be present in over half the mine waste samples and sphalerite was present in four of the eight mine waste samples. The highest concentrations of galena and sphalerite were found to be present in samples from the central portion of Gunnerside Gill, both in the vicinity of Sir Francis Level which was a major processing site. Sphalerite ranged from <10 vol % in Gun 5 and Gun 8, and between 10 and 25 vol % in Gun 7. Pyrite and Zn-, Cd- and Cu-bearing Fe oxyhydroxides were observed by EMP in the majority of the samples. Calcite was only noted to be present in some of the more upstream samples.

Several of the samples including Gun 1, Gun 2, Gun 4, and Gun 5 had Fe oxyhydroxide grains (possibly as a result of weathering pyrite) containing Cd-Cu-Zn within the grain structure with a rim of clay minerals around the outer edge. The Cd-Cu-Zn concentrations appeared to be relatively uniform across the grains, which could imply they are impurities within the original grains. Further mineral rims were observed including pyrite grains with a corner of Cd-Cu-Mn bearing Pb oxide or carbonate, surrounded by a rim of Ba oxide or carbonate.

Another interesting grain was noted in some of the mine waste samples (e.g. Gun 3, Gun 5, Gun 6 and Gun 7) comprising of core of Cd- bearing Zn sulfide, with weathering on the outer rim appearing less bright and surrounded by a layer of clay minerals. The Cd showed some zonation or variation across the grains. Several further noteworthy grains comprised of a core of galena surrounded by Pb oxide or carbonate and then a thin layer of Si-Al-K clay minerals.

A grain of galena with concentrations of Cu and Cd rather than inclusions, surrounded by an outer rim of barite and then a thin layer of possibly secondary Pb was noted in one of the mine waste samples (Gun 5). A thin outer rim of

Pb oxide or carbonate was present around the barite, with a final layer of K-Al-Si clay minerals around the outermost edge, this particular grain had four secondary halos.

A sphalerite grain with some Cd zoning was recorded (Gun 5) and it also had an outer barite rim, protecting it from further weathering. Clay minerals were often noted as thin outer rims on ore mineral grains.

Calcite was only detected by XRD in three of the waste samples, Gun 1, Gun 2 and Gun 4 and was not found to be present in either of the sediment samples by XRD. Fluorite was found to be more common, with concentrations of 10 to 25 % in the mine wastes samples Gun 3, Gun 5 and Gun 7, and less than 10 % in Gun 2, Gun 4, Gun 6 and Gun 8.

None of the samples had the same mineralogical composition, making the prediction of the overall behaviour of the metallic elements at Gunnerside Gill difficult. This is likely to be a reflection of the use of hushing and the evolution of mining and processing techniques as the technology progressed throughout the mining period, which as a physical control will have resulted in mixing and density separation of minerals and the release of mine waste and sediments directly into the waters of Gunnerside Gill. In addition, the physical erosion of upstream spoil heaps and deposition of sediments at different points along Gunnerside Gill as a function of the flow conditions at the time. Furthermore, the location of the samples (i.e. near the mining areas, Sir Francis Level or overbank sediments) the types of ore mined, processing techniques used historically, and subsequent weathering of the minerals would have played important roles in the observed mineralogy of the samples.

6.1.2.2 Sediment Mineralogy

The sediments were also dominated by quartz, with barite and clays present. Galena was not found to be present in either of the sediment samples. Sphalerite was recorded in Gun 9, but was absent from Gun 10. Gun 9 was also noted to contain fluorite, sphalerite and Fe oxyhydroxides. In addition, Gun 9 included a grain of Pb-Zn phosphate with associated Cd as identified by EMP.

Along with quartz, barite and clay minerals, Gun 10 was also found to contain grains of cerussite, Fe oxyhydroxides, pyrite and smithsonite. A Zn-, Cd-, Na- and Cu- bearing Pb oxide or carbonate grain was also noted in Gun 10 by EMP. There was a distinct absence of S, but the concentrations of O, Al and Fe varied across the grain, suggesting it could have been differentially weathered. Overall, Gun 10 is be considered to be relatively weathered and / or derived from weathered mine wastes given the absence of primary ore minerals.

The alluvial sediments could potentially be covered and buried by further sedimentation or continue within the sediment cycle to be transported and re-deposited downstream or within the adjoining River Swale.

6.1.3 Bulk Geochemistry

The total digestions show that all the samples predominantly were composed of Al, Ba and Ca with relatively low concentrations of Cu and Mn. As might be expected Pb, Zn and S showed the largest variations in total concentrations of the elements tested throughout the samples.

Calcium concentrations varied greatly between samples and did not appear to show any trends in relation to the source material. However, the highest total Ca concentrations were found to be present in Gun 7 and Gun 8, just downstream from Sir Francis Level dressing floor, possibly as a result of the ore processing and gangue mineral separation undertaken at the location. Concentrations of Pb are highest in Gun 1 (70,000 mg/kg) and Gun 5 (49,300 mg/kg), whereas Zn is highest in Gun 5 (64,300 mg/kg) and Gun 7 (60,900 mg/kg) (Figure 5.2). Gun 5 and Gun 7 also have the highest concentrations of S (11,700 mg/kg and 17,100 mg/kg, respectively) supporting the presence of primary ZnS minerals as identified by the XRD.

6.1.4 Solid Phase-Speciation of Metallic Elements

The results of the sequential extraction show Pb was mostly present in the exchangeable (operationally defined carbonate and CEC sites) fraction in Gun 1 and Gun 2 (Figure 5.6). By contrast Pb was mainly present in the residual fraction in Gun 3, Gun 5 and Gun 7. In Gun 4, Gun 6, Gun 8, Gun 9 and Gun 10 Pb was largely present in the reducible (Mn/Fe oxyhydroxides) fraction with slightly lower relative proportions present in the exchangeable fraction. In Gun

1, Gun 2, Gun 4, Gun 9 and Gun 10 Zn was mostly present in the exchangeable fraction (Figure 5.6), whereas the Zn in Gun 6 and Gun 8 predominantly occurred in the oxidisable fraction. Gun 3, Gun 5 and Gun 7 were dominated by Zn in the residual phase. Sulfur was mainly present in the residual fraction, with lower relative proportions recorded in the oxidisable fraction. Overall, the partitioning of Pb varied between all the operationally defined fractions. By contrast, Zn occurred mainly in the exchangeable and residual fractions, implying the Zn was relatively mobile in half of the ten samples tested or may be controlled by reactions involving S.

Total carbon concentrations varied from 0.98 wt. % (Gun 6) to 2.57 wt. % (Gun 3), with an average of 1.75 %. Metallic elements that are sorbed to organic matter are generally more strongly bound than those sorbed to Fe oxyhydroxides (Warren and Haack, 2001). Total carbon concentrations within both the mine waste and sediment samples were found to be relatively low, generally less than 2 wt. % based on the combustion analysis of the samples. It is likely that the concentrations of organic matter such as plants, roots and bacteria vary greatly, given the waste rock piles are adjacent to the river and subject to wind, water erosion and varying degrees of vegetation by metallophyte plants. Anecdotal evidence suggests that the river is browner in colour after heavy precipitation, which would indicate that natural dissolved and / or colloidal organic matter is being mobilised from the surrounding peat beds. However, the R^2 values for carbon vs both Pb and Zn were calculated as < 0.01 . This does not conclusively mean that organic matter is not involved in mobility and retention of metallic elements in Gunnerside Gill, but perhaps is a less significant mechanism in the waste rock piles and sediments.

Manganese was mainly present in the exchangeable fraction in Gun 5, Gun 7, and Gun 8, and in the reducible fraction in Gun 1, Gun 2, Gun 4, Gun 6, Gun 9, and Gun 10. The presence of Mn in the reducible fraction is to be expected as the reagents of the BCR procedure target Fe and Mn oxyhydroxides in this step (Rauret et al., 1999). Similar to Mn, Fe was mainly found to be present in the reducible fraction with slightly lower relative proportions in the residual fraction.

The total digestions were repeated on the post column leaching solids, CGun 1, CGun 2, CGun 3 and CGun 9. The results generally showed a reduction in concentration of Pb and Zn, which is not unexpected. What is slightly unexpected is the magnitude of the reduction. Gun 1 showed a reduction of 21 % Pb between the pre and post-column solids; however, there the concentrations within the leachate remained low throughout the 40 week experiment. CGun 2 and CGun 3 recorded reductions of Pb of 32 % and 60 %, respectively. In all three of the mine waste samples (Gun 1 to Gun 3) the Pb concentrations in the column leachate remained relatively low, implying that Pb was being mobilised, but at a slower rate than within the sediment sample (Gun 9). Surprisingly, the Pb concentrations in CGun 9 increased by approximately 42 % at the end of the experiment; this is likely to be an effect of the inhomogeneity of the material rather than representing an actual increase of Pb in the post column sample. In all of the post column samples the Zn concentrations were lower than in the pre column samples. The changes ranged from 2 % in CGun 1 to 49 % in CGun 3. Several studies have recorded higher concentrations of Zn than Pb in the mining discharges (e.g. Hammarstrom et al., 2002; Desbarats and Dirom, 2007; Palumbo-Roe and Colman, 2010; Navarro et al. 2015; Valencia-Avellan et al., 2017). Suave et al. (1998) found that Pb solubility shows a linear reduction from pH 3 to 6.5, independent of soil organic matter within that pH range. However, given that some metallic elements, such as As, Co, Ni, Sb and Zn, are soluble at near-neutral pH (Plante et al., 2011), it is therefore possible Zn is more mobile in the waters than Pb in the neutral mine drainage conditions in this study. This is true even when the total concentrations of Pb and Zn within the solids are similar.

6.1.5 pH of Solids and Column Leachate

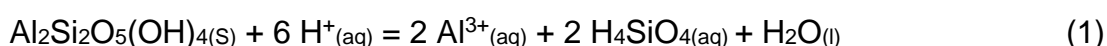
Neutral mine drainage has been classified as having a pH of 6.0 to 8.0 (Nordstrom 2011, Figure 2.3). The pH of the solid samples ranged from 6.8 to 8.0, with the majority between 7.0 and 7.6 (Table 5.1). Given the pH of the blank the most interesting samples were Gun 7, which recorded the most alkaline pH of 8 and Gun 9, which was the most acidic pH (6.8) of all the samples. Gun 7 was recovered from the dressing floor of Sir Francis Level

alongside Gun 8. It could be that the area around Sir Francis Level dressing floor contains gangue minerals with some remaining neutralisation capacity (calcite, barite, quartz and clays) alongside any residual ore minerals. Gun 9 is representative of the floodplain sediments located downstream of the mining areas and interestingly recorded the lowest pH values of both the solid samples and during the column leachate experiment.

Both the mine wastes and sediment showed evidence of neutralisation reactions during the column leaching experiment. As shown in Figure 5.21, Gun 1 to Gun 3 (mine wastes) generally maintained stable pH values of between 6.5 to 7.0. At around week 22 the pH values reduced slightly (to 6.5), as the pH of the blank reduced. However, at week 32 Gun 1 to Gun 3 showed evidence of neutralisation by increasing the pH to 7.0 to 7.5. Gun 9 (sediment) had an initial low pH value of 4.4 before rising to 6.7 in week 3. The pH values then remained at around 6.5 to 7.0, reducing to 6.0 between week 22 and week 32. The pH values then increased slightly from week 33 onwards to 6.4, similar to the pH of the blank.

It appears that the mine waste samples have more neutralisation capacity remaining than the sediments. Although calcite was only found to be present by XRD in Gun 1, Gun 2 and Gun 4 at concentrations of <10 vol. %. Fluorite was found to be much more common and present in eight out of the ten samples, including Gun 9.

It has been noted that silicates also have neutralisation capacity (Banks et al., 2002; Hammarstrom et al., 2002; Lottermoser, 2010). The weathering of silicates results in the consumption of hydrogen ions, either by completely dissolving the mineral or altering it to a different phase. Secondary clay phases produced may dissolve further and again consume hydrogen ions in the process (equation 1) (Lottermoser, 2010).



Given the proportion of quartz and clays within the majority of the samples, it is likely that there is some neutralisation capacity coming from these minerals within Gunnerside Gill. Furthermore, although the CEC was not directly measured in this study this is a known mechanism for the neutralisation. For

examples Ca^{2+} within a CEC site could be exchanged for H^+ (Lottermoser, 2010).

There are various ways of calculating the potential neutralisation capacity of soils and sediment based on the calcite content. Lottermoser (2010) described net neutralisation potential (NNP) as the maximum potential acidity (MPA) (assumed that total S all becomes H_2SO_4) subtracted from the neutralisation potential (NP) (total inorganic carbon). The more negative the result, the higher the potential for acid generation. Unfortunately, it was not possible to undertake total inorganic carbon analysis as part of this study due to financial and logistical constraints. White et al. (1999) defined a different methodology which uses the concentration of S to determine how much calcium carbonate would be required to neutralise the potential acidity produced. This is based on a 1 to 1 mole ratio of S (32 g/mole) to CaCO_3 (100 g/mole), which gives a weight ratio of 1:3.125. Therefore, multiplying the weight percent S contained in the mine waste or sediment by 3.125 gives the S to weight percent calcium carbonate required to neutralise the produced acid and multiplying by 31.25 gives the amount of calcium carbonate required in parts per thousand. (White et al. 1999). The average S of the mine waste samples is 0.77 wt. % and 0.44 wt. % for the sediments. This converts to 2.40 wt % and 1.36 wt % of calcium carbonate, respectively. This shows that the mine waste samples have higher concentrations of S which require more calcium carbonate to neutralise any potential acidity. This is not unexpected as the mine waste samples generally contain higher concentrations of ore minerals resulting in higher total S concentrations. The mine waste samples on average were found to contain almost double the total Ca of the sediment samples, 49,400 mg/kg and 25,900 mg/kg respectively, therefore the mine wastes do appear to have at least some neutralisation capacity remaining. Neutralisation capacity based on static tests do have some limitations, including acid generated may be neutralised by alternative sources in addition to the NP (total inorganic carbon) and the neutralisation capacity of silicates may be underestimated (Chatwin et al., 2014). Some acid potential calculations assume that the reactive sulfide mineral is only pyrite, when it could be pyrrhotite or any number other sulfide

bearing minerals (Morrin and Hutt, 2001), however these minerals are largely absent in Gunnerside Gill or present in very low concentrations.

6.1.6 Comparison of Samples

The following sub sections detail the characterisation of all the samples (Gun 1 to Gun 10).

6.1.6.1 Gun 1

The most northerly mine waste sample, Gun 1, was recovered just upstream of the Old Gang mines and near to the location of the first EA water sample. In Gun 1 both Pb and Zn were mostly present within the exchangeable fraction. The total digestions show that Gun 1 contained the highest concentration of Pb (70,000 mg/kg) of all the tested samples, Zn concentrations were low, with a concentration of 4,100 mg/kg. The main metallic element bearing minerals identified were cerussite and Fe oxyhydroxides. During the column leaching experiment Pb was generally recorded at around 100 µg/L and Zn at around 70 µg/L in the resultant leachate, the lowest of all the column leachate concentrations.

The total digestions of the post column solids had a slight reduction in Pb, however Zn remained largely unchanged. EMP analysis of the samples indicated weathering rims on some grains, including Pb oxide / carbonate around a galena core and a Pb oxide / carbonate grain with a rim of clay minerals. In addition, Pb showed an increase in the exchangeable fraction in the post column solids. The exchangeable fraction of the sequential extraction aims to represent relatively easily available carbonate and CEC sites.

In Gun 1 it would seem all the most readily available Pb and Zn had been weathered prior to the column experiments, with the remaining ore mineral grains having rims and coatings to protect them from further weathering reactions. Also the pH in Gun 1 was almost always the highest in the column leaching experiment with a mean value of 7.1.

Gun 1

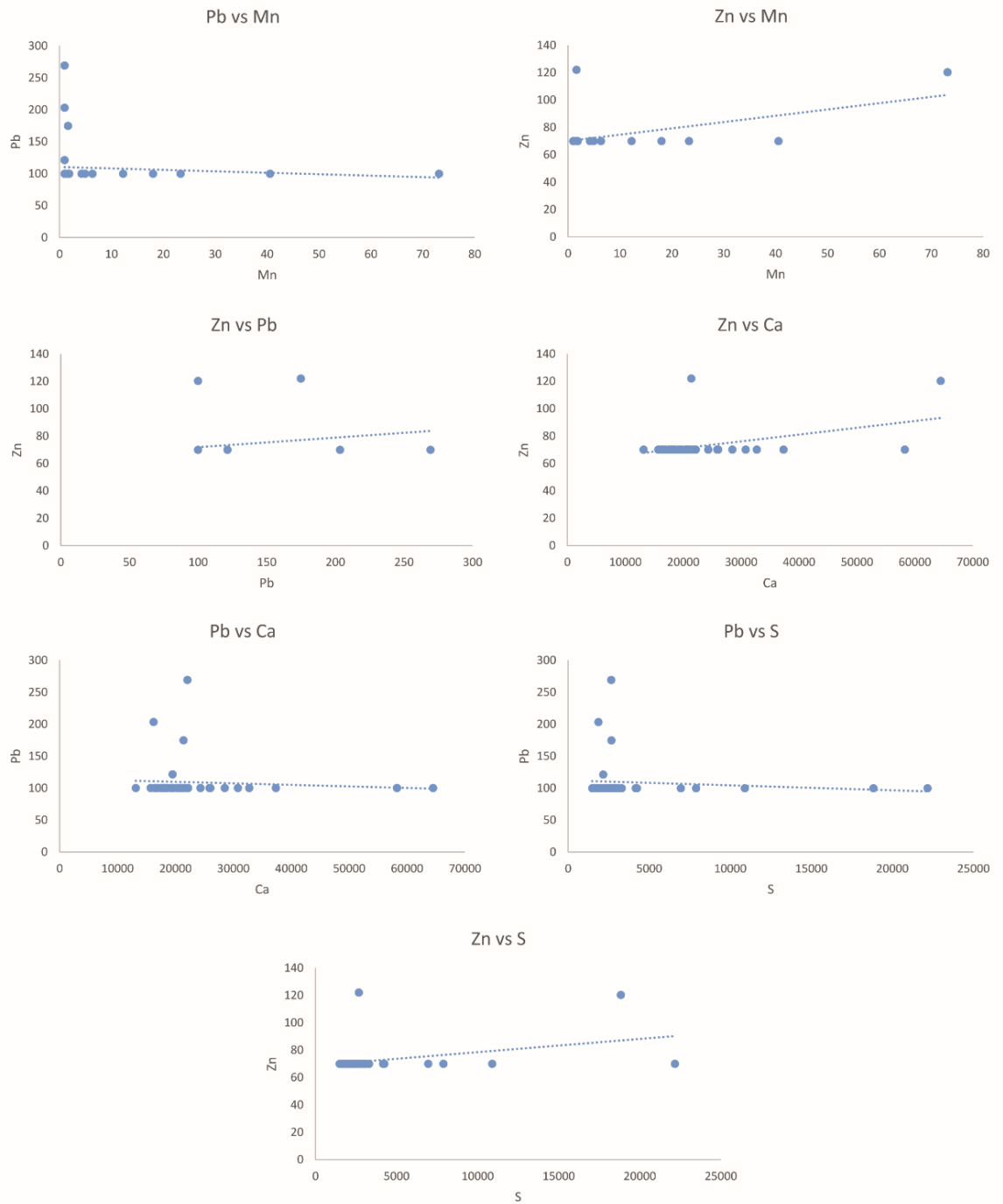


Figure 6.1: Correlation graphs for various pairs of elements from Gun 1 leachate ($\mu\text{g/L}$)

There is limited correlation between elements (Figure 6.1), which reflects the low concentrations of Pb and Zn within the column leachate and therefore are not considered to be particularly conclusive when determining correlation relationships within Gun 1.

6.1.6.2 Gun 2

The second mine waste sample, Gun 2, was recovered just south of the Old Gang Mines. Similar to Gun 1 both Pb and Zn were found to be mostly present within the exchangeable fraction. The concentrations of Pb and Zn were found to be a factor of 4 less than the highest concentrations, recorded in Gun 1 (Pb) and Gun 5 (Zn). The main metallic element bearing minerals in Gun 2 included galena, cerussite and Fe oxyhydroxides. The EMP analysis showed some of the Fe oxyhydroxides contained Cd, Cu and Zn and were surrounded by a rim of clay minerals. The EMP also showed a grain of galena surrounded by a rim of Pb oxide / carbonate and then again surrounded by clay minerals.

Lead concentrations remained low in the leachate during the column leaching experiment. Zinc had an initial concentration of 33,500 µg/L before reducing in week 3 to around 8,000 µg/L and gradually reducing again for the remaining 37 weeks of the experiment. Following the column leaching study the post column solids were found to contain galena, Pb oxide / carbonate and sphalerite. Sphalerite was not detected in the pre column solids, but grains were noted using EMP analysis following the column leaching experiment. It is likely sphalerite was present in low concentrations in the pre column solids, however was not detected at the time. Again the EMP identified galena surrounded by Pb oxide / carbonate and then clay minerals in both the pre and post column solids. The results of the sequential extraction showed Pb to increase slightly in the reducible fraction and reduce slightly in the exchangeable fraction, by around 4 % following the column leachate experiment. Zinc showed a 9 % reduction in the exchangeable and reducible fractions and a 9 % increase in the oxidisable and residual fractions. This implies the Zn within the column leachate was removed from carbonate / CEC sites and Fe / Mn oxyhydroxides. Similarly the limited Pb leached was likely to have been from the carbonate / CEC sites. Within the leachate of Gun 2, S had an initial peak of 500,000 µg/L before reducing in week 8, this could also be part of the mechanism controlling Zn release into the waters of the catchment.

Gun 2

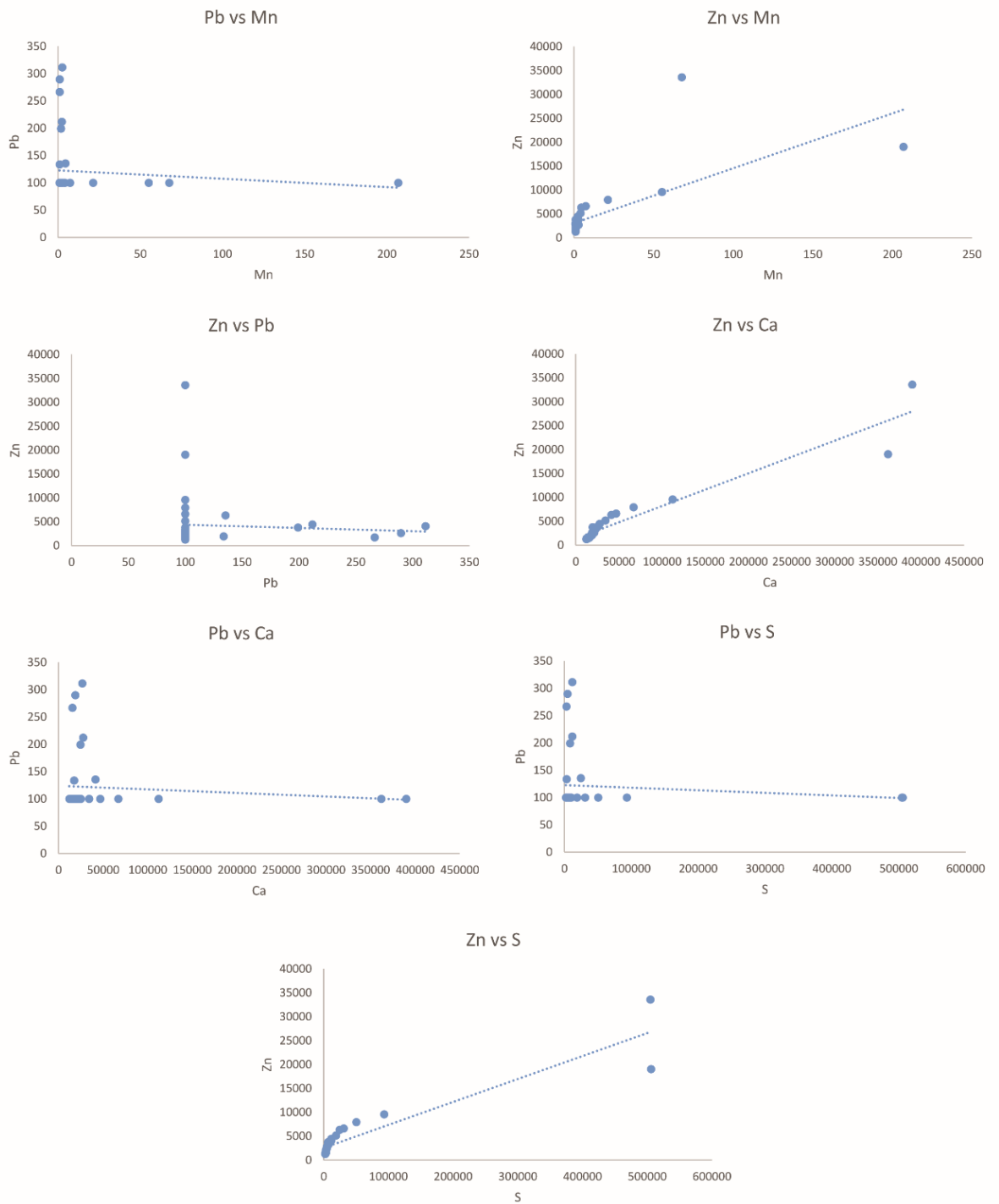


Figure 6.2: Correlation graphs for various pairs of elements from Gun 2 leachate ($\mu\text{g/L}$)

Similar to Gun 1 the concentrations of Pb were relatively low reflected in the limited correlation values noted in Figure 6.2. Zinc however, shows strong correlations with both S, Mn and Ca, which indicate that both primary and

secondary minerals are involved in its mobility in this setting. More Pb and Zn were mobilised from Gun 2 than Gun 1, even though Gun 1 recorded higher total concentrations. This is considered to be related to the slightly lower pH values recorded during the leaching experiment, with a mean value of 6.8 against 7.1 in Gun 1

6.1.6.3 Gun 3

Gun 3 was recovered from the central section of Gunnerside Gill. The gap between Gun 2 and Gun 3 is largely due to access to the stream itself. Both Zn and Pb were found to be present largely within the residual fraction following the sequential extraction. Galena, sphalerite and pyrite were all found to be present within Gun 3. The EMP revealed a Zn bearing sulfide with a core containing Cd. The total concentration of Pb was the lowest of all the samples tested (1,840 mg/kg) and Zn was relatively low (8,100 mg/kg) compared to the other mine waste samples, a factor of 8 less than the highest total concentration (recorded in Gun 5).

During the column leaching experiment Zn concentrations peaked in week 2 at 55,000 µg/L, before reducing steadily until week 10 and then again gradually over the remaining weeks. This trend was also noted in the Mn concentration, which peaked in week 2 at 1,400 µg/L before reducing over the next 10 to 15 weeks. Within the leachate Gun 3 had an initial S concentration of 143,300 µg/L in week 1 and reducing to 43,000 µg/L by week 7. Further reductions in S concentration were noted during the remaining weeks to 15,000 to 20,000 µg/L by week 20 and then 5,000 to 6,000 µg/L from week 30 to week 40. The post column leaching solids contained sphalerite and barite with some weathering textures, and sphalerite containing Cd surrounded by a rim of barite then an outer rim of clay minerals. Relative proportions of Pb decreased in the oxidisable fraction and increased in the reducible fraction by 8 % and 9 % respectively. The proportions of Zn reduced in exchangeable and residual fractions, by 6 % and 30 % respectively, and increased by 6 % in reducible and by 30 % in the oxidisable fractions. This indicates a significant movement of Zn from the residual to oxidisable fraction, again probably controlled by sphalerite dissolution.

Gun 3

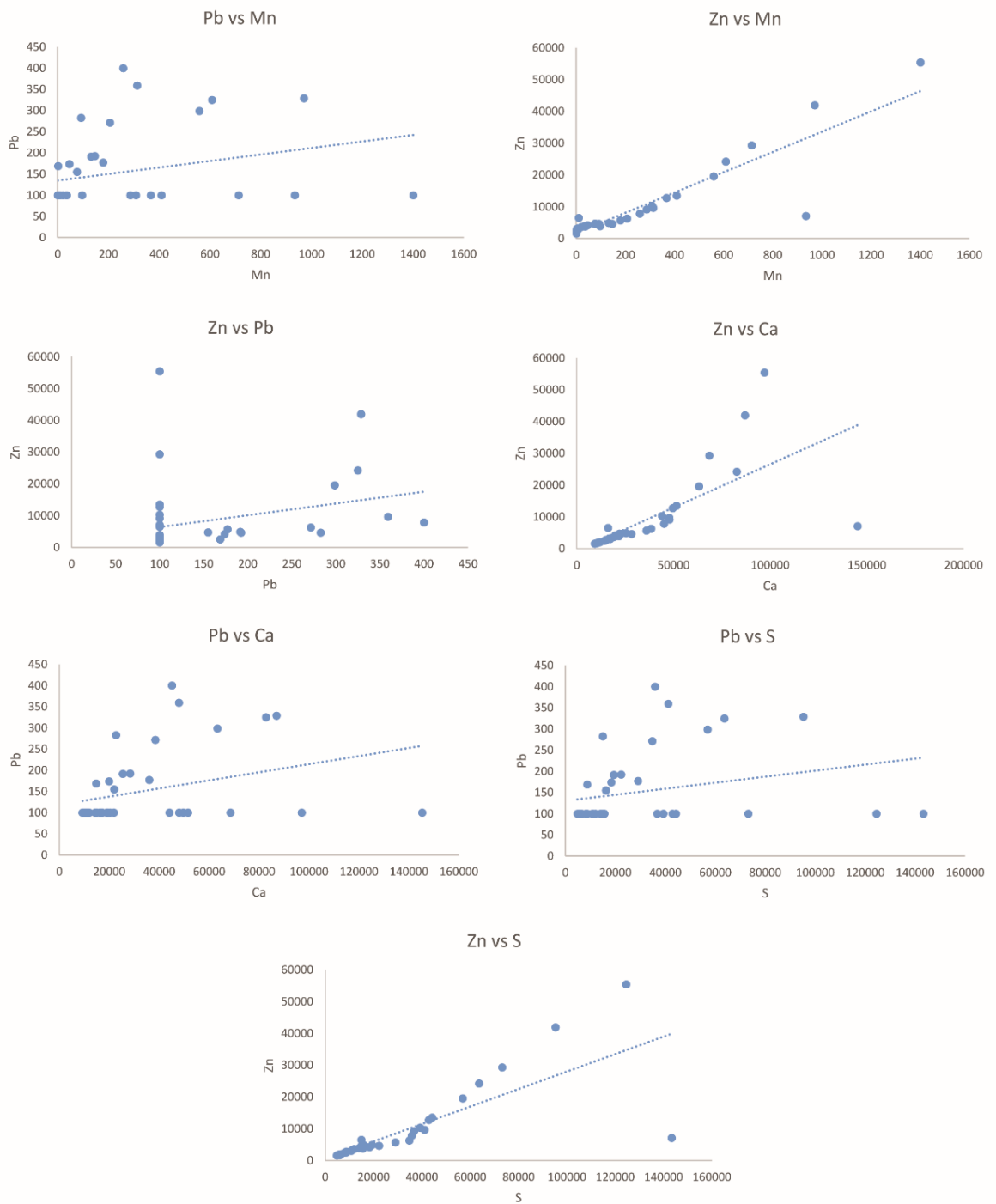


Figure 6.3: Correlation graphs for various pairs of elements from Gun 3 leachate ($\mu\text{g/L}$)

The correlations of the leachate are shown in Figure 6.3, which show very similar trends to those in Gun 2. Again Gun 3 recorded a slightly lower mean pH of 6.6 during the column leaching experiment, which would go some way

to explain the higher metallic element concentrations within the resultant leachate, even though the total concentrations in the solids were lower.

6.1.6.4 Gun 4

Gun 4 was found to contain low concentrations of Pb (5,430 mg/kg) and the lowest concentration of Zn of all the samples (2,000 mg/kg). The sequential extraction showed that Pb was mostly present in the reducible fraction and Zn in the exchangeable fraction. There was no evidence of any galena or sphalerite in the sample. The EMP did show grains of Fe oxyhydroxide containing Cd, Cu and Zn with a rim of clay minerals. Gun 4 was recovered in line with Sir Francis Level adit and was browner in colour than most of the other mine waste samples. The colour difference may reflect a lower concentration of ore minerals within the browner samples, and a higher concentration in the grey coloured samples. The column leachate experiment did not include Gun 4.

6.1.6.5 Gun 5

The concentrations of Zn within Gun 5 were found to be the highest (64,300 mg/kg) and Pb was the second highest (49,300 mg/kg), and both elements were mostly present in the residual phase. The minerals present in Gun 5 included galena, sphalerite, cerussite and pyrite. The EMP showed a Zn sulfide with Cd with an outer rim of barite and clay minerals. In addition, grains of sphalerite with some Cd zoning and outer barite rim, protecting it from further weathering, were also noted by EMP analysis. A thin outer rim of Pb oxide or carbonate was present around the barite, with a final layer of clay minerals around the outermost edge. Gun 5 was recovered from a possible burning or smelted layer of mine waste in the central portion of the study area. Gun 5 was not part of the column leaching experiment.

6.1.6.6 Gun 6

Gun 6 was recovered from a different strata, notably browner in colour, directly below Gun 5. Gun 6 had relatively low concentrations of Pb (2,400 mg/kg) and Zn (2,900 mg/kg), mostly found within the reducible and oxidisable fractions. Key minerals within Gun 6 included galena, cerussite and grains pyrite noted by EMP. The EMP revealed grains of Cd bearing Zn sulfide with a weathered

outer rim surrounded by a layer of clay minerals. Gun 6 was not included in the column leachate experiment.

6.1.6.7 Gun 7

Within Gun 7 both the Pb (6,260 mg/kg) and Zn (61,000 mg/kg) were present mainly in the residual fraction. Galena, Fe oxyhydroxides and grains of pyrite were all found to be present in the sample, in addition Gun 7 had the highest concentration of sphalerite (10 to 25 %) of all the samples. A grain of Cd bearing Zn sulfide was noted by EMP analysis, with an outer rim of Ba oxide and clay minerals. The concentration of Pb was within the lower range of the mine waste samples, with a relative proportion of 3.6 %, and the Zn concentration was the second highest at 34.3 % of the total concentration. Gun 7 was recovered from Sir Francis Level dressing floor and was predominantly grey in colour. Gun 7 was also not part of the column leachate experiment.

6.1.6.8 Gun 8

Gun 8 was located adjacent to Gun 7 and just downstream of Sir Francis Level dressing floor and in contrast to Gun 7 was orange / brown in colour. Total concentrations of Zn were in the middle of the range (14,600 mg/kg) and Pb concentrations were low (14,600 mg/kg). Both sphalerite and cerussite were noted to be present by XRD and EMP respectively. Lead was mostly present in the reducible fraction and Zn in the oxidisable fraction. Gun 8 did not form part of the column leachate experiment.

6.1.6.9 Gun 9

Moving further down Gunnerside Gill Gun 9 was recovered from an area of grey over-bank sedimentation. The concentrations of Pb and Zn within Gun 9 were both in the mid-range compared to the mine wastes, at 8,710 mg/kg and 4,950 mg/kg respectively. Lead was found to be mostly present in the reducible fraction and Zn in the exchangeable fraction. Key minerals present were identified as sphalerite, Fe oxyhydroxides and Pb phosphate (identified by EMP analysis). Gun 9 was included as the fourth and final sample in the column leaching experiment. During the leaching experiment Gun 9 recorded the highest Pb concentrations in the column leachate, starting at around 6,000 µg/L. This reduced rapidly to 460 µg/L in week 3, before increasing to between 1,670-3,070 µg/L from week 10 to week 35, and then reducing again to around

1,700 µg/L from week 36 to week 40. Manganese shows a similar trend to Pb during the leaching experiment in Gun 9, with an initial peak of 340 µg/L in week 1. The concentration of Mn then reduced to 35 µg/L by week 3 and increased to 418 µg/L in week 13 before remaining between 260 and 320 µg/L until week 33. After this the concentration of Mn gradually reduced to around 70 µg/L in week 40. Zinc had an initial peak concentration of 50,200 µg/L, which reduced rapidly to around 4,400 to 5,700 µg/L from week 3 onwards. Concentrations of S peaked in week 3 and 4 at 6,400 µg/L, before reducing to around 3,000 µg/L in week 11 and then generally remaining between 2,500 and 2,000 µg/L for the remainder of the experiment.

Following the completion of the column leaching experiment the post column from Gun 9 solids showed minor changes of <3 % between the exchangeable, oxidisable, reducible and residual fractions with regards to the relative Pb proportions. Zinc showed slight reductions in the exchangeable and residual fractions and slight increases in the reducible and oxidisable fractions.

The correlations for Gun 9 leachate data are shown in Figure 6.4 for various pairs of elements. There appears to be a limited correlation between Pb vs Mn and Zn vs Mn. The correlations are skewed by some high initial concentrations, however it appears there is some correlation between Zn vs Pb and Pb vs Ca. This implies that there is a combination of reactions controlling the mobility of the metallic elements within the alluvial sediments including dissolution of Mn oxyhydroxides and secondary carbonate phases.

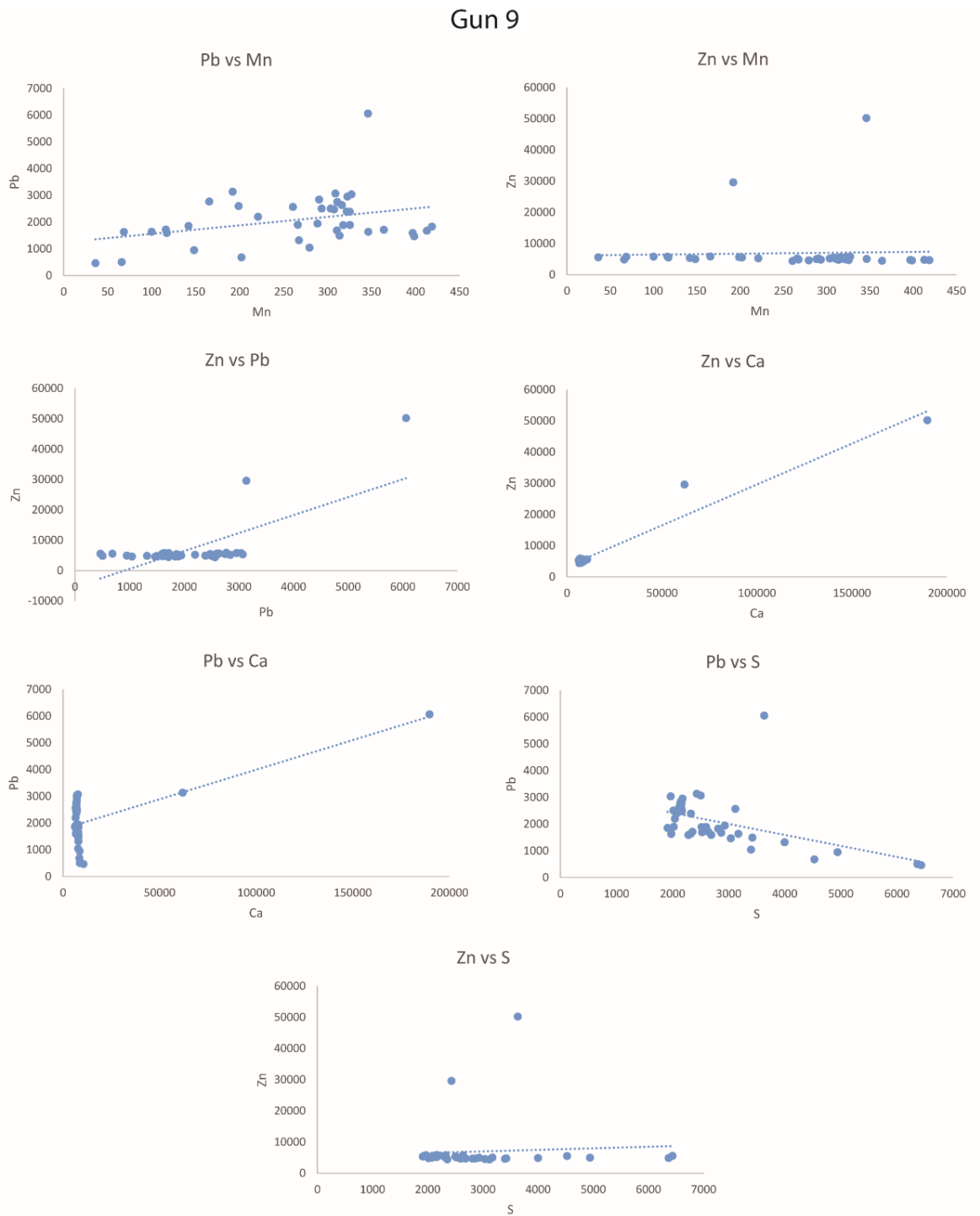


Figure 6.4: Correlation graphs for various pairs of elements from Gun 9 leachate ($\mu\text{g/L}$)

6.1.6.10 Gun 10

The last alluvial sediment sample was recovered from the channel edge, located close to the confluence of Gunnerside Gill and the River Swale. The sample contained Pb concentrations of 6,590 mg/kg within the mid-range

when compared to the mine waste samples and low concentrations of Zn (3,280 mg/kg). Lead was mainly present in the reducible fraction and Zn in the exchangeable fraction. Minerals of interest in Gun 10 include cerussite, Fe oxyhydroxides, pyrite and smithsonite. Using EMP analysis a Zn-, Cd-, Na- and Cu- bearing Pb oxide / carbonate was present with a distinct absence of S within the grain. In addition, concentrations of O, Al and Fe varied across the grain indicating it could be undergoing different weathering reactions.

6.1.6.11 Summary of Sample Comparison

The column leaching study suggested that Gun 1 was likely to be the oldest mine waste sampled and had probably been extensively leached and weathered, as the experiments yielded low amounts of Pb and Zn in the column leachate. Within the mine waste samples the metallic element concentrations in the leachate, specifically Pb and Zn, were Gun 3 > Gun 2 > Gun 1. This suggests that the mine wastes could still leach Pb but in lower amounts than from the alluvial sediments. This could also be a function of variations in the mineral processing techniques or the wastes could be from different stages of the process operations. This is difficult to quantify given the lack of accurate historical records of when the waste rock piles were generated. However, it was noted that the mean pH values reduced from 7.1 in Gun 1, to 6.8 in Gun 2 and 6.6 in Gun 3, this could at least in part account for the differences in the release of metallic elements from the mine waste samples.

The majority of available Pb is associated with secondary minerals. The highest total concentrations of Pb were not reflected in the column leachate concentrations, for example Gun 1 had the highest total Pb in the solid but the lowest Pb concentration in the column leachate. Often when galena and sphalerite are present in the environment together, sphalerite is preferentially weathered (Urbano et al., 2007). This is likely to be related to sphalerite being more soluble in the pH conditions of the column leaching experiment than galena. Galena and sphalerite are considered to have relatively low resistance to alteration when they are present in oxidised tailings (Moncur et al., 2009), and as a result the surface of galena is known to oxidise to an “anglesite-like”

phase (Pb oxide) (Lara et al., 2011), which acts as a protective barrier for the galena underneath. The anglesite-like phase may then go on to form cerussite-like phases (Pb carbonate) (Lara et al., 2011). Lead mobilisation is heavily influenced by pH. If the pH is maintained around pH 5 to 8 then Pb mobilisation is reduced. If the pH drops, calcite may be able to raise the pH, this results in slower reduction in pH and therefore a slower release rate of Pb to the surroundings (Gee et al., 2001). Lead oxides, sulfates and carbonates are soluble in pHs that are acidic to circum-neutral (Traina and Laperche, 1999), which means Pb can be mobilised from secondary mineral phases within a neutral mine drainage setting.

The results of the column leaching experiment indicate that Pb is leaching more from the alluvial floodplain sediments than the mine waste piles within Gunnerside Gill. This could be related to the fact the alluvial sediments are likely to be derived from older mine wastes that have been mobilised / weathered previously, and weathering of the ore minerals present to less stable forms over time. The release of Pb seems to be controlled by Mn oxyhydroxide dissolution at least in part. Furthermore, Gun 9 was noted to contain grains of a Pb/Zn phosphate. Phosphate is commonly used as a remediation option for Pb and Zn, as Pb phosphates are relatively stable over a wide pH range and less soluble than Pb oxides, sulfides and carbonates (Traina and Laperche, 1999). Although not formally identified in this study, it is considered the mineral present may be pyromorphite, a Pb chlorophosphate. Pyromorphite is a secondary mineral that has been found in the oxidised zones of Pb deposits (mindat.org, 2019). Cotter-Howells et al. (1994) undertook a study of Pb impacted mine waste soils in Derbyshire, which is present within the South Pennine Orefield. They found that Ca-rich pyromorphite was an important secondary Pb mineral within the study area. Pyromorphite has not previously been reported in the sediment samples recovered from Gunnerside Gill located within the North Pennine Orefield, but as it is often very poorly crystalline (e.g., Cotter-Howells et al., 1994) it may have been overlooked.

A study of the River Tees (Hudson-Edwards et al., 1997) looked at the mineralogy of the mining catchment. Four groups of contaminant-bearing minerals were identified: sulfides such as galena, sphalerite and chalcopyrite;

secondary minerals including cerussite, smithsonite and occasional Pb phosphates; Fe oxyhydroxides (most common contaminant-bearing mineral group); and Mn oxides.

The Fe and Mn oxyhydroxides were both found to be pseudomorphs of sphalerite, cerussite, chlorite, siderite, pyrite and augite (Hudson-Edwards et al., 1997). This four group classification could also be applied to the minerals of Gunnerside Gill. In the River Tees study, the secondary minerals were found as rims or as pseudomorphs of the primary sulfide mineral (Hudson-Edwards et al., 1997). A similar trend is also noted within the Gunnerside Gill samples, most commonly with respect to the galena grains detected by EMP.

Other locations within the north Pennines have also been studied to better understand NMD. Holden Beck, a tributary of the River Wharfe in the north Pennines was also mined by hushing (Valencia-Avellan et al., 2017). Within the solid phases the highest concentrations of Pb and Zn were recorded within the spoil samples and within the sediment samples the highest Pb and Zn concentrations were from the headwaters of the catchment. The concentrations of Pb and Zn decreased downstream within the sediment samples. The researchers concluded that metallic element mobility is controlled by the pH and weathering reactions which are in turn influenced by the underlying limestone geology. Within Holden Beck dissolved Pb and Zn were derived from galena and sphalerite, respectively, but their concentrations were found to be typically controlled by the cerussite and smithsonite. Both these secondary minerals and were continuously leaching (Valencia-Avellan et al., 2017).

In order to better understand the relationships between certain elements in Gunnerside Gill the total digestion results from the solid phases were plotted against each other.

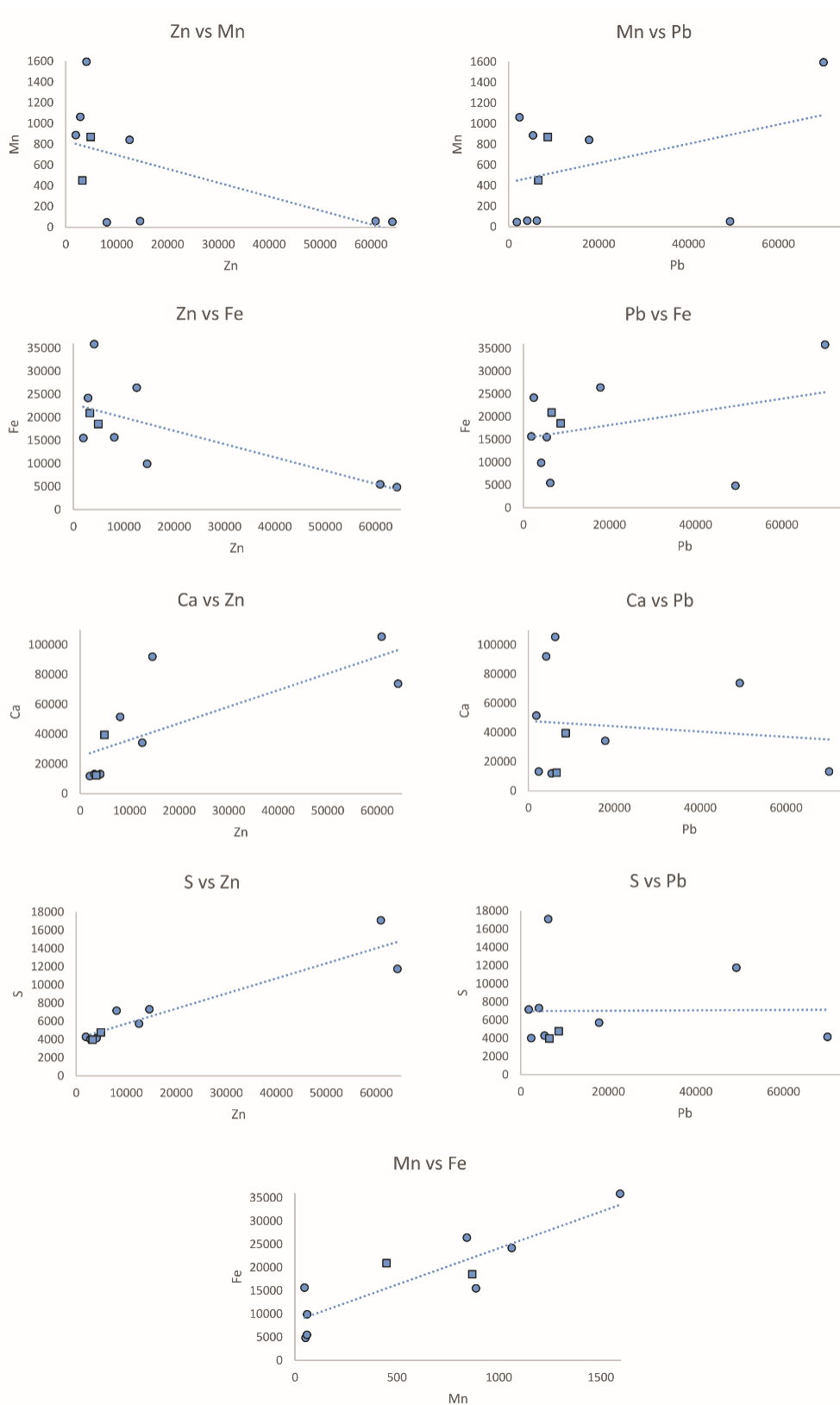


Figure 6.5: Correlation graphs for various pairs of elements from the solid phases of Gun 1 to Gun 10 (mg/kg)

The graphs in Figure 6.5 show that Ca vs Zn and S vs Zn appear to show a positive correlation within the solid phases. As expected Fe vs Mn show a strong correlation. Overall the correlations between the elements vary, which reflects the different mechanisms controlling the mobility of the metallic elements in Gunnerside Gill.

The results of this study suggests that the dissolution of Mn oxyhydroxides within the alluvial sediments is a more important source of Pb than the mine wastes. Using the column leachate data for Gun 9, the alluvial sediment sample, Spearman and Pearson correlations were calculated (Table 6.1). While the Pearson values shows some strong positive correlations, this method is better applied to normally distributed data. In this case the data are not normally distributed and therefore the Spearman correlation is more applicable.

Table 6.1: Spearman and Pearson correlation for Gun 9 leachate

| Spearman | Mn | Pb | Zn | Ca |
|----------|-------|-------|-------|------|
| Mn | 1.00 | | | |
| Pb | 0.25 | 1.00 | | |
| Zn | -0.41 | 0.37 | 1.00 | |
| Ca | 0.15 | -0.35 | -0.12 | 1.00 |

| Pearson | Mn | Pb | Zn | Ca |
|---------|------|------|------|------|
| Mn | 1.00 | | | |
| Pb | 0.35 | 1.00 | | |
| Zn | 0.04 | 0.70 | 1.00 | |
| Ca | 0.09 | 0.70 | 0.98 | 1.00 |

The Spearman values show that there is a weak positive correlation between Mn vs Pb and Zn vs Pb the leachate of Gun 9 and weak negative correlations between Zn vs Mn, Pb vs Ca and Zn vs Ca.

Given that the sediments in the southern part of Gunnerside Gill are largely derived from the upstream mine wastes or processing wastes it would be expected that the mineralogy is similar between both sample types. Although Gun 1 (a mine waste sample) had the highest total Pb concentration, Gun 9, the alluvial floodplain sediment sample, was found to release significantly more (around 17 times) Pb into the column leachate. During the column leaching experiment Pb release from Gun 2 and Gun 3 were 10 times and 13 times less, respectively, than from Gun 9. In the case of Gun 9 the Pb release can be attributed mainly to dissolution of Mn oxyhydroxides, secondary Pb

minerals and possibly Fe oxyhydroxides, although evidence for the latter is weak. Given the limited concentrations of Pb released during the column leaching experiment in the mine waste samples, it is difficult to attribute the exact mechanism for Pb mobilisation. It is considered likely, based on the EMP elemental maps, that most of the galena remaining has undergone some degree of weathering, resulting in rims of secondary minerals. This then reduces the contact of the galena to atmospheric conditions reducing the direct weathering. Furthermore, outer rims of clay minerals were often noted on the weathered grains, further reducing the potential to mobilise Pb from the primary phases. It would seem the secondary mineral or non-sulfide phases, including anglesite and cerussite, are likely to be the main control the mobility of Pb from the mine wastes (Gun 9) in Gunnerside Gill. BGS records indicate that cerussite may have been mined in the North Pennine Orefield historically (BGS 1996), suggesting that it could be present as both a primary and secondary mineral within Gunnerside Gill.

The highest total concentrations of Zn were recorded in the central portion of Gunnerside Gill, attributed to inputs from Sir Francis Level dressing floor. The mobility of Zn is considered to be largely related to the dissolution of sphalerite based on S release during the column leaching experiments, especially within the mine waste samples of Gun 2 and Gun 3. The initial Zn peak in Gun 9 coincides with Ca and Ba.. It would appear sphalerite controls Zn mobility in the mine wastes and secondary minerals such as smithsonite are a more important control mechanism in the sediments.

6.2 Comparison to Published Threshold Values

The mine wastes, sediments, column leachate and EA water monitoring data were compared to available published values to determine if the concentrations of Pb and Zn might be hazardous to human health and / or the wider environment.

6.2.1 Mine Wastes and Sediments

The concentrations of Pb in the mine wastes ranged from 1,840 mg/kg (Gun 3) to 70,000 mg/kg (Gun 1). Gun 1 was recovered from the most northerly part

of Gunnerside Gill in this study and was located in the vicinity of Lownathwaite and Old Gang mines. Gun 5 recorded the second highest Pb concentration of 49,300 mg/kg was located in the central portion of the study area, in the vicinity of Sir Francis Level adit. The mean of the eight mine waste samples was calculated as 19,700 mg/kg, significantly in excess of the GBASE (BGS 2009a/2009b) mean concentration of 84.6 mg/kg for UK sediments (Table 2.1). The two floodplain sediment samples recovered from the southern portion of Gunnerside Gill recorded Pb concentrations of 8,710 mg/kg (Gun 9) and 6,590 mg/kg (Gun 10), indicating a general reduction in Pb concentrations downstream, with a peak at Sir Francis Level. However, these are again significantly above the GBASE mean concentration for Pb in UK sediments. The concentrations of Pb exceeded published guideline values for the US, Canada, Australia and England (Table 2.2). Although these guidelines do not directly address the concentrations of Pb within a mining catchment setting, they do give an indication that the levels of Pb could have adverse impacts on human health.

Similarly, concentrations of Zn in all ten samples also exceeded the mean GBASE concentrations for UK sediments of 152.4 mg/kg. The concentrations in the mine waste ranged from 2,000 mg/kg (Gun 4) to 64,300 mg/kg (Gun 5). The second highest concentration of Zn was recorded in Gun 7 at 60,900 mg/kg, which was located in the vicinity of Sir Francis Level dressing floor. The concentrations of Zn within the sediments were recorded as 4,950 mg/kg and 3,280 mg/kg in Gun 9 and Gun 10, respectively.

With regards to the worldwide soil guideline values two of the mine samples, Gun 5 and Gun 7, recorded Zn concentrations that exceeded the USA threshold of 23,500 mg/kg. All of the samples exceeded the Canadian threshold and five of the eight mine waste samples exceeded the Australia threshold value. Both sediment samples recorded concentrations of Zn below the published Australian acceptable level of 7,000 mg/kg. Six of the mine waste samples and one of the sediments recorded concentrations of Zn in excess of the UK assessment criteria for residential end use.

The post column solids were also found to contain total concentrations of Pb in excess of the published guidance values. Total Zn concentrations in the post

column solids all exceeded Canadian guidance values, three out of four (all the mine waste samples) exceeded the UK published thresholds, one exceeded the Australian threshold and all were below the American threshold concentration. Although these samples were subjected to 10 modelled years of weathering, the total concentrations of Pb and Zn still remained at potentially hazardous levels.

The published threshold values (in Table 2.2) are based on residential use of a site, which is considered to be most sensitive and include direct contact with the soils and even ingestion of home grown vegetables. While this scenario is very unlikely given that mine wastes and sediments were sampled, it does indicate that both the Gunnerside mine wastes and sediments could pose a risk to human health. However, based on the column leaching experiment and sequential extractions Pb and Zn were not always in an available form.

6.2.1 Column Leachate

The monthly calculated values for the leachate were calculated by averaging the concentrations from week 15 onwards and then dividing by three (the number of month in each modelled season) to account for the seasonal additions of water, shown in Table 6.2. The averages were calculated from week 15 onwards as this was when the concentrations of metallic elements in the leachate largely stabilised.

The EA calculated the EQS (annual averages) for Gunnerside Gill based on a hardness of 70 mg/L sampled in February 2010 as 50 µg/L for Zn, 7.2 µg/L for Pb and 0.09 µg/L Cd (EA 2013). The EQS were updated to bioavailability rather than hardness (WFD-UKTAG, 2014), for Gunnerside Gill this means the EQS values have reduced to 6.1 µg/L for Pb and 28 µg/L for Zn. The calculated concentrations of Pb exceeded the EQS in all four column leachate samples and three of the four samples exceeded the EQS for Zn.

Table 6.2: Average aqueous concentrations of Pb and Zn from the column leachate experiment

| Location | Pb | Zn |
|----------------------|------|------|
| | µg/L | |
| Gun 1 | 37.1 | 23.3 |
| Gun 2 | 38.3 | 700 |
| Gun 3 | 40.6 | 1010 |
| Gun 9 | 758 | 1760 |
| EQS (EA 2013) | 7.2 | 50 |
| EQS (WFD-UKTAG 2014) | 6.1 | 28 |

The published thresholds for Pb in drinking water ranged from 1 µg/L (DWI 2009) to 15 µg/L (USEPA, 2009). Only two of the five sources have thresholds for Zn, ranging from 3,000 µg/L (Australia Drinking Water Guidelines, 2015) to <5,000 µg/L (Health Canada, 2014). All the thresholds are detailed in Table 2.3 and relate specifically to drinking water. All four samples recorded Zn concentrations below the published threshold values and all four samples exceeded the Pb thresholds. This is a reflection of the sensitivity of Pb on human health (Korn et al., 2006) and Zn on aquatic life (Tiruta-Barna et al., 2007).

6.3 Column Leachate vs EA Monitoring Data

The EA data from the monthly monitoring water at Gunnerside Gill undertaken in 2010 / 2011 and the calculated values from the column leaching experiment were compared (EA, 2013). This was done to see if the column leaching could predict the concentrations recorded within the waters of Gunnerside Gill. The EA concentrations and data from the study were plotted to indicate how the locations relate to each other, also shown on Figure 4.2. A summary of the EA data can be found in Appendix A.

The six EA monitoring locations were GG1 - to the north of the main mining areas; GG2 - adit at Bunton Level; GG3 - river monitoring point; GG4 - Sir

Francis Level; GG5 - river monitoring point; and GG6 - downstream river monitoring point at the village of Gunnerside.

The EA report (2013) concluded that 92 % of the concentrations of Pb and Zn exceeded the respective calculated EQS values. At GG1 the concentrations of Pb exceeded the EQS by a factor of 1.5 and Zn by a factor of 2.4 as a result of considered to be resulting from inputs from the Blakenthwaite Mines situated upstream of the study area. Concentrations of Pb were 4 times higher than the EQS at GG6, Zn concentrations are a factor of 3.4 higher and Cd was 18 times higher. The highest concentrations of Pb and Zn were recorded in the mine discharges from Bunton Level and Sir Francis Level. When considering flow along with the metallic element concentrations the EA concluded that point sources are more important for Zn at higher flows and it was likely the Pb was emanating from diffuse inputs including contaminated sediments and run off from spoil heaps.

The EA water monitoring data and column leachate concentrations are shown schematically for Pb, Zn, Mn, Ca and Fe in Figures 6.6 to 6.10.

The modelled monthly Pb concentrations were one to four times above the concentrations recorded during the EA monitoring, with the exception of Gun 9. The leachate from Gun 9 recorded concentrations of around 17 times greater than at the downstream monitoring location of GG5. GG5 was a river monitoring location and not targeting any of the main mining areas. Gun 9 was recovered from alluvium which was likely to be a combination of mobilised upstream and local sediment. These over bank sediments do not appear to have been fully weathered. Concentrations of Pb within the waters of Gunnerside Gill ranged between 13.8 µg/L (GG1) to 51.9 µg/LL (GG2) and remained between 25 µg/L to 45 µg/L further downstream. The column leachate concentrations were recorded as 2.7 times higher between Gun 1 and GG1, 0.7 times lower in Gun 2 than GG2, 1.1 times higher in Gun 3 than GG3 and 17 times higher in Gun 9 than GG5.

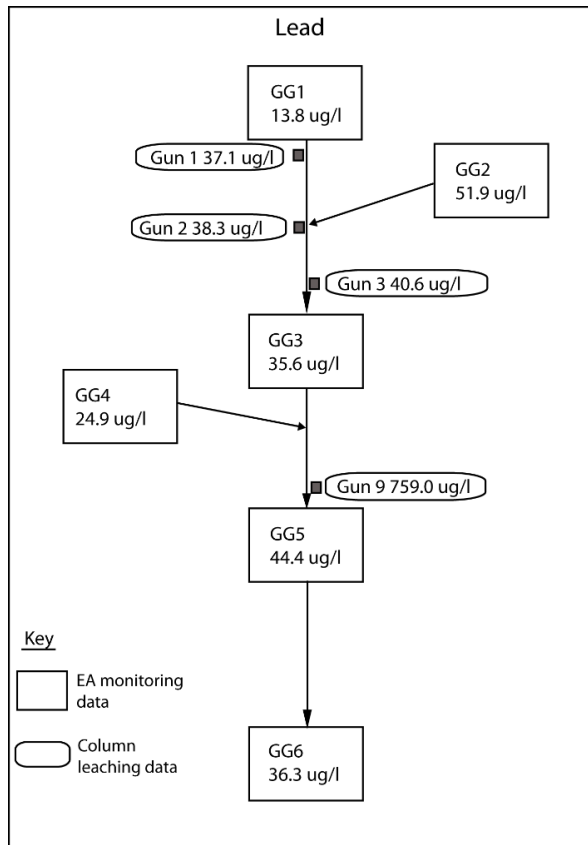


Figure 6.6: Column leachate concentrations vs EA monitoring data for Pb

Concentrations of Zn broadly agreed with the direct monitoring data (Figure 6.7). Gun 9 has similar concentrations to GG4 (Sir Francis Level direct mine drainage) located upstream rather than GG5 a river monitoring point. The Zn concentrations were 8.2 times above GG5 but only 1.05 times above GG4. This could imply a coincidental relationship or possibly that the mine waters emanating from Sir Francis Level are in contact with rocks that have a somewhat similar mineralogy to the mine wastes. Given that any readily exposed ore minerals would have been removed out first this would leave behind a higher gangue to ore mineral ratio in the remaining rocks that have also been weathered over the last century due to the cessation of the mining. Gun 2 and Gun 3 both recorded Zn concentrations similar to GG2 (adit at Bunton Level), although Gun 3 is closer to GG3 which is slightly further downstream. Concentrations of Zn were 1.1 times GG1 in Gun 1, Gun 2 was 13 % less than GG2, and Gun 3 was 13.7 times above GG3 but only 1.3 times above GG2. The EA monitoring data shows that the Zn concentrations are lowest at GG1, peaking at the mine discharge point sources of GG2 (Bunton Level) and GG4 (Sir Francis Level) and then reducing downstream.

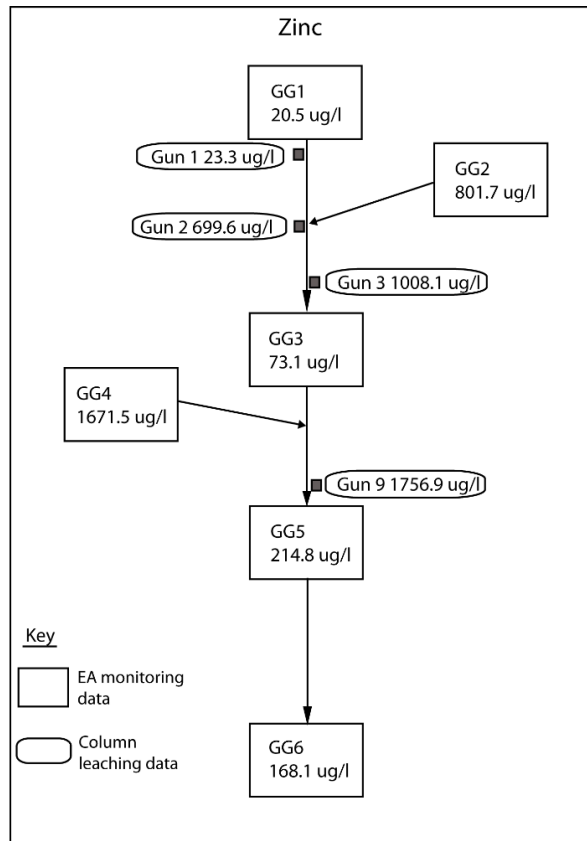


Figure 6.7: Column leachate concentrations vs EA monitoring data for Zn

Concentrations of Mn during the EA water monitoring remained low, specifically less than 2.5 µg/L (Figure 6.8). Gun 1 and Gun 2 both recorded concentrations of 0.3 µg/L compared to 2.48 µg/L in GG1 and 0.0 µg/L in GG2. However, Gun 3 is around 5.8 times higher than the concentration reported in GG3. This is probably because Gun 3 is from mine wastes and GG3 is a river monitoring point. The implication is that the mine wastes of Gun 3 aren't fully weathered yet. The highest Mn concentration was recorded in Gun 9 at 85.7 µg/L, significantly above (around 85 times) the value reported during the water monitoring.

The highest concentration of Mn in Gun 9 coincides with the highest concentration of Pb in the column leachate of the sediment sample, this trend is not noted within the EA data. This would imply that the dissolution of Mn oxyhydroxides are involved in the release of Pb in the alluvial sediment samples.

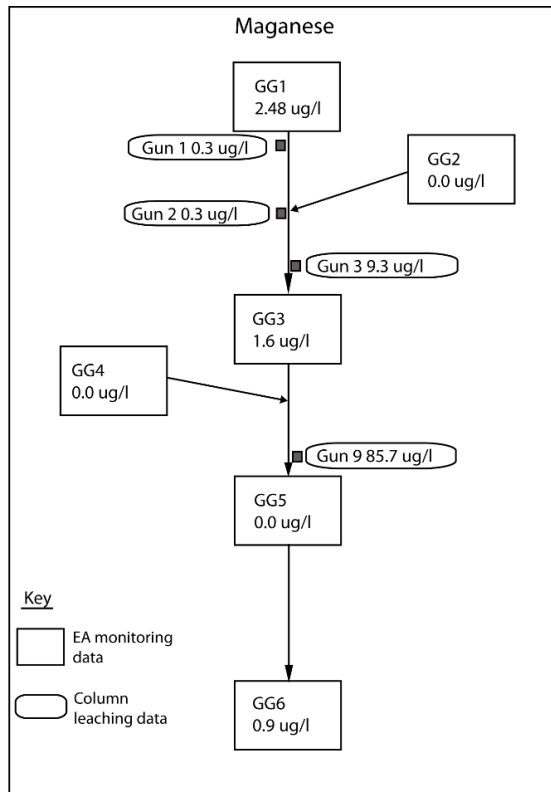


Figure 6.8: Column leachate concentrations vs EA monitoring data for Mn

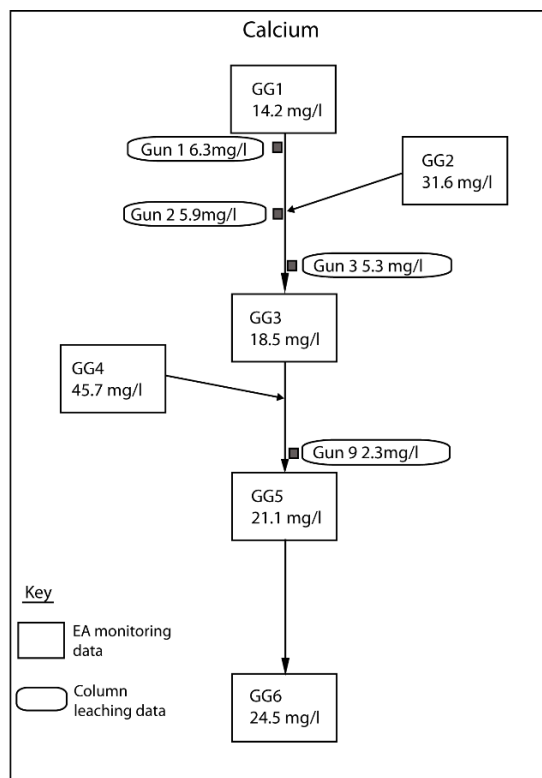


Figure 6.9: Column leachate concentrations vs EA monitoring data for Ca

The Ca concentrations are recorded in mg/L and are an order of magnitude higher in the monitored samples when compared to the modelling data (Figure 6.9). Gun 1 recorded concentrations of 2.3 times less than GG1, Gun 2 was 5.4 times less than GG2, Gun 3 3.6 times less than GG3 and Gun 9 9.2 times below GG5. This could be because the waters within Gunnerside Gill have already been in contact with the underlying carbonate country rocks, allowing for higher Ca concentrations in the catchment water due to dissolution reactions further upstream and from the groundwater/ mine water discharges coming from Bunton and Sir Francis Levels.

The recorded concentrations of Fe within the column leachate were largely below the limit of detection, therefore do not accurately reflect the EA river monitoring data.

In summary, the column leachate experiment was able to give a good estimate of Pb concentrations with regards to the mine waste samples and the water monitoring data from the northern portion of Gunnerside Gill. The alluvial sediment sample, however seemed to overestimate the concentration of Pb when compared to the concentrations recorded in the water of Gunnerside Gill. This is likely to reflect the location of Gun 9 which was recovered from an area of overbank sedimentation, indicating the sediments within Gunnerside Gill likely act as a temporary sink of Pb. Also the column leachate experiment recorded the lowest mean pH value in Gun 9 of 6.5, compared to 6.6 to 7.1 in the other column samples. Some of the water monitoring locations specifically targeted sources of contamination including GG2 at Bunton Level and GG4 at Sir Francis Level, both direct mine water discharges. GG1 was located upstream of the main mining areas and GG6 downstream of the mining areas at Gunnerside village, the remaining two points GG3 and GG5 were river monitoring points.

The first two column leachate experiments again showed similar concentrations of Zn when compared to the EA monitoring data and could be a useful tool at predicting the longer term leachability of Zn in the northern portion of Gunnerside Gill. Gun 3 shows a similar modelled concentration to GG2, which implies the mine wastes are similar to those further up the gill. Gun 9 appears to be more similar to the mine discharges GG4. This could

imply that the rocks remaining within the underlying mine have a similar mineralogical composition to the alluvial sediments or could just be a coincidence that the leachate has similar concentrations to the direct mine discharge.

Manganese concentrations from the column leachate experiment show reasonable agreement with those of the mine waste samples but similar to Pb, Gun 9 overestimated concentrations recorded within the water monitoring samples. This is considered to be a function of Mn oxyhydroxide dissolution during the column leachate experiment, which appeared to be one of the main controls of Pb mobilisation from the sediment sample.

Calcium concentrations were low in comparison to the column leaching experiment when compared to the EA monitoring data. This is perhaps as a result of the water being in direct contact with the underlying carbonate county rocks increasing the Ca concentrations of the water. Again Fe was largely underestimated by the column leachate experiment, possibly because the Fe within the columns was being dissolved and then re-precipitated, and as a result, not recorded in the leachate.

The mine wastes Gun 1 to Gun 3 samples relatively well represented the weathered materials whose leaching resulted in low but constant mobilisation of Pb and Zn. The sediment sample was more representative of a point source whose dissolution resulted in higher concentrations of Pb and Zn being released into the waters of Gunnerside Gill.

6.4 Geochemical Modelling

In order to model which mineral phases may precipitate or dissolve saturation indices (SI) were calculated for both the EA monitoring data and the column leachate data. Saturation indices calculations were undertaken using PHREEQC version 3 (Parkhurst and Appelo, 2013). Negative values indicate minerals that are undersaturated and are likely to dissolve in river waters, and positive values predict that the minerals are oversaturated and therefore likely to precipitate. The more negative or positive the number then the more undersaturated or oversaturated the mineral is likely to be. Values close to

zero indicate the mineral is likely to be in or near equilibrium. There may be some uncertainty in relation to the calculated saturation indices as a result of the estimates used within the thermodynamic data of the database within PHREEQC, these are within 1-2 units as described by Stefánsson et al. (2001).

The calculated saturation indices based on the EA monitoring data are shown in Table 6.3. The results show that the waters are generally undersaturated with respect to the majority of the minerals with the exception of barite, Fe oxyhydroxides and gibbsite ($\text{Al}(\text{OH})_3$). Hematite records the highest SI values and therefore could be precipitating in Gunnerside Gill. Goethite has the second highest SI values in all six sampling locations.

Anglesite is predicted to be undersaturated in five of the six locations (and absent from GG1 as sulfate was below the limit of detection in this sample) and cerussite is also undersaturated in all six locations but the values are closer to zero indicating it is nearer to equilibrium. The lowest SI of cerussite is recorded in GG1, where no SI value for anglesite was recorded reflecting the absence of sulfate in this sample. This is probably a function of its location upstream of the main mining areas away from the most mineralised zones. A Pb hydroxide (PbOH_2) is also undersaturated in all six locations. The PHREEQC results suggest that anglesite may have been the main mineral controlling the mobility of Pb in Gunnerside Gill based on the actual EA monitoring data.

Table 6.3: Saturation indices of key minerals from EA monitoring data (EA 2013)

| Phase | GG1 | GG2 | GG3 | GG4 | GG5 | GG6 |
|-------------------------------------|--------------|--------------|-------------|--------------|-------------|--------------|
| Lead minerals | | | | | | |
| Anglesite | - | -4.22 | -5.08 | -4.40 | -5.20 | -4.96 |
| Cerussite | -1.12 | -0.52 | -0.71 | -0.85 | -0.60 | -0.69 |
| Pb(OH) ₂ | -1.79 | -1.36 | -1.34 | -2.19 | -1.62 | -1.42 |
| Zinc minerals | | | | | | |
| Smithsonite | -2.80 | -0.99 | -2.09 | -0.72 | -1.40 | -1.66 |
| Zn(OH) ₂ | -2.61 | -0.95 | -1.92 | -1.24 | -1.64 | -1.61 |
| Sulfate minerals | | | | | | |
| Jarosite-K | - | -8.21 | -5.84 | -7.44 | -5.69 | -6.00 |
| Gypsum | - | -2.38 | -3.41 | -2.15 | -3.20 | -3.08 |
| Anhydrite | - | -2.89 | -3.91 | -2.65 | -3.69 | -3.58 |
| Iron oxyhydroxides | | | | | | |
| Fe(OH) ₃ (a) | 3.32 | 1.82 | 3.18 | 1.6 | 3.07 | 2.94 |
| Goethite | 8.53 | 7.03 | 8.44 | 6.84 | 8.34 | 8.21 |
| Hematite | 18.98 | 15.97 | 18.8 | 15.61 | 18.6 | 18.35 |
| Manganese oxyhydroxides | | | | | | |
| Hausmannite | -17.74 | - | -17.32 | - | - | - |
| Manganite | -5.41 | - | -5.34 | - | - | - |
| Pyrochroite | -7.07 | - | -7.10 | - | - | - |
| Pyrolusite | -12.7 | - | -12.33 | - | - | - |
| Rhodochrosite | -2.30 | - | -2.30 | - | - | - |
| Carbonate and other minerals | | | | | | |
| Aragonite | -1.18 | -0.51 | -0.84 | -0.42 | -0.4 | -0.62 |
| Barite | - | 0.30 | -0.38 | 0.76 | 0.04 | 0.17 |
| Calcite | -1.02 | -0.35 | -0.69 | -0.25 | -0.25 | -0.47 |
| Dolomite | -2.95 | -1.76 | -2.30 | -1.34 | -1.14 | -1.91 |
| Gibbsite | 2.19 | 1.48 | 1.93 | 1.44 | 1.86 | 1.76 |
| Siderite | -0.84 | -2.27 | -1.08 | -1.66 | -0.78 | -1.12 |
| Witherite | -3.19 | -2.84 | -2.83 | -2.53 | -2.19 | -2.39 |
| % Error | 6.2 | 0.4 | 4.3 | -0.3 | -29.9 | 5.2 |

With regards to Zn, smithsonite and Zn hydroxide record similar undersaturated SI values at all six locations. Jarosite-K, gypsum and anhydrite are sulfate minerals that are also undersaturated within Gunnerside Gill, but these are not likely to be present in the field area as they form and are stable only under very acidic conditions.

Various Mn oxyhydroxides recorded negative SI values in GG1 and GG3, located to the north of the main mining area and a river monitoring point, however, and were absent from the other locations. Aragonite, barite and calcite all reported SI values close to zero indicating relative equilibrium.

The column leachate data was also used to calculate the SI values using PHREEQC (Table 6.4). The first column in Table 6.4 for each location has been charge balanced by the software. The second column shows results of the SI modelling for the raw leachate data, which have high error values as shown in the last row. This is likely to be related to the fact that the data is experimental and that not all elements or not enough were included in the analysis to balance the charges. Although there is a discrepancy in the % error overall the trends are largely the same for both sets of data with the exception of $\text{Pb}(\text{OH})_3$ and $\text{Zn}(\text{OH})_2$, which are slightly oversaturated when charge balanced and slightly undersaturated when not. The SI values generally remain close to zero indicating that they are relatively close to equilibrium and based on the calculations would likely remain in the solid phase. The majority of the mineral phases identified are undersaturated, this is especially true for sphalerite, pyrite and mackinawite (Fe_9S_8). Similar to the EA monitoring data, goethite and hematite are both over saturated in all four columns. There is some discrepancy in the results for the Mn oxyhydroxides between the balanced and unbalanced data. The balanced results indicate the Mn oxyhydroxide phases present are more likely to be oversaturated, while the unbalanced results show an understaturation. Anglesite is predicted to be undersaturated in five of the six locations and cerussite was suggested to not be present based on the column leaching data.

Table 6.4: Saturation indices from column leachate experiments

| | Gun 1 | | Gun 2 | | Gun 3 | | Gun 9 | |
|-------------------------------------|--------------|------------------|--------------|------------------|--------------|------------------|--------------|------------------|
| | Raw data | PHREEQC balanced |
| Lead minerals | | | | | | | | |
| Anglesite | -9.48 | -3.94 | -8.82 | -3.65 | -7.34 | -3.08 | -5.76 | -1.92 |
| Pb(OH) ₂ | 1.38 | -1.36 | 1.52 | -1.91 | 1.87 | -1.75 | 3.68 | -0.36 |
| Zinc minerals | | | | | | | | |
| Sphalerite | -87.69 | -53.08 | -82.83 | -48.54 | -88.61 | -47.98 | -83.14 | -46.73 |
| Zn(OH) ₂ (e) | -1.18 | -3.99 | 0.77 | -2.67 | 0.99 | -2.53 | 1.27 | -2.65 |
| Sulfate minerals | | | | | | | | |
| Jarosite-K | -26.47 | -11.36 | -24.26 | -11.68 | -21.01 | -10.55 | -22.06 | -13.91 |
| Gypsum | -3.56 | -3.53 | -3.35 | -3.33 | -2.99 | -2.98 | -3.92 | -3.93 |
| Anhydrite | -3.92 | -3.89 | -3.71 | -3.69 | -3.35 | -3.34 | -4.28 | -4.29 |
| Pyrite | -168.9 | -96.81 | -163.0 | -91.24 | -173.7 | -90.42 | -164.1 | -88.67 |
| Mackinawite | -102.4 | -60.47 | -98.81 | -57.53 | -105.4 | -57.12 | -99.51 | -56.34 |
| Iron oxyhydroxides | | | | | | | | |
| Fe(OH) ₃ (a) | -0.73 | 0.16 | -0.32 | -0.42 | 0.02 | -0.43 | 0.00 | -1.22 |
| Goethite | 4.98 | 5.87 | 5.39 | 5.29 | 5.73 | 5.28 | 5.71 | 4.49 |
| Hematite | 11.95 | 13.73 | 12.77 | 12.56 | 13.45 | 12.54 | 13.4 | 10.96 |
| Manganese oxyhydroxides | | | | | | | | |
| Hausmannite | 6.35 | -24.27 | 6.54 | -25.3 | 11.95 | -20.12 | 12.86 | -18.47 |
| Manganite | 2.42 | -9.0 | 2.38 | -9.45 | 4.48 | -7.72 | 4.56 | -7.23 |
| Pyrochroite | -2.08 | -9.86 | -1.82 | -10.01 | -0.61 | -8.28 | 0.15 | -7.59 |
| Pyrolusite | 0.21 | -14.85 | -0.13 | -15.6 | 2.86 | -13.87 | 2.27 | -13.59 |
| Carbonate and other minerals | | | | | | | | |
| Barite | -0.3 | -0.27 | -0.3 | -0.29 | -0.08 | -0.08 | -0.18 | -0.19 |
| Gibbsite | -2.21 | 1.73 | -1.87 | 0.48 | -1.31 | -0.28 | -0.65 | 0.42 |
| Alunite | -28.46 | -4.19 | -26.46 | -6.51 | -22.54 | -7.62 | -21.53 | -6.52 |
| Fluorite | -1.2 | -1.19 | -0.37 | -0.38 | 0.27 | 0.25 | -0.53 | -0.66 |
| % Error | 0 | 82 | 0 | 62 | 0 | 28 | 0 | 48 |

6.4.1 Changes in pH

Using PHREEQC the EA monitoring data and column leachate data were subject to changes in pH to see what the effects of mineral dissolution and precipitation might be. The pH range covers the general range recorded during the EA monitoring and the column leaching experiment.

The decreasing pH generally results in a reduction of the SI indices of both the saturated and undersaturated phases (Table 6.5), which is not unexpected. Anglesite is predicted to be present and undersaturated in 5 of the 6 monitoring locations. Furthermore, anglesite becomes less undersaturated as the pH decreases, implying that it will dissolve less in lower pH conditions.

Table 6.5: Summary of the saturation indices from EA monitoring data for pH's 8, 7.5, 7, 6.5, 6, and 5.5

| GG1 | pH value | | | | | |
|-------------|--------------|--------------|--------------|--------------|-------------|-------------|
| | 8.0 | 7.5 | 7.0 | 6.5 | 6.0 | 5.5 |
| Calcite | -0.82 | -1.32 | -1.81 | -2.31 | -2.81 | -3.31 |
| Cerussite | -1.11 | -1.14 | -1.25 | -1.47 | -1.83 | -2.27 |
| Goethite | 8.70 | 7.96 | 6.56 | 5.07 | 3.57 | 2.07 |
| Hematite | 19.32 | 17.84 | 15.04 | 12.05 | 9.05 | 6.05 |
| Manganite | -4.83 | -6.29 | -7.78 | -9.28 | -10.8 | -12.3 |
| Smithsonite | -2.67 | -3.05 | -3.51 | -4.00 | -4.49 | -4.99 |

| GG2 | pH value | | | | | |
|-------------|--------------|--------------|--------------|-------------|-------------|-------------|
| | 8.0 | 7.5 | 7.0 | 6.5 | 6.0 | 5.5 |
| Anglesite | -4.32 | -3.85 | -3.44 | -3.13 | -2.97 | -2.9 |
| Calcite | -0.25 | -0.74 | -1.24 | -1.74 | -2.24 | -2.74 |
| Cerussite | -0.52 | -0.54 | -0.63 | -0.83 | -1.16 | -1.59 |
| Goethite | 7.10 | 6.31 | 4.9 | 3.41 | 1.91 | 0.41 |
| Hematite | 16.12 | 14.55 | 11.72 | 8.73 | 5.73 | 2.73 |
| Smithsonite | -0.94 | -1.28 | -1.73 | -2.22 | -2.71 | -3.21 |

| GG3 | pH value | | | | | |
|-------------|-------------|-------------|-------------|-------------|-------------|-------------|
| | 8.0 | 7.5 | 7.0 | 6.5 | 6.0 | 5.5 |
| Anglesite | -5.18 | -4.72 | -4.31 | -4.02 | -3.86 | -3.8 |
| Calcite | -0.59 | -1.08 | -1.58 | -2.08 | -2.58 | -3.08 |
| Cerussite | -0.70 | -0.73 | -0.83 | -1.03 | -1.37 | -1.81 |
| Goethite | 8.50 | 7.82 | 6.43 | 4.94 | 3.44 | 1.94 |
| Manganite | -5.05 | -6.51 | -7.99 | -9.49 | -10.9 | -12.5 |
| Smithsonite | -2.03 | -2.39 | -2.85 | -3.33 | -3.83 | -4.33 |

| GG4 | pH value | | | | | |
|-------------|--------------|--------------|--------------|-------------|-------------|-------------|
| | 8.0 | 7.5 | 7.0 | 6.5 | 6.0 | 5.5 |
| Anglesite | -4.78 | -4.31 | -3.88 | -3.55 | -3.35 | -3.27 |
| Calcite | 0.13 | -0.36 | -0.86 | -1.36 | -1.86 | -2.36 |
| Cerussite | -0.84 | -0.86 | -0.93 | -1.1 | -1.4 | -1.82 |
| Goethite | 7.37 | 6.61 | 5.2 | 3.71 | 2.21 | 0.71 |
| Hematite | 16.66 | 15.14 | 12.33 | 9.35 | 6.35 | 3.35 |
| Smithsonite | -0.50 | -0.80 | -1.22 | -1.7 | -2.19 | -2.69 |

| GG5 | pH value | | | | | |
|-------------|--------------|--------------|--------------|--------------|-------------|-------------|
| | 8.0 | 7.5 | 7.0 | 6.5 | 6.0 | 5.5 |
| Anglesite | -5.30 | -4.82 | -4.38 | -4.04 | -3.84 | -3.75 |
| Calcite | -0.15 | -0.64 | -1.14 | -1.64 | -2.14 | -2.64 |
| Cerussite | -0.60 | -0.61 | -0.68 | -0.84 | -1.13 | -1.54 |
| Goethite | 8.40 | 7.69 | 6.3 | 4.81 | 3.31 | 1.81 |
| Hematite | 18.73 | 17.31 | 14.53 | 11.55 | 8.55 | 5.55 |
| Smithsonite | -1.36 | -1.64 | -2.06 | -2.54 | -3.03 | -3.52 |

| GG6 | pH value | | | | | |
|-------------|--------------|--------------|--------------|--------------|-------------|-------------|
| | 8.0 | 7.5 | 7.0 | 6.5 | 6.0 | 5.5 |
| Anglesite | -5.06 | -4.59 | -4.18 | -3.87 | -3.7 | -3.63 |
| Calcite | -0.37 | -0.86 | -1.36 | -1.86 | -2.36 | -2.86 |
| Cerussite | -0.69 | -0.72 | -0.8 | -0.99 | -1.32 | -1.75 |
| Goethite | 7.59 | 8.27 | 6.21 | 4.72 | 3.22 | 1.72 |
| Hematite | 18.47 | 17.12 | 14.35 | 11.37 | 8.37 | 5.37 |
| Smithsonite | -1.60 | -1.95 | -2.4 | -2.88 | -3.38 | -3.87 |

Table 6.6: Summary of saturation indices from column leachate data for pH's 8, 7.5, 7, 6.5, 6, and 5.5

| Gun 1 | pH value | | | | | |
|------------|--------------|--------------|--------------|--------------|-------------|-------------|
| | 8.0 | 7.5 | 7.0 | 6.5 | 6.0 | 5.5 |
| Anglesite | -4.31 | -4.06 | -3.94 | -3.89 | -3.87 | -3.87 |
| Goethite | 6.94 | 6.78 | 5.87 | 4.43 | 2.94 | 1.44 |
| Hematite | 15.87 | 15.55 | 13.73 | 10.85 | 7.86 | 4.86 |
| Manganite | -6.0 | -7.5 | -9.0 | -10.5 | -12.0 | -13.5 |
| Pyrite | -114 | -105 | -96.8 | -88.8 | -80.8 | -72.8 |
| Sphalerite | -61.2 | -57.1 | -53.0 | -49.1 | -45.1 | -41.1 |

| Gun 2 | pH value | | | | | |
|------------|--------------|--------------|--------------|-------------|-------------|-------------|
| | 8.0 | 7.5 | 7.0 | 6.5 | 6.0 | 5.5 |
| Anglesite | -4.06 | -3.81 | -3.69 | -3.64 | -3.63 | -3.62 |
| Goethite | 7.21 | 7.04 | 6.13 | 4.7 | 3.2 | 1.7 |
| Hematite | 16.39 | 16.07 | 14.25 | 11.4 | 8.39 | 5.39 |
| Manganite | -5.55 | -7.05 | -8.55 | -10.1 | -11.6 | -13.1 |
| Pyrite | -114 | -104 | -96.1 | -88.0 | -80.0 | -72.0 |
| Sphalerite | -59.0 | -54.9 | -50.9 | -46.9 | -42.9 | -38.9 |

| Gun 3 | pH value | | | | | |
|------------|--------------|--------------|-------------|-------------|-------------|-------------|
| | 8.0 | 7.5 | 7.0 | 6.5 | 6.0 | 5.5 |
| Anglesite | -3.48 | -3.23 | -3.12 | -3.07 | -3.06 | -3.05 |
| Goethite | 7.20 | 7.04 | 6.12 | 4.69 | 3.19 | 1.69 |
| Hematite | 16.39 | 16.06 | 14.2 | 11.4 | 8.37 | 5.37 |
| Manganite | -3.82 | -5.32 | -6.82 | -8.32 | -9.82 | -11.32 |
| Pyrite | -113 | -104 | -95.3 | -87.2 | -79.2 | -71.2 |
| Sphalerite | -58.5 | -54.4 | -50.4 | -46.4 | -42.4 | -38.4 |

| Gun 9 | pH value | | | | | |
|------------|-------------|-------------|-------------|-------------|--------------|--------------|
| | 8.0 | 7.5 | 7.0 | 6.5 | 6.0 | 5.5 |
| Anglesite | -2.35 | -2.09 | -1.97 | -1.92 | -1.91 | -1.9 |
| Gibbsite | 1.80 | 2.25 | 1.84 | 0.42 | -1.08 | -2.58 |
| Hematite | 15.9 | 15.6 | 13.8 | 11.0 | 7.97 | 4.97 |
| Manganite | -2.73 | -4.32 | -5.73 | -7.23 | -8.73 | -10.2 |
| Pyrite | -115 | -105 | -96.7 | -88.7 | -80.7 | -72.7 |
| Sphalerite | -58.8 | -54.7 | -50.7 | -46.7 | -42.7 | -38.7 |

The SI of the column leachate data (Table 6.6) are based on the unbalanced water analysis data, so although the exact SI may be incorrect it conveys the overall trends.

The mineral phases vary from the EA monitoring data, as do the changes in SI based on changes in the pH values. Anglesite shows a similar, if less pronounced trend, of slightly increasing SI values.

6.5 Comparison to Previous Studies

One of the main reasons Gunnerside Gill was selected as the area of study for this work is due to the previous studies undertaken by other researchers including Dennis et al. (2009). Further studies were also conducted on the sediments within the Upper Swale by Macklin et al. (1994), Walling et al. (2003), and Dennis et al. (2003). The potential volume of mine wastes present in Gunnerside Gill is difficult to quantify. It has previously been estimated that at least 100,000 tonnes of mine waste was dumped along Old Rake Vein, located in the Lownathwaite / Old Gang mining area (Dunham and Wilson, 1985).

A DEFRA commissioned study (Brewer et al., 2005) found the following within the wider River Swale catchment:

- 91% of topsoil and 94 % of sub-surface samples were elevated in Pb above the background concentrations;
- between 90 % and 95 % of samples exceeded the background concentrations of Cd and Zn;
- calculated 'pre-mining' background concentrations of 212 mg/kg for Pb, 105 mg/kg for Zn and 1.0 mg/kg for Cd.

Table 6.7 shows that total concentration of Pb within the ten samples recovered from Gunnerside Gill are all in excess of the background concentrations from the wider River Swale catchment.

Table 6.7: Total Pb and Zn concentrations (mg/kg) compared to calculated 'pre-mining' background values from Brewer et al. (2005).

| | Gun 1 | Gun 2 | Gun 3 | Gun 4 | Gun 5 | Gun 6 | Gun 7 | Gun 8 | Gun 9 | Gun 10 | Back-ground |
|-----------|-------|-------|-------|-------|-------|-------|-------|-------|-------|--------|-------------|
| Pb | 70000 | 17900 | 1840 | 5430 | 49300 | 2400 | 6260 | 4140 | 8710 | 6590 | 212 |
| Zn | 4100 | 12600 | 8100 | 2000 | 64300 | 2900 | 61000 | 14600 | 4950 | 3280 | 105 |

The Pb concentrations are between 8.6 and 330 times higher than the calculated 'pre-mining' background values. Similarly, all the Zn concentrations also exceeded the background concentrations by a factor of 27 to 612. The upper reaches of the River Swale have been subjected to mining inputs from the tributaries including Gunnerside Gill. However, given that there is no published threshold value for Pb and Zn contamination within sediments these values give a reasonable baseline for Gunnerside Gill.

Dennis et al. (2009) reported concentrations of Pb within the clay and silt fraction of the overbank sediments of 11,000 to 14,500 mg/kg and 21,500 to 22,400 mg/kg within the sand sized fraction. These were sampled from Sir Francis Level and the Old Gang / Lownathwaite mining areas. Concentrations of Zn were not reported as part of the study and the samples were recovered from active channel sediments between Blakenthwaite mines and the River Swale. The sediment samples from Gun 9 and Gun 10 recorded Pb concentrations of 8,710 mg/kg and 6,590 mg/kg respectively, both below the concentrations reported by Dennis et al. (2009) in sediment samples of both size fractions. With regard to locations Gun 2 and Gun 5 might be more comparable to the solids analysed by Dennis et al. (2009) as they are from similar localities. Although these are mine waste samples, they recorded Pb concentrations of 17,900 mg/kg and 49,300 mg/kg, respectively. Given that the alluvial sediments are largely derived from the mine wastes and former mining activities (e.g. hushing), elevated concentrations of Pb within the sediments near the former mining areas are not unexpected. Dennis et al. (2009) used the data to estimate the Pb storage within the floodplain of the River Swale, there was no discussion with regards to the potential

mechanisms to mobilise Pb in from the sediments to the water or mineralogy. This does indicate that concentrations of metallic elements may be higher in the channel sediments when compared to the over bank sediments. This shows the heterogeneity of the metallic element concentrations of all the river sediments, both in channel and on the surrounding floodplain. However, it was noted that concentrations of Pb, Zn and Cd increased downstream of the main mining areas, including; Blakenthwaite dressing floor, Old Gang and Lownthwaite hushes and dressing floors, and Sir Francis Level dressing floor (Dennis et al., 2009). The concentrations of metallic elements reduce rapidly downstream, but this was noted to be less obvious in the lower sections of the river.

As a result of the EA monitoring programme (EA, 2013) at Gunnerside Gill it was concluded that the main source of Zn was Sir Francis Level under all flow conditions. It was more difficult to define a point source for Pb, the diffuse sources identified included sediments within the river, waste from Bunton Mine and wastes Sir Francis Level.

Based on the current study it appears that the alluvial sediments are more important than the mine wastes for the release of Pb into Gunnerside Gill. The mine wastes have been present for around 100 years and have therefore been subject to both physical and chemical erosion. This has resulted in the mobilisation of the mine wastes including ore minerals downstream but also the formation of secondary minerals and scavenging of Pb by Mn oxyhydroxides. In this case the results suggest that the dissolution of Mn oxyhydroxides could be one of the main controls resulting in mobilisation of Pb into the waters of Gunnerside Gill and further downstream into the River Swale.

[6.6 Controls on Weathering Reactions](#)

The second objective of the study was to determine the major factors influencing the transfer of metallic elements from solids into the waters, e.g. mineralogy, grain-size, location of the mine tips and/or contaminated sediments, pH, or the reductive dissolution of the Fe / Mn oxyhydroxides.

Key mechanisms related to the controls on weathering reactions include pH, mineralogy, CEC, Mn / Fe oxyhydroxides, organic matter, microbiology, oxic

and anoxic conditions, and physical controls. Due to time and financial constraints CEC, organic matter and microbiological analysis were excluded from this study.

6.6.1 Eh-pH from Column Leaching Experiment

During the column leaching experiment the pH and Eh of the leachate were recorded (Figure 5.19). The system was open so the Eh cannot be fully relied on as the leachate was allowed to equilibrate with the surrounding atmosphere. However, in Gunnerside Gill is also not a closed system. The leachate from Gun 9 often had the highest Eh and Gun 1 often has the lowest Eh, opposite to the pH results. The Eh concentrations generally ranged between 150 and 280 mV. These values are suggestive of Mn(IV) reduction as shown in Table 2.5, based on a pH of 7.

The overall Eh trend (Figure 5.21) began relatively high, around 240 mV, reducing to week 11 when the lowest values were recorded at around 180 mV. The Eh values then crept up again and remain relatively consistent at 220 mV. Week 11 was week commencing 31st March 2014, so the overall drop in Eh could reflect a seasonal variation related to when the experiment was undertaken.

As shown in Figure 5.21 and Table 5.6, the overall pH values of the column leachate generally ranged from 6.5 to 7.5 in the first 28 weeks. The pH dropped around week 28 to 6.0 to 7.0 and then the pH of the blank input water continued to drop throughout the remaining weeks to 5.5 in week 40. From week 30 to week 40 the column leachate showed buffering reactions, reflected in the pH increasing back to 6.5 to 7.5. The drop in pH of the input water is as a result of a change of source, which although adding an extra variable. It shows that the mine wastes and sediment are still able to maintain a neutral pH and buffer acidic conditions.

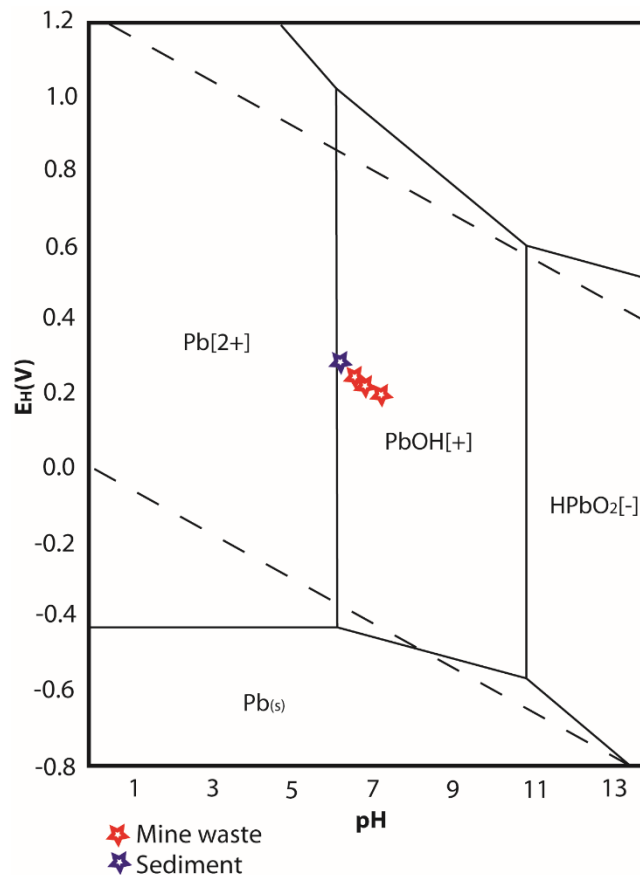


Figure 6.10: Eh-pH diagram for Pb-O-H (after Takeno 2005))

Within the four modelled samples (Gun 1, Gun 2, Gun 3 and Gun 9), cerussite was found to be present at <10 % in Gun 1 and as grains by EMP in Gun 2, and galena was present in Gun 2 by EMP and in Gun 3 at <10 %. Interestingly Gun 9, was not found to contain either cerussite or galena but did contain Pb/Zn phosphate grains as identified by EMP analysis. Figure 6.10 shows that within the mine wastes Pb is present potentially in a hydroxide form and within the sediment sample is on the boundary with aqueous Pb[2+]. Galena is stable over a wide pH range when in sulfidic conditions, Pb sulfate (anglesite) is stable at low pH and oxidising environments and Pb carbonates (e.g. cerussite) is stable at near-neutral to slightly alkaline conditions (USEPA, 2007). Sulfate reduction occurs at around -217 mV (at pH 7) (Langmuir, 1997), given the Eh of the column leachate was never recorded below 90 mV sulfate reduction is not considered to play an important control within the modelled system in relation to Pb release. This implies that galena is likely to be, or was historically, relatively unstable in these conditions, and likely to undergo or have previously been weathered to cerussite and / or anglesite. From the EMP

analysis it appeared that often grains of galena would have an outer protective rim of Pb oxide / carbonate, barite or clay minerals. As a result the dissolution of galena is not the primary source of Pb in the catchment waters currently, it is likely to have been a more important control on Pb mobility historically. Gun 9 released the most Pb during the column leaching experiment, which after an initial peak in week 1 and sharp drop in concentration by week 3, which then gradually increased for the remainder of the experiment. A similar if less pronounced trend was noted in weeks 1 to 3 in Mn concentrations, which also increased and plateaued before gradually decreasing again from week 32 onwards. The Eh-pH diagram for Mn is discussed below.

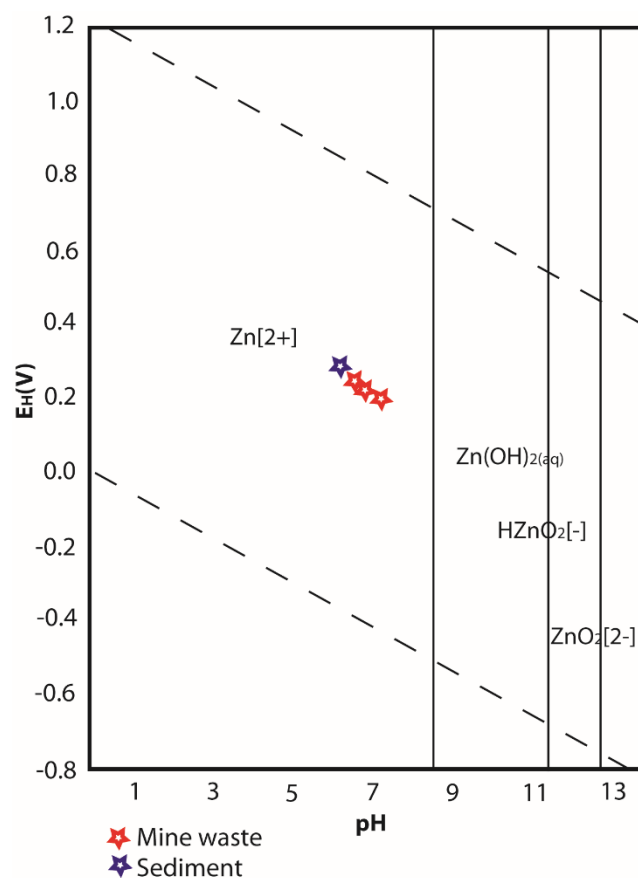


Figure 6.11: Eh-pH diagram for Zn-O-H (after Takeno 2005)

The recorded Eh and pH from the column leachates plot within the Zn²⁺ zone, (Figure 6.11) implying that Zn is likely to be in the oxide or aqueous phase. Both Gun 2 and Gun 3 recorded initial peaks of Zn within the leachate of 33,500 and 55,000 µg/L/L respectively. This was mirrored by similar peaks of S within Gun 2 and Gun 3 of 500,000 and 143,000 µg/L, respectively. This implies that within the mine waste samples the dissolution of sphalerite is an

important mechanism in the mobility of Zn. Sphalerite was detected in Gun 2 and Gun 3 by EMP analysis. Gun 9 also contains sphalerite (<10 %) and had an initial peak concentration of Zn, but this was not mirrored within the S concentrations.

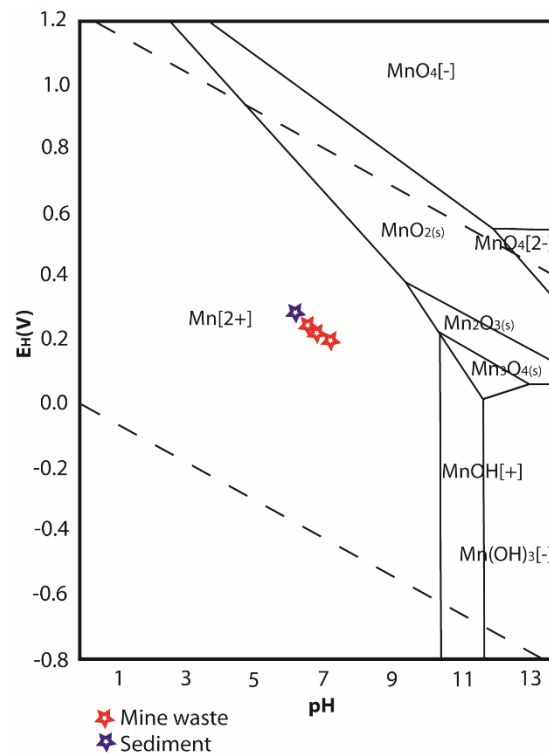


Figure 6.12: Eh-pH diagram for Mn-O-H (after Takeno 2005)

Manganese appears to have an important role in the release of Pb from the sediment sample (Gun 9). Based on the Eh and pH of the column leachate from Gun 9 Mn is largely present in the aqueous Mn[2+] form (Figure 6.12). The leachate from the mine waste samples maintained a slightly higher pH and slightly lower Eh so tend to be just within the Mn oxide boundary of the Eh-pH diagram.

Given the recorded pH and Eh of the column leachate, it may be possible the Fe was undergoing dissolution and precipitation reactions and therefore remains at a low concentration within the leachate itself. The Eh and pH values from the column leachate plot within the Fe₂(OH)₃ section of the Eh-pH diagram (Figure 6.13), which is a Fe oxide. Ferric Fe oxide is actually produced as a powder, granules or slurry to remove metallic elements from soils and water (Reade International, 2018). Ferrihydrite, is a poorly crystalline Fe oxide that is often found in natural waters. It can sorb metallic elements (e.g. Cd, Pb

and Zn) and as it ages become more crystalline transforming into goethite or hematite to become a more permanent sink (Arthur et al., 1999). This indicates the importance of Fe oxyhydroxides in the cycling of metallic elements within mining impacted catchments.

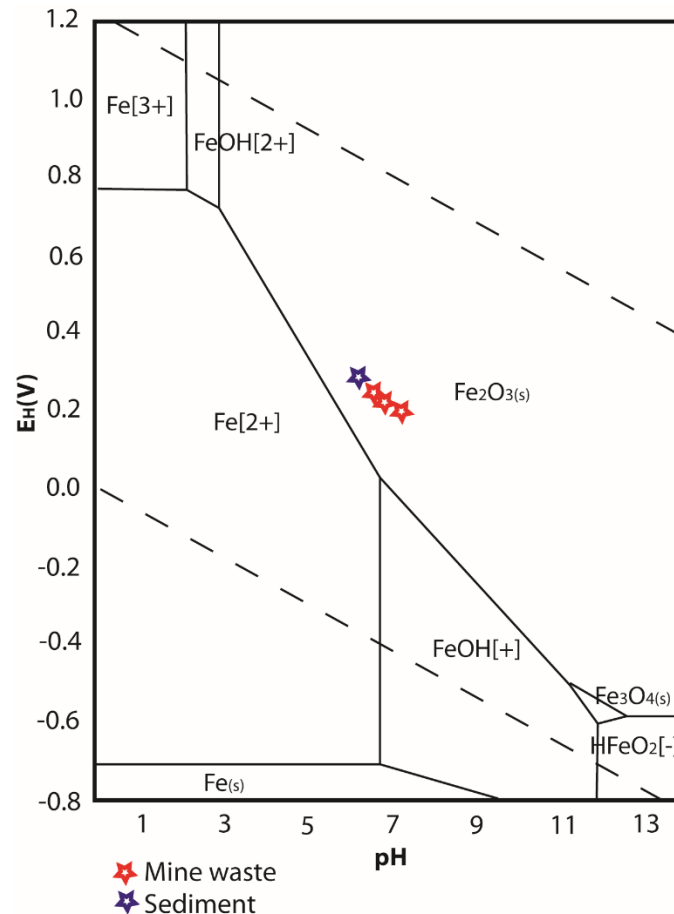


Figure 6.13: Eh-pH diagram for Fe-O-H (after Takeno 2005)

6.6.2 pH from EA Monitoring Data

The Eh data were not supplied with the water monitoring data from the EA so it is not possible to determine the controls of metallic element mobility in the waters of Gunnerside Gill directly. However, a summary of the pH values is shown in the table below.

Table 6.8: pH values reported following EA water monitoring campaign (EA 2013)

| Sampling Location | Features of Note | pH | | |
|-------------------|---|-----|------|-----|
| | | Min | Mean | Max |
| GG1 | Upstream of Bunton Mine | 7.5 | 7.8 | 8.0 |
| GG2 | Bunton Level | 7.3 | 7.9 | 8.1 |
| GG3 | Upstream of Sir Francis Level | 7.7 | 7.9 | 8.2 |
| GG4 | Sir Francis Level | 7.5 | 7.6 | 7.7 |
| GG5 | Downstream of Sir Francis Level and spoil | 7.6 | 7.9 | 8.2 |
| GG7 | Tributary from Kining Level | 7.8 | 7.8 | 8.0 |
| GG6 | At Gunnerside village bridge | 6.8 | 7.8 | 8.4 |

The pH values recorded during the EA monitoring ranged between 6.8 to 8.4, with a mean range of 7.6 to 7.8 (Table 6.8). These values are generally slightly more alkaline than those measured during the column leaching experiment which averaged between 6.5 to 7.1, this is likely to be related to the source of the water.

Rainwater has a pH of around 5.6 (Blowes et al., 2013), but the waters within Gunnerside Gill are not pure rainwater. The gill waters will be mixtures of rainwater and runoff from the surrounding landscapes that has percolated through the surrounding rock piles, and emanated from further up Gunnerside Gill. This means that the waters themselves have undergone various reactions, including neutralisation by the underlying carbonate and silicate rocks.

The deionised water used in the column leachate study had a pH of between 5.5 and 7.7 (Table 5.6) before being added to the mine wastes and sediments. This means that the pH was often lower than that directly measured in the water of Gunnerside Gill. Consequently the leachate pH values are also lower overall. However, there is evidence of buffering reactions during the second half of the experiment. The pH of the deionised water was generally between 5.5 and 7.0, with the solids buffering the pH to between 6.0 and 7.0.

6.6.3 Ficklin Classification

Ficklin et al. (1992) created a classification scheme by using the metallic element content (Zn, Cu, Cd, Pb, Co and Ni) of mine drainage and plotting it against pH. In the case of this study Co and Ni were not tested for as they are not likely to be present in significant concentrations within the samples, so the metallic element content excludes these elements. Figure 6.14 shows the water of Gunnerside Gill plotted from the EA data and the column leachate from the four tested samples.

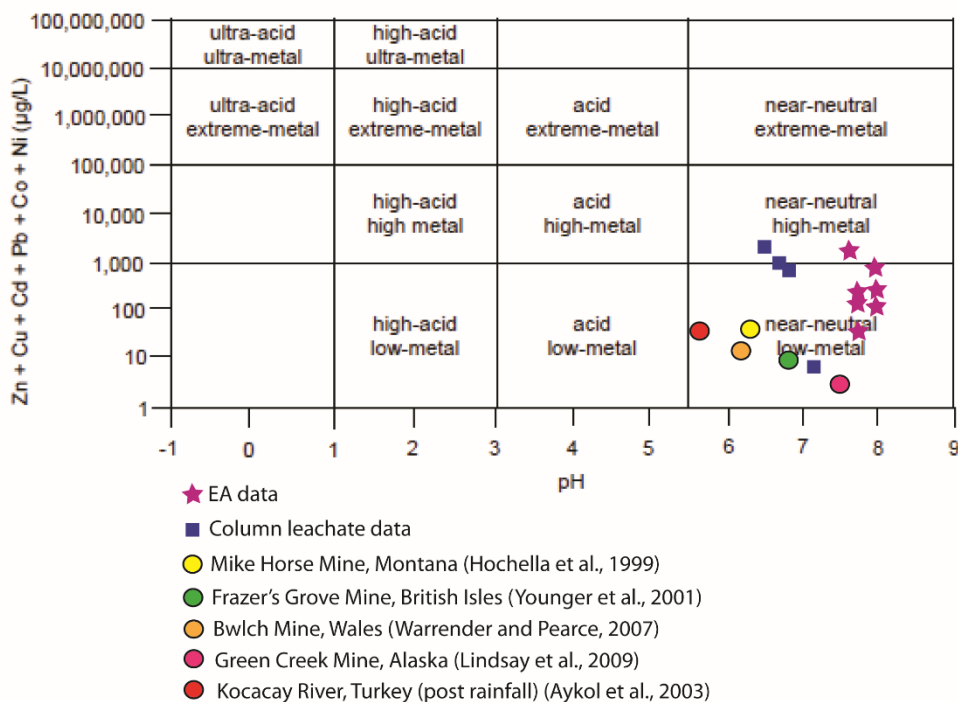


Figure 6.14: Ficklin plot of EA data, column leaching data and other localities (from Table 2.6)

The majority of the EA water samples plotted within the 'near-neutral, low-metal' classification, with the exception of GG4. GG4 plotted in the 'near-neutral, high metal' classification. This sample was recovered from Sir Francis Level mine water adit and interestingly also has the lowest pH of the monitoring samples. The sample with second the highest metallic element concentration was located at Bunton Lead Level mine water adit (GG2). The metallic element concentrations from GG2 and GG4 are made up of 93 % and 98 % Zn, respectively. This corroborates the findings of the EA report, which were that Sir Francis Level minewater adit is the most significant source of Zn (and Cd) within Gunnerside Gill (EA, 2013).

The column leachate samples also plotted in the ‘near-neutral, low metal’ to ‘near-neutral, high-metal’ section similar to the EA data. The main difference between the monitoring data and the leachate samples is the pH, but the overall concentrations of metallic elements are comparable. Again Zn was found to be the main contributor to the recorded concentrations with Gun 2 and Gun 3 comprising 91 % and 95 % Zn respectively, in the mine wastes. Zn comprised 70 % of the metallic elements of the Gun 9 leachate. This could be because significant amounts of Pb were leached from Gun 9 compared to Pb leached from the mine waste samples Gun 1 to Gun 3.

6.6.4 Mineralogy

The mineralogy of a mine site and associated mining affected catchment are considered to be key in determining the potential for AMD or NMD.

Table 6.9: Summary of key primary and secondary minerals for mine wastes (Gun 1 to Gun 8) and sediments (Gun 9 and Gun 10) from Gunnerside Gill (XX = 10-25%, X = minor component – <10%, x_g = individual grains identified by EMP)

| | Galena | Sphalerite | Cerussite | Pb/Zn Phosp. | Pyrite | Fe Oxi | Smithsonite |
|--------|------------------|------------------|----------------|-----------------|----------------|----------------|----------------|
| Gun 1 | X _g * | | X | | X _g | X _g | |
| Gun 2 | X _g | X _g * | X _g | | | X _g | |
| Gun 3 | X | X _g | | | X _g | | |
| Gun 4 | | | | | | X _g | |
| Gun 5 | X | X | X _g | | X _g | X _g | |
| Gun 6 | X | | X _g | | X _g | | |
| Gun 7 | X | X | | | X _g | X _g | |
| Gun 8 | | X | X _g | | | | |
| Gun 9 | | X | | X _g | | X _g | |
| Gun 10 | | | X _g | | X _g | X _g | X _g |

* identified in the post column leaching solids by EMP

The full mineralogical summary table is in Section 5.3.3, and Table 6.9 is a summary of the key primary and secondary minerals found within the ten samples recovered from Gunnerside Gill.

Overall Gunnerside Gill is considered to be representative of a low Fe NMD type. This is confirmed by the low concentrations of pyrite present, only noted as grains by EMP five of the mine waste samples and one of the sediment

samples. In addition, the EMP mapping of various grains indicated limited concentrations of Fe within the sphalerite present in the solid samples.

Sphalerite was noted to be present within the alluvial overbank sample, Gun 9. This is likely to be as a result of transportation of ore rich minerals from Sir Francis Level, where the highest concentrations of sphalerite were present within the gill.

Oxyhydroxides of Mn / Fe were found to be present within the sediment samples. In oxidised tailings as the system matures the Fe oxyhydroxides gradually become more crystalline reducing their ability to sorb metallic elements (Moncur et al., 2009). Poorly crystalline and microcrystalline Mn and Fe oxyhydroxides have a large sorption capacity for metallic elements, in a dry oxidising environment they become more stable with greater capacities for immobilising their incorporated metallic elements (Tack et al., 2006). Gun 9 was located on an area of overbank sediments, this could be considered to be a relatively 'dry oxidising' environment, which may have resulted in some recrystallisation of the Fe / Mn oxyhydroxides and therefore have a higher immobilisation capacity for Pb and Zn.

6.6.5 Location of Mine Wastes and Impacted Sediments

The nature and volume of tailings and waste rock can vary enormously depending upon the mineral of interest, the types of processes involved and the mineralogy of the area being mined. These variations result from many factors including particle size, permeability, secondary mineral formation, and the concentration and distribution of metallic elements (Palumbo-Roe and Colman, 2010). The mine waste piles along Gunnerside Gill frequently lie adjacent to the water's edge (Figure 3.9). This is a function of the historical mining techniques used including hushing and gravity separation using water. Furthermore, historically mine wastes would have been disposed of by the cheapest and easiest method possible, often by dumping in or close to the nearest watercourse (Hochella et al., 2005; Palumbo-Roe and Colman, 2010). This is most evident along the northern portion of the study area in Gunnerside Gill.

Based on the results much of the mine waste in the north of the study area has been significantly weathered and are contributing low concentrations of metallic elements to the waters of Gunnerside Gill, however they are still leaching. Remediation options are difficult given the dispersed nature of the mine waste piles.

The sediments in this study were samples from the southern portion of Gunnerside Gill. Gun 9 was located to the south of Sir Francis Level, this would indicate that the metallic elements present within the sediments are likely to be derived from here and further up the gill. The mine wastes become part of the sediment load within mining affected catchments and then are cycled through the system. Mechanical erosion of the waste piles and tailings results in the metallic element associated sediments entering the fluvial system (Audry et al., 2006). Gun 9 was recovered from an area of overbank sedimentation with limited vegetation. Overbank deposition on floodplains represents a loss of sediment in the system as it enters long-term storage, conversely channel storage is usually shorter-term and serves to convey sediment to the catchment outlet (Walling et al., 2003), in this case the River Swale.

During the winters of 2013-2014 and 2015-2016 there was an unprecedented volume of rainfall which resulted in widespread flooding not only of this catchment, but also across the British Isles. Further flash flooding occurred in north Yorkshire in July 2019. It is likely these flooding events will have increased the erosion and redistribution of mine wastes and sediments down Gunnerside Gill and on into the River Swale. Should these flooding events become more common in the future, this will have a significant impact on the mobilisation of metallic elements in mining affected catchments.

The EA are in the process of undertaking a consultation on river basin management (EA, 2019), which includes a section on pollution from abandoned mines and future climate change. The UK government set up a climate research group in 2018 called the UK Climate Projections (UKCP18). The UKCP18 predicts there to be hotter drier summers, milder wetter winters, increasing sea levels and more common extreme weather events (UKCP18

2020). The EA used this data to inform the potential impacts on mining impacted river catchments in the future. It was considered that:

- diffuse metallic element sources are more important after heavy rainfall / higher river flow rates as infiltration of the rain through mine wastes may increase mobilisation and the rate of erosion of mine wastes may increase;
- at higher river flows diffuse sources are found to be the main contributor of metallic elements, as a result of predicted climate change these sources will become a more significant;
- lower river flows following hotter drier summers mean that direct mine water discharges will contribute more to baseflow and therefore become a more important source of metallic elements as there will be less dilution by rain water;
- higher river flows may reduce the metallic element concentrations but increase the overall flux (kg per day);
- extreme rainfall events may erode mine waste piles increasing the mobilisation of metallic elements into the river waters and may also disturb impacted sediments from within the channel;
- severe rainfall events may also cause the collapse of mine shafts, causing a wash out effect and a temporary increase of metallic elements in the effected catchment (EA, 2019).

It was concluded that climate change is likely to impact rainfall intensity and river flows resulting in an increase of the movement of metallic elements in mining affected catchments (EA, 2019).

Dennis et al. (2003) studied the effects of the 2000 flooding event on the metallic element dispersal within the River Swale. The flooding resulted in deposition of channel edge and overbank sediments, identified as they covered the existing vegetation. Furthermore, the highest concentrations of Pb and Zn within the sediments were noted in the middle and lower sections of the River Swale as a result of the erosion of previously contaminated floodplain materials (Dennis et al., 2003). This implies that flood events result in the physical mobilisation of mine wastes downstream from the waste rock piles

but also the mobilisation of contaminated sediments, which would likely be deposited on the floodplains further downstream. This is likely to be most pronounced downstream the Lownathwaite and Old Gang mining areas and Sir Francis Level. In fact, this scenario probably describes the mechanism which formed the overbank sediments samples at Gun 9. Downstream of Sir Francis Level where mining was limited, it could be that the addition of some uncontaminated sediments could actually dilute the metallic element concentrations. This effect is noted between Gun 9 and Gun 10, however a larger sample set would need to be tested to confirm this.

6.6.6 Grain Size

Interestingly, in the study undertaken at Gunnerside Gill by Dennis et al. (2009) higher concentrations of Pb were present in the sand sized sediment fraction, rather than the clay and silt fraction. The mine waste and alluvial sediment samples recovered from Gunnerside Gill for this study were also dominated by sand sized particles. This could be as a result of the finer particles having been washed out of the system previously, given that Gunnerside Gill has not been mined for over a century. It could also be a function of extracting the ore by hushing that the finer particles of galena and sphalerite remained in suspension and were mobilised to the River Swale, while the larger grains were deposited and remained in Gunnerside Gill. Also, the ore minerals are denser than the gangue minerals and would have settled from the water more quickly and were therefore buried by further sediment input. Macklin et al. (1994) indicated the highest concentrations of Pb were around 1.1 to 0.6 m below ground level, which was carbon dated to the late 18th century when the mines were booming. Furthermore, galena was noted to have rims of Pb oxide / carbonate, barite or even clay minerals. At pH values above 8 Pb carbonates are very insoluble, but below pH 6 they can become very soluble (USEPA, 2007). It is possible that galena is not as readily reduced to clay or silt sized grains as it is partially protected from further weathering and that the presence of carbonate is able to maintain a more neutral pH.

6.6.7 Prediction of Metallic Element Mobility

Not all of the solid samples collected from Gunnerside Gill were subjected to the column leaching experiment. Based on the characterisation data of the other samples, namely Gun 4 to 8 and Gun 10, and the column leaching results it might be possible to predict the impact of these samples on Gunnerside Gill.

Gun 4 did not contain any notable concentrations of metallic element bearing minerals with the exception of grains of Fe oxyhydroxides as identified by EMP. It is possible that these oxyhydroxides may act as a sink for Pb and Zn mobilised from the upstream mining areas of Lowanthwaite and Old Gang. However, they are unlikely to represent a significant source of Pb and Zn given the low concentrations present in Gun 4.

Within Gun 5 Pb and Zn were found to be largely associated with the residual fraction based on the sequential extraction data. This corresponds with the presence of galena and sphalerite identified by XRD analysis. This shows that although Pb and Zn are present they are unlikely to result in significant input into the catchment waters as they are contained within the primary minerals. Weathering textures show the primary minerals to have protective coatings or rims of oxides, carbonates and even clay minerals, thereby reducing the dissolution of the galena and sphalerite. Grains of cerussite, Fe oxyhydroxides and pyrite were observed by EMP. This could mean that there was some localised minor acidity produced by the dissolution of pyrite, which was likely to be neutralised by the presence of silicate minerals.

The Pb in Gun 6 was found to be mostly associated with Fe / Mn oxyhydroxides. Similar to Gun 4 these oxyhydroxides are likely to act as a short-term sink for Pb, changes in the environmental conditions may result in the dissolution and therefore mobilising Pb. Cerussite and pyrite were noted to be present as grains by EMP, given the low concentrations they are unlikely to have a significant effect on the metallic element mobility within Gunnersdie Gill.

Gun 7 was recovered from Sir Francis Level and showed similar mineralogy to Gun 5, with the exception that cerussite was not noted. This includes very similar BCR results for Pb and Zn when compared with Gun 5. Galena and sphalerite were also recorded by EMP indicating limited weathering to date,

again probably as a result of protective coatings and rims. It is therefore considered under the current conditions that these wastes are unlikely to be leaching significant concentrations of Pb or Zn.

Gun 8 was recovered from Sir Francis Level but was a brown orange colour. Gun 8 was found to contain sphalerite and cerussite, with Pb and Zn present mostly in the reducible and residual fractions respectively. It is considered that there is the potential for Pb to be more mobile than Zn within this sample given the presence of their associations with primary and secondary minerals, respectively.

The last sample from Gunnerside Gill, Gun 10, was the second alluvial sediment sample tested. It was found to contain cerussite and smithsonite, both secondary minerals and carbonates, in low concentrations. The BCR results are similar for Pb and Zn when compared to Gun 9, with Pb mostly present in the reducible and exchangeable fractions and Zn in the exchangeable fraction. Based on the column leaching experiment it could be inferred that Gun 10 is likely to release more Pb than the mine wastes due to the mineralogical similarities with Gun 9.

6.7 Comparison to Worldwide Drainage

Although there are worldwide examples of NMD as a result of buffering from surrounding carbonate rocks, including Alaska, US (Kelley and Taylor, 1997; Lindsay et al., 2009), Sardinia, Italy (Fanfani et al., 1997), Canada (Desbarats and Dirom, 2007) and the British Isles (Nuttall and Younger, 2000; Johnson and Younger, 2002; Warrender and Pearce, 2007; Palumbo-Roe and Colman, 2010), mine drainage is complex and may also be neutralised by aluminosilicate country rocks, such as in Idaho, US (Hammarstrom et al., 2002) or by a combination of dolomitic limestones and clayey schist as in Tuscany, Italy (Drescher-Schneider et al., 2007; Tesser et al., 2011).

There are other examples of similar mineralogical associations as those found within Gunnerside Gill. Fanfani et al. (1997) used SEM to show that galena had been oxidised to anglesite and cerussite and the Fe-rich sphalerite had rims of Zn-rich oxyhydroxides in a Pb-Zn historical mining area in Sardinia. In

the Salafossa mining area, Italy, metallic elements including As, Cd, Pb, Tl and Zn were found to accumulate within the Fe-Mn oxyhydroxides and carbonates within the sediments of the mine galleries themselves (Pavoni et al., 2018). In Namibia, a Zn-Pb-Cu mine hosted in black shale, arenites and carbonates was found to have a near neutral pH within the soils and sediments. The metallic elements were generally reported to be bound to Fe-Mn oxyhydroxides and carbonates (Nejeschlebová et al., 2015). Within Holden Beck, north Pennines, dissolved Pb and Zn were found to result from the weathering of primary minerals galena and sphalerite respectively but also from secondary minerals including cerussite and smithsonite. These secondary minerals continue to contribute to the Pb and Zn concentrations within the catchment due to continuous leaching (Valencia-Avellan et al., 2017). The continuous leaching of secondary minerals is likely to be important within Gunnerside Gill given the geological similarities and comparable historical mining techniques used to extract the ore.

Another interesting comparison is the fractionation of the metallic elements with regards to the use of sequential extractions. Soils from Pb-Zn Amizour-Bejaia mining area, Algeria, were found to have a pH of 7.5 to 8.3 and a low organic matter content. The Pb and Zn present were found to be associated mostly with the organic and reducible (Mn / Fe oxyhydroxides) fractions, and less than 20 % with the residual fraction (Mouni et al., 2017). The Zanjan province of Northern Iran is an area known for Pb-Zn mining and smelting. The National Iranian Lead and Zinc (NILZ) smelter is located some 11 km east of Zanjan. Following a four-stage BCR sequential extraction Pb was found to be mostly present within the Fe / Mn oxyhydroxide fraction, similarly Zn and Cd were also found to be mostly present within the reducible fraction (Gharyoraneh and Qishlaqi, 2017). A study on smelter-impacted soil in the north of France looked at the geochemical speciation and oral bioaccessibility of Pb, Zn and Cd. The soils were found to have a pH of 6.7 to 8.2. It was found the metallic elements were found to be bioaccessible in the gastric and gastrointestinal stages generally in soluble forms, bound to organic matter and associated with carbonates and Fe / Mn oxyhydroxides (Waterlot et al., 2017). The use of sequential extractions in these cases implies that the metallic

elements are relatively mobile, as they are often associated with organic matter, Fe / Mn oxyhydroxides and / or carbonates. In the case of Gunnerside Gill Pb was found to be mostly present in the reducible (Mn / Fe oxyhydroxides) fraction. Interestingly in the two most upstream mine waste samples, Gun 1 and Gun 2, Pb was mainly found to be present in the exchangeable fraction, this could indicate these waste rock piles are older than the others and are therefore more weathered. Zinc was found to be mostly present in the exchangeable (CEC sites / carbonates) fraction in half of the tested samples, the second most common association was the residual fraction. The results of the sequential extractions from both this study and the literature indicate that the key metallic element associations are as a result of weathering of the primary sulfide minerals. As a result the concentrations of sulfide minerals present at a site are likely not to be the best indicator of availability of metallic elements within a mine drainage setting.

Based on the wider literature it is clear that mine drainage is strongly influenced by the ore minerals present, the presence of Fe-rich minerals, the geology of the host rock, the type of mining techniques used, and the time that has lapsed since mining ceased. Rather than comparisons to worldwide drainage it might be more useful to initially compare to more local mines, in this case, the northern and southern Pennine Orefields.

Valencia-Avellan et al. (2017) undertook a study of Holden Beck, a tributary of the River Wharfe in the north Pennines. The study concluded that the limestone bedrock has a strong control on the pH and weathering reactions, and therefore metallic element mobility within similar catchments; point sources were regular contributors of dissolved Zn in all flow conditions, whereas diffuse sources like spoil wastes produced higher contribution of dissolved Zn and Pb in flooding conditions following dry periods; Zn and Pb mobilisation are a function of specific biogeochemical and hydrogeological conditions at each different site; contributions of dissolved Zn and Pb were not derived directly from oxidation of sphalerite and galena, but from secondary minerals such as smithsonite and cerussite, which are continuously leaching into the catchment (Valencia-Avellan et al. 2017).

Gunnerside Gill appears to show similar controls on the mobility of Pb and Zn to that of Holden Beck, which is geologically similar given both sites are located within the north Pennines. Within Gunnerside Gill the sphalerite and galena grains were often noted to have weathering rims and / or coatings of clay minerals, which reduce the dissolution of the primary ore minerals within the mine waste samples. Some of the weathering rims comprise secondary minerals, such as cerussite and smithsonite, that are likely to be continuously leaching to the waters, which is the same mechanism described by Valencia-Avellan et al. (2017).

6.8 Summary

Although these samples have been subjected to 10 modelled years of weathering the total concentrations of Pb and Zn still remain at potentially hazardous levels. In summary:

- There was no significant relationship between grain size and the metallic element concentrations of the solid samples;
- None of the samples had the same mineralogical composition, making the prediction of the overall behaviour of the metallic elements at Gunnerside Gill difficult. This is considered to be a reflection of the mining and processing techniques used, which would have changed significantly throughout the mining history;
- Both the mine wastes and sediment showed evidence of neutralisation reactions during the column leaching experiment;
- Within the mine waste samples the metallic element concentrations in the leachate, specifically Pb and Zn, were Gun 3 > Gun 2 > Gun 1. The pH values were the opposite, Gun 1 was the highest and Gun 3 the lowest;
- The results of the column leaching experiment indicate that Pb is leaching more from the alluvial floodplain sediments than from the mine waste piles within Gunnerside Gill;
- The control of mobilisation of Pb within the mine wastes is dominated by secondary minerals, which often formed rims on the primary ore grains. The control of mobilisation of Pb within the sediment sample is considered

to be a combination of dissolution of secondary minerals and Mn oxyhydroxides;

- The mobilisation of Zn is considered to be largely as a result of the dissolution of sphalerite in the mine wastes and secondary minerals such as smithsonite within the sediments;
- Overall the sediment sample (Gun 9) was found to release significantly more Pb into the column leachate when compared to the mine waste samples (Gun 1 to Gun 3);
- The column leachate experiment was able to give a good estimate of Pb concentrations with regards to the mine waste samples and the water monitoring data from the northern portion of Gunnerside Gill;
- The first two column leachate experiments (Gun 1 and Gun 2) again showed similar concentrations of Zn when compared to the EA monitoring data and could be a useful tool at predicting the longer term leachability of Zn in the northern portion of Gunnerside Gill;
- Climate change is likely to impact rainfall intensity and river flows resulting in an increase of the movement of metallic elements in mining affected catchments (EA, 2019).

Chapter 7

Conclusions and Recommendations

Contents

| | |
|---------------------------------------|-----|
| Chapter 7..... | 245 |
| 7.1 Conclusion..... | 245 |
| 7.2 Recommendations..... | 248 |
| 7.3 Further Work and Limitations..... | 251 |

7.1 Conclusion

The overarching objective of this study was to increase the understanding of the mechanisms controlling NMD in a historically mined catchment in the North Pennines.

The data collected during this study has been used to address the specific objectives outlined in Section 1.3.

The first objective was to characterise the solid-phase speciation of the metallic elements present in mine waste and sediments. This was achieved by collecting samples of mine wastes and sediments from along the length of Gunnerside Gill, starting upstream of the main mining areas and finishing to the south of Gunnerside Village. These samples were subjected to various analytical techniques including total digestion, sequential extraction, particle size analysis XRD and EMP analysis. The results indicate that none of the samples have the same mineralogical or metallic element composition. This, therefore, makes the overall behaviour of the metallic elements at Gunnerside Gill difficult to predict. The metallic elements were found to be associated with primary ore minerals, secondary mineral phases and Mn oxyhydroxides.

The second objective was to determine the factors influencing the transfer of metallic elements from the solids into the waters. This was done by undertaking a column leaching experiment using three mine waste samples (Gun 1 to Gun 3) and one alluvial sediment sample (Gun 9). The column leaching experiment was designed and undertaken over a 40 week period to model 10 years of weathering. The concentrations of Pb and Zn released into

the leachate were highest in Gun 9 > Gun 3 > Gun 2 > Gun 1. This coincided with average pH values of the column leachate from lowest to highest, Gun 9 > Gun 3 > Gun 2 > Gun 1. Gun 1 was found to have the highest total concentration of Pb in the solid sample but released the least during the column leaching experiment, this implies that pH is the main control on the dissolution of ore minerals within Gunnerside Gill. No specific relationship was determined between grain size and the concentration or mobility of metallic elements from the samples. The control of Zn mobility is largely governed by the dissolution of primary and secondary minerals, for example sphalerite and smithsonite, within the mine waste samples, and from the dissolution of secondary minerals within the alluvial sediments. Within the mine waste samples Pb mobility was largely controlled by the dissolution of secondary minerals, including cerussite and anglesite. Weathering rims were often noted on the primary ore grains. The mobility of Pb within the alluvial sediment sample appeared to be controlled by the dissolution of primary and secondary ore minerals, but also Mn oxyhydroxides.

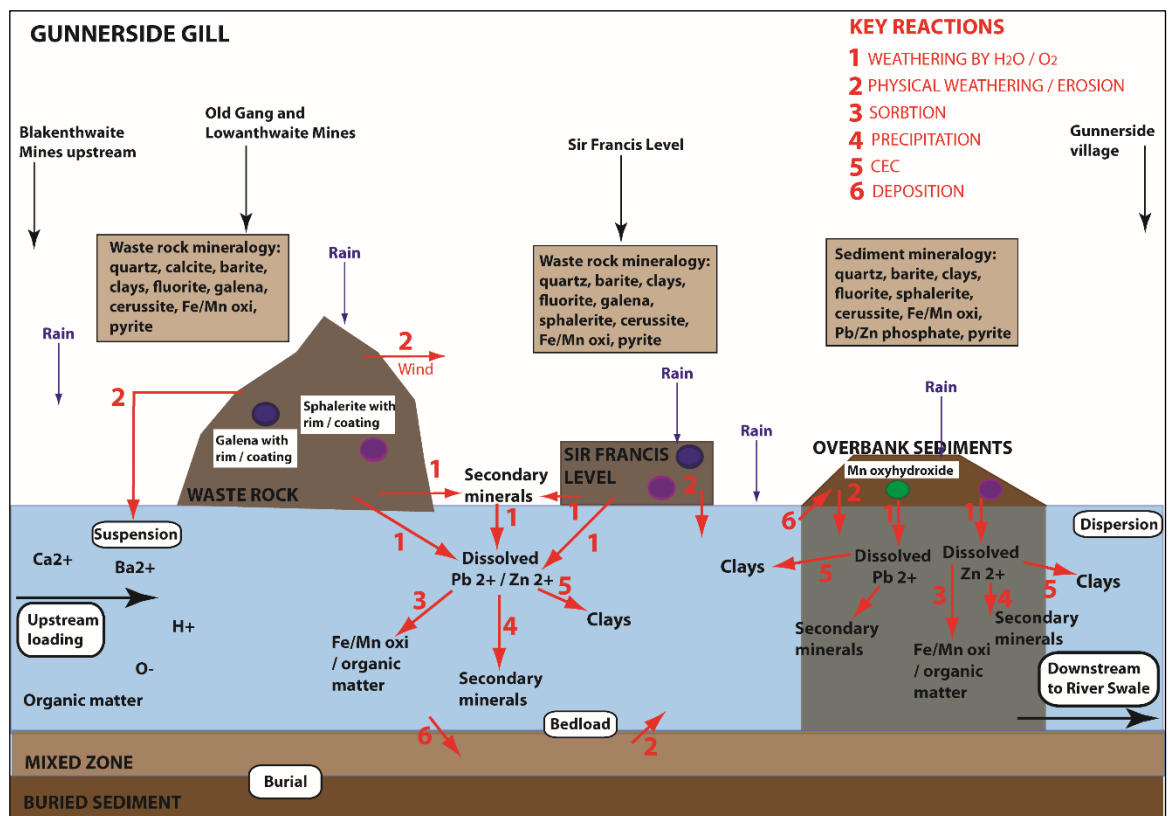


Figure 7.1: Conceptual site model for the reactions at Gunnerside Gill

The locations of the mine waste are largely a function of the historical mining techniques and use of water in the processing of the ore. Some of the dressing floors and mine waste tips are protected as they are scheduled ancient monuments (EA, 2013). These are concentrated in the northern and central areas of Gunnerside Gill near Lowanthwaite and Old Gang Mines and Sir Francis Level (Figure 3.9). The mine wastes become part of the sediment load within mining affected catchments and then are cycled through the system to be deposited and re-mobilised further down the gill depending upon the flow of the water (Figure 7.1).

The mine wastes Gun 1 to Gun 3 samples represented the weathered materials whose leaching results in low but constant mobilisation of Pb and Zn. The alluvial sediment sample was more representative of a diffuse source whose dissolution resulted in higher concentrations of Pb and Zn being released into the waters of Gunnerside Gill (Figure 7.1).

The final objective was to use the data from the column leaching experiments, EA monitoring data and geochemical modelling to predict the influence of changes in the environmental setting, including pH and the effects of climate change. The EA river monitoring data reported an average range of pH 7.6 to 7.9. The data were used to calculate the saturation indices of the mineral and to model the effects of changes in pH (8.0 to 5.5) on mineral saturation. The exact minerals present depended upon the location and chemistry of the sample. Where present goethite and hematite become less oversaturated as the pH reduced. Calcite, cerussite and smithsonite became less undersaturated as the pH reduced. The modelling of the column leachate data recorded different mineralogical composition but similar trends to the EA data. Goethite and hematite again both become less oversaturated.

The EA are in the process of undertaking a consultation which so far has concluded that climate change is likely to impact rainfall intensity and river flows resulting in an increase of the movement of metallic elements in mining affected catchments (EA, 2019). This is backed up by a study undertaken by Dennis et al. (2003) which found that the 2000 floods resulted in the deposition of channel edge and overbank sediments, and the increased mobilisation of

mine wastes downstream. It is considered that the increase in extreme weather events including heavy rainfall and flooding is likely to result in the increased transportation of both mine wastes and contaminated sediments.

The original hypothesis was that 'higher concentrations of metallic elements are released from the solid mine wastes than the sediments into the catchment waters of Gunnerside Gill as a result of historical mining activities'. This hypothesis was found to be incorrect in this setting. The alluvial sediment sample was found to leach between 10 to 17 times more Pb than the mine waste samples. Similarly a higher concentration of Zn was mobilised from the sediment sample than the mine wastes. This is considered to be a function of age of the mine wastes and the location of the alluvial sample downstream of both the main mining and processing areas.

7.2 Recommendations

The research has shown that there are elevated concentrations of Pb and Zn within the leachate of the column study when compared to the EQS. Concentrations of Pb, Zn and Cd were also recorded within the waters of Gunnerside Gill during the EA monitoring campaign.

The treatment of low-Fe NMD is considered to be more difficult than AMD, which often uses the co-precipitation of metallic elements with Fe oxyhydroxides, due to the characteristic low Fe concentrations (Warrender and Pearce, 2007). AMD has been more extensively studied than NMD and as a result has been remediated using a variety of methods. These include active treatment technologies using the addition of acid neutralising and metallic element precipitating chemicals, constructed wetlands, phytoremediation by phytoextraction and / phytostabilisation (RoyChowdhury et al., 2015). Additional remedial and management options to try and reduce the impact of metallic elements in mining impacted catchment, include water treatment schemes, civil engineering projects, or to reduce the erosion of mine wastes (EA, 2019).

As part of the monitoring undertaken within Gunnerside Gill in 2010 / 2011 by the EA the following recommendations were made:

- treatment of the point sources, primarily Sir Francis Level. This would lead to a reduction in Zn and Cd concentrations within Gunnerside Gill;
- treatment of Pb is more problematic as it was considered to result from more diffuse sources including in-river sediments and mine wastes. There was no specific recommendation given to try and reduce Pb concentrations because of this;
- investigate the impact from Gunnerside Gill on the downstream River Swale, particularly the direct mine water discharges from Sir Francis Level (EA, 2013).

Examples of treatment of UK NMD sites include Force Crag, a Pb-Zn mine located within the Lake District. Coledale Beck was found to be contaminated by both diffuse sources, including processing and mining wastes, but also point sources from direct mine water drainage resulting in NMD (Jarvis et al., 2015). A passive treatment system was installed with the aim of reducing Zn concentrations in the water. The results so far indicate the passive compost-based ponds have removed approximately 0.5 tonne of Pb, Zn and Cd annually from the waters of Coledale Beck (EA, 2019).

Warrender and Pearce (2007) undertook a study in the use of reactive materials to reduce the metallic element concentrations within NMD settings. The materials used included Zero Valent Iron, activated carbon, limestone chippings, compost and fly ash, all of which were found to be effective at removing Pb, Zn and Cd from the two NMD waters and one AMD water. The study showed that removal of the metallic elements from the NMD waters was more rapid and in higher concentrations than the AMD sample. The use of reactive materials was found to have a relatively quick reaction rate and would reduce the land area required by traditional passive treatment systems (Warrender and Pearce, 2007).

Other studies include testing the use of 'pelletised recovered hydrous ferric oxide' (HFO) in a pilot study to see how effective it would be in removing Zn from NMD (Mayes et al., 2009). The results indicated that HFO was effective at removing Zn by forming secondary precipitates and possibly microbial activity associated with an algal colony present during part of the experiment.

It was concluded that HFO could be developed into a low-cost, small area option for the removal of Zn from NMD impacted waters (Mayes et al., 2009).

All of the above remediation schemes are possible in Gunnerside Gill, but the difficulty of implementing any remedial options here is increased by the fact that some of the mine waste piles are scheduled monuments, it is located within a national park, within the North Pennines Moor Special Protection Area and Special Area of Conservation, and three Sites of Special Scientific Interest (Arkengarthdale, Gunnerside and Reeth Moors) for blanket bog, heather moorland and their breeding bird populations (EA, 2013). This means the removal of the waste piles from the edge of Gunnerside Gill is unlikely to be an agreeable option.

It may be possible to install localised reactive barriers in the vicinity of the Sir Francis and Bunton Level adits to reduce the concentrations of metallic elements in Gunnerside Gill from these point sources. However, this study showed that both the mine wastes and alluvial sediments are acting as diffuse sources, and both are continuing to contribute to the Pb and Zn concentrations within the water. In order to try and manage these sources a management strategy rather than full remediation approach is likely to be required. In this case the use of phytostabilisation may immobilise the metallic elements by containing them in plant root zones and the roots themselves can protect the soils against further erosion and leaching (RoyChowdhury et al., 2015). By using metallophyte plants it may be possible to reduce the impact of the diffuse sources of Pb and Zn without radically disturbing the mine wastes or sediments or creating an undesirable alteration to the landscape. Logistically this would also be easier than trying to physically move the mine waste piles from the edge of Gunnerside Gill.

In order to stop the direct mobilisation of mine wastes into the River Nent a new river wall was installed. Although relatively simple it was reported to stop 1 tonne of Pb, Zn and Cd annually (EA, 2019). Again a river wall may be considered too drastic an option due to the designations within Gunnerside Gill. However, it might be possible to install localised structures to reduce direct erosion of the mine wastes and sediments. This could include gabions or walls

constructed from locally sourced materials so that they remain in keeping with the landscape. Within the mining portion of Gunnerside Gill several historical walls and structures remain, it may be possible to use similar techniques to install small localised river walls in suitable locations.

7.3 Further Work and Limitations

The research has highlighted a number of areas that require further research to continue the understanding of NMD mechanisms within Gunnerside Gill but could also be applied to other NMD impacted rivers:

- Continue the column leaching experiment to include the remaining six samples. This could aid the prediction of metallic element mobility going forward and could give more data on the spatial variations down Gunnerside Gill. Additional samples could also be included from the River Swale, both upstream and downstream from Gunnerside Gill to determine the wider environmental impacts;
- Undertake sampling from the channel sediments within Gunnerside Gill to see how much the metallic element concentrations vary from the mine wastes and alluvial bank sediments and to determine if the same mechanisms control their mobility;
- Investigate the concentrations of metallic elements within the underlying soils and sediments by sampling vertical profiles through the adjacent river banks. This could give an indication as to the processes involved in the sediment cycling within Gunnerside Gill;
- Use additional analytical techniques to look at the effects of organic matter, CEC and microbiology on the mobility of Pb and Zn in an NMD setting. This work would go some way to complete the overall understanding of what processes dominate within Gunnerside Gill;
- Undertake groundwater monitoring to assess the risks to the wider environment and potentially potable water resources.

Overall this study has shown the importance of understanding the metallic element mobility from both the mine wastes and derived sediments. In order

to better understand NMD in general it is considered that a range of analysis should be undertaken with a minimum of bulk mineralogy by XRD and EMP, leachate testing, and river water / direct mine water discharge monitoring. Based on this study the key factors include the pH of the samples during the column leaching experiment and the mineralogical composition of the samples, including weathering rims.

Following the completion of the study some limitations became apparent. The first would have been to use single source of water during the column leachate experiment. Although the change in source and therefore pH values demonstrated that the samples still had some neutralisation capacity remaining, so even though it was an additional variable it also gave useful information. It would have been useful to include additional elements during the ICP analysis, specifically P. This would have allowed further information of which Pb-Zn phosphate was present within the alluvial sediment sample (Gun 9). In addition, given the low concentrations of some elements below the LoD it would have been useful to analyse some elements from the column leaching experiment and total digestions using an ICP-MS. This would have given a better idea of the concentrations of various elements but mainly Fe and Cd, as Cd is harmful at very low concentrations. Density separation was undertaken on the ten samples during the early part of the research, however the separated grains were not analysed. It would have been useful to have more information on the ore minerals present and perhaps a more accurate concentration of these phases. Additionally, in order to reduce the potential heterogeneity of the solids and increase reproducibility it would have been useful to powder the samples prior to some of the analyses. At some points it was logistically and financially difficult to complete some of the techniques, this included inorganic carbon concentrations within the solid samples and XRD analysis on the post column solids.

References

- Abumaizar, R. J. and Smith, E. H. (1999) 'Heavy metal contaminants removal by soil washing', *Journal of Hazardous Materials*, 70(1–2), pp. 71–86. doi: 10.1016/S0304-3894(99)00149-1.
- Acero, P., Cama, J. and Ayora, C. (2007) 'Sphalerite dissolution kinetics in acidic environment', *Applied Geochemistry*, pp. 1872–1883. doi: 10.1016/j.apgeochem.2007.03.051.
- Al, T. A., Martin, C. J. and Blowes, D. W. (2000) 'Carbonate-mineral/water interactions in sulfide-rich mine tailings', *Geochimica et Cosmochimica Acta*, 64(23), pp. 3933–3948. doi: 10.1016/S0016-7037(00)00483-X.
- Álvarez-Ayuso, E., Otones, V., Murciego, A., García-Sánchez, A. and Santa Regina, I., (2013). Zinc, cadmium and thallium distribution in soils and plants of an area impacted by sphalerite-bearing mine wastes. *Geoderma*, 207, pp.25-34.
- Alves, C. M., Ferreira, C. M. H. and Soares, H. M. V. M. (2018) 'Relation between different metal pollution criteria in sediments and its contribution on assessing toxicity', *Chemosphere*. Elsevier Ltd, 208, pp. 390–398. doi: 10.1016/j.chemosphere.2018.05.072.
- Amos, R.T., Blowes, D.W., Bailey, B.L., Sego, D.C., Smith, L. and Ritchie, A.I.M., (2015). Waste-rock hydrogeology and geochemistry. *Applied Geochemistry*, 57, pp.140-156.
- Andrés, N. F. and Francisco, M. S. (2008) 'Effects of sewage sludge application on heavy metal leaching from mine tailings impoundments', *Bioresource Technology*, 99(16), pp. 7521–7530. doi: 10.1016/j.biortech.2008.02.022.
- Anju, M. and Banerjee, D. K. (2010) 'Comparison of two sequential extraction procedures for heavy metal partitioning in mine tailings', *Chemosphere*. Elsevier Ltd, 78(11), pp. 1393–1402. doi: 10.1016/j.chemosphere.2009.12.064.
- Argane, R., Benzaazoua, M., Bouamrane, A. and Hakkou, R., (2015). Cement hydration and durability of low sulfide tailings-based renders: A case study in Moroccan constructions. *Minerals Engineering*, 76, pp.97-108.
- Arthur, S. E., Brady, P. V., Cygan, R. T., Anderson, H. L., Westrich, H. R., and Nagy, K. L. (1999) Irreversible sorption of contaminants during ferrihydrite transformation. In *Proceedings of the Waste Management Conference, WM'99*, 1-14.
- Audry, S., Grosbois, C., Bril, H., Schäfer, J., Kierczak, J. and Blanc, G., (2010). Post-depositional redistribution of trace metals in reservoir sediments of a mining/smelting-impacted watershed (the Lot River, SW France). *Applied Geochemistry*, 25(6), pp.778-794.
- Audry, S., Blanc, G. and Schäfer, J. (2006) 'Solid state partitioning of trace metals in suspended particulate matter from a river system affected by smelting-waste drainage', *Science of the Total Environment*. doi: 10.1016/j.scitotenv.2005.05.035.
- Australia Drinking Water Guidelines 6 2011, updated 2017. National Water Quality Management Strategy Version 3.4. Australian Government, National Health and Medical Research Council and National Resource Management Ministerial Council.
- Aykol, A., Budakoglu, M., Kumral, M., Gultekin, A.H., Turhan, M., Esenli, V., Yavuz, F. and Orgun, Y., (2003). Heavy metal pollution and acid drainage from the abandoned Balya Pb-Zn sulfide Mine, NW Anatolia, Turkey. *Environmental Geology*, 45(2), pp.198-208.
- Banks, D., Parnachev, V.P., Frengstad, B., Holden, W., Vedernikov, A.A. and Karnachuk, O.V., (2002). Alkaline mine drainage from metal sulphide and coal mines: examples from Svalbard and Siberia. *Geological Society, London, Special Publications*, 198(1), pp.287-296.
- Banwart, S. A., Evans, K. A. and Croxford, S. (2002) 'Predicting mineral weathering rates at field scale for mine water risk assessment', *Geological Society, London, Special Publications*. doi: 10.1144/gsl.sp.2002.198.01.10.

- Barančíková, G. and Makovníková, J. (2003) 'The influence of humic acid quality on the sorption and mobility of heavy metals', *Plant, Soil and Environment*.
- Bell, F. G. (2004) *Engineering Geology and Construction, Engineering Geology and Construction*. doi: 10.1201/9781482264661.
- Bernard, A. (2008) 'Cadmium & its adverse effects on human health RID A-6511-2010', *Indian Journal of Medical Research*, 128(4), pp. 557–564. doi: 10.1016/j.ympv.2012.12.001.
- Bevins, R.E., Young, B., Mason, J.S., Manning, D.A.C. and Symes, R.F. (2010), Mineralization of England and Wales, Geological Conservation Review Series, No. 36, Joint Nature Conservation Committee, Peterborough
- Blowes, D. W., Ptacek, C. J., Jambor, J. L., Weisener, C. G., Paktunc, D., Gould, W. D., and Johnson, D. B. (2013) *The Geochemistry of Acid Mine Drainage*, in Turekian, K.K. & Holland, H.D. Treatise on Geochemistry: Second Edition doi: 10.1016/B978-0-08-095975-7.00905-0.
- Brewer, P. A., Dennis, I. A. and Macklin, M. G. (2005) 'The use of geomorphological mapping and modelling for identifying land affected by metal contamination on river floodplains'.
- Brewer, P. A. and Taylor, M. P. (1997) 'The spatial distribution of heavy metal contaminated sediment across terraced floodplains', *Catena*, 30(2–3), pp. 229–249. doi: 10.1016/S0341-8162(97)00017-9.
- Bright, D. A.; Sandys, N. (2015) 'Beyond ML/ARD : the many faces of neutral mine drainage in the context of mine closure', in *British Columbia Mine Reclamation Symposium*. doi: <http://dx.doi.org/10.14288/1.0305865>.
- British Geological Survey 2009a. Lead in stream sediments: Great Britain. G-BASE Geochemical Map. Keyworth, Nottingham. UK.
- British Geological Survey 2009b. Zinc in stream sediments: Great Britain. G-BASE Geochemical Map. Keyworth, Nottingham. UK.
- British Geological Survey website 2017, Gunnerside Gill geology map - <http://mapapps.bgs.ac.uk/geologyofbritain/home.html?location=gunnerside&gobBtn=go>
- British Geological Survey website 2020, Lexicon of named rock units - <https://www.bgs.ac.uk/lexicon/lexicon.cfm?pub=SMGP>
- British Geological Survey (BGS) 1996 – Regional Geochemical Atlas 22, [Mineralisation and mining, continued]. Askrigg Block. Mineralisation in the Craven area. Mineralisation in the Richmond area. Mineralisation in post-Dinantian rocks, 1996
- Bromly, M., Hinz, C. and Aylmore, L. a G. (2007) 'Relation of dispersivity to properties of homogeneous saturated repacked soil columns', *European Journal of Soil Science*, 58(1), pp. 293–301. doi: 10.1111/j.1365-2389.2006.00839.x.
- Burckhard, S. R., Schwab, A. P. and Banks, M. K. (1995) 'The effects of organic acids on the leaching of heavy metals from mine tailings', *Journal of Hazardous Materials*. doi: 10.1016/0304-3894(94)00104-O.
- Calmano, W., Hong, J. and Forstner, U. (1993) 'Binding and mobilization of heavy metals in contaminated sediments affected by pH and redox potential', *Water Science and Technology*, pp. 223–235. doi: 10.15480/882.450.
- Cann, J.R. and Banks, D.A., 2001. Constraints on the genesis of the mineralization of the Alston Block, Northern Pennine Orefield, northern England. *Proceedings of the Yorkshire Geological Society*, 53(3), pp.187-196.
- Cappuyns, V., Swennen, R. and Niclaes, M. (2007) 'Application of the BCR sequential extraction scheme to dredged pond sediments contaminated by Pb-Zn mining: A combined geochemical and mineralogical approach', *Journal of Geochemical Exploration*, 93(2), pp.

78–90. doi: 10.1016/j.gexplo.2006.10.001.

Carroll, S. A., O'Day, P. A. and Piechowski, M. (1998) 'Rock-water interactions controlling zinc, cadmium, and lead concentrations in surface waters and sediments, U.S. Tri-State Mining District. 2. Geochemical interpretation', *Environmental Science and Technology*, 32(7), pp. 956–965. doi: 10.1021/es970452k.

Caussy, D., Gochfeld, M., Gurzau, E., Neagu, C. and Ruedel, H., (2003). Lessons from case studies of metals: investigating exposure, bioavailability, and risk. *Ecotoxicology and environmental safety*, 56(1), pp.45-51.. doi: 10.1016/S0147-6513(03)00049-6.

Cave, R.R., Andrews, J.E., Jickells, T. and Coombes, E.G., (2005). A review of sediment contamination by trace metals in the Humber catchment and estuary, and the implications for future estuary water quality. *Estuarine, Coastal and Shelf Science*, 62(3), pp.547-557.. doi: 10.1016/j.ecss.2004.09.017.

CEH webpage - Centre for Ecology and Hydrology (CEH) website consulted 2017 – www.ceh.ac.uk

Chappell, D. A. and Craw, D. (2002) 'Geological analogue for circumneutral pH mine tailings: Implications for long-term storage, Macraes Mine, Otago, New Zealand', in *Applied Geochemistry*, pp. 1105–1114. doi: 10.1016/S0883-2927(02)00002-1.

Chatwin, T., Ferguson, K., Verburg, R., & Bezuidenhout, N. (2014) 'Global Acid Rock Drainage Guide', INAP: The International Network for Acid Prevention', pp. 198–203. Available at: <http://www.gardguide.com>.

Chen, A. *et al.* (2010) 'Chemical dynamics of acidity and heavy metals in a mine water-polluted soil during decontamination using clean water', *Journal of Hazardous Materials*, 175, pp. 638–645. doi: 10.1016/j.jhazmat.2009.10.055.

Cheong, Y.-W. *et al.* (2012) 'Seasonal effects of rainwater infiltration on volumetric water Content and water quality in mine wastes at the Gyopung mine, South Korea', *Journal of Geochemical Exploration*. Elsevier B.V., 116–117, pp. 8–16. doi: 10.1016/j.gexplo.2011.05.003.

Ciccu, R., Ghiani, M., Serci, A., Fadda, S., Peretti, R. and Zucca, A., (2003). Heavy metal immobilization in the mining-contaminated soils using various industrial wastes. *Minerals Engineering*, 16(3), pp.187-192. doi: [http://dx.doi.org/10.1016/S0892-6875\(03\)00003-7](http://dx.doi.org/10.1016/S0892-6875(03)00003-7).

Cidu, R., Dadea, C., Desogus, P., Fanfani, L., Manca, P.P. and Orrù, G., (2012). Assessment of environmental hazards at abandoned mining sites: a case study in Sardinia, Italy. *Applied geochemistry*, 27(9), pp.1795-1806.. doi: 10.1016/j.apgeochem.2012.02.014.

CIRIA 2019 – C758D Abandoned mine workings manual, CIRIA. Edited by Parry D and Chiverrell, C. ISBN: 978-0-86017-765-4.

Clausen, J.L., Bostick, B. and Korte, N., 2011. Migration of lead in surface water, pore water, and groundwater with a focus on firing ranges. *Critical reviews in environmental science and technology*, 41(15), pp.1397-1448.

coolgeography.com 2017 - http://www.coolgeography.co.uk/A-level/AQA/Year%2012/Rivers_Floods/Flooding/York%20Flooding.htm

Cotter-Howells, J. (1996) 'Lead phosphate formation in soils', *Environmental Pollution*, 93(1), pp. 9–16. doi: 10.1016/0269-7491(96)00020-6.

Covelo, E. F., Vega, F. a. and Andrade, M. L. (2007) 'Competitive sorption and desorption of heavy metals by individual soil components', *Journal of Hazardous Materials*, 140(1–2), pp. 308–315. doi: 10.1016/j.jhazmat.2006.09.018.

Crystal Impact 2019 –Match Phase Identification from Powder Diffraction Version 2 - <https://www.crystalimpact.de/match/>

Davidson, C.M., Duncan, A.L., Littlejohn, D., Ure, A.M. and Garden, L.M., (1998). A critical evaluation of the three-stage BCR sequential extraction procedure to assess the potential

- mobility and toxicity of heavy metals in industrially-contaminated land. *Analytica Chimica Acta*, 363(1), pp.45-55. doi: 10.1016/S0003-2670(98)00057-9.
- Dempsey 2016 - Proceedings of the OUGS 2 2016, 33–7. Proceedings of the Open University Geological Society Volume 2
- Dennis, I. (2005) *The impact of historical metal mining on the river Swale catchment, North Yorkshire, U.K.* University of Wales, Aberystwyth.
- Dennis, I.A., Macklin, M.G., Coulthard, T.J. and Brewer, P.A., (2003) 'The impact of the October-November 2000 floods on contaminant metal dispersal in the River Swale catchment, North Yorkshire, UK', *Hydrological Processes*, 17(January), pp. 1641–1657. doi: 10.1002/hyp.1206.
- Dennis, I.A., Coulthard, T.J., Brewer, P. and Macklin, M.G., (2009) 'The role of floodplains in attenuating contaminated sediment fluxes in formerly mined drainage basins', *Earth Surface Processes and Landforms*, 34(3), pp. 453–466. doi: 10.1002/esp.1762.
- Department of Environment and Conservation 2010. Assessment levels for Soil, Sediment and Water. Contaminated Site Management Series. Western Australia.
- Department of Environment Food and Rural Affairs (2010) 'Environmental Permitting Guidance The Mining Waste Directive For the Environmental Permitting (England and Wales)', (May), p. 100.
- Desbarats, A. J. and Dirom, G. C. (2005) 'Temporal variation in discharge chemistry and portal flow from the 8-Level adit, Lynx Mine, Myra Falls Operations, Vancouver Island, British Columbia', *Environmental Geology*, 47, pp. 445–456.
- Desbarats, A. J. and Dirom, G. C. (2007) 'Temporal variations in the chemistry of circum-neutral drainage from the 10-Level portal, Myra Mine, Vancouver Island, British Columbia', *Applied Geochemistry*, 22(2), pp. 415–435. doi: 10.1016/j.apgeochem.2006.09.008.
- Deutsch, W. J. and Siegel, R. (1997) *Groundwater geochemistry: fundamentals and applications to contamination*, *Choice Reviews Online*. doi: 10.5860/CHOICE.35-3883.
- Dold, B. (2005) 'Basic concepts of environmental geochemistry of sulfide mine-waste', in *XXIV Curso Latinoamericano de Metalogenia UNESCO-SEG*.
- Drescher-Schneider, R., de Beaulieu, J.L., Magny, M., Walter-Simonnet, A.V., Bossuet, G., Millet, L., Brugiapaglia, E. and Drescher, A., (2007) 'Vegetation history, climate and human impact over the last 15,000 years at Lago dell'Accesa (Tuscany, Central Italy)', *Vegetation History and Archaeobotany*, 16(4), pp. 279–299. doi: 10.1007/s00334-006-0089-z.
- Drinking Water Safety* (2009) *The Drinking Water Inspectorate*. doi: 10.1001/jama.282.6.519.
- Duffus, J. H. (2002) "'Heavy metals" a meaningless term? (IUPAC Technical Report)', *Pure and Applied Chemistry*, 74(5), pp. 793–807. doi: 10.1351/pac200274050793.
- Dunham, K. C. (1959) 'Epigenic mineralization in Yorkshire', *Proceedings of the Yorkshire Geological Society*, 32, pp. 1–30.
- Dunham, K. C. and Wilson, A. A. (1985) *Geology of the Northern Pennine Orefield: Volume 2, Stainmore to Craven*. H.M.S.O. London.
- Earthwise British Geological Survey 2018 - http://earthwise.bgs.ac.uk/index.php/Bedrock_Geology_UK_North:_Carboniferous
- Edwards, W. and Trotter, F. M. (1954) *British Regional Geology: The Pennines & Adjacent Areas*. H.M.S.O. London.
- Environment Agency (2004) *Model Procedures for the Management of Land Contamination CLR11*
- Environment Agency (2013) *Humber River Basin District Investigation. Mining Pollution: Catchment Characterisation Report for Gunnerside Gill*.

Environment Agency; catchment data explorer (consulted 2018) - <http://environment.data.gov.uk/catchment-planning/>

Environment Agency 2019. 2021 Mine waters Challenge; River Basin Management Plan. 22/10/2019 Environment Agency, UK.

European Parliament (2006) 'DIRECTIVE 2006/21/EC OF THE EUROPEAN PARLIAMENT AND OF THE COUNCIL of 15 March 2006 on the management of waste from extractive industries and amending Directive 2004/35/EC', (1882). doi: L 102/15.

European Parliament, C. (2000) 'Directive 2000/60/EC of the European Parliament and of the Council of 23 October 2000 establishing a framework for Community action in the field of water policy', *Official Journal of the European Parliament*.

El Azhari, A., Rhoujjati, A., El Hachimi, M.L. and Ambrosi, J.P., (2017) 'Pollution and ecological risk assessment of heavy metals in the soil-plant system and the sediment-water column around a former Pb/Zn-mining area in NE Morocco', *Ecotoxicology and Environmental Safety*, 144, pp. 464–474. doi: 10.1016/j.ecoenv.2017.06.051.

Fanfani, L., Zuddas, P. and Chessa, A. (1997) 'Heavy metals speciation analysis as a tool for studying mine tailings weathering', *Journal of Geochemical Exploration*. doi: 10.1016/S0375-6742(96)00059-3.

Fernandez, A. and Borrok, D. M. (2009) 'Fractionation of Cu, Fe, and Zn isotopes during the oxidative weathering of sulfide-rich rocks', *Chemical Geology*. doi: 10.1016/j.chemgeo.2009.01.024.

Fernández-Ondoño, E., Bacchetta, G., Lallena, A.M., Navarro, F.B., Ortiz, I. and Jiménez, M.N., (2017) 'Use of BCR sequential extraction procedures for soils and plant metal transfer predictions in contaminated mine tailings in Sardinia', *Journal of Geochemical Exploration*. Elsevier B.V., 172, pp. 133–141. doi: 10.1016/j.gexplo.2016.09.013.

Ficklin, W.H. & Plumlee, Geoffrey & Smith, Kathleen & McHugh, J. B. (1992) 'Geochemical classification of mine drainages and natural drainages in mineralized areas', in *Water-Rock Interaction 7*, pp. 81–384.

Filgueiras, a. V., Lavilla, I. and Bendicho, C. (2004) 'Evaluation of distribution, mobility and binding behaviour of heavy metals in surficial sediments of Louro River (Galicia, Spain) using chemometric analysis: A case study', *Science of the Total Environment*, 330(1–3), pp. 115–129. doi: 10.1016/j.scitotenv.2004.03.038.

Flores, A. N. and F. Sola, M. (2010) 'Evaluation of Metal Attenuation from Mine Tailings in SE Spain (Sierra Almagrera): A Soil-Leaching Column Study', *Mine Water and the Environment*, 29(1), pp. 53–67.

Freitas, R.M., Perilli, T.A. and Ladeira, A.C.Q., 2013. Oxidative precipitation of manganese from acid mine drainage by potassium permanganate. *Journal of Chemistry*, 2013.

Gandy, C. J., Smith, J. W. N. and Jarvis, A. P. (2007) 'Attenuation of mining-derived pollutants in the hyporheic zone: A review', *Science of the Total Environment*, pp. 435–446. doi: 10.1016/j.scitotenv.2006.11.004.

Gao, Y. and Bradshaw, A. D. (1995) 'The containment of toxic wastes: II. Metal movement in leachate and drainage at Parc lead-zinc mine, North Wales', *Environmental Pollution*. doi: 10.1016/0269-7491(95)00011-F.

García-Sánchez, A., Alastuey, A. and Querol, X. (1999) 'Heavy metal adsorption by different minerals: Application to the remediation of polluted soils', *Science of the Total Environment*. doi: 10.1016/S0048-9697(99)00383-6.

Gee, C., Ramsey, M. H. and Thornton, I. (2001) 'Buffering from secondary minerals as a migration limiting factor in lead polluted soils at historical smelting sites', *Applied Geochemistry*, 16(9–10), pp. 1193–1199. doi: 10.1016/S0883-2927(01)00025-7.

Geological Conservation Review 2018 -

<http://www.thegcr.org.uk/GIA/17/Figures/JPEGsLoRes/GCRv17c04f001.jpg>

- Ghayoraneh, M. and Qishlaqi, A. (2017) 'Concentration, distribution and speciation of toxic metals in soils along a transect around a Zn/Pb smelter in the northwest of Iran', *Journal of Geochemical Exploration*. Elsevier, 180(August), pp. 1–14. doi: 10.1016/j.gexplo.2017.05.007.
- Gieré, R., Sidenko, N. . and Lazareva, E. . (2003) 'The role of secondary minerals in controlling the migration of arsenic and metals from high-sulfide wastes (Berikul gold mine, Siberia)', *Applied Geochemistry*, 18(9), pp. 1347–1359. doi: 10.1016/S0883-2927(03)00055-6.
- Gill, M. C. (2001) *Swaledale: its mines and smelt mills*. Landmark Publishing Ltd.
- De Giudici, G. and Zuddas, P. (2001) 'In situ investigation of galena dissolution in oxygen saturated solution: evolution of surface features and kinetic rate', *Geochimica et Cosmochimica Acta*, 65(9), pp. 1381–1389. doi: 10.1016/S0016-7037(00)00605-0.
- Gomes, M.E.P., Antunes, I.M.H.R., Silva, P.B., Neiva, A.M.R. and Pacheco, F.A.L., (2010) 'Geochemistry of waters associated with the old mine workings at Fonte Santa (NE of Portugal)', *Journal of Geochemical Exploration*, 105(3), pp. 153–165. doi: 10.1016/j.gexplo.2010.05.001.
- Gomes, M. E. P. and Favas, P. J. C. (2006) 'Mineralogical controls on mine drainage of the abandoned Ervedosa tin mine in north-eastern Portugal', *Applied Geochemistry*, 21(8), pp. 1322–1334. doi: 10.1016/j.apgeochem.2006.06.007.
- Government of Alberta (2016) *Alberta Tier 1 Soil and Groundwater Remediation Guidelines, Land and Forestry Policy Branch, Policy Division*. Available at: <https://open.alberta.ca/dataset/842becf6-dc0c-4cc7-8b29-e3f383133ddc/resource/1b851705-0622-485d-beee-752a627bdfc4/download/2016-albertatier1guidelines-feb02-2016a.pdf>.
- Graham, D.J. and Midgley, N.G., 2000. Graphical representation of particle shape using triangular diagrams: an Excel spreadsheet method. *Earth Surface Processes and Landforms*, 25(13), pp.1473-1477.
- Gutiérrez, M., Mickus, K. and Camacho, L. M. (2016) 'Abandoned Pb Zn mining wastes and their mobility as proxy to toxicity: A review', *Science of The Total Environment*, 565, pp. 392–400. doi: 10.1016/j.scitotenv.2016.04.143.
- Hammarstrom, J. M., Eppinger, R. G., van Gosen, B. S., Briggs, P. H., and Meier, A. L. (2002) *Case study of the environmental signature of a recently abandoned, carbonate-hosted replacement deposit; the Clayton Mine, Idaho. Open-File Report 2002-10.*
- Hauser, L., Tandy, S., Schulin, R. and Nowack, B., (2005) 'Column extraction of heavy metals from soils using the biodegradable chelating agent EDDS.', *Environmental science & technology*, 39(17), pp. 6819–24. doi: 10.1021/es050143r.
- Health Canada (2017) 'Guidelines for Canadian Drinking Water Quality Summary Table Prepared by the Federal-Provincial-Territorial Committee on Drinking Water of the Federal-Provincial-Territorial Committee on Health and the Environment March 2006', *Environments*, (October 2014), pp. 1–16.
- Helgen, S. O. and Moore, J. N. (1996) 'Natural background determination and impact quantification in trace metal-contaminated river sediments', *Environmental science & technology*, 30(1), pp. 129–135.
- Hering, D., Borja, A., Carstensen, J., Carvalho, L., Elliott, M., Feld, C.K., Heiskanen, A.S., Johnson, R.K., Moe, J., Pont, D. and Solheim, A.L., (2010) 'The European Water Framework Directive at the age of 10: A critical review of the achievements with recommendations for the future', *Science of the Total Environment*. doi: 10.1016/j.scitotenv.2010.05.031.
- Hibbert, C. (2017) 'Controls on seasonal elemental variation in tropical rivers in Goa, India', (July), p. 345. Available at: <http://bbktheses.da.ulcc.ac.uk/275/>.

- Hirsche, D.T., Blaskovich, R., Mayer, K.U. and Beckie, R.D.. (2017) 'A study of Zn and Mo attenuation by waste-rock mixing in neutral mine drainage using mixed-material field barrels and humidity cells', *Applied Geochemistry*. doi: 10.1016/j.apgeochem.2017.06.005.
- Michael F. Hochella, Johnnie N. Moore, Ute Golla, Andrew Putnis, A TEM study of samples from acid mine drainage systems: metal-mineral association with implications for transport, *Geochimica et Cosmochimica Acta*, Volume 63, Issues 19–20, 1999, Pages 3395–3406, Hochella Jr, M.F., Moore, J.N., Putnis, C.V., Putnis, A., Kasama, T. and Eberl, D.D., (2005) 'Direct observation of heavy metal-mineral association from the Clark Fork River Superfund Complex: Implications for metal transport and bioavailability', *Geochimica et Cosmochimica Acta*, 69(7), pp. 1651–1663. doi: 10.1016/j.gca.2004.07.038.
- Hodson, M. E. (2004) 'Heavy metals - Geochemical bogey men?', *Environmental Pollution*, 129(3), pp. 341–343. doi: 10.1016/j.envpol.2003.11.003.
- House, W. A. and Warwick, M. S. (1998a) 'A mass-balance approach to quantifying the importance of in-stream processes during nutrient transport in a large river catchment', *Science of the Total Environment*, 210–211, pp. 139–152. doi: 10.1016/S0048-9697(98)00047-3.
- House, W. A. and Warwick, M. S. (1998b) 'Intensive measurements of nutrient dynamics in the River Swale', *Science of the Total Environment*, 210–211, pp. 111–137. doi: 10.1016/S0048-9697(98)00046-1.
- Hoyle, B. and Beveridge, T. J. (1983) 'Binding of metallic ions to the outer membrane of *Esherichia coli*', *Appl. Environ. Microbiol.*, 46(3), pp. 749–752.
- Hudson-Edwards, K. A. (2003) 'Sources, mineralogy, chemistry and fate of heavy metal-bearing particles in mining-affected river systems', *Mineralogical Magazine*, 67(2), pp. 205–217. doi: 10.1180/0026461036720095.
- Hudson-Edwards, K., Macklin, M. and Taylor, M. (1997) 'Historic metal mining inputs to Tees River sediment', *Science of the Total Environment*, 194–195(96), pp. 437–445. doi: 10.1016/S0048-9697(96)05381-8.
- Hudson-Edwards, K.A., Macklin, M.G., Brewer, P.A. and Dennis, I.A., (2008) *Assessment of metal mining-contaminated river sediments in England and Wales*. Available at: <http://eprints.bbk.ac.uk/1279/>.
- Ixer, R. A. and Vaughan, D. J. (1993) 'Lead-zinc-fluorite-baryte deposits of the Pennines, North Wales and the Mendips.', in Pattrick, R. A. D. and Polya, D. A. (eds) *Mineralization in the British Isles*. Chapman and Hall, London, pp. 355–418.
- Jamieson, H. E., Walker, S. R. and Parsons, M. B. (2015) 'Mineralogical characterization of mine waste', *Applied Geochemistry*. Elsevier Ltd, 57, pp. 85–105. doi: 10.1016/j.apgeochem.2014.12.014.
- Järup, L. (2003) 'Hazards of heavy metal contamination.', *British medical bulletin*.
- Järup, L. and Åkesson, A. (2009) 'Current status of cadmium as an environmental health problem', *Toxicology and Applied Pharmacology*. doi: 10.1016/j.taap.2009.04.020.
- Jarvie, H. P., Neal, C. and Robson, A. J. (1997) 'The geography of the Humber catchment', *Science of The Total Environment*, 194–195, pp. 87–99. doi: 10.1016/S0048-9697(96)05355-7.
- Jarvis, A.P., Davis, J.E., Orme, P.H., Potter, H.A. and Gandy, C.J., (2018). Predicting the benefits of mine water treatment under varying hydrological conditions using a synoptic mass balance approach. *Environmental science & technology*, 53(2), pp.702-709.
- Jarvis, A., Fox, A., Gozzard, E., Hill, S., Mayes, W.M. and Potter, H., (2007) 'Prospects for Effective National Management of Abandoned', (May).
- Jarvis, A., Gandy, C., Bailey, M., Davis, J., Orme, P., Malley, J., Potter, H. and Moorhouse, A., 2015. Metal removal and secondary contamination in a passive metal mine drainage treatment system. In *10th International Conference on Acid Rock Drainage* (pp. 1-9).

- Jennings, A. A. (2013) 'Analysis of worldwide Regulatory Guidance Values for less frequently regulated elemental surface soil contaminants', *Journal of Environmental Management*. doi: 10.1016/j.jenvman.2013.05.062.
- Johnson, K. L. and Younger, P. L. (2002) 'Hydrogeological and geochemical consequences of the abandonment of Frazer's Grove carbonate hosted Pb/Zn fluorspar mine, north Pennines, UK', *Geological Society, London, Special Publications*. doi: 10.1144/gsl.sp.2002.198.01.24.
- Johnston, D., Potter, H., Jones, C., Rolley, S., Watson, I., and Pritchard, J. (2008) *Abandoned mines and the water environment*, *Science Report*. doi: 978-1-84432-894-9.
- Joubert, A.V.P., Lucas, L., Garrido, F., Joulian, C. and Jauzein, M., (2007) 'Effect of temperature, gas phase composition, pH and microbial activity on As, Zn, Pb and Cd mobility in selected soils in the Ebro and Meuse Basins in the context of global change', *Environmental Pollution*. doi: 10.1016/j.envpol.2007.01.031.
- Jung, M. C. (2001) 'Heavy metal contamination of soils and waters in and around the Imcheon Au-Ag mine, Korea', *Applied Geochemistry*, 16(11–12), pp. 1369–1375. doi: 10.1016/S0883-2927(01)00040-3.
- Jung, M. C. and Thornton, I. (1996) 'Heavy metal contamination of soils and plants in the vicinity of a lead-zinc mine, Korea', in *Applied Geochemistry*, pp. 53–59. doi: 10.1016/0883-2927(95)00075-5.
- Kalbitz, K. and Wennrich, R. (1998) 'Mobilization of heavy metals and arsenic in polluted wetland soils and its dependence on dissolved organic matter', *Science of the Total Environment*, 209(1), pp. 27–39. doi: 10.1016/S0048-9697(97)00302-1.
- Kelley, K. D. and Taylor, C. D. (1997) 'Environmental geochemistry of shale-hosted Ag-Pb-Zn massive sulfide deposits in northwest Alaska: Natural background concentrations of metals in water from mineralized areas', *Applied Geochemistry*, 12(4), pp. 397–409. doi: 10.1016/S0883-2927(97)00009-7.
- Kerolli–Mustafa, M., Fajković, H., Rončević, S. and Ćurković, L., (2015) 'Assessment of metal risks from different depths of jarosite tailing waste of Trepča Zinc Industry, Kosovo based on BCR procedure', *Journal of Geochemical Exploration*, 148, pp. 161–168. doi: 10.1016/j.gexplo.2014.09.001.
- Kim, B. S. *et al.* (1995) 'Scanning Tunneling Microscopy Studies of Galena: The Mechanisms of Oxidation in Aqueous Solution', *Langmuir*, 11(7), pp. 2554–2562.
- Klarup, D. G. (1997) 'The influence of oxalic acid on release rates of metals from contaminated river sediment', *Science of the Total Environment*. doi: 10.1016/S0048-9697(97)00183-6.
- Kleszczewska-Zębala, A., Manecki, M., Bajda, T., Rakovan, J. and Borkiewicz, O.J., (2016) 'Mimetite Formation from Goethite-Adsorbed Ions', *Microscopy and Microanalysis*. doi: 10.1017/S1431927616000829.
- Kossoff, D., Hudson-Edwards, K.A., Dubbin, W.E. and Alfredsson, M.A., (2011) 'Incongruent weathering of Cd and Zn from mine tailings: A column leaching study', *Chemical Geology*, 281(1–2), pp. 52–71. doi: 10.1016/j.chemgeo.2010.11.028.
- Laing, G., Rinklebe, J., Vandecasteele, B., Meers, E. and Tack, F.M., (2009) 'Trace metal behaviour in estuarine and riverine floodplain soils and sediments: A review', *Science of the Total Environment*. doi: 10.1016/j.scitotenv.2008.07.025.
- Langmuir, D. (1997) *Aqueous Environmental Geochemistry*. Prentice Hal.
- Lara, R.H., Briones, R., Monroy, M.G., Mullet, M., Humbert, B., Dossot, M., Naja, G.M. and Cruz, R., (2011) 'Galena weathering under simulated calcareous soil conditions', *Science of the Total Environment*, 409(19), pp. 3971–3979. doi: 10.1016/j.scitotenv.2011.06.055.
- Lecce, S. A. and Pavlowsky, R. T. (2001) 'Use of mining-contaminated sediment tracers to investigate the timing and rates of historical flood plain sedimentation', *Geomorphology*.

doi: 10.1016/S0169-555X(00)00071-4.

Ledin, M. and Pedersen, K. (1996) 'The environmental impact of mine wastes - Roles of microorganisms and their significance in treatment of mine wastes', *Earth-Science Reviews*. doi: 10.1016/0012-8252(96)00016-5.

Lefebvre, R., Hockley, D., Smolensky, J. and Gélinas, P., (2001) 'Multiphase transfer processes in waste rock piles producing acid mine drainage. 1: Conceptual model and system characterization', *Journal of Contaminant Hydrology*, 52(1–4), pp. 137–164. doi: 10.1016/S0169-7722(01)00156-5.

Lewin, J., Davies, B. E and Wolfenden, P. J. (1977) 'Interactions between channel change and historic mining sediments', *River Channel Changes*, pp. 353–367.

Lewin, J. and Macklin, M.G. (1987) 'Metal mining and floodplain sedimentation in Britain', *International geomorphology*, pp. 1009–1027.

Lewis, J. and Sjöström, J. (2010) 'Optimizing the experimental design of soil columns in saturated and unsaturated transport experiments', *Journal of Contaminant Hydrology*, 115(1–4), pp. 1–13. doi: 10.1016/j.jconhyd.2010.04.001.

Li, J. and Naidu, R. (2005) 'Risk assessment of heavy metal contaminated soil in the vicinity of a lead/zinc mine', *Journal of Environmental Sciences*, 17(6), pp. 881–885.

Li, X. and Thornton, I. (1993) 'Multi-element contamination of soils and plants in old mining areas, U.K.', *Applied Geochemistry*, 8, pp. 51–56. doi: 10.1016/S0883-2927(09)80010-3.

Li, X. and Thornton, I. (2001) 'Chemical partitioning of trace and major elements in soils contaminated by mining and smelting activities', *Applied Geochemistry*. doi: 10.1016/S0883-2927(01)00065-8.

Lindsay, M.B., Condon, P.D., Jambor, J.L., Lear, K.G., Blowes, D.W. and Ptacek, C.J., (2009) 'Mineralogical, geochemical, and microbial investigation of a sulfide-rich tailings deposit characterized by neutral drainage', *Applied Geochemistry*, 24(12), pp. 2212–2221. doi: 10.1016/j.apgeochem.2009.09.012.

Lindsay, M.B., Moncur, M.C., Bain, J.G., Jambor, J.L., Ptacek, C.J. and Blowes, D.W., (2015) 'Geochemical and mineralogical aspects of sulfide mine tailings', *Applied Geochemistry*. Elsevier Ltd, 57, pp. 157–177. doi: 10.1016/j.apgeochem.2015.01.009.

Liu, J., Aruguete, D.M., Jinschek, J.R., Rimstidt, J.D. and Hochella Jr, M.F., (2008) 'The non-oxidative dissolution of galena nanocrystals: Insights into mineral dissolution rates as a function of grain size, shape, and aggregation state', *Geochimica Et Cosmochimica Acta*, 72(24), pp. 5984–5996. doi: DOI 10.1016/j.gca.2008.10.010.

Lottermoser, B. G. (2010) 'Mine Wastes', in *Mine wastes*, p. 12419.

Ma, L. Q. and Rao, G. N. (2010) 'Effects of Phosphate Rock on Sequential Chemical Extraction of Lead in Contaminated Soils', *Journal of Environment Quality*. doi: 10.2134/jeq1997.00472425002600030028x.

Ma, Y. B. and Uren, N. C. (1997) 'The fate and transformations of zinc added to soils', *Australian Journal of Soil Research*. doi: 10.1071/S96102.

Macklin, M. G. (1992) 'Metal pollution of soils and sediments: a geographical perspective', *Managing the human impact on the natural environment: patterns and processes*. Belhaven Press, London, 172, p. 195.

Macklin, M.G., Ridgway, J., Passmore, D.G. and Rumsby, B.T., (1994) 'The use of overbank sediment for geochemical mapping and contamination assessment: results from selected English and Welsh floodplains', *Applied Geochemistry*, 9(6), pp. 689–700. doi: 10.1016/0883-2927(94)90028-0.

Macklin, M.G., Brewer, P.A., Hudson-Edwards, K.A., Bird, G., Coulthard, T.J., Dennis, I.A., Lechler, P.J., Miller, J.R. and Turner, J.N., (2006) 'A geomorphological approach to the management of rivers contaminated by metal mining', *Geomorphology*, 79(3–4), pp. 423–

447. doi: 10.1016/j.geomorph.2006.06.024.

Macklin, M. G., Hudson-Edwards, K. A. and Dawson, E. J. (1997) 'The significance of pollution from historic metal mining in the Pennine orefields on river sediment contaminant fluxes to the North Sea', *Science of The Total Environment*, 194–195(96), pp. 391–397. doi: 10.1016/S0048-9697(96)05378-8.

magic.defra.co.uk consulted 2017- <https://magic.defra.gov.uk/MagicMap.aspx>

Maria das Graças, A.K., de Andrade, J.B., de Jesus, D.S., Lemos, V.A., Bandeira, M.L., dos Santos, W.N., Bezerra, M.A., Amorim, F.A., Souza, A.S. and Ferreira, S.L., . (2006) 'Separation and preconcentration procedures for the determination of lead using spectrometric techniques: A review', *Talanta*, 69(1), pp. 16–24. doi: 10.1016/j.talanta.2005.10.043.

Martin, S. and Griswold, W. (2009) 'Human Health Effects of Heavy Metals: Briefs for Citizens', *Environmental Science and Technology*.

Matos, A.T., Fontes, M.P.F., Da Costa, L.M. and Martinez, M.A., (2001) 'Mobility of heavy metals as related to soil chemical and mineralogical characteristics of Brazilian soils.', *Environmental pollution*, 111(3), pp. 429–35. doi: 10.1016/S0269-7491(00)00088-9.

Mayes, W.M., Johnston, D., Potter, H.A.B. and Jarvis, A.P., (2009) 'A national strategy for identification, prioritisation and management of pollution from abandoned non-coal mine sites in England and Wales. I. Methodology development and initial results', *Science of the Total Environment*. Elsevier B.V., 407(21), pp. 5435–5447. doi: 10.1016/j.scitotenv.2009.06.019.

McKillop, S. and Dyar, M.D., 2010. *Geostatistics explained: an introductory guide for earth scientists*. Cambridge University Press.

MET Office 2017 / 2019 <https://www.metoffice.gov.uk/research/climate/maps-and-data/uk-temperature-rainfall-and-sunshine-time-series>

Miller, J. R. (1997) 'The role of fluvial geomorphic processes in the dispersal of heavy metals from mine sites', *Journal of Geochemical Exploration*, 58, pp. 101–118. doi: 10.1016/S0375-6742(96)00073-8.

Miller, J. R. and Orbock Miller, S. M. (2007) 'Contaminated Rivers: An Overview', in *Contaminated Rivers*, pp. 1–31. doi: 10.1007/1-4020-5602-8_1.

Mills, C., Simpson, I. and Adderley, W.P., 2014. The lead legacy: the relationship between historical mining, pollution and the post-mining landscape. *Landscape History*, 35(1), pp.47-72

mindat.org consulted 2019: <https://www.mindat.org/min-3320.html>

Moncur, M.C., Jambor, J.L., Ptacek, C.J. and Blowes, D.W., (2009) 'Mine drainage from the weathering of sulfide minerals and magnetite', *Applied Geochemistry*, 24(12), pp. 2362–2373. doi: 10.1016/j.apgeochem.2009.09.013.

Moncur, M.C., Ptacek, C.J., Lindsay, M.B., Blowes, D.W. and Jambor, J.L.. (2015) 'Long-term mineralogical and geochemical evolution of sulfide mine tailings under a shallow water cover', *Applied Geochemistry*. Elsevier Ltd, 57, pp. 178–193. doi: 10.1016/j.apgeochem.2015.01.012.

Monhemius, A.J., 2016. THE IRON ELEPHANT: A Brief History of Hydrometallurgists' Struggles with Element No. 26.

Morin, G., Ostergren, J.D., Juillot, F., Ildefonse, P., Calas, G. and Brown, G.E., (1999) 'XAFS determination of the chemical form of lead in smelter-contaminated soils and mine tailings: Importance of adsorption processes', *American Mineralogist*. doi: 10.2138/am-1999-0327.

- Morin, K.A. and Hutt, N.M., 2001. *Environmental geochemistry of minesite drainage: Practical theory and case studies, Digital Edition*. MDAG Publishing (www.mdag.com), Surrey, British Columbia.
- Mossop, K. F. and Davidson, C. M. (2003) 'Comparison of original and modified BCR sequential extraction procedures for the fractionation of copper, iron, lead, manganese and zinc in soils and sediments', *Analytica Chimica Acta*, 478(1), pp. 111–118. doi: 10.1016/S0003-2670(02)01485-X.
- Mouni, L., Belkhiri, L., Bouzaza, A. and Bollinger, J.C., (2017) 'Interactions between Cd, Cu, Pb, and Zn and four different mine soils', *Arabian Journal of Geosciences*. Arabian Journal of Geosciences, 10(4). doi: 10.1007/s12517-017-2864-9.
- Munk, L., Faure, G. and Koski, R. (2006) 'Geochemical evolution of solutions derived from experimental weathering of sulfide-bearing rocks', *Applied Geochemistry*. doi: 10.1016/j.apgeochem.2006.04.003.
- Nathanail, C.P.; McCaffrey, C.; Gillett, A.G.; Ogden, R.C. & Nathanail, J.F., *The LQM/CIEH S4ULs for Human Health Risk Assessment*, 201, Land Quality Press, Nottingham.
- National Parks website 2015 - https://nationalparks.uk/quick-guide-to-the-uks-national-parks#q_15
- National River Flow Archive 2015 - nrfa.ceh.ac.uk/
- Navarro, M.C., Pérez-Sirvent, C., Martínez-Sánchez, M.J., Vidal, J., Tovar, P.J. and Bech, J., (2008) 'Abandoned mine sites as a source of contamination by heavy metals: A case study in a semi-arid zone', *Journal of Geochemical Exploration*, 96(2–3), pp. 183–193. doi: 10.1016/j.gexplo.2007.04.011.
- Nejeschlebová, L., Sracek, O., Mihaljevič, M., Ettlér, V., Křibek, B., Knésl, I., Vaněk, A., Penížek, V., Dolníček, Z. and Mapani, B., (2015) 'Geochemistry and potential environmental impact of the mine tailings at Rosh Pinah, southern Namibia', *Journal of African Earth Sciences*. doi: 10.1016/j.jafrearsci.2015.02.005.
- Nichols, G. (2004) 'Sedimentology and Stratigraphy', in *Sedimentology and Stratigraphy*.
- Nordstrom, D. K. (2011) 'Mine waters: Acidic to circumneutral', *Elements*. doi: 10.2113/gselements.7.6.393.
- Nordstrom, D. K. (2015) 'Baseline and premining geochemical characterization of mined sites', *Applied Geochemistry*. Elsevier Ltd, 57, pp. 17–34. doi: 10.1016/j.apgeochem.2014.12.010.
- Nordstrom, D. K., Blowes, D. W. and Ptacek, C. J. (2015) 'Hydrogeochemistry and microbiology of mine drainage: An update', *Applied Geochemistry*. Elsevier Ltd, 57, pp. 3–16. doi: 10.1016/j.apgeochem.2015.02.008.
- Northern Mines Research Group 2017 - www.nmrs.co.uk
nrfa.ceh.ac.uk/ consulted 2015 - National River Flow Archive
- Nuttall, C. a. and Younger, P. L. (2000) 'Zinc removal from hard, circum-neutral mine waters using a novel closed- bed limestone reactor', *Water Research*, 34(4), pp. 1262–1268. doi: 10.1016/S0043-1354(99)00252-3.
- Nuttall, C. A. and Younger, P. L. (2002) 'Secondary minerals in the abandoned mines of Nenthead, Cumbria as sinks for pollutant metals', *Geological Society, London, Special Publications*. doi: 10.1144/gsl.sp.2002.198.01.15.
- Ódor, L., Wanty, R.B., Horváth, I. and Fügédi, U., (1998) 'Mobilization and attenuation of metals downstream from a base-metal mining site in the Matra Mountains, northeastern Hungary', *Journal of Geochemical Exploration*. doi: 10.1016/S0375-6742(98)00056-9.
- Ongley, E. (1996) 'SEDIMENT MEASUREMENTS - Chapter 13', *United Nations Environment Programme and the World Health Organization (UNEP/WHO)*.

- Ordnance Survey, OS Open River (consulted 2018) - <https://www.ordnancesurvey.co.uk/business-and-government/products/os-open-rivers.html>
- Palumbo-Roe, B. and Colman, T. (2010) 'The nature of waste associated with closed mines in England and Wales'. Available at: <http://nora.nerc.ac.uk/10083/>.
- Parkhurst, D.L. and Appelo, C.A.J., 2013. *Description of input and examples for PHREEQC version 3: a computer program for speciation, batch-reaction, one-dimensional transport, and inverse geochemical calculations* (No. 6-A43). US Geological Survey.
- Pavoni, E., Covelli, S., Adami, G., Baracchini, E., Cattelan, R., Crosera, M., Higuera, P., Lenaz, D. and Petranich, E., (2018) 'Mobility and fate of Thallium and other potentially harmful elements in drainage waters from a decommissioned Zn-Pb mine (North-Eastern Italian Alps)', *Journal of Geochemical Exploration*, 188, pp. 1–10. doi: 10.1016/j.gexplo.2018.01.005.
- Petrunic, B. M., MacQuarrie, K. T. B. and Al, T. A. (2005) 'Reductive dissolution of Mn oxides in river-recharged aquifers: A laboratory column study', *Journal of Hydrology*. doi: 10.1016/j.jhydrol.2004.06.022.
- Pirajno, F., Burlow, R. and Huston, D. (2010) 'The Magellan Pb deposit, Western Australia; a new category within the class of supergene non-sulphide mineral systems', *Ore Geology Reviews*, 37(2), pp. 101–113. doi: 10.1016/j.oregeorev.2010.01.001.
- Plante, B., Benzaazoua, M. and Bussière, B., 2011. Predicting geochemical behaviour of waste rock with low acid generating potential using laboratory kinetic tests. *Mine Water and the Environment*, 30(1), pp.2-21.
- Plante, B., Bussière, B. and Benzaazoua, M. (2014) 'Lab to field scale effects on contaminated neutral drainage prediction from the Tio mine waste rocks', *Journal of Geochemical Exploration*, 137, pp. 37–47. doi: 10.1016/j.gexplo.2013.11.004.
- Plumlee, Geoffrey & Smith, Kathleen & Ficklin, W.H. & Briggs, P. H. (1992) 'Geological and geochemical controls on the composition of mine drainages and natural drainages in mineralized areas', *Low Temperature Environments*, 1, pp. 419–122.
- Plumlee, G. and Nash, J. (1995) *Geoenvironmental models of mineral deposits—fundamentals and applications*.
- Pope, J., Rait, R., Cavanagh, J., Harding, J., Trumm, D., Craw, D., Champeau, O., Buxton, R., Haffert, L., Niyogi, D. and Clemens, A., (2009) 'A framework to assist decision making on mine drainage related environmental issues in New Zealand .', *Geology*, pp. 1–11.
- Postawa, A. and Motyka, J. (2019) 'Selected trace elements and metals in groundwater within Permian sediments near Olkusz (Zn-Pb ore mining region, S Poland)', *Environmental Science and Pollution Research*, 26(1), pp. 34–43. doi: 10.1007/s11356-018-2953-7.
- Potter, H.A.B. and Johnston, D., 2014. Inventory of closed mine waste facilities. Version 2. Environment Agency.
- Pueyo, M. *et al.* (2008) 'Use of the modified BCR three-step sequential extraction procedure for the study of trace element dynamics in contaminated soils', *Environmental Pollution*, 152(2), pp. 330–341. doi: 10.1016/j.envpol.2007.06.020.
- Pulford, I.D., MacKenzie, A.B., Donatello, S. and Hastings, L., (2009) 'Source term characterisation using concentration trends and geochemical associations of Pb and Zn in river sediments in the vicinity of a disused mine site: Implications for contaminant metal dispersion processes', *Environmental Pollution*. doi: 10.1016/j.envpol.2008.12.018.
- Pulford, I. and Flowers, H. (2006) *Environmental chemistry at a glance*. Blackwell.
- Raistrick, A. (1975) *The Lead Industry of Wensleydale and Swaledale. Volume 1: The Mine*. Moorland Publishing Company, Hartington.
- Raistrick, A. and Jennings, B. (1965) *A History of Lead Mining in the Pennine*. Longmans, Green and Co., London.

Ramos Arroyo, Y. R. and Siebe, C. (2007) 'Weathering of sulphide minerals and trace element speciation in tailings of various ages in the Guanajuato mining district, Mexico', *Catena*, 71(3), pp. 497–506. doi: 10.1016/j.catena.2007.03.014.

Rauret, G., Lopez-Sanchez, J.F., Sahuquillo, A., Rubio, R., Davidson, C., Ure, A. and Quevauviller, P., (1999) 'Improvement of the BCR three step sequential extraction procedure prior to the certification of new sediment and soil reference materials.', *Journal of environmental monitoring: JEM*, 1(1), pp. 57–61. doi: 10.1039/a807854h.

Reade International consulted 2018 -

<https://www.reade.com/products/ferric-iii-iron-hydroxide-fe-oh-3-granular-powder-slurry>

Reid, I., Bathurst, J.C., Carling, P., Walling, D. E., and Webb, B. (1997) 'Sediment erosion, transport, and deposition', (July 2017).

Resongles, E., Casiot, C., Freydier, R., Dezileau, L., Viers, J. and Elbaz-Poulichet, F., (2014) 'Persisting impact of historical mining activity to metal (Pb, Zn, Cd, Tl, Hg) and metalloid (As, Sb) enrichment in sediments of the Gardon River, Southern France', *Science of the Total Environment*, 481(1), pp. 509–521. doi: 10.1016/j.scitotenv.2014.02.078.

Riba, I., DelValls, T.A., Forja, J.M. and Gómez-Parra, A., (2002) 'Influence of the Aznalcóllar mining spill on the vertical distribution of heavy metals in sediments from the Guadalquivir estuary (SW Spain)', *Marine Pollution Bulletin*. doi: 10.1016/S0025-326X(01)00171-0.

Rodríguez, L., Ruiz, E., Alonso-Azcárate, J. and Rincón, J., (2009) 'Heavy metal distribution and chemical speciation in tailings and soils around a Pb-Zn mine in Spain', *Journal of Environmental Management*, 90(2), pp. 1106–1116. doi: 10.1016/j.jenvman.2008.04.007.

RoyChowdhury, A., Sarkar, D. and Datta, R. (2015) 'Remediation of Acid Mine Drainage-Impacted Water', *Current Pollution Reports*, 1(3), pp. 131–141. doi: 10.1007/s40726-015-0011-3.

Salomons, W. (1995) 'Environmental impact of metals derived from mining activities: Processes, predictions, prevention', *Journal of Geochemical Exploration*, 52(1–2), pp. 5–23. doi: 10.1016/0375-6742(94)00039-E.

Salomons, W. and Forstner, U., 1984. *Metals in the hydrocycle*, Springer Berlin Heidelberg. ISBN 10: 3540127550

Sanusi, K.A., Hassan, M.S., Abbas, M.A. and Kura, A.M., (2017) 'Assessment of heavy metals contamination of soil and water around abandoned Pb-Zn mines in Yelu, Alkali Local Government Area of Bauchi State, Nigeria', *International Research Journal of Public and Environmental Health*, 4(5), pp. 72–77. doi: 10.15739/irjpeh.17.010.

Sauvé, S., Dumestre, A., McBride, M. and Hendershot, W., 1998. Derivation of soil quality criteria using predicted chemical speciation of Pb²⁺ and Cu²⁺. *Environmental Toxicology and Chemistry: An International Journal*, 17(8), pp.1481-1489.

Satarug, S. *et al.* (2003) 'A global perspective on cadmium pollution and toxicity in non-occupationally exposed population', in *Toxicology Letters*. doi: 10.1016/S0378-4274(02)00381-8.

Schwab, a P., He, Y. and Banks, M. K. (2005) 'The influence of organic ligands on the retention of lead in soil.', *Chemosphere*, 61(6), pp. 856–66. doi: 10.1016/j.chemosphere.2005.04.098.

Satarug, S., Baker, J.R., Urbenjapol, S., Haswell-Elkins, M., Reilly, P.E., Williams, D.J. and Moore, M.R., (2008) 'Environmental geochemistry of a Kuroko-type massive sulfide deposit at the abandoned Valzinco mine, Virginia, USA', *Applied Geochemistry*, 23(2), pp. 320–342. doi: 10.1016/j.apgeochem.2007.10.001.

Shaheen, S. M. (2009) 'Sorption and lability of cadmium and lead in different soils from Egypt and Greece', *Geoderma*. doi: 10.1016/j.geoderma.2009.07.017.

- Sharafi, A., Ardejani, F.D., Rezaei, B. and Sargheini, J., (2018) 'Environmental geochemistry of near-neutral waters and mineralogy of zinc and lead at the Angouran non-sulphide zinc mine, NW Iran', *Journal of Geochemical Exploration*. doi: 10.1016/j.gexplo.2017.11.020.
- Singh, B.R. and Oste, L., 2001. In situ immobilization of metals in contaminated or naturally metal-rich soils. *Environmental Reviews*, 9(2), pp.81-97.
- Sipos, P., Németh, T., Kis, V.K. and Mohai, I., (2008) 'Sorption of copper, zinc and lead on soil mineral phases', *Chemosphere*. doi: 10.1016/j.chemosphere.2008.06.046.
- Smith, K.S., Ficklin, W.H., Plumlee, G.S. and Meier, A. . (1992) 'Metal and arsenic partitioning between water and suspended sediment at mine-drainage sites in diverse geologic settings', in *Water-rock interaction*. Balkema, Rotterdam, pp. 443–447.
- Smith, K. S., Plumlee, G. S., and Ficklin, W. H., (1992) 'Metal and arsenic partitioning between water and suspended sediment at mine-drainage sites in diverse geologic settings', in *Water-Rock Interaction: 7th International Symposium on Water-Rock Interaction, Park City, Utah*, pp. 443–447.
- Smith R and Murphy S 2011 - Smith, R. and Murphy, S., 2011. *Mines of the West Pennines*. Northern Mine Research Society.
- SoBRA - Society of Brownfield Risk Assessment (2011) *SOCIETY OF BROWNFIELD RISK ASSESSMENT SUMMER WORKSHOP REPORT 2011 - Human health risk assessment of lead in soil- the key issues*.
- Sparks, D. L. (2003) *Environmental Soil Chemistry, Soil Science*. doi: 10.1097/00010694-199703000-00009.
- Sparks, D. L. (2005) 'Toxic Metals in the Environment: The Role of Surfaces', *Elements*, 1(4), pp. 193–197. doi: 10.2113/gselements.1.4.193.
- Stracek, O., Filip, J., Mihaljevič, M., Kříbek, B., Majer, V. and Veselovský, F. (2011) 'Attenuation of dissolved metals in neutral mine drainage in the Zambian Copperbelt', *Environmental Monitoring and Assessment*, 172(1–4), pp. 287–299. doi: 10.1007/s10661-010-1334-6.
- Stanton, M.R., Gemery-Hill, P.A., Shanks III, W.C. and Taylor, C.D., (2008) 'Rates of zinc and trace metal release from dissolving sphalerite at pH 2.0–4.0', *Applied Geochemistry*, 23(2), pp. 136–147. doi: 10.1016/j.apgeochem.2007.10.005.
- Stefanowicz, A. M., Woch, M. W. and Kapusta, P. (2014) 'Inconspicuous waste heaps left by historical Zn-Pb mining are hot spots of soil contamination', *Geoderma*, 235–236, pp. 1–8. doi: 10.1016/j.geoderma.2014.06.020.
- Stefánsson, A., Gíslason, S.R. and Arnórsson, S., 2001. Dissolution of primary minerals in natural waters: II. Mineral saturation state. *Chemical Geology*, 172(3-4), pp.251-276.
- Stephenson, D., Bevins, R.E., Millward, D., Stone, P., Parsons, I., Highton, A.J. & Wadsworth, W.J., (2000), *Caledonian Igneous Rocks of Great Britain*, Geological Conservation Review Series, No. 17, Joint Nature Conservation Committee, Peterborough, 648 pages, illustrations, A4 hardback, ISBN 1 86107 471 9
- Sterckeman, T., Douay, F., Proix, N. and Fourrier, H., (2000) 'Vertical distribution of Cd, Pb and Zn in soils near smelters in the North of France', *Environmental Pollution*, 107(3), pp. 377–389. doi: 10.1016/S0269-7491(99)00165-7.
- Strzebońska, M., Jarosz-Krzemińska, E. and Adamiec, E. (2017) 'Assessing Historical Mining and Smelting Effects on Heavy Metal Pollution of River Systems over Span of Two Decades', *Water, Air, and Soil Pollution*, 228(4). doi: 10.1007/s11270-017-3327-3.
- Swennen, R. and Van Der Sluys, J. (1998) 'Zn, Pb, Cu and As distribution patterns in overbank and medium-order stream sediment samples: Their use in exploration and environmental geochemistry', *Journal of Geochemical Exploration*, 65, pp. 27–45. doi: 10.1016/S0375-6742(98)00057-0.

Tack, F.M.G., Van Ranst, E., Lievens, C. and Vandenberghe, R.E., (2006) 'Soil solution Cd, Cu and Zn concentrations as affected by short-time drying or wetting: The role of hydrous oxides of Fe and Mn', *Geoderma*. doi: 10.1016/j.geoderma.2006.07.003.

Takeo, N., 2005. Atlas of Eh-pH diagrams. *Geological survey of Japan open file report*, 419, p.102.

Taylor, M. P. and Hudson-Edwards, K. a (2008) 'The dispersal and storage of sediment-associated metals in an arid river system: the Leichhardt River, Mount Isa, Queensland, Australia.', *Environmental pollution (Barking, Essex : 1987)*, 152(1), pp. 193–204. doi: 10.1016/j.envpol.2007.05.011.

Tesser, E., D'Amato, E., Gori, R. and Lubello, C., (2011) 'Conventional and innovative processes for neutral mine drainage treatment and reuse of residuals', in *Mine Water – Managing the Challenges*. IMWA. Aachen, Germany.

Tessier, A, Campbell, P. G. C. and Bisson, M. (1979) 'Sequential Extraction Procedure for the Speciation of Particulate Trace Metals', *Analytical Chemistry*, 51(7), pp. 844–851. doi: 10.1021/ac50043a017.

The Yorkshire Dales 2017 - Yorkshire-Dales.com

Tiruta-Barna, L., Benetto, E. and Perrodin, Y. (2007) 'Environmental impact and risk assessment of mineral wastes reuse strategies: Review and critical analysis of approaches and applications', *Resources, Conservation and Recycling*, 50(4), pp. 351–379. doi: 10.1016/j.resconrec.2007.01.009.

Traina, S.J. and Laperche, V., 1999. Contaminant bioavailability in soils, sediments, and aquatic environments. *Proceedings of the National Academy of Sciences*, 96(7), pp.3365-3371.

UKCP18, consulted 2020 -

<https://www.metoffice.gov.uk/research/approach/collaboration/ukcp/about>

Urbano, G., Meléndez, A.M., Reyes, V.E., Veloz, M.A. and González, I., (2007) 'Galvanic interactions between galena-sphalerite and their reactivity', *International Journal of Mineral Processing*, 82(3), pp. 148–155. doi: 10.1016/j.minpro.2006.09.004.

USEPA (1994) 'Acid generation prediction in mining', *Environmental Protection Agency*.

USEPA (2007) Monitored Natural Attenuation of Inorganic Contaminants in Ground Water, Volume 2. Assessment for non-radionuclides including arsenic, cadmium, chromium, copper, lead, nitrate, perchlorate, and selenium. Ref: EPA/6006r-07/140

USEPA (2009) United States Environmental Protection Agency; national primary drinking water regulations, EPA 816-F-09-004, May 2009 - <https://www.epa.gov/ground-water-and-drinking-water/national-primary-drinking-water-regulations>

USEPA (2018) United States Environmental Protection Agency; regional screening level online calculator (consulted 2018) - https://epa-prgs.ornl.gov/cgi-bin/chemicals/csl_search

Valencia-Avellan, M., Slack, R., Stockdale, A. and Mortimer, R.J.G., (2017) 'Understanding the mobilisation of metal pollution associated with historical mining in a carboniferous upland catchment', *Environmental Science: Processes and Impacts*. doi: 10.1039/c7em00171a.

Vaněk, A., Ettler, V., Grygar, T., Borůvka, L., Šebek, O. and Drábek, O., (2008) 'Combined Chemical and Mineralogical Evidence for Heavy Metal Binding in Mining- and Smelting-Affected Alluvial Soils', *Pedosphere*. doi: 10.1016/s1002-0160(08)60037-5.

Vega, F.A., Covelo, E.F., Andrade, M.L. and Marcet, P., (2004) 'Relationships between heavy metals content and soil properties in minesoils', in *Analytica Chimica Acta*. doi: 10.1016/j.aca.2004.06.073.

Verner, J.F., Ramsey, M.H., Helios-Rybicka, E. and Jeźdrzejczyk, B., (1996) 'Heavy metal contamination of soils around a Pb-Zn smelter in Bukowno, Poland', in *Applied*

Geochemistry. doi: 10.1016/0883-2927(95)00093-3.

Viers, J., Oliva, P., Dandurand, J. L., Dupre, B., and Gaillardet, J., (2013) 'Chemical Weathering Rates, CO₂ Consumption, and Control Parameters Deduced from the Chemical Composition of Rivers', *Treatise on Geochemistry: Second Edition*, 7, pp. 175–194. doi: 10.1016/B978-0-08-095975-7.00506-4.

Voegelin, A., Barmettler, K. and Kretzschmar, R. (2003) 'Heavy metal release from contaminated soils: comparison of column leaching and batch extraction results.', *Journal of environmental quality*, 32(3), pp. 865–875.

Edwards, W. and Trotter, F. M. E. (1954) *The Pennines and Adjacent Areas*.

Walling, D.E., Owens, P.N., Waterfall, B.D., Leeks, G.J. and Wass, P.D., (2000) 'The particle size characteristics of fluvial suspended sediment in the Humber and Tweed catchments, UK', *Science of the Total Environment*. doi: 10.1016/S0048-9697(00)00384-3.

Walling, D.E., Owens, P.N., Carter, J., Leeks, G.J.L., Lewis, S., Meharg, A.A. and Wright, J., (2003) 'Storage of sediment-associated nutrients and contaminants in river channel and floodplain systems', *Applied Geochemistry*, 18(2), pp. 195–220. doi: 10.1016/S0883-2927(02)00121-X.

Warren, L. a. and Haack, E. a. (2001) 'Biogeochemical controls on metal behaviour in freshwater environments', *Earth-Science Reviews*, 54(4), pp. 261–320. doi: 10.1016/S0012-8252(01)00032-0.

Warrender, R. and Pearce, N. J. G. (2007) 'Remediation of Circum-Neutral , Low-Iron Waters By Permeable Reactive Media', *Analysis*, (May).

Waterlot, C., Douay, F. and Pelfrène, A. (2017) 'Chemical Availability of Cd, Pb and Zn in Anthropogenically Polluted Soil: Assessing the Geochemical Reactivity and Oral Bioaccessibility', *Pedosphere*. doi: 10.1016/S1002-0160(17)60356-4.

Waters, C.N., Dean, M.T., Jones, N.S. and Somerville, I.D., 2011. Cumbria and the northern Pennines. *A Revised Correlation of Carboniferous Rocks in the British Isles*, (26), p.82..

Waychunas, G. A., Kim, C. S. and Banfield, J. F. (2005) 'Nanoparticulate iron oxide minerals in soils and sediments: Unique properties and contaminant scavenging mechanisms', in *Journal of Nanoparticle Research*. doi: 10.1007/s11051-005-6931-x.

Weisener, C. G., Smart, R. S. t. C. and Gerson, A. R. (2003) 'Kinetics and mechanisms of the leaching of low Fe sphalerite', *Geochimica et Cosmochimica Acta*, 67(5), pp. 823–830. doi: 10.1016/S0016-7037(02)01276-0.

Weng, L., Temminghoff, E.J., Lofts, S., Tipping, E. and Van Riemsdijk, W.H., (2002) 'Complexation with dissolved organic matter and solubility control of heavy metals in a sandy soil', *Environmental Science and Technology*. doi: 10.1021/es0200084.

WFD-UKTAG, 2014. Updated Recommendations on Environmental Standards, River Basin Management (2015-21). UK Technical Advisory Group on the Water Framework Directive

White III, W.W., Lapakko, K.A. and Cox, R.L., 1999. Static-test methods most commonly used to predict acid-mine drainage: practical guidelines for use and interpretation. *The Environmental Geochemistry of Mineral Deposits, Part A, Processes, Techniques, and Health Issues: Littleton, CO, Society of Economic Geologists, Reviews in Economic Geology A*, 6, pp.325-338.

Wilson, M. J. and Bell, N. (1996) 'Acid deposition and heavy metal mobilization', in *Applied Geochemistry*. doi: 10.1016/0883-2927(95)00088-7.

World Health Organization (2011) 'Guidelines for Drinking-water Quality 4th ed., WHO, Geneva, p. 340.', *World Health Organization*. doi: 10.1016/S1462-0758(00)00006-6.

Wu, S.C., Luo, Y.M., Cheung, K.C. and Wong, M.H., (2006) 'Influence of bacteria on Pb and Zn speciation, mobility and bioavailability in soil: A laboratory study', *Environmental Pollution*. doi: 10.1016/j.envpol.2006.02.022.

Yong, R. N. *et al.* (2001) 'Partitioning of heavy metals on soil samples from column tests', *Engineering Geology*, 60(1–4), pp. 307–322. doi: 10.1016/S0013-7952(00)00111-3.

Yorkshire-dales.com consulted 2017

Younger, P. L. (2000) 'Nature and practical implications of heterogeneities in the geochemistry of zinc-rich, alkaline mine waters in an underground F–Pb mine in the UK', *Applied Geochemistry*, 15(9), pp. 1383–1397. doi: 10.1016/S0883-2927(00)00010-X.

Younger, P. L. (2001) 'Mine water pollution in Scotland: Nature, extent and preventative strategies', *Science of the Total Environment*, 265, pp. 309–326. doi: 10.1016/S0048-9697(00)00673-2.

Younger, P. L., Banwart, S. and Hedin, R. S. (2002) *Mine Water: Hydrology, Pollution, Remediation*, *Journal of Chemical Information and Modeling*. doi: 10.1017/CBO9781107415324.004.

Younger, P. L. and Robins, N. S. (2002) *Mine water hydrogeology and geochemistry*, *Geological Society Special Publications*.

Yukselen, M. A. and Alpaslan, B. (2001) 'Leaching of metals from soil contaminated by mining activities', *Journal of Hazardous Materials*. doi: 10.1016/S0304-3894(01)00277-1.

Zhang, P., Ryan, J. A. and Bryndzia, L. T. (1997) 'Pyromorphite formation from goethite adsorbed lead', *Environmental Science and Technology*. doi: 10.1021/es970087x

APPENDIX A – SUMMARY OF EA DATA

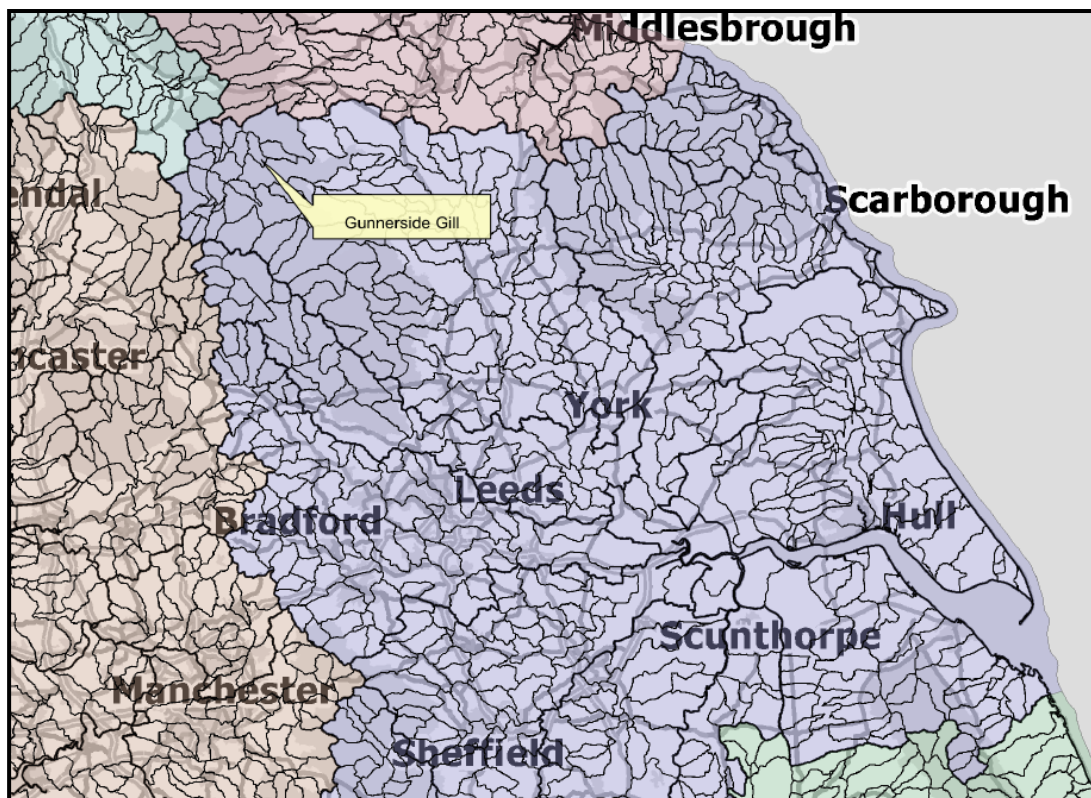
Project details

| | |
|----------------------------------|--|
| Project name | Gunnerside Gill catchment characterisation |
| Contact | John Barber, GWCL-Yorkshire Area |
| NoCam assessment | Probably Not Impacted - Score = 1 – Rank = 355 |
| River length impacted | Gunnerside Gill = 5.6km downstream of mines |
| Mining Waste Directive inventory | Yes (Bunton Lead Mine) |

Water body summary information

| | |
|-------------------------|--|
| Surface Water Body ID | GB104027069090 (Humber River Basin District) |
| Surface Water Body Name | Gunnerside Gill (Gunnerside Beck) |
| Surface Water Catchment | Swale, Ure, Nidd & Upper Ouse (SUNO) |
| Surface Water Body Type | Mid, Small, Siliceous (Secondary River) |
| Groundwater Body ID | GB40402G701900 (Humber River Basin District) |
| Groundwater Body Name | SUNO: Millstone Grit & Carboniferous Limestone |
| RBP Measure | None (Good Status - but see below) |
| RFF Database | No |

Figure 1. Gunnerside Gill location within the Humber River Basin District (in blue)

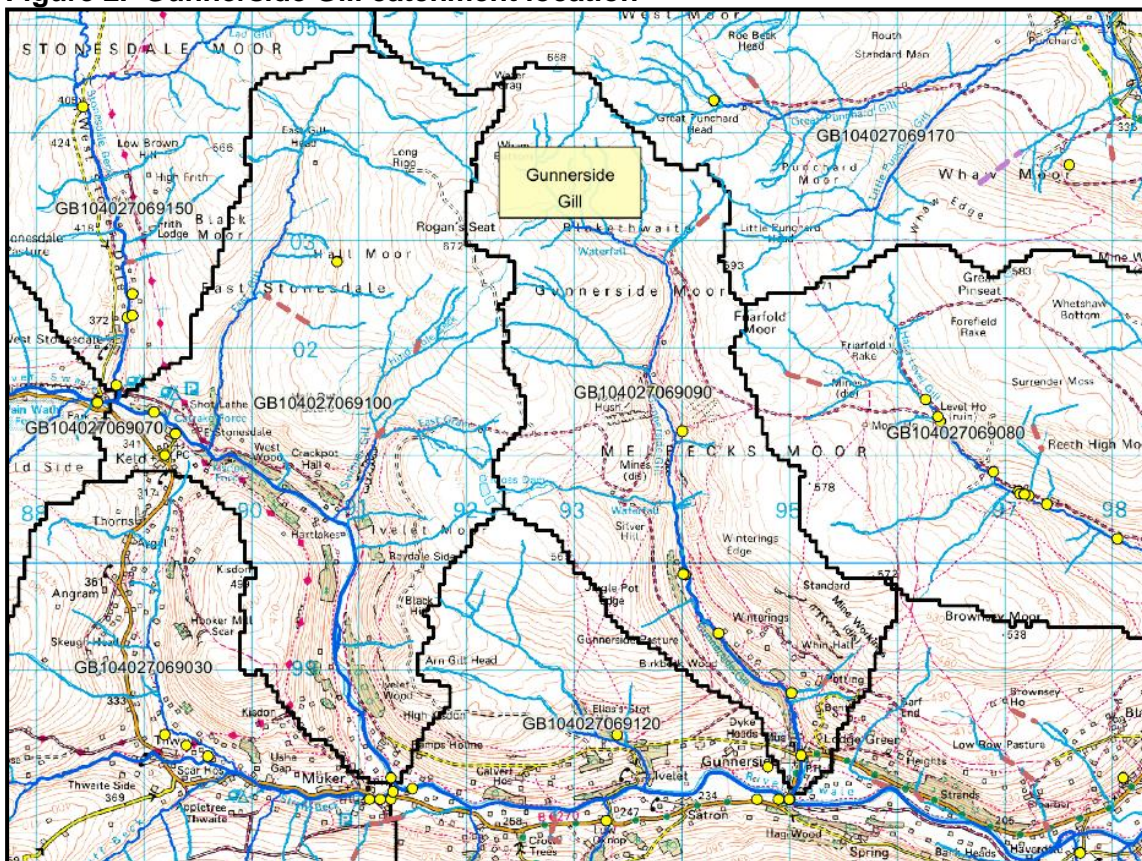


Background information

| Surface water body classification | Status in 2009 |
|-----------------------------------|-----------------------------------|
| Ecological Status | Good |
| Biological Status | Good |
| General Physico-Chemical Status | High |
| Hydromorphological Status | Not High |
| Hydromorphological Designation | Not a Heavily Modified Water Body |
| Specific Pollutants Overall | High |
| Chemical Status | Does Not Require Assessment |

| Groundwater body classification | Status in 2009 | Confid-ence | Predicted Status | Reason for not achieving good status |
|---------------------------------|----------------|-------------|------------------|---|
| Chemical Status Overall | Poor | High | Good by 2027 | Disproportionate cost Technically infeasible |
| Saline Intrusion | Good | High | Good | - |
| Surface Water Impacts | Poor | Low | Good by 2027 | Technically infeasible |
| Wetland (GWDTE) Impacts | Good | Low | Good | - |
| Drinking Water Protected Area | Poor | High | Good by 2027 | Disproportionate cost |
| General Chemical Assessment | Poor | Low | Good by 2027 | Technically infeasible |
| Upward Pollutant Trend | Yes | - | - | - |

Figure 2. Gunnerside Gill catchment location



Gunnerside Gill, located in the northern part of the Humber River Basin District (see **Figure 1** above), is a tributary of the River Swale in the Yorkshire Dales National Park; with the confluence some 29km upstream of Richmond. Gunnerside Gill catchment (13km²) is shown in **Figure 2** above, with recent water quality monitoring points shown as yellow circles. Gunnerside Gill drains a former lead mining area, where the minerals extracted included galena (PbS), sphalerite (ZnS) and barite (BaSO₄).

Gunnerside Gill was identified with elevated metal concentrations (Pb, Cd, Zn, Ba) in the EA Yorkshire Metal Mines Study (2010). This was based on a single surface water sampling event at the confluence of Gunnerside Gill with the River Swale conducted in February 2010. These results were subsequently confirmed by a sampling programme conducted by Hull University in 2010 and by the EA in 2011 for the MWD project. These previous water quality results are summarised in the table below, where the metals identified are consistent with the ores formerly mined in the catchment; cadmium being an impurity in the main lead and zinc mineral ores

The metal concentrations were compared to annual average EQS values with exceedences high-lighted in pink in the table below. The EQS values for zinc, cadmium and copper are variable and depend on the hardness of the receiving waters. The mean hardness in the samples shown below was 67mg/L and in all the samples in this project the mean hardness was 74mg/L. These fall into the hardness band from 50-100mg/L and so the relevant EQS values are: 50µg/L for zinc; 0.09µg/L for cadmium; and 6µg/L for copper.

| Date | Location | NGR | Pb (µg/L) | Zn (µg/L) | Cd (µg/L) | Ni (µg/L) | Cu (µg/L) | Flow (L/s) |
|----------------------------------|---------------------------------------|----------|------------|-----------|-------------|-----------|-----------|------------|
| Feb-10 | Gunnerside Beck at Gunnerside | SD951983 | 22 | 199 | 1.7 | 1.1 | <1 | 500 |
| Jul-10 | Bunton Level Discharge | NY940012 | 54 | 1285 | 10 | 2 | 2 | 2 |
| Jul-10 | Sir Francis Level Discharge | NY934000 | 72 | 2003 | 12 | 5 | 2 | 12 |
| Jul-10 | Bank Discharge to Gunnerside Beck | SD941999 | 183 | 679 | 6 | 7 | 2 | 0.1 |
| Feb-11 | Gunnerside Beck u/s Bunton Level | NY939014 | 7 | 18 | 0.1 | 1.1 | <1 | - |
| Feb-11 | Bunton Level Discharge | NY940012 | 41 | 780 | 8.3 | 3.6 | <1 | ~10 |
| Feb-11 | Gunnerside Beck d/s Bunton Level | NY939012 | 10 | 40 | 0.4 | 1.3 | <1 | - |
| Feb-11 | Water Sykes | NY940011 | 4 | 51 | 0.3 | <1 | <1 | - |
| Feb-11 | Gunnerside Beck u/s Sir Francis Level | NY940000 | 19 | 56 | 0.6 | 1.1 | <1 | - |
| Feb-11 | Gunnerside Beck d/s Sir Francis Level | SD941998 | 22 | 140 | 1.3 | 1.4 | <1 | - |
| Feb-11 | Gunnerside Beck at Gunnerside | SD951984 | 26 | 194 | 1.7 | 1.3 | <1 | - |
| EQS Annual Average (µg/L) | | | 7.2 | 50 | 0.09 | 20 | 6 | - |

The above water quality monitoring identified significant metal pollutants in Gunnerside Gill that were not originally identified in the first RBMP of 2009, because of the limited range of parameters in the routine analysis suite.

Mining Waste Directive

The following sites in the Gunnerside Gill catchment are on the MWD Article 20 Inventory.

| URN | Site Name | Mine Type | Reason | Easting | Northing |
|--|------------------|---------------|-----------------|---------|----------|
| MWD Inventory | | | | | |
| 1229 | Bunton Lead Mine | Metalliferous | Water pollution | 394258 | 501303 |
| Potential MWD Inventory | | | | | |
| - | none | - | - | - | - |
| Other Potential Sites not on MWD Inventory | | | | | |
| - | none | - | - | - | - |

Mining History Summary

Gunnerside Gill drains an area of former lead mining, which was carried out extensively throughout the catchment from about 1700 to 1900, most actively in the 1800s, followed by some reworking of spoil tips until the 1990s. The orefield comprises lead-zinc mineral deposits within Carboniferous Limestone and Millstone Grit host rocks. Galena (PbS) is the most common mineral with associated 'gangue' minerals including sphalerite (ZnS), chalcopyrite (CuFeS₂), barite (BaSO₄), fluorite (CaF₂) and calcite (CaCO₃). These minerals occur mostly in vertical veins along fault planes, as shown on **Figure 3**, **Figure 4** and on **Figure 5** below.

Early mine workings were open cuts, with shafts used to work deeper in later years, but exploitation was initially limited by the water table. The scouring technique of hushing was used until about 1850 to expose mineral veins at the surface by the erosive power of water released from temporary dams. Horizontal drainage levels (adits) were driven from the valley bottoms to enable deeper working and for easier removal of minerals from the mines. The ore was crushed and dressed at the surface close to the mines to further concentrate the metal before smelting at sites close to the mines. Water power was used at ore dressing floors and smelt mills and so these sites and their spoil tips are often located next to rivers.

The main mining features in Gunnerside Gill catchment are as follows.

| Lead Mines | NGR | Adits/Levels | Hushes | Spoil Tips | Smelters |
|--------------|--------------|--------------|-----------|-------------|--------------|
| Blakethwaite | NY 9387 0295 | B Upper | | | Blakethwaite |
| | | B Lower | | | |
| Lownathwaite | NY 9330 0133 | Lownathwaite | North | | Lownathwaite |
| | | Sun Hush | Sun | | |
| | | Dolly | | Dolly | |
| | | Woodward | | | |
| | | Priscilla | | | |
| | | Blind Gill | | | |
| Bunton | NY 9398 0123 | Bunton | Bunton | Bunton | |
| | | Water Sikes | Friarfold | | |
| | | Sir George | Gorton | | |
| | | Barbara | | | |
| Sir Francis | SD 9402 9996 | Sir Francis | | Sir Francis | |
| | | Silver Hill | | Gunnerside | |
| Kining | SD 9563 9926 | Kining | | Kining | |

Figure 3. Aerial photograph showing mining scars along mineralised faults

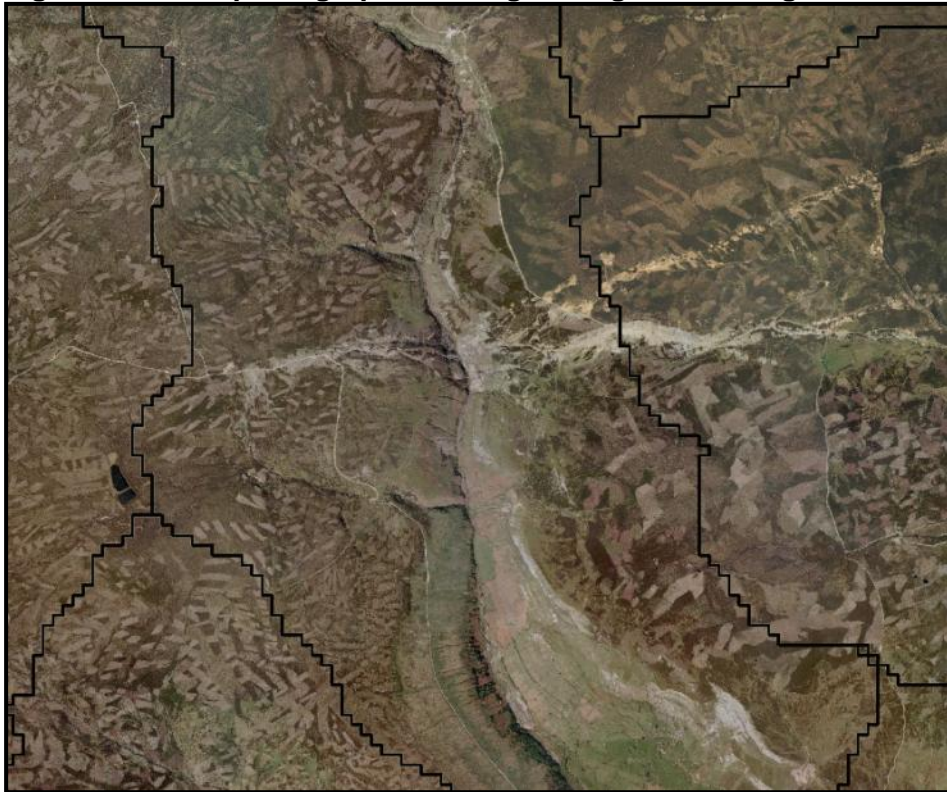


Figure 4. BGS map detail (1985) showing levels and mineral veins

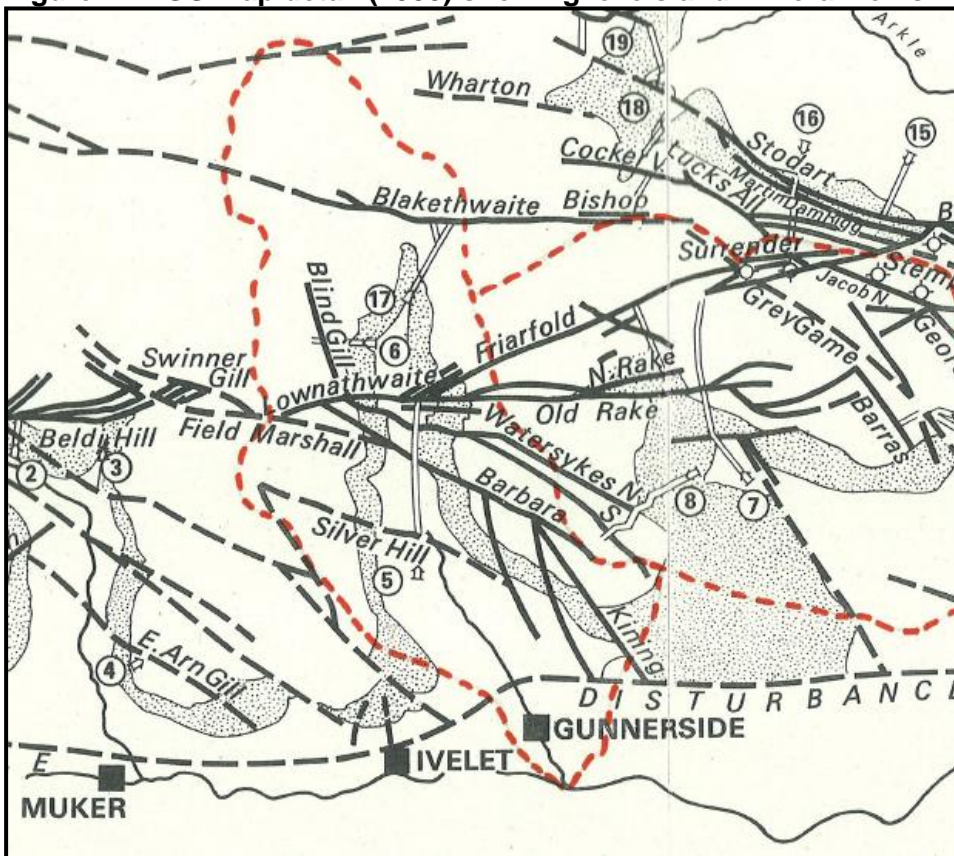
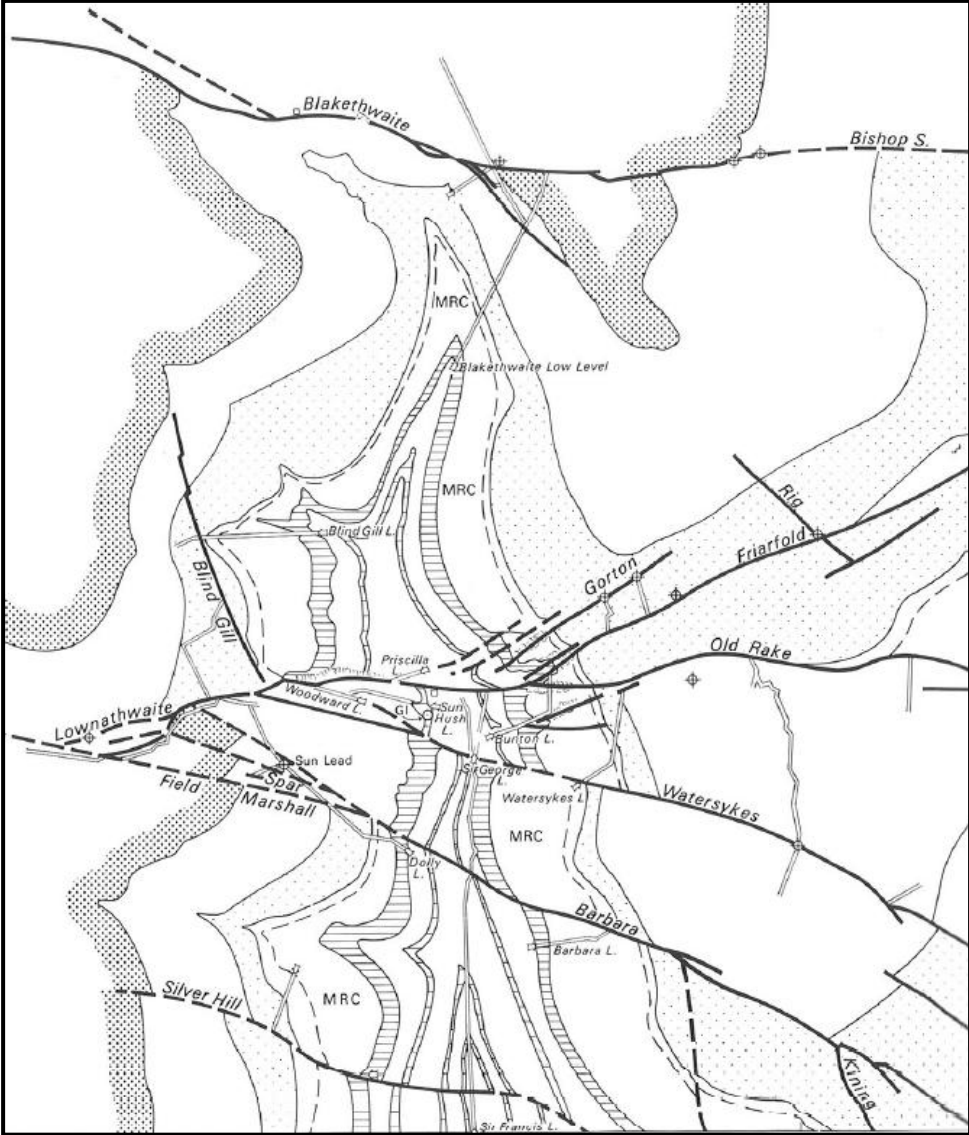


Figure 5. BGS map (1985) showing levels and mineral veins



Historical Ecological Data

Prior to the current project ecological sampling has generally been sporadic at best and Gunnerside Gill has not been sampled since the early 1990s. Prior to the project ecological sampling was primarily undertaken as part of the 'headline indicator' programme which formed part of the General Quality Assessment (GQA) classification. However as the GQA network was reduced Gunnerside Gill was removed from the programme. From 2013 routine sampling has been reinstated under the new Ecological Status Indicator (ESI) programme and will form the basis of WFD classification from 2014 onwards.

Historic ecological monitoring events in the Gunnerside catchment are shown below.

| Site Ref | Site Name | Date | Diatoms | Invertebrates | Macrophytes | Fish | Reason |
|----------|-------------------------------|----------|---------|---------------|-------------|------|--------------------|
| 165 | Gunnerside Gill at Gunnerside | 14/05/90 | YES | NO | NO | ? | Headline Indicator |
| 165 | Gunnerside Gill at Gunnerside | 15/08/90 | YES | NO | NO | ? | Headline Indicator |
| 165 | Gunnerside Gill at Gunnerside | 30/10/90 | YES | NO | NO | ? | Headline Indicator |
| 165 | Gunnerside Gill at Gunnerside | 09/04/91 | YES | NO | NO | ? | Headline Indicator |
| 165 | Gunnerside Gill at Gunnerside | 02/03/92 | YES | NO | NO | ? | Headline Indicator |
| 165 | Gunnerside Gill at Gunnerside | 29/07/92 | YES | NO | NO | ? | Local Routine |

Despite coming back onto the WFD assessment programme the impact of metal pollution may not show up through WFD classification. This is because both of the relevant WFD classification tools, River Invertebrate Classification Tool (RICT) and Diatom Assessment of River and Lake Ecological Quality (DARLEQ), are underpinned by indices designed to assess specific pressures, but none of these are metal pollution.

For invertebrates RICT uses two indices, Average Score Per Taxon (ASPT) and Number of scoring Taxa (NTAXA). ASPT is designed to measure the impact of organic pollution on an invertebrate community, so will not pick up the impact to metals. In fact many species that are known to be tolerant of metal pollution are intolerant of organic pollution. NTAXA is the number of different species present in a sample and is thus a measure of diversity of the invertebrate community. It is possible that impacts of severe metal pollution that would reduce invertebrate diversity may show up in WFD classification through NTAXA. However NTAXA is not abundance weighted and works on a presence/absence basis and thus will not be sensitive to scenarios where metal intolerant species are present but in very reduced numbers.

For diatoms the DARLEQ tool is underpinned by the Trophic Diatom Index (TDI), which is designed to measure nutrient enrichment. Thus it is unlikely that any impacts of metal pollution on the diatom community will show up through WFD classification.

Designations

The Gunnerside Gill catchment is entirely located in the Yorkshire Dales National Park. Almost all of the catchment forms part of the Arkengarthdale, Gunnerside and Reeth Moors SSSI, designated for blanket bog, heather moorland and for their breeding bird populations; and is also part of the coincident North Pennine Moors SPA and SAC. A small area of

woodland (11ha) alongside Gunnerside Gill near to the Swale confluence is designated as Ancient and Semi-Natural Woodland.

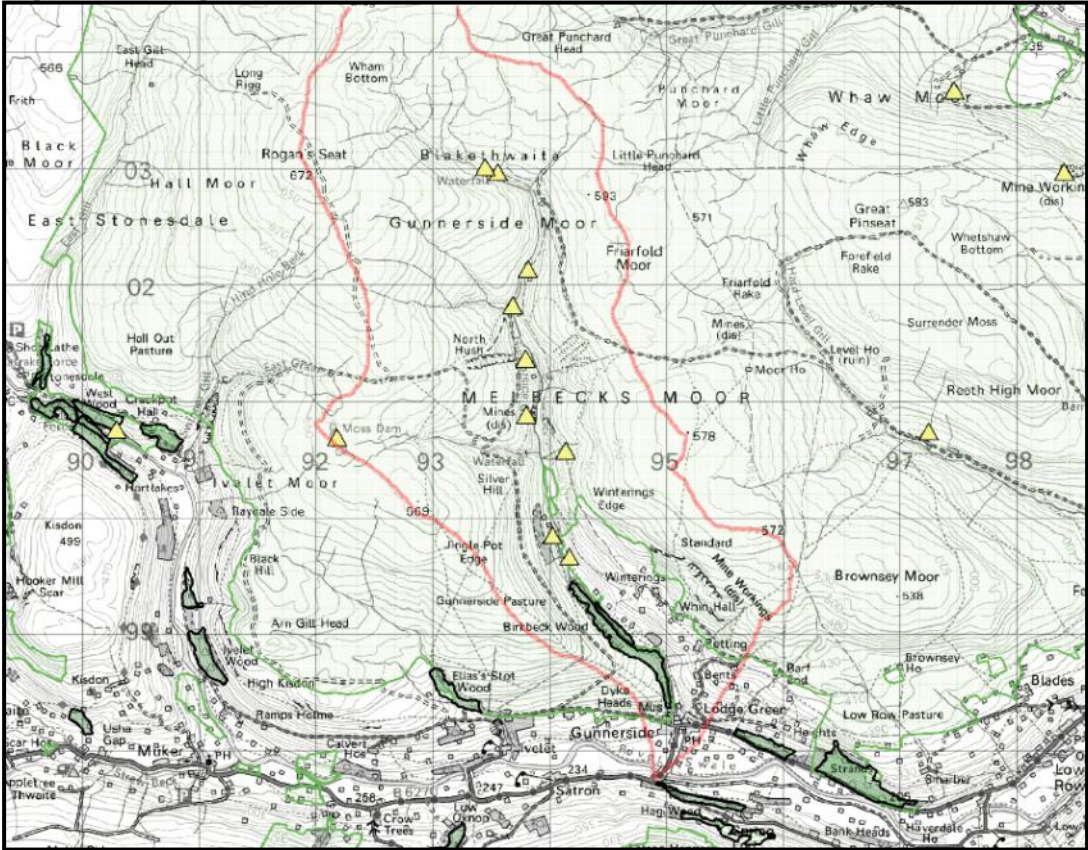
There are 9 Scheduled Ancient Monuments in the catchment, these are:

- Blakethwaite Dams (x2)
- Blakethwaite Smelt Mill
- Blakethwaite Ore Dressing Floor
- Lownathwaite and Bunton Mine Complex
- Dolly Mine, Level and Spoil Tip
- Moss Moor Dams
- Barbara Level and Spoil Tip
- Sir Francis Level and Ore Dressing Floor
- Winterings Ore Dressing Floor

There are no licensed abstractions in the catchment.

Designated sites are shown on **Figure 6** below, where the coincident SSSI, SPA and SAC are shown by light green shading, ancient woodland is dark green and the Scheduled Ancient Monuments are shown as yellow triangles.

Figure 6. Designated sites in Gunnerside Gill



Photographs

Dolly Level spoil tips looking southwards down Gunnerside Gill



Bunton Level Portal



Sir Francis Level Portal

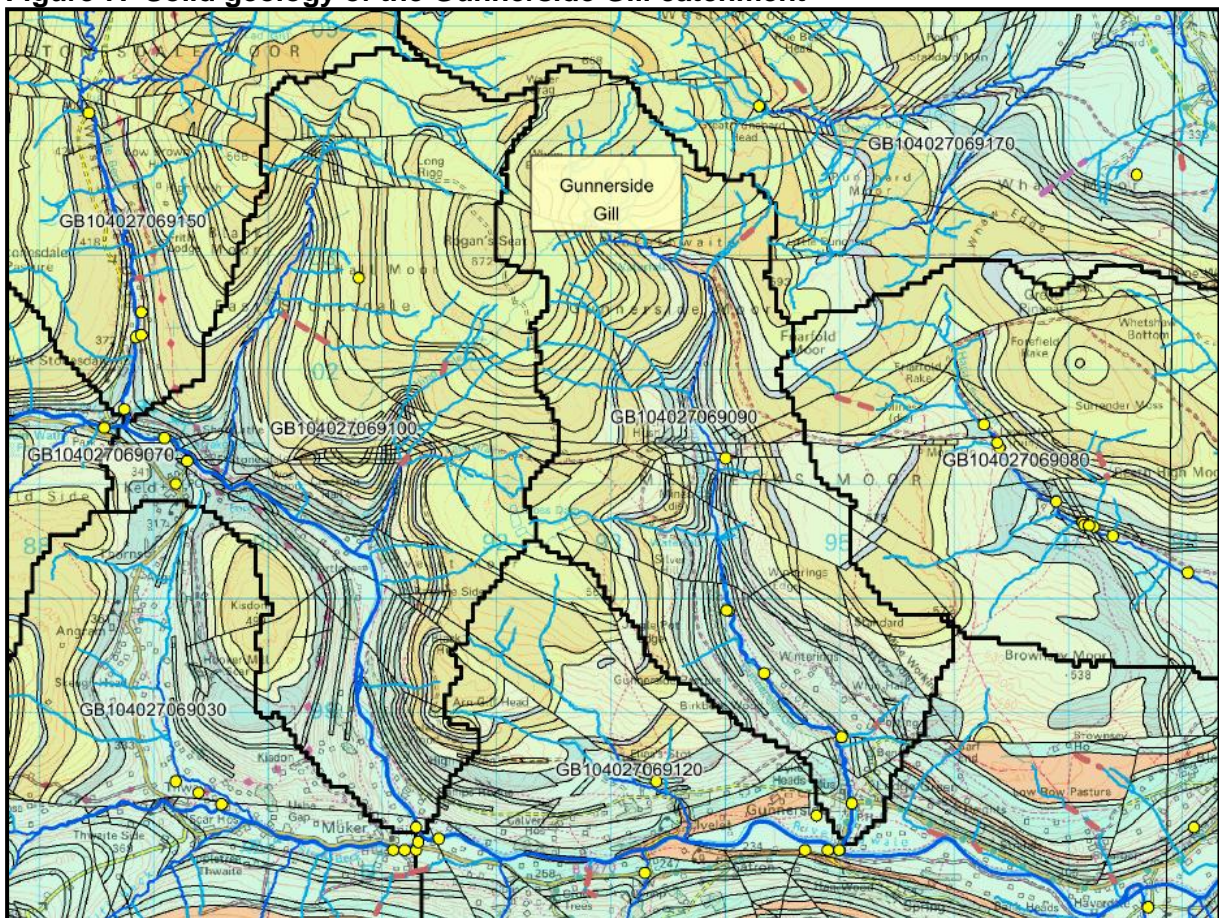


Geology

The solid geology of the Gunnerside Gill catchment (13km²) is shown on **Figure 7** below, comprising mostly Millstone Grit (green) on the higher ground in the north, overlying a smaller portion of Carboniferous Limestone (blue) exposed in the valley bottom in the south. Millstone Grit covers 70% of the catchment (9km²) while Carboniferous Limestone covers 30% (4km²) and includes all of the sampling locations for this project.

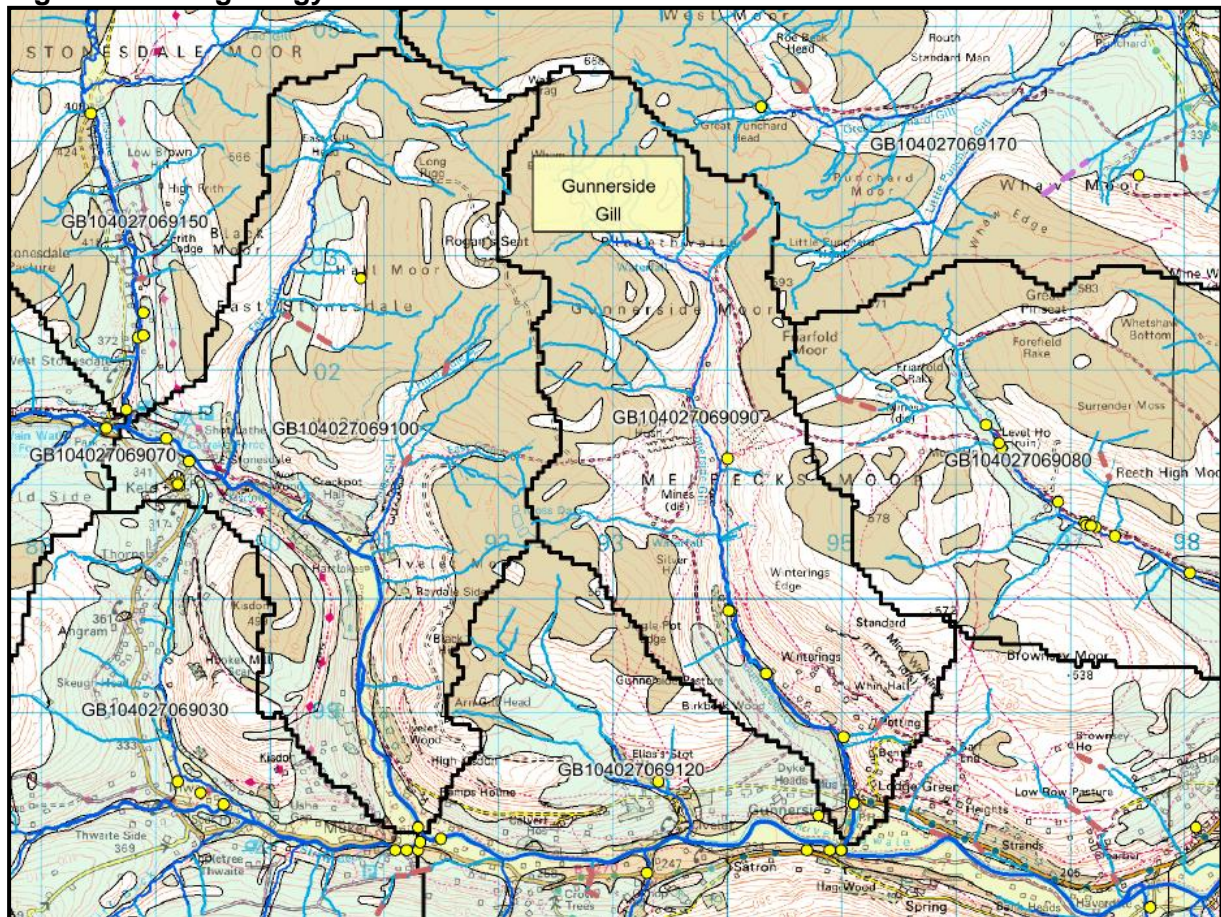
A number of W-E and NW-SE trending faults cross the catchment; many of these are mineralised, and are likely to have a significant effect on surface water quality and groundwater flow conditions. The extensive mining voids in the upper part of the catchment have permanently altered the hydrogeological conditions, creating fast pathways for rainwater infiltration to pass through the mined areas and enter the river.

Figure 7. Solid geology of the Gunnerside Gill catchment



The drift geology of the Gunnerside Gill catchment (13km²) is shown on **Figure 8** below, comprising mostly Peat (in brown) on the higher ground and a smaller portion of Glacial Till (in light blue) in the south. Peat covers 48% of the catchment (6km²), resting mostly upon Millstone Grit, and is located upstream of the sampling locations. Glacial Till covers 4% (<1km²), sitting upon Carboniferous Limestone, with a further 48% (6km²) of the catchment where superficial deposits are absent.

Figure 8. Drift geology of the Gunnerside Gill catchment



Monitoring programme

This study is designed to characterise the Gunnerside Gill catchment by investigating the impact of former metal mining on river water quality and aqueous ecology. Mining records were used to identify potential monitoring sites, followed by a catchment visit to identify safe and practical locations for water quality sampling, ecological sampling and flow measurement. Sources of elevated metal concentrations will be identified to help the design of potential mitigation and remediation measures.

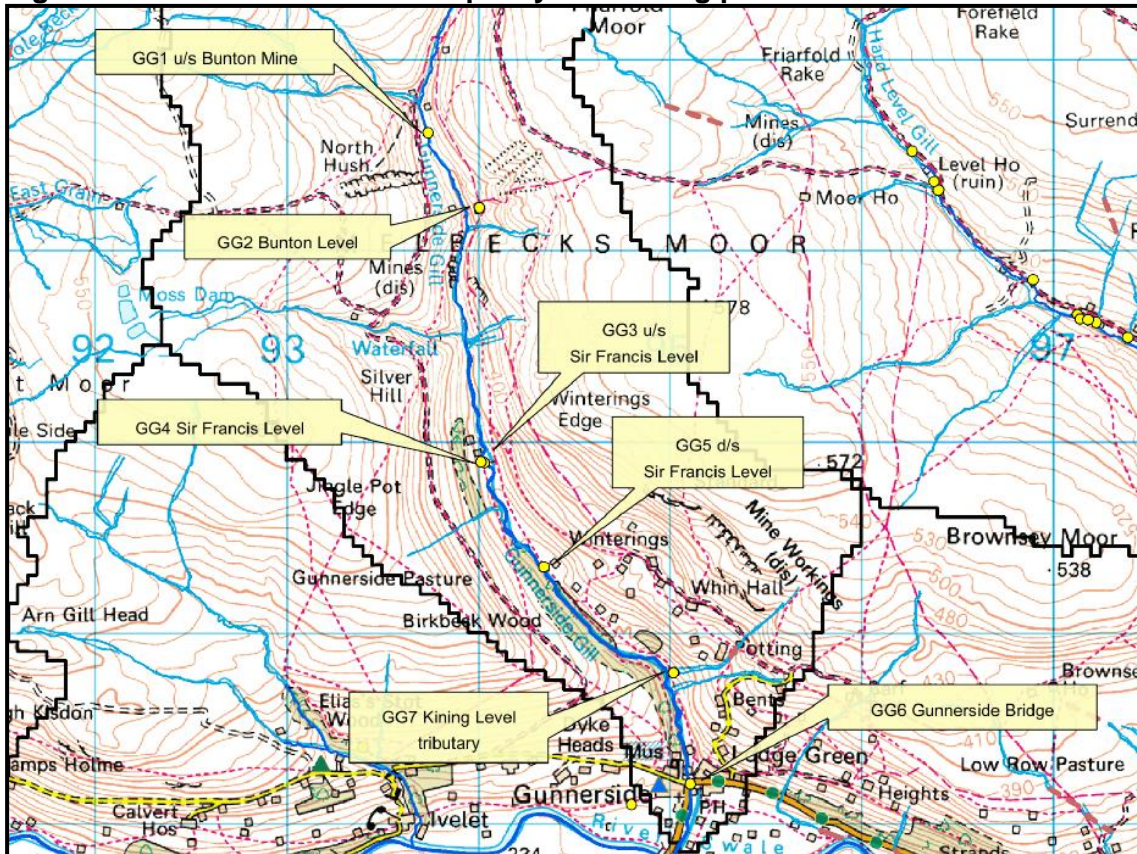
The sampling programme began in March 2012 and comprised water quality sampling with simultaneous flow measurement at 6 locations from GG1 (upstream) to GG6 (downstream), planned for 12 monitoring visits at monthly intervals. GG1, GG3, GG5 and GG6 are river monitoring points, GG1 is the upstream location, GG3 is 1.8km downstream, GG5 is 2.5km downstream and GG6 is 4.1km downstream of GG1. Adits are monitored at Bunton Level (GG2) and Sir Francis Level (GG4). The water quality and flow measurements were used to calculate metal loading to identify the contribution from each inflow into Gunnerside Gill.

An extra monitoring point (GG7) was added in December 2012 at the confluence between Gunnerside Gill and a tributary draining the mine workings from Kining Level in the south-east of the catchment. The current water quality and flow monitoring points (GG1 to GG7) are shown as yellow circles and labelled in **Figure 9** below. All of the monitoring points are located on the Carboniferous Limestone bedrock, as also shown on **Figure 7**, above.

The water quality and flow monitoring points are shown on **Figure 9** below and also listed from upstream (GG1, WSB1) to downstream (GG6, WSB2) in the table below, with the ecological control catchment, West Stonesdale Beck, high-lighted in blue.

| Site Ref | URN | Location | Easting | Northing | Distance (km) |
|----------|----------|--|---------|----------|---------------|
| GG1 | 49905130 | Gunnerside Gill u/s Bunton Mine | 393739 | 501615 | 0 |
| GG2 | 49905131 | Bunton Level minewater drainage adit | 394006 | 501223 | 0.5 |
| GG3 | 49905132 | Gunnerside Gill u/s Sir Francis Level | 394033 | 499888 | 1.8 |
| GG4 | 49905133 | Sir Francis Level minewater drainage adit | 394015 | 499893 | 1.8 |
| GG5 | 49905134 | Gunnerside Gill d/s Sir Francis Level & Spoil | 394343 | 499343 | 2.5 |
| GG7 | 49905170 | Gunnerside Gill tributary from Kining Level | 395020 | 498790 | 3.5 |
| GG6 | 49905126 | Gunnerside Beck at Gunnerside village bridge | 395108 | 498208 | 4.1 |
| WSB1 | 49905144 | West Stonesdale Beck at Stonesdale Bridge | 388440 | 504240 | 0 |
| WSB2 | 49905145 | West Stonesdale Beck u/s Currack Force | 388750 | 501650 | 2.8 |

Figure 9. Gunnerside Gill water quality monitoring points



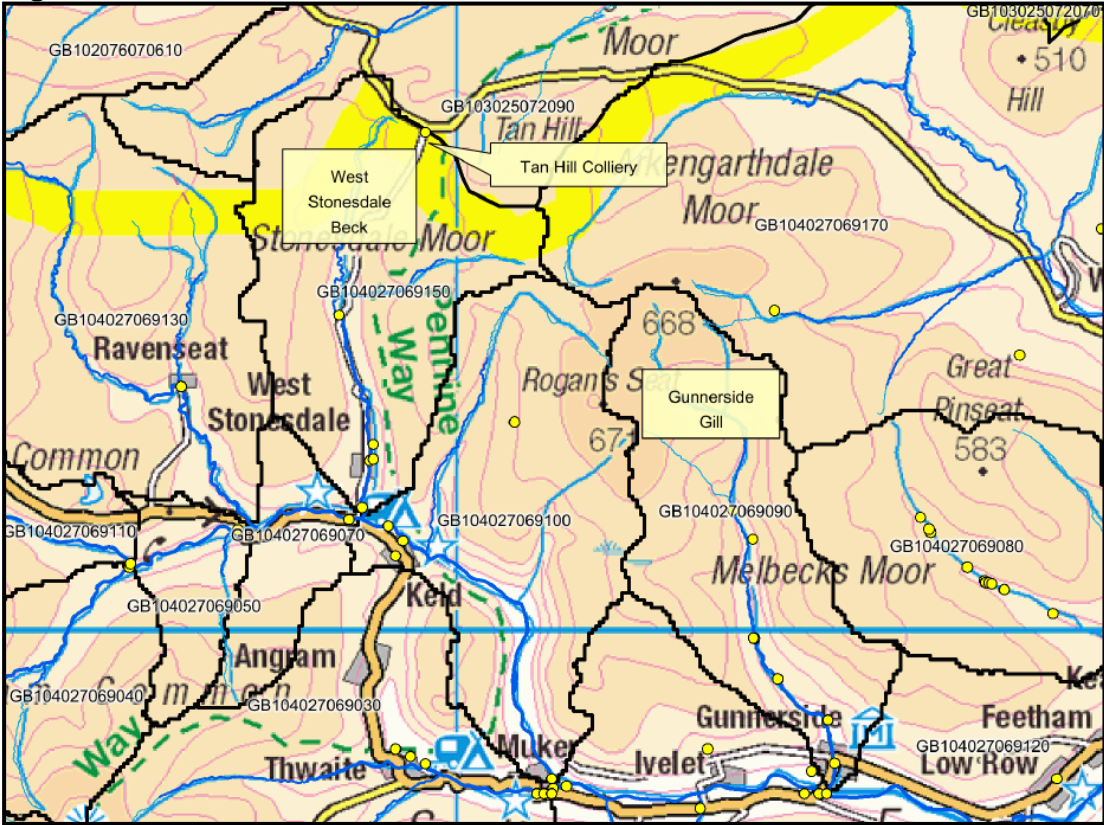
The water quality analysis suites were selected as follows.

| Site Ref | Analysis Suite | Field Determinands | Laboratory Determinands | Metals (Dissolved and Total) |
|--|---------------------------------|---|---|--|
| GG1 GG3 GG5 GG6 WSB1 WSB2 | METSTR for surface waters | pH, EC, Alkalinity, Redox | pH, Hardness as CaCO ₃ , Suspended Solids, DoC, SO ₄ | Al, B, Ba, Ca, Cd, Cr, Cu, Fe, K, Li, Mg, Mn, Na, Ni, Pb, Sr, Zn |
| GG2 GG4 GG7 | METPR for adits | pH, EC, Alkalinity, Redox, DO, DO% | pH, EC Hardness as CaCO ₃ , Alkalinity @ pH4.5, Cl, NO ₂ , NH ₃ , SiO ₂ , SO ₄ | |

Ecological monitoring was undertaken upstream and downstream of the main mining areas on Gunnerside Gill upstream of Sir Francis Level (GG3) and at Gunnerside village, downstream of the mines (GG6), to assess whether the historical mining activity has adversely affected the aqueous ecology.

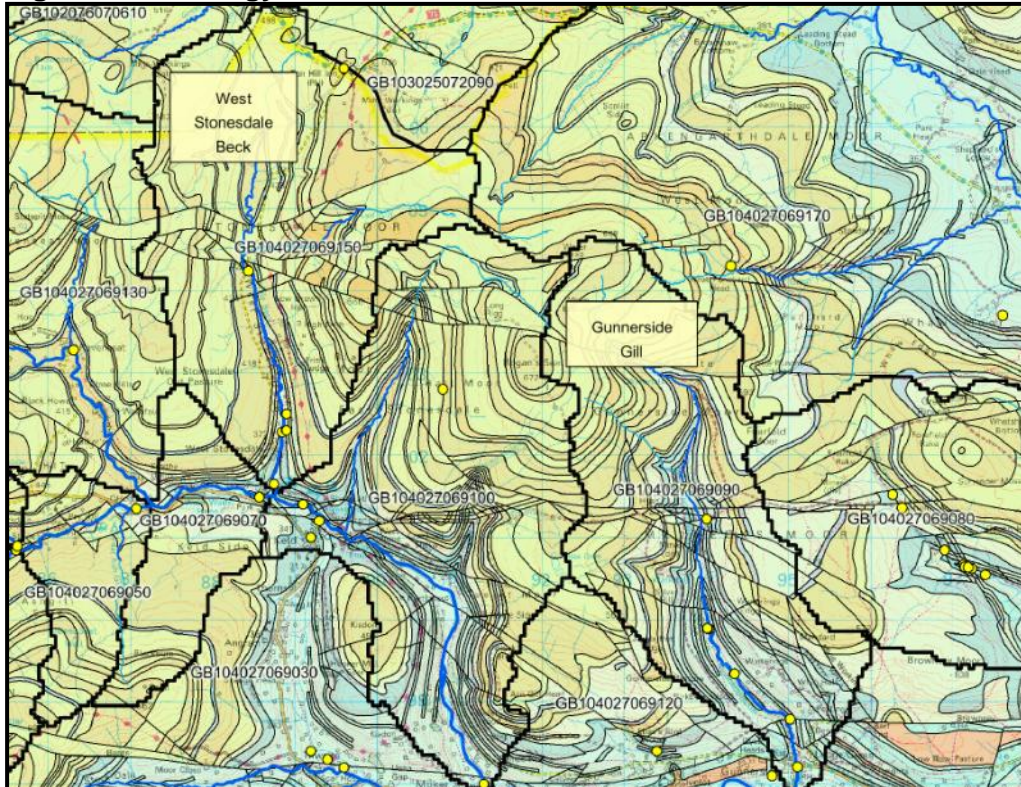
Additional ecological monitoring was also carried out in a neighbouring control catchment located to the west of Gunnerside Gill, shown in **Figure 10** below. West Stonesdale Beck (GB104027069150) is another north bank tributary of the River Swale, with its confluence 9km upstream of the confluence between Gunnerside Gill and the River Swale. Lead mining was not carried out extensively in the West Stonesdale Beck catchment, but small coal mines, such as Tan Hill Colliery (operated from about 1880 to 1940) are located at the very top of the catchment, as shown on **Figure 10** below.

Figure 10. West Stonesdale Beck catchment location



West Stonesdale Beck has similar geology and geomorphology to Gunnerside Gill, as shown in **Figure 11** below, but there has been almost no mining in the West Stonesdale catchment.

Figure 11. Geology of the West Stonesdale and Gunnerside catchments



The current ecological and water quality monitoring points at West Stonesdale Beck (WSB1 and WSB2) are shown as yellow circles and labelled in **Figure 12** below. WSB2 is located 2.8km downstream of WSB1.

Figure 12. West Stonesdale Beck sampling points



The monitoring visits were conducted with simultaneous water quality sampling (Q), spot flow measurements (F), and ecological sampling (E) as follows.

| Date | GG1 | GG2 | GG3 | GG4 | GG5 | GG6 | GG7 | WSB1 | WSB2 |
|-------------------|------------------------|--------------|---------------------|--------------|--------------|---------------------|-----|------------|------------|
| 27/03/12 | Q+F | Q+F | Q+F | Q+F | Q+F | Q+F | - | - | - |
| 24/04/12 | Q+F | Q+F | Q+F | Q+F | Q+F | Q+F | - | - | - |
| 08/05/12 | | | E | | | E | | E | E |
| 14/05/12 | Q+F | Q+F | Q+F | Q+F | Q+F | Q+F | - | - | - |
| 20/06/12 | Q+F | Q+F | Q+F | Q+F | Q+F | Q+F | - | - | - |
| 16/07/12 | Q+F | Q+F | Q+F | Q+F | Q+F | Q+F | - | - | - |
| 31/07/12 | - | - | E | | | E | - | Q+E | Q+E |
| 14/08/12 | Q+F | Q+F | Q+F | Q+F | Q+F | Q+F | - | - | - |
| 12/09/12 | Q+F | Q+F | Q+F | Q+F | Q+F | Q+F | - | - | - |
| 15/10/12 | Q+F | Q+F | Q+F | Q+F | Q+F | Q+F | - | - | - |
| 23/10/12 | - | - | E | | | E | - | Q+E | Q+E |
| 20/11/12 | Q+F | Q+F | Q+F | Q+F | Q+F | Q+F | - | - | - |
| 17/12/12 | Q+F | Q+F | Q+F | Q+F | Q+F | Q+F | Q | - | - |
| 28/01/13 | Q | Q | Q | Q | Q | Q | Q | | |
| 27/02/13 | Q+F | Q+F | Q+F | Q+F | Q+F | Q+F | - | | |
| 20/03/13 | Q+F | Q+F | Q+F | Q+F | Q+F | Q+F | Q | | |
| 28/05/13 | - | - | Q+E | - | - | Q+E | - | Q+E | Q+E |
| 05/08/13 | | | Q+E | - | - | Q+E | - | Q+E | Q+E |
| Sub-totals | Q=13 F=12 | Q=13 F=12 | Q=15 F=12 E=5 | Q=13 F=12 | Q=13 F=12 | Q=15 F=12 E=5 | Q=3 | Q=4 E=5 | Q=4 E=5 |
| TOTALS | Q = 93, F = 78, E = 20 | | | | | | | | |

Ecological Monitoring

The ecological monitoring part of this project is on-going, but the interim findings reported by Dave Barber are as follows.

Conclusions

- Diatom data **does** indicate an ecological impact of elevated metal levels in both Gunnerside Gill and Barney Beck. However, in terms of WFD status, metals are **not** currently impacting on the diatom status. Diatom data indicates there are no impacts of nutrients or acidity.
- Invertebrate populations at five out of the six sites (including one control site) are failing to meet WFD standards due to low species diversity. The exact pressures or combination of pressures leading to these failures are unclear and requires further investigation. However the species composition indicates that metals or acidity are not currently major drivers of this failure.
- This highly mobile, cobble and boulder dominated habitat, coupled with a high number of spate events in 2012 is likely to have impacted species diversity in all catchments covered in this study

Recommendations

- Continue the diatom and invertebrate sampling regimes for an additional year. Currently diatoms are the only ecological tool showing a clear ecological response to metal concentrations through valve deformities, further data would allow more robust testing of the significance of the levels of deformities seen between control and impact catchments.
- Whilst invertebrate populations are not currently showing a clear response to metal levels, populations are failing to meet WFD requirements. This failure is likely to be due to a complex interaction of pressures including metals, low pH, habitat and spate flows. Additional data particularly through a more 'normal' flow year will allow more sophisticated analysis to be applied to the data and attempt to tease apart the different pressures acting on the community.
- Alongside any future diatom and invertebrate collection an assessment and collection of any green algae growth should be made. Conspicuous growths of green algae such as *Klebsormidium* and *Stigeoclonium* are commonly associated with high concentrations of metals (Kelly et al 2012). Identification of these algae will aid our interpretation of the ecological impact of metals.
- More detailed analysis of the invertebrate and diatom data using appropriate statistical packages should be undertaken when more data is available to tease out more subtle trends and test the significance of any patterns seen in the data.

Flow Measurements

The 6 flow monitoring sites comprise 4 locations on Gunnerside Gill (GG1, GG3, GG5, GG6) and 2 inflows from mine drainage adits (GG2, GG4). The spot flow gauging results after 12 rounds of monitoring using the velocity/area method at 6 locations are shown in the table below, with the river locations high-lighted in grey. As expected, the flows in Gunnerside Gill increase steadily downstream from GG1 on the left of the table to GG6 on the right. This shows that significant quantities of flow are not lost into the underlying Carboniferous Limestone bedrock, on which all of the monitoring points are located.

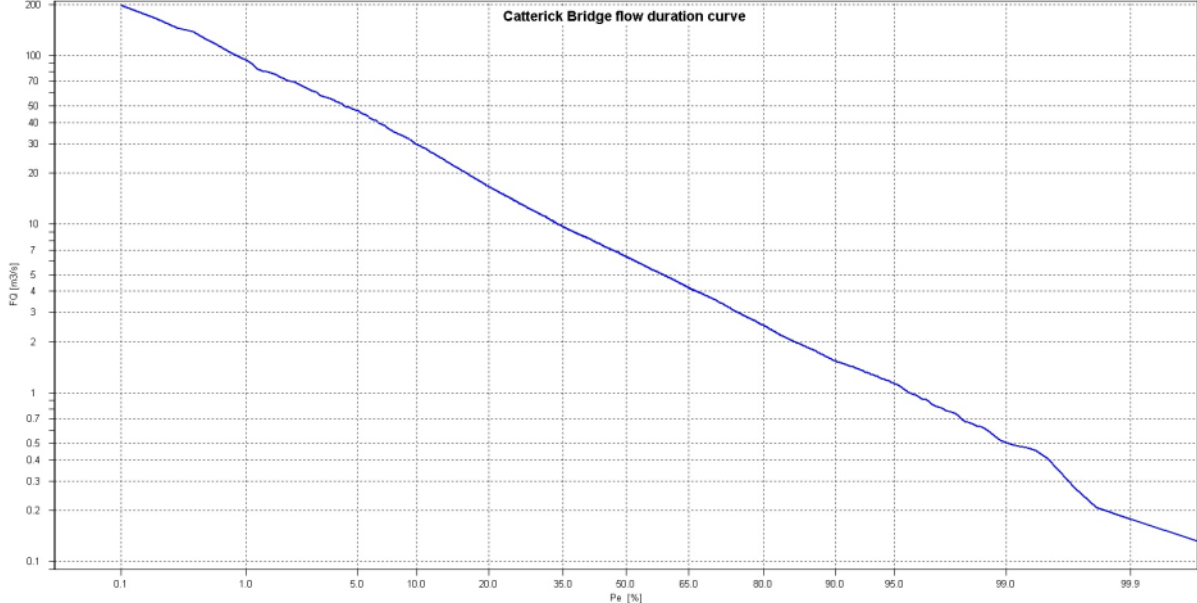
| Date | Spot flow measurements at Gunnerside (L/s) | | | | | | Catterick Bridge Flow Gauge F2306 | | Grinton Level Gauge L2309 (%ile) |
|-------------|--|------------|-------------|------------|-------------|-------------|-----------------------------------|------------------|----------------------------------|
| | GG1 (river) | GG2 (adit) | GG3 (river) | GG4 (adit) | GG5 (river) | GG6 (river) | Daily mean (L/s) | Percent ile Flow | |
| 27/03/12 | 18 | 4 | 38 | 24 | 51 | 62 | 1390 | Q93 | Q93 |
| 24/04/12 | 85 | 8 | 146 | 17 | 168 | 188 | 7550 | Q44 | Q42 |
| 14/05/12 | 108 | 9 | 194 | 19 | 246 | 278 | 11,900 | Q29 | Q29 |
| 20/06/12 | 58 | 7 | 110 | 20 | 131 | 152 | 6530 | Q50 | Q54 |
| 16/07/12 | 52 | 11 | 102 | 22 | 133 | 169 | 5970 | Q53 | Q56 |
| 14/08/12 | 38 | 6 | 58 | 17 | 68 | 78 | 2340 | Q82 | Q90 |
| 12/09/12 | 72 | 6 | 119 | 14 | 139 | 143 | 8340 | Q40 | Q27 |
| 15/10/12 | 88 | 8 | 171 | 18 | 173 | 227 | 9660 | Q35 | Q31 |
| 20/11/12 | 248 | 10 | 592 | 19 | 964 | 915 | 22,800 | Q14 | Q10 |
| 17/12/12 | 291 | 11 | 449 | 27 | 483 | 506 | 17,600 | Q19 | Q16 |
| 27/02/13 | 37 | 6 | 78 | 17 | 99 | 110 | 5590 | Q55 | Q58 |
| 20/03/13 | 58 | 5 | 116 | 16 | 135 | 178 | 10,700 | Q33 | Q36 |
| Mean | 96 | 8 | 181 | 19 | 233 | 250 | - | - | - |

The nearest flow gauging station with continuous measurement is located on the River Swale at Catterick Bridge (F2306), some 38km downstream and east of Gunnerside Gill. Estimates of the percentile values for the spot flow measurements at Gunnerside Gill can be obtained from the long term flow duration curve (or table) at F2306. Daily mean flows at Catterick Bridge were obtained for the dates of the Gunnerside monitoring visits and the percentile values of these flows were determined from the flow duration curve shown in **Figure 13** below. These range from Q14 to Q93, where the lowest flow at Catterick Bridge (Q93) is exceeded 93% of the time, and the highest flow (Q14) is exceeded only 14% of the time.

The nearest level gauging station to Gunnerside on the River Swale at Grinton Bridge (L2309) is located 11km downstream of the confluence between the Swale and Gunnerside Gill. Daily mean levels at Grinton Bridge were obtained for the dates of the Gunnerside monitoring visits and the percentile values of these flows were determined from the level duration curve. The table above shows there is good correlation between the long-term flow and level duration curves at Grinton and Catterick, except where high-lighted in pink.

The flow conditions at Catterick Bridge give a good indication of flow conditions at Gunnerside, but localised rainfall events at either location could make this correlation less useful. Grinton Bridge at 11km is much closer to Gunnerside than the flow gauging station at Catterick Bridge at 38km, so the Grinton percentile values are more applicable to the Gunnerside catchment.

Figure 13. Long-term flow duration curve for Catterick Bridge (F2306)



When the percentile levels at Grinton Bridge (L2309) are ranked in order, they correlate fairly well with the spot measured flows at the most downstream monitoring point on Gunnerside Gill (GG6) and the flows at Catterick Bridge (F2306), as shown in the table below. The main exception is high-lighted in pink, where there is also the least good correlation between the percentile flows at Catterick and the percentile levels at Grinton.

| Date | Spot flow at GG6 (m ³ /s) | Daily mean flow at F2306 (m ³ /s) | Percentile flow at F2306 | Percentile Level at L2309 |
|----------|--------------------------------------|--|--------------------------|---------------------------|
| 27/03/12 | 62 | 1390 | Q93 | Q93 |
| 14/08/12 | 78 | 2340 | Q82 | Q90 |
| 27/02/13 | 110 | 5590 | Q55 | Q58 |
| 16/07/12 | 169 | 5970 | Q53 | Q56 |
| 20/06/12 | 152 | 6530 | Q50 | Q54 |
| 24/04/12 | 188 | 7550 | Q44 | Q42 |
| 20/03/13 | 178 | 10,700 | Q33 | Q36 |
| 15/10/12 | 227 | 9660 | Q35 | Q31 |
| 14/05/12 | 278 | 11,900 | Q29 | Q29 |
| 12/09/12 | 143 | 8340 | Q40 | Q27 |
| 17/12/12 | 506 | 17,600 | Q19 | Q16 |
| 20/11/12 | 915 | 22,800 | Q14 | Q10 |

Low Flows Enterprise Software could also be used to estimate flows in a catchment, but this tool only provides long-term monthly or annual averages and doesn't give information for specific dates, which would be needed for this study.

Spot flow gauging using the velocity-area method is generally considered to only be accurate under laminar flow conditions, but flow in natural rivers with irregular shape and granular substrate is typically turbulent. A graphical method using a time series of measured concentrations of a known spike of salt (NaCl) added to the river could be more accurate.

Flow Balances

A schematic conceptual model of the Gunnerside Gill catchment and the monitoring locations is shown in **Figure 14** below.

River flow measurement is subject to uncertainty, however carefully undertaken, whether by manual spot gauging or at continuous flow gauging stations and this will also vary between low and high flow conditions. Therefore, significant discrepancies in the flow correlations may be explained by unknown inputs, but may also be due to measurement errors.

Flow balance calculations from the conceptual model can be used as a check on the accuracy of the spot flow gauging measurements, as follows:

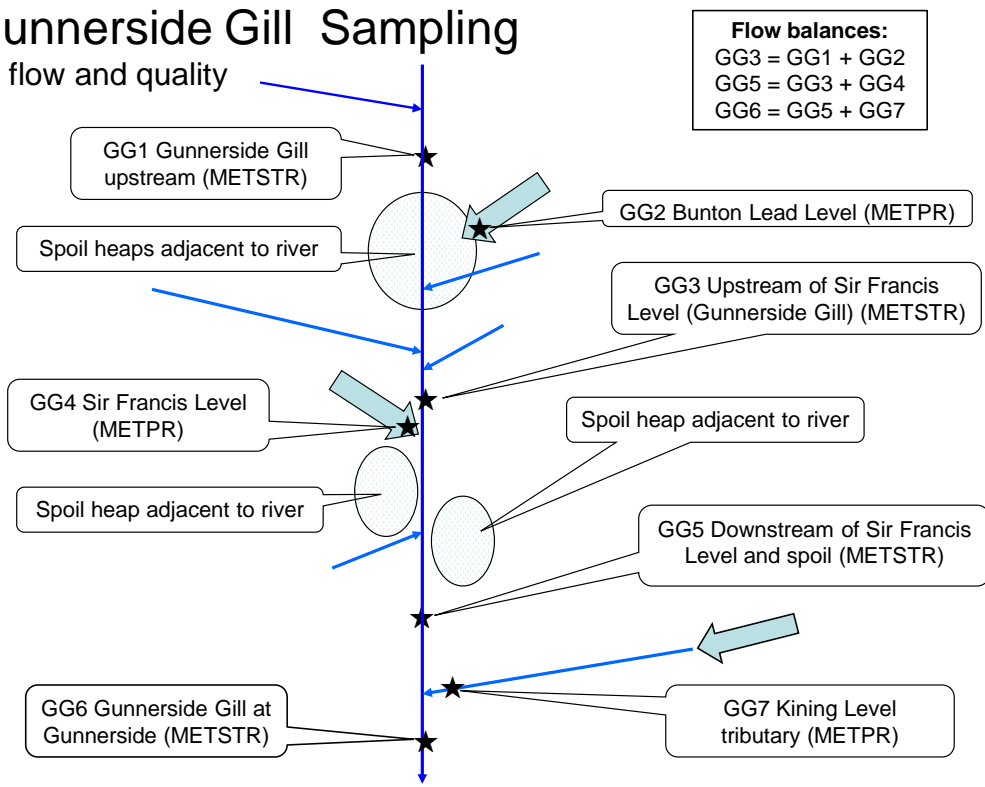
- $GG3 = GG1 + GG2 + \text{Water Sikes} + \text{Botcher Gill} + \text{un-named tributary (not measured)}$
- $GG5 = GG3 + GG4 + \text{un-named tributary (not measured)}$

The calculations and correlations assume there are no other flow inputs into the system that have not been accounted for, either from point sources such as small tributaries and unknown adits or via diffuse baseflow (including baseflow via spoil). However, at Gunnerside Gill at least 5 tributaries are easily identified that have not been measured for flow (see **Figure 14** above), including the tributary at GG7, that was not monitored for flow.

Figure 14. Conceptual model of catchment flows

Gunnerside Gill Sampling

All flow and quality



In the tables below, correlation within 10% is rated as good and within 20% is rated as OK, while correlation errors of more than 20% error are rated as poor.

| Date | GG1 | GG2 | GG1 + GG2 | GG3 | % Error | Correlation |
|------------------------|-----------|----------|------------|------------|------------|-------------|
| 27/03/12 | 18 | 4 | 22 | 38 | 58% | Poor |
| 24/04/12 | 85 | 8 | 93 | 146 | 64% | Poor |
| 14/05/12 | 108 | 9 | 117 | 194 | 60% | Poor |
| 20/06/12 | 58 | 7 | 65 | 110 | 59% | Poor |
| 16/07/12 | 52 | 11 | 63 | 102 | 62% | Poor |
| 14/08/12 | 38 | 6 | 44 | 58 | 76% | Poor |
| 12/09/12 | 72 | 6 | 78 | 119 | 66% | Poor |
| 15/10/12 | 88 | 8 | 96 | 171 | 56% | Poor |
| 20/11/12 | 248 | 10 | 258 | 592 | 44% | Poor |
| 17/12/12 | 291 | 11 | 302 | 449 | 67% | Poor |
| 27/02/13 | 37 | 6 | 43 | 78 | 55% | Poor |
| 20/03/13 | 58 | 5 | 63 | 116 | 54% | Poor |
| Mean flow (L/s) | 96 | 8 | 104 | 181 | 57% | Poor |

It is not surprising that this flow balance shows a consistently poor correlation because at least 2 un-gauged tributaries of Gunnerside Gill, Botcher Gill and Water Sikes, are identified between GG2 and GG3.

| Date | GG3 | GG4 | GG3 + GG4 | GG5 | % Error | Correlation |
|------------------------|-----|-----|-----------|-----|---------|-------------|
| 27/03/12 | 38 | 24 | 62 | 51 | 122% | Poor |
| 24/04/12 | 146 | 17 | 163 | 168 | 97% | Good |
| 14/05/12 | 194 | 19 | 213 | 246 | 87% | OK |
| 20/06/12 | 110 | 20 | 130 | 131 | 99% | Good |
| 16/07/12 | 102 | 22 | 124 | 133 | 93% | Good |
| 14/08/12 | 58 | 17 | 75 | 68 | 110% | Good |
| 12/09/12 | 119 | 14 | 133 | 139 | 96% | Good |
| 15/10/12 | 171 | 18 | 189 | 173 | 109% | Good |
| 20/11/12 | 592 | 19 | 611 | 964 | 63% | Poor |
| 17/12/12 | 449 | 27 | 476 | 483 | 99% | Good |
| 27/02/13 | 78 | 17 | 95 | 99 | 96% | Good |
| 20/03/13 | 116 | 16 | 132 | 135 | 98% | Good |
| Mean flow (L/s) | 181 | 19 | 200 | 233 | 86% | OK |

This flow balance calculation shows generally good correlation in spite of an identified, but rather small un-named tributary of Gunnerside Gill located between GG4 and GG5.

Water quality results

Water quality results for Gunnerside Gill and the control catchment of West Stonesdale Beck (high-lighted in blue) are summarised below for 95 samples from 13 sampling rounds at 9 locations. The analysis suites contained 17 metals; where the concentrations of Ni, Al, Cr, Li, B, Ba, Sr, Na, Ca, K, Mg were not significant; but the other 6 metals have been selected with the more significant concentrations, and EQS exceedences. The selected metals are divided into 2 tables: the first shows Pb, Zn and Cd, along with pH and flow; while the second table shows Cu, Fe and Mn along with hardness and sulphate. The tables show the minimum, mean and maximum concentrations, with the mean values high-lighted in bold. The monitoring points are listed from upstream (GG1, WSB1) to downstream (GG6, WSB2).

The concentrations were compared to available EQS values with exceedences high-lighted in increasing saturations of pink. Strictly, metal EQS values should be compared to either total or dissolved concentrations, but these were broadly similar for all sample results in this project, so both total and dissolved concentrations have been compared in the tables below. The current (2013) EQS values for Zn, Cd and Cu are hardness-based. The mean hardness of the river samples (see below) mostly fell into the hardness band from 50-100mg/L and so the relevant EQS values were determined as 50µg/L for Zn, 0.09µg/L for Cd and 6µg/L for Cu. However GG1, the upstream monitoring point, had mean hardness of 42mg/L giving lower EQS values of 8µg/L for Zn, 0.08µg/L for Cd and 1µg/L for Cu.

| Site Ref | Monitoring Point | Stats | Pb Diss | Pb Total | Zn Diss | Zn Total | Cd Diss | Cd Total | pH | Flow (L/s) |
|---------------------------------------|--|-------------|--------------|--------------|-------------|-------------|----------------|----------------|------------|------------|
| GG1 | Gunnorside Gill u/s Buntun Mine | Min | 4 | 5 | 14 | 14 | 0.1 | 0.1 | 7.5 | 18 |
| | | Mean | 11 | 14 | 19 | 21 | 0.2 | 0.2 | 7.8 | 96 |
| | | Max | 26 | 27 | 29 | 27 | 0.3 | 0.3 | 8.0 | 291 |
| GG2 | Buntun Lead Level Minewater Adit | Min | 39 | 41 | 597 | 577 | 6.1 | 6.1 | 7.3 | 4 |
| | | Mean | 45 | 52 | 790 | 802 | 8.3 | 8.3 | 7.9 | 8 |
| | | Max | 57 | 77 | 981 | 971 | 10.5 | 10.2 | 8.1 | 11 |
| GG3 | Gunnorside Gill u/s Sir Francis Level | Min | 11 | 14 | 39 | 40 | 0.4 | 0.5 | 7.7 | 38 |
| | | Mean | 31 | 36 | 71 | 73 | 0.7 | 0.7 | 7.9 | 181 |
| | | Max | 97 | 81 | 253 | 244 | 2.2 | 2.3 | 8.3 | 592 |
| GG4 | Sir Francis Level Minewater Adit | Min | 11 | 16 | 1270 | 1460 | 10.5 | 11.8 | 7.5 | 14 |
| | | Mean | 21 | 25 | 1632 | 1672 | 13.7 | 13.9 | 7.6 | 19 |
| | | Max | 36 | 35 | 1810 | 1800 | 15.1 | 15.0 | 7.7 | 27 |
| GG5 | Gunnorside Gill d/s Sir Francis Level & Spoil | Min | 13 | 21 | 127 | 135 | 1.1 | 1.2 | 7.6 | 51 |
| | | Mean | 36 | 44 | 208 | 215 | 2.0 | 2.0 | 7.9 | 233 |
| | | Max | 98 | 98 | 276 | 268 | 2.7 | 2.6 | 8.2 | 964 |
| GG7 | Gunnorside Gill tributary from Kining Level | Min | 17 | 58 | 26 | 29 | 0.5 | 0.7 | 7.8 | - |
| | | Mean | 28 | 113 | 36 | 47 | 0.7 | 0.8 | 7.8 | - |
| | | Max | 38 | 185 | 56 | 69 | 0.8 | 1.1 | 8.0 | - |
| GG6 | Gunnorside Beck at Gunnorside village bridge | Min | 9 | 11 | 91 | 99 | 0.7 | 0.7 | 6.8 | 62 |
| | | Mean | 29 | 33 | 171 | 177 | 1.6 | 1.6 | 7.8 | 250 |
| | | Max | 88 | 95 | 282 | 300 | 2.2 | 2.3 | 8.4 | 915 |
| WSB 1 | West Stonesdale Beck at Stonesdale Bridge | Min | <2 | <2 | <5 | <5 | <0.1 | <0.1 | 7.2 | - |
| | | Mean | <2 | <2 | 4 | 2 | <0.1 | <0.1 | 7.5 | - |
| | | Max | <2 | <2 | 6 | 5 | <0.1 | <0.1 | 7.7 | - |
| WSB 2 | West Stonesdale Beck u/s Currack Force | Min | <2 | <2 | 6 | 6 | <0.1 | <0.1 | 6.6 | - |
| | | Mean | <2 | <2 | 8 | 6 | <0.1 | <0.1 | 7.7 | - |
| | | Max | <2 | <2 | 9 | 7 | <0.1 | <0.1 | 8.2 | - |
| EQS (Annual Average) at GG1 | | | 7.2 | | 8 | | 0.08 | | 6-9 | - |
| EQS (Annual Average) elsewhere | | | | | 50 | | 0.09 | | | |

All units are in µg/L except where indicated.

| Site Ref | Monitoring Point | Stats | Cu Diss | Cu Total | Fe Diss | Fe Total | Mn Diss | Mn Total | Hardness | SO ₄ |
|--------------------------------|---|-------|---------|----------|---------|----------|---------|----------|----------|-----------------|
| GG1 | Gunnorside Gill u/s Buntun Mine | Min | <1 | <1 | 69 | 97 | <10 | <10 | 20 | <10 |
| | | Mean | 0.2 | 0.3 | 304 | 362 | <10 | 2 | 42 | <10 |
| | | Max | 1.3 | 2.2 | 943 | 1020 | <10 | 11 | 66 | <10 |
| GG2 | Buntun Lead Level Minewater Adit | Min | <1 | <1 | <30 | <30 | <10 | <10 | 78 | 17 |
| | | Mean | <1 | 0.2 | <30 | 9 | <10 | <10 | 88 | 22 |
| | | Max | <1 | 1.2 | <30 | 90 | <10 | <10 | 98 | 27 |
| GG3 | Gunnorside Gill u/s Sir Francis Level | Min | <1 | <1 | 32 | 45 | <10 | <10 | 29 | <10 |
| | | Mean | 1.4 | 0.3 | 205 | 237 | <10 | 2 | 54 | 3 |
| | | Max | 13.8 | 2.0 | 784 | 705 | <10 | 12 | 78 | 12 |
| GG4 | Sir Francis Level Minewater Adit | Min | <1 | <1 | <30 | <30 | <10 | <10 | 119 | 27 |
| | | Mean | 0.3 | 1.0 | 3 | 18 | <10 | <10 | 135 | 31 |
| | | Max | 1.4 | 1.4 | 39 | 55 | <10 | <10 | 144 | 34 |
| GG5 | Gunnorside Gill d/s Sir Francis Level & Spoil | Min | <1 | <1 | <30 | <30 | <10 | <10 | 33 | <10 |
| | | Mean | 0.4 | 0.7 | 158 | 196 | <10 | <10 | 61 | 5 |
| | | Max | 1.5 | 1.6 | 501 | 553 | <10 | <10 | 90 | 15 |
| GG7 | Gunnorside Gill tributary from Kining Level | Min | <1 | <1 | <30 | 42 | <10 | <10 | 61 | 8 |
| | | Mean | <1 | 0.6 | <30 | 97 | <10 | 5 | 72 | 11 |
| | | Max | <1 | 1.8 | <30 | 155 | <10 | 16 | 79 | 15 |
| GG6 | Gunnorside Beck at Gunnorside village bridge | Min | <1 | <1 | <30 | <30 | <10 | <10 | 24 | <10 |
| | | Mean | 0.5 | 0.6 | 118 | 143 | <10 | 1 | 65 | 5 |
| | | Max | 1.5 | 1.5 | 407 | 526 | <10 | 12 | 94 | 16 |
| WSB 1 | West Stonesdale Beck at Stonesdale Bridge | Min | 1.6 | 1.5 | 999 | 1190 | 35 | 33 | 33 | 14 |
| | | Mean | 1.7 | 1.7 | 1593 | 1953 | 46 | 47 | 57 | 28 |
| | | Max | 1.9 | 2.0 | 2400 | 2890 | 66 | 70 | 85 | 47 |
| WSB 2 | West Stonesdale Beck u/s Currack Force | Min | 1.2 | 1.5 | 551 | 708 | <10 | <10 | 40 | 13 |
| | | Mean | 1.5 | 1.6 | 1024 | 1286 | 9 | 10 | 57 | 20 |
| | | Max | 1.8 | 1.7 | 1500 | 1780 | 16 | 18 | 78 | 31 |
| EQS (Annual Average) at GG1 | | | 1 | | 1000 | | 30 | | - | 400 |
| EQS (Annual Average) elsewhere | | | 6 | | | | | | | |

All units are in µg/L, except hardness and sulphate concentrations in mg/L.

Concentrations of Pb, Zn and Cd were very elevated in all samples within this project, with 92% of Pb and Zn results and 100% of Cd results above EQS values. However, concentrations of Cu, Fe and Mn in Gunnorside are not significant and will not be considered further in this report.

The metal concentrations in Gunnorside Gill upstream of GG1 exceed the EQS values for Pb (1.5x), Zn (2.4x) and Cd (2.5x) because of inputs from the mining areas located upstream of the study area (Blakethwaite Mines). However, metal concentrations leaving the catchment at GG6 also significantly exceed the EQS values for Pb (4x), Zn (3.4x) and Cd (18x) despite additional dilution from un-impacted tributaries. Overall, from the inflow at GG1 to the outflow at GG6, Pb, Zn and Cd concentrations within Gunnorside Gill increase downstream through the study area. Pb concentration increases at GG5 located 700m downstream of Sir Francis Level, indicating some input from the intervening spoil tips.

The highest concentrations of Pb, Zn and Cd are in the discharges from Buntun Level and Sir Francis Level.

The control catchment of West Stonesdale Beck, with just one lead-zinc mine, as expected shows much lower concentrations of Pb, Zn, Cd, but has exceedences of Fe. This may result from former coal mining located at the very top of the catchment, such as at Tan Hill Colliery, as shown on **Figure 10**.

Parameter values in the adit discharges are as follows.

| Site Ref | Monitoring Point | Stats | Flow (L/s) | pH | Pb Diss | Cd Diss | Zn Diss | Cu Diss | Fe Diss | SO ₄ mg/L |
|----------|--|-------------|------------|------------|-----------|-------------|-------------|--------------|---------------|----------------------|
| GG2 | Bunton Lead Level Minewater Adit | Min | 4 | 7.3 | 39 | 6.1 | 597 | <1 | <30 | 17 |
| | | Mean | 8 | 7.9 | 45 | 8.3 | 790 | <1 | <30 | 22 |
| | | Max | 11 | 8.1 | 57 | 10.5 | 981 | <1 | <30 | 27 |
| GG4 | Sir Francis Level Minewater Adit | Min | 14 | 7.5 | 11 | 10.5 | 1270 | <1 | <30 | 27 |
| | | Mean | 19 | 7.6 | 21 | 13.7 | 1632 | 0.3 | 3 | 31 |
| | | Max | 27 | 7.7 | 36 | 15.1 | 1810 | 1.4 | 39 | 34 |
| GG7 | Gunnarside Gill tributary from Kining Level | Min | - | 7.8 | 17 | 0.5 | 26 | <1 | <30 | 8 |
| | | Mean | - | 7.8 | 28 | 0.7 | 36 | <1 | <30 | 11 |
| | | Max | - | 8.0 | 38 | 0.8 | 56 | <1 | <30 | 15 |

All units are in µg/L unless where indicated.

Metal bioavailability assessment

Assessment of water quality using current hardness-based EQS values for metals may be over- or under-protective of freshwater aquatic life, and new EQS based on bioavailability are being developed. The bioavailable concentration of Cu, Zn, Mn and Pb can be estimated from the concentrations of dissolved metal, dissolved organic carbon (DOC), Ca and pH; the standard for Ni is in development. The bioavailable metal is compared with Predicted No Effect Concentrations (PNEC) for Cu (1µg/L), Zn (10.9µg/L), Mn (123µg/L) and Pb (1.2µg/L) to calculate a Risk Characterisation Ratio (RCR) for each water quality sample. If the RCR is >1 the sample fails the bioavailable EQS. A summary of the results is shown below (there were no failures for Cu or Mn).

| Site Ref | Monitoring Point | No. of Samples | No. Zn EQS Failures | No. Zn PNEC Failures | No. Pb EQS Failures | No. Pb PNEC Failures |
|----------|---|----------------|---------------------|----------------------|---------------------|----------------------|
| GG1 | Gunnarside Gill u/s Bunton Mine | 13 | 13 | 0 | 9 | 11 |
| GG3 | Gunnarside Gill u/s Sir Francis Level | 14 | 12 | 14 | 14 | 14 |
| GG5 | Gunnarside Gill d/s Sir Francis Level & Spoil | 13 | 13 | 13 | 14 | 14 |
| GG6 | Gunnarside Beck at Gunnarside village bridge | 14 | 14 | 14 | 14 | 14 |

The bioavailability assessment did not make a great difference to the interpretation of the results, but was most significant at GG1, the upstream monitoring point, where the current EQS failures for Zn did not result in any failures of the bioavailable EQS.

The bioavailable concentrations of Zn and Pb in all sample results at the river monitoring sites (GG1, GG3, GG5, GG6) were calculated using the MBAT Excel spreadsheet and these are shown in the table below with failures of hardness-based EQS and bioavailable PNEC high-lighted in red. Pb fails throughout the catchment whereas Zn only fails downstream of the Bunton Level and spoil heaps.

| Site Ref | Monitoring Point | Date | Measured Zn (diss) | Zn (RCR) | Zn estimated PNEC | Measured Pb (diss) | Pb (RCR) | Pb estimated PNEC |
|----------|---------------------------------------|-------------|--------------------|-------------|-------------------|--------------------|-------------|-------------------|
| GG1 | Gunnerside Gill u/s Bunton Level | 27/03/12 | 16.5 | 0.99 | 16.68 | 7.69 | 2.93 | 2.63 |
| | | 24/04/12 | 22.1 | 0.65 | 33.89 | 10.50 | 1.26 | 8.33 |
| | | 14/05/12 | 18.5 | 0.54 | 34.53 | 10.80 | 1.34 | 8.05 |
| | | 20/06/12 | 16.9 | 0.63 | 26.97 | 9.09 | 1.60 | 5.66 |
| | | 16/07/12 | 17 | 0.65 | 26.33 | 11.10 | 1.97 | 5.63 |
| | | 14/08/12 | 21 | 0.72 | 28.98 | 16.10 | 2.62 | 6.14 |
| | | 12/09/12 | 28.8 | 0.41 | 70.92 | 26.10 | 1.42 | 18.36 |
| | | 15/10/12 | 18.6 | 0.48 | 38.49 | 15.40 | 1.68 | 9.16 |
| | | 20/11/12 | 23 | 0.83 | 27.64 | 13.40 | 2.02 | 6.65 |
| | | 17/12/12 | 15.9 | 0.49 | 32.51 | 6.17 | 0.78 | 7.93 |
| | | 28/01/13 | 17.4 | 0.70 | 24.76 | 6.12 | 0.94 | 6.52 |
| | | 27/02/13 | 13.9 | 0.90 | 15.41 | 3.87 | 1.64 | 2.36 |
| | | 20/03/13 | 16.5 | 0.87 | 18.92 | 5.59 | 1.67 | 3.35 |
| | Mean | 18.9 | 0.7 | 30.5 | 10.9 | 1.68 | 6.98 | |
| GG3 | Gunnerside Gill u/s Sir Francis Level | 27/03/12 | 39.3 | 2.60 | 15.09 | 15.70 | 7.61 | 2.06 |
| | | 24/04/12 | 57.5 | 1.98 | 29.08 | 32.00 | 5.01 | 6.38 |
| | | 14/05/12 | 57.0 | 1.73 | 33.02 | 37.60 | 5.20 | 7.22 |
| | | 20/06/12 | 47.4 | 2.05 | 23.15 | 20.40 | 4.79 | 4.26 |
| | | 16/07/12 | 51.8 | 2.34 | 22.16 | 24.30 | 5.85 | 4.15 |
| | | 14/08/12 | 50.0 | 2.18 | 22.93 | 28.70 | 6.81 | 4.21 |
| | | 12/09/12 | 108.0 | 1.71 | 63.00 | 97.30 | 6.65 | 14.64 |
| | | 15/10/12 | 57.8 | 1.82 | 31.77 | 45.40 | 6.70 | 6.78 |
| | | 20/11/12 | 60.5 | 1.32 | 46.00 | 36.80 | 3.32 | 11.08 |
| | | 17/12/12 | 50.4 | 1.60 | 31.59 | 22.10 | 3.14 | 7.04 |
| | | 28/01/13 | 56.3 | 2.04 | 27.55 | 21.10 | 3.68 | 5.74 |
| | | 27/02/13 | 54.8 | 3.94 | 13.92 | 11.40 | 6.13 | 1.86 |
| | | 20/03/13 | 56.6 | 3.52 | 16.06 | 16.00 | 6.41 | 2.50 |
| 28/05/13 | 253.0 | 14.00 | 18.07 | 22.20 | 7.28 | 3.05 | | |
| | Mean | 71.5 | 3.1 | 28.1 | 30.8 | 5.6 | 5.8 | |
| GG5 | Gunnerside Gill d/s Sir Francis Level | 27/03/12 | 230 | 16.44 | 13.99 | 19.30 | 11.74 | 1.64 |
| | | 24/04/12 | 202 | 7.55 | 26.74 | 39.20 | 6.97 | 5.63 |
| | | 14/05/12 | 196 | 7.09 | 27.66 | 43.10 | 7.38 | 5.84 |
| | | 20/06/12 | 232 | 11.00 | 21.10 | 25.70 | 6.69 | 3.84 |
| | | 16/07/12 | 245 | 11.97 | 20.47 | 27.90 | 7.62 | 3.66 |
| | | 14/08/12 | 268 | 13.09 | 20.47 | 30.90 | 8.73 | 3.54 |
| | | 12/09/12 | 276 | 5.35 | 51.55 | 98.30 | 8.22 | 11.96 |
| | | 15/10/12 | 213 | 7.57 | 28.14 | 54.30 | 9.33 | 5.82 |
| | | 20/11/12 | 127 | 2.57 | 49.36 | 48.00 | 4.00 | 12.00 |
| | | 17/12/12 | 143 | 4.90 | 29.20 | 28.70 | 4.50 | 6.37 |
| | | 28/01/13 | 143 | 5.70 | 25.08 | 26.30 | 5.07 | 5.18 |
| | | 27/02/13 | 234 | 16.77 | 13.96 | 13.20 | 7.48 | 1.76 |
| | | 20/03/13 | 201 | 11.51 | 17.46 | 18.80 | 6.67 | 2.82 |
| | Mean | 208 | 9.3 | 26.6 | 36.44 | 7.3 | 5.4 | |
| GG6 | Gunnerside Gill at Gunnerside | 27/03/12 | 137 | 9.71 | 14.11 | 13.90 | 8.33 | 1.67 |
| | | 24/04/12 | 158 | 6.48 | 24.39 | 33.80 | 6.92 | 4.88 |
| | | 14/05/12 | 156 | 5.91 | 26.40 | 34.90 | 6.61 | 5.28 |

| | | | | | | |
|-------------|------------|------------|-------------|-------------|------------|------------|
| 20/06/12 | 155 | 7.75 | 20.00 | 26.80 | 7.84 | 3.42 |
| 16/07/12 | 170 | 8.67 | 19.61 | 23.00 | 6.97 | 3.30 |
| 14/08/12 | 170 | 8.71 | 19.52 | 22.40 | 7.04 | 3.18 |
| 12/09/12 | 236 | 4.91 | 48.09 | 87.50 | 8.07 | 10.84 |
| 15/10/12 | 172 | 6.88 | 25.00 | 44.90 | 9.28 | 4.84 |
| 20/11/12 | 135 | 2.90 | 46.51 | 53.40 | 4.83 | 11.06 |
| 17/12/12 | 136 | 4.86 | 28.00 | 30.40 | 5.16 | 5.89 |
| 28/01/13 | 130 | 5.46 | 23.80 | 23.80 | 5.07 | 4.69 |
| 27/02/13 | 180 | 12.99 | 13.85 | 10.10 | 5.93 | 1.70 |
| 20/03/13 | 166 | 10.47 | 15.85 | 16.50 | 7.16 | 2.30 |
| 28/05/13 | 182 | 10.37 | 17.54 | 17.20 | 6.18 | 2.78 |
| Mean | 163 | 7.6 | 24.5 | 31.3 | 6.8 | 4.7 |

All units are in µg/L.

Metal loading

Metal loading (in µg/s) at each monitoring point is calculated by multiplying the filtered metal concentration (in µg/L) by the measured flow rate (in L/s).

The table below shows the concentration and loading results for Pb, Zn and Cd from 6 individual monitoring events listed from the lowest measured flows (Q93) exceeded 93% of the time, to the highest flows (Q10) only exceeded 10% of the time. The monitoring points are listed from upstream (GG1) to downstream (GG6). GG1, GG3 and GG6 are river samples while GG2 and GG4 (in bold) are adit samples from Bunton Level and Sir Francis Level. The loading values for GG1 to GG5 are compared to the loading at the downstream monitoring point, GG6 and those exceeding the loading at GG6 are high-lighted in pink.

| Flow %ile and Date | Site Ref | Flow Rate L/s | Pb µg/L | Pb Load | | Zn µg/L | Zn Load | | Cd µg/L | Cd Load | |
|--------------------|------------|---------------|-----------|------------|-----------|-------------|---------------|------------|--------------|------------|------------|
| | | | | µg/s | % of GG6 | | µg/s | % of GG6 | | µg/s | % of GG6 |
| Q93 27/03/12 | GG1 | 18 | 8 | 139 | 16 | 17 | 298 | 4 | 0.2 | 3 | 4 |
| | GG2 | 4 | 45 | 170 | 20 | 981 | 3684 | 43 | 10.5 | 39 | 40 |
| | GG3 | 38 | 16 | 602 | 70 | 39 | 1506 | 18 | 0.6 | 21 | 22 |
| | GG4 | 24 | 19 | 461 | 54 | 1660 | 39,884 | 471 | 13.5 | 324 | 330 |
| | GG5 | 51 | 19 | 992 | 115 | 230 | 11,828 | 140 | 2.5 | 128 | 130 |
| | GG6 | 62 | 14 | 859 | 100 | 137 | 8471 | 100 | 1.6 | 98 | 100 |
| Q81 14/08/12 | GG1 | 38 | 16 | 612 | 35 | 27 | 1,026 | 8 | 0.24 | 9 | 6 |
| | GG2 | 6 | 52 | 311 | 18 | 971 | 5,826 | 44 | 9.89 | 59 | 40 |
| | GG3 | 58 | 29 | 1,665 | 95 | 64 | 3,712 | 28 | 0.64 | 37 | 25 |
| | GG4 | 17 | 24 | 401 | 23 | 1750 | 29,750 | 224 | 14.70 | 250 | 169 |
| | GG5 | 68 | 31 | 2,101 | 120 | 265 | 18,020 | 136 | 2.71 | 184 | 124 |
| | GG6 | 78 | 22 | 1,747 | 100 | 170 | 13,260 | 100 | 1.90 | 148 | 100 |
| Q58 27/02/12 | GG1 | 37 | 4 | 145 | 13 | 14 | 520 | 3 | 0.1 | 5 | 3 |
| | GG2 | 6 | 45 | 258 | 23 | 792 | 4525 | 23 | 8.6 | 49 | 27 |
| | GG3 | 78 | 11 | 889 | 80 | 55 | 4274 | 22 | 0.6 | 44 | 25 |
| | GG4 | 17 | 11 | 190 | 17 | 1590 | 26,499 | 134 | 13.4 | 223 | 125 |
| | GG5 | 99 | 13 | 1308 | 118 | 234 | 23,188 | 118 | 2.1 | 212 | 119 |
| | GG6 | 110 | 10 | 1107 | 100 | 180 | 19,723 | 100 | 1.6 | 179 | 100 |
| Q53 16/07/12 | GG1 | 52 | 11 | 577 | 15 | 18 | 957 | 3 | 0.19 | 10 | 3 |
| | GG2 | 11 | 49 | 540 | 14 | 891 | 9,801 | 33 | 8.92 | 98 | 34 |
| | GG3 | 102 | 24 | 2,479 | 64 | 57 | 5,834 | 20 | 0.64 | 65 | 22 |
| | GG4 | 22 | 22 | 473 | 12 | 1670 | 36,740 | 124 | 14.40 | 317 | 108 |
| | GG5 | 133 | 28 | 3,711 | 95 | 257 | 34,181 | 115 | 2.31 | 307 | 105 |
| | GG6 | 169 | 23 | 3,887 | 100 | 176 | 29,744 | 100 | 1.73 | 292 | 100 |

| | | | | | | | | | | | |
|-----------------|------------|-----------|-----------|------------|-----------|-------------|---------------|------------|--------------|------------|------------|
| Q49 20/06/12 | GG1 | 58 | 9 | 527 | 13 | 18 | 1,032 | 4 | 0.21 | 12 | 5 |
| | GG2 | 7 | 44 | 305 | 7 | 918 | 6,426 | 26 | 8.88 | 62 | 25 |
| | GG3 | 110 | 20 | 2,244 | 55 | 51 | 5,555 | 23 | 0.60 | 65 | 26 |
| | GG4 | 20 | 23 | 466 | 11 | 1800 | 36,000 | 148 | 15.10 | 302 | 121 |
| | GG5 | 131 | 26 | 3,367 | 83 | 234 | 30,654 | 126 | 2.25 | 295 | 118 |
| | GG6 | 152 | 27 | 4,074 | 100 | 160 | 24,320 | 100 | 1.64 | 249 | 100 |
| Q42 24/04/12 | GG1 | 85 | 11 | 893 | 14 | 22 | 1879 | 6 | 0.2 | 16 | 6 |
| | GG2 | 8 | 41 | 320 | 5 | 725 | 5659 | 19 | 7.8 | 61 | 22 |
| | GG3 | 146 | 32 | 4663 | 73 | 58 | 8379 | 28 | 0.6 | 83 | 30 |
| | GG4 | 17 | 31 | 513 | 8 | 1670 | 27,637 | 93 | 13.9 | 230 | 84 |
| | GG5 | 168 | 39 | 6584 | 104 | 202 | 33,929 | 114 | 1.8 | 304 | 111 |
| | GG6 | 188 | 34 | 6353 | 100 | 158 | 29,696 | 100 | 1.5 | 274 | 100 |
| Q29 14/05/12 | GG1 | 108 | 11 | 1168 | 12 | 19 | 2000 | 5 | 0.2 | 20 | 5 |
| | GG2 | 9 | 39 | 351 | 4 | 704 | 6329 | 15 | 7.4 | 66 | 16 |
| | GG3 | 194 | 38 | 7296 | 75 | 57 | 11,060 | 26 | 0.6 | 112 | 27 |
| | GG4 | 19 | 22 | 423 | 4 | 1630 | 31,762 | 73 | 13.8 | 269 | 65 |
| | GG5 | 246 | 43 | 10,617 | 110 | 196 | 48,283 | 111 | 1.8 | 453 | 110 |
| | GG6 | 278 | 35 | 9695 | 100 | 156 | 43,336 | 100 | 1.5 | 411 | 100 |
| Q16 17/12/12 | GG1 | 291 | 6 | 1798 | 12 | 16 | 4633 | 7 | 0.1 | 38 | 6 |
| | GG2 | 11 | 41 | 454 | 3 | 645 | 7075 | 10 | 6.9 | 76 | 13 |
| | GG3 | 449 | 22 | 9924 | 64 | 50 | 22,633 | 33 | 0.4 | 195 | 33 |
| | GG4 | 27 | 15 | 407 | 3 | 1540 | 41,758 | 61 | 13.8 | 374 | 63 |
| | GG5 | 483 | 29 | 13,848 | 90 | 143 | 68,999 | 100 | 1.2 | 593 | 100 |
| | GG6 | 506 | 30 | 15,394 | 100 | 136 | 68,869 | 100 | 1.2 | 592 | 100 |
| Q10 20/11/12 | GG1 | 248 | 13 | 3324 | 7 | 23 | 5706 | 5 | 0.2 | 59 | 5 |
| | GG2 | 10 | 49 | 481 | 1 | 713 | 6959 | 6 | 7.6 | 74 | 7 |
| | GG3 | 592 | 37 | 21,793 | 45 | 61 | 35,829 | 29 | 0.5 | 300 | 27 |
| | GG4 | 19 | 28 | 521 | 1 | 1630 | 30,648 | 25 | 13.5 | 254 | 23 |
| | GG5 | 964 | 48 | 46,266 | 95 | 127 | 122,412 | 99 | 1.1 | 1051 | 94 |
| | GG6 | 915 | 53 | 48,850 | 100 | 135 | 123,498 | 100 | 1.2 | 1116 | 100 |

Pb concentrations and loadings increase at GG5 some 700m downstream of Sir Francis Level. There is one west bank tributary entering Gunnerside Gill in this stretch, but there are no identified mining sites within its catchment. However, there is 500m of mining spoil in the intervening stretch located on the valley bottom, comprising the Sir Francis and the Winterings ore dressing floors (see **Figure 9** and **Figure 14**). Gunnerside Gill flows through this mining spoil and is actively eroding it. The increase in Pb concentration and loading may be related to the presence of this spoil, but there are no similar increases in Zn and Cd concentration and loading, which might be expected. Pb concentrations and loading then decrease at GG6, located 1.6 km downstream of GG5.

GG1 and GG6 are upstream and downstream samples from Gunnerside Gill and so represent the flows and metal loading entering and leaving the study area, while GG2, GG4 and GG7 represent metal loading inflows from mine drainage adits.

When loadings are considered, the relative impact of each inflow can be compared, so that high concentrations in relatively low flows, such as Bunton Level (GG2), may not be contributing a significant proportion of the overall metal loading in the catchment.

At low to medium flows (up to ~Q40), the most significant source of Zn and Cd is the Sir Francis Level. However at higher river flows, diffuse sources become more important although the Sir Francis Level remains the single largest source.

Under the highest river flows, the Zn, Pb and Cd concentration at GG6 increases with flow leading to a significant increase in loading. No point source of Pb has been identified and it is

most likely arising from diffuse inputs such as contaminated sediments and run-off from spoil heaps.

| Site Ref | Monitoring Point | Mean Flow (L/s) | Mean Concentrations (µg/L) | | | Mean Loadings (µg/s) | | |
|----------|-------------------|-----------------|----------------------------|------|----|----------------------|--------|-----|
| | | | Pb | Zn | Cd | Pb | Zn | Cd |
| GG2 | Bunton Level | 8 | 45 | 790 | 8 | 360 | 6320 | 64 |
| GG4 | Sir Francis Level | 19 | 21 | 1632 | 14 | 399 | 31,008 | 266 |

The mean metal loadings (in kg/yr) leaving the catchment at GG6 are as follows; calculated from the mean of individual sampling events with the range in parentheses.

| Site Ref | Monitoring Point | Mean Flow (L/s) | Mean Concentrations (µg/L) | | | Mean Loadings (kg/year) | | |
|----------|--|-----------------|----------------------------|-----|-----|-------------------------|----------------------|----------------|
| | | | Pb | Zn | Cd | Pb | Zn | Cd |
| GG6 | Gunnerside Beck at Gunnerside village bridge | 250 | 29 | 171 | 1.6 | 226 (27 – 1540) | 1349 (267 – 3894) | 12 (3 – 35) |

Potential water quality improvements from treating point sources

The accompanying spreadsheet (“Gunnerside Gill display data.xlsm”) has been used to calculate the water quality improvement predicted by treating the two main point sources identified in the Gunnerside catchment, Bunton Level and Sir Francis Level. The benefits of various treatment options have been calculated to show the reduction in metal concentration and loading at the downstream monitoring point (GG6) representing the predicted metal impacts leaving the catchment and entering the River Swale. The predictions were made assuming that 70% and 90% of the Pb, Zn and Cd could be removed from the two adit discharges, individually and both in combination. These were considered for the 12 monitoring events at GG6 from low flow (Q93) to high flow (Q10). The treatment predictions were calculated using the expression:

$$\text{Loading } (\mu\text{g/s}) = \text{Concentration } (\mu\text{g/L}) \times \text{Flow (L/s)}$$

Treatment predictions were made by reducing the metal concentrations by 70% or 90% at one or both adits as required, and deriving the metal load reduction that was passed on downstream. The expression above was then used again, to back-calculate the resultant downstream concentrations under the reduced loading. The measured concentrations and flows occasionally resulted in downstream load values that were predicted to be negative, but these were altered to zero, indicating that the adit treatment had been 100% successful at the location concerned. The predicted improvement in EQS failure rates at the downstream monitoring point on Gunnerside Gill (GG6) are shown in the table below for the various treatment options under all 12 flow conditions. The concentrations predicted to be below the EQS values were all at flows less than the 50th percentile.

| Treatment Option | No. Samples | No. Measured EQS Failures | | | No. Predicted EQS Failures | | |
|----------------------|-------------|---------------------------|----|----|----------------------------|----|----|
| | | Pb | Zn | Cd | Pb | Zn | Cd |
| Bunton 70% | 12 | 12 | 12 | 12 | 12 | 12 | 12 |
| Bunton 90% | 12 | 12 | 12 | 12 | 12 | 12 | 12 |
| Francis 70% | 12 | 12 | 12 | 12 | 12 | 9 | 10 |
| Francis 90% | 12 | 12 | 12 | 12 | 12 | 7 | 8 |
| Bunton & Francis 70% | 12 | 12 | 12 | 12 | 11 | 7 | 8 |
| Bunton & Francis 90% | 12 | 12 | 12 | 12 | 10 | 6 | 6 |

The predicted treatment results for each of the treatment options and metal removal rates are shown below in 3 tables for the individual problematic metals (Pb, Zn, Cd). The results with 50% or more reduction in concentration and loading are high-lighted in orange and those showing 100% reduction are high-lighted in green.

The treatment predictions show the following.

- Treatment of Zn and Cd is much more successful at low flows.
- Treatment is not effective at the highest flows (>~Q40).
- Treating both adits is better than treating just one.
- If only one adit is treated, Sir Francis will be more effective.
- Treating Sir Francis alone should lead to compliance with the bioavailable EQS for Zn and hardness-based EQS for Cd under medium to low flows..
- Since Pb appears to arise from diffuse sources, treating the mine water discharges does not make a significant improvement in water quality.

Predicted reductions in Pb concentration and loading at GG6 are shown in the table below.

| Q-Flow %ile | Flow (L/s) | Bunton 70% | Bunton 90% | Francis 70% | Francis 90% | Bunton & Francis 70% | Bunton & Francis 90% |
|-------------|------------|------------|------------|-------------|-------------|----------------------|----------------------|
| Q93 | 62 | 14% | 18% | 38% | 48% | 51% | 66% |
| Q90 | 78 | 13% | 17% | 16% | 20% | 29% | 37% |
| Q58 | 110 | 16% | 21% | 12% | 15% | 28% | 36% |
| Q56 | 169 | 10% | 13% | 9% | 11% | 18% | 24% |
| Q54 | 152 | 5% | 7% | 8% | 10% | 13% | 17% |
| Q42 | 188 | 4% | 5% | 6% | 7% | 9% | 12% |
| Q36 | 178 | 6% | 7% | 5% | 6% | 11% | 14% |
| Q31 | 227 | 3% | 3% | 2% | 3% | 5% | 6% |
| Q29 | 278 | 3% | 3% | 3% | 4% | 6% | 7% |
| Q27 | 143 | 2% | 2% | 3% | 4% | 5% | 6% |
| Q16 | 506 | 2% | 3% | 2% | 2% | 4% | 5% |
| Q10 | 915 | 1% | 1% | 1% | 1% | 1% | 2% |

Predicted reductions in Zn concentration and loading at GG6 are shown in the table below.

| Q-Flow %ile | Flow (L/s) | Bunton 70% | Bunton 90% | Francis 70% | Francis 90% | Bunton & Francis 70% | Bunton & Francis 90% |
|-------------|------------|------------|------------|-------------|-------------|----------------------|----------------------|
| Q93 | 62 | 30% | 39% | 100% | 100% | 100% | 100% |
| Q90 | 78 | 32% | 41% | 100% | 100% | 100% | 100% |
| Q58 | 110 | 16% | 21% | 94% | 100% | 100% | 100% |
| Q56 | 169 | 24% | 31% | 90% | 100% | 100% | 100% |
| Q54 | 152 | 17% | 22% | 100% | 100% | 100% | 100% |
| Q42 | 188 | 13% | 17% | 65% | 84% | 78% | 100% |
| Q36 | 178 | 10% | 12% | 60% | 77% | 70% | 89% |
| Q31 | 227 | 12% | 15% | 49% | 63% | 61% | 78% |
| Q29 | 278 | 10% | 13% | 51% | 66% | 62% | 79% |
| Q27 | 143 | 11% | 14% | 51% | 66% | 62% | 80% |
| Q16 | 506 | 7% | 9% | 42% | 55% | 50% | 64% |
| Q10 | 915 | 4% | 5% | 17% | 22% | 21% | 27% |

Predicted reductions in Cd concentration and loading at GG6 are shown in the table below.

| Q-Flow %ile | Flow (L/s) | Bunton 70% | Bunton 90% | Francis 70% | Francis 90% | Bunton & Francis 70% | Bunton & Francis 90% |
|-------------|------------|------------|------------|-------------|-------------|----------------------|----------------------|
| Q93 | 62 | 28% | 36% | 100% | 100% | 100% | 100% |
| Q90 | 78 | 30% | 38% | 100% | 100% | 100% | 100% |
| Q58 | 110 | 19% | 25% | 88% | 100% | 100% | 100% |
| Q56 | 169 | 24% | 31% | 76% | 98% | 100% | 100% |
| Q54 | 152 | 17% | 22% | 84% | 100% | 100% | 100% |
| Q42 | 188 | 16% | 20% | 59% | 75% | 74% | 96% |
| Q36 | 178 | 11% | 14% | 53% | 68% | 64% | 82% |
| Q31 | 227 | 13% | 17% | 44% | 56% | 57% | 73% |
| Q29 | 278 | 11% | 14% | 46% | 59% | 57% | 73% |
| Q27 | 143 | 12% | 16% | 45% | 58% | 57% | 74% |
| Q16 | 506 | 9% | 12% | 44% | 57% | 53% | 68% |
| Q10 | 915 | 5% | 6% | 16% | 20% | 21% | 26% |

Benefits

The Stage 1 cost-benefit tool calculates that moving the Gunnerside Gill water body from moderate to good status would deliver ~£1,684k in benefits over 40 years. More significantly, it would contribute to cleaning up pollution in the River Swale which will fail the bioavailable Zn EQS for tens of kilometres downstream due to Gunnerside Gill and other mining-impacted tributaries.

Constraints

Land owners and occupiers

The main landowners in the Gunnerside catchment are as follows:

West bank: Gunnerside Estates, Ivelet, North Yorkshire, DL11 6JH.

East Bank: Reeth Sporting Society, The Estate Office, Rothwell, Market Rasen, Lincolnshire, LN7 6BJ.

There are a number of smaller landowners at farms in the lower valley, but these should not be significant in terms of any potential remedial treatment works at the mine sites. Contact details for the landowners are available from John Barber or from Robert White at YDNPA (see below).

Conservation and heritage designations

The designations within Gunnerside Gill catchment are listed on **page 8** of this report and shown on **Figure 6**. The Yorkshire Dales National Park Authority has produced a report detailing the conservation and heritage issues.

In summary, all of the catchment is in the Yorkshire Dales National Park, most is also a SSSI. SPA and SAC, there is 11ha of ancient woodland just above Gunnerside village and there are 9 Scheduled Ancient Monuments amongst the mine sites.

Recommendations

- The main sources of Zn and Cd are:
 - Sir Francis Level (GG4): this is the most significant source under all flow conditions (25-470% of Zn flux at GG6; 23-330% of Cd flux at GG6).

- Treatment of Sir Francis Level (70-100% decrease in flux) should lead to compliance with the Cd and (bioavailable) Zn EQS under low to medium flow conditions (flows <Q40).
2. Pb arises from three main diffuse sources:
 - Contaminated in-river sediments.
 - Wastes around Bunton mine.
 - Wastes around Sir Francis Level area.
 - There is little prospect of significantly improving the water quality with respect to Pb.
 3. Share final report with the Coal Authority:
 - Carry out scoping study for 14/15 focussed on Sir Francis Level.
 - Flows requiring treatment are 14-27 l/s; a flow measurement logger should be installed to establish the true range in flows.
 - Using the Newcastle University look-up table for a vertical flow pond, this would require ~7-10,000 m² of land.
 - Yorkshire Dales National Park Authority are keen to help reduce further erosion of mining wastes.
 4. EA to investigate Zn, Pb and Cd pollution in the downstream River Swale
 - Establish the extent of EQS failure and the contribution of Gunnerside Gill, and specifically, the Sir Francis Level mine water discharge.

Stakeholders

Robert White, Senior Historic Environment Officer
Yorkshire Dales National Park Authority,
Yoredale, Bainbridge, Leyburn, North Yorkshire, DL8 3EL

Steve Hill, Principal Technical Manager,
The Coal Authority, 200 Lichfield Lane, Mansfield, Nottinghamshire, NG18 4RG

Summary of source apportionment study

| | | Comment |
|--|---|------------------------------------|
| # water bodies impacted | One = confirmed 4 d/s = contribution to be confirmed | |
| Length of river impacted (km) | 6km confirmed Up to 100km (contributes to) | |
| Metals failing current EQS | Zn = 3.4x Cd = 18x Pb = 4x | At d/s catchment sampling point. |
| Metals failing bioavailable EQS | Zn = 7.6x Pb = 6.8x | |
| Is there an outbreak risk? | No | |
| # of sources | Two point, several diffuse. | One key point source. |
| Metal loading – point sources (kg/yr) | Zn = 977 (800 – 1,300) Cd = 8 (7 – 10) Pb = 12 (6 – 16) | GG4: Sir Francis Level |
| Metal loading – river (d/s) kg/yr | Zn = 1349 (267 – 3894) Cd = 12 (3 – 35) Pb = 226 (27 – 1540) | GG6: Gunnerside Gill in Gunnerside |
| How many sources need to be treated to achieve EQS (good status) ? | One source needs treatment for Zn. No obvious source of Pb. | |
| Length of river improved by treatment (km) | 4 km but would contribute to up to 100 km. | |
| NWEBS benefit (£m over 40 years) | £1,684,000 (single water body) £30,471,989 (including 4 d/s wbs) | |
| Potential contribution from others? | Not known. | |

Recommendations

| Options | Comment |
|--|--|
| Feasibility: sources defined, move to feasibility | <ol style="list-style-type: none"> The main sources of Zn and Cd are: <ul style="list-style-type: none"> Sir Francis Level (GG4): this is the most significant source under all flow conditions (25-470% of Zn flux at GG6; 23-330% of Cd flux at GG6). Treatment of Sir Francis Level (70-100% decrease in flux) should lead to compliance with the Cd and (bioavailable) Zn EQS under low to medium flow conditions (flows <Q40). Pb arises from three main diffuse sources: <ul style="list-style-type: none"> Contaminated in-river sediments. Wastes around Bunton mine. Wastes around Sir Francis Level area. There is little prospect of significantly improving the water quality with respect to Pb. In principle, the Yorkshire Dales National Park Authority are keen to reduce erosion, particularly around Sir Francis Level dressing floor area – this should be explored. |

| | |
|--|---|
| | <p>3. Share final report with the Coal Authority:</p> <ul style="list-style-type: none"> • Carry out scoping study for 14/15 focussed on Sir Francis Level. • Flows requiring treatment are 14-27 l/s; a flow measurement logger should be installed to establish the true range in flows. • Using the Newcastle University look-up table for a vertical flow pond, this would require ~7-10,000 m² of land. <p>4. EA to investigate Zn, Pb and Cd pollution in the downstream River Swale</p> <ul style="list-style-type: none"> • Establish the extent of EQS failure and the contribution of Gunnerside Gill, and specifically, the Sir Francis Level mine water discharge. |
| Monitor: sources not defined, more monitoring needed | |
| Suspend: sources too complicated, not feasible with current technology/costs | |
| National delivery team decision | Priority High |

Conclusion

This catchment should be forwarded to the Coal Authority for a feasibility study.

| | | | |
|-------|--|-------|----------|
| Name: | John Barber, Technical Specialist in Land Contamination, Yorkshire Area Groundwater & Contaminated Land Team | Date: | 10/09/13 |
|-------|--|-------|----------|

Approval

- Pass to Coal Authority for scoping study.
- Conduct monitoring investigation in wider Swale catchment.

| | | | |
|-------|---|-------|----------|
| Name: | Hugh Potter, Technical Advisor on Pollution from Abandoned Mines National Operations, Geoscience Team | Date: | 10/10/13 |
|-------|---|-------|----------|

APPENDIX B – SUMMARY OF BCR DATA

BCR SUM VS TOTAL DIGESTION DATA - Gun 1 to 10 – pre column solids

| | Pb (mg/kg) | | Zn (mg/kg) | | Fe (mg/kg) | |
|--------|------------|-----------|------------|-----------|------------|-----------|
| | BCR Sum | Total Dig | BCR Sum | Total Dig | BCR Sum | Total Dig |
| Gun 1 | 79899 | 70046 | 4583 | 4105 | 4868 | 35881 |
| Gun 2 | 24280 | 17897 | 9109 | 12583 | 12566 | 26445 |
| Gun 3 | 4219 | 1841 | 9185 | 8096 | 5742 | 15684 |
| Gun 4 | 4969 | 5425 | 2111 | 1976 | 9581 | 15529 |
| Gun 5 | 64460 | 49250 | 67056 | 64252 | 3487 | 4866 |
| Gun 6 | 2958 | 2402 | 3182 | 2891 | 10793 | 24213 |
| Gun 7 | 16549 | 6263 | 61917 | 60939 | 1913 | 5486 |
| Gun 8 | 6198 | 4142 | 9731.1 | 14639 | 3936 | 9916 |
| Gun 9 | 14882 | 8705 | 3667 | 4952 | 9380 | 18536 |
| Gun 10 | 5430 | 6589 | 2636 | 3280 | 7993 | 20915 |

| | Mg (mg/kg) | | Mn (mg/kg) | | S (mg/kg) | |
|--------|------------|-----------|------------|-----------|-----------|-----------|
| | BCR Sum | Total Dig | BCR Sum | Total Dig | BCR Sum | Total Dig |
| Gun 1 | 2926 | 2860 | 1067 | 1595 | 7314 | 4152 |
| Gun 2 | 2847 | 2585 | 792 | 843 | 8006 | 5720 |
| Gun 3 | 2980 | 3351 | 47 | 47 | 13133 | 7158 |
| Gun 4 | 2957 | 3010 | 818 | 888 | 6857 | 4286 |
| Gun 5 | 359 | 373 | 50 | 52 | 42567 | 11747 |
| Gun 6 | 1422 | 1220 | 941 | 1063 | 4309 | 4022 |
| Gun 7 | 476 | 666 | 60 | 59 | 30483 | 17092 |
| Gun 8 | 1761 | 1414 | 59 | 60 | 12493 | 7309 |
| Gun 9 | 1709 | 1421 | 1014 | 870 | 7181 | 4763 |
| Gun 10 | 1806 | 1698 | 510 | 450 | 4499 | 3967 |

| | Al (mg/kg) | | Ca (mg/kg) | |
|--------|------------|-----------|------------|-----------|
| | BCR Sum | Total Dig | BCR Sum | Total Dig |
| Gun 1 | 36728 | 33547 | 32087 | 12962 |
| Gun 2 | 47362 | 37627 | 19848 | 33615 |
| Gun 3 | 16873 | 63963 | 51818 | 50549 |
| Gun 4 | 43624 | 41716 | 30775 | 11683 |
| Gun 5 | 5842 | 6033 | 8604 | 72402 |
| Gun 6 | 29920 | 24779 | 20834 | 12925 |
| Gun 7 | 8120 | 11022 | 13769 | 103409 |
| Gun 8 | 35021 | 23782 | 20353 | 90245 |
| Gun 9 | 30890 | 21562 | 27400 | 38696 |
| Gun 10 | 28557 | 23566 | 21412 | 12080 |

Gun 1,2,3 and 9 and CGun 1,2,3 and 9 – pre and post column solids

| | Pb (mg/kg) | | Zn (mg/kg) | | Fe (mg/kg) | |
|---------|------------|-----------|------------|-----------|------------|-----------|
| | BCR Sum | Total Dig | BCR Sum | Total Dig | BCR Sum | Total Dig |
| Gun 1 | 79899 | 70046 | 4583 | 4105 | 4868 | 35881 |
| C Gun 1 | 65469 | 55379 | 4170 | 4008 | 39795 | 38972 |
| Gun 2 | 24280 | 17897 | 9109 | 12583 | 12566 | 26445 |
| C Gun 2 | 16229 | 12109 | 8289 | 7534 | 19508 | 16699 |
| Gun 3 | 4219 | 1841 | 9185 | 8096 | 5742 | 15684 |
| C Gun 3 | 1867 | 738 | 4529 | 4161 | 26529 | 27857 |
| Gun 9 | 14882 | 8705 | 3667 | 4952 | 9380 | 18536 |
| C Gun 9 | 16787 | 12345 | 3402 | 3069 | 21988 | 2756 |

| | Mn (mg/kg) | | S (mg/kg) | |
|---------|------------|-----------|-----------|-----------|
| | BCR Sum | Total Dig | BCR Sum | Total Dig |
| Gun 1 | 1067 | 1595 | 7314 | 4152 |
| C Gun 1 | 1377 | 1622 | 5794 | 5141 |
| Gun 2 | 792 | 843 | 8006 | 5720 |
| C Gun 2 | 493 | 615 | 7008 | 6915 |
| Gun 3 | 47 | 47 | 13133 | 7158 |
| C Gun 3 | 43 | 39 | 9282 | 6479 |
| Gun 9 | 1014 | 870 | 7181 | 4763 |
| C Gun 9 | 961 | 29 | 5467 | 4167 |

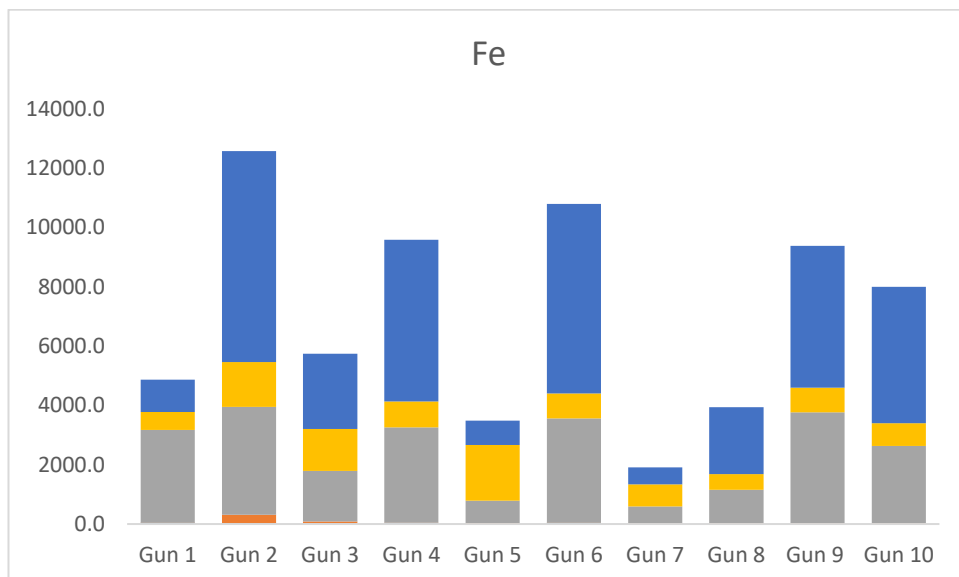
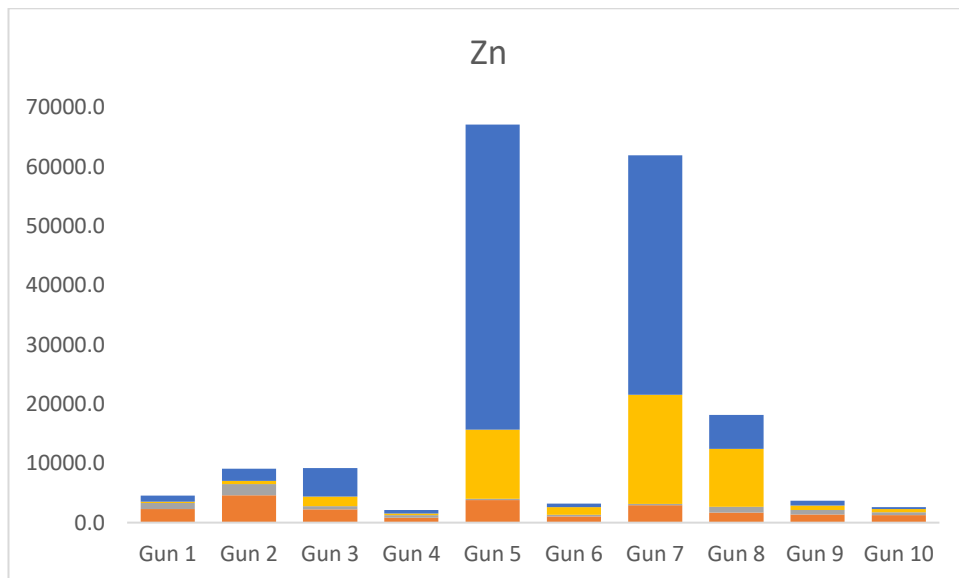
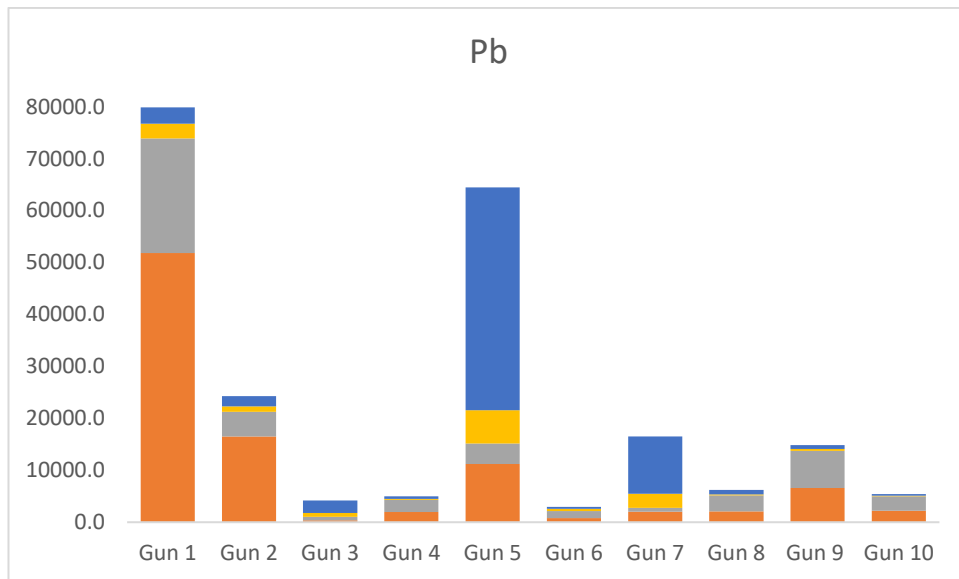
BCR DATA ($\mu\text{g/L}$)

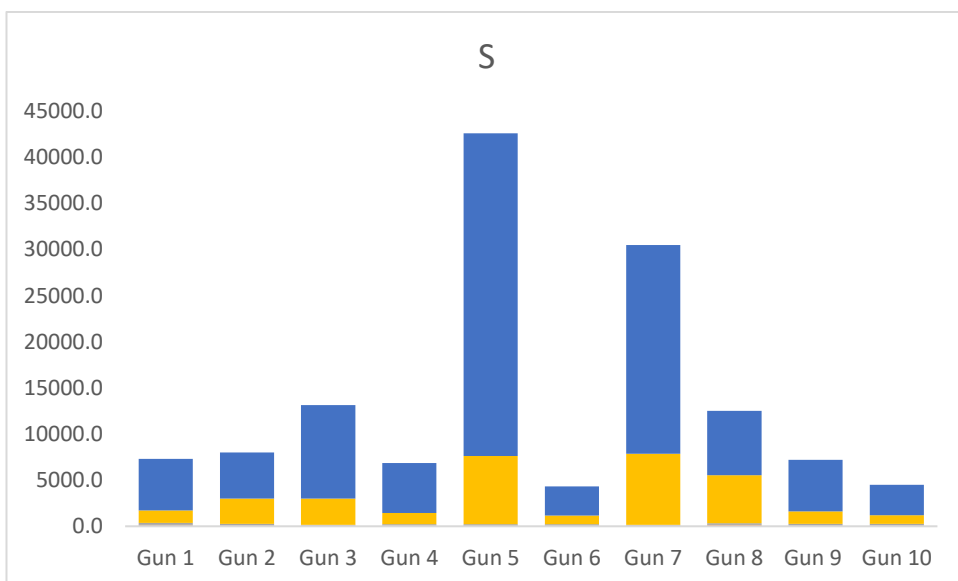
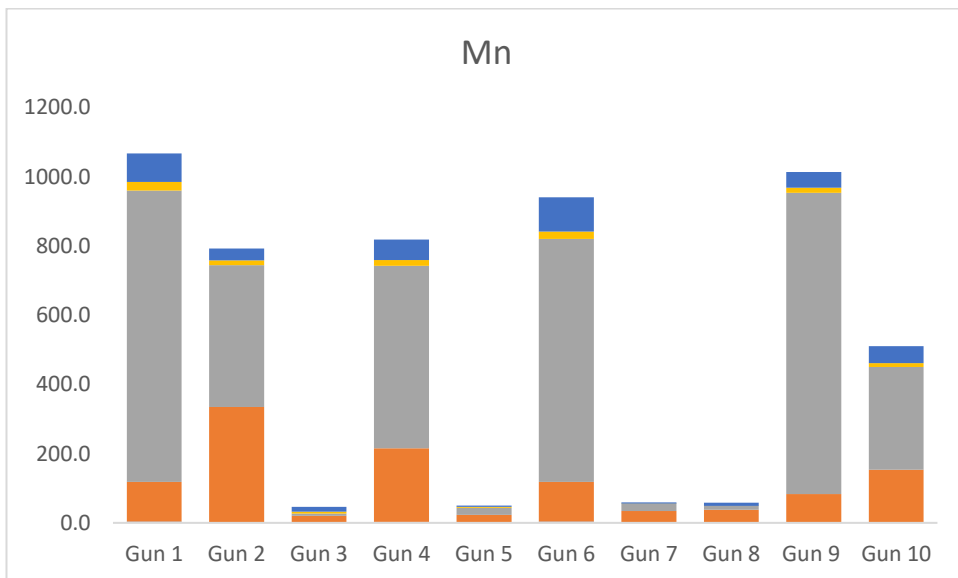
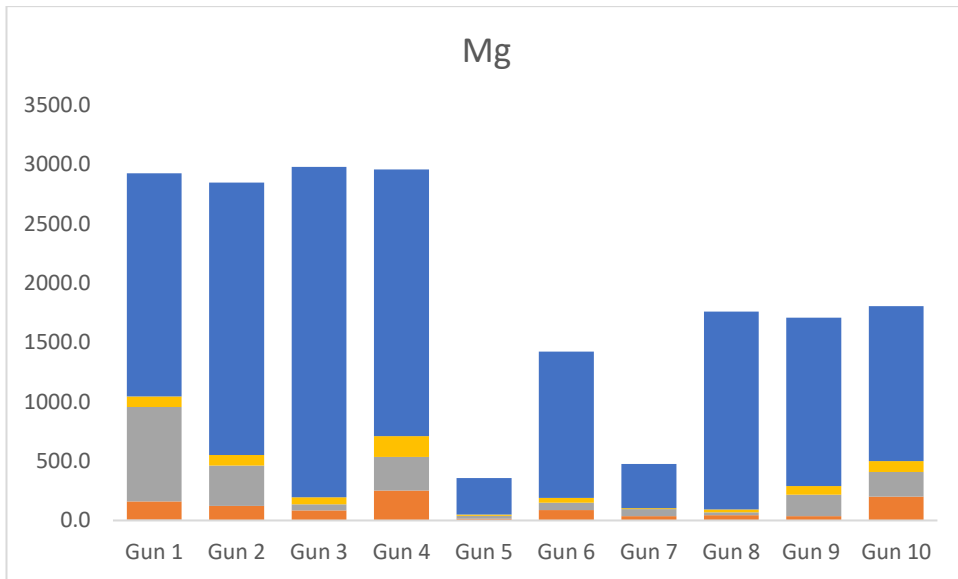
| Pb | Water | Step 1 | Step 2 | Step 3 | Res |
|-----------|----------|----------|----------|----------|----------|
| C Gun 1 | 1.659975 | 1307.748 | 274.1779 | 14.96041 | 2755.939 |
| C Gun 2 | 1.298969 | 258.5256 | 98.74685 | 12.88927 | 2484.836 |
| C Gun 3 | 0.166579 | 3.852659 | 12.3454 | 3.449429 | 2080.339 |
| C Gun 9 | 2.301337 | 201.4907 | 190.1141 | 6.759959 | 1386.255 |
| C Gun 2 A | 1.364473 | 243.1751 | 103.0968 | 14.48367 | 2410.918 |
| | | | | | |
| Gun 1 | 1.940119 | 1294.124 | 551.3796 | 57.26814 | 6278.458 |
| Gun 2 | 0.48294 | 412.3615 | 119.4667 | 20.35143 | 3940.59 |
| Gun 3 | 0.148422 | 8.5047 | 17.68002 | 14.75702 | 2484.836 |
| Gun 4 | 0.286308 | 48.71095 | 58.92793 | 3.680179 | 936.6844 |
| Gun 5 | 0.955857 | 279.2862 | 98.09916 | 129.1097 | 85775.87 |
| Gun 6 | 0.315217 | 19.45864 | 33.74136 | 9.370519 | 697.6879 |
| Gun 7 | 0.286547 | 50.9739 | 17.72051 | 53.89378 | 22199.38 |
| Gun 8 | 0.223799 | 51.9893 | 77.72047 | 3.112043 | 1691.337 |
| Gun 9 | 0.784693 | 163.3188 | 179.9475 | 6.751718 | 1565.836 |
| Gun 10 | 0.174746 | 55.53889 | 68.4664 | 2.404362 | 684.6881 |
| | | | | | |
| Zn | Water | Step 1 | Step 2 | Step 3 | Res |
| C Gun 1 | 0.680262 | 48.54373 | 26.50144 | 4.214426 | 1860.68 |
| C Gun 2 | 1.483474 | 85.07673 | 25.87183 | 23.16133 | 5270.126 |
| C Gun 3 | 0.601958 | 20.57747 | 13.41802 | 42.9291 | 1998.614 |
| C Gun 9 | 1.644365 | 21.50573 | 18.42676 | 22.39366 | 1239.652 |
| C Gun 2 A | 1.458287 | 92.65436 | 27.64611 | 22.57957 | 7407.331 |
| | | | | | |
| Gun 1 | 0.723359 | 57.18215 | 25.40253 | 4.493105 | 2052.125 |
| Gun 2 | 0.881958 | 114.0803 | 46.82078 | 11.01297 | 4175.248 |
| Gun 3 | 0.346437 | 55.37378 | 14.33339 | 31.97704 | 9571.429 |
| Gun 4 | 0.13734 | 20.34617 | 10.90986 | 5.905193 | 1120.144 |
| Gun 5 | 0.453821 | 94.53256 | 5.436109 | 232.9796 | 102821.3 |
| Gun 6 | 0.237726 | 25.76202 | 6.737403 | 26.56133 | 1089.698 |
| Gun 7 | 0.514529 | 72.81805 | 6.066818 | 366.9378 | 80820.25 |
| Gun 8 | 1.679035 | 40.69371 | 24.65069 | 2432.773 | 11516.14 |
| Gun 9 | 0.733415 | 33.93109 | 18.98996 | 14.77572 | 1563.834 |
| Gun 10 | 0.153466 | 31.75997 | 12.26705 | 10.19427 | 717.7207 |
| | | | | | |
| Cd | Water | Step 1 | Step 2 | Step 3 | Res |
| C Gun 1 | 0.010192 | 0.171083 | 0.107437 | 0.03253 | 10.92391 |
| C Gun 2 | 0.016953 | 0.360276 | 0.140049 | 0.19394 | 75.04991 |
| C Gun 3 | 0.013505 | 0.122116 | 0.089657 | 0.307638 | 13.06984 |
| C Gun 9 | 0.009153 | 0.03791 | 0.053082 | 0.159179 | 12.04618 |
| C Gun 2 A | 0.014405 | 0.387339 | 0.137766 | 0.19792 | 49.93943 |
| | | | | | |

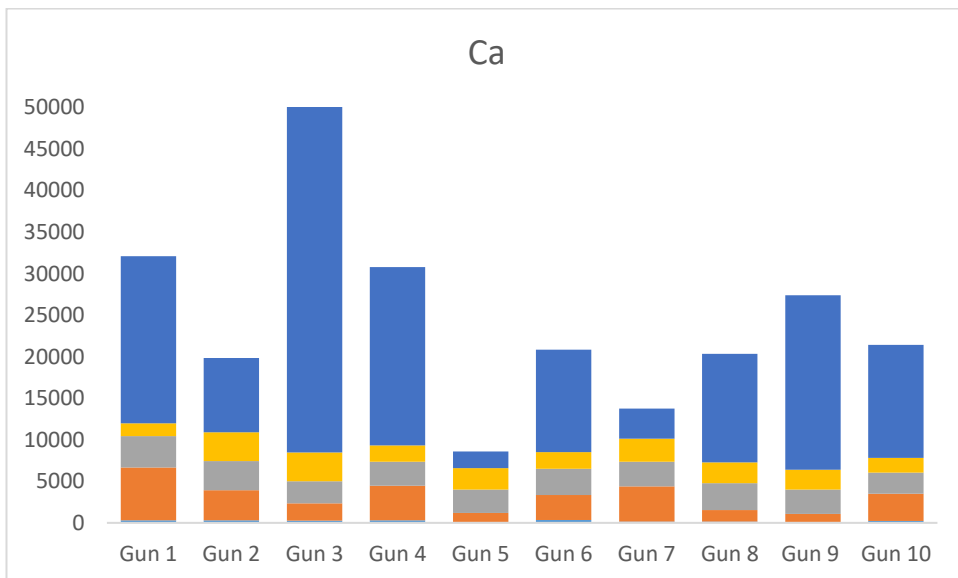
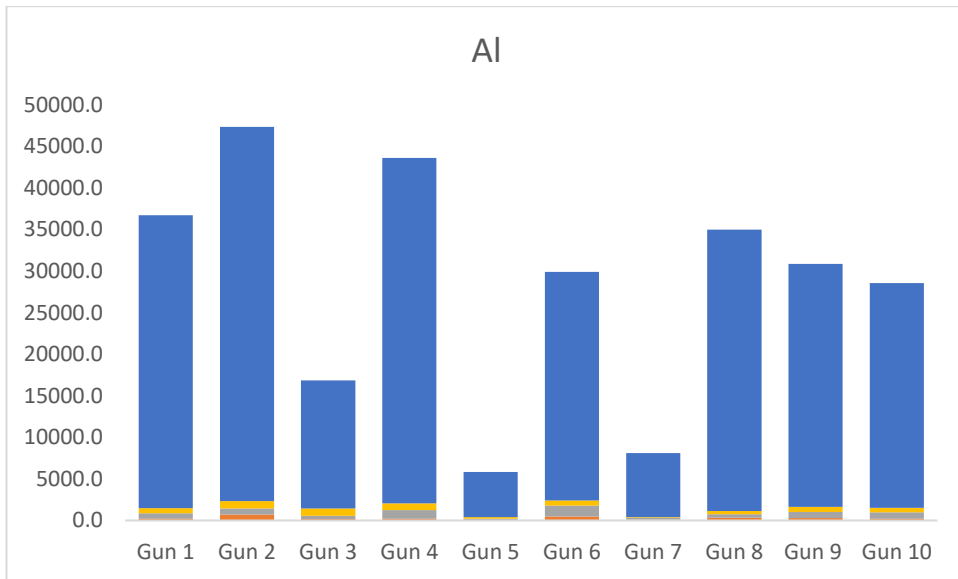
| | | | | | |
|-----------|----------|----------|----------|----------|----------|
| Gun 1 | 0.001419 | 0.136806 | 0.086263 | 0.029551 | 10.77574 |
| Gun 2 | 0.004144 | 0.542895 | 0.280877 | 0.108468 | 36.58429 |
| Gun 3 | 0.001088 | 0.278374 | 0.11914 | 0.214156 | 71.42857 |
| Gun 4 | #VALUE! | 0.087818 | 0.057502 | 0.049622 | 26.6281 |
| Gun 5 | 0.002688 | 0.278426 | 0.046787 | 1.749874 | 709.5902 |
| Gun 6 | 0.001339 | 0.169003 | 0.076156 | 0.187754 | 8.610827 |
| Gun 7 | 0.001335 | 0.222881 | 0.063293 | 2.615721 | 649.9261 |
| Gun 8 | 0.008682 | 0.119033 | 0.038377 | 1.779156 | 77.41211 |
| Gun 9 | 0.002266 | 0.038095 | 0.044426 | 0.094439 | 38.13768 |
| Gun 10 | #VALUE! | 0.161244 | 0.07899 | 0.068735 | 5.261344 |
| | | | | | |
| Fe | Water | Step 1 | Step 2 | Step 3 | Res |
| C Gun 1 | 0.319446 | 0.107868 | 96.31878 | 21.26008 | 69753.2 |
| C Gun 2 | 0.360509 | 0.811624 | 66.23387 | 28.13065 | 30823.07 |
| C Gun 3 | 0.37342 | 1.054762 | 50.61201 | 18.90333 | 47024.11 |
| C Gun 9 | 0.410651 | 0.479083 | 102.3808 | 21.4553 | 33581.92 |
| C Gun 2 A | 0.327732 | 0.678126 | 66.60537 | 29.28674 | 30557.92 |
| | | | | | |
| Gun 1 | 1.041204 | 0.136565 | 78.10868 | 12.19623 | 8922.35 |
| Gun 2 | 0.485776 | 7.366338 | 90.94796 | 30.21416 | 58319.22 |
| Gun 3 | 0.415557 | 1.676349 | 42.68544 | 28.20388 | 20857.14 |
| Gun 4 | 0.714611 | 0.41212 | 80.38123 | 17.34407 | 44775.08 |
| Gun 5 | 0.093779 | 0.733046 | 18.94384 | 37.41921 | 6774.086 |
| Gun 6 | 0.949098 | 0.173463 | 87.89261 | 16.77703 | 52491.37 |
| Gun 7 | 0.111148 | 0.529341 | 14.24956 | 14.86903 | 4713.657 |
| Gun 8 | 0.207654 | 0.531831 | 28.03506 | 10.63526 | 18498.95 |
| Gun 9 | 0.288896 | 0.463641 | 93.46352 | 16.5847 | 39265.13 |
| Gun 10 | 0.331236 | 0.388063 | 65.09327 | 15.36314 | 37704.33 |
| | | | | | |
| Mg | Water | Step 1 | Step 2 | Step 3 | |
| C Gun 1 | 0.671761 | 5.765783 | 19.58062 | 1.953357 | 5308.57 |
| C Gun 2 | 0.47774 | 1.749542 | 2.430849 | 1.099154 | 6177.064 |
| C Gun 3 | 0.311384 | 0.662756 | 0.811385 | 0.805882 | 8203.19 |
| C Gun 9 | 0.226313 | 0.52203 | 3.910556 | 1.288129 | 2929.878 |
| C Gun 2 A | 0.316664 | 1.617369 | 2.568719 | 1.187684 | 5982.746 |
| | | | | | |
| Gun 1 | 0.136805 | 3.88163 | 19.91946 | 1.73511 | 3764.894 |
| Gun 2 | 0.085823 | 2.966376 | 8.501202 | 1.815195 | 4589.923 |
| Gun 3 | 0.122213 | 1.998365 | 1.273312 | 1.192584 | 5571.429 |
| Gun 4 | 0.110413 | 6.212026 | 7.084482 | 3.511272 | 4491.29 |
| Gun 5 | 0.043306 | 0.313157 | 0.599751 | 0.220961 | 619.1793 |
| Gun 6 | 0.059554 | 2.122464 | 1.584899 | 0.772807 | 2465.907 |
| Gun 7 | 0.0447 | 0.890647 | 1.450234 | 0.148392 | 746.0763 |
| Gun 8 | 0.079044 | 1.052366 | 0.619088 | 0.455438 | 3337.186 |
| Gun 9 | 0.072769 | 0.871191 | 4.481954 | 1.449917 | 2840.12 |

| | | | | | |
|-----------|----------|----------|----------|----------|----------|
| Gun 10 | 0.068287 | 4.929247 | 5.197745 | 1.854114 | 2611.207 |
| | | | | | |
| Mn | Water | Step 1 | Step 2 | Step 3 | |
| C Gun 1 | 0.087605 | 3.616602 | 27.68442 | 0.563888 | 186.9641 |
| C Gun 2 | 0.037628 | 3.580067 | 7.959886 | 0.158292 | 43.84538 |
| C Gun 3 | 0.007423 | 0.291918 | 0.191702 | 0.056872 | 41.13711 |
| C Gun 9 | 0.052175 | 2.036276 | 20.5078 | 0.257051 | 88.73043 |
| C Gun 2 A | 0.03228 | 3.261219 | 7.749353 | 0.16891 | 48.61083 |
| | | | | | |
| Gun 1 | 0.09399 | 2.86397 | 21.04999 | 0.483554 | 165.8183 |
| Gun 2 | 0.029375 | 8.351729 | 10.2375 | 0.266222 | 68.15399 |
| Gun 3 | 0.006149 | 0.497846 | 0.168527 | 0.10695 | 28.57143 |
| Gun 4 | 0.065582 | 5.312367 | 13.18063 | 0.348082 | 116.6454 |
| Gun 5 | 0.008396 | 0.57425 | 0.510466 | 0.046539 | 7.735257 |
| Gun 6 | 0.085581 | 2.878079 | 17.54813 | 0.427688 | 198.1408 |
| Gun 7 | 0.00661 | 0.850331 | 0.520213 | 0.003328 | 8.797182 |
| Gun 8 | 0.056664 | 0.896917 | 0.262763 | 0.016252 | 18.22832 |
| Gun 9 | 0.049683 | 2.04098 | 21.74145 | 0.294997 | 91.58062 |
| Gun 10 | 0.030416 | 3.810464 | 7.40951 | 0.236905 | 97.06541 |
| | | | | | |
| S | Water | Step 1 | Step 2 | Step 3 | |
| C Gun 1 | 1.593553 | 1.757925 | 5.594349 | 30.91946 | 7784.281 |
| C Gun 2 | 1.611379 | 0.592457 | 4.923813 | 45.85984 | 8864.097 |
| C Gun 3 | 2.444231 | 0.231701 | 5.855911 | 48.82717 | 13004.11 |
| C Gun 9 | 1.148845 | 0.214979 | 5.756004 | 32.20445 | 7146.17 |
| C Gun 2 A | 1.364556 | 0.576394 | 5.058735 | 49.0111 | 11361.08 |
| | | | | | |
| Gun 1 | 1.890595 | 1.74974 | 5.673699 | 26.70262 | 11216.64 |
| Gun 2 | 2.051168 | 0.636817 | 4.016791 | 54.37849 | 10041.07 |
| Gun 3 | 1.747976 | 0.47443 | 1.883411 | 56.59538 | 20285.71 |
| Gun 4 | 1.214243 | 0.800219 | 4.046079 | 23.81629 | 10852.37 |
| Gun 5 | 1.958151 | 0.506246 | 3.526388 | 147.7275 | 69910.4 |
| Gun 6 | 0.711093 | 0.548396 | 4.514073 | 18.84723 | 6273.891 |
| Gun 7 | 0.982537 | 0.847321 | 1.87288 | 154.2605 | 45261.7 |
| Gun 8 | 1.30918 | 2.244472 | 4.380745 | 104.2514 | 13931.54 |
| Gun 9 | 0.830713 | 0.397035 | 5.351139 | 27.29054 | 11111.98 |
| Gun 10 | 1.268449 | 0.651258 | 4.248502 | 18.93696 | 6612.838 |

CONCENTRATION GRAPHS







APPENDIX C – SUMMARY OF COLUMN LEACHATE DATA

pH DATA

| Week_pH | Blank | Gun 1 | Gun 2 | Gun 3 | Gun 9 |
|---------|-------|-------|-------|-------|-------|
| | 7.26 | 7.21 | 6.52 | 5.53 | 4.36 |
| 2 | 6.93 | 7.63 | 6.66 | 6.25 | 6.10 |
| | 7.67 | 7.43 | 6.92 | 6.53 | 6.77 |
| 4 | 7.58 | 7.37 | 6.93 | 6.61 | 6.69 |
| | 7.26 | 7.60 | 7.02 | 6.86 | 6.71 |
| 6 | 6.75 | 7.30 | 7.03 | 6.77 | 6.85 |
| | 7.24 | 6.96 | 6.71 | 6.57 | 6.61 |
| 8 | 7.48 | 7.07 | 6.85 | 6.76 | 6.68 |
| | 7.29 | 7.07 | 6.79 | 6.82 | 6.73 |
| 10 | 7.16 | 7.18 | 6.81 | 6.96 | 6.60 |
| | 7.11 | 7.16 | 6.84 | 6.92 | 6.64 |
| 12 | 7.45 | 7.07 | 6.86 | 6.88 | 6.78 |
| | 7.36 | 7.26 | 6.96 | 6.97 | 6.85 |
| 14 | 7.34 | 7.19 | 6.88 | 6.90 | 6.81 |
| | 7.32 | 7.18 | 6.94 | 6.99 | 6.84 |
| 16 | 7.09 | 7.24 | 6.98 | 6.91 | 6.71 |
| | 7.24 | 7.25 | 6.95 | 6.98 | 6.80 |
| 18 | 7.33 | 7.09 | 6.96 | 6.94 | 6.66 |
| | 7.09 | 7.20 | 6.97 | 6.86 | 6.71 |
| 20 | 7.37 | 7.37 | 7.10 | 6.87 | 6.83 |
| | 7.19 | 7.21 | 6.98 | 6.93 | 6.74 |
| 22 | 7.06 | 7.27 | 6.95 | 6.90 | 6.92 |
| | 7.02 | 7.12 | 6.96 | 6.87 | 6.69 |
| 24 | 6.82 | 7.20 | 6.91 | 6.86 | 6.70 |
| | 6.65 | 7.15 | 6.89 | 6.84 | 6.71 |
| 26 | 6.58 | 6.99 | 6.86 | 6.82 | 6.65 |
| | 6.54 | 6.92 | 6.77 | 6.70 | 6.48 |
| 28 | 6.62 | 6.93 | 6.71 | 6.62 | 6.54 |
| | 6.30 | 6.67 | 6.59 | 6.31 | 6.33 |
| 30 | 6.59 | 6.58 | 6.27 | 6.37 | 6.01 |
| | 6.33 | 6.40 | 6.25 | 6.21 | 5.94 |
| 32 | 6.29 | 7.04 | 6.91 | 6.84 | 6.59 |
| | 6.12 | 6.82 | 6.60 | 6.40 | 6.14 |
| 34 | 6.23 | 6.99 | 6.61 | 6.64 | 6.29 |
| | 6.35 | 7.08 | 6.52 | 6.66 | 6.30 |
| 36 | 6.12 | 6.91 | 6.56 | 6.48 | 6.13 |
| | 6.22 | 6.95 | 6.58 | 6.50 | 6.27 |
| 38 | 6.01 | 6.95 | 6.64 | 6.40 | 6.21 |
| | 6.29 | 7.13 | 6.61 | 6.35 | 6.05 |
| 40 | 5.65 | 6.88 | 6.39 | 6.21 | 6.20 |

E_H DATA (mV)

| Week_EH | Blank | Gun 1 | Gun 2 | Gun 3 | Gun 9 |
|---------|-------|-------|-------|-------|-------|
| 1 | 177 | 198 | 269 | 282 | 306 |
| 2 | 208 | 225 | 266 | 235 | 283 |
| 3 | 244 | 263 | 303 | 311 | 299 |
| 4 | 191 | 217 | 236 | 268 | 247 |
| 5 | 216 | 221 | 254 | 281 | 255 |
| 6 | 149 | 186 | 218 | 232 | 219 |
| 7 | 170 | 171 | 209 | 217 | 222 |
| 8 | 216 | 215 | 236 | 242 | 240 |
| 9 | 180 | 188 | 214 | 217 | 223 |
| 10 | 198 | 183 | 216 | 228 | 233 |
| 11 | 142 | 93 | 137 | 192 | 152 |
| 12 | 149 | 173 | 188 | 184 | 209 |
| 13 | 174 | 133 | 191 | 211 | 212 |
| 14 | 168 | 162 | 192 | 211 | 218 |
| 15 | 174 | 183 | 216 | 216 | 228 |
| 16 | 154 | 169 | 200 | 218 | 228 |
| 17 | 179 | 180 | 214 | 218 | 229 |
| 18 | 219 | 220 | 243 | 254 | 280 |
| 19 | 190 | 224 | 262 | 273 | 283 |
| 20 | 236 | 234 | 267 | 276 | 284 |
| 21 | 254 | 216 | 249 | 253 | 263 |
| 22 | 222 | 228 | 260 | 265 | 264 |
| 23 | 221 | 220 | 250 | 255 | 267 |
| 24 | 234 | 219 | 239 | 247 | 276 |
| 25 | 184 | 178 | 209 | 218 | 232 |
| 26 | 218 | 204 | 235 | 242 | 256 |
| 27 | 191 | 173 | 181 | 222 | 238 |
| 28 | 190 | 182 | 220 | 225 | 238 |
| 29 | 196 | 180 | 207 | 212 | 236 |
| 30 | 190 | 192 | 221 | 231 | 248 |
| 31 | 199 | 160 | 234 | 257 | 271 |
| 32 | 232 | 198 | 238 | 243 | 264 |
| 33 | 254 | 173 | 212 | 215 | 235 |
| 34 | 262 | 228 | 250 | 251 | 270 |
| 35 | 189 | 217 | 169 | 243 | 197 |
| 36 | 220 | 206 | 230 | 243 | 252 |
| 37 | 219 | 187 | 220 | 235 | 243 |
| 38 | 255 | 184 | 224 | 214 | 254 |
| 39 | 260 | 216 | 257 | 263 | 269 |
| 40 | 235 | 197 | 233 | 248 | 252 |

VOLUME DATA (mL)

| Week | Water In | Gun 1 | Gun 2 | Gun 3 | Gun 9 |
|------|----------|-------|-------|-------|-------|
| | 580 | 500 | 500 | 500 | 500 |
| 2 | 635 | 610 | 630 | 620 | 630 |
| | 801 | 800 | 750 | 710 | 790 |
| 4 | 745 | 685 | 690 | 685 | 690 |
| | 580 | 550 | 570 | 565 | 575 |
| 6 | 635 | 615 | 580 | 610 | 620 |
| | 801 | 800 | 800 | 790 | 795 |
| 8 | 745 | 745 | 700 | 710 | 720 |
| | 580 | 575 | 580 | 535 | 570 |
| 10 | 635 | 620 | 625 | 615 | 605 |
| | 801 | 770 | 760 | 685 | 735 |
| 12 | 745 | 720 | 710 | 645 | 645 |
| | 580 | 560 | 555 | 540 | 545 |
| 14 | 635 | 615 | 610 | 595 | 615 |
| | 801 | 780 | 770 | 765 | 740 |
| 16 | 745 | 725 | 695 | 720 | 715 |
| | 580 | 580 | 570 | 545 | 545 |
| 18 | 635 | 620 | 625 | 615 | 565 |
| | 801 | 760 | 775 | 750 | 745 |
| 20 | 745 | 745 | 660 | 710 | 695 |
| | 580 | 560 | 530 | 555 | 490 |
| 22 | 635 | 625 | 570 | 575 | 560 |
| | 801 | 790 | 735 | 710 | 760 |
| 24 | 745 | 725 | 670 | 710 | 710 |
| | 580 | 570 | 525 | 535 | 535 |
| 26 | 635 | 630 | 590 | 615 | 600 |
| | 801 | 780 | 750 | 770 | 760 |
| 28 | 745 | 720 | 685 | 740 | 690 |
| | 580 | 545 | 550 | 530 | 550 |
| 30 | 635 | 595 | 555 | 575 | 650 |
| | 801 | 795 | 720 | 695 | 710 |
| 32 | 745 | 740 | 685 | 710 | 715 |
| | 580 | 560 | 535 | 545 | 545 |
| 34 | 635 | 595 | 605 | 610 | 595 |
| | 801 | 790 | 770 | 680 | 690 |
| 36 | 745 | 680 | 705 | 715 | 685 |
| | 580 | 560 | 510 | 510 | 545 |
| 38 | 635 | 625 | 590 | 595 | 595 |
| | 801 | 780 | 790 | 760 | 750 |
| 40 | 745 | 715 | 710 | 720 | 705 |

ELEMENT DATA (µg/L)

| GUN 1 | | | | | | | | | | | | |
|-------|--------|---------|---------|----------|---------|---------|---------|-----------|-----------|----------|---------|----------|
| Week | Sample | Al | Ba | Ca | Cd | Cu | Fe | Mg | Mn | Pb | S | Zn |
| | | 396.152 | 233.527 | 317.933 | 214.439 | 327.395 | 259.940 | 279.553 | 257.610 | 217.000 | 180.669 | 206.200 |
| | LOD | 100.00 | 5.00 | 600.00 | 2.00 | 20.00 | 100 | 30 | 1 | 100 | 100 | 70 |
| 1 | 1 g1 | 100.00 | 112.34 | 64488.37 | 2.00 | 20.00 | 100 | 12331.377 | 73.140672 | 100 | 18834.8 | 120.2891 |
| 2 | 2 g1 | 100.00 | 71.91 | 58268.27 | 2.00 | 20.00 | 100 | 6846.081 | 40.575869 | 100 | 22167.8 | 70 |
| 3 | 3 g1 | 100.00 | 114.18 | 37339.79 | 2.00 | 20.00 | 100 | 4365.2507 | 23.339358 | 100 | 10898.3 | 70 |
| 4 | 4 g1 | 100.00 | 184.99 | 32727.32 | 2.00 | 20.00 | 100 | 3988.5079 | 18.035471 | 100 | 7888.3 | 70 |
| 5 | 5 g1 | 100.00 | 276.29 | 30801.91 | 2.00 | 20.00 | 100 | 3704.2889 | 12.264126 | 100 | 6950.75 | 70 |
| 6 | 6 g1 | 100.00 | 281.78 | 24325.80 | 2.00 | 20.00 | 100 | 2948.8871 | 4.2358806 | 100 | 4170.39 | 70 |
| 7 | 7 g1 | 100.00 | 242.59 | 17957.81 | 2.00 | 20.00 | 100 | 2155.1287 | 1.8779269 | 100 | 3012.41 | 70 |
| 8 | 8 g1 | 100.00 | 392.00 | 25890.07 | 2.00 | 20.00 | 100 | 3126.8237 | 4.9385762 | 100 | 4242.88 | 70 |
| 9 | 9 g1 | 100.00 | 467.04 | 28506.72 | 2.00 | 20.00 | 100 | 3423.5553 | 6.3556878 | 100 | 4222.89 | 70 |
| 10 | 10 g1 | 100.00 | 394.65 | 22183.01 | 2.00 | 20.00 | 100 | 2579.2125 | 1.6556379 | 100 | 3043.17 | 70 |
| 11 | 11 g1 | 100.00 | 393.41 | 21356.30 | 2.00 | 20.00 | 100 | 2401.4673 | 1.0848741 | 100 | 2717.06 | 70 |
| 12 | 12 g1 | 100.00 | 390.99 | 19652.00 | 2.00 | 20.00 | 100 | 2161.2845 | 1 | 100 | 2494.59 | 70 |
| 13 | 13 g1 | 100.00 | 438.96 | 20823.52 | 2.00 | 20.00 | 100 | 2221.1668 | 1.1392159 | 100 | 2894.96 | 70 |
| 14 | 14 g1 | 100.00 | 470.24 | 21396.05 | 2.00 | 20.00 | 100 | 2273.8225 | 1.6350652 | 174.8471 | 2672.26 | 122.0237 |
| 15 | 15 g1 | 100.00 | 380.68 | 16470.98 | 2.00 | 20.00 | 100 | 1752.8418 | 1 | 100 | 1874.52 | 70 |
| 16 | 16 g1 | 100.00 | 516.77 | 21957.47 | 2.00 | 20.00 | 100 | 2314.7862 | 1 | 100 | 2917.35 | 70 |
| 17 | 17 g1 | 100.00 | 372.50 | 15734.57 | 2.00 | 20.00 | 100 | 1668.631 | 1 | 100 | 3090.84 | 70 |
| 18 | 18 g1 | 100.00 | 682.42 | 26044.73 | 2.00 | 20.00 | 100 | 2816.7471 | 1 | 100 | 3304.95 | 70 |

| | | | | | | | | | | | | |
|----|-------|--------|--------|----------|------|-------|-----|-----------|---|----------|---------|----|
| 19 | 19 g1 | 100.00 | 507.21 | 18556.14 | 2.00 | 20.00 | 100 | 1926.3122 | 1 | 100 | 2273.49 | 70 |
| 20 | 20 g1 | 100.00 | 458.69 | 16478.23 | 2.00 | 20.00 | 100 | 1711.3111 | 1 | 100 | 2135.08 | 70 |
| 21 | 21 g1 | 100.00 | 558.07 | 20362.32 | 2.00 | 20.00 | 100 | 2053.8319 | 1 | 100 | 2447.17 | 70 |
| 22 | 22 g1 | 100.00 | 509.08 | 17809.35 | 2.00 | 20.00 | 100 | 1850.5365 | 1 | 100 | 2100.44 | 70 |
| 23 | 23 g1 | 100.00 | 549.44 | 18391.09 | 2.00 | 20.00 | 100 | 1880.1892 | 1 | 100 | 2450.99 | 70 |
| 24 | 24 g1 | 100.00 | 579.84 | 19571.56 | 2.00 | 20.00 | 100 | 1968.7985 | 1 | 100 | 2308.89 | 70 |
| 25 | 25 g1 | 100.00 | 673.22 | 20810.86 | 2.00 | 20.00 | 100 | 2079.533 | 1 | 100 | 2480.72 | 70 |
| 26 | 26 g1 | 100.00 | 653.52 | 20424.55 | 2.00 | 20.00 | 100 | 2038.2638 | 1 | 100 | 2411.58 | 70 |
| 27 | 27 g1 | 100.00 | 603.88 | 19281.05 | 2.00 | 20.00 | 100 | 1932.9079 | 1 | 100 | 2132.85 | 70 |
| 28 | 28 g1 | 100.00 | 622.85 | 19212.51 | 2.00 | 20.00 | 100 | 1942.5848 | 1 | 100 | 2255.99 | 70 |
| 29 | 29 g1 | 100.00 | 740.77 | 22079.55 | 2.00 | 20.00 | 100 | 2249.7119 | 1 | 269.279 | 2664.48 | 70 |
| 30 | 30 g1 | 100.00 | 663.41 | 19501.40 | 2.00 | 20.00 | 100 | 1909.9476 | 1 | 121.3947 | 2160.98 | 70 |
| 31 | 31 g1 | 100.00 | 440.82 | 13160.62 | 2.00 | 20.00 | 100 | 1314.8928 | 1 | 100 | 1493.9 | 70 |
| 32 | 32 g1 | 100.00 | 554.93 | 16217.34 | 2.00 | 20.00 | 100 | 1586.457 | 1 | 203.3626 | 1867 | 70 |
| 33 | 33 g1 | 100.00 | 732.06 | 20337.18 | 2.00 | 20.00 | 100 | 2003.4503 | 1 | 100 | 2489.88 | 70 |
| 34 | 34 g1 | 100.00 | 747.62 | 21270.88 | 2.00 | 20.00 | 100 | 2087.814 | 1 | 100 | 2821.03 | 70 |
| 35 | 35 g1 | 100.00 | 810.21 | 22017.64 | 2.00 | 20.00 | 100 | 2235.1536 | 1 | 100 | 2648.42 | 70 |
| 36 | 36 g1 | 100.00 | 537.49 | 15711.96 | 2.00 | 20.00 | 100 | 1499.0421 | 1 | 100 | 1635.3 | 70 |
| 37 | 37 g1 | 100.00 | 591.78 | 16874.79 | 2.00 | 20.00 | 100 | 1588.8744 | 1 | 100 | 1984.84 | 70 |
| 38 | 38 g1 | 100.00 | 623.68 | 17525.48 | 2.00 | 20.00 | 100 | 1645.1631 | 1 | 100 | 2144.2 | 70 |
| 39 | 39 g1 | 100.00 | 614.40 | 16512.23 | 2.00 | 20.00 | 100 | 1554.1 | 1 | 100 | 2171.21 | 70 |
| 40 | 40 g1 | 100.00 | 574.24 | 15743.52 | 2.00 | 20.00 | 100 | 1444.3952 | 1 | 100 | 1777.21 | 70 |

| GUN 2 | | | | | | | | | | | | |
|-------|---------------|---------------|---------------|---------------|---------------|---------------|---------------|---------------|---------------|---------------|--------------|---------------|
| | Sample Labels | Al 396.152 | Ba 233.527 | Ca 317.933 | Cd 214.439 | Cu 327.395 | Fe 259.940 | Mg 279.553 | Mn 257.610 | Pb 217.000 | S 180.669 | Zn 206.200 |
| | LOD | 100.00 | 5.00 | 600.00 | 2.00 | 20.00 | 100 | 30 | 1 | 100 | 100 | 70 |
| 1 | 1 g2 | 280.32 | 21.15 | 390000.00 | 996.85 | 20.00 | 100 | 25027.13 | 67.69214 | 100 | 505000 | 33579.95 |
| 2 | 2 g2 | 204.62 | 47.51 | 362000.00 | 708.10 | 20.00 | 100 | 16059.25 | 206.9943 | 100 | 506000 | 19002.93 |
| 3 | 3 g2 | 133.92 | 78.53 | 112329.83 | 310.51 | 20.00 | 100 | 5619.748 | 55.24099 | 100 | 93355.82 | 9546.815 |
| 4 | 4 g2 | 127.72 | 91.12 | 67016.39 | 221.85 | 20.00 | 100 | 3487.278 | 21.34899 | 100 | 50527.69 | 7913.727 |
| 5 | 5 g2 | 111.65 | 73.59 | 46751.48 | 181.66 | 24.58 | 100 | 2521.786 | 7.411562 | 100 | 30894.5 | 6599.705 |
| 6 | 6 g2 | 118.53 | 67.26 | 41329.01 | 164.21 | 20.00 | 100 | 2234.963 | 4.585853 | 135.471 | 24679.15 | 6307.772 |
| 7 | 7 g2 | 100.00 | 56.74 | 34285.44 | 131.85 | 24.45 | 100 | 1831.274 | 4.162541 | 100 | 18900.97 | 5146.832 |
| 8 | 8 g2 | 112.08 | 53.97 | 26648.06 | 105.85 | 20.00 | 100 | 1459.059 | 2.558478 | 311.3248 | 11691.57 | 4078.061 |
| 9 | 9 g2 | 100.00 | 59.86 | 27558.69 | 103.56 | 20.00 | 100 | 1416.919 | 2.370267 | 211.9002 | 11733.15 | 4421.847 |
| 10 | 10 g2 | 100.00 | 74.84 | 25027.28 | 89.47 | 20.00 | 100 | 1293.126 | 2.714903 | 100 | 10255.59 | 3740.901 |
| 11 | 11 g2 | 100.00 | 89.86 | 19465.80 | 87.21 | 20.00 | 100 | 1250.98 | 1.9988 | 100 | 6677.17 | 3734.011 |
| 12 | 12 g2 | 100.00 | 123.01 | 24577.08 | 86.18 | 20.00 | 100 | 1209.337 | 1.839192 | 199.1969 | 8492.237 | 3789.14 |
| 13 | 13 g2 | 100.00 | 130.86 | 22027.87 | 76.71 | 20.00 | 100 | 1066.265 | 1.277426 | 100 | 7458.736 | 3261.796 |
| 14 | 14 g2 | 100.00 | 154.81 | 23126.53 | 79.43 | 20.00 | 100 | 1151.459 | 1.578664 | 100 | 6846.858 | 3367.086 |
| 15 | 15 g2 | 100.00 | 166.38 | 21135.17 | 63.10 | 20.00 | 100 | 1092.662 | 0.964511 | 100 | 6186.143 | 3014.525 |
| 16 | 16 g2 | 100.00 | 184.35 | 20588.51 | 60.83 | 20.00 | 100 | 982.561 | 0.896638 | 100 | 5878.454 | 2942.282 |
| 17 | 17 g2 | 100.00 | 154.41 | 24935.42 | 40.14 | 20.00 | 100 | 782.7519 | 1 | 100 | 9359.794 | 3798.446 |
| 18 | 18 g2 | 100.00 | 219.67 | 20922.83 | 48.24 | 20.00 | 431.2251 | 1124.424 | 2.893487 | 100 | 4789.822 | 2685.311 |
| 19 | 19 g2 | 100.00 | 253.18 | 20715.65 | 58.26 | 20.00 | 100 | 989.4381 | 0.946044 | 100 | 4907.021 | 2760.842 |
| 20 | 20 g2 | 100.00 | 251.99 | 18895.50 | 55.39 | 20.00 | 100 | 914.1884 | 1 | 289.722 | 4729.375 | 2586.985 |

| | | | | | | | | | | | | |
|----|-------|--------|--------|----------|-------|-------|-----|----------|---------|----------|----------|----------|
| 21 | 21 g2 | 100.00 | 259.51 | 19547.39 | 49.45 | 20.00 | 100 | 972.6558 | 1 | 100 | 4198.971 | 2440.284 |
| 22 | 22 g2 | 100.00 | 311.83 | 21488.37 | 54.50 | 20.00 | 100 | 1055.616 | 1.19384 | 100 | 4664.444 | 2632.589 |
| 23 | 23 g2 | 100.00 | 330.82 | 19592.66 | 54.75 | 20.00 | 100 | 911.9895 | 1 | 100 | 4449.736 | 2357.832 |
| 24 | 24 g2 | 100.00 | 317.19 | 18372.97 | 51.62 | 20.00 | 100 | 859.4488 | 1 | 100 | 4213.728 | 2286.527 |
| 25 | 25 g2 | 100.00 | 331.93 | 18253.22 | 50.07 | 20.00 | 100 | 887.0794 | 1 | 100 | 3907.356 | 2243.476 |
| 26 | 26 g2 | 100.00 | 355.13 | 18833.82 | 51.10 | 20.00 | 100 | 883.1526 | 1 | 100 | 3952.709 | 2186.963 |
| 27 | 27 g2 | 100.00 | 333.64 | 16902.70 | 44.30 | 20.00 | 100 | 780.4593 | 1 | 100 | 3515.186 | 1888.318 |
| 28 | 28 g2 | 100.00 | 253.95 | 12308.15 | 33.12 | 20.00 | 100 | 565.4062 | 1 | 100 | 2336.523 | 1375.753 |
| 29 | 29 g2 | 100.00 | 381.29 | 18939.16 | 46.87 | 20.00 | 100 | 885.5866 | 1 | 100 | 3637.04 | 2058.764 |
| 30 | 30 g2 | 100.00 | 392.67 | 17505.20 | 46.55 | 20.00 | 100 | 808.4174 | 1 | 133.7434 | 3348.739 | 1939.793 |
| 31 | 31 g2 | 100.00 | 367.07 | 15649.69 | 42.52 | 20.00 | 100 | 721.8929 | 1 | 266.6036 | 3082.063 | 1713.239 |
| 32 | 32 g2 | 100.00 | 340.05 | 14230.64 | 39.25 | 20.00 | 100 | 645.295 | 1 | 100 | 3034.758 | 1571.868 |
| 33 | 33 g2 | 100.00 | 433.80 | 17287.38 | 43.95 | 20.00 | 100 | 851.5128 | 1 | 100 | 3137.041 | 1979.885 |
| 34 | 34 g2 | 100.00 | 400.29 | 15654.06 | 37.38 | 20.00 | 100 | 728.6749 | 1 | 100 | 3033.83 | 1649.75 |
| 35 | 35 g2 | 100.00 | 319.14 | 12109.18 | 28.42 | 20.00 | 100 | 542.2538 | 1 | 100 | 2456.685 | 1231.837 |
| 36 | 36 g2 | 100.00 | 336.73 | 12516.03 | 31.88 | 20.00 | 100 | 565.5081 | 1 | 100 | 2447.665 | 1257.273 |
| 37 | 37 g2 | 100.00 | 423.97 | 15744.94 | 35.41 | 20.00 | 100 | 757.5813 | 1 | 100 | 3348.506 | 1533.209 |
| 38 | 38 g2 | 100.00 | 464.56 | 16217.50 | 38.99 | 20.00 | 100 | 784.2424 | 1 | 100 | 3191.533 | 1635.26 |
| 39 | 39 g2 | 100.00 | 407.01 | 13906.18 | 33.56 | 20.00 | 100 | 635.6839 | 1 | 100 | 2893.324 | 1362.128 |
| 40 | 40 g2 | 100.00 | 432.68 | 14083.80 | 32.85 | 20.00 | 100 | 656.1321 | 1 | 100 | 2547.217 | 1437.571 |

| GUN 3 | | | | | | | | | | | | |
|-------|---------------|---------------|---------------|------------|---------------|---------------|---------------|---------------|---------------|---------------|--------------|---------------|
| | Sample Labels | Al 396.152 | Ba 233.527 | Ca 317.933 | Cd 214.439 | Cu 327.395 | Fe 259.940 | Mg 279.553 | Mn 257.610 | Pb 217.000 | S 180.669 | Zn 206.200 |
| | LOD | 100.00 | 5.00 | 600.00 | 2.00 | 20.00 | 100 | 30 | 1 | 100 | 100 | 70 |
| 1 | 1 g3 | 11900.00 | 35.80 | 145338.40 | 35.37 | 45.79 | 405.76 | 29800 | 934.9947 | 100 | 143352 | 7061.277 |
| 2 | 2 g3 | 6813.03 | 50.81 | 97094.46 | 618.89 | 20.00 | 100 | 11999.3 | 1401.626 | 100 | 124566.9 | 55382.54 |
| 3 | 3 g3 | 1612.25 | 65.09 | 87031.06 | 371.72 | 20.00 | 100 | 9232.613 | 970.9094 | 328.7741 | 95312.55 | 41936.89 |
| 4 | 4 g3 | 1006.67 | 52.24 | 68539.16 | 250.12 | 22.00 | 100 | 7215.617 | 714.1233 | 100 | 73261.49 | 29277.64 |
| 5 | 5 g3 | 584.07 | 58.49 | 82766.85 | 212.59 | 57.82 | 100 | 6424.602 | 608.9601 | 325.0752 | 63656.08 | 24170.38 |
| 6 | 6 g3 | 563.17 | 62.80 | 63299.32 | 171.73 | 20.00 | 210.9199 | 6212.599 | 559.1 | 298.8623 | 56919.69 | 19557.6 |
| 7 | 7 g3 s2 | 296.65 | 50.06 | 51548.94 | 120.51 | 20.00 | 100 | 4930.303 | 409.5705 | 100 | 44286.65 | 13494.9 |
| 8 | 8 g3 | 316.38 | 55.08 | 49635.53 | 114.69 | 20.00 | 100 | 4657.92 | 367.8735 | 100 | 42910.59 | 12748.36 |
| 9 | 9 g3 | 208.58 | 60.36 | 44114.99 | 90.61 | 20.00 | 100 | 4083.698 | 309.2829 | 100 | 39227.01 | 10261.19 |
| 10 | 10 g3 | 218.02 | 84.42 | 47906.75 | 92.03 | 20.00 | 100 | 4292.004 | 313.9034 | 359.2505 | 41169.19 | 9655.108 |
| 11 | 11 g3 | 171.37 | 84.63 | 48013.97 | 86.21 | 20.00 | 100 | 4144.2 | 287.0091 | 100 | 36759.53 | 9163.512 |
| 12 | 12 g3 | 120.53 | 76.63 | 45129.10 | 78.54 | 20.00 | 100 | 3719.554 | 258.8704 | 400.0934 | 35910.48 | 7829.666 |
| 13 | 13 g3 | 133.21 | 78.69 | 38487.78 | 61.50 | 20.00 | 100 | 3120.389 | 207.1859 | 271.6021 | 34813.86 | 6280.508 |
| 14 | 14 g3 | 150.61 | 87.35 | 36051.39 | 60.43 | 20.00 | 100 | 2799.023 | 180.162 | 177.0361 | 29046.83 | 5646.752 |
| 15 | 15 g3 | 111.95 | 85.55 | 28394.49 | 49.31 | 20.00 | 100 | 2285.199 | 147.1571 | 192.4818 | 22334.29 | 4601.418 |
| 16 | 16 g3 | 130.74 | 115.54 | 25468.70 | 56.41 | 20.00 | 100 | 2057.594 | 132.2561 | 191.4375 | 19399.9 | 4880.37 |
| 17 | 17 g3 | 100.00 | 125.08 | 20376.82 | 47.97 | 20.00 | 100 | 1674.78 | 97.00627 | 100 | 14031.08 | 3872.372 |
| 18 | 18 g3 | 147.06 | 164.49 | 22746.19 | 54.88 | 20.00 | 100 | 1830.073 | 92.84419 | 282.8474 | 15000 | 4621.56 |
| 19 | 19 g3 | 160.91 | 157.75 | 22021.60 | 49.52 | 20.00 | 100 | 1805.541 | 77.06127 | 154.9868 | 16207.77 | 4692.515 |
| 20 | 20 g3 | 144.97 | 153.53 | 19947.24 | 50.23 | 20.00 | 100 | 1644.497 | 46.80955 | 173.7456 | 18401.8 | 4189.512 |

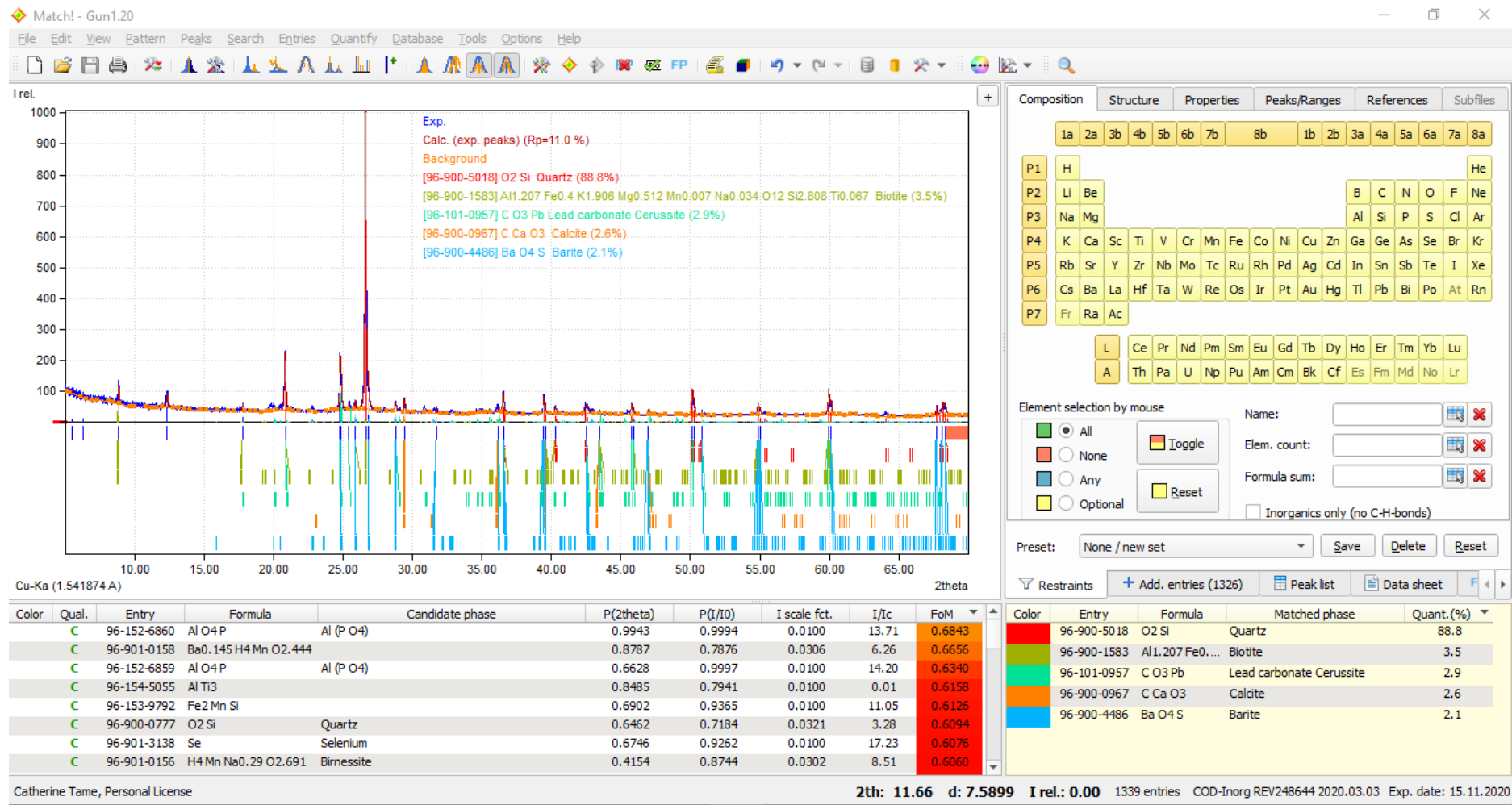
| | | | | | | | | | | | | |
|----|-------|--------|--------|----------|-------|-------|----------|----------|----------|----------|----------|----------|
| 21 | 21 g3 | 100.00 | 170.73 | 19430.98 | 42.89 | 20.00 | 100 | 1593.801 | 36.8324 | 100 | 15624.99 | 3760.037 |
| 22 | 22 g3 | 113.06 | 191.49 | 21859.25 | 43.57 | 20.00 | 100 | 1759.789 | 33.92419 | 100 | 14707.75 | 3917.101 |
| 23 | 23 g3 | 120.49 | 201.77 | 18994.52 | 35.90 | 20.00 | 100 | 1555.701 | 20.52142 | 100 | 11972.99 | 3586.391 |
| 24 | 24 g3 | 126.36 | 172.01 | 16877.25 | 36.63 | 20.00 | 100 | 1357.844 | 7.916772 | 100 | 11062.54 | 3216.615 |
| 25 | 25 g3 | 102.27 | 170.32 | 16223.81 | 23.03 | 20.00 | 100 | 1183.909 | 10.90578 | 100 | 14967.56 | 6498.037 |
| 26 | 26 g3 | 100.00 | 212.21 | 17213.53 | 28.24 | 20.00 | 100 | 1405.995 | 2.856906 | 100 | 10735.88 | 2992.575 |
| 27 | 27 g3 | 101.09 | 203.17 | 15027.69 | 24.77 | 20.00 | 100 | 1231.13 | 1.797994 | 100 | 8753.285 | 2708.852 |
| 28 | 28 g3 | 139.50 | 190.91 | 14796.11 | 25.02 | 20.00 | 248.9233 | 1240.955 | 2.491158 | 168.7116 | 8735.008 | 2508.82 |
| 29 | 29 g3 | 100.00 | 240.57 | 14832.81 | 23.63 | 20.00 | 100 | 1241.049 | 1.013795 | 100 | 8652.224 | 2505.794 |
| 30 | 30 g3 | 100.00 | 247.53 | 14398.22 | 22.62 | 20.00 | 100 | 1179.219 | 1 | 100 | 8089.433 | 2448.588 |
| 31 | 31 g3 | 100.00 | 207.96 | 10992.59 | 17.45 | 20.00 | 100 | 895.2793 | 1 | 100 | 5856.906 | 1848.297 |
| 32 | 32 g3 | 100.00 | 228.75 | 11476.22 | 20.29 | 20.00 | 100 | 929.9182 | 1 | 100 | 6388.517 | 1927.128 |
| 33 | 33 g3 | 105.51 | 265.40 | 12031.12 | 21.27 | 20.00 | 100 | 1005.946 | 1 | 100 | 6535.427 | 2003.981 |
| 34 | 34 g3 | 106.22 | 279.91 | 11178.42 | 20.29 | 20.00 | 100 | 910.1574 | 1 | 100 | 6293.725 | 1883.67 |
| 35 | 35 g3 | 100.00 | 249.66 | 10462.61 | 17.52 | 20.00 | 100 | 858.5435 | 1 | 100 | 5493.415 | 1729.708 |
| 36 | 36 g3 | 100.00 | 239.63 | 9497.01 | 16.68 | 20.00 | 100 | 730.4525 | 1 | 100 | 4912.432 | 1563.26 |
| 37 | 37 g3 | 100.00 | 284.49 | 10485.03 | 18.76 | 20.00 | 100 | 859.3318 | 1 | 100 | 6178.144 | 1728.752 |
| 38 | 38 g3 | 100.00 | 299.89 | 10723.83 | 20.68 | 20.00 | 100 | 879.4669 | 1 | 100 | 5718.245 | 1796.038 |
| 39 | 39 g3 | 100.00 | 332.24 | 9977.16 | 16.50 | 20.00 | 100 | 790.5225 | 1 | 100 | 5698.903 | 1623.8 |
| 40 | 40 g3 | 100.00 | 290.96 | 9304.83 | 17.25 | 20.00 | 100 | 729.7171 | 1 | 100 | 4818.966 | 1531.903 |

| GUN 9 | | | | | | | | | | | | |
|-------|---------------|---------------|---------------|------------|---------------|---------------|---------------|---------------|---------------|---------------|--------------|---------------|
| | Sample Labels | Al 396.152 | Ba 233.527 | Ca 317.933 | Cd 214.439 | Cu 327.395 | Fe 259.940 | Mg 279.553 | Mn 257.610 | Pb 217.000 | S 180.669 | Zn 206.200 |
| | LOD | 100.00 | 5.00 | 600.00 | 2.00 | 20.00 | 100 | 30 | 1 | 100 | 100 | 70 |
| 1 | 1 g9 | 945.99 | 7026.81 | 189742.70 | 289.10 | 20.00 | 100 | 25300 | 346.0212 | 6061.048 | 3633.119 | 50200 |
| 2 | 2 g9 | 469.45 | 2702.31 | 61901.37 | 138.22 | 20.00 | 100 | 9526.608 | 192.1881 | 3136.445 | 2431.268 | 29590.18 |
| 3 | 3 g9 | 432.72 | 766.43 | 10579.77 | 34.79 | 20.00 | 100 | 1723.27 | 36.16568 | 466.0469 | 6433.856 | 5564.361 |
| 4 | 4 g9 | 501.35 | 676.64 | 8635.10 | 25.41 | 20.00 | 100 | 1468.943 | 66.10595 | 506.8681 | 6365.366 | 4846.055 |
| 5 | 5 g9 | 527.42 | 692.08 | 8602.28 | 33.39 | 20.00 | 100 | 1409.432 | 148.2938 | 949.5757 | 4939.359 | 4957.568 |
| 6 | 6 g9 | 396.54 | 692.07 | 8520.94 | 34.26 | 20.00 | 100 | 1381.951 | 202.2176 | 685.0949 | 4525.988 | 5534.496 |
| 7 | 7 g9 | 539.79 | 663.79 | 7989.40 | 27.83 | 20.00 | 100 | 1319.638 | 267.5694 | 1320 | 3997.452 | 4856.863 |
| 8 | 8 g9 | 417.49 | 571.13 | 7821.54 | 24.32 | 20.00 | 100 | 1214.164 | 279.4621 | 1044.658 | 3399.034 | 4584.414 |
| 9 | 9 g9 | 422.58 | 613.44 | 8058.62 | 28.39 | 20.00 | 100 | 1255.864 | 313.6668 | 1492.669 | 3423.22 | 4767.585 |
| 10 | 10 g9 | 345.48 | 594.14 | 7705.86 | 25.57 | 21.88 | 100 | 1236.351 | 346.2612 | 1639.156 | 3171.658 | 5051.632 |
| 11 | 11 g9 | 381.81 | 608.06 | 7791.45 | 23.05 | 20.00 | 100 | 1199.395 | 398.6133 | 1469.646 | 3036.667 | 4570.031 |
| 12 | 12 g9 | 304.24 | 563.59 | 7827.02 | 24.57 | 20.00 | 100 | 1144.15 | 413.0201 | 1673.015 | 2869.048 | 4744.281 |
| 13 | 13 g9 | 298.76 | 595.86 | 7932.78 | 22.76 | 20.00 | 100 | 1113.822 | 418.7244 | 1829.861 | 2810.992 | 4681.983 |
| 14 | 14 g9 | 313.56 | 578.10 | 7916.03 | 24.78 | 20.00 | 100 | 1129.793 | 396.8092 | 1595.87 | 2689.464 | 4713.239 |
| 15 | 15 g9 | 326.48 | 584.69 | 7200.94 | 21.46 | 20.00 | 100 | 1045.16 | 364.0094 | 1714.364 | 2353.914 | 4459.887 |
| 16 | 16 g9 | 331.76 | 565.97 | 7665.59 | 22.59 | 20.00 | 100 | 1034.925 | 325.4371 | 1891.951 | 2596.951 | 4674.103 |
| 17 | 17 g9 | 329.11 | 523.68 | 6474.35 | 21.90 | 20.00 | 100 | 925.8656 | 260.6118 | 2567.161 | 3117.856 | 4382.998 |
| 18 | 18 g9 | 310.82 | 694.27 | 7736.04 | 23.42 | 20.00 | 100 | 1094.511 | 308.979 | 3070.244 | 2500.879 | 5340.31 |
| 19 | 19 g9 | 315.76 | 641.31 | 7340.24 | 22.54 | 20.00 | 100 | 1052.413 | 310.596 | 1691.335 | 2526.937 | 5104.182 |
| 20 | 20 g9 | 343.17 | 611.35 | 6824.75 | 26.13 | 20.00 | 100 | 973.03 | 321.8063 | 2395.773 | 2327.082 | 4919.505 |

| | | | | | | | | | | | | |
|----|----------|--------|--------|---------|-------|-------|-----|----------|----------|----------|----------|----------|
| 21 | 21 g9 | 284.85 | 633.06 | 7095.06 | 28.59 | 20.00 | 100 | 988.4002 | 290.5211 | 2843.393 | 2144.516 | 5177.142 |
| 22 | 22 g9 | 253.44 | 633.84 | 8003.01 | 18.92 | 20.00 | 100 | 1019.654 | 288.5273 | 1945.054 | 2931.328 | 4973.06 |
| 23 | 23 g9 | 273.27 | 645.71 | 7260.00 | 23.20 | 20.00 | 100 | 993.2058 | 317.9491 | 1885.907 | 2516.955 | 5077.009 |
| 24 | 24 g9 | 284.17 | 619.09 | 7028.29 | 21.85 | 20.00 | 100 | 960.1767 | 325.2294 | 2385.129 | 2066.582 | 4925.274 |
| 25 | 25 g9 | 270.16 | 591.30 | 6807.87 | 23.19 | 20.00 | 100 | 920.8424 | 293.3618 | 2504.355 | 2014.009 | 4790.048 |
| 26 | 26 g9 | 299.38 | 695.66 | 7191.31 | 22.74 | 20.00 | 100 | 978.9614 | 303.7135 | 2505.077 | 2164.29 | 5167.73 |
| 27 | 27 g9 | 279.39 | 671.30 | 7167.63 | 21.92 | 20.00 | 100 | 1003.041 | 307.4966 | 2475.27 | 2163.618 | 5463.08 |
| 28 | 28 g9 s2 | 245.98 | 706.76 | 7168.88 | 29.26 | 20.00 | 100 | 981.1745 | 327.1622 | 3039.471 | 1967.042 | 5767.181 |
| 29 | 29 g9 | 342.69 | 673.63 | 6863.70 | 26.30 | 20.00 | 100 | 961.7805 | 310.9505 | 2753.321 | 2135.392 | 5414.938 |
| 30 | 30 g9 | 302.41 | 704.91 | 7172.61 | 21.68 | 20.00 | 100 | 979.2274 | 322.5836 | 2957.386 | 2176.65 | 5751.943 |
| 31 | 31 g9 | 304.16 | 681.45 | 6924.72 | 26.83 | 20.00 | 100 | 954.7485 | 316.258 | 2639.796 | 2118.445 | 5604.831 |
| 32 | 32 g9 | 240.48 | 657.63 | 6506.30 | 24.85 | 20.00 | 100 | 866.67 | 266.1247 | 1902.445 | 2019.392 | 5186.258 |
| 33 | 33 g9 | 299.75 | 647.44 | 6546.59 | 16.83 | 20.00 | 100 | 892.4339 | 221.0795 | 2199.729 | 2039.351 | 5240.467 |
| 34 | 34 g9 | 277.71 | 682.74 | 6692.67 | 26.74 | 20.00 | 100 | 898.2507 | 198.924 | 2598.006 | 2157.248 | 5593.484 |
| 35 | 35 g9 | 286.94 | 679.79 | 7015.83 | 27.17 | 20.00 | 100 | 1011.588 | 165.6493 | 2771.395 | 2160.652 | 5856.018 |
| 36 | 36 g9 | 212.98 | 639.74 | 6191.62 | 22.52 | 20.00 | 100 | 791.045 | 141.969 | 1857.02 | 1910.67 | 5361.48 |
| 37 | 37 g9 | 232.65 | 682.30 | 6669.88 | 26.99 | 20.00 | 100 | 839.913 | 117.3098 | 1593.091 | 2281.116 | 5507.41 |
| 38 | 38 g9 | 216.56 | 700.73 | 7378.30 | 26.95 | 20.00 | 100 | 1006.997 | 116.144 | 1717.526 | 2637.317 | 5780.723 |
| 39 | 39 g9 | 206.37 | 693.06 | 6739.92 | 25.61 | 20.00 | 100 | 863.4896 | 100.1129 | 1638.939 | 2324.262 | 5775.806 |
| 40 | 40 g9 | 210.19 | 701.65 | 7016.29 | 33.00 | 20.00 | 100 | 826.8933 | 68.53805 | 1630.138 | 1974.506 | 5747.257 |

APPENDIX D – SUMMARY OF XRD DATA

GUN 1



GUN 2

Match!* - □ ×

File Edit View Pattern Peaks Search Entries Quantify Database Tools Options Help

Exp.
Calc. (exp. peaks) (Rp=11.5 %)
Background
[96-710-3015] O2 Si (80.2%)
[96-230-0450] Ca F2 calcium fluoride fluorite (6.7%)
[96-900-0651] Ba O4 S Barite (6.4%)
[96-101-1050] Al3 H2 K O12 Si3 Potassium aluminium silicate hydroxide * Muscovite 2M1 (5.8%)
[96-901-6707] C Ca O3 Calcite (0.8%)
[96-900-6515] W Tungsten

Composition Structure Properties Peaks/Ranges References Subfiles

1a 2a 3b 4b 5b 6b 7b 8b 1b 2b 3a 4a 5a 6a 7a 8a

P1 H He
P2 Li Be B C N O F Ne
P3 Na Mg Al Si P S Cl Ar
P4 K Ca Sc Ti V Cr Mn Fe Co Ni Cu Zn Ga Ge As Se Br Kr
P5 Rb Sr Y Zr Nb Mo Tc Ru Rh Pd Ag Cd In Sn Sb Te I Xe
P6 Cs Ba La Hf Ta W Re Os Ir Pt Au Hg Tl Pb Bi Po At Rn
P7 Fr Ra Ac

L Ce Pr Nd Pm Sm Eu Gd Tb Dy Ho Er Tm Yb Lu
A Th Pa U Np Pu Am Cm Bk Cf Es Fm Md No Lr

Element selection by mouse
 All None Any Optional
 Toggle Reset
 Name:
 Elem. count:
 Formula sum:
 Inorganics only (no C-H-bonds)

Preset: None / new set

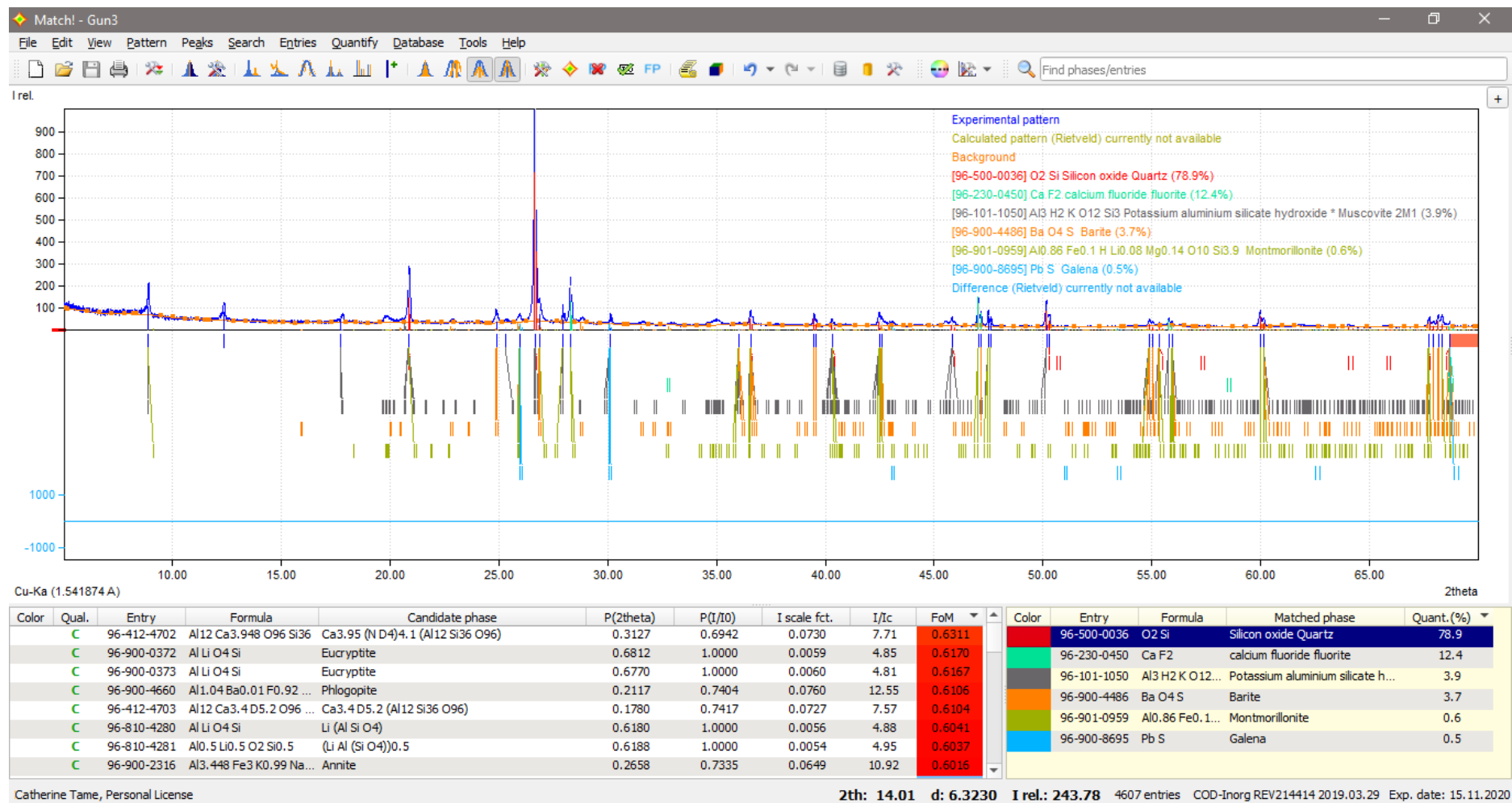
Restraints + Add. entries Peak list Data sheet FP Rietveld

| Color | Qual. | Entry | Formula | Candidate phase | P(2theta) | P(I/I0) | I scale fct. | I/Ic | FoM |
|-------|-------|-------------|-------------------------|-------------------------|-----------|---------|--------------|-------|--------|
| C | | 96-210-1329 | B17 Be N2 | | 0.9956 | 0.9664 | 0.0164 | 1.19 | 0.6940 |
| C | | 96-900-6615 | Fe0.91 Si0.09 | | 0.9935 | 0.9340 | 0.0164 | 12.49 | 0.6876 |
| C | | 96-153-7809 | Hf0.66 Mo1.32 | (Hf Mo2)0.66 | 0.9911 | 1.0000 | 0.0061 | 28.53 | 0.6722 |
| C | | 96-152-3509 | Hf Ru | | 0.9903 | 1.0000 | 0.0061 | 32.34 | 0.6721 |
| C | | 96-900-6514 | W | Tungsten | 0.9863 | 1.0000 | 0.0061 | 41.96 | 0.6713 |
| C | | 96-152-2743 | Hf Rh | | 0.9603 | 1.0000 | 0.0061 | 32.79 | 0.6663 |
| C | | 96-900-6509 | W | Tungsten | 0.9485 | 1.0000 | 0.0061 | 41.96 | 0.6641 |
| C | | 96-221-1740 | Al1.44 Li1.44 O6 Si1.56 | lithium aluminosilicate | 0.4027 | 0.9183 | 0.0830 | 4.99 | 0.6629 |

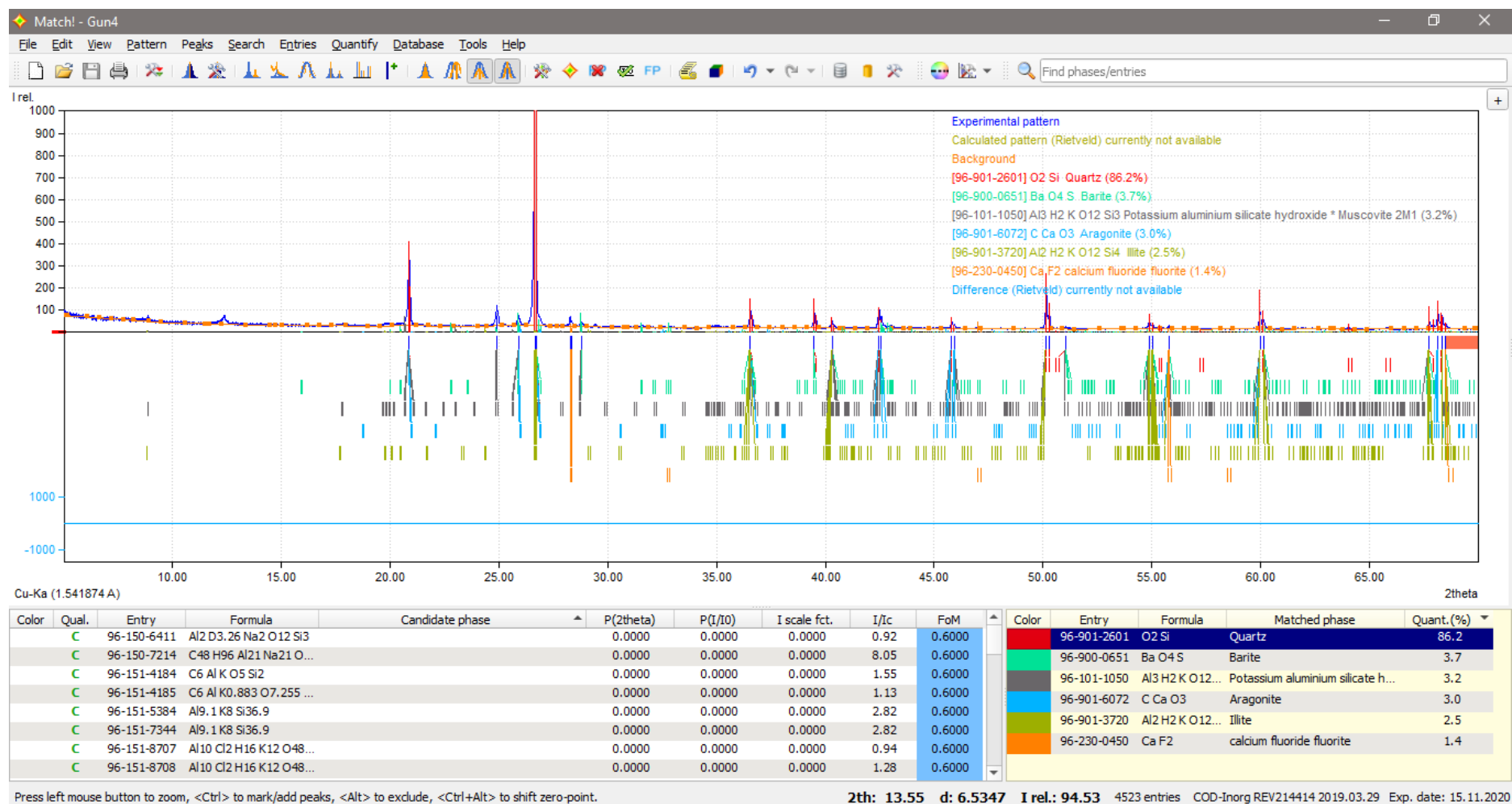
| Color | Entry | Formula | Matched phase | Quant.(%) |
|--------|-------------|-----------------|-----------------------------------|-----------|
| Red | 96-710-3015 | O2 Si | | 80.2 |
| Green | 96-230-0450 | Ca F2 | calcium fluoride fluorite | 6.7 |
| Orange | 96-900-0651 | Ba O4 S | Barite | 6.4 |
| Grey | 96-101-1050 | Al3 H2 K O12... | Potassium aluminium silicate h... | 5.8 |
| Blue | 96-901-6707 | C Ca O3 | Calcite | 0.8 |

Catherine Tame, Personal License 2th: 18.42 d: 4.8160 I rel.: 0.00 98 entries COD-Inorg REV248644 2020.03.03 Exp. date: 15.11.2020

GUN 3



GUN 4



GUN 5

Match!* _ □ ×

File Edit View Pattern Peaks Search Entries Quantify Database Tools Options Help

Exp.
Calc. (exp. peaks) (Rp=17.3 %)
Background
[96-230-0450] Ca F2 calcium fluoride fluorite (29.4%)
[96-710-3015] O2 Si (26.9%)
[96-900-4486] Ba O4 S Barite (22.5%)
[96-500-0088] Pb S Lead sulfide Galena (13.1%)
[96-900-0108] S Zn Sphalerite (8.2%)
[96-900-0662] Fe Iron

Composition* Structure Properties Peaks/Ranges References Sul

1a 2a 3b 4b 5b 6b 7b 8b 1b 2b 3a 4a 5a 6a 7a 8a

P1 H He
P2 Li Be B C N O F Ne
P3 Na Mg Al Si P S Cl Ar
P4 K Ca Sc Ti V Cr Mn Fe Co Ni Cu Zn Ga Ge As Se Br Kr
P5 Rb Sr Y Zr Nb Mo Tc Ru Rh Pd Ag Cd In Sn Sb Te I Xe
P6 Cs Ba La Hf Ta W Re Os Ir Pt Au Hg Tl Pb Bi Po At Rn
P7 Fr Ra Ac

L Ce Pr Nd Pm Sm Eu Gd Tb Dy Ho Er Tm Yb Lu
A Th Pa U Np Pu Am Cm Bk Cf Es Fm Md No Lr

Element selection by mouse
 All None Any Optional
 Toggle Reset
 Name:
 Elem. count:
 Formula sum:
 Inorganics only (no C-H-bonds)

Preset: None / new set

Restraints + Add. entries (317)

| Color | Qual. | Entry | Formula | Candidate phase | P(2theta) | P(I/I0) | I scale fct. | I/Ic | FoM |
|-------|-------|-------------|-------------------------|-------------------------|-----------|---------|--------------|-------|--------|
| C | | 96-900-0662 | Fe | Iron | 0.9904 | 0.9330 | 0.0389 | 13.23 | 0.7246 |
| C | | 96-152-4168 | Co0.75 Fe0.25 | (Co0.75 Fe0.25) | 0.9904 | 0.9320 | 0.0389 | 13.77 | 0.7244 |
| C | | 96-152-4429 | Cr0.1 Fe0.63 Si0.27 | (Cr Fe6.3 Si2.7)0.1 | 0.9904 | 0.9315 | 0.0389 | 11.14 | 0.7243 |
| C | | 96-221-1740 | Al1.44 Li1.44 O6 Si1.56 | lithium aluminosilicate | 0.4932 | 0.8874 | 0.2195 | 4.99 | 0.7236 |
| C | | 96-152-5707 | O2 Zr | Zr O2 | 0.5677 | 0.6675 | 0.2710 | 11.19 | 0.7230 |
| C | | 96-901-0020 | Fe0.725 Ni0.025 Si0.25 | Suessite | 0.9827 | 0.9312 | 0.0389 | 11.50 | 0.7227 |
| C | | 96-900-6592 | Fe | Iron | 0.9785 | 0.9330 | 0.0389 | 13.23 | 0.7223 |
| C | | 96-901-1982 | K | Potassium | 0.6499 | 0.6174 | 0.3352 | 9.73 | 0.7216 |

| Color | Entry | Formula | Matched phase | Quant.(%) |
|-------|-------------|---------|---------------------------|-----------|
| | 96-230-0450 | Ca F2 | calcium fluoride fluorite | 29.4 |
| | 96-710-3015 | O2 Si | | 26.9 |
| | 96-900-4486 | Ba O4 S | Barite | 22.5 |
| | 96-500-0088 | Pb S | Lead sulfide Galena | 13.1 |
| | 96-900-0108 | S Zn | Sphalerite | 8.2 |

Save the current status to a so-called "document" file 2th: 16.04 d: 5.5243 I rel.: 286.54 1076 entries COD-Inorg REV248644 2020.03.03 Exp. date: 15.11.2020

GUN 6

Match!* - □ ×

File Edit View Pattern Peaks Search Entries Quantify Database Tools Options Help

Composition Structure Properties Peaks/Ranges References Subfiles

1a 2a 3b 4b 5b 6b 7b 8b 1b 2b 3a 4a 5a 6a 7a 8a

P1 H He
P2 Li Be B C N O F Ne
P3 Na Mg Al Si P S Cl Ar
P4 K Ca Sc Ti V Cr Mn Fe Co Ni Cu Zn Ga Ge As Se Br Kr
P5 Rb Sr Y Zr Nb Mo Tc Ru Rh Pd Ag Cd In Sn Sb Te I Xe
P6 Cs Ba La Hf Ta W Re Os Ir Pt Au Hg Tl Pb Bi Po At Rn
P7 Fr Ra Ac

L Ce Pr Nd Pm Sm Eu Gd Tb Dy Ho Er Tm Yb Lu
A Th Pa U Np Pu Am Cm Bk Cf Es Fm Md No Lr

Element selection by mouse
 All None Any Optional
 Toggle Reset
 Name:
 Elem. count:
 Formula sum:
 Inorganics only (no C-H-bonds)

Preset: None / new set

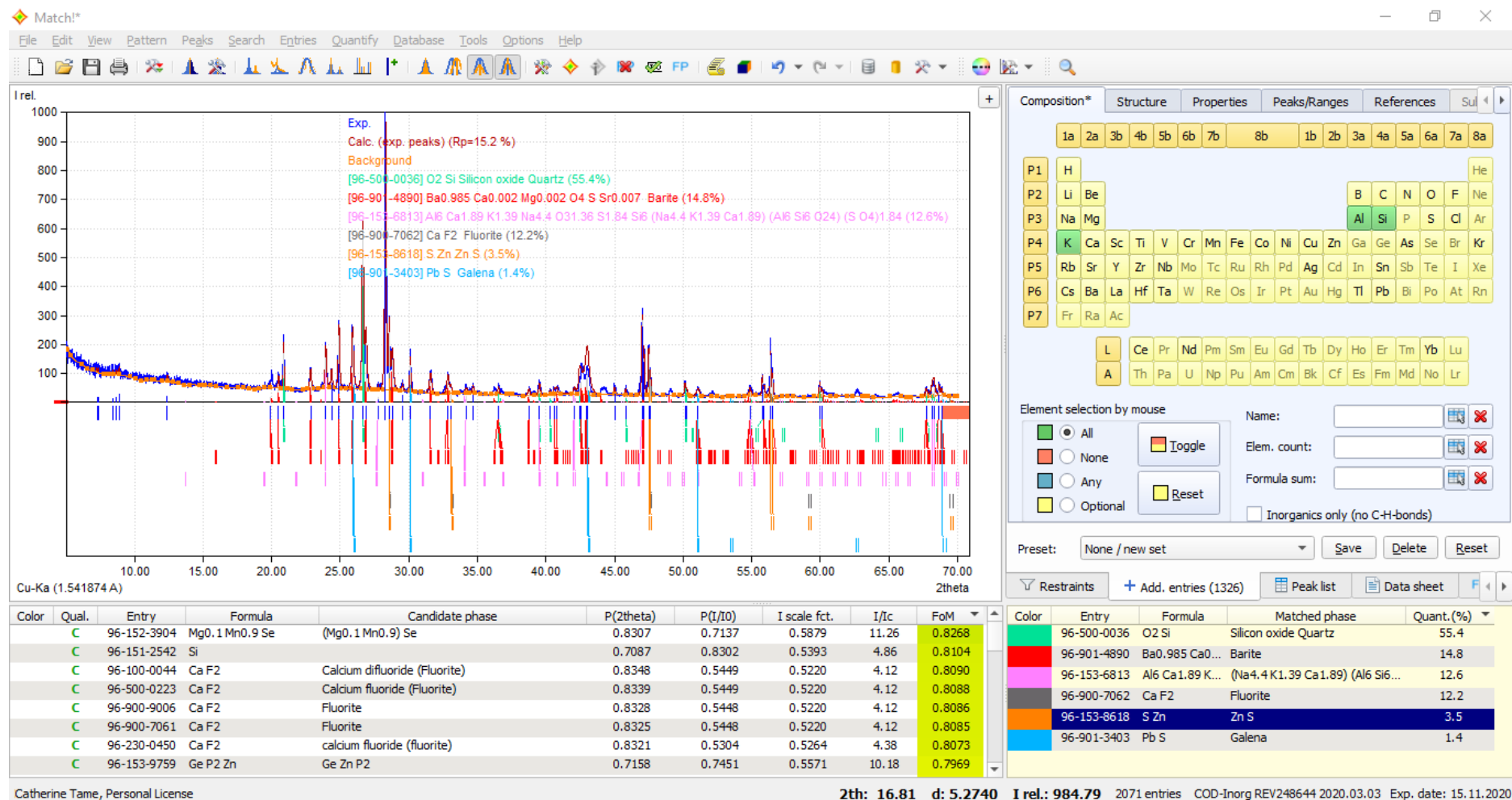
Restraints + Add. entries Peak list Data sheet FP Rietveld

| Color | Qual. | Entry | Formula | Candidate phase | P(2theta) | P(I/I0) | I scale fct. | I/Ic | FoM |
|-------|-------|-------------|-----------------|-----------------|-----------|---------|--------------|-------|--------|
| C | | 96-901-4020 | Ni0.493 Ti0.507 | | 0.9903 | 0.9350 | 0.0169 | 6.02 | 0.6923 |
| C | | 96-152-7279 | Si0.2 Tc0.8 | (Tc0.8 Si0.2) | 0.9897 | 0.9174 | 0.0169 | 19.07 | 0.6888 |
| C | | 96-151-7938 | Au Cs | | 0.9336 | 1.0000 | 0.0100 | | 0.6876 |
| C | | 96-152-3685 | Ir0.18 V0.82 | (Ir0.18 V0.82) | 0.9553 | 0.9200 | 0.0169 | 16.49 | 0.6827 |
| C | | 96-152-3921 | Ga Ru | | 0.9553 | 0.9188 | 0.0169 | 20.19 | 0.6825 |
| C | | 96-900-6615 | Fe0.91 Si0.09 | | 0.9986 | 1.0000 | 0.0060 | 12.49 | 0.6774 |
| C | | 96-210-1329 | B17 Be N2 | | 0.9811 | 1.0000 | 0.0060 | 1.19 | 0.6740 |
| C | | 96-152-5522 | Cd Li3 | | 0.9835 | 0.7374 | 0.0197 | 5.21 | 0.6696 |

| Color | Entry | Formula | Matched phase | Quant.(%) |
|--------|-------------|-----------------|----------------------|-----------|
| Red | 96-500-0036 | O2 Si | Silicon oxide Quartz | 96.3 |
| Orange | 96-900-2308 | Al1.24 Fe1.4... | Biotite | 1.8 |
| Green | 96-900-7061 | Ca F2 | Fluorite | 1.8 |
| Blue | 96-900-0002 | Pb S | Galena | 0.1 |

Catherine Tame, Personal License 2th: 29.13 d: 3.0661 I rel.: 0.00 84 entries COD-Inorg REV248644 2020.03.03 Exp. date: 15.11.2020

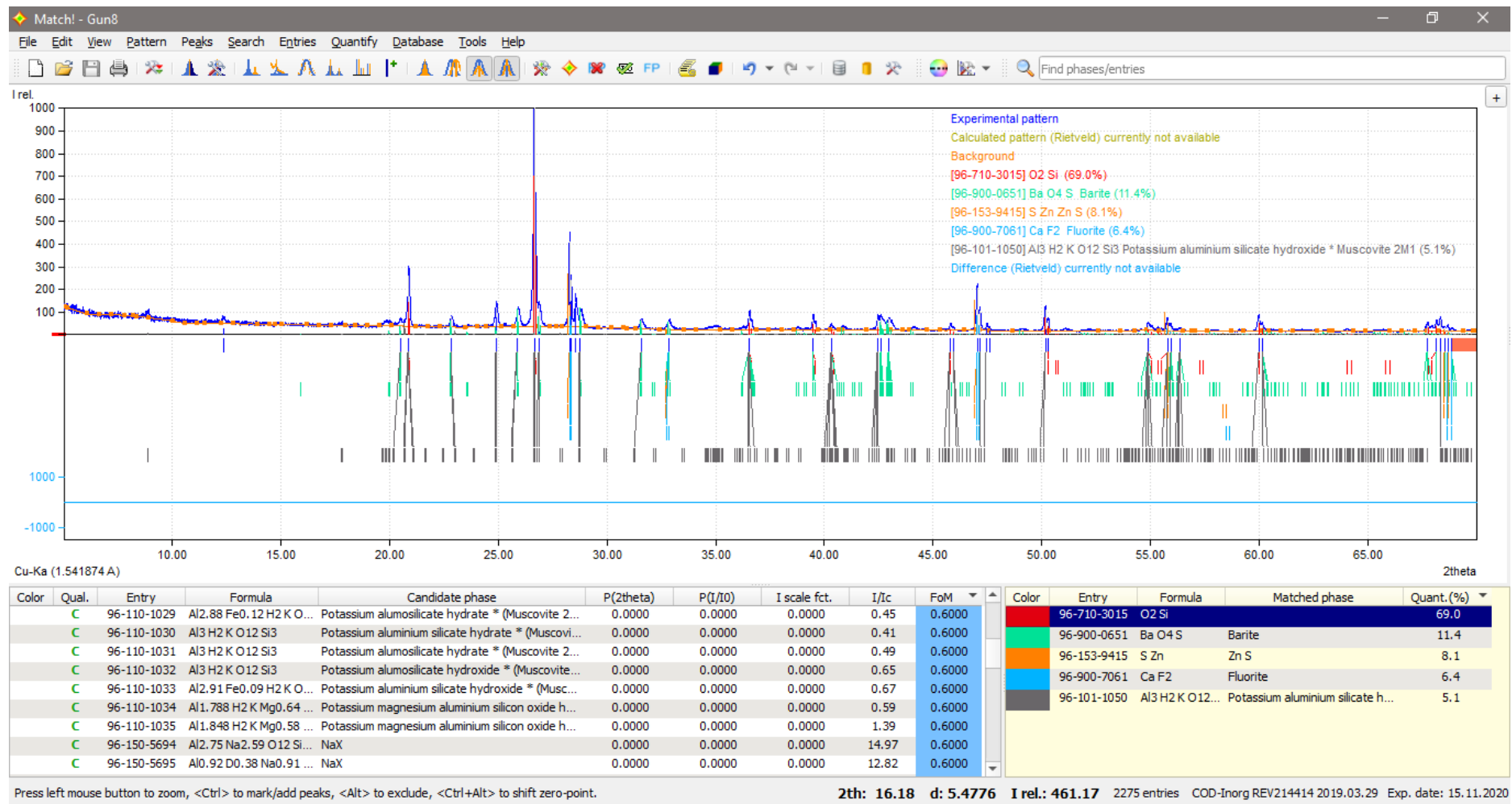
GUN 7



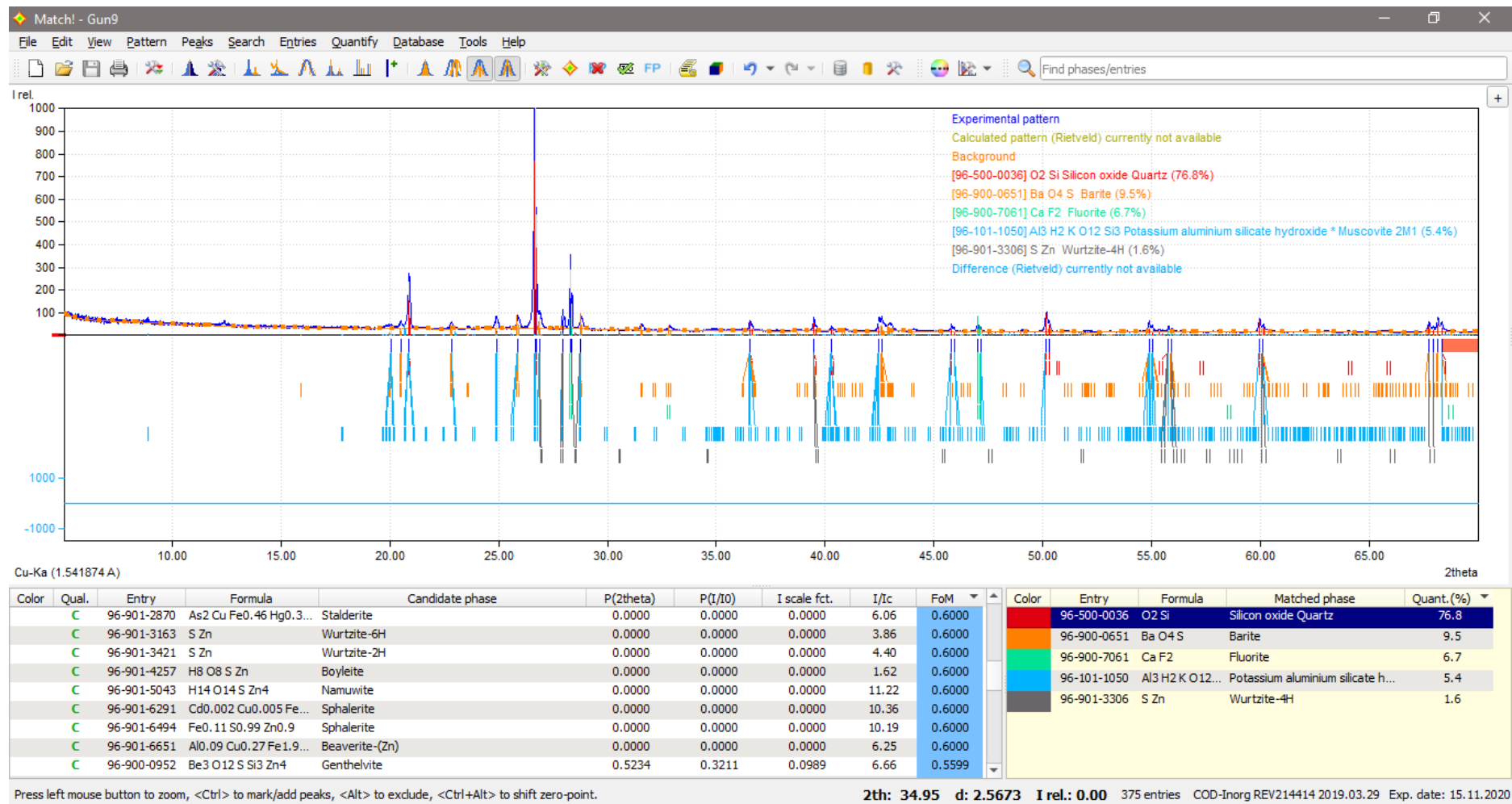
Catherine Tame, Personal License

2th: 16.81 d: 5.2740 I rel.: 984.79 2071 entries COD-Inorg REV248644 2020.03.03 Exp. date: 15.11.2020

GUN 8



GUN 9



GUN 10

